Pathways as spheres of long-term interaction between Humans and our natural environment. A multiscalar and cross-regional analysis.

Freie Universität Berlin

Dissertation

zur Erlangung des akademischen Grades
Doktor der Naturwissenschaften
am Fachbereich Geowissenschaften
der Freien Universität Berlin

vorgelegt von:

Nadav Nir

Gutacherin:

Univ.-Prof. Dr. Brigitta Schütt

Freie Universität Berlin

Fachbereich Geowissenschaften

Institut für Geographische Wissenschaften

Physische Geographie

Das Ziel ist der Weg

Erstgutachterin:

Univ.-Prof. Dr. Brigitta Schütt
Freie Universität Berlin
Fachbereich Geowissenschaften
Institut für Geographische Wissenschaften
Physische Geographie

Zweitgutachterin:

Jun-Prof. María Piquer-Rodríguez
Freie Universität Berlin
Fachbereich Geowissenschaften
Institut für Geographische Wissenschaften
Modellierung von Mensch-Umwelt Interaktionen

21.10.2022

Verteidigung der Doktorarbeit Disputation / Defence - 23.01.23

Acknowledgments

I would like to express my deep sympathy for my research partners in Tigray in hopes of a sustainable resolution to the current conflict. Constant and irreplaceable guidance throughout was given to me by my supervisor Prof. Brigitta Schütt. Thank you. Jacob Hardt, Mareike Stahlschmidt and Robert Busch were three brilliant minds guiding and holding my hand scientifically and otherwise during the entire working process. I additionally want to thank Daniel Knitter for allowing me to undertake a pathway through R and for always being a beacon of scientific light. I would like to thank Christopher Eichhorn (GIZ) for valuable fieldwork assistance and Peter Schad, Ariel Malinsky-Buller, Ruth Shahack-Gross, Zack Rothbart and Fabian Kirsten for their helpful advice and valuable input. Other irreplaceable coworkers on this project were Mika Ulman (HUJI), Uri Davidovich (HUJI), Sonja Bepita, Vincent Haburaj and Kristina Pfeiffer (DAI). Continuous support at Freie Universität Berlin was given by: Manuela Abendroth, Christiane Reuter, Ralf Milke, Moriz Nykamp, Philipp Hoelzmann, Fabian Becker, Frank Kutz, Silvan Schmieg and my fellow PhD students. I would like to thank the Studienstiftung des deutschen Volkes for fanatically supporting me for three years. I acknowledge the support of the Authority for Research and Conservation of Cultural Heritage (የቅርስ ባለስልጣን ተወካይ) of the Federal Democratic Republic of Ethiopia given by Halenessg Desta Ayalew, Tsegazeab Mezgebe and Haftum Birhane. I additionally value the technical and personal assistance of Anna Shraer, Julius Schröder, Nick McCann Karolina el Lobo, Anja Jens, Natica Moreno, Marcus Cieslak, Balthasar Busmann and Chezi Bepita . My family across the seas (Mem, Pey, Rody, Tomer, Shira, Alon, Noa, Buda and Bass) were all very supportive and insightful. In memory of Prof. Georges Stoops and Amiram Nir.

"כִּי שְׁכֵחֻנִי עַמִּי לַשָּׁוְא יְקַטֵּרוּ וַיַּכְשִׁלוּם בְּדַרְכֵיהֶם שְׁבִילֵי עוֹלָם לָלֶכֶת נְתִיבוֹת דָּרֶךְ לֹא סְלוּלָה"[1]

ירמיהו י״ח פס׳ טו

[1] "Yet my people have forgotten me… stumble… in the ancient paths. They made them walk in byways, on roads not built up"
Jeremiah 18, 15

Abstract

Pathways are an early occurring and widespread interface through which humans have influenced the landscape. These not decidedly built routes mark a meaningful milestone in our relationship with the natural world. The following thesis depicts environmental changes resulting from the formation of pathways, across different climatic zones, topographic units, and land uses. Two case studies involving 9 footpaths under temperate, sub-humid and arid climatic zones are used to evaluate the long-term interaction between footpaths and the underlying soil. The latter case studies are located in eastern Germany, Tigray (Ethiopia) and the Judean Desert (Israel) accordingly. Recreational and daily travelled footpaths are studied for current use impacts while footpaths attributed to an archaeological period are used to evaluate residues of the long-termed use of paths. For the archaeologically attributed footpaths, geomorphological effects related to linear soil erosion or changes in surface colour are also addressed, depending on the local dynamics. Following the understanding of footpath formation and effects, using a third case study (Tigray, Ethiopia), a wider look into the interaction of pathways (i.e., including unpaved roads) with human society is presented. The latter investigation focuses on the geosocial dynamic and feedback mechanism between the cost of movement and gully erosion. Scientific methods implemented in the field work included geomorphological surveying, footpath mapping, undisturbed soil sampling and penetration resistance measurements. Laboratory methods used include micromorphology, automated porosity image analysis, sedimentary analysis (XRF, XRD, grain sizes, TOC, etc.), selective Fe extraction and sedimentary colour analysis. Beyond, remote sensing was frequently applied using satellite and Unmanned Aerial Vehicle (UAV) imagery while following analysis were conducted applying Frequency Ratio (FR) and Least Cost Path (LCP) analysis.

Kurzfassung

Wanderwege sind eine früh vorkommende und weit verbreitete Schnittstelle, durch die der Mensch die Landschaft beeinflusst hat. Diese unbebauten Routen markieren einen bedeutenden Meilenstein in unserer Beziehung zur Natur. Die folgende Untersuchung zeigt Umweltveränderungen, die sich aus der Bildung von Wanderwegen ergeben, über verschiedene Klimazonen, topografische Einheiten und Landnutzungen hinweg. Zwei Fallstudien mit 9 Fußwegen in gemäßigten, subhumiden und ariden Klimazonen werden verwendet, um die langfristige Wechselwirkung zwischen Fußwegen und dem darunter liegenden Boden zu bewerten. Letztere Fallbeispiele sind entsprechend in Ostdeutschland, Tigray (Äthiopien) und der Judäischen Wüste (Israel) angesiedelt. Freizeit- und täglich begangene Fußwege werden auf Auswirkungen der aktuellen Nutzung untersucht, während Fußwege, die einer archäologischen Epoche zugeordnet sind, verwendet werden, um Reste der langfristigen Nutzung von Wegen zu bewerten. Für die archäologisch zugeordneten Fußwege werden je nach lokaler Dynamik auch geomorphologische Effekte im Zusammenhang mit linearer Bodenerosion oder Veränderungen der Oberflächenfarbe behandelt. Nach dem Verständnis der Fußwegbildung und -effekte wird anhand einer dritten Fallstudie (Tigray, Äthiopien) ein breiterer Einblick in die Wechselwirkung von Wegen (d. h. einschließlich unbefestigter Straßen) gegeben. Die letztgenannte Untersuchung konzentriert sich auf die geosoziale Dynamik und den Rückkopplungsmechanismus zwischen den Kosten der Bewegung und Gully Erosion. Zu den in dieser Arbeit implementierten Werkzeugen gehören Mikromorphologie, automatisierte Porositätsbildanalyse in R, Sedimentanalyse, selektive Fe-Extraktion, Sedimentfarbanalyse, Fernerkundung mit Satelliten- und unbemannten Luftfahrtfahrzeugen (UAV), Frequency Ratio (FR) und Least Cost Path (LCP) Analyse.

Table of Contents

List of Figures

List of Tables

List of abbreviations and terms

BCE – Before Common Era

CE – Common Era

DEM - Digital Elevation Model

GIS - Geographic Information System

LCP - Least Cost Path

LGM - Last Glacial Maximum

LP - Lower Paleolithic

MP - Middle Paleolithic

NEH - North Ethiopian Highlands

OIL – Oblique incident light

R - Open-source statistical software environment (written in C and C+)

SRO – Short-Range Order iron oxides, mostly pedogenic and mobile

UP - Upper Paleolithic

Footpath - An unconstructed route going through the open landscape formed by trampling and used by humans and animals (i.e., Trampelpfad).

Pathway / Trail– A footpath or an unpaved road

Gully – A linear depression that is the result of erosion, cannot be filled by regular tillage and that is deeper than 30 cm

Sunken lane – An elongated depression through the landscape that is the result of traveling, usually due to the use of wheeled transport. Also termed a hollow way and a road gully

Chapter 1

Introduction

1.1 A human environment

> *"The Anthropocene represents the beginning of a very rapid human-driven trajectory of the Earth System away from the glacial–interglacial limit cycle toward new, hotter climatic conditions and a profoundly different biosphere"*
>
> (Steffen et al., 2018)

Climate change is the most recent human-inflicted ecological crisis to stand on the world stage as an impact of planetary dimensions. However, the emission of carbon dioxide and other greenhouse gasses is far from being a unique example of a large-scale human influence on our ecosystems. On the contrary, the latter phenomena join the dramatic human-inflicted changes to the global sulfur, phosphorus and nitrogen cycles as well as vast deforestation, soil stability, and other land cover changes (Certini and Scalenghe, 2022). Together, these processes are possibly leading the earth towards the sixth major extinction event in its history (Thomas et al., 2004). These impacts, and particularly the change in atmospheric concentrations of carbon dioxide and methane since the middle of the 19th century and an average global temperature increase of 0.6 degrees Celcius during the 20th century, have promoted the conceptualization of a new human-induced geological era beyond the Holocene (Waters et al., 2016). The Anthropocene as a term, therefore implies that humans have recently reached an influence on the planet of geological dimensions to produce among others, completely human landscapes (Lewis and Maslin, 2015). How and when have we separated ourselves from the natural world to possess such an influence? The answer to that, if such exists, is complex and of multi-disciplinary nature. Some biologists and physical anthropologists suggest it was an increase in brain size, resulting in increasingly complex social skills in the genus *homo,* that marked the point from which we differed from other mammals (Isler and van Schaik, 2012, Gibson, 2002, Kappelman, 1996). In the archaeological record, behavioral attributes, inferred through the use of complex tools (requiring planning and conceptualization), are regarded as features that made us stand out from other species over a million years ago (Ambrose, 2001, Shea, 2016). The threshold humans crossed to possess such influence, could also result from our ability to adapt to changing environments or to move elsewhere when we can no longer

adapt (Coop et al., 2009, Moran, 2018). During the late Pleistocene and early Holocene, some of these 'adaptations' included intense interaction with the landscape through large-scale burning and the emergence of agricultural practices (Fairbairn et al., 2006, Duncan et al., 2021). It was the latter abilities, namely adaptation, innovation, and migration, that have allowed humans to spread across the globe, eventually entering almost every ecological niche and resulting in multiple anthropogenic landscapes (Tarolli et al., 2019). A distinct part of these 'human landscapes' that often connects different ecological zones is the pathway.

1.2 Trails

"Trails, paths and roads are essential structures of the human landscape"
(Snead et al., 2009)

As anthropogenic features, or 'fingerprints', pathways are observed from the Arctic to the deserts, from tropical jungles to temperate zones, crossing hillslopes and highlands, valleys, and plains (Pounder, 1985). Narrow trails and trampling ways are not exclusively human attributes. Boelhouwers and Scheepers (2004) have mentioned that animal trampling along tracks can cause soil erosion by initiating cutback development downslope from the path. However, the morphological effect of trails due to animal trampling was recognized to be substantial in specific mountainous environments where animals are forced to use specific routes (Boelhouwers and Scheepers, 2004). Similarly, humans have long been forming animal-like trails with evidence for linear trampling dated to 350 Ka BP (Panarello et al., 2017). Later in prehistory, as humans began to repeatedly use a certain locality, the routine use of a specific track resulted in long-term environmental costs. This effect has likely been more dominant following the introduction of farming and the use of domesticated pack animals (van Andel et al., 1990, Ullah, 2011). In one experimental work, it was shown that the impact made by pack animals on the local flora is at least double that resulting strictly from human trampling (Barros and Pickering, 2015). The latter results strengthen the argument that it was domestication that, in the footpath prism, had resulted in the difference between the effect animals and humans hold on the landscape. Therefore, footpaths make an excellent example of such human-landscape interaction, which is both geographically widespread as well as likely early occurring in human (pre)history. Trails and trampling have been thoroughly investigated for decades (Liddle, 1975). However, while various aspects of trails have been addressed in the literature through the years, the path has been treated as an agent of either recreational activities (Salesa

and Cerdà, 2020, Rodway-Dyer and Ellis, 2018, Yaşar Korkanç, 2014, Wimpey and Marion, 2010) or soil erosion in agricultural contexts (Zhang et al., 2019, Ziegler et al., 2001, Ziegler et al., 2000). A holistic, multi-scalar approach that includes both temporal and spatial variabilities is needed to address trails as the impactful historic and present-day features of anthropogenic landscapes that they are.

1.3 Objectives

In the current work, I investigate the development and effects of pathways, i.e., including both footpaths and unpaved roads. The prisms examined include the micro investigation of soil development on the surface and subsurface of footpaths as well as larger-scale evidence of sedimentation and erosion, specifically looking into linear soil erosion expressed by the formation of gullies and sunken lanes. The hereby presented research question is therefore a processual one: What are the long-term ecological effects footpaths produce under different land use and climatic zones and how do such effects further interact with human behavior? To answer this question, the following hypothesis and objectives are brought forward: Hypothesis: Pathways have specific long-term effects on the sub surface and the landscape under different climatic zones

Objective 1: Determine the effect of modern footpaths on soil formation

Objective 2: Determine the effect of long-term used footpaths on soil formation Objective 3: Determine the effect of modern and long-term used footpaths on the landscape Objective 4: Determine the effect of modern and long-term used pathways on the landscape

Figure 1.1. A forest recreational footpath south of Berlin (Germany) and a daily transportation footpath in central Tigray (Ethiopia).

Chapter 2

State of the art

2.1 The natural setting

Landscape formation and processes taking place on the earth's surface, are usually treated within the framework of geomorphology (Strahler, 1952). The three building blocks, lithology, tectonics, and climate, set the stage for other types of landscape inputs (e.g., relief, hydrology, soil type) and shape the complex processes that compose the interaction between these units (Ahnert et al., 1965). The solid cover of the earth surface could be divided into bare rock, soils, and sediments. In geomorphological research, the latter are also considered as archives, which we can measure, sample and analyze - usually to understand the interaction between different natural forces forming an evolving landscape (Goudie, 2004). Similar to a mathematical equation, geomorphological interest could be focused on different unknown variables, whether it may be the sediments' origin, information on past climate or the depositional (accumulation) or denudational (erosional) processes themselves (Leopold et al., 2020, Calvet et al., 2021). Colluvial, fluvial and aeolian processes are used for describing the accumulation and erosion of matter on the earth's surface (Goudie, 2004). The former process describes mass gravity-driven transport on steep slopes while the latter describes wind-based processes, e.g., wind erosion, dust transport and dune formation (Livingstone and Warren, 1996, Staff, 1999). Fluvial processes incorporate stream driven transport of material and the landscape it subsequently generates (Ahnert et al., 1965). As landscapes are open systems, these three accumulating, transporting and eroding agents constantly interact with one another. Such combinations also result in difficulties to define certain deposits, e.g., a mixed fluvial-colluvial deposit could be named alluvium while other reserve the term strictly for water transported material on a floodplain (Miller and Juilleret, 2020). Depending upon climatic inputs and geomorphological stability, and the resulting availability of organic inputs and time, the accumulated material can transform to soil.

Soil formation comprises a number of processes that lead to the formation of soil horizons along a soil profile. The soil horizons are usually defined according to specific diagnostic characteristics e.g., the accumulation of secondary carbonates, highly humified organic matter, andic properties, high amounts of readily soluble salts, organic layer etc. (Devos et al., 2022, Coleman et al., 2017, Gilley, 2005, McLennan, 1995). The interaction between soils and sediments on a slope for example, is highly dynamic. Scientific definitions for the resulting

material are still under debate with the World Reference Base for soil resources (WRB) and the United States Department of Agriculture (USDA), the two major international soil taxonomy classification systems, assessing colluvial soils differently (Zádorová and Pení žek, 2018).

Our landscape is, therefore, a complex and highly dynamic system in which geology (including both lithology and tectonics) and climate affect surface processes which in turn transport, deposit or erode sediments and soils, and expose bare rock (McLennan, 1995). The resulting earth surface is composed of different geomorphons, i.e., geometrical classification of landform elements, and landscape units such as hillslopes, valleys, highlands, riverbeds, and terraces (Ahnert et al., 1965, Leopold et al., 2020).

2.2 Human landscapes

Into the dynamic natural system of geological time scale, arrived a most recent but influential factor: humans (Werner and Mcnamara, 2007). On the one hand, humans are heavily dependent on the earth's surface, e.g., available water, fertile soils, timber, petroleum and minerals (Smith, 1968, Kopittke et al., 2019). On the other hand, humans have disrupted the morphoclimatic equilibrium in most environments and affected practically all types of landscapes and resources as well as generated new types of human made landscapes, both agricultural (e.g., terraces) and urban, (Harden et al., 2014). One example are Small Natural Features (SNF) or 'human niche constructions', these can generate hotspots of biodiversity that are the result of agricultural landscapes and other human land uses in areas that may otherwise support little biodiversity (Snead et al., 2009, Snead, 2006, Smith and Zeder, 2013, Zgłobicki et al., 2021). From a natural resource perspective, one main concern addressed by the geomorphological community is soil erosion, the removal of surface soil cover by wind and, for most environments, water induced soil erosion (Zachar, 2011).

"Water erosion occurs if the combined power of the rainfall energy and overland flow exceeds the resistance of soil to detachment"

(Bocco, 1991)

Overland flow (or surface runoff) occurs either as hortonian (more common in arid zones) or saturated (more common in humid zones) water flow (Leopold et al., 2020). After surface runoff develops, certain physical threshold conditions are to be crossed to detach soil particles and initiate erosion. The latter occurs according to various factors among which the surface infiltration capacity, the shear strength and cohesion of the surface and the frequency, intensity, and viscosity of the fluid (Ahnert et al., 1965, Leopold et al., 2020, Schumm, 1979). These

mechanical and physical attributes are controlled by several variables including human impact (e.g., land use changes and pollution), topography (as dictated by lithology and tectonics) and climatic conditions (Borrelli et al., 2017). Adding clay or increasing aggregation, for example, can make soil more resistant to erosion (Smerdon and Beasley, 1959). Water soil erosion can be divided into three categories, according to its spatial behavior and related to agricultural activities; The first category, wash or sheet soil erosion or in agricultural context, interrill erosion, involves the removal of a soil layer practically evenly on a large surface (Ahnert et al., 1965). The second category, rill erosion, depicts linear soil erosion that can be leveled by tillage and that is not deeper than 30 cm. Gully erosion marks the third category. The resulting landform, gullies, are linear depressions that cannot be filled by regular tillage and are deeper than 30 cm. Gullies can reach dozens of meters in depth and kilometers in length. Soil loss through gulling is a global problem that has long been investigated (Imeson and Kwaad, 1980, Bennett et al., 2000). From a depositional perspective, gully erosion is an important sediment source on the watershed level. Gullies transfer sediment to valley bottoms as well as to permanent river channels. Therefore, after gullies form, similar to permeant streams, they can increase the connectivity in the landscape (Poesen et al., 2003). However, also similar to river channels, when it comes to the ecological connectivity and the transition between niches, deep elongated gullies can potentially be berries to the movement of both humans and other animals and contribute to a fragmented landscape (Laurance, 2004). Other, similarly elongated, landscape features that can serve humans as ecological corridors while at the same time constitute a barrier for other animals, are trails.

2.3 The geomorphology of trails

Whether due to traveling on a (pre)historic scale or more recently for tourism, the resulting effects of trails on the natural environment has been assessed within different disciplinesand from various perspectives (Brandolini et al., 2006, Snead, 2006, Wimpey and Marion, 2010, Buchwał and Rogowski, 2010a, Snead et al., 2011, Fonseca Filho et al., 2018, Sidle et al., 2019, Phillips et al., 2021). It should be noted that many of those works do not distinguish between footpaths and unpaved roads that are driven on by motored vehicles. The basic starting point of most of the effects trails have on the landscape is soil compaction. Soil compaction can change the structure of the soil, it causes the reduction and breakage of soil aggregates and decreases soil porosity and infiltration capacity. The latter in turn results in surface overland flow and soil erosion (Coulon and Bruand, 1989, Soane and Van Ouwerkerk, 1994, Yaşar Korkanç, 2014). Therefore, one important impact of trails, especially in slopy areas, is

downslope soil erosion due to overland flow and surface runoff. This can result in sheet, rill, or gully erosion outside the trail or cause erosion within it (Sutherland et al., 2001, Brandolini et al., 2006, Buchwał and Rogowski, 2010a, Sidle et al., 2019, Salesa and Cerdà, 2020). When a path is heavily eroded and/or intensely used (usually by vehicles), it can become a linear depression called sunken lane. From a historical and agricultural point of view, sunken lanes are probably the most striking and intuitive example of human movement residue on the landscape;

"Sunken lanes are roads or tracks, 2 m or more wide, that are incised at least 0.5 m, but often by several meters, below the general level of the surrounding land surface. They are formed by the passage of people, animals, vehicles and erosion by water and gravity"

(Zgłobicki et al., 2021)

Recently studied sunken lanes in southern England, occurred due to wheels passage and animal trampling compacting the Mesozoic soil cover, following centuries of use and reoccurring rain events and overland flow that contribute to the erosion of the entire lane up to several meters in depth (Boardman, 2022). In historic contexts, sunken lanes are usually termed hollow ways and have been suggested to hold a great deal of importance from a cultural heritage perspective (Boardman, 2022, Kirchner et al., 2020). The resulting elongated features can be well compared to a gully, similarly the natural requirements for a sunken lane to form are erodible sedimentary cover (e.g., the European loess belt) and usually a hilly environment (Zgłobicki et al., 2021). Also similar to a gully, a sunken lane acts as a channel during extreme rain events and it can increase landscape connectivity and sedimentation (Boardman, 2013). Different to gullies, no clear slope-area threshold has been found to initiate sunken lanes and they do not seem to be heavily dependend on surface runoff (Geeter et al., 2020). However, in other climatic zones, sunken lanes, also sometimes termed "road gullies" may be less common but remain very visible and compose a unique part of the landscape (Zgłobicki et al., 2021). Two early hollow ways structures, dating back to the Bronze Age, were discovered in Syria and northern Jazeera. In the latter case study, sunken lanes have been continuously forming for 5000 years. The depth and length of the hollow ways has been suggested to correlate with the size of settlements they lead to. I.e., deeper or longer sunken lanes tend to cross larger settlements than shorter or shallower ones do (de Gruchy and Cunliffe, 2020, Wilkinson et al., 2010). However, trails can influence the landscape even when such striking geomorphological effects are not observed. Looking at the effect of tourism on the landscape and specifically the biosphere, multiple authors have tried to understand the relationship between trails and the local vegetation and erosion. Based on those studies, it is generally agreed that footpaths and

roads decrease the local flora and biota, and increase surface runoff (Harden, 1992, Ziegler et al., 2000, Ziegler et al., 2001, Ayres et al., 2008, Pounder, 1985, Morrocco and Ballantyne, 2008, Buchwał and Rogowski, 2010a, Tejedo et al., 2016a, Rodway-Dyer and Ellis, 2018, Loor and Evans, 2021). In the arctics for example, the rare footpaths have been shown to decrease local biogenic activities and increase bulk density under the trail (Pounder, 1985, Ayres et al., 2008, Tejedo et al., 2016a). In Europe, trails have shown to affect the local vegetation by both compaction and the direct destruction of plants along the route. Some plants have shown regrowth during seasons of lower activities while others were not as resilient and were later absent from the micro environment of the trail (Bernhardt-Römermann et al., 2011). On the same note, the abundance of Organic matter, N and C tent to decrease due to tourists trampling repeatedly on a surface to form a trail (Ballantyne and Pickering, 2015, Fonseca Filho et al., 2018). Qualitative work in the USA has shown that biking, off road motor sports and walking have all resulted in soil compaction. However, compaction resulting from hiking and biking is lower and increases slowly over repetitive use compared with that caused by motor vehicles (Lei, 2004). In tourism, the different ways trails are used and their position in the landscape can both affect the width of the trail and the local biosphere. It has been suggested that for recreational purposes it is preferable that tourists use one trail intensively rather than generate several moderately used footpaths within a given environment (Wimpey and Marion, 2010, Salesa and Cerdà, 2020).

2.4 The mineralogy of soil compaction

Several studies evaluate the effect of recreational trails on the underlying soil. Most of these works have focused on soil erosion and the surrounding biosphere while the effect footpaths may have on the local soil formation including structure, Fe oxides and mineralogy have rarely been looked into (Ballantyne and Pickering, 2015, Fonseca Filho et al., 2018, Sherman et al., 2019b). In contrast, considering the latter topics, for over half a century a great deal of work has been done investigating soils compacted by heavy machinery in agricultural and forestry contexts (Coulon and Bruand, 1989, Lull, 1959, Nawaz et al., 2013, Soane and Van Ouwerkerk, 1994). It is well known that in Europe, for example, silty Cambic horizon become compacted under different crops. In one experimental work it has been shown that following compaction, compound packing voids (>75µm) disappeared while similar sized channels resulting from earthworm remained. The amount of smaller sized voids (50 µm to 75µm) appearing between the micro aggregates, have also been reduced. However, on the smallest scale, the arrangement of clays remained isotropic and was not affected by compaction (Bresson and Zambaux, 1990).

Contrastingly, Kooistra and Tovey (1994) have concluded that soil microstructure is affected by compaction at all levels including the rearrangement of clays, i.e., compaction results in the clay and fine silt sizes particles being squeezed between sands and larger silt sized grains (Kooistra and Tovey, 1994). In both urban and open environments, tree growth constrained by roots activities has also been decreased by changes in soil crusts and reduction of loose soils, resulting from compaction (Jim, 1993). More recently, other authors have further investigated the structural changes in soils using micromorphology as well as the concentration of organic carbon, nitrogen, and iron oxides in compacted soils. (Herbin et al., 2011, Silva et al., 2011, Bagheri et al., 2012, Nawaz et al., 2016, Shah et al., 2017, Wang et al., 2020). In one experimental work, under controlled pressure on loamy sandy soils (bulk density of 1.6 Mg m–3), carbon mineralization rate was found to be lower than in both uncompacted soil samples. This decrease in mineralization implies that such degree of compaction would result in higher amounts of organic carbon in the soil. As N mineralization in the same experiment has not shown a significant decrease, it has been suggested that the accumulated organic matter in the compacted soil would have higher C : N ratios than in the uncompacted soil (Neve and Hofman, 2000). One important group of agents that affect the accumulation of organic carbon, clay minerals and various elements as well as the overall structure of the soil, are metal- and namely iron- oxides (e.g., Wüstite, Hematite). Fe (and to some extent Mn) oxides in sediments and soils could be the result of geogenic weathering i.e., originating from the bedrock, or they can be pedogenic oxides, usually Short-Range Order (SRO), resulting from soil forming processes, whether *in situ* or transported. SRO iron oxides or hydroxides are dependent on the amount of water and Organic Carbon (OC) and, quite intuitively, on the availability of oxygen. Changes between phases of Fe(II) and Fe(III) and the transition from a reduced to an oxidized state are therefore dependent on the environment being aerobic or anaerobic. For example, with lower supply of oxygen (anoxic environment) ferrous Fe(II) can transform into ferric Fe(III) and vice versa (Stumm and Sulzberger, 1992, Davison, 1993, Jim, 1993, Doyle and Otte, 1997, Bigham et al., 2002, Gilley, 2005, Coward et al., 2017). Going back to compaction, as it reduces the pore size between aggregates and grains, and with it the availability of air, the amount of oxygen in the soil is decreased. The latter in turn can change the type of Fe oxides accumulated in the soil (Coulon and Bruand 1989). In studies it has been shown that in soils under compaction, a higher amount of SRO or pedogenic Fe is expected than that in similar but uncompacted soils. In one case it has been suggested that the appearance of puddle on soils compacted by heavy machinery generates a reducing environment that allows the formation of some SRO Fe oxides, increasing their abundance compared with a non-compacted soil (Nawaz

et al., 2016, Wang et al., 2020). Depending on the local environment, both the oxidation as well as the reduction of Fe oxides can affect Organic Carbon Cycle and cause the release of CO2 from the soil to the atmosphere (Song et al., 2022). To further understand the relationship between the inorganic and organic components of the soil, one approach that is commonly used in both soil sciences and archaeology, is the microscopic investigation of undisturbed soil samples, i.e., micromorphology (Courty et al., 1989, Berna et al., 2007, YLI-HALLA et al., 2009, Goldberg and Berna, 2010, Williams et al., 2012, Rasa et al., 2012a, Nicosia and Stoops, 2017, Rentzel et al., 2017, Goldberg, 2018, Menzies and Meer, 2018).

2.5 Micromorphology of archaeology and trampling

"We are able to investigate a watch in very different ways.
We can put it into a mortar and pound it to a very fine powder.
The chemical analysis of this powder gives us complete information
on the nature and quantity of the elements used for the construction of the whole…
A second, mechanical, analysis will be necessary to sort these isolated components...
A third mode of analysis would be to investigate its works without destruction…examine
every part in its place and determine the nature of their connection... Micropedology
deals with the morphology, genesis, general dynamics and biology of soils"

(Kubïena, 1939)

As Walter Kubïena pioneered the sampling of undisturbed soils and the petrographic analysis of their thin section, the focus of his (and following early micromorphologists) studies was aimed at understanding pedological processes. Questions regarding soil fertility and the interaction between various organic and inorganic components were at the forefront of the micropedological research (Collins and McGown, 1974, Babel, 1975, Frei and Cline, 1949). Following macro pedology, the concept of fabric was key to understanding micromorphological processes (FitzPatrick, 1984, Coleman et al., 2017). The fabric includes the organization of the different units of the soil. The way in which larger (e.g., sand, gravel), and smaller (clay, silt) grains, interact with each other, can shed light on much of the soil-forming process (Kubïena, 1939). Beyond the fabric, pedogenic features (e.g., voids, Fe oxides, cement) and Organic Matter (OM) as well as the form and shape of the independent features and grains, have been crucial for the understanding and reconstruction of soil formation (FitzPatrick, 1984). In archeology, micromorphology was applied as early as the 1950s when it was used to distinguish anthropogenic deposits from natural ones (Dalrymple, 1958). The method, however, involved a long preparation time with the impregnation of the undisturbed

soil samples which was (and still is) followed by cutting using a rock saw and a long analysis under the microscope. While in the soil sciences interest in the method peaked during the 1970s-80s, micromorphology has emerged as a commonly used technique in prehistoric-archaeological research since the early 1990s (Courty et al., 1989, Berna et al., 2007, Goldberg and Berna, 2010, Nicosia and Stoops, 2017, Goldberg, 2018). In caves, post-depositional chemical processes, that at times hold severe effects on the archaeological records (e.g., preservation of organic and bone remains, are ash layers in situ or transported) are far better-understood following the application of micromorphology and other micro-archaeological methods (Binford et al., 1985, Goldberg, 2000, Henshilwood et al., 2001, Stiner et al., 2001). Outside caves, micromorphology can be used in various ways, among them is to uncover phases of construction or the early Holocene technologies behind the preparation of plaster (Friesem et al., 2020, Karkanas and Van de Moortel, 2014). For all types of thin section investigations, it is important to remember that micromorphology is a team player, i.e., relying on data supplied by complementary micro- and geo-archaeological techniques such as Fourier-transform infrared spectroscopy (FTIR) and common sedimentary and geological analyses (Shahack-Gross, 2017). In some cases, it is micromorphology that can supply the confirmation of context and state of preservation for other methods in focus. Recently, micromorphology was successfully applied to assess archeological and sedimentary contexts while dating desert cisterns using Optically Stimulated Luminesce (OSL) and by the extraction of ancient DNA samples in multiple paleolithic locations (Junge et al., 2021, Massilani et al., 2022). Today, soil micromorphologists combine various technologies to better-recognized elements (e.g., micro Scanning Electron Microscope (SEM)) and minerals (e.g., microscope adjustable FTIR) directly on the thin section (Verrecchia and Trombino, 2021a). Additionally, the preparation of the slides has also substantially improved and is now possible in some cases on-site and within days (Asscher and Goren, 2016). When it comes to trampling in micromorphology, Rentzel et al. (2017) defined it as the action of humans and animals passing on dry surfaces while the word poaching would suggest trampling on water-saturated soils. The understanding of the trampled surfaces (also named trample) from the micromorphological point of view can be subdivided into two prisms: (1) the effect of trampling on the archaeological remains (e.g., bones, ash) and (2) the effect of trampling on the soil (e.g., compaction, porosity). In the archaeological record, the former is used as a common proxy for trampling while the latter is rarely applied outside experimental investigations. This is mainly due to the difficulty of distinguishing compaction resulting from trampling from that caused by agents such as overlaying soil burden and non-trampling human activities (Miller et al., 2010, Rentzel et al.,

2017). Natural trampled surfaces can result in complex packing voids and plant remains organized in a linear horizontal structure. At limes micro laminations of fine material (silt and clay) can also result from slightly sunken surfaces (puddles) that are part of a trampled path (Rentzel et al., 2017).

2.6 Reconstructing (pre)historical routes

Ancient movement patterns have long been in the focus of the prehistorical research, applying geochemical methods for tracing the origins of different raw materials (de Mendoza and Jester, 1978). For later archaeological periods, excavated and surveyed historical road networks have been intensely investigated in order to reconstruct past routes and deduct anthropological and geographical insights (Harel, 1967, Ward-Perkins, 1962). However, in most archaeological case studies it is only the points of interest that are known based on either excavations or their mentioning in the historical records. In arid environments, locating routes from direct evidence could be based on indicative sherds ('travel waste') collections along trails (Rothenberg, 1970). However, for most historic and prehistoric routes, reconstructed movement networks are suggested by some authors based on travelers reports, local knowledge or pure imagination (Bent, 1893, Crawford, 2019, Caraman, 1985, Henze, 2000, Nyssen et al., 2020, Woldekiros, 2019).

In recent decades, a geographic cost-based tool was developed and intensely used for modeling the routes of human and animals traveling through landscapes. The latter, Least Cost Path analysis (LCP) uses topographic data sets and, based on one of several cost theories and algorithms, it calculates the cost humans pay to travel across landscape units (Rees, 2004, Herzog, 2010, Tobler, 1993). The cost is commonly defined as a combination of distance and slope angels, reflecting required energy. In its most used form today, a LCP analysis is based on a Digital Elevation Model (DEM) of a given landscape. The DEM is transformed into squares of difficulties corresponding to the degree of elevation difference between neighboring pixels i.e., a cost matrix (Johnson, 1977). One can calculate a cost matrix using different numbers of neighboring pixels (e.g., 8, 12) depending on the needs of the LCP and computation limitations (Schild, 2016, Nakoinz and Knitter, 2016). Following the formation of the cost matrix, at least two archaeological or historically known points are placed on the grid and the least cost path between the two or more points is calculated (Herzog, 2010). As our understanding of the algorithm progressed, various tools have been developed to improve and adjust the projected LCP so that it is more realistic. Some of the theories and algorithms take

into account energy output, several of them put an emphasis on road traveling while others are focused only on topography (Alberti, 2019, Herzog, 2014). A few models offer multipoint or grid-based LCPs. The latter tend to focus on junction or travel hierarchy calculation to understand where would an optimal connection between several historical locations pass or explain why do some historical point of interest positioned in certain locations (Herzog, 2014, Seifried and Gardner, 2019). Recently, historical maps, high resolution Lidar (Light detection and ranging) DEMs and LCP modeling were successfully combined to assess the locations of pre-industrialization routes in Germany (Herzog, 2017). Similarly in Ethiopia, the reconstruction of the ancient salt trade routes between Afar depression and the Ethiopian highlands has been suggested based on archaeological and historical evidences coupled with LCP modeling (Woldekiros, 2019). However, as the use of LCP analysis has been intensified, criticism was raised addressing the over simplifications of the theories and the quality of the DEM (Verhagen et al., 2019). Others have mentioned the notion of a 'black box' used by archaeologists who do not fully understand the meaning behind the selection of a LCP (Nakoinz and Knitter, 2016, Verhagen et al., 2019). On the other hand, complex solutions have already been proposed to some of the issues in an attempt to make these routes more realistic and overcome DEM related errors (Gowen and de Smet, 2020, Herzog, 2021, McLean and Rubio-Campillo, 2022, Crandell, 2020). As part of the ongoing effort to improve LCP analysis, many researchers are using the script based open-source R environment. The latter tends to offer more flexibility in LCP modeling than a GIS (Geographical Information System) does, making it more adjustable to the site specific limitations and research questions (Alberti, 2019, Flückiger et al., 2022, Verhagen et al., 2019).

Chapter 3

Methodological structure

3.1 Experimental design

An experimental design was planned in order to understand the long-term ecological effects footpaths and pathways produce under different land use and climatic zones and how do such effects further interact with human behaviour. The design is extrapolated from

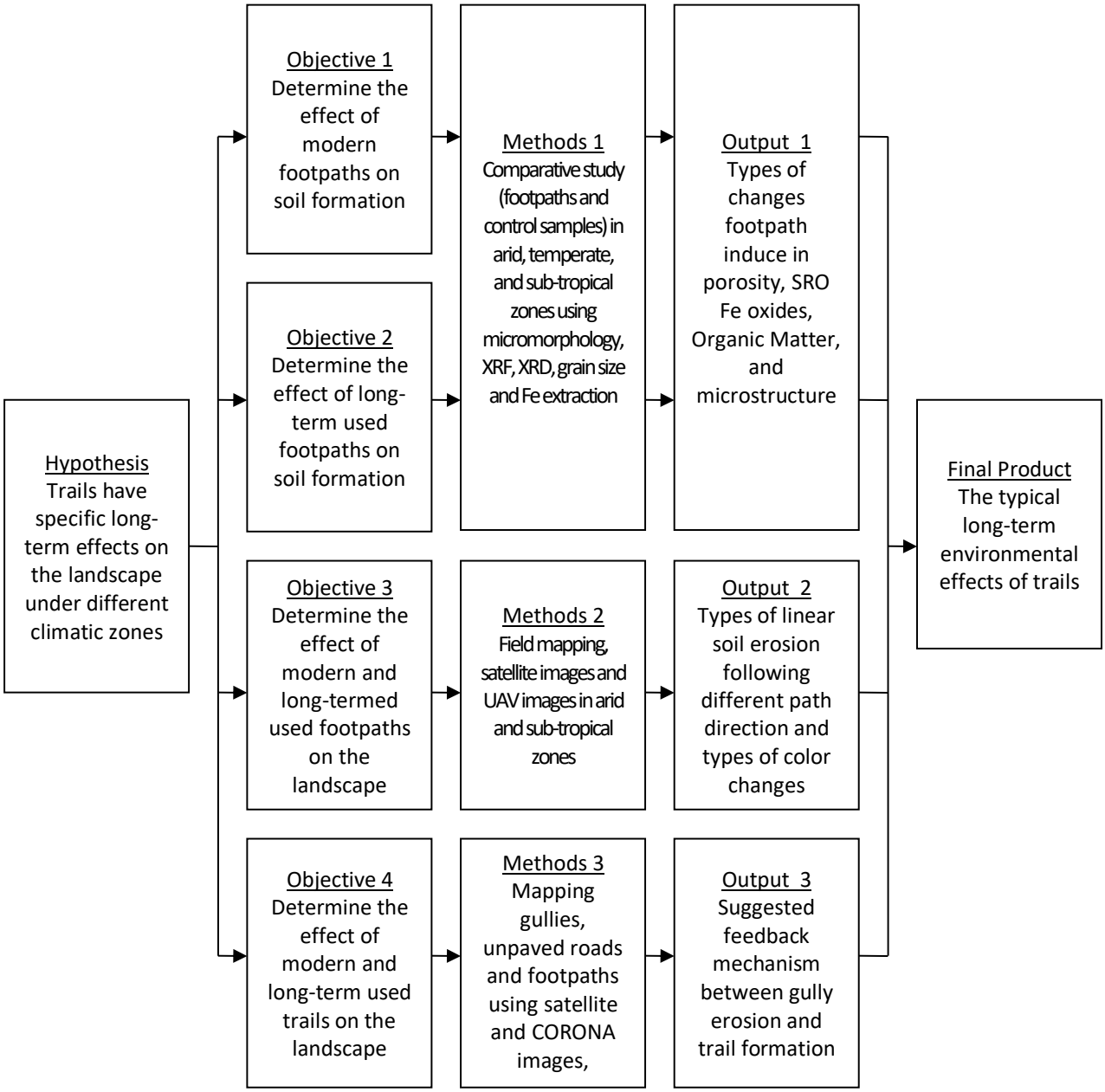

Figure 3.1. Methodological structure of the research presented as a processual chart. See further illustration of the methodological approach in chapter 4: figure 5.

3.2 Methods

Fieldwork

Geomorphological field observations compose a significant and elementary part of this work. For all environments, early observations made on the dynamics between the natural environment and trails have contributed to forming the hypothesis later tested using other methods (Baker and Twidale, 1991). Footpaths selected for sampling were either 1) in an environment where no traffic is evident or 2) not accessible to motored vehicles due to slope angle or natural or human barriers. Long-term used footpaths were selected based on their proximity to archaeological sites, or the archaeological finds documented along the footpaths, with preferences for sunken paths, a geomorphological character which also served as an indication of long-termed use. Field observations during surveying, land use documentation, and assessing the interaction between trails and gullies, were all typed and directly uploaded to the FU cloud so that they are accessible, editable, and safely stored. For measuring width and angles, two instruments were used 1) a Leica DISTO device (for further description see chapter 4.3 in Nir et al. (2022)), and 2) an I-phone device with measurement features including calculating the distance between points, angle and tilt (Breitbarth et al., 2019). The exact locations of survey points and features were generated using a Garmin GPS instrument and processed using Garmin Base Camp (for further description see method chapter in Nir et al. (2022)). An Unmanned Arial Vehicle (UAV) was used above several footpath segments in the arid zone for the long-termed used footpaths to produce a high resolution for color and geomorphological analysis, for further descriptions see Nir et al. (manuscript).

The sampling of naturally exposed soil profiles (undercut by gully erosion) and footpaths were conducted according to conventional geomorphological practices (Leopold et al., 2020). These included field descriptions of the area and the sedimentary and soil horizons (e.g., texture, color, and grain size) and sampling of ca. 150 g of disturbed samples into designated plastic bags at 5-10 cm intervals. For further description see the method chapters in Nir et al. (2022) and Hardt et al. (submitted manuscript). The sampling of footpaths was conducted with references, i.e., control samples for each path, to understand the possible change compared with the natural setting. The exact positioning of these control samples varies. For further descriptions see Nir et al. (2022) and Nir et al. (manuscript). Footpath and control surfaces were dug to a depth of ca. 50 cm and similarly described and sampled. OSL and 14C sampling

followed common procedures (Boaretto, 2009, Yukihara and McKeever, 2011). The sampling of undisturbed soil samples for micromorphological analysis followed Stoops (2021). Additionally, the sampling process of undisturbed soil and of OSL and 14C datable material is further elaborated in Nir et al. (2022), within the method chapter. For footpaths located in the temperate and arid zones, a penetrometer was used on the footpath surface and outside it, i.e., on the non-path area. For further information see chapters 3.2 and 4.2, Nir et al. (2022) and Nir et al. (manuscript).

Laboratory analysis

In the Freie Universität Berlin (FU Berlin), common sedimentological tools were used for investigating footpaths in all environments and climatic zones. For soil acidity and degree of salinity pH and electric conductivity tests were carried out. In order to validate micromorphological observations and understand the deposition grain size analyses were conducted. For comparable data between footpaths and control samples in regard to iron and other common oxide composing elements, X-Ray Fluorescence (XRF) was performed. Total Carbon and Total Organic Carbon (TC and TOC) were used to understand the degree of soil formation processes and the effect of compaction on the organic components. Following XRF analysis, Inductively Coupled Plasma (ICP) was carried out to gain higher resolution on the abundance of Fe and Mn in the samples. Several representative samples from each footpath were additionally mineralogically examined using X-Ray Diffraction (XRD). See elaborations on these analyses in the methods and supplementary chapters of Nir et al. (2022) and Nir et al. (manuscript). For footpaths in the temperate and the sub-humid zones, further analysis was held regarding the change in the types of iron on footpath surfaces. Short-Range Order (SRO) Fe oxides are mostly the result of pedogenic processes rather than weathering material of a geogenic origin. They are inorganic so they can survive for as long as the environment allows, and they affect both nutrients and organic components in soils (Stumm and Sulzberger, 1992, Bigham et al., 2002, Kilbride et al., 2006, Coward et al., 2017, Chen et al., 2020). Therefore, SRO Fe oxides can be an important long-term result of compaction and footpath formation. The extraction of SRO Fe oxides was performed using three different approaches. Further details regarding the chemical methods and approaches are provided in Nir et al. (2022).

Some micromorphological samples were impregnated and cut while others were sent to an external laboratory for the complete preparation process (chapter 4.2). The analysis of the

resulting thin sections was held in the microscopy laboratory at the FU Berlin using a polarizing microscope in 4 magnifications following common procedures (Stoops, 2021). It is important to notice that micromorphology was applied focusing on the existence or hindering of pedogenesis with most studied samples coming from soil surfaces. Therefore, to some extent, the application of micromorphology in this work resembles those applied for answering research questions of the soil sciences rather than ones of archaeological nature (FitzPatrick, 1984, Rasa et al., 2012a). However, micro-features implying human activities have been etherealness targeted during the microscopic analyses. One challenge of sampling outside archaeological sites and on the surface is that indicators such as pottery, bones, charcoal, and construction materials are of limited use outside the archaeological context (Goldberg and Berna, 2010). Hence, the approach used here compares between an outside control and the path itself. When the control sampling location is carefully chosen, surface and sub-surface changes from the natural (or anthropogenic) landscapes to those experiencing linear trampling (i.e., footpaths) could potentially be observed. Further elaboration regarding the micromorphological analyses could be found in Nir et al. (2022) and Nir et al. (manuscript) under the micromorphology method chapters.

An automated pore size recognition technique is applied in this work to generate comparable data on changes in surface porosity, resulting from footpath formation. Recent attempts to use automated image analysis in order to understand porosity in soils have been fruitful (Pires et al., 2009b, Rasa et al., 2012a). However, some of the software used for the latter investigations are either no longer available or unaffordable to some scholars. Firstly, images were taken at 1 cm intervals on the thin section slide in various magnifications. Following which, the open-source environment R was used for assessing changes in porosity. The latter offers a simple and reproducible method, one that all can apply while investigating voids using micromorphology (R Core Team, 2013). This would also make different publications more comparable. Further information could be found in Nir et al. (2022) under the method chapter. After establishing that changes in porosity are significant and recognizable using the smallest magnification, i.e., with the most visible slide area in the image, the latter magnification alone was used, in triplicates, along the first 5 cm of each slide. For further information see the methods chapter in Nir et al. (manuscript).

Computation and spatial analysis

Spatial analysis performed here is based on publicly available satellite images along with digitalized historical, geological and soil maps and UAV images (USGS, Panagos et al., 2011).

For all three case studies (Eastern Germany, the Ethiopian Highlands and the Judean Desert), raw and processed Shuttle Radar Topography Mission (SRTM) data and other DEMs were available at USGS (https://earthexplorer.usgs.gov).

For the North Ethiopian Highlands case study (Tigray), four 10x10 km rectangular sample units with their center positioned around 1st Millenia Before Common Era (BCE) archaeological sites where formed. For the Tigray case study, several additional inputs were used; Normalized Difference Vegetation Index (NDVI) was calculated using Sentinel-2 satellite imagery (T37PDR, T37PER; 2020/06/25; https://scihub.copernicus.eu) while Land use-land cover (LULC) data were provided by the European Space Agency (ESA) Climate Change Initiative (CCI), also based on Sentinel-2 data (http://2016africalandcover20m.esrin.esa.int/download.php). Soil types were mapped and calculated by Dewitte et al. 2013 while the Drainage network was deducted from a world bank online database in cooperation with the Ethiopian government (https://datacatalog.worldbank.org/dataset/ethiopia-rivers). Geological maps of the Ethiopian Highlands were provided by the Ethiopian geological survey unit at a scale of 1:250,000 (ND 37-6, ND 37-7) and later digitalized. Three USSR topographic maps (D37-13, D37-21, D37-28 (http://loadmap.net) were processed and digitalized to reflect the main roads and pathways during the second half of the 20th century. Similarly, CORONA satellite images originally taken by the US Central Intelligence Agency (KH4B, 1967; DS1102-2106DF072_c) were used to assess the premodern landscape and the antiquity of some of the studied trails and gullies. Based on these inputs, the online mapping of gullies, roads, trails, and other natural and anthropogenic landscape units was conducted using an open-access Geographic Information System (QGIS.org, 2021). Settlements, gullies, roads, and trails were validated during fieldwork, to reflect the reality of the surface dynamics and the exact appearances and social significance of the above-mentioned features. Calculating the effect of all inputs (variables) on the location of gullies was performed using the Frequency Ratio (FR) equation, incorporating 12 variables (Senanayake et al., 2020). For a detailed description of the mapping resolution and methodologies as well as FR calculations see Nir et al. (2021) within the method chapter and supplementary data.

In the Judean Desert, UAV was used for obtaining higher resolution than that reached by using satellite images in the case study of the Ethiopian Highlands (d'Oleire-Oltmanns et al., 2012). A UAV Real Time Kinematics (RTK) drone was provided by the spatial archaeology laboratory at the Hebrew University of Jerusalem and operated by Dr. Uri Davidovich. Images were then processed and used for manually mapping geomorphological units (i.e.,

geomorphons), and in particular, trails and gullies. Further computational analysis using the UAV images as inputs was conducted to calculate the values of the three visible color bands (RGB) on the surface of trails and on the surface outside the trails. For the latter values extraction and calculation, a script was developed in an R environment (R Core Team, 2013). The color values were combined and normalized to form a non-satellite image estimation of the albedo values following similar works with UAV (Ryan et al., 2017, Cao et al., 2018). Detailed methodological description and R scripts are to be found in the method add supplementary chapters in Nir et al. (manuscript) accordingly.

Within the four 10x10 km rectangular sample units in Tigray, a methodological use of Least Cost Path (LCP) analysis was applied (Rees, 2004, Herzog, 2014, Alberti, 2019). One thousand LCPs started from the south going to the north and from the east heading to the west of each rectangular. The start and end points of the LCPs were randomly located on the rectangular' border strips accordingly. The result was 1000 LCPs crossing each rectangular case study for each of the two directions, i.e., a total of 2000 LCPs per area. LCPs were then recalculated following the introduction of the mapped gullies as uncrossable obstacles to the LCPs. The difference in lengths of each LCP following the introduction of gullies is the focus of this method. For performing these calculations, an R script was formulated and run using the high-capacity supercomputer of the FU Berlin. The calculations are described in the method chapter while images and scripts can be found in the supplementary section of Nir et al. (2021).

Dating methods

For dating methods implemented indirectly through external collaborations, were used to assess the age of footpaths in the cases of Tigray and the Judean Desert. Unfortunately, none of these methods can independently validate the antiquely of footpaths and therefore an attempt is made to combine multiple methods wherever it is possible. Two of the dating methods are relative or qualitative while the remaining two are based on chemical and elemental extractions, i.e., absolute dating. Firstly, the antiquity of footpaths was archaeologically evaluated in cooperation with Kristina Pfeiffer, Sarah Japp and Iris Gerlach from the Deutsches Archäologisches Institut (DAI) and with Mika Ulman and Uri Davidovich from the Hebrew University of Jerusalem Israel (HUJI). In Tigray this meant that selected footpaths were regionally long-distanced intertown paths in the proximity of 1st millennium BCE archaeological sites (Leclant, 1959, Fattovich, 2009). Based on the assumption that with little modern road constructions, apart from short phase of Italian occupation, these paths are relics of archaeological routes. In the Judean Desert, both the first Century CE and the 3-4th millennia

BCE attributed footpaths, were archaeologically surveyed. Typical indicative pottery sherds and “travel waste” of the corresponding periods were found on their surfaces while nearby archeological sites dated to periods were excavated (Davidovich, 2014, Yekutieli, 2009, Yekutieli, 2005). See further elaboration on the relative chronologies in the case studies sub-chapter 3.3. and within the method sub-chapters for each of the case studies (Nir et al., 2022, Nir et al., manuscript, Nir et al., 2021).

The second, and rather qualitative, relative dating method is based on geomorphological observations made by Jacob Hardt from the Freie Universität Berlin (FU Berlin) and Uri Davidovich (HUJI). For Tigray, these observations mainly consisted of path-incision and its transformation into a sunken lane or the initiation of gullies downslope from the footpath. The affiliation of these observations with antiquity is based on the assumption that long-termed used footpaths have underwent more rain events generating surface runoff and in turn higher intensity of path use and erosion dynamics, than younger footpaths have. However, many other factors can influence the incisions of trails and unpaved roads, therefore this method is to be used cautiously (Zgłobicki et al., 2021, Geeter et al., 2020). For the Judean Desert, a deep truncation of the Roman path by the Nahal Zeelim active stream serves as a validation tool of the former’s relative antiquity. Less dramatic interaction with gullies of both archaeologically affiliated footpaths in the Judean Desert, also serves as geomorphological evidence of their likely long-term use. Further discussions regarding temporal-geomorphological understandings of trails could be found in sub-chapter 3.3. and within the method and discussion sub-chapters of each case study (Nir et al., 2022, Nir et al., manuscript, Nir et al., 2021).

The third method for assessing the ages of trails, is a well-established absolute dating technique for determining the age of any object containing organic material, by using the radioactive isotope of carbon, 14C. Based upon the last uptake of atmospheric carbon by the dated object, the relative abundance of the decaying 14C compared with the concentration of the stable isotope 12C, produces an age estimation (Hajdas et al., 2021). The radiocarbon based direct dating on the sediments of the footpaths using 14C. The latter was conducted to give a general estimation of the age of the organic materials buried on the surface. The results were used to evaluate and validate or disprove of the above mentioned archaeological and geomorphological methods. As the context and origins of these subsurface sediments are unclear, micromorphology was used to give some form of validation for the dated sediments, i.e., that

the latter were in fact produced by footpath use. However, as no macroscopically distinguishable organic material was found, the soil organic carbon from the bulk samples was the dated material and therefore these samples could not be considered as a reliable independent source for the antiquity of the paths (Boaretto, 2009). Following the sampling, radiocarbon dating was done at the Poznan Radiocarbon Laboratory (Poland) using accelerator mass spectrometry (AMS) and calibrating with the OxCal version 4.3.2. Further details could be found in Nir et al. (2022).

Similar to radiocarbon, the fourth dating method implemented in this study, Optically Stimulated Luminesces (OSL), is a long-time used absolute dating technique (Yukihara and McKeever, 2011). This method evaluates the time passed from a grain's exposure to the sunlight or to extreme heat. From the time of burial, the radioactive decay several isotopes (e.g., 40K) release beta and gamma radiation contributing to trapping of electrons in the lattice of silicate minerals, namely quartz or feldspar. As soon as the latter are exposed to the light, most of these trapped electrons are released. Therefore, measuring the radiation produced by these electrons can, in many cases, give the last point in time in which the sediments were "zeroed" by exposure to the sunlight i.e., the age of deposition (McKeever, 2011). This method was applied in Tigray on a fan deposit of a small gully, the OSL samples were extracted by Jacob Hardt (FU Berlin). The gully "head" (i.e., initiation point) is located downslope from one of the main footpaths were crossing a watershed which was survey by Robert Busch and myself in Tigray. Such gullies, that are initiated by surface runoff promoted by paved and unpaved roads are a known phenomenon in the Ethiopian Highlands and elsewhere (Cao et al., 2021, Sidle et al., 2019, Zhang et al., 2019, Seutloali et al., 2016, Nyssen et al., 2002, Schütt et al., 2005) . Therefore, assuming this gully has been initiated due to surface runoff generated by the footpath-use, the age of the gully's fan deposits should be later than the time of the footpath-formation. Following this logic, OSL as well as micromorphological samples were taken from the upper 50 cm of the fan deposits. Sampling of the OSL was conducted using a hammer and plastic tubes inserted to the exposed profile, the tubes were covered by tape from the external side and following extraction from the internal side. Additional bags with the surrounding sediments were extracted for each sample in order to assess the current local radiation while calculating the Gamma radiation of the sample. The processing and dating of the OSL samples were conducted by Christopher Lüthgens in the Institute of Applied Geology, University of Natural Resources and Life Sciences, Vienna. Further information regarding the process of

OSL dating could be found in the supplementary section of Nir et al. (2022) as it was described by Christopher Lüthgens.

3.3 Sampling design

Three case studies were chosen for the analysis of footpaths and unpaved roads, their environmental effect, and in one case, their interaction with human behavior. These case studies correspond to three different climatic zones and three different types of human trail use. As the different natural settings are independently described within each case study, i.e., Nir et al. (2022), Nir et al. (manuscript), Nir et al. (2021), in the environmental background chapters, a brief overview of the locations and types of footpaths is given below. It is worth mentioning that not all case studies are equally described. For the eastern German case study, two sub-areas were chosen for sampling while the footpaths are treated from a soil-formation perspective only. For Tigray in the Northern Ethiopian Highlands, four sub-areas (units) are used while the trails are analyzed for geomorphological and soil formation effects as well as the proximity to archaeological sites. In the Judean Desert west of the Dead Sea, footpaths are observed geomorphologically and from a soil formatting prism with some of them being directly archaeologically affiliated.

In the temperate-transitional climate of Eastern Germany, three footpaths were studied from a pedogenetic perspective. Two of them are in the capital city of Berlin, ca. 35 meters above sea level (m a.s.l.), where, similar to most of northeastern Germany, Quaternary glaciofluvial sandy deposits dominant the surface (Eissmann, 2002). Of the two paths, one footpath was sampled in the sandy forest area at the city outskirts while the other footpath was sampled within an urban park environment. The third footpath in eastern Germany was sampled in a forest at the outskirts of a small town in the metamorphic bedrock-covered Ore mountains anticline. There, close to the border of the Czech Republic, steep slopy rocks are common while recently weathered silts and clays rich in Fe, Mn, and Al, compose the building blocks for the shallow local soils (Seifert and Baumann, 1994). The three studied footpaths in eastern Germany are used for recreational purposes, two of them, in the Berlin and Ore Mountain forests, are inaccessible by vehicles. The footpath located in the urban park in Berlin is very unlikely to have been driven on, and if so, the control sample (1 m away) to which it is compared, would have undergone a similar experience.

In the sub-humid to semi-arid climates of the Tigray region in the North Ethiopian Highlands (NEH), four 10x10 km rectangular sample units, mostly centered around archaeological sites, were mapped for their gullies, trails, and roads applying remote sensing techniques based on satellite imagery. Although all were visited, systematic validation occurred within one of the four rectangular sample units, where a watershed was chosen and intensely surveyed for its footpaths and linear soil erosion. Within three of the sample units, one footpath was studied from a pedogenetic perspective, i.e., three footpaths in total, one for each sample unit (apart from one unit that had none). The NEH are composed of a variety of geological structures which, coupled with a bimodal rain distribution, result in geomorphologically different landscapes. Volcanic activities are responsible for cone-shaped mountains as well as basaltic plateaus, while tectonics has left its mark with several grabens and eroded anticlines, dissecting the highlands (Beyth, 1972, Hofmann et al., 1997, Coltorti et al., 2007, Konka et al., 2012). At ca. 1900 m a.s.l, the rectangular sample unit is chosen around the archaeological site and 1st Millennium BCE temple Wuqro. The sample unit is located directly north of the district's capital Mekelle and it is composed of Paleozoic to Mesozoic dolomite and limestone (Asrat et al., 2003). The latter sample unit has only been studied using remote sensing and was shortly visited for basic ground validation and impression of the landscape. The three other sample units are located 75-80 km northwest of the Wuqro sample unit and are generally 5-10 km apart from each other. The southernmost unit among the three is situated in the Daraga area (at c. 2,000 m a.s.l.), around the Hawelti-Melazo 1st Millennium BCE temples, directly south of the outskirts of the city Axum. The latter is best known for its archaeological 1st millennium CE steles (Phillipson, 2012). The Daraga sample unit is located on the Axum basaltic plateau basalt. Within the fine-grained clayey soils, one incised footpath, leading from the area of the Melazo temple towards the ancient temple of Yeha was sampled (French et al., 2009). The third sample unit is located 5 km to the northeast of Daraga, around the latter ancient temple (Yeha). It is situated at 2000-2400 m a.s.l. in a cone-shaped extrusive environment dominated by metamorphic sand- and siltstones (Gebremariam, 2009). One, incised and several km long, footpath (N-S) was sampled within this unit at two locations. The fourth sample unit, 10 km further to the north, close to the Eritrean border, is located at 1200 m a.s.l. and is composed mainly of a N-S elongated depression, likely a graben. Within this depression, covered by quaternary fluvial sediments and granitic hills, is the modern town of Rama. No archaeological sites were excavated in the sample unit. However, archaeological evidence for 1st Millenia BCE occupation was sporadically discovered on the graben's surface and in a test pit (Pfeiffer and Gerlach, 2020). One watershed within the Rama sample unit was surveyed for its gullies,

footpaths and incised footpaths, while one of the latter was the third footpath sampled for pedogenetic analysis. Two of the sampled footpaths, in the Daraga and Yeha units, are considered here as long termed and long distanced used footpaths, active until today, while the Rama sample unit footpath, is used daily by local farmers and is considered as recent.

In the arid (60-80 mm y) Judean Desert (Israel), three footpaths were studied for their possible pedogenetic and geomorphological influences in the landscape. The Judean Desert serves as the western boundary of the Dead Sea depression. Within a 20 km width (W-E) the limestone cliffs and narrow draining canyons form a ca. 1500 m descent towards the Dead Sea (Garfunkel and Ben-Avraham, 1996). Approximately 3 km west of the current Dead Sea (ca. 330 m a.s.l.), on the fan deposits of the Wadi Seiyal (Nahal Zeelim), two of the three footpaths were sampled. The sediments of the fan, forming its multiple terraces, are composed of Pleistocene colluvial, Lisan formation and floodplain deposits (Lisker et al., 2010, Davidovich, 2013). Of the two footpaths sampled on the Nahal Zeelim fan, one is intensely used for recreational purposes while the other is unmarked, far less accessible to tourism, and is rarely walked on today. The latter footpath has been surveyed and based on archaeological evidence it has been attributed to the Roman siege on the nearby archaeological site of Masada taken place in the late 1st century CE (Harel, 1967, Hirschfeld, 2006, Eshel, 2003, Davidovich, 2014). A third footpath is situated directly above and south of the canyon 'Nahal Zohar' and is consequently locally named the Zohar ascend. This footpath is located ca. 17 km south of the two footpaths sampled in the Nahal Zeelim fan. There, the Har Hemar anticline replaces the western Dead Sea Escarpment (Lisker et al., 2010, Garfunkel and Ben-Avraham, 1996). The Zohar ascend footpath (ca. 150 m b.s.l.) is positioned on weathered carbonate rock and sedimentary pockets and was sampled several meters below the watershed line. The path has been attributed to the Early Bronze Age (EBA, ca. 3200-2500 BCE) following archaeological surveys directly on the footpath's surface and excavations on the ridge overlooking the footpath (Yekutieli, 2005, Yekutieli, 2006).

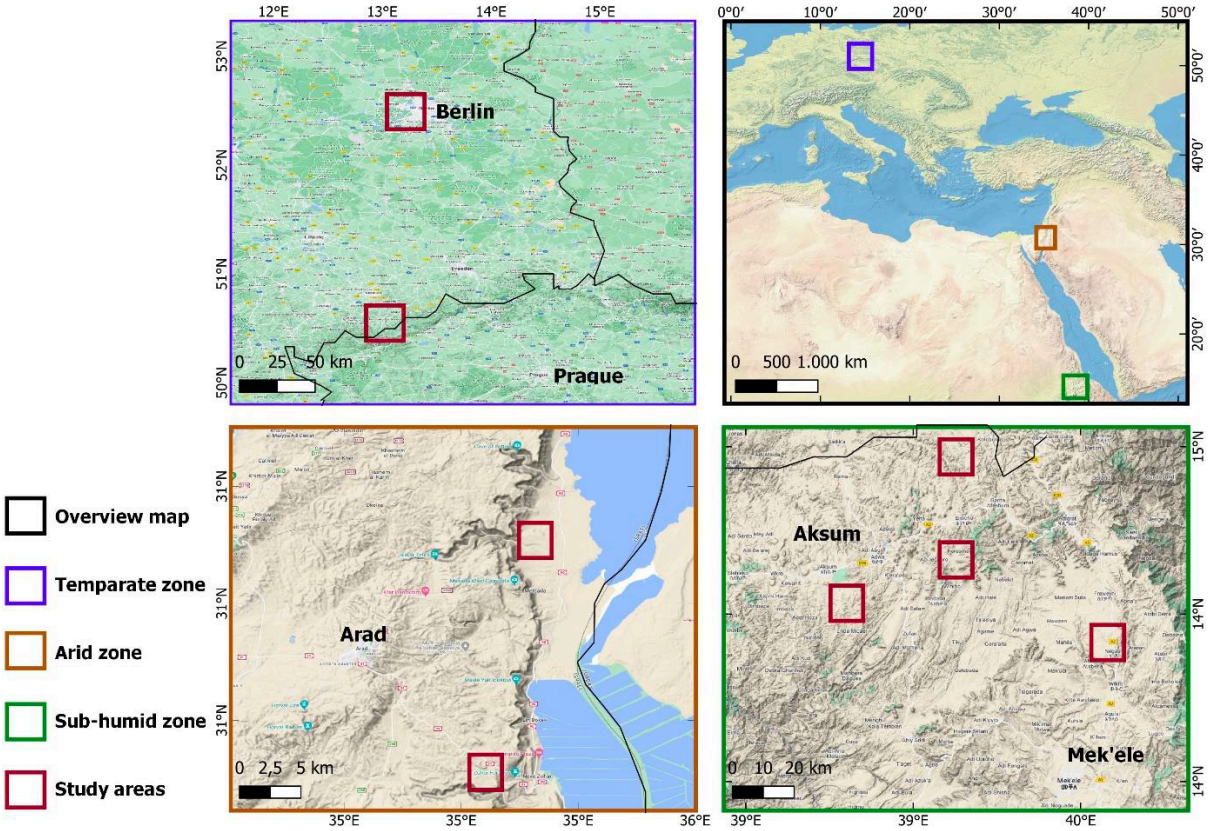

Figure 3.2 Overview maps of the research areas. Rectangular region maps correspond to their colors in the main overview map. Natural Earth open-source data available at naturalearthdata.com.

Chapter 4

Footpath formation and resulting morphodynamics

Nir, N., Stahlschmidt, M., Busch, R., Lüthgens, C., Schütt, B. and Hardt, J., 2022.
Footpaths: Pedogenic and geomorphological long-term effects of human trampling.
CATENA, *215*, p.106312.
https://doi.org/10.1016/j.catena.2022.106312

Abstract

Footpaths are of the oldest and most widely distributed forms of human imprint on the landscape. These elongated features are the result of continuous usage of a certain route for walking, at time scales ranging from days to centuries or millennia. In this qualitative investigation, we take a holistic approach combining micromorphology (including voids analysis), chemical soil parameters (such as selective iron oxide dissolution), and remote sensing (spatial distribution and orientation of footpaths in the landscape) to evaluate the long-term residues and environmental effects resulting from the formation of footpaths. Our diverse case studies incorporate footpaths used for recreational and transport purposes in temperate and sub-humid climates from both a modern and historical perspectives. Footpath formation affects the physical and chemical properties of subjacent layers (up to ~3 cm below surface), resembling effects caused by heavy agricultural machinery and tree logging. A reduction of pores as was observed down to 3 cm below surface compared to control areas without footpaths. Higher amounts of both Fe oxides and either macro or micro organic residues under footpaths, are likely due to the lower porosity, hindering the supply of oxygen and/or water into the sub-surface. As an additional result of the compaction, surface runoff is promoted. This may either trigger the initiation of gullies in proximity to the footpaths, or lead to incision of the footpaths themselves. Incised footpaths are more likely to occur when the footpath is oriented parallel to the stream network. Once an incised footpath is formed, it may reduce gully erosion susceptibility downslope as the incised footpath acts as a channel that decreases overbank flow. Based on these results, we point out that footpaths can have both positive and negative environmental effects; in temperate forests footpaths may promote organic carbon storage and hinder soil formation while on steeper slopes and in open sub-humid zones, footpaths can cause major (gully) or minor (path incision) linear soil erosion. With a better

understanding of footpaths as landscape units we can (1) pose archaeological questions related to human environmental interaction, and (2) use incised footpaths as possible measures against gully erosion.

Keywords: footpaths, gully erosion, sunken lanes, micromorphology, porosity, pedogenic iron

4.1 Introduction

Humans have historically affected and continue to have an effect on soil formation, erosion and degradation (Butzer 2005; Storozum et al. 2021). Historical changes in land cover triggered by land use requirements, such as the removal of natural vegetation and its replacement with agricultural crops, have shown to promote soil erosion as early as the first millennia BCE (van Andel et al. 1990). A special type of land cover that has dominated areas used by humans are footpaths. In the Near East, the latter have been evident at least since the early Bronze age (Snead et al. 2009). Pathways have been intensely investigated in archaeological contexts from a route network perspective, with a growing use of remote sensing techniques (Verhagen et al. 2019). Since the time of road construction and usage of pavements, pathways are considered as archaeological features (Zedeño and Stoffle 2003). However, footpaths, the unconstructed predecessors of paved pathways and roads, might have influenced the landscape far before the Bronze age. Although spatially and temporally widely distributed, footpaths as a landscape archaeological feature have gained little attention in the archaeological research with few exceptions (Snead et al. 2009). Recreational trails having been investigated for their possible effect on vegetation cover and soil erosion. However, data remains scarce, distinctions between wheeled and non-wheeled paths are inconsistent, and little is known on footpaths relationship with soil formation or the drainage basin dynamics (Sidle et al. 2019; Wimpey and Marion 2010; Buchwał and Rogowski 2010; Cole 2004).

Trampling and soil compaction

The process of modifying surfaces and sub-surfaces as a consequence of repeated human and animal movement is usually referred to as “trampling”. Human trampling has long been in the focus of micro-archaeological investigations (Rentzel et al. 2017). Micromorphological experiments and investigations of archaeological records suggest that the structure of sediments, soils and human residues is affected by trampling. This is expressed by texture characters such as the breakage of bones and ash layers and general compaction of

archaeological materials. In soils, indications of trampling can be platy microstructures and horizontal to polyconcave voids and reduction of overall porosity (Miller et al. 2010; Goldberg and Berna 2010; Rentzel et al. 2017). For organic components, it is suggested that trampling re-organizes plant fibres originating from dung, resulting in a sub-parallel platy macrostructure (Shahack-Gross et al. 2003). Additionally, complex packing voids, a lack of void structures and massive microstructures were evident in different open areas occupied by humans and cattle (Pietola et al. 2005). The pressures adult humans can induce on the underlying ground depends on their static versus moving positioning. The range incorporating both, standing and moving, lies between 60 and 500 kPa (Asmi et al. 2020; Rodgers 1988). Bernhardt-Römermann et al. (2011) concluded for 35 trails in European forests, that historical human land use and local climate strongly affected the resilience and resistance of plants to human trampling and that this process differs for different environments (Bernhardt-Römermann et al. 2011).

Agricultural soils have long been investigated for the effect of compaction due to heavy machinery (Coulon and Bruand 1989). Few of these studies have used micromorphology as a tool to understand the effect pressure has on the soil and sub-soil. Results show that changes in voids' structure reach well into the first centimetres of the soil. It has been observed that vertical voids are blocked from reaching the surface - at the same time, concentrated voids are formed in the sub-soil (Rasa et al. 2012; Iraj et al. 2011).

An experiment by Silva el al. (2011) studied the effects of direct pressure on soil nitrogen (N) and carbon (C) contents. For pressure levels up to 240 kPa, soil density increased between 20-22%. However, in one occasion, the rate of Total Organic Carbon (TOC) loss through mineralization decreased and TOC concentration increased starting at a pressure of 120 kPa (Silva et al. 2011). This degree of pressure is within the range applied by walking human adults and cattle. Other experiments imply that lower extents of pressure might result in higher Total Carbon (TC) and Total Nitrogen (TN) compared to those induced by heavy compaction (Blumfield et al. 2005; Wang et al. 2020).

Some authors explain the changes in TOC and N concentration as the result of changes in the density of both macro- and micro-porosity of the soil which in turn affects microbial activity, mostly through the supply of oxygen and the degree of photosynthesis (Neve and Hofman 2000; Silva et al. 2011). Following this notion, it has been found that a large portion of soil organic matter (SOM) is stabilized within the entrance of small pores (Kawahigashi et al. 2006; Kaiser et al. 2002). It was subsequently suggested that reducing porosity and therefore microbial activity affects C and N cycling (Mikutta et al. 2006). Further experimental work found that SOM stability is affected by the changes in aggregate types and heavy compaction

(Silva et al. 2011; Guimarães et al. 2013; Mikutta et al. 2006). The carbon mineralization rate decreases as bulk densities increase, up to some extent, indicating that carbon mineralization in moderately compacted soils can lead to an increase in the accumulation of organic matter (Neve and Hofman 2000). Additionally, identifying changes in the relative amounts of poorly crystalized pedogenic iron oxides serves as an indicator for long-term residues of compaction as they are affected by water and air availability and relate to organic matter decomposition (Chen et al. 2020; Coward et al. 2017).

To date, no micromorphological or selective Fe extraction studies have directly addressed the formation of footpaths. Recreational tracks and footpaths studies were focused predominantly on vegetation cover and on aspects of soil erosion (Sherman et al. 2019; Ayres et al. 2008; Cole 2004). Experimental works and investigations looking into vegetation response to trampling have shown that compaction by human induced pressure may decrease biomass and increase soil density especially in the upper 5 cm of the soil but might also reach down as far as 20 cm (Sherman et al. 2019). Soil moisture and organic matter have shown a mixed reaction to pressure while soil pH has slightly increased in soils under footpaths (Kissling et al. 2009; Sherman et al. 2019).

Gully erosion and pathways

Soil erosion has been correlated with geological, topographic, climatic and human induced variables (Addisie et al. 2018; Vandaele et al. 1996; Valentin et al. 2005). One point of origin for soil erosion are roads and pathways. Due to the high compaction of their surfaces, runoff generation is favoured and gullies, a linear form of soil erosion exceeding 30 cm depth, can initiate downslope (Ziegler et al. 2000; Nyssen et al. 2002; Nir et al. 2021). Mostly in silty environments and presumably when a pathway is oriented down slope, a different linear erosional process may occur: the erosion and incision of the path itself, usually termed a *sunken lane* or, in historical and archaeological context named as *holloway* (Bell and Leary 2020). Similar to other forms of pathways, sunken lanes are seen as the result of the movement of people, animals, and different types of transport (Nir et al. 2021). The additional factor differentiating it from a pathway is the water induced mass transport, controlled by the slope angle (Boardman 2013). The elongated and gully-like sunken lanes are usually defined as such when they are incised at least 0.5 m into the surrounding surface, a threshold related to the crossing abilities of agricultural vehicles (Geeter et al. 2020; David et al. 2011; Zgłobicki et al. 2021). The threshold for the development of sunken lanes is heavily dependent on human activities and does not necessarily require steep slopes as gullies often do. However, steeper

slopes may generate deeper sunken lanes (Geeter et al. 2020). Shallow forms of sunken lanes, ca. <0.5 m "sunken" into the surrounding surface, are also prominent features in the landscape resulting from the incision of footpaths (Zgłobicki et al. 2021). Throughout the course of a single footpath, it can change from being levelled with its surroundings to being slightly incised (c. <0.5 m) or to form a sunken lane (> 0.5 m). During flash flood events in the non-sunken section, surface runoff may occur that in turn could trigger gully erosion in its downslope vicinity. Hence, both types of footpath-related linear erosional forms can initiate within the course of one path (Busch et al. 2021; Nir et al. 2021).

Objectives

In the present study we investigate the formation processes of footpaths as they affect and are affected by surface runoff and soil formation. We aim to determine differences and similarities between the erosion attributes when historically used footpaths are incised. We expect to find differences in the amount of voids and pedogenic Fe oxide contents in the topsoils of currently used and historical footpaths, as both are influenced by compaction and the supply of water and oxygen, and relate to each other. An initial and multi-method qualitative investigation follows a holistic approach in order to better understand the effects of human movement on top-soil characters and erosion dynamics. Using the case studies from both temperate and sub-humid zones, we examine the modern and historical long-term effects of footpaths. Our aim is to (1) recognize possible patterns and changes in the top-soil of footpaths and incision of footpaths using micromorphology, focussing on void pattern image analyses in the top-soils and selected chemical characters of the top-soils (2) asses these patters under different climatic conditions and in different soil types, and (3) evaluate the interplay of long-term used (and subsequently incised) footpaths with soil erosion on a drainage basin scale.

4.3 Case studies

The Tigray region of the Ethiopian highlands, representing a developing nation under sub-humid climate, has been intensively studied for both its gully erosion (Billi and Dramis 2003; Busch et al. 2021; Frankl et al 2012) and pathway systems (Nir 2021; Nyssen et al 2020) as well as its substantial archaeological records (Nyssen et al. 2004; Fattovich 2010; Nyssen et al. 2020). Against this backdrop, Tigray appears as a perfect study area to conduct research into the soil properties of pathways. As a counterpoint and as a subject of comparison in a different climate zone and with completely different soil conditions, we identified three currently used footpaths in different soil types under temperate climate in Germany. The selection of a number

of highly diverse study sites aims to provide robust data to assess the formation of currently used and historical footpaths and their possible effect on landscape dynamics (Figure 4.1).

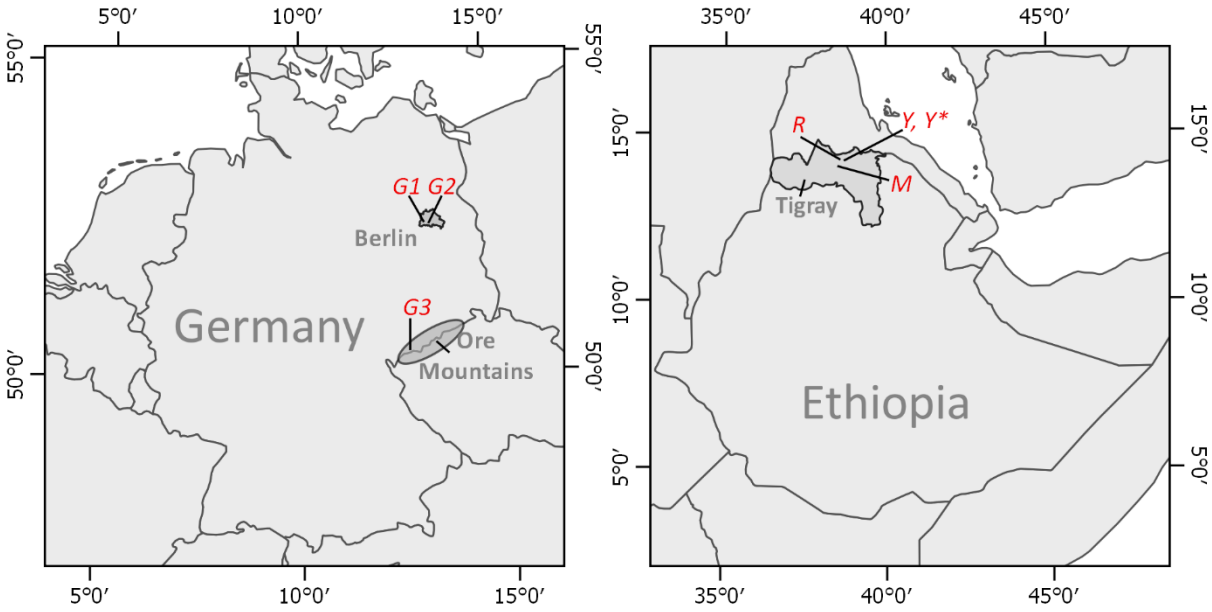

Figure 4.1 Overview maps indicating the locations (marked red) of sampled footpaths from a. Germany: Grunewald Forest Berlin (G1),s Urban Park Berlin (G2) and Ore mountains (G3) and b. Tigray, Ethiopia: Rama ®, Yeha (Y), Yeha margins (Y*) and Melazo-Hawelti. Red marked G1-G3 (map a) mark overviewing the sampling locations in Germany. Red rectangle in map b corresponds to the map section shown in Figure 4.4. Natural Earth open source data available at *naturalearthdata.com*.

The selection of the six case study sites and the slightly differing methods applied at the various locations, were chosen to identify the different environmental and temporal effects of footpath use. In Germany, the currently used footpaths result from recreational use. We selected a sandy forest environment, a clayey forest environment and a loamy urban park environment. In Tigray, incised footpaths in proximity to 1st millennium BCE archaeological sites were chosen to represent a likely historical use of footpaths (Figure 4.2). The two likely historical footpaths reflect long distance and daily short distance travel in clayey soils. Another footpath in Tigray represents modern use in an agricultural context (narrow path used by farmers between fields), although the path is located within a watershed where first millennia BCE pottery sherds were found (archaeological survey, Pfeifer et al. in press). Therefore, although most study sites share the same methodological approach, the three German case study sites are interpreted rather as currently used footpaths, while the Tigray footpaths are regarded more as likely historical use indicators. Subsequently, footpaths in Germany were always micromorphologically studied from 0 cm below surface and measured for surface resistance, while in the Tigray case study sites, the focus was put on the lower 5-20 cm below surface (apart from the likely modern

footpath). Additionally, the geomorphological aspect of footpaths, attributed to long term use, has been investigated by analysing remote rensing data and accompanying field surveys for the sites in Tigray.

Figure 4.2 Sampling sites on footpaths in Germany (samples G1-G3) and Tigray, sample R, sample Y, sample Y* and sample M. Red circle marks the micromorphological sampling point.

Germany

Berlin footpaths

Two of the investigated footpaths are located in Berlin (Germany; Figures 4.1-4.2), one in the Grunewald Forest (sample G1, Figure 4.3) and one in an urban park in south Berlin (Gemeindepark Lankwitz) (sample G2, Figure 4.3). The annual precipitation of the region averages 577 mm and the average annual temperature amounts 8.9°C. The Grunewald Forest marks the western margins of Berlin. Here, sandy soils (*Haplic Arenosol*) with an organic horizon reaching up to 8 cm thickness developed in Pleistocene glaciofluvial sediments. The sampled footpath (sample G1) is situated at the margins of a ridge (100 m asl), continuing on a slope that sharply (>20°) descends west towards the River Havel. In the urban park a footpath (sample G2) was selected for sampling which is oriented semi-diagonally and at times parallel to a paved way. The urban park was constructed and opened to the public in 1912. The soils of the park developed in mixed sands and silts with cultivated lawns dominating most of the area (Wessolek et al. 2008; Umweltamt Steglitz-Zehlendorf von Berlin 2016).

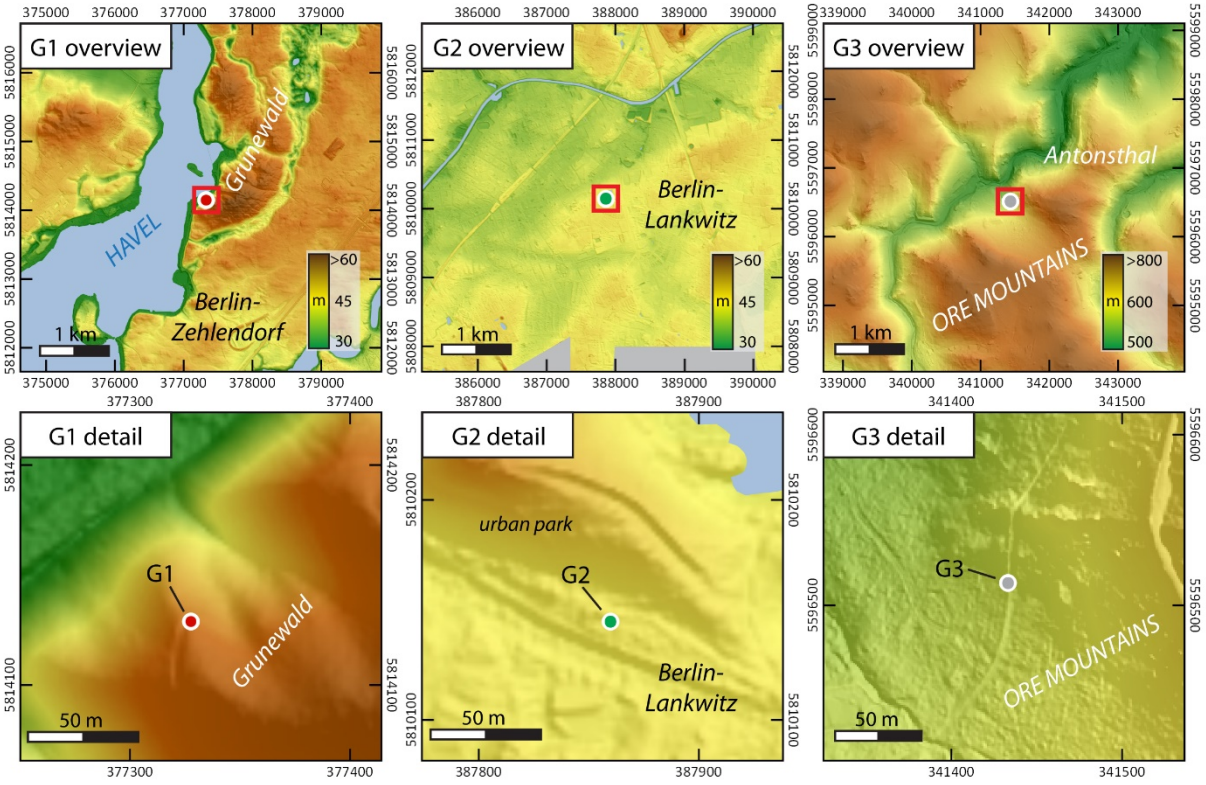

Figure 4.3 Overview (top row) and detail (bottom row) maps of sampled footpaths in Germany. Coloured dots indicate the sampling sites. (Hill shade maps based on open source Lidar data (Geoportal Berlin) for G1 and G2; https://www.stadtentwicklung.berlin.

Ore Mountains footpath

In the Ore Mountains (Figures 4.1-4.2) a footpath situated in a forest outside Anthonstal at the border between Germany and the Czech Republic was investigated (sample G3, Figure 4.3). Podzolic and eutrophic brown earth soils are characteristic for the region while forests are characterized by short rotation pine and mature spruce forests. Annual precipitation amounts to 820-950 mm and mean air temperature is ca. 5-7.2°C (Tichomirowa et al. 2019; Drauschke et al. 2015). The footpath is perpendicular to the slope (c. 40°) while the bare schist bedrock is exposed at different locations directly above the footpath.

Tigray, Ethiopia

In central Tigray in the Northern Ethiopian Highlands three incised footpaths were studied. The sample names – Rama (sample R), Yeha (sample Y) and Melazo-Hawelti (sample M) – correspond to the archaeological sites in their surroundings (Figure 4.4). Today's climate in Tigray is sub-humid to semi-arid and driven by the monsoon with yearly average daytime temperatures across Tigray varying from 20°C to 35 °C. For central Tigray, the mean annual precipitation during the 20th century varied between 500-800 mm following a bimodal yearly pattern (Harrower et al. 2020); at times, rainfall occurs within massive storm events

(Gebrehiwot and van der Veen 2013; Berhane et al. 2020). In 2005 about 43.2 % of Tigray was covered by low woodlands and shrublands while about 0.2 % of the total Tigray area (~ 5 million ha) was covered by high woodlands and forests (FAO Forest Department 2010). Land use today is mainly characterized by tef, wheat, barley and millet cultivation (Asfaha et al. 2021). Multiple soil conservation measures have been applied to prevent soil erosion, mainly using earth bunds, furrows and grassed lynchets (locally known as *daget*). Placing stone bunds and planting of trees and bushes to stabilize larger earth bunds have been implemented since the early 1990s (Dagnew et al. 2015; Frankl et al. 2013; Nyssen et al. 2000; Nyssen et al. 2020).

Two of the oldest and most dominant archaeological sites in Tigray are the Pre-Aksumitic (early first millennium BCE) sites of Yeha and Melazo-Hawelti (Breton 2011; Contenson 1961). Archaeological evidence discovered in Yeha indicates almost three millennia long continuous occupation of this area including a unique and well-known temple attributed to the Ethio-Sabean material culture of the pre-Aksumite period (Weiß et al. 2016). The Melazo-Hawelti archaeological sites similarly include a temple attributed to the Ethio-Sabean culture (Contenson 1961; Leclant 1959). The continuous human presence around these sites and the fact that today people still predominantly use footpaths (personal observation), make this an ideal research location. In order to identify possible older footpaths, we concentrated on the detection of incised footpaths. Three incised footpaths were selected for the current work: one selected footpath is assumed to be 'modern' (Rama incised footpath), two of the selected footpaths are incised and considered as being in historical use and consistently used until today (Yeha and Melazo-Hawelti incised footpaths; Figures 4.2 and 4.4). The mere incision of a footpath does not directly infer its age. However, the combination of their long-distance course between ancient centres, their incision and their location within the vicinity of the pre-Aksumite archaeological sites, brought about these assumptions and selections (see Results chapter for further confirmation of the antiquity of the incised footpaths in Tigray).

Rama incised footpath (sample R)

The Rama incised footpath is situated ca. 3 km SE of the modern town of Rama (Figures 4.2 and 4.4). Both the footpath and the town are located within a depression that covers an area approximately 3 km wide and 10 km long, striking S-N with an average elevation of 1300 m asl. The flanks of the structure are dominated by metamorphic siltstones and granitic domes; locally granitic domes also appear in the depression as isolated positive landforms while the depression is widely infilled by Cenozoic sediments. Within the generally sub-humid Tigray, the micro-climate dominating the depression can reach characteristics of a semi-arid zone

(Busch et al. 2021). The Rama incised footpath is considered as a modern example of a footpath that locally forms a shallow sunken lane (<0.5 m incised). The footpath starts at the eastern escarpments of the depression (at ca. 20° slope) and descends ca. 50 m into the planes, where it is disturbed and redirected by a gully and 46adlands. It continues through farmland until it ends in the Inda Shawit River where animals and humans cross (Busch et al. 2021). Extraction of sample R (Table 1) took place in the planes, east of the Inda Shawit River where the incised footpath is also affected by overflow of field irrigation.

Yeha incised footpath (samples Y, Y)*

The incised footpath close to the archaeological Yeha site is presumably 'ancient'. It is a 16 km long north-south connection between the monastery of Mariyam Shewit and the village Ihsa'a through the modern town of Sehul (Figure 4.4). The footpath runs ca. 6-9 km (varies) east of the early 1st Millennium BCE archaeological site of Yeha. The region is dominated by cone shaped hills made of volcanic plugs and domes (Machado 2015) the footpath runs in the foot zone and in the colluvial deposits of these hills. Locally the footpath runs parallel to a modern road, mostly perpendicular to the slope of the hills and has an inclination of ca. 5-15°. The path is used today on a daily basis by locals traveling by foot or with pack animals. This footpath usually forms a shallow sunken lane (<0.5 m incised) with local incisions deeper than 0.5 m.

Melazo-Hawelti incised footpath (sample M)

The sampling site of the Melazo-Hawelti footpath is located where the path reaches the modern villages of Melazo and Hawelti in the municipality of May-Weiny (Figure 4.4). The flat to hilly plateau region is composed of metamorphic sandstones and basalts (Beyth 1972). The footpath investigated classifies as a shallow sunken lane and is located in ca. 700 m distance to the temple of Melazo. It is part of a currently daily used track from the local villages in the area towards the cities of Yeha and Adwa. The footpath has an inclination ranging between ca. 7-11°.

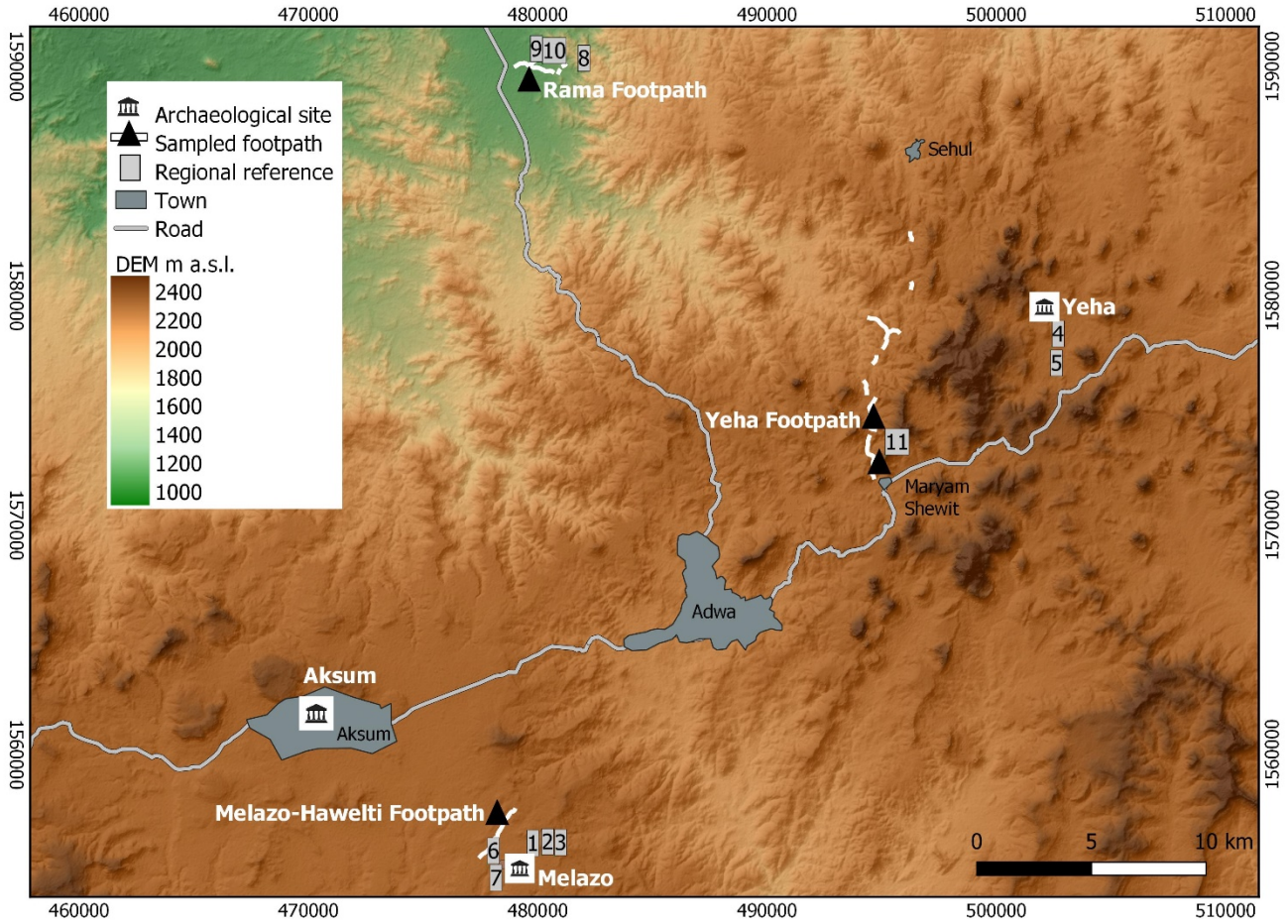

Figure 4.4 Regional overview map of the study sites in Tigray, Ethiopia. White lines: One currently used incised footpath Rama (sample R), and two likely historical incised footpath 1) Yeha samples: Y (north) and Y* (south) and 2) Melazo-Hawelti: sample

4.4 Materials and methods

A holistic multi-scale approach was selected including micro (micromorphology, sedimentary and image analyses and extraction of pedogenic Fe), meso (field description, surface resistance) and macro (remote sensing) scales, as these different scales each offer different approaches to assess the effects of footpaths on top-soil formation and erosion processes (Figure 4.5).

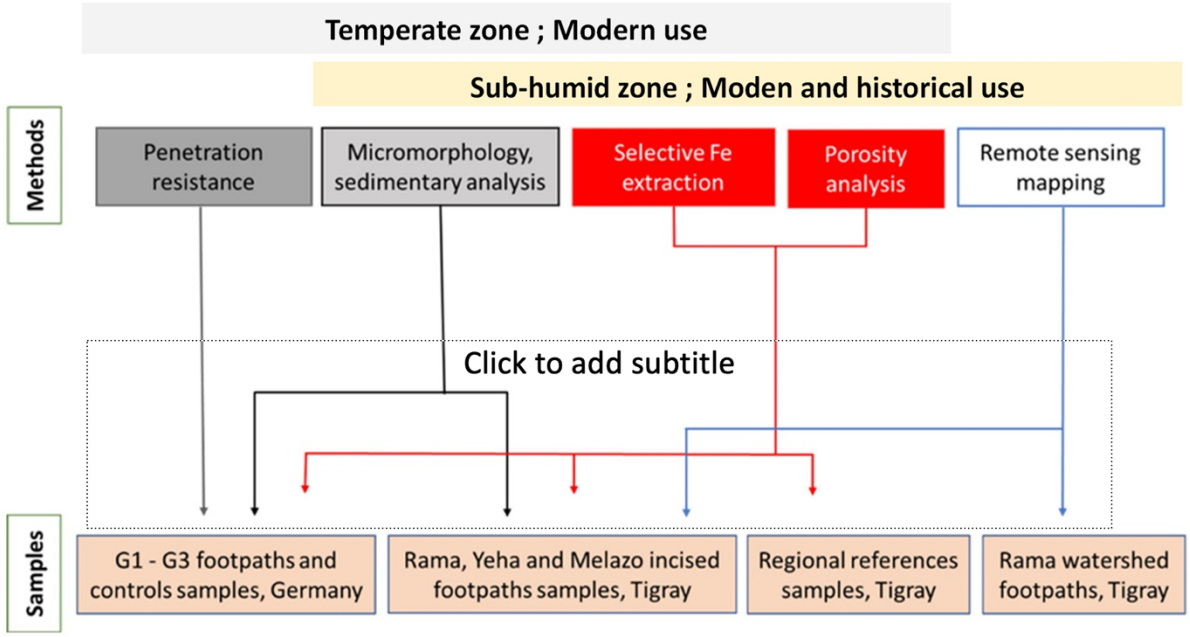

Figure 4.5. Flowchart summarizing the various methods and analyzed samples. Sedimentary analysis includes grain size analysis, pH, electric conductivity (EC), X-ray fluorescence (XRF) and Total Organic Carbon (TOC).

Sampling

Micromorphological (MM) undisturbed, stabilized soil samples were extracted at the centres of the three footpaths (G1-3F) in Germany at a depth of 0-30 cm (Figure 4.2). For control, a non-footpath sample (G1-3C) was taken at similar depth in ca. 1 m distance off-site of each footpath sampling location (n=6). Complementary, soil penetration resistance measurements using a manual penetrometer (pocket penetrometer ELE International-29-3729) were obtained to receive information on soil compaction of the soil surface; for each sampling location three replicas were measured (Tejedo et al. 2016). Bulk material was extracted from footpath and non-footpath (control) locations from the topsoil (c. 0-5 cm depth) and the underlying stratum (c. 10-15 cm depth) below strata boundaries (n=12) for laboratory analysis. In Tigray, incised footpaths were confined by active agricultural fields characterized by ploughing and sowing activities, so that these areas were unsuitable for taking the non-footpath control samples. Therefore, the control samples used for the Tigray region reflect a landscape perspective, using several micromorphological and geochemical control samples from natural exposures (named here 'regional reference samples'). A total of four micromorphological samples in Tigray were extracted from the three footpath sites along with 11 regional bulk and 10 MM reference samples represented by different numbers (i.e., non-footpaths) (Figure 4.4,5). The Rama footpath sample (sample R) was extracted from a levelled segment of the footpath, the footpath is both-sided flanked by agricultural fields. The Yeha footpath sample (sample Y) was extracted at the centre of the footpath. A second sample from this footpath (sample Y*) was

taken 1.8 km south of the first sampling Y. The sample Y* was extracted at a locality where a large boulder covers part of the footpath, acting as an obstacle for runoff and trampling; the sample was taken close to the boulder where less trampling is expected than at the central path. The Melazo-Hawelti (Melazo) footpath sample (sample M) was extracted at the centre of the footpath, where it runs through agricultural fields.

Table 4.1. Sampling sites in Germany (G) and Tigray. UTM zone (WGS84) for coordinates in Germany: 33U; UTM zone for coordinates in Ethiopia: 37N.

Site	Sample name	Sample description	Easting	Northing
G1 Grunewald Forest Berlin, Germany	Sample G1 footpath (G1F)	Upper 15 cm at the footpath's centre	377310	5814150
	Sample G1 control (G1C)	Upper 15 cm, 1 meter off the footpath	377312	5814150
G2 urban park Berlin, Germany	Sample G2 footpath (G2F)	Upper 15 cm at the footpath's centre	387871	5810170
	Sample G2 control (G2C)	Upper 15 cm, 1 meter off the footpath	387870	5810172
G3 Ore Mountains, Germany	Sample G3 footpath (G3F)	Upper 15 cm at the footpath's centre	341430	5596508
	Sample G3 control (G3C)	Upper 15 cm, 1 meter off the footpath	341429	5596502
Rama depression, Tigray	Sample Rama footpath (sample R)	1.5-8.5 cm below surface at the footpath's centre	479263	1590134
Yeha archaeological site area, Tigray	Sample Yeha footpath (sample Y)	6-19 cm below surface, at the footpath's centre	494455	1574326
	Sample Yeha footpath margin (sample Y*)	3-10 cm below surface, at the footpath's margins	494639	1572953
Hawelti-Melazo archaeological sites area, Tigray	Sample Melazo footpath (sample M)	6-13 cm below surface at the footpath's centre.	478804	1557436

Most of the micromorphological regional reference samples (n=10) were extracted from natural outcrops close to the footpath sampling locations of archaeological sites (Mussi et al. 2021). One additional reference sample from the sub-surface (5 cm below surface) was sampled from the Yeha incised footpath between the two sampling spots (Y and Y*); this sample was exclusively used for geochemical analysis (Figure 4.5). The micromorphological reference samples were extracted from different depths to be able to assess different pressures caused by the overburden (supplementary Table 2).

Analysis

Micromorphological analysis

Undisturbed block samples were extracted using jackets of gypsum bandages (plaster of Paris) or plastic boxes, depending on the sediment type and cohesion. Samples were processed in the Physical Geography Laboratory of Freie Universität Berlin where they were dried for several days at room temperature (c. 18° C) and later heated to 40°C for 30 hours. Subsequently, sediments were impregnated using a 6:4 (v:v) mixture of polyester resin and acetone and a small amount of hardener (5-10 ml hardener to 1 l of polyester resin and acetone mixture). Due to the heavy saturation and cracking of the clay enriched sediments, acetone removal was performed and amounts and ratios were changed according to the reactions and impregnation of the sediments. After several weeks of repeated sample impregnation and drying, sampled blocks were cut with a slab saw to ca. 6x5 cm 'hand' size slabs. These units were sent for preparation of 30µm thick sections to the Quality Thin Section labs, Arizona. The processing of the footpath samples from Germany (samples G1-3) was completely conducted at the MKfactory labs in Stahnsdorf, Germany. Analysis of the slides was performed using four objective lenses (x2.5, x10, x20 and x40), along with x10 ocular lenses, resulting in four magnifications (x25, x100, x200 and x400) in plane and cross polarized lights (PPL and XPL) on a Zeiss polarizing microscope following common micromorphological studies (Stoops 2021; Verrecchia 2021).

Voids analysis

Voids quantification and measuring the extent of porosity has been used by micromorphologists for several decades (Pires et al. 2009). Here, we analysed voids at five scales according to objective lens: x2.5 (field of view: 20,200 µm), x5 (field of view: 18,500 µm), x10 (field of view: 11,100 µm), x20 (field of view: 5,700 µm) and x40 (field of view: 2,900 µm). For each of these objective lenses, pictures were taken in 1 cm steps, starting at 0.1 cm below the upper border of each slide, reaching 5 cm. Each segment in all scales was photographed in plane polarized light (PPL) and at cross polarized light (XPL). The locations chosen were at a vertical line along the horizontal centre of the slides. For the higher objective lenses (x10, x20, x40) the image was directed to a matrix area were voids fit within the objective lens frame (except for planes where these could cross the borders to some extent) to be able to analyse the 'micro-voids'. The quantification of the number of voids for each scale

was conducted using R basic package in environment (R Core Team 2013), using 'cimg' and 'greyscale' functions for both, PPL and XPL images ('imager' package). A major task was to differentiate between quartz minerals and voids, as both appear alike in the plane polarized light. In cross polarized light the quartz minerals show a characteristic colour sequence when rotating due to the reorientation of the light (white, light grey, dark colours), while the voids remain dark grey. The XPL image was subsequently subtracted from the PPL image so that the white and very light grey coloured quartz minerals are not considered as voids. The resulting image was converted into a binary black and white image using the 'threshold' function ('imager' package). The ratio between voids and non-voids was calculated in R environment (R Core Team 2013). The different types of voids in the samples were analysed by manual micromorphological observations considering each objective lens size at each 1 cm step, classifying voids into seven classes (simple packing voids, complex packing voids, close complex packing voids, channels and vesicles, chambers, vughs and planes) based on the types of relevant voids (Stoops 2021).

Sedimentary analysis

The bulk samples were dried at 105° C in a drying cabinet and aggregates were disintegrated using a porcelain mortar. By dry-sieving sample material was subdivided into grain-size classes with diameters >2mm, ≤2mm and ≤1mm. The grain-size fraction with diameters ≤1mm was further measured using a LS 13320 PIDS Beckmann Coulter Laser particle size analyser to obtain the grain size distributions. The ≤1mm fraction was additionally chemically analysed. The respective sample preparation and measurement steps were conducted according to previously published workflows (Nykamp et al. 2020; Kirsten et al. 2021). Measurement of the electrical conductivity (µS cm^{-1}) and pH values of the water saturated samples was determined in a 1:2.5 solution of air-dried sediment and bi-distilled water using handheld electrical conductivity and pH meters accordingly (Hanna Instruments). Total carbon content (mass-% TC) was determined using a LECO Truspec CHN and an add-on elemental analyser. Total Organic Carbon (mass-% TOC) was measured following $CaCO_3$ dissolution using katalytic oxidation at 680° C and subsequent Non-Dispersive Infra-Red detection using a TOC-L Shimadzu device. Elemental analysis was carried out using the portable energy-dispersive X-ray fluorescence analyser (p-ED-XRF) Thermoscientific Niton XLt3 measuring the sample in plastic cups sealed by a mylar foil (0.4 µm). The prepared sample-cups were measured for 120 seconds by p-ED-XRF with different filters. Measurements included four known reference standards (RF3, RF25, RF87, RF89) for device error assessment and calibration (Hoelzmann et al. 2017). Preliminary age assessments were conducted on incised footpaths in Tigray using;

1) carbon dating on the footpath sub surfaces and 2) Optically Stimulated Luminescence (OSL) dating of fan deposits of a gully initiating from one of the footpaths (Supplementary Text 2). Extraction of Short-Range Order (SRO) and pedogenic iron oxides was done following Coward et al. (2017) using 1) Sodium dithionite (0.05 M), 2) Ammonium oxalate/oxalic acid 4:3 (0.2 M) and 3) Sodium pyrophosphate (0.1 M). 50 ml of each solvent was shaken in the dark with 0.5 g of homogenized sample material in a tube for 16 hours. Subsequently, samples were centrifuged for 150 min at 4400 rpm and filtered through 0.2 mm nylon membrane filters. The extract supernatants were shortly stored in the dark and Fe contents were measured for the filtered extractant solutions applying Inductively Coupled Plasma Mass Spectrometry (ICP-MS) (Coward et al. 2017). Fe content in soils measured by ICP-MS (ppm) and p-ED-XRF (ppm) has shown high correlation (Kilbride et al. 2006) therefore Fe concentration was normalized and divided by the total Fe concentration evaluated using the XRF. Results for all three extraction methods are given as a ratio between the extracted Fe (Fe_{ex}) in the footpath sample and the respective Fe_{ex} from the control or regional reference samples.

Spatial analysis

In central Tigray, continuous human occupation is expressed by the archaeological records, while geomorphological observations revealed shallow sunken lanes and gullies occupying and accompanying footpaths. Industrialized agriculture and infrastructure are rare, thus in many areas human-made terraces and footpaths are the main human impact on the landscape. In Germany, in contrast, the intense modern land use and high settlement density did not allow for straightforward mapping of incised footpaths. Therefore, only in Tigray a spatial analysis was conducted to study possible long term geomorphological effects resulting from likely historical footpaths. Incised footpaths, and streams in Tigray were mapped at a scale of 1:1500 using 1 m/pixel resolution provided by CNES/Airbus Maxar Technologies Map data @2020 as they appeared on Google Maps via the Quick map service extension in QGIS version 3.4.5-Madeira (R Core Team 2013; Jammalamadaka and Sengupta 2001; QGIS.org 2021). The imagery was used to map the three incised Ethiopian footpaths that were sampled (Rama, Yeha and Melazo footpaths) as well as for high resolution mapping of streams and footpaths in the watershed of the Rama footpath. All mapped incised footpaths were validated and distinguished from non-incised footpaths by field surveys in November 2019. The mapping results were compared with CORONA satellite images, produced by US Central Intelligence Agency (KH4B, 1967; DS1102-2106DF072_c) dating to 1967 (USGS) in order to confirm that only footpaths with a minimum age of ca. 50 years were considered in the analyses. The

orientations and lengths of non-incised footpaths, incised footpaths and streams were analysed in the R software environment using circular statistics and rose diagrams, while 'Mean Resultant Lengths' (MRL) was used to indicate the intensity of directionality (R Core Team 2013; Jammalamadaka and Sengupta 2001; QGIS.org 2021).

4.5 Results

Macroscopic observations

G1 samples (Grunewald Forest Berlin). In the G1 control sample, the upper 3 cm consist of loose organic material, roots and grasses in particular. These are embedded in sandy humus, while below 3 cm depth a sandy matrix occurs with only occasionally grass roots occurring. The G1 footpath sample had a 5 cm thick upper layer of mixed sands and silts and more diverse and smaller sized organic components than the upper part of the G1 control sample. These top 5 cm are also far more compacted than the upper layer of the G1 control samples (Figures 4.6-4.7, Table 2). Below 5 cm depth a sandy matrix occurs, but different to the G1 control sample it is dominated by leaves and other poorly decomposed organic materials. The profile of the G1 footpath sample is subsequently subdivided into three layers where the topmost layer (0-5 cm depth) is highly compacted, the middle layer (5-15 cm depth) is composed of loose sand with abundance of organic material and an underlying layer (>15 cm depth), which is similar to the middle layer but without large organic remains (Figure 4.6).

G2 samples (Urban park Berlin). The G2 samples (G2 footpath and control samples) have similar upper organic and lower sandy sequences as the G1 footpath and control samples. Except for a higher degree of compaction of the G2 footpath sample compared to the G2 control sample (Table 2), and some grasses growing on the G2 control sample's surface, no clear difference between the material characteristics of both samples is macroscopically evident.

G3 samples (Ore Mountains). The G3 control sample shows a clear indication of soil forming processes with undecomposed organic material corresponding to an Oe horizon (0-10 cm depth) followed by an organic humified layer corresponding to an Oa horizon (10-16 cm) (Figures 4.5-4.6). Although components of these two horizons of the G3 control sample were also evident in the G3 footpath sample, clear soil forming indicators were absent in the G3 footpath sample. The G3 footpath sample shows two distinct layers with sharp contact, with dark grey colour dominating the upper 9 cm while stark orange accumulation occupies the underlying layer (9-17 cm depth). In contrast to all other samples, in the G3 footpath sample, the bedrock was reached at a depth of 17 cm (Figure 4.7).

R sample (Rama footpath Tigray). Macroscopically the material of the Rama footpath sample (sample R) showed a homogenous silt-loam texture and did not allow any vertical differentiation.

Y and Y* samples (Yeha footpath Tigray). Sediments extracted from the central part of the main Yeha footpath (sample Y) were silty in the upper part of the subsurface (0-11 cm depth). At the lower part of the subsurface the sediment interchanges between sandy silts and gravels with semi-horizontal orientations (11-25 cm depth). Compared to the sample Y the sediments of sample Y* originating from a protected location of the footpath were finer and more homogenous (mainly fine sand-silt) excluding only fine gravels (Figures 4.6-4.7).

M sample (Melazo footpath Tigray). In the sample extracted from the Melazo footpath (sample M) heavy clay mixed with low amounts of silts dominated. Occasionally large (3-10 cm long) semi rounded pebbles were embedded into the clayey matrix.

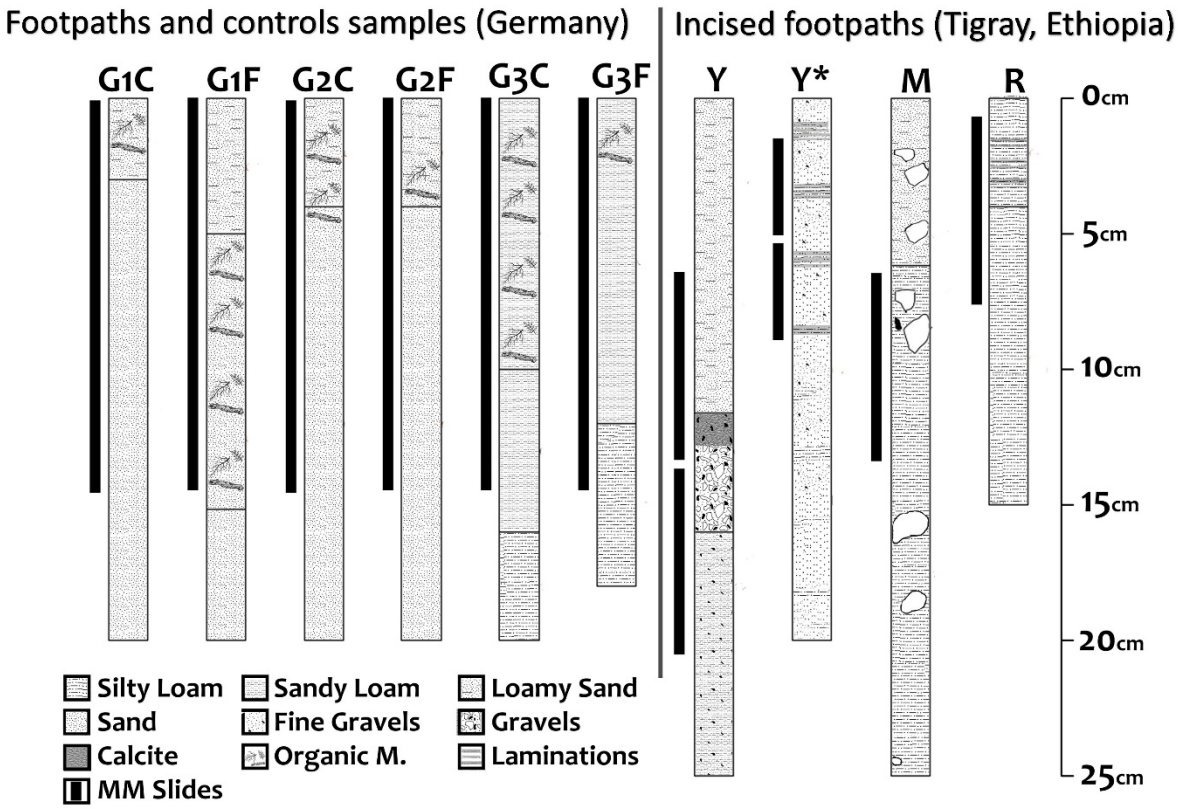

Figure 4.6. Section logs of sediment profiles sampled in temperate (Germany; G) and sub-humid (Tigray, Ethiopia; Y, Y*, M, R). Coverage of micromorphological slides (MM) is marked by a black bar. "F" marks samples taken from footpaths, "C" marks non-footpath control samples taken from the undisturbed vicinity of the corresponding footpath sample. (Germany - G1: sampling location in Grunewald Forest, Germany , G2: sampling location at the urban park in Berlin, G3: sampling location in the Ore Mountains, Germany; Tigray, Ethiopia - Y: sampling locations west of the Yeha archaeological site, at the central part of an incised footpath (sample Y) and

at the margins of the same incised footpath (sample Y*), M: sampling location at an incised footpath near the Melazo archaeological sites, R: sampling location at a incised footpath in the Rama depression.

Table 4.2. Penetration resistance, pH and electric conductivity for G1-G3 footpath and control samples.
Penetration resistance error margins are due to an average of n=3 at each sampling location using a pocket penetrometer.

Sample	**Penetration Resistance** kg*cm^{-2}	**cm depth** below surface	**pH**	**EC** µS*cm^{-1}
Sample G1 footpath (G1F)	4.3 ±0.1	0-3.5	5.1	153
		3.5+	5.4	73
Sample G1 control (G1C)	2. 0 ± 0.2	0-1.5	4.8	150
		1.5+	4.9	56
Sample G2 footpath (G2F)	4.4±0.1	0-6	6.8	58
		6+	7.1	73
Sample G2 control (G2C)	2±0.4	0-6	6.2	31
		6+	6.6	67
Sample G3 footpath (G3F)	3.5 ±0.5	0-7	4.6	354
		7-13	4.3	310
Sample G3 control (G1C)	0.75 ±0.3	0-8	3.5	378
		8-15	3.4	377

Micromorphological observations

Micromorphological analysis showed distinctive material differences between the footpaths and structural differences with the control samples (see Supplementary Table 3 for a detailed micromorphological description). Surfaces of all three footpath samples in Germany have massive microstructures as opposed to more granular or crumb microstructures in the surfaces of the control samples (Supplementary Table 3, Figure 4.8). The footpath samples G1 (Grunewald Forest Berlin) and G2 (urban park Berlin) show darker and more brown colours compared to the respective more greyish non-footpath control samples (Figure 4.7). Additionally, the G2 footpath sample holds a grano-striated (rearrangement of clay particles around grains) and speckled b-fabric causing the brown colour in this footpath (Figure 4.8). The brown colour of the G1 footpath sample results from high contents of micro- and macro-organic residues, which are lacking in the more greyish G1 control sample (Supplementary Table 3, Figures 4.7-4.8). Differences between the control and footpath sample, are most striking for context G3 (Figure 4.8): While the structure in the G3 control slide shows loose and relatively homogenous composition, the G3 footpath's slide discloses two district strata (0-9 cm depth: dark grey, 9-17 cm depth: yellow-brown) with a clear contact between them.

The surface of the G3 control site has an enaulic c/f related distribution with pellets and mesofaunal droppings that are typical of an upper O horizon (Figure 4.8). In contrast, the surface of the G3 footpath sample shows a massive microstructure of clayey-silty micromass with an abundance of coarser (medium sand sized) minerals and rock fragments and black-opaque minerals which are black to silver in Oblique Incident Light (OIL), a composition corresponding to the local lithology and possibly affected by modern pollution (Supplementary Table 3, Figures 4.7-4.8).

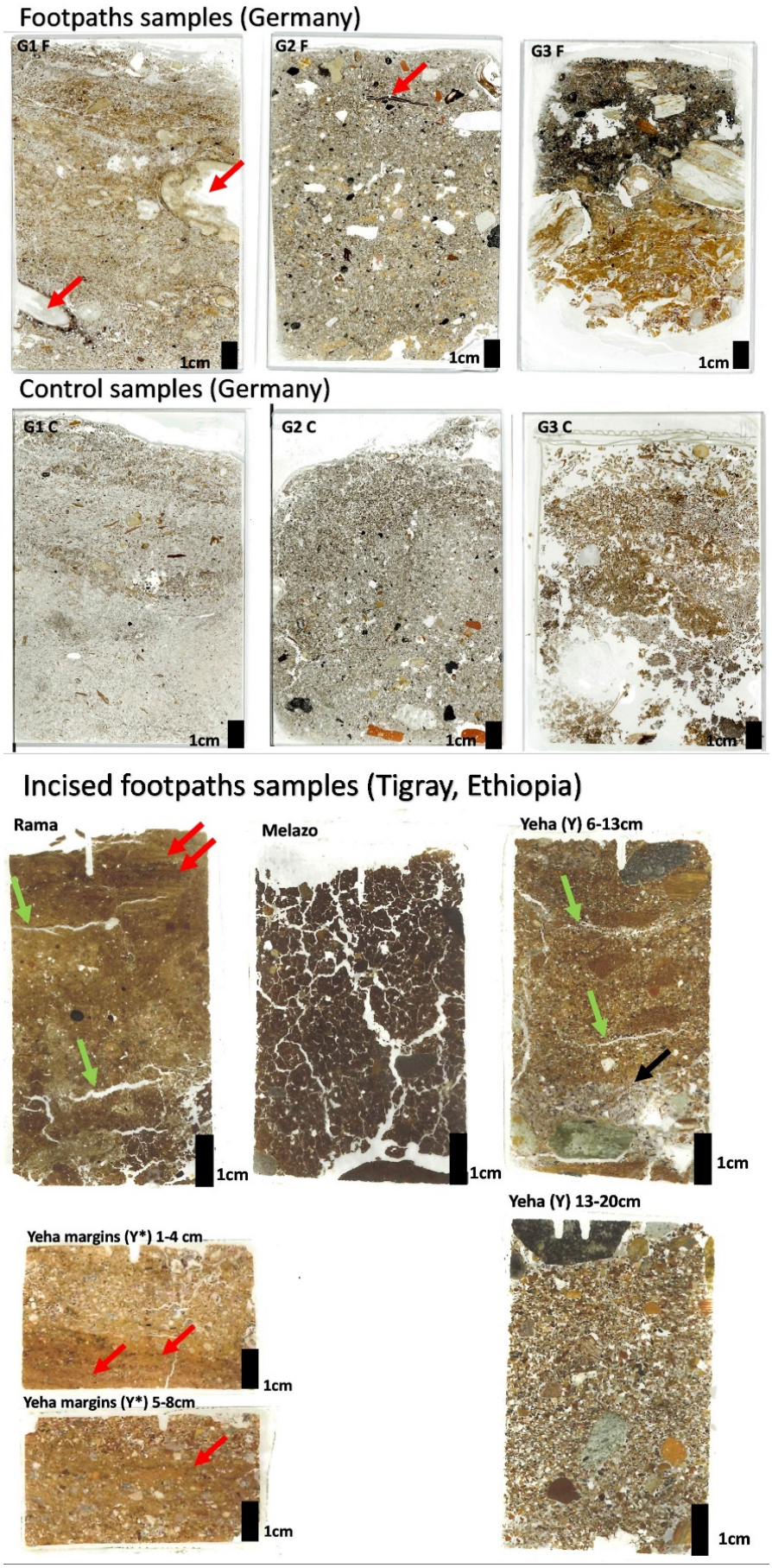

Figure 4.7. Upper part: Sampled footpaths from Germany (G1 F, G2 F, G3 F) and their control samples (G1C, G2 C, G3 C). Notice roots in footpath sample G1 (red arrows) and in footpath sample G2 a horizontal thin wooden/charcoal piece that is slightly fractured at its centre (red arrow). Lower part: Samples from incised footpaths from Tigray, Ethiopia (Rama, Melazo, Yeha, Yeha margins,). Notice bedded fine material in both Rama and Yeha margins samples (red arrows) and some horizontal planes in the Rama and Yeha (6-13 cm) samples (green arrow). For the Yeha sample a black arrow points at the contact between the upper fine material and the lower sands and gravel size minerals cemented by calcium carbonate. The latter coarse-grained unit is likely re-deposited and compacted construction material.

In the samples originating from the three footpaths sampled in the sub-

humid climatic zone (R, Y, M), various forms of massive microstructure and compacted matrixes with partially radiant or semi-horizontal fissure patterns were observed (Figures 4.7 and 4.9). The Rama footpath shows a banded and massive microstructure resulting from layers of clay impregnated with Fe oxide (Figure 4.9). The Yeha and Melzao incised footpaths were sampled at a depth of ca. 6 cm below surface in order to recognize possible paleo-surfaces of the footpaths. The sample from Yeha footpath centre (sample Y) shows a massive microstructure very heterogeneous in grain size and mineral content and possibly containing redeposited calcitic construction materials (Figures 4.7 and 4.9). The underlying stratum of the Yeha footpath sample Y (12-18 cm below surface) is more homogeneous than the upper stratum, with coarse sands and gravels dominating than the overlying (6-12 cm depth) (Figures 4.7 and 4.9).

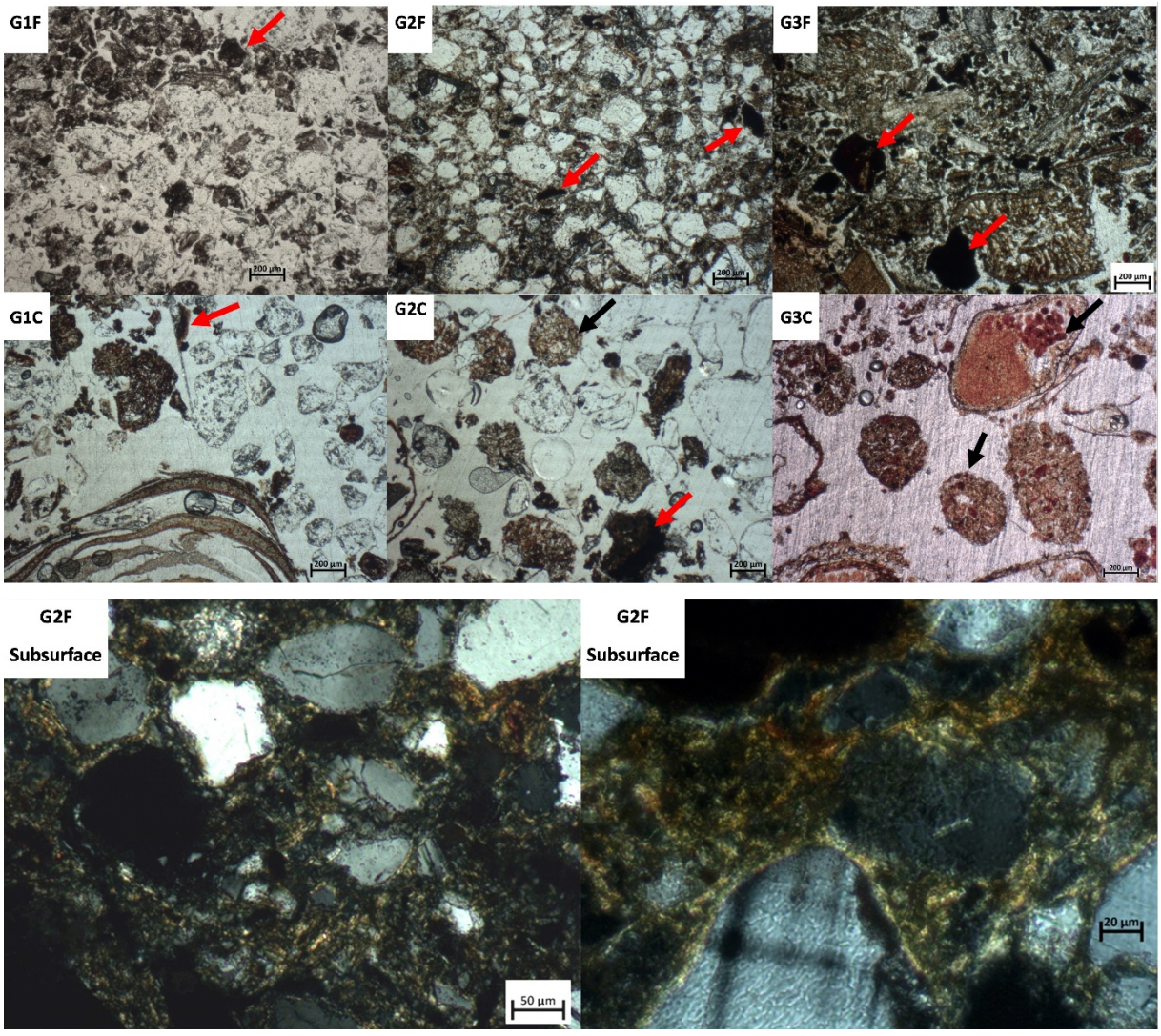

Figure 4.8. Surface strata (c. 0.5 cm below surface) of footpath (F) and control samples (C) of footpaths from the case studies in a temperate zone (Germany; samples G1-G3) in PPL. Microstructures of the three footpaths (samples G1F, G2F and G3F) are massive, while control samples present single grain to crumb and granular microstructures. Notice Fe and Mn nodules and impregnated fine material (red arrows) and organic pellets for the control samples (black arrows). The G2F subsurface images are taken in XPL. Notice the yellow clay particles arranged mostly around grains.

). Lower part: Samples from incised footpaths from Tigray, Ethiopia (Rama, Melazo, Yeha, Yeha margins,).

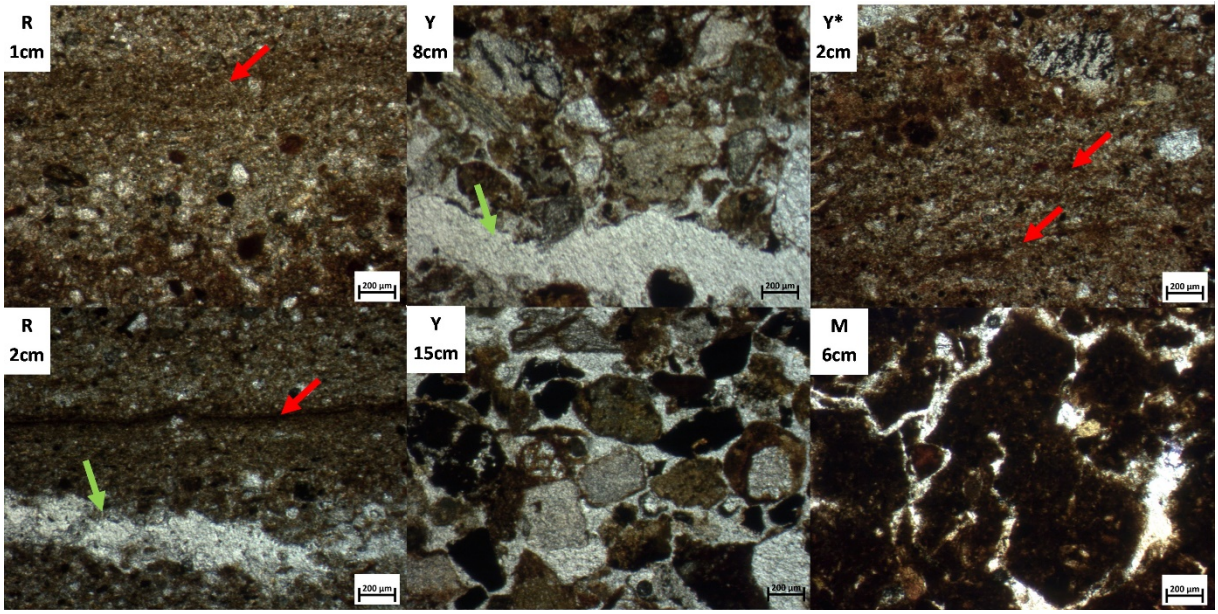

Figure 4.9. Different depths below present surface for incised footpath samples from the sub-humid zone case studies (Tigray, Ethiopia). Rama (sample R), Yeha (sample Y), Yeha margins (sample Y*) and Melazo (sample M) incised footpaths. Red arrows point at laminations and bedding suggesting surfaces in the Rama (sample R) and Yeha margins (sample Y*) footpath samples. Green arrows point at horizontal planes found in the Rama (sample R) and Yeha (sample Y) samples. Notice the loose nature of the Y sample at 15 cm below surface as opposed to massive compound upper stratum at 8 cm below surface. Vertical and semi-vertical directions for planes are evident in the Melazo (sample M) footpath sample.

Void analysis

Void frequencies were analysed as a measure for evaluating soil porosity. Differences in porosity between all footpath samples and their respective control samples (samples G1, G2 and G3) or incised footpaths and their regional reference samples (samples R, Y, Y*, M and regional reference samples 1-10) are compiled in Figure 4.10. Trends of decreasing relative porosity with increasing depth can be observed for currently used footpaths by analysing the macro voids visible in x2.5 and x5 objective lenses (Figure 4.10). For the incised footpaths that were sampled below the current surface (samples Y and M), abrupt changes of macro porosity (x2.5 and x5 objective lenses) are evident. Meso porosity (x10 objective lens) in currently used footpaths (samples G1-G3), and the Rama footpath sample (sample R) is lower than their

respective control samples and the regional reference samples for the first 3 cm depth below surface (Figure 4.10). Consistent differences in micro porosity (visible in x20 and x40 objective lenses) were not observed. A test was conducted to examine whether there is significantly lower porosity in footpaths from Germany (samples G1F, G2F, G3F) compared with their control samples (samples G1C, G2C, G3C) and for the sample from the (currently used) incised footpath in Tigray (sample R) compared with its regional reference samples (samples 4-8). The T-test considers the entire upper 5 cm of each footpath and control sample (Supplementary Figure 4.5). Results show that the sample from the Ore Mountains forest footpath (sample G3F) has significantly less voids than its control sample (sample G3C) independent from the objective lens sizes while the sample from the Grunewald Forest footpath (sample G1F) has significantly less voids than its control sample (sample G1C) considering the macro and meso voids objective lenses x5 and x10. Differences in porosity between the footpath sample from the urban park (sample G2F) and its control sample (sample G2C) are not significant for the entire 5 cm below surface ($p>0.5$; Supplementary Figure 4.5). The sample from the Rama incised footpath (sample R) from Tigray, shows significantly less voids than two of its regional reference samples (samples 6, 7) applying all objective lens sizes and significantly less voids are visible in the objective lens sizes x2.5, x5, x10, x20 than in the regional reference sample (sample 4). Compared with regional reference sample 5, significantly lower void cover in the sample originating from the Rama footpath (sample R), only occurs for voids visible at objective lens sizes x10 and x20. Compared with regional reference sample 8, footpath sample R has significantly lower micro porosity as visible at objective lens size x20 (Supplementary Figure 4.5).

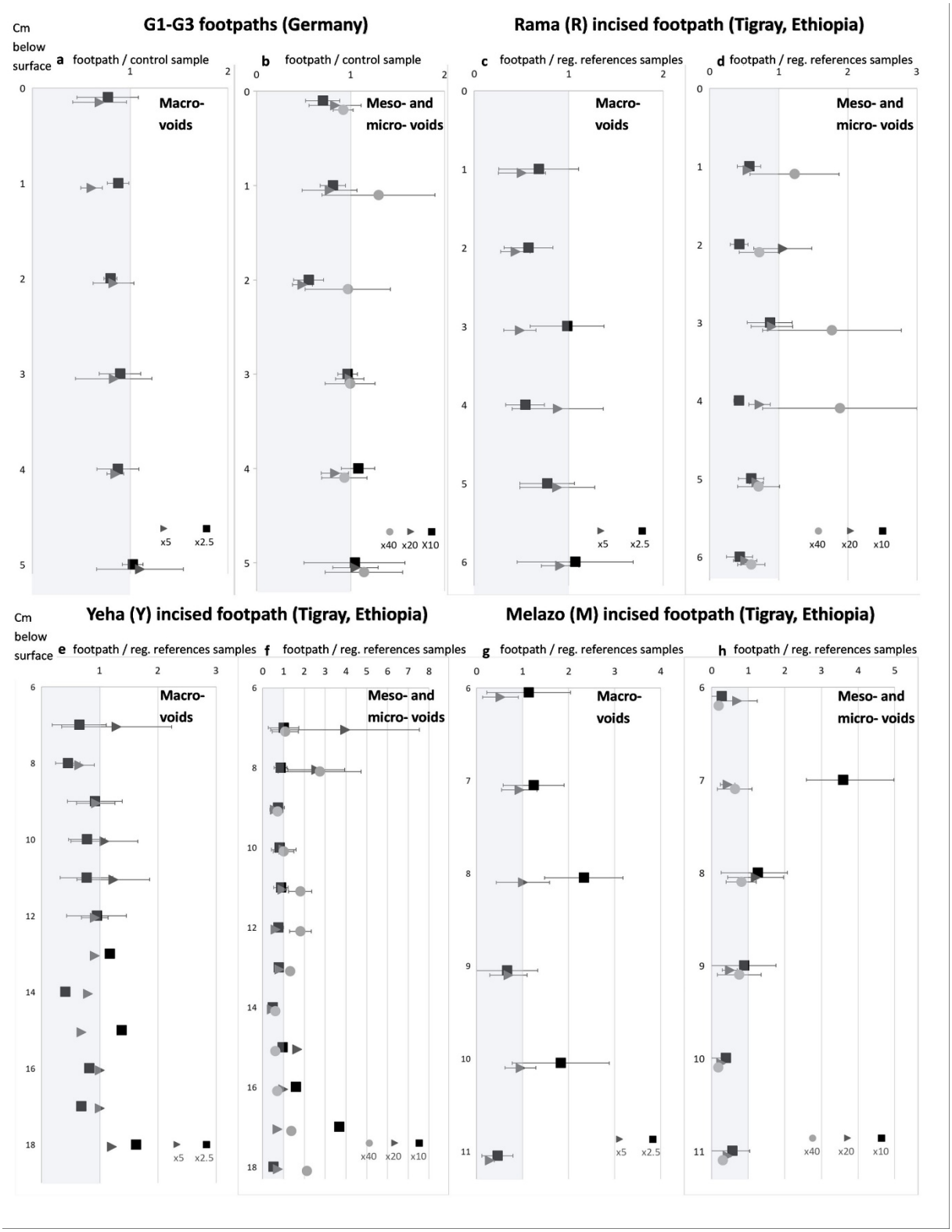

Figure 4.10. Relative differences in porosity between samples originating from footpaths, and their respective control samples and regional reference samples (reg. references), as measured using voids frequency difference analysis ('imager' package in R environment). Grey area below 1 indicates footpath has less voids than its non-footpath control sample or regional reference sample. a-b: Comparison between footpath and control samples from Germany (n=3) in different objective lenses. c-d: Incised footpath (sample R) in Tigray, Ethiopia compared with regional reference samples in different objective lenses. e-h: incised footpath samples (Y and M) in Tigray,

Ethiopia compared with regional reference samples in different objective lenses. Regional reference samples: Rama n=5, Yeha (sample Y) upper slide n=5, Yeha (sample Y) bottom slide n=1 (with comparable grain sizes and structure), Melazo n=7.

For the samples originating from recreational footpaths located in the temperate zone, less planes are recognized in the lower objective lens (x5), when compared with their control samples (Supplementary Figure 4.6). For the samples originating from the incised footpaths and reference sites in the sub-humid (to semi-arid) zone, an increase in planes and decrease in channels occurs in the samples originating from footpaths compared with the respective regional reference samples (Supplementary Figure 4.6). Applying the objective lens (x40), focusing on the smallest recognizable micro voids in samples G1F-G3F, channels appear, while they are far less represented in the respective control samples (samples G1C-G3C). In the samples originating from Tigray (samples R, Y, Y* and M), planes and complex packing voids are more dominant in the samples extracted from incised footpaths compared with those of their regional reference samples (Supplementary Figure 4.6).

Elemental and chemical components

X-Ray Fluorescence (XRF) analyses are presented for the samples from Germany (G1-G3) differentiating between surface and subsurface samples (Table 3). XRF results reveal higher amounts of Pb in the footpath's surface compared with all other samples and that Fe and Al are abundant in all G1 samples (Table 3). The G2 samples have no distinct differences between the footpath (G2F) and control samples (G2C) in XRF data. Fe, Al and Mn are abundant in all G2 samples. For the G3 footpath samples, XRF data shows differences between the G3F sample surface and the G3 control samples with ca. twice as much Fe and three times higher Al contents in the G3F surface sample compared to the respective G3 control samples (Table 3).

Table 4.3. Selected chemical components based on X-Ray Fluorescence (XRF) and Total Organic Carbon (TOC) determination in both strata of currently used footpaths and their control samples in Germany

Sample		**Fe** ppm	**Al** ppm	**Mn** ppm	**Pb** ppm	**P** ppm	**TOC** mg/L
G1C	Surface	4062 ±52	9435 ±476	<d.l.	<d.l.	<d.l.	177
	Subsurface	3555 ±50	10011 ±526	<d.l.	<d.l.	<d.l.	75

G1F	Surface	4746 ±59	8138 ±500	<d.l.	13±2.2	<d.l.	214
	Subsurface	5252 ±68	10816 ±638	<d.l.	<d.l	<d.l.	147
G2C	Surface	13493±104	20614±671	<d.l.	79±4	<d.l.	72
	Subsurface	7631±100	15657±1001	173±39	<d.l.	<d.l.	215
G2F	Surface	14365±107	23747±717	<d.l.	110±4	<d.l.	61
	Subsurface	16733±116	25961±697	55±28	29±3	<d.l.	40
G3C	Surface	36804±243	20903±1078	130±36	99±4.8	1953±118	988
	Subsurface	51648±247	52276±1156	<d.l.	213±5.54	419±73	654
G3F	Surface	101603±434	78418±1581	555±37	98±4.85	596±69	355
	Subsurface	67029±313	83804±1653	398±35	72±3.97	318±71	247

Error margins - XRF device error per sample. <d.l – Values for element are lower than the device's detection limit.

Pedogenic Fe oxides

Pedogenic iron contents (Fe_{ex}) are higher in the surface samples of G1F-G3F footpaths than Fe_{ex} contents of their respective control surface samples (Figure 4.11a). In contrast, Fe_{ex} contents of subsurface samples were lower in the samples originating from the footpaths than in their control samples (Figure 4.11a). The Fe_{ex} contents measured following the pyrophosphate extraction method in sample G1 are an exception as Fe_{ex} contents in the surface sample of the control site (sample G1C) are higher than in the surface sample originating from the footpath (sample G1F; Figure 4.11a). All samples extracted from incised footpaths show higher Fe_{ex} contents than the respective regional reference samples (Figure 4.11a). Figure 4.11b presents Fe_{ex} values normalized to total Fe concentration measured using XRF (Fe_{ex}/Fe XRF). Considering the total Fe XRF concentrations, sodium dithionite extracted Fe_{ex}, that includes most crystalline pedogenic Fe(III) oxides, shows higher contents in all surface samples from footpaths than in their control samples and higher Fe contents in all incised footpath samples compared to their regional reference samples (Figure 4.11b). The oxalic acid extraction method shows a decrease in relative Fe_{ex}/Fe XRF content with depth in footpaths (samples G1F-G3F) compared with their respective control samples (samples G1C-G3C; Figure 4.11b). Oxalic acid extraction accounts for both Short-Range Order (SRO) Fe(III) as well as some pedogenic crystalline Fe(III) oxides.

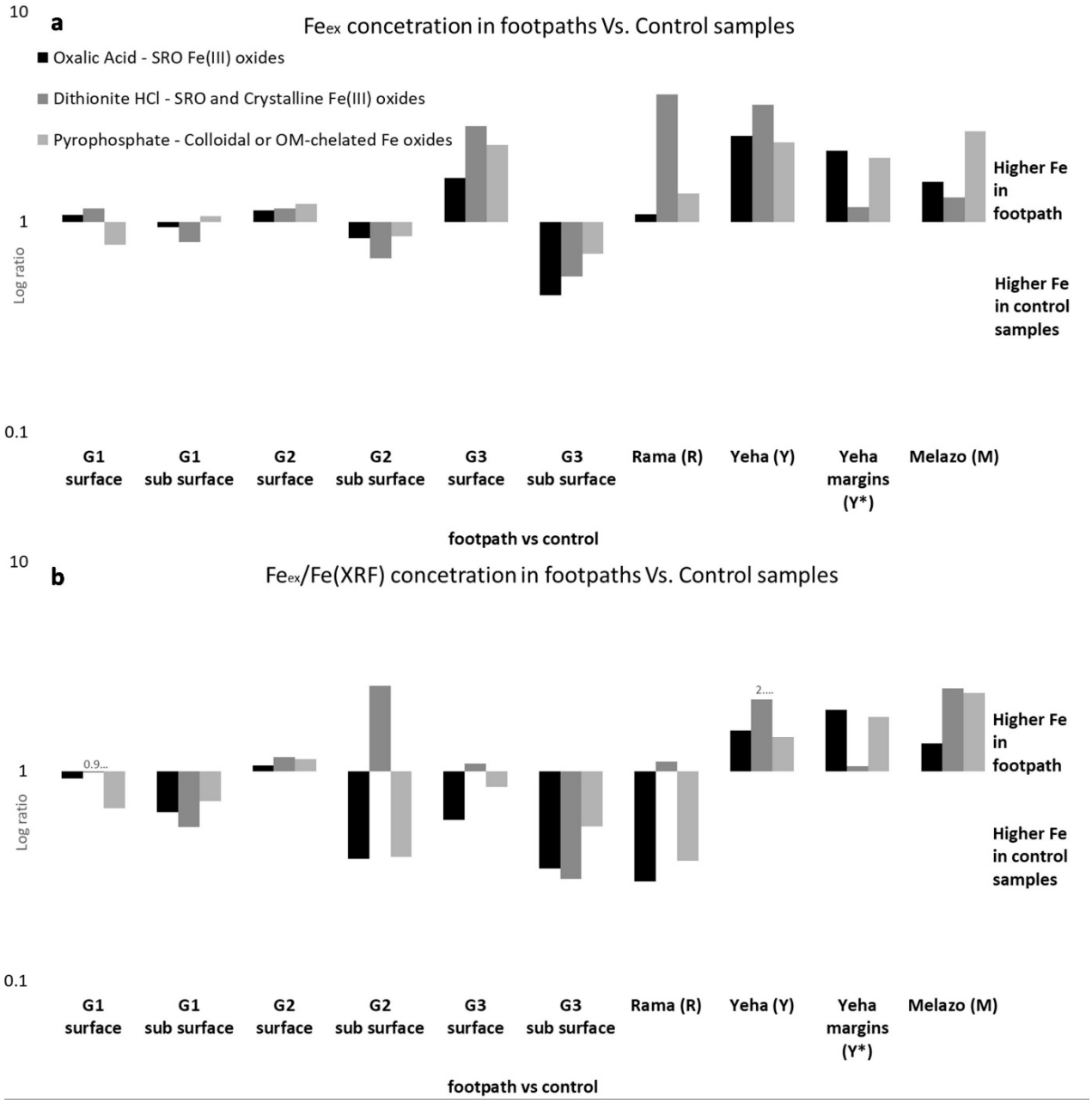

Figure 4.11. Three types of Fe extraction (Fe_{ex}); Oxalic Acid (black), Sodium Dithionite HCl (dark grey) and Sodium Pyrophosphate (light grey). For G1-G3 Fe_{ex} from currently used footpaths, Fe_{ex} is divided by their control samples for the surface (ca. 0-7cm) and subsurface (ca. 7-15cm) of each location. For the incised footpath samples, Rama (sample R), Yeha (sample Y), Yeha margins (sample Y*) and Melazo (sample M), Fe was extracted at 1-8, 2-5, 6-12 and 6-15 cm below surface accordingly. The Fe_{ex} values were divided by Fe_{ex} values extracted from the subsurface of the closest and most similar in grain size regional reference sample (regional reference 9 for R, 11 for both samples Y and Y* and at the location of reference 6 for sample M). All values are in logarithmic ratio. Fig. a. shows Fe_{ex} values and b. Shows Fe_{ex} values normalized to total Fe, obtained using X-Ray Fluorescence; Fe_{ex}/Fe (XRF).

Antiquity and spatial analysis

In Tigray, non-industrialized land use and cover enables the spatial analysis of the studied incised footpaths (Rama, Yeha and Melazo footpaths). The latter were subsequently mapped and spatially characterized on a watershed scale (Supplementary Table 6). Identifying these footpaths on basis of CORONA satellite images from 1967 (USGS) reveals that the historically used incised footpaths in Tigray already existed to various extents at least 50 years ago; however, the degree of incision remains unclear due to image resolution. For the Yeha footpath (sample Y), it seems that the agricultural area around the footpath had decreased dramatically along with the construction of the nearby road which was also constructed on top of parts of the older footpath. While accurate dating of footpaths use is challenging, preliminary ^{14}C dates, likely indicating carbon formation or burial and subsequently - the latest possible time of accumulation, were carried out under footpaths surfaces. Based on two samples from 5 and 20 cm below the surface of the Yeha incised footpaths (Y), this accumulation occurred between 1285-215 years BP. The single ^{14}C obtained for the depths of 12 cm below surface of the Melazo incised footpath, gave a date of 995 years BP (Supplementary text 2). Especially for the Yeha footpath, the ^{14}C sampling locations exhibited footpath related features (see micromorphology), suggesting these dates account for the use of the surface as a footpath. Using ^{14}C results in this context can only serve as supportive circumstantial evidence for the likely antiquity of footpaths, as older ^{14}C bearing organic matter could have been eroded and redeposited. Separately, in the Rama watershed, fan deposits of a gully which initiates from a footpath, was dated using OSL (Supplementary text 2).

Figure 4.12 Field photographs from the Rama drainage basin: a. a typical non-incised footpath, b. an incised foot path (shallow sunken lane), c. a segment of the sampled Rama incised footpath.

In the Rama drainage basin (Figure 12), orientations of incised footpaths show clear and distinct similarities to the orientation of the stream network as opposed to the unoriented non-

incised footpaths (Figure 4.13). Additionally, 57 gullies have initiated ('gully heads') in the 5 meters away from non-incised footpaths while only 5 gully heads were found within the same distance from incised footpaths. Normalizing these values using the lengths of footpaths, indicates that the amount of gully heads per 100 meters of non-incised footpaths are one order of magnitude higher than that of gullies initiating next to incised footpaths (Supplementary Table 7).

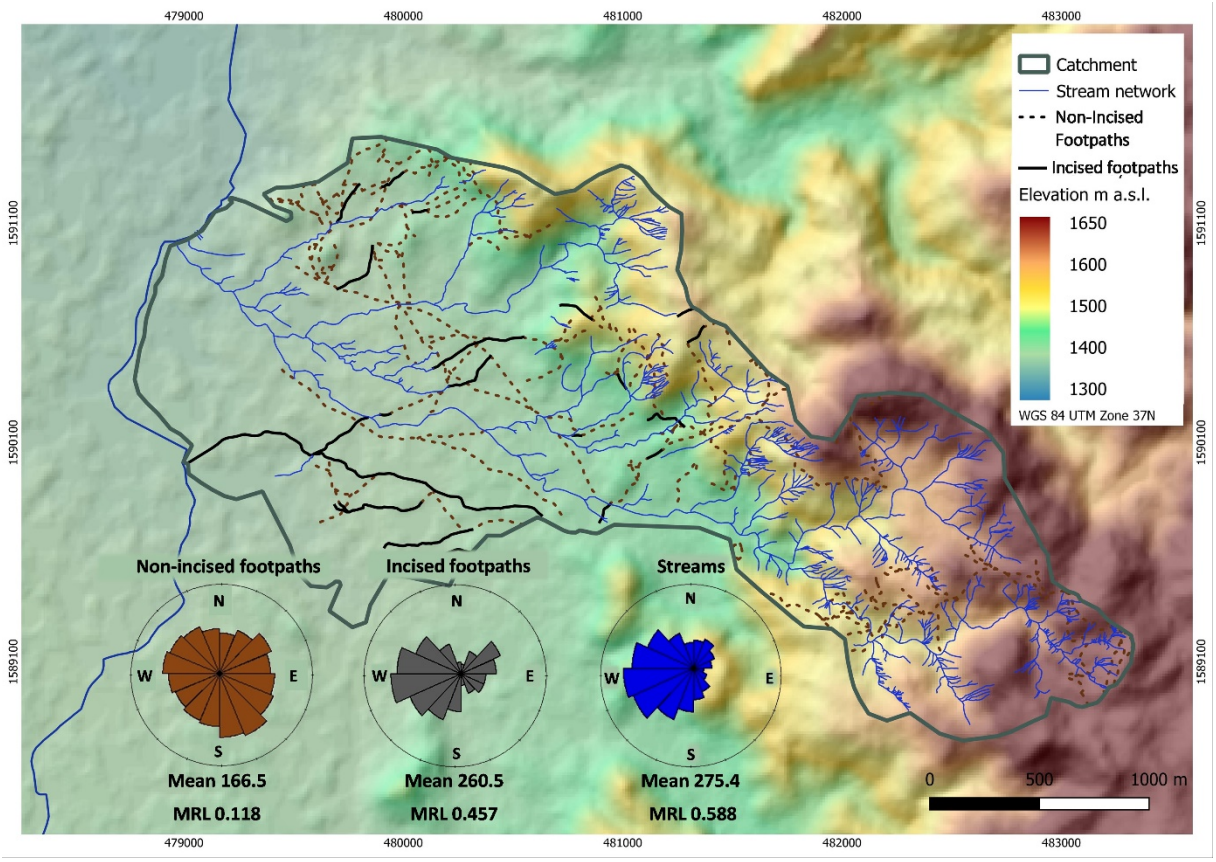

Figure 4.13. The Rama watershed case study. Rose diagrams indicating directions of non-incised footpaths, incised footpaths and streams. Mean averaged direction was calculated for each feature. Mean Resultant Lengths (MRL) indicates the intensity of directionality, with 0 representing no preferred orientation and 1 a unidirectional model (Agostinelli and Lund 2013; Jammalamadaka S.R. and Sengupta A 2001).

4.6 Discussion

Structural patterns

Footpaths located in different climatic zones and under different land uses, hinder or promote natural surface processes distinctively and to various extents. However, from their comparison, some common patterns do emerge. Similar to the effect of heavy machinery usage in forests as well as pressure caused by farming vehicles (Bagheri et al. 2012; Batey 2009; Silva et al. 2011), footpaths show 462a tendency for lower porosity compared to the control samples in both sub-humid and temperate climate zones (Figure 4.10, Supplementary Figure 4.5).

Micromorphology confirms a similar observation made on compaction by humans or animals, which affects the soil and vegetation of footpaths at similar depths (Yaşar Korkanç 2014; Tejedo et al. 2016; Sherman et al. 2019; Roovers et al. 2004). Trampling appears to be one of the main processes influencing macro- and micro differences in the temperate environment, while the interaction between trampling and sedimentation is dominant in the sub-humid Tigray region. This difference can have great impact on a possible positive or negative effect of footpaths on the topsoil. Footpaths from the sandy soils in the temperate zone (GF1-2) are more compacted, with finer grains and have a more massive microstructure than their control samples (Figures 4.7-8). Similarly, there is a massive microstructure evident in the upper stratum of the likely historical sunken lane Yeha (footpath sample Y, Figures 4.7-4.9). Although channels and Fe oxides (indication of pedogenesis) are evident, much of the contacts between units and features in the Y footpath sample indicate that the groundmass organisation is more of a result of compaction than bioturbation (Figure 4.9). Additionally, the underlying stratum of the Y footpath sample is different than the upper one. It is more homogeneous, with coarse sands and gravels dominating (Figures 4.7 and 4.9). This clearly sedimentary deposition lower stratum suggests that medium energy running water was responsible for the deposition of the earlier phase of the Yeha footpath (sample Y) sediments (Leopold et al. 2020). Apart from the massive microstructure in several footpaths, partially radiant or semi-horizontal fissure patterns were observed as a result of trampling (Figures 4.7-4.9). The Rama footpath (sample R) shows similarities (Figures 4.7 and 4.9) to footpaths in lake marl sediments, where trampling initiated the formation of a flat depression and was subsequently filled with laminated puddles and fine sediments (Rentzel et al. 2017). Additionally, the banded and massive microstructure with fine layers of clay impregnated with Fe oxide in the R footpath in Tigray (Figure 4.8), is likely an indication of a buried surface horizon (Verrecchia 2021; Rentzel et al. 2017). Grain size seems to play an important role in both climatic zones, as the pattern of lower porosity in footpaths compared to the control samples is unclear for the clay rich sample in the sub-humid zone while the other samples show similarities to the temperate zone footpaths (Figure 4.10). One explanation is that smectite undergoes seasonal shrink and swell cycles that have shown to affect soil porosity (Rasa et al. 2012; Pires et al. 2009). Such cycles may have impeded the preservation of a possible imprint resulting from the footpath formation. However, micromorphological experimental work by Bresson and Zambaux (1990), imitating heavy machinery pressure, showed three main factors influencing the intensity of fissures; (1) the degree of applied pressure, (2) water content, and (3) gravel content and heterogeneity. It was found that higher applied pressure and higher water content generated

more fissures. The most distinct case of fissures in our study was observed for the R footpath sample, which receives overbank flow on a weekly basis from the surrounding field irrigation system. Bresson and Zambaux (1990) further concluded that the occurrence of gravels, or a non-homogenous soil matrix, may redirect the pressure, resulting in less fissures. For the M footpath sample, the fine homogenous sediments under the footpath resulted in many fissures and a dense packing, while for footpath samples from Germany (samples G1-G3), which are coarser, we observed the least amount of fissures. Both findings are in good agreement with the aforementioned experimental work (Bresson and Zambaux 1990).

Pedo-features

In all currently used footpaths (in Germany and Tigray), there is little indication of soil formation/bioturbation in the upper 3 cm (apart from the few mentioned pedogenic Fe oxides in Tigray, Figures 4.7 and 4.9). In the Ore mountains (G3), the control sample shows enaulic c/f related distribution with pellets, mesofaunal droppings and higher organic carbon (Figure 4.8, Table 3) that are typical of an upper O horizon, which are absent in the footpath (Verrecchia 2021). In the latter footpath sample (G3F), both structure and organic materials in the subsurface stratum have likely developed prior to the surface being compacted and used as a footpath. This stratum has a clear contact to the surface layer, suggesting the missing O horizon may have been eroded along the footpath. In the temperate zone sandy footpaths (Berlin), the darker colours (in visible light, Figure 4.7) as opposed to light grey in their respective control samples, has to do both with higher clay and organic matter contents in the footpaths. The higher clay content is likely resulting from direct pressure rearmament (Figure 4.8). Organic matter is stabilized by trampling as reduced pore volume impedes microbial activity (Silva et al. 2011; Guimarães et al. 2013; Mikutta et al. 2006). Neve and Hoffmann (2000) showed that the carbon mineralization rate decreases with specific bulk densities, indicating that carbon mineralization in compacted soils can lead to an increase in the accumulation of organic matter (Neve and Hofman 2000). Therefore, by decreasing air and water supply, trampling hinders the degradation, humification and mineralization of organic matter. Following this, it appears that in the sandy soils, footpaths preserve organic material due to hindering of air and water supply while still receiving leafs and organic deposits from nearby sources. In silty-clayey soils of both climatic zones, an opposite outcome emerges, with less organic material than in the control samples, due to erosion and removal of vegetation. Another aspect found in the temperate zone sandy footpaths, is the higher Pb concentration in footpaths than in controls which is likely related to modern traffic pollution (Bartkowiak et al. 2017) and its accumulation

may be favoured on footpath surfaces due to compaction as well as comparably lower biogenic activity compared to the control sites (Table 3).

Void types

Unlike the larger voids, smaller void types in footpaths do not show a clear decrease compared with control samples (Figure 4.10). From a soil mechanic perspective, the smaller voids may be protected by larger grains and aggregates from pressure applied to the surface, hindering the effect of compaction on porosity. If water supply is a factor responsible for the decrease in porosity under footpath samples, it has been observed that during wet-dry cycles the larger voids are those mainly experiencing enlargement. In the case of footpaths, lack of such cycles under the footpath, while they occur in control samples, may present the opposing side of a similar process (Pires et al. 2009). Looking into the type of voids, it should be stated that images gained in 1 cm steps to classify void types as conducted here (Supplementary Figure 4.6), could produce slightly different results compared with a manual qualitative assessment of void types along a slide (Supplementary Table 3). Furthermore, both types of observations are limited in producing a representative database as a micromorphological slide captures only several cm in depth and incorporates a two-dimensional view (Stoops 2021). In the temperate climate zone, footpaths have higher relative number of vughs than their control samples where planar voids occupy more of the relative space (Supplementary Figure 4.6). This difference could be a direct result of compaction, by which elongated voids, such as planes or channels, are destroyed and more disconnected patterns, such as vughs, occur (Nicosia and Stoops 2017; Stoops 2021; Rentzel et al. 2017). Differently appearing but perhaps a result of a similar process, in sub-humid footpaths, planes are more abundant in the footpaths compared with the regional reference samples (R1-R10). This effect is mostly at the expense of channels, which are more abundant in the reference samples (Supplementary Figure 4.6). Although the two patterns may seem contrary, the footpath-related compaction in the finer and drier sediments of Tigray, would have altered the more rounded channels to form the rather angular planes, in accordance with the effect of compaction of finer grain sizes (Bresson and Zambaux 1990). However, the formation of channels, that are largely related to bioturbation, is also dependent on the availability of water and the infiltration capacity (Pietola et al. 2005; Sherman et al. 2019; Jim 1993; Ayres et al. 2008). This is in agreement with results of Shipitalo et al. (2004) who observed for finer grain sizes that larger voids result from the works of burrows, earthworms and cracking (Shipitalo et al. 2004). Therefore, a lower number of larger planar and channel voids (Supplementary Figure 4.6) could also be due to a decreasing effect of bio- and pedo-

features, rather than strictly from direct surface pressure (trampling). The latter process supports aninterpretation as for the hindering of soil formation in footpaths under temperate climate. The other agent likely having the strongest effect on the formation of larger voids are large surface roots. Reduction of surface vegetation on footpaths reduces roots, increases the bulk density and reduces water permeability (Sherman et al. 2019; Ayres et al. 2008; Cole 2004).

Formation of pedogenic Fe oxides

Pedogenic iron oxides relate to the amount of oxygen, SOM and water availability affected by soil porosity (Chen et al. 2020; Coward et al. 2017). Compaction and the resultant impeded oxygen supply could be behind the higher Fe_{ex} content in footpaths surfaces compared with their control samples in both temperate and sub-humid climate zones. Chen et al. (2020) demonstrated how Fe(II) under anoxic conditions generates SRO Fe(III) oxides (Chen et al. 2020). Independently, pedogenic metal oxides have been long known to strongly relate to anoxic and reducing conditions and therefore to changes due to water and air conductivity and supply (Bigham et al. 2002). Independently, changes in Fe oxides have shown to be a direct result of compaction (Coulon and Bruand 1989). Likely historical footpaths have higher amounts of SRO and poorly-crystalline Fe(III) oxides than their closest regional reference samples at similar depth (Figure 4.11). This is in contrast to sub-surfaces of the modern footpaths from the temperate zone, suggesting that the former were in fact past surfaces of the footpaths. Following normalisation using XRF measured Fe concentrations, the most crystalline pedogenic Fe(III) oxides (extracted using sodium dithionite) show higher Fe_{ex} contents in all footpath surface samples compared to their control samples in the sub-humid and temperate climate zones (Figure 4.11). Using the ammonium oxalate Fe_{ex} extraction, a pattern of higher relative Fe_{ex} in footpath surface samples compared with their sub-surfaces emerges. The latter may imply a reducing zone of water stagnation on the surface and lack of water supply in the subsurface. In machinery compacted forest soils, citrate bicarbonate extracted Fe is higher in compacted soils than in non-compacted control samples for ca. the upper 30 cm (Nawaz et al. 2016). The authors argue that due to compaction, water resides longer on the compacted surface, reducing the availability of oxygen and changing the Fe lability through reduction from Fe(III)+ to Fe(II)+ i.e., from well crystallised to poorly crystalized Fe oxides(Nawaz et al. 2016). This is similar to the observation made in an experimental trampling site (Rentzel et al. 2017). In the current work, another explanation is possible beyond the *in-situ* pedogenic process. The most consistent Fe_{ex} increase in the

temperate climate zone footpaths' surfaces, is for the well crystalized Fe(III), suggesting more than just pedogenic origins for the Fe. Therefore, these well crystalized Fe oxides could have actually been transported and trampled into the footpaths' surfaces by humans and animals rather than being illuviated or bioturbated to the sub surface in the control samples.

Footpaths and linear soil erosion

Unlike the temperate and industrialized central Europe, in the Tigray region, mechanized agriculture, modern infrastructure and urban settlements, have not significantly impacted much of the local landscape. It has been previously shown for the Ethiopian Highlands and elsewhere, that both, pathways and roads, promote the formation of gullies downslope and the formation of sunken lanes due to incision (Nir et al. 2021; Busch et al. 2021; Nyssen et al. 2002; Sidle et al. 2019), as compacted and thus less permeable surfaces result in increased surface runoff (Boardman 2013; Sidle et al. 2004; Ziegler et al. 2000; Zgłobicki et al. 2021). The onset of incision along a footpath is likely to initiate only in one (or several) specific location along the path, comparable to trigger factors of gullies, where slope and catchment area thresholds are crossed (Belachew 2020). In this sense, it differs from a gully as several locations and thresholds can initiate different types of soil erosion, e.g., gullies and sunken lanes. Sunken lanes can play an important role in a catchment's drainage system (Zgłobicki et al. 2021). It is therefore not surprising that within the Rama watershed case study, incised footpaths follow similar general directions as the stream network (Figure 4.13). It has been recently shown that unpaved roads may develop different rill structures, depending on the road slope angle (Cao et al. 2021). This mechanism may also govern the incision of footpaths (Figure 4.12). It is evident that less gullies tend to form in the vicinity of incised footpaths than near non-incised footpaths (Supplementary Table 6). Changes in surface runoff patterns could be responsible for this observation. When a footpath is parallel to the stream network direction, at least for some of its course, incision along the footpath may occur due to surface runoff either during one or multiple events (Zgłobicki et al. 2021). This type of erosion is depending on the slope angle, suggested to initiate at ca. 7% (Cao et al. 2021). Incised footpaths would subsequently canalize the surface runoff downslope along the footpath. However, in cases where the footpath is not incised, likely when it is perpendicular to the slope, surface runoff due to the footpath's lower permeability (Figures 4.7-4.10), would continue directly downslope from the footpath. Such runoff can initiate gully erosion. These gullies would be perpendicular to the footpath downslope. Due to their compaction and resulting different morphology, it is likely that most

incised footpaths, similar to shallow sunken lanes (< 0.5 m deep), tend to incise slower than gullies in a similar environment (Zgłobicki et al. 2021). Additionally, it has been observed that incised footpaths in the Rama watershed do not have banks steep enough to collapse (Figure 4.12). As a result, in the study area, gullies are usually deeper than incised footpaths. Subsequently, soil erosion and sediment supply resulting from these gullies should be higher than that resulting from incised footpaths. In contrast, similar to gullies, incised footpaths could lower the groundwater Table and can decrease biomass production along the footpath banks. However, for some incised footpaths, concentrations of bushes along the footpath banks were observed (Figure 4.12). The latter observation, coupled with compositional and micromorphological differences between footpaths and non-footpaths (i.e., more uncomposed organic matter, Figures 4.7-4.10), suggests that footpaths could be considered as Small Natural Features (SNF) that hold the potential to increase local biodiversity (Zgłobicki et al. 2021).

4.7 Conclusions

The long-term residues of footpaths were evaluated, using different scales in a variety of climatic, sedimentary and land-use contexts. Comparing footpaths in a temperate industrialized European environment with that of the sub-humid, extensive agricultural region of the Ethiopian Highlands, have allowed to observe several common trends. Trampling decreases the porosity of the top 3 cm of the soil while the type of voids under the footpath are more angular than outside the path. Footpaths result in the reduction of biogenic activities due to hindering of oxygen and water supply from the surface. Most extractable pedogenic Fe values are consistently higher on footpaths surfaces than in non-path control samples, likely due to surface processes (e.g. puddles, overland flow, Fe transport) or the result of the lower pedogenesis on the footpath. Differences between the various climatic and sedimentary environments are striking; In temperate environments, footpath formation can erode or hinder soil formation while specifically in sandy forest environments it can also result in burial of organic matter (e.g., leaves), hindering organic decomposition and carbon discharge. Trampling results in higher overland flow and erosion dynamics in all environments with the intensity of these processes depending mainly on the topographic position of the footpath. However, in a sub-humid zone, footpath-erosion interaction seems more dominant and possible to systematically observe. Incised footpaths follows the direction of the stream network and hinder gully erosion downslope from paths. The incision of footpaths rather than the development of gullies, may result in lower soil erosion on a watershed level. Historically used

incised footpaths in a sub-humid environment can be recognized and are dominated by the interaction between erosion and compaction, while recreational footpaths in a temperate climate zone can hinder soil formation and may also result in lower decomposition of organic matter under the footpath. These preliminary results call for future research into the behaviour of footpaths under different environmental conditions. Such investigations may hold implications for the recognition of older footpaths in archaeological contexts as well as recommendations for pathway management to prevent soil loss on a watershed scale.

Chapter 5

Footpath formation under arid conditions

Nir, N., Davidovich, U., Ullman, M., Schütt, B. and Stahlschmidt, M. *Manuscript*

The environmental footprint of Holocene societies: a multi-temporal study of footpaths in the Judean Desert, Israel

https://doi.org/10.3389/feart.2023.1148101

Abstract

The global distribution of footpaths and their inferred antiquity, imply they are widespread spatial and temporal anthropogenic landscape units. Arid environments are of special interest for investigating historically used footpaths as older routes may preserve better due to minimal modern impact and slower pedogenic processes. Here we examine footpaths in the Judean Desert of the southern Levant, a human hotspot throughout the Holocene. We studied one modern and two archaeological footpaths (one attributed to the Early Bronze age and one to the Roman period) using micromorphology, sedimentary analysis, and remote sensing. Macroscopically, our results indicate that footpaths in the studied arid limestone environment, can result in brighter surface colour than their non-path surroundings. Similar color changes are reflected both using sedimentary analysis and high-resolution remote sensing, where the difference is also significant. Microscopically, the footpaths studied tend to be less porous and with less biogenic activities when compared to their non-path controls. However, the two ancient footpaths studied, do exhibit minimal biogenic indicators that is not detectable in the modern footpath sample. Our study shows that high-resolution remote sensing coupled with micromorphology, while using appropriate local modern analogies, can assist to locate and assess both the environmental effect and the antiquity of footpaths.

5.2 Introduction

Trails are common human marks on the landscape, occurring practically in all environments (Loor and Evans, 2021, Rodway-Dyer and Ellis, 2018). In the social sciences, it has been argued that both paved and unarmored roads are an important part of our cultural heritage (Zedeño and Stoffle, 2003, Jackson, 1984), while geomorphological research shows that the environmental effects of trails through soil erosion is a problem on a global scale, reaching

values of 2090 Mg ha−1 y−1 (Salesa and Cerdà, 2020). Linear soil erosion in particular, has recently been suggested to interact with the establishment of new pathways, affecting human routes selection through a positive feedback mechanism (Nir et al., 2021). From a temporal perspective, both gully erosion due to farming as well as the initiation of sunken lanes (i.e., holoways), resulting from erosion and deepening of the pathway, have been dated well into the Holocene (Dotterweich, 2005, Wilkinson et al., 2010, Dotterweich et al., 2012).

As with other types of human-made environmental impacts, it is difficult to assess the timing of the earliest occurrence of footpaths, which went beyond the environmental imprint produced by other animals (Boelhouwers and Scheepers, 2004, Foley and Lahr, 2015). During the late Pleistocene, human groups underwent long distances traveling for obtaining raw materials, and hunter-gatherers likely used similar routes at least on a seasonal basis (Winterhalder, 1981, Malinsky-Buller et al., 2021). However, with the appearance of sedentism, the foundation of settlements and growth of population would have been accompanied by processes of intensive and repetitive use of trails. Therefore, with the onset of so called 'human niche construction' behavior, an environmental imprint through the repetitive use of trails, would become more dominant (Snead et al., 2009, Snead, 2006, Smith and Zeder, 2013). Archaeological evidence for the domestications of both plants and animals with the emergence of sedentary societies in the Near East, dates to ca. 10-8 ka cal. BCE (Gibling, 2018). In our study area, this is evident for example, by the monumental walls and tower of Jericho, located in the Dead Sea basin and dated to ca. 8 ka BCE (Bar-Yosef, 1986). Therefore, a minimum age for a unique human imprint on the landscape, by the formation of footpaths, could be situated within the Early Holocene. With respect to long term residues of such imprints, i.e., geomorphological and pedological changes related to footpath formation, we here present the study of three footpaths in the Judean Desert.

In landscape-archaeology, the majority of attempts to track down possible prehistoric routes have focused on Least Cost Path (LCP) analysis, or the archaeological finds (i.e., pottery, installations, stone tools) discovered along a specific research area (Yekutieli, 2006, Schild, 2016), rather than pedogenic or geomorphological evidence. In micro- and geo-archaeology, paved or wheeled driven tracks have often been investigated using construction materials and micromorphological residues as proxies (Tsokas et al., 2009, Charbonnier and Cammas, 2018). Recently micromorphology has been used to reveal the application of similar construction methods for centuries of roman road paving (Gutiérrez-Rodríguez et al., 2022). Within archaeological sites, the effect of trampling on pathways and surfaces was thoroughly examined by Rentzel et al. (2017) while others have used the in situ fracturing of microscopic

artifacts embedded in sediment as proxies for trampling (Goldberg, 2018, Miller et al., 2010, Devos et al., 2022, Pawłowska and Shillito, 2022). Off-site footpaths, however, have been until recently neglected in the geoarchaeological literature (Nir et al., 2022).

Here we consider non-wheeled pathways, i.e., footpaths, as trails (> 30cm width) that are reused by humans and at times pack animals (Pounder, 1985, Morrocco and Ballantyne, 2008, Tejedo et al., 2016b, Buchwał and Rogowski, 2010b). Identification of archaeological footpaths is difficult due to post depositional overprinting, later sedimentary accumulation, and modern land use (Goldberg and Macphail, 2008). In arid environments however, the influences of these processes are limited, which frequently allows to recognize archaeological non- or partially constructed routes. The duration of construction and use of these routes can be constrained using material culture, i.e., movement wastes and/or road-related structures (Dregne, 2011, Yekutieli, 2009, Davidovich et al., 2016, Fanning et al., 2009).

Following this notion, in this work we attempt to develop tools to document and test the occurrence and preservation of ancient footpaths in arid environments and their impact on these environments. The Judean Desert, a small arid region in the eastern flank of Cisjordan, is a perfect laboratory for the study of ancient pathways in the Ancient Near East due to its limited land use and aridity. Here, we address three footpaths located in the Judean Desert (southern Levant). A modern footpath (M), a footpath which shows evidence of use during the Early Bronze Age (EBA) and a third path, which has an early use phase attributed to the Roman period (R) (Figures 1 and 2). We use sedimentology, micromorphology and Unmanned Aerial Vehicle (UAV) imagery to examine how Holocene societies influenced the environment by repetitively walking from one location to the other. Following observation of gullies next to footpaths and pathways being brighter than their surroundings, we expected to find differenced in the micro-landscape and color around on the surface trails compared with non-path areas.

5.3 Study area

Geographical and natural setting

The Judean Desert is a 20 km wide (W-E) and ca. 70 km long (N-S) desert in the rain shadow of the Judean Highlands. It is framed by the Judean Highlands to the west and the Dead Sea to the east, while the Negev Highlands marks its southern border. The Judean Desert marks the western flank of the morphotectonic Dead Sea depression, created by normal as well as strike-slip faulting since the Miocene (Garfunkel and Ben-Avraham, 1996). A remarkable attribute of the Judean Desert area is its strong relief, ranging from ca. 800-1000 m above sea level (a.s.l.) in the west to ca. 400 m below sea level (b.s.l.) to the east. The area is flanked by high

escarpments in the east (Dead Sea graben) and dissected by multiple W-E draining canyons, which tend to be very steep and narrow as they approach the Dead Sea. Locally exposed bedrock units include dolomite, chalk, marl, limestone and cherts deposited during the Upper Cretaceous, and conglomerates and lacustrine formations attributed to the Pleistocene and Holocene (Lisker et al., 2010, Davidovich, 2013). Some of the lithological units as well as the current Dead Sea water incorporate different salts (e.g., NaCl, $CaSO_4$) that are distributed on the Desert's surface through both alluvial and aeolian processes. Morphodynamics in the region are characterized by few yearly flash flood events with exceptionally high sedimentary yield and deposition of slack water deposits and flood-out sediments. The latter result in the abundancy of typical arid environment vegetation such as Zygophyllum dumosum (Lisker et al., 2010, Cohen and Laronne, 2005, Zituni et al., 2021). The average annual rainfall in the south-eastern region of the Judean Desert, where research was conducted, averages 60-80 mm. At the sampling areas, where the modern and Roman period footpaths are located, the surface is composed of a regolith soil and coarse grain alluvium, while to the south, at the Early Bronze Age (EBA) footpath sampling location, bare rock predominate with poorly developed lithosol (Steinberger et al., 1999, Singer, 2007).

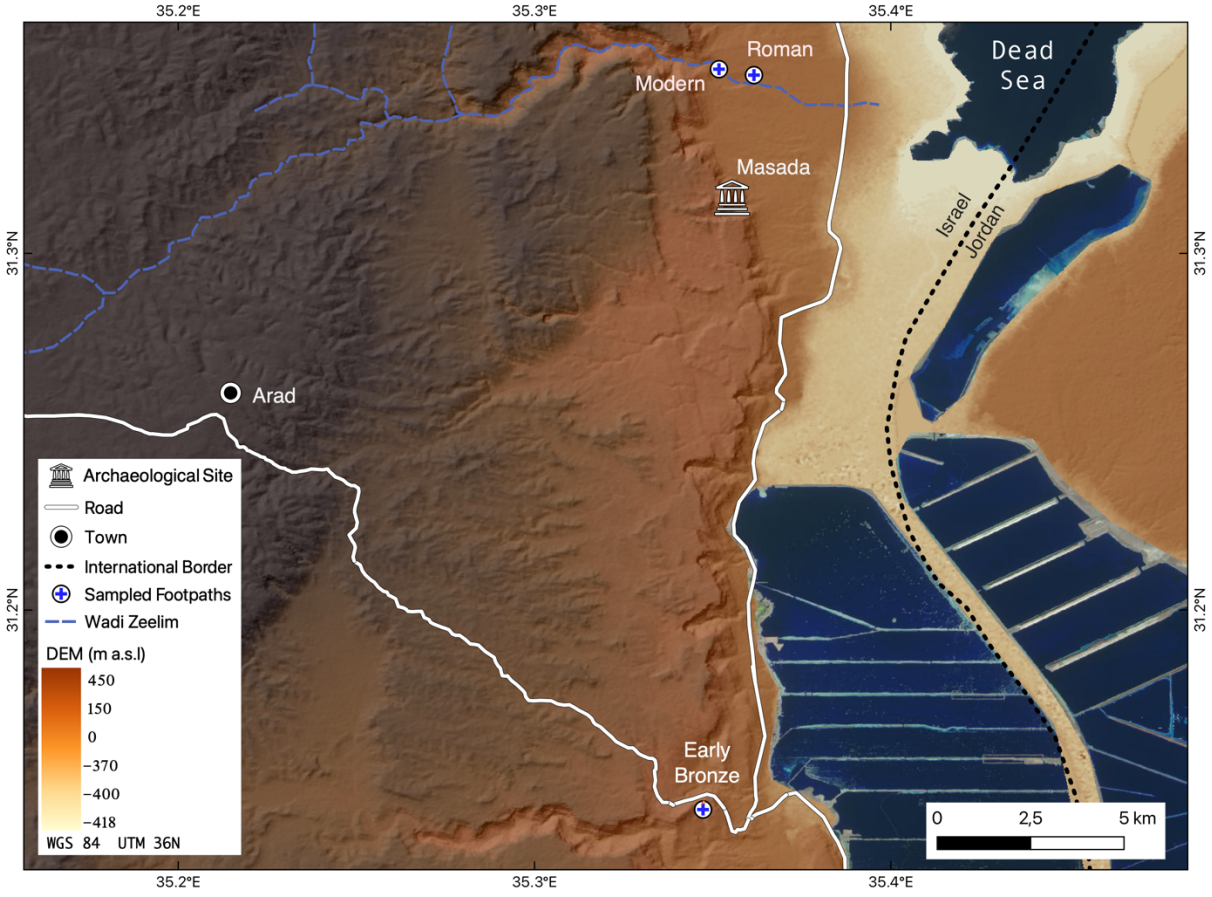

Figure 5.1. An overview map of the study area. Footpath attributed to the modern and Roman period are located within the Dead Sea plain (northern edge of the figure) while the footpath attributed to the Early Bronze Age ascend from the lake shore to the desert uplands (southern edge of the figure). Digital Elevation Model is based on SRTM (1N31E035V3) available at USGS . Satellite imagery of the water bodies are extracted using the visible light bands from Sentinal-2 satellite (European Space Agency) available at . The underlying slope aspect layer was generated using QGIS (QGIS.org, 2021)

Archaeological Framework

As a desert strip bounded by settled zones on the west (The Judean Highlands) and east (the Transjordanian Plateau beyond the Dead Sea), the Judean Desert has been used intermittently throughout the Holocene as a bridge connecting both sides of the Dead Sea Rift (Davidovich, 2014). Moreover, local Dead Sea Valley products (e.g., salt, bitumen) and commercial cash-crops grown in the oases along the lake shores (palm dates, perfumes) served as important commodities in certain epochs in the history of the greater region, enhancing the development of road networks to mobilize goods and labor in addition to other activity patterns typifying this region, e.g. refuge in cliff caves (Mazar et al., 1966, Connan et al., 1992, Hirschfeld, 2006, Davidovich, 2013). In tandem, the severe topographical obstacles created as part of the tectonic faulting along the western margins of the Dead Sea Transform, limited the use of wheeled traffic in this area. Thus, routes ascending from the rift valley to the desert uplands were used for movement on foot, associated with pack animals (namely donkeys and camels). The Early Bronze Age footpath of the Zohar Ascent (EBA footpath) (Yekutieli, 2009) is part of an east-west route connecting two settled provinces – Arad to the west (Amiran and Ilan, 1978) and the Southeastern Dead Sea communities on the east (Rast, 2001). The ascent is located in the southern part of the Judean Desert, in a segment where the western Dead Sea Escarpment is replaced by a bend scarp (The Har Hemar anticline; fig. 1, 2C), locally known as the Wadi Zohar/Zeron Outlet. The EBA ascent is the southernmost in a series of routes from multiple periods that pass through this outlet. The footpath has a modern (but seldomly used) marked trail along part of its course; however, these modern parts are easily distinguishable both by extreme bright color as well as modern waste from the ancient footpath. The EBA route was identified in a high-resolution regional survey headed by Y. Yekutieli through the observation of a quasi-linear distribution pattern of sherd scatters dated to this period, that were interpreted as movement wastes (Yekutieli, 2005, Yekutieli, 2006). Furthermore, an EBA built site was excavated on the ridge overlooking the footpath, interpreted as a military outpost (Yekutieli, 2009). In later periods, this route was abandoned and more northerly routes were chosen (e.g. Aharoni and Rothenberg (1960)). For the present study, we selected a segment of the ascent

directly downslope a local watershed where a narrow saddle marks a necessary crossing point for movement (fig. 3C).

The Roman period in the southern Judean Desert is best known for the construction of the Herodian palace-fortress at Masada, and the historically-documented Roman siege on the Jewish rebels entrenched in the fortress during the Great Revolt between 66 and 73/74 CE (Yadin, 1966). The Roman-era road system around Masada was briefly described by several scholars over the years (e.g., Schulten et al. (1933), and was lately archaeologically surveyed as part of a regional survey project (Davidovich, 2014). In this study, we examined a segment of the route connecting Masada with the large oasis of Ein Gedi located ca. 20 km north of the palace-fortress; the trail was most probably established in association with the Roman siege efforts of Masada, and was not used since, other than by occasional travelers. Where the path crosses the Pleistocene alluvial deposits (<5°) of Wadi Seiyal (Nahal Zeelim) (fig. 1 and 2B) it is marked by a curbstones along both its sides. As the path is abruptly truncated (>7m vertically) by the current active stream (Figure 5.3B), it is clear that it was not used in recent centuries.

.

5.4 Materials and Methods

Selection of footpaths

The criteria for selecting the archaeological paths to be explored in this study were, 1) evidence of archaeological use of the paths based on structures, stones arrangements and scatters of pottery shards along them, 2) distance from currently used trails for recreational proposes, 3) a distinct period in which the footpath was established, preferably without evidence of restructure or extensive usage during later periods. Contrastingly, the sampling site of the modern footpath is located on an extensively used recreational route (Wikiloc, 2022). This latter footpath was selected based on its relative proximity and environmental similarities to the Roman footpath (figures 1 and 2). All selected trails were sampled in areas where passing of vehicles could be excluded (or in the case of the Roman segment on the plain - where it is highly unlikely).

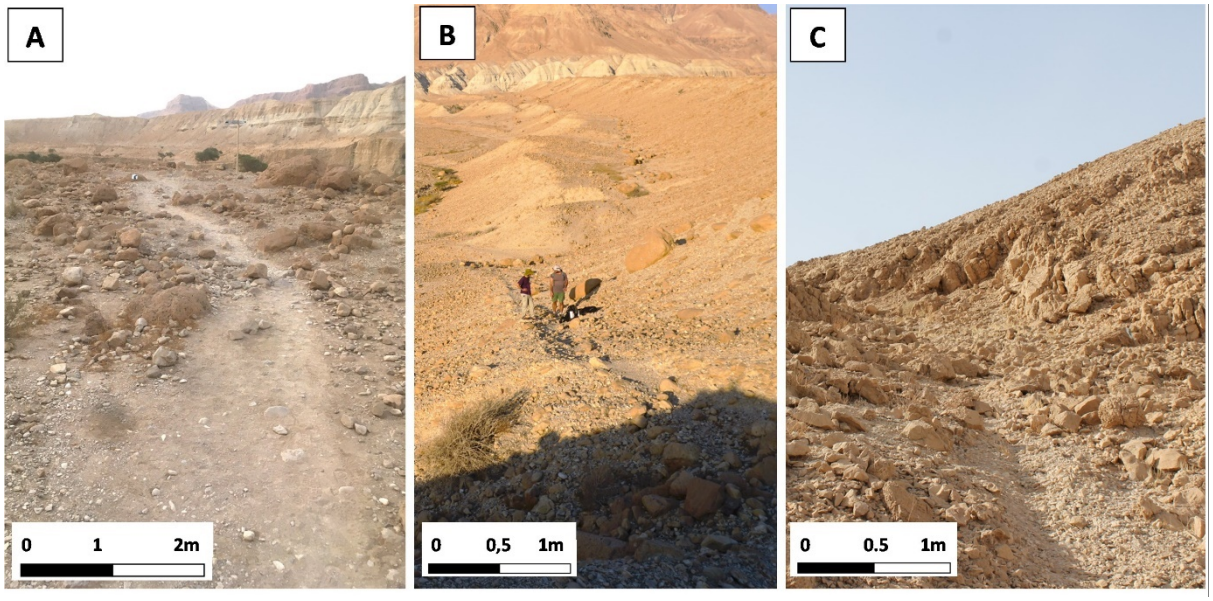

Figure 5.2. Studied Footpaths. A. The modern hiking trail. B. The Roman footpath and C. The Early Bronze Age footpath. Carbonate of Lake Lisan formation (Pleistocene) characterize the bedrock of the modern footpath as well as of the Roman footpath. Both stretch through alluvial-colluvial sediments in the foot slope and ravine fan areas, while the EBA footpath in the Zohar Ascent stretches along a debris covered backslope position.

Field observations, mapping and sampling

Sampling included extraction of undisturbed block samples for micromorphological analysis and a bulk sample for sedimentary analysis. Following field description, each footpath was measured along ca. 20 m for its width and slope angle, of both the footpath's course and the slope at its location, using a Leica DISTO device. Surface resistance was obtained using a manual penetrometer (ELE pocket penetrometer), with three replicas measured at all sampling locations (Tejedo et al., 2016a). Surface resistance was measured in $kp*cm^{-1}$. For each measurement at a footpath location a control, ca. 1-2 m outside the path's course, was measured. Micromorphological samples from the footpaths were taken starting always directly at the uncleaed surface (0 cm) and reaching 5 to 10 cm depth, depending on the state of the material as it affects sampling depth (n=5). Also, outside each footpath, a nearby, undisturbed control was collected (ca. 1-4 m away from the sample within the path), where disturbances due to trampling were not evident (n=5). Block samples were extracted using plaster of Paris. Bulk samples for sedimentary analysis were taken at each micromorphological sampling point and at two additional locations along the paths and at the respective additional off-footpath control samples (table 5.1). These bulk samples were extracted each from 0-5 and 5-10 cm below surface (n=38); additionally, bulk samples from 10-15 cm below surface were taken

where unconsolidated fines occurred in sufficient thickness forming the subsurface material at some footpaths (n=12).

Remote sensing

Remote sensing data was derived from Unmanned Air Vehicle (UAV) imagery using a DJI Phantom 4, RTK. Visible spectrum images above the areas of the two archaeological footpaths provided a resolution of ca. 1 cm. For mapping the course of footpaths, the images were geocoded applying Agisoft Metashape Pro software. Three archaeologically affiliated footpath segments where measured; Roman path on the slope, Roman path on the plain and Early Bronze path. Footpaths and non-path RGB values per pixel were extracted and summed for each line (ca. 5000-10000 pixels) and then averaged (n=3 for each footpath and n=6 for each non-footpath area). Albedo values estimations were conducted following common UAV calculation (Wang et al., 2016). However, unlike other UAV studies, the normalization by Landsat 8 values was excluded and replaced by RGB normalization. The latter is sufficient for comparison purposes, between path and non-path areas, while additionally, the resolution of a 0.5 m wide path would not be detectable by Landsat data (Cao et al., 2018). Therefore albedo values were calculated using the formula Eq. 1 $\alpha vis = (0.5621R + 0.1479G + 0.2512B - 0.0015)/256$ (Wang et al., 2016). Remote sensing data were processed in R environment using 'raster' package for image processing and the 'base' package for significant tests (t-test at a significance level α=0.05), graphs and boxplots visualization (R Core Team, 2013).

Table 5.1. Sites sampled in the Judean Desert, their coordinate's location (UTM zone WGS84), and sampling method/parameters.

Site	Footpath name	Sample name	Easting	Northing	Bulk samples depths	Micromorphological Samples Depth
Zeelim Wadi Modern recreational trail (surrounding slope angle <10)	Modern footpath	Modern footpath (on a plane) Modern F	35.35175931°	31.35166544°	0-5 cm, 5-10 cm, 10-15 cm	0-10 cm at the footpath's centre
		Modern control (on a plane) Modern C	35.35176387°	31.35165660°	0-5 cm, 5-10 cm, 10-15 cm	0-10cm deep - 4 meter off the footpath
Zeelim Wadi Modern recreational trail on		Modern footpath (on a hillslope)	35.3520385°	31.3520789°	0-5 cm, 5-10 cm	None – path structure likely altered for accessibility

hillslope-(surrounding slope angle >20°)		Modern control (on a hillslope)	35.35213670°	31.35215208°	0-5 cm, 5-10 cm	None – path structure likely altered for accessibility
Zeelim Wadi Roman footpath on plane – (surrounding slope angle <10°)	Roman footpath	Roman footpath (on a plane) Roman F (1)	35.35889727°	31.34908704°	0-5 cm, 5-10 cm	0-10cm at the footpath's center
		Roman control (on a plane) Roman C (1)	35.35882316°	31.34918540°	0-5 cm, 5-10 cm	0-10 cm, 1 meter off the footpath
Zeelim Wadi Roman attributed footpath on hillslope (surrounding slope angle >20°)		Roman footpath (on a hillslope) Roman F (2)	35.36418741°	31.35092990°	0-5 cm, 5-10 cm, 10-15 cm	0-10 cm at the footpath's center
		Roman control (on a hillslope) Roman C (2)	35.36415034°	31.35094688°	0-5 cm, 5-10 cm, 10-15 cm	0-10 cm, 1 meter off the footpath
Maale Zohar Early Bronze attributed footpath – under saddle	Early Bronze footpath	Early Bronze footpath 1 EB F (1)	35.34729954°	31.14631249°	0-5 cm, 5-10 cm, 10-15 cm	0-10 cm at the footpath's center
		Early Bronze control 1 EB C (1)	35.34732569°	31.14629184°	0-5 cm, 5-10 cm, 10-15 cm	0-10 cm, 1 meter off the footpath
Maale Zohar Early Bronze attributed footpath at hill slope		Early Bronze footpath 2 EB F (2)	35.34720145°	31.14619651°	0-5 cm, 5-10 cm, 10-15 cm	0-10 cm at the footpath's center
		Early Bronze control 2 EB C (2)	35.34717363°	31.14617519°	0-5 cm, 5-10 cm, 10-15 cm	0-10 cm, 1 meter off the footpath

Laboratory analysis

Undisturbed block samples for micromorphological analysis (n=10) were impregnated, cut and ground to 30µm thick, thin sections (7x5 cm) at the MKfactory in Stahnsdorf, Germany. Thin sections were started from the top down of the samples, so they include the recent surface.

Analysis of the slides was performed using four magnification ranges (x25, x100, x200 and x400) in oblique incident plane- and cross-polarized light (OIL, PPL, and XPL) on a Zeiss polarizing microscope following standard micromorphological procedures (Stoops, 2021, Verrecchia and Trombino, 2021b). To characterize porosity we used optical digitalized void analysis (Pires et al., 2009a, Rasa et al., 2012b). Images were taken at 1 cm intervals starting at 0.1 cm below surface reaching 5 cm below surface (n=6 depths). At each depth, using x25 magnification, a triplicate was taken (n=18 per MM slide). The resulting images were then processed using imager' package in R environment (R Core Team, 2013) where void cover was automatically assessed. The resulting data indicate the relative porosity of each image (Nir et al., 2022).

For sedimentary analysis, bulk samples were dried at 105° C in a drying cabinet and aggregates were disintegrated using a porcelain mortar. Samples were sieved into coarse (Ø >2mm) and fine material (Ø ≤ 2mm). The Ø ≤ 2mm fraction was further measured using a LS 13320 PIDS Beckmann Coulter Laser particle size analyser to obtain the grain size distributions. The Ø ≤ 2mm fraction was additionally used for further geochemical and mineralogical analyses (n=60). The respective sample preparation and measurement steps were conducted according to previously published workflows (Nykamp et al. 2020; Kirsten et al. 2021). Measurement of the electrical conductivity (µS cm−1) and pH values of the water saturated samples (n=50) was determined in a 1:2.5 solution of 10 g of air-dried sediment and 25 ml of bi-distilled water, using handheld electrical conductivity and pH (with a resolution of 0.1) meters accordingly (Hanna Instruments). Total carbon (TC) was determined using a LECO Truspec CHN and an add-on elemental analyzer (n=50). Total Organic Carbon (TOC) was measured following CaCO3 dissolution using katalytic oxidation at 680° C and subsequent Non-Dispersive Infra-Red detection using a TOC-L Shimadzu device (n=50). Mineralogical X-Ray Diffraction (XRD) values were determined inserting flat-surfaced samples on metal pellets into a Rigaku Mini-flex 600 X-Ray Diffractometer (n=15). Elemental analysis was carried out using the p-ED-XRF (portable energy-dispersive X-ray fluorescence) analyzer Thermo scientific Niton XLt3. Each XRF sample was placed in plastic cups and sealed with a mylar foil (0.4 µm). The prepared sample-cups were placed on the p-ED-XRF and measured for 120 seconds with different filters for detecting specific elements (n=60). Measurements included four known reference standards (RF3, RF25, RF87, RF89) measured prior to and following sample measurements, for device error assessment and calibration. Further elemental analysis was conducted using Inductively Coupled Plasma- Optical Emission Spectrometry (ICP-OES) following digestion in aqua regia (HNO3 + 3 HCl). ICP-OES measurements were conducted

in the Julius Kuhn Institute (JKI) Berlin (n=50). Measurements included three references materials and a black sample. Color bands values were obtained using Minolta Portable Spectrophotometer CM-2600d. A triplicate was measured for each sample under three different runs of the instrument which included white and room light measurements for calibration. The data was further normalized dividing each color band by the total RGB sum and placed on logarithmic ratio in R environment (R Core Team, 2013).

5.5 Results

Field observations

Modern footpath (Zeelim Wadi)

The part of the modern footpath examined, includes segment where the footpath is descending on a south facing slope of ca. >15º ('hillslope'), from a plateau like area (in Pleistocene floodplain and colluvial deposits), towards a lower plane area of ca. <5º inclination ('plane'), one that is truncated by the current Zeelim channel (table 1). The examined segment of the path on the hillslope is ca. 80 m long, while on the plane area the examined footpath segment is ca. 150 m long. The non-path areas were generally occupied by large (ca. 10-80 cm Ø), dark brown (dust and bacterial cover), angular boulders. These boulders were sparsely dispersed and in the areas between them, homogeneous fine material was present. The ca. 0.5 - 1 m wide (table 2) footpath surface is covered with subrounded limestone and chert boulders and large pebbles (ca. 5-30 cm Ø) within and overlaying compacted fine sands and silt (table 2, Figure 5.3). At some locations along the plane, the path is ca. 2-4 cm deeper than its surrounding (i.e., sunken). One minor gully (10-50 cm deep and 1 m wide) evolves directly below the path at the hillslope (>15º) segment (Figure 5.3b).

Roman footpath (Zeelim Wadi)

The Roman footpath is similarly compiled of two segments, running on a hillslope (>15º) and on a plane (<5º) area, ca. 1 km southeast of the modern footpath sampling point (Table 1). On the hillslope, the footpath runs for approximately 200 m (ca. 1 m wide) semi diagonal along a south facing slope in NE-SW direction and descends south westwards to a lower Pleistocene terrace plane area. On the plane, the footpath runs for 450 m; here the footpath is generally ca. 5 m wide and at parts it is marked by a line of >20 cm curbstones on both sides (See Figure 5.2). The path occasionally crosses gullies, 1-2 m deep, functioning as first to second order ephemeral streams. As it continues southwest, at one of its better-preserved areas, the path is abruptly truncated by a > 7 m deep incision of the active stream cutting into its own deposits (supplementary Figure 5.1). The areas adjacent to the path are covered by boulders (ca. 6-40

cm Ø) and shrubs, while boulders lying on the paths generally show sizes of ca. 3-20 cm Ø and are not accompanied by vegetation.

Early Bronze Age footpath (Zohar Ascent)

The Early Bronze age (EBA) footpath stretches on mostly bare bedrock from northwest and crosses a watershed line through a saddle. In the current study, the footpath was examined where it crosses the saddle and continues to run on the east facing hillslope (Table 1). The footpath is ca. 1 m wide and 75 m long in the sampling area. Under the saddle, it is composed of ca. 3 broken segments of ca. 10 m long paths. These path segments descend semi perpendicular to the slope on bare rock and patches of sediments. Some of these segments had coarse and fine grains cemented together in a 'breccia-like' surface. From the area below the saddle, on the southeast facing hillslope, an officially marked modern trail, which does not show intense usage, continues to the northeast. A second segment of the path continues to the southwest on the hillslope. On the latter segment, as the path runs perpendicular to the slope, a gully evolves directly from the surface of the footpath. The footpath surface is covered with subangular pebbles (ca. 5-60 cm Ø) within sands and silt (supplementary table 1). Poorly sorted debris of angular rock fragments reaching up to boulders sizes cover most of the non-path surface while silt-fine sands occupy the areas between the boulders (figures 2C and 3C).

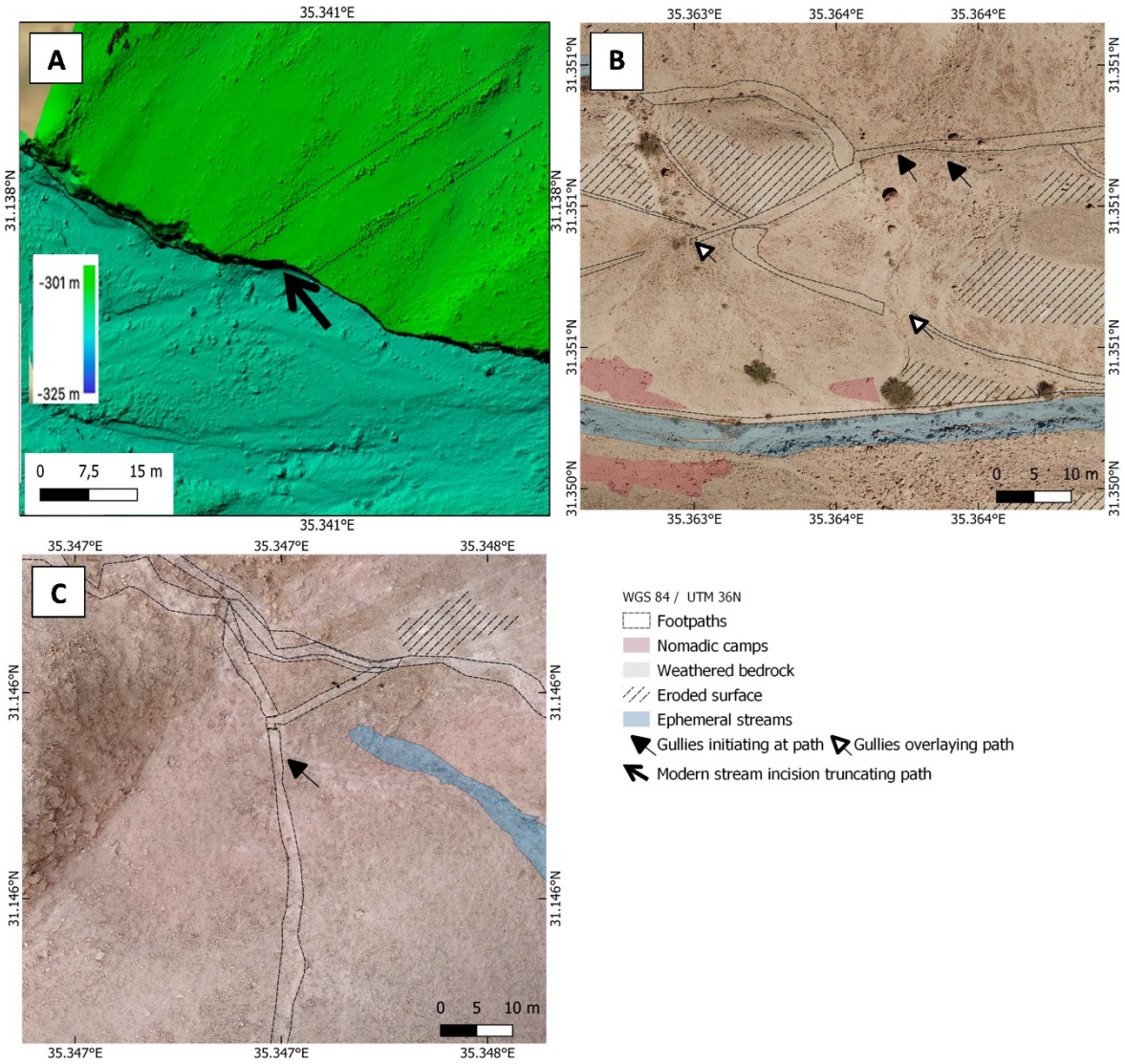

Figure 5.3. UAV image of selected geomorphological features on the archaeologically attributed footpaths. A. DEM of the Roman path on the plane. Notice the ca. 7m deep truncation by the active stream marked by the black arrow and the curbstones arranged to the sides of the path. B. Orthophoto image of the Roman path segment on the hillslope. Notice gully fan covering the path's course. C. Orthophoto image of the Early Bronze Age footpath. Notice the gully initiating directly below the path.

Surface penetration resistance was measured for footpaths (n=22) and for non-paths areas (on both sides of the footpaths, n=22). Results show footpath surfaces hold significantly higher resistance than non-footpath surfaces (t test $p<0.05$, supplementary table 2, supplementary Figure 5.1). Additionally, the two footpaths attributed to archaeological periods (Early Bronze Age and Roman period) were mapped for their main geomorphological attributes (Figure 5.3).

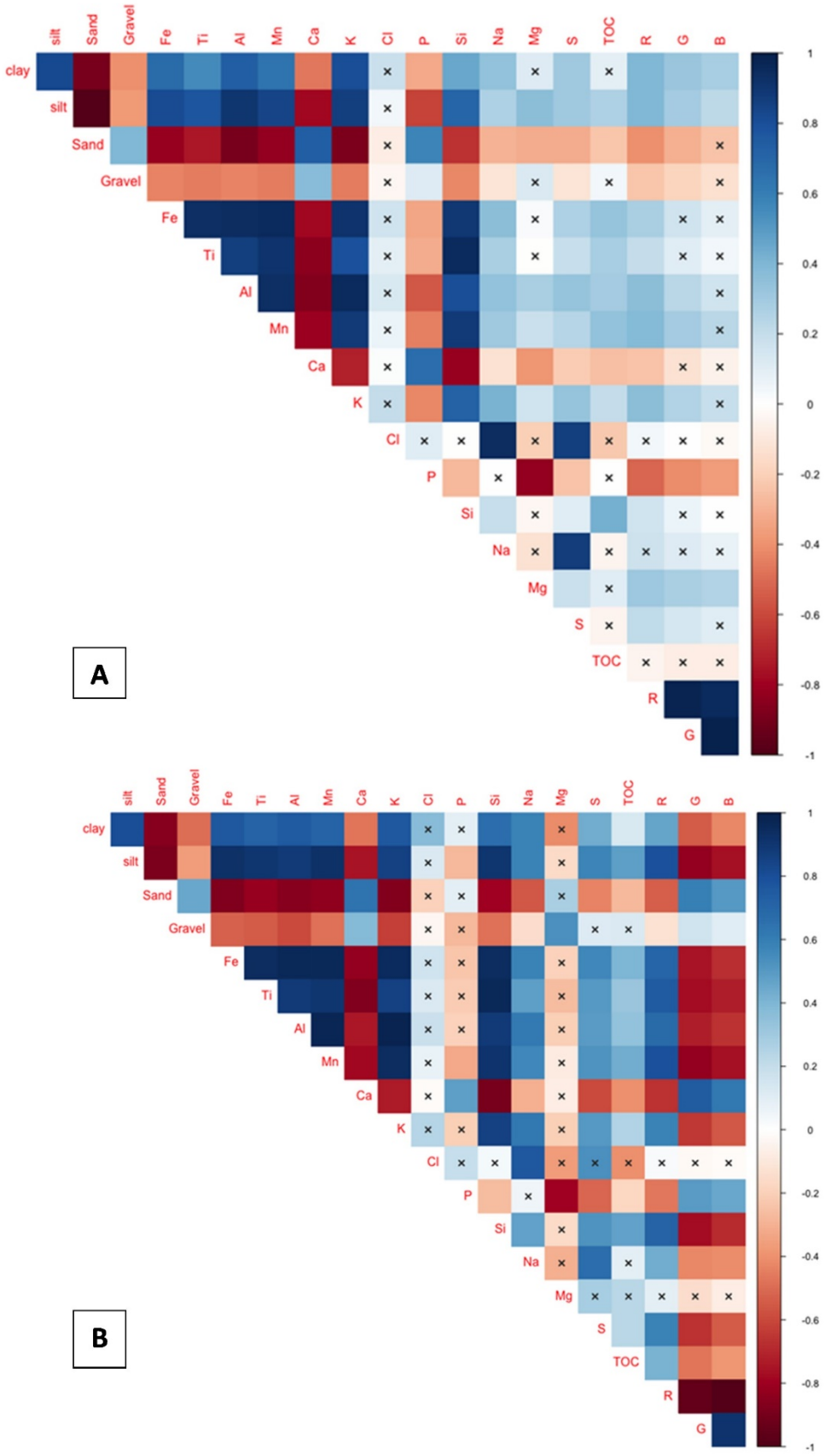

Figure 5.4. Correlation analysis (R 'corrplot' package) between various sedimentary data for A. all samples and B. surface samples (n=50 and n=20 accordingly). X marks insignificant correlation (p>0.01). Positive correlations

are marked in blue (max=1) while negative ones are marked in red (max=-1). Grain sizes were assessed using a Coulter Laser particle size analyzer while elemental data was obtained using ICP-OES following digestion in aqua regia (HNO3 + 3 HCl), apart from Cl which was measured in p-ED-XRF. Gravels were calculated by weight based on sieving. TOC was directly measured using Non-Dispersive Infra-Red detection. Color bands values were obtained using a Minolta Portable Spectrophotometer.

Sedimentary analysis

Sedimentary analysis for all surface (0-5 cm) and subsurface (5-15 cm) samples (n=50) finer grain sizes (silt and clay) shows the dominance of Ca and Si in all samples (supplementary Figure 5.2). All samples fall into the category of sandy loam, although in the modern footpath samples, silt was more abundant on the surface (0-5 cm) than on the subsurface (5-15) while for the archaeological footpaths this difference was not evident. The finer fraction tends to positively correlate with Fe, Ti, Al and Mn (figure 4). Contrastingly, Ca concentrations are positively correlated with the occurrence of sand fraction and negatively to the occurrence of the silt fraction. Sodium and chloride and sulfur are strongly correlated with each other, although Na and Cl occur in low concentrations (supplementary Figure 5.2). Spectral data referring to the RGB color space do not show strong relationships to any of the elements or grain sizes looking at the total samples (n=50) although for the surface samples some correlation is evident. Within all surface samples (n=20), red band values are positively correlated with silt, Mn and Si, and negatively correlated with Ca; while green and blue bands values show a mirror image (Figure 5.4).

Micromorphology

Similar mineralogical composition, originating from the exposed weathered bedrock and soil surfaces, is evident in all samples (Figure 5.4). Particularly abundant are carbonate minerals (e.g., calcite), rock fragments (limestone, dolomite, shells) and silicates (chert, quartz). For the **Modern footpath**, the control sample (from outside the path) shows silty-clayey crumbs in its upper 1 mm that are absent from the footpath sample (Figure 5.5). For the uppermost 2 cm, the modern footpath sample contains more fine grains (silt, clay) than at its control sample, although both samples share a generally massive microstructure. Therefore, although both control and footpath samples present complex packing voids, in the footpath samples much of the void space is filled by the finer fraction (silt-clay). In consequence, the micromorphology sample from the modern footpath is matrix supported, while its control sample is grain supported (Figure 5.5 and supplementary table 2). Light grey fine grained biogenic cementation, with rounded and irregular borders, were evident at the control sample of the

modern footpath, at times these features were occupied by vesicular voids (Figure 5.8A). Both macro and microscopically, in the modern footpath sample, a clear contact is evident at 4 cm below the surface. At the this depth, a ca. 0.7 cm thick bedding is observed and below it sands and gravels appear in a grain supported matrix. In the control sample, such bedding and clear contact is absent and large sands and gravels dominate throughout the profile (Figure 5.5 scanned images).

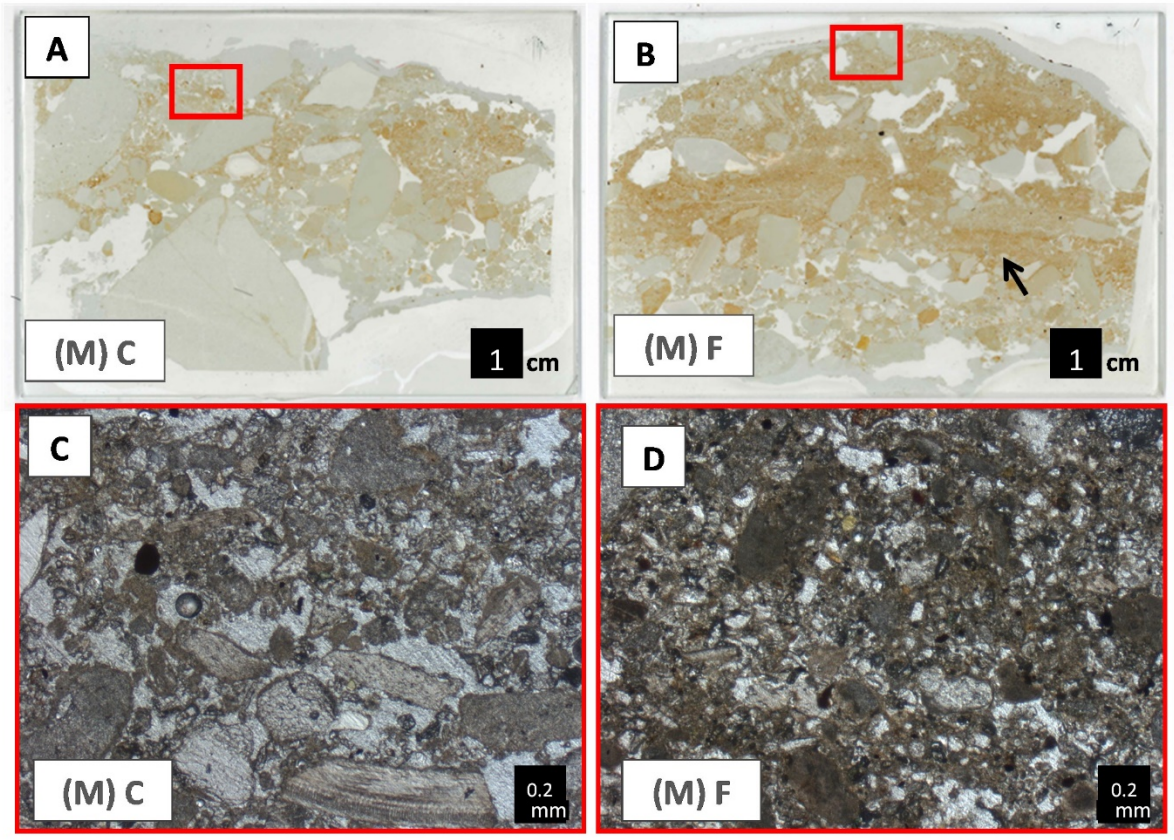

Figure 5.5. Scanned images of the micromorphological slides and microphotographs of the Modern footpath (M). A. Showing non-path control (M) C sample and B. The footpath (M) F sample with red boxes indicating the location of microphotographs in C. Control (C) Sample micrograph and D. Footpath (F) sample micrograph . Notice the large sand and gravels dominating the control sample scanned image and open microstructure observed in the control micrograph. This stands in contrast to the dominance of fine fraction (silt and clay) in the footpath scanned image and the closed massive microstructure seen in the footpath micrograph. Note also a clear contact between the upper, matrix supported, and lower grain supported layers (marked with an arrow) in the scanned image of the modern footpath.

The footpath attributed to the Roman period was sampled both on a (1) plane (Figure 5.6) and a (2) hillslope (Figure 5.7) area. For the upper 1 cm of the footpath located on the plane, **Roman footpath (1)**, the control sample has an open aggregated structure while inside the footpath we observed localized micritic cementation, comparably smaller aggregates and a closed-complex microstructure (figures 6a-d and 8a). Interestingly in the control sample, at 3 cm below surface,

a ca. 1 cm thick, horizontal silty-clay microlayer is present (figures 6a and 8b). Below this microlayer is a clear contact with bedded sediments, where fine and coarse layers with open and closed structures are interchanging. Neither the 1 cm thick fine microlayer, nor such bedding, were observed in the footpath sample (Figure 5.6a-b and supplementary table 2). At 2 cm depth, the plane Roman footpath (1) contains small clay aggregates and sand grains with some clay illuviation between the sand grains and generally obseverd porosity in the slide is decreasing with depth (supplementary table 2).

At the hillslope area, **Roman footpath (2)**, a slightly different pattern concerning the general microstructure appears. At the control sample, the upper 1 cm contains few aggregates in an open microstructure (figures 6e and 6g).. The footpath sample presents an enaulic to gefuric microstructure, similar to the control sample. One difference between the control and the foootpath two is the more homogenous distribution of silts and clays in the upper 3 cm of the footpath sample while they have more aggregated appearance in the control sample. Another difference lies in the degree of bioturbation. The footpath shows less developed bioturbation features while the control sample contains a fine 0.7 cm thick horizon with planes, channels and vesicles. The planes could also be slacking crusts resulting from trapped air (Figure 5.8c). A third difference between the footpath and control samples lies in the orientation of large grains. In the hillslope footpath, large (size) elongated grains show a sub-horizontal orientation that generally follows the slope. In the control sample of the Roman footpath (2), however, there is no distinct orientation (Figure 5.6 E and F).

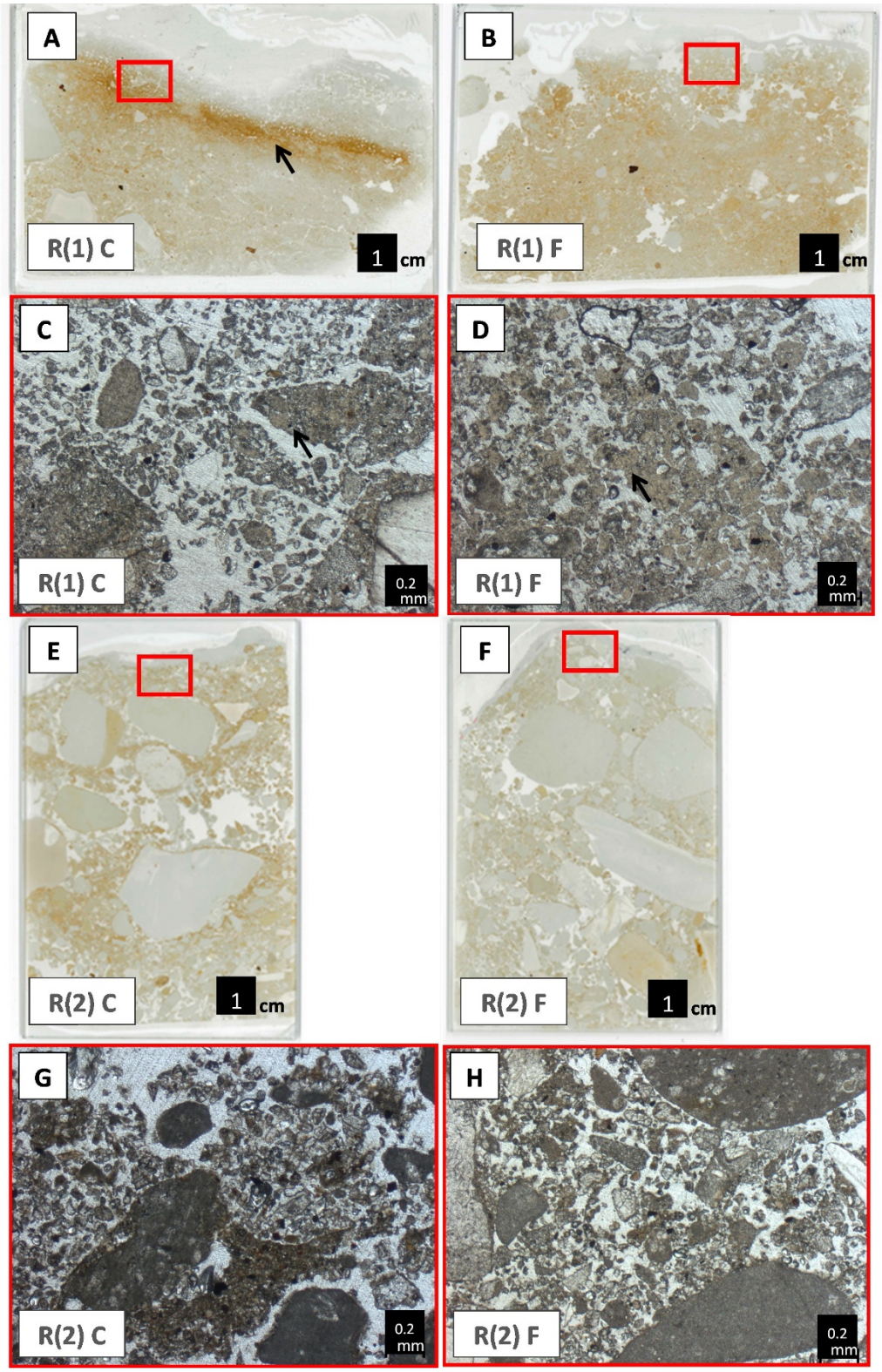

Figure 5.6. Scanned images of the micromorphological slides and microphotographs of the Roman path on the plane area R(1); A. Non-footpath control. Note the silty-clayey layer marked by an arrow. B. Footpath sample. Micrograph images (microphotograph location is marked on the slide by a red box) of Roman Footpath R(1); C. Control sample. D. Footpath sample. Notice aggregates in figure C and cementation in figure D are marked with arrows. Scanned images of the micromorphological slides of the Roman path on the hillslope area R(2); E. Non-footpath control. F. Footpath sample. Micrograph images (microphotograph location is marked on the slide) of

Roman Footpath R(2); G. Control sample includes one large clayey-silty aggregate at the lower part of the micrograph with a semi rounded contact to the fine sand size minerals directly above it. H. Footpath sample includes different sands sized minerals and no indication of bioturbation or cementation.

The footpath associated to the Early Bronze Age is located close to the watershed line. The footpath was sampled in two locations on the south facing slope, both with steep slope angles (>15°). The first Early Bronze footpath segment was sampled directly below the saddle (EB footpath (1), while the second was sampled on the hillslope (EB footpath (2). For **EB footpath (1)**, the control sample has a chitonic to open porphyric coarse to fine (c/f) related distribution, in a complex microstructure, with few coarse gravels at 0.1 cm below surface (Figure 5.7c). Similarly the footpath shows at 0.1 cm a chitonic to closed porphyric c/f related distribution in a massive microstructure, but it is more compacted with individual voids being smallercompared to the control,. Additionally, the control sample exhibited changes in grain size and micro facies along the examined depth (ca. 5 cm), unlike the footpath sample, where the microstructure remains similar throughout the slide (Figure 5.7b, supplementary table 2) apart from a minor increase in porosity and clay aggregation with increasing depth. Another difference between the footpath and the control samples is the grain size. In the control large sand grains dominate over common silts and clay until a depth of 7 cm below surface when it changes to fine sands. In the footpath the fine (silt and clay) fraction is always dominant at these depths.

For the samples on the hillslope, **EB footpath (2)**, a different pattern emerges (Figure 5.7e-h). Both footpath and control samples exhibit grey calcific matrix and biogenic activity related voids (figures 8d and 8f), although the calcitic crystallitic matrix is more dominant in the control sample. A clayey Fe rich, 1-7 mm thick, *in situ* slacking crusts is apparent in all EB footpaths' samples, although they are observed more often in the control samples of EB footpath (1) and footpath sample of EB footpath (2) (figures 5.7C and). However, under the footpath, the crusts are more common, better preserved, and show greater disturbance by pressure from the surface. For the 0-2 cm below surface, the control sample of EB 2? is dominated by biogenic-calcitic cementing material with a enaulic to chitonic c/f related distribution while large voids as well as very large gravels are abundant. The EB 2 footpath shows a different microstructure than its control. In the upper 2 cm it is supported by a calcitic fine fraction (clay-silt), which is dissimilar to the bio-calcitic cementobserved in the control, with a c/f distribution of closed porphyric. Additionally, the massive microstructure at the EB footpath (2) sample is more compacted than that of the control sample where it is slightly more open with channels and planes. Below 2 cm, both EB (2) footpath and control samples have

changes in microstructures resulting in several different units, with the footpath showing higher variability between its units, including open microstructures and slacking crusts (Figure 5.7e-h), while the control shows XYZ.

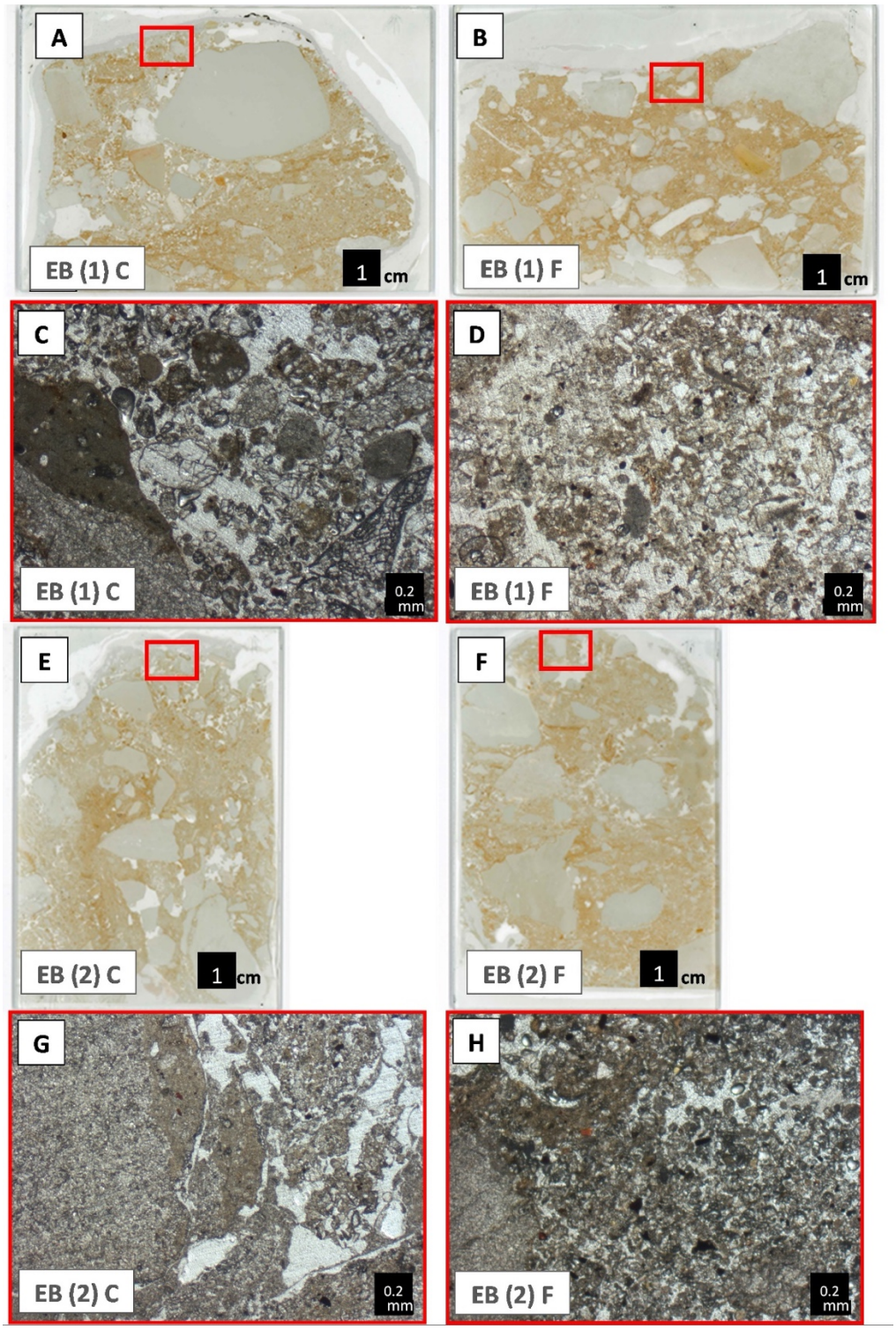

Figure 5.7. Scanned images of the micromorphological slides and microphotographs of the Early Bronze Age footpath directly below the saddle area EB(1); A. Non-footpath control. Notice the pebble and the gravels following the slope angle while below these are fine grained sediments a common observed structure for non footpath areas. B. Footpath sample. Notice the distribution of fine gravels throughout the slide and the preserved

slope angel. Micrograph images (micrograph location is marked on the slide) of Early Bronze Age Footpath EB(1); C. Control sample with rounded medium and large sands and the three different grains sizes in a dominating grey calcitic matrix. D. Footpath sample. Notice the massive microstructure and the brown-dark organic features and metal oxides distributed throughout . Scanned images of the micromorphological slides of the Early Bronze Age path on the hillslope area EB(2); E. Non-footpath control. Notice the concentrations of gravels on the surface similar to the control sample of EB(1). F. Footpath sample. Notice the well preserved but truncated slack crusts. Micrograph images (micrograph location is marked on the slide) of Roman Footpath EB(2); G. Control sample. Notice the large gravel and calcitic cementing material with fine sands and an unusual void structure with calcitic (quasi)coatings. H. Footpath sample. Notice the massive microstructure and the brown-dark organic features and metal oxides distributed throughout the micrograph.

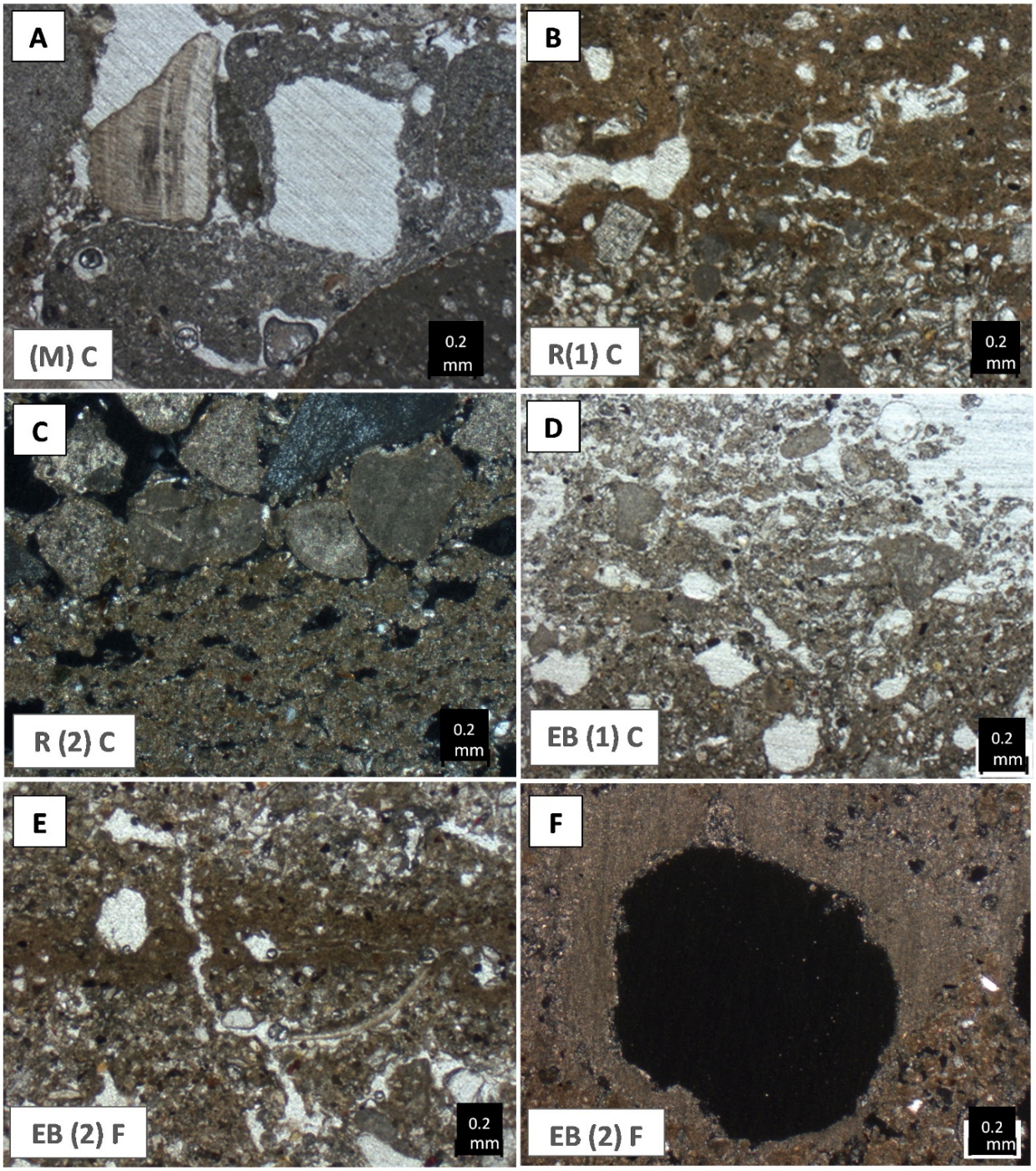

Figure 5.8. Microphotographs showing biogenic activities on the different footpaths' samples. A. Modern footpath (M) control (C) sample (PPL) with calcific biogenic cement with irregular rounded edges (mosses-lichen). B. Roman footpath (R(1)) sample (PPL) with planes. C. Roman footpath (R(2)) sample (XPL) with vesiclse in calcific biogenic matrix. D. Early Bronze Age footpath (EB (1)) sample (PPL) showing channels and interconnected vesicles in calcitic and clay matrix. E. Early Bronze Age footpath (EB (2)) sample (PPL) showing channel and vertical plane in a slacking crust. F. Early Bronze footpath (EB (2)) sample (XPL) showing the cross section of a large channel with a calcareous hypocoating .

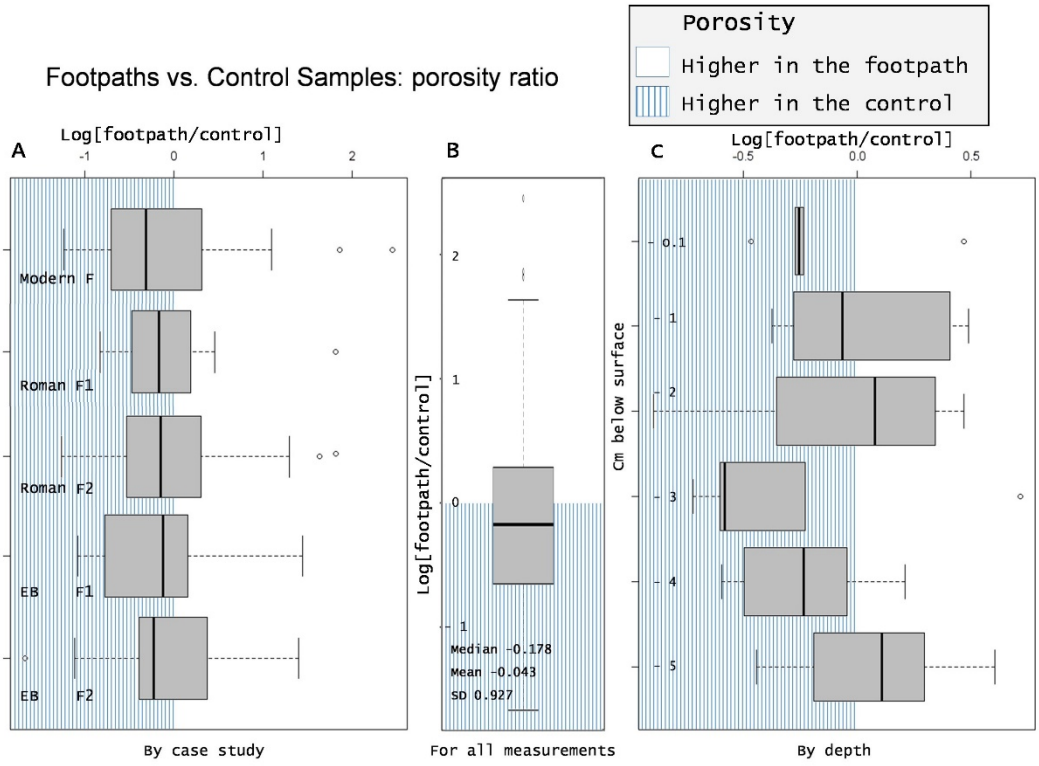

Figure 5.9. Porosity ratios of footpaths and their corresponding control samples (log(footpath/control) along 5 cm for each micromorphological slide. Presented according to A. The individual paths, B. Combined and C. Depth (n=180, $p>0.05$).

Micromorphological sub-surface samples (0-5 cm) extracted from footpaths in the Judean Desert, tend to be less porous than their respective control samples (Figure 5.9b). This is especially true for the uppermost 0.1 cm where all footpaths are less puros ($p<0.05$) than their controls samples (Figure 5.9c). The modern footpath sample shows the lowest porosity of all case studies compared with its control sample, especially for the upper 3 cm below surface. Deeper than 3 cm, the modern footpath's control sample is less porous than the footpath sample. For all samples, variations along depth in the relative porosity between footpath and control samples, are observed and are also partly responsible for the variability within each footpath while incorporating the entire 5 cm (Figure 5.9a). A trend of relative increased porosity in the control samples along depth is evident between 0.1-2 cm and then again between 3-5 cm below surface (Figure 5.9c).

Color values

Color measurements of the fine fraction (<2mm) using the CIELAB color space (D65 European midday standards) show consistent difference between footpaths and their control samples

(Figure 5.10). It is evident that footpaths have brighter color value and higher values for the green and blue bands than their controls (Figure 5.10A). Differences of the blue spectrum values between samples extracted from footpaths and their control samples are significant ($p<0.05$) while the green are insignificantly different between footpath and non-footpath areas ($p>0.05$). Additionally, three sections were mapped using UAV orthophoto image to extract the RGB signature of the footpaths and their neighboring areas; Roman footpath (1) situated on the plane topography, Roman footpath (2), its continuation on the hillslope, and the Early Bronze footpath segment. The extracted RGB values from triplicate lines marked on the footpaths show higher RGB values than the same lines placed ca. 1 m on both sides of the paths (Figure 5.10B). Based on the RGB values, albedo values were calculated to assess possible reflection effect of the footpaths. There are higher albedo values on the surfaces of the footpaths compared to the non-path control areas (Figure 5.10). This difference is relatively small with a median of +2.7% and with a highest difference value lying at +5.7% for the EB footpath, however it is significant ($P<0.05$).

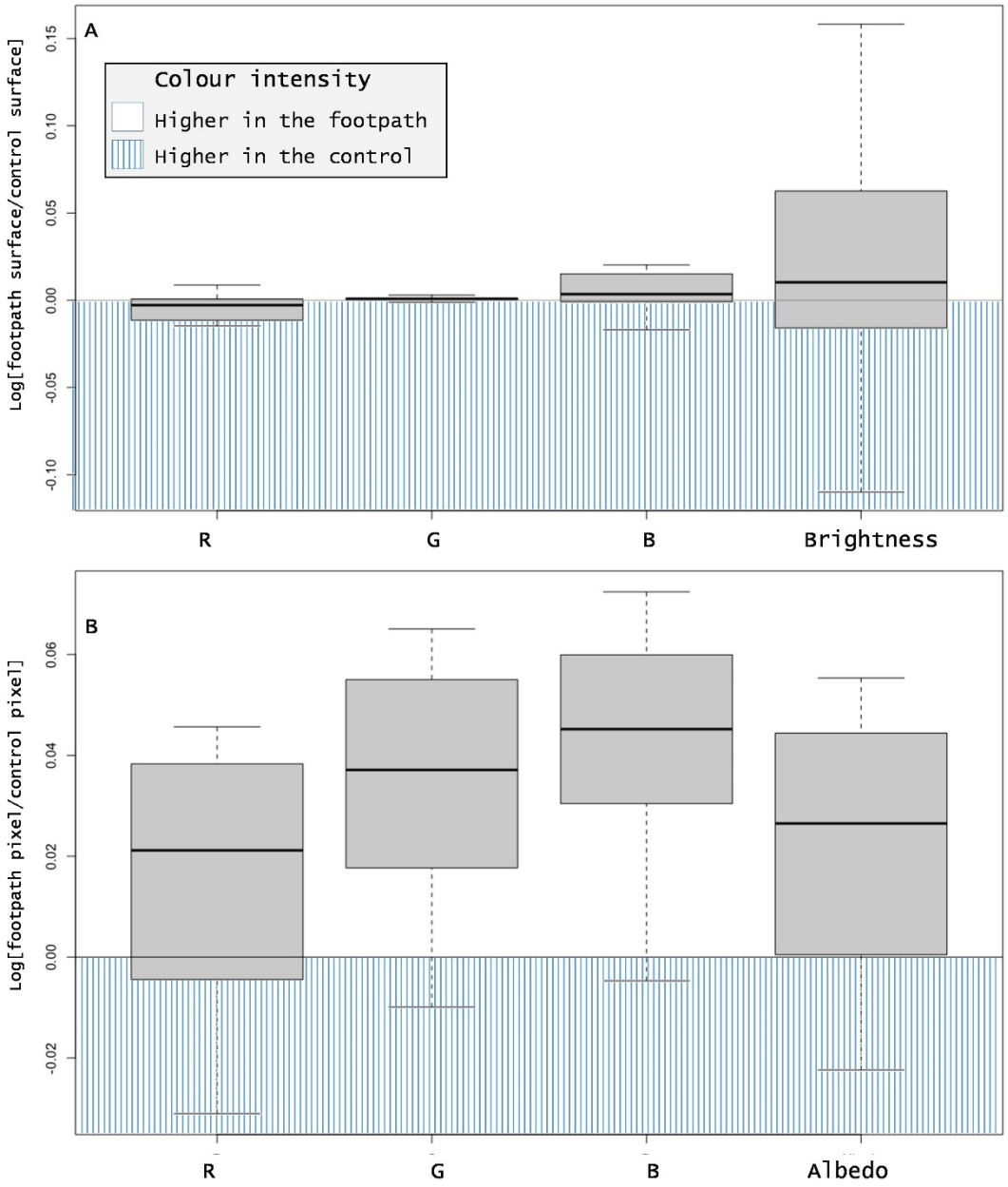

Figure 5.10. Color evaluations of two archaeological and one recently used footpaths plotted against their corresponding non-path areas in logarothmic scale. The median avarage is marked by a black horizontal line within the boxplot. A. RGB (Red, Green, Blue) and brightness values of the fine fraction (<2mm) originating from footpaths (n=30) vs. its respective control samples (n=30). B. RGB and calculated albedo orthophoto values originating from footpaths vs. its respective control samples (each n>10000 pixels). Notice both brightness ($p>0.05$) and albedo ($p<0.05$) values are higher on the footpath surfaces than on the non-path areas.

5.6 Discussion

Establishing long-term used footpaths

The Early Bronze Age and the Roman period are regarded here as dominant phases within the lifespan of the two archaeologically attributed footpaths. Subsequently, any later (including

recent) use of these trails could not be excluded, as recurrent use of existing trail systems is a well know phenomena (Jackson, 1994). Geomorphologically, the relative antiquity of the footpaths could be assessed through the interaction between linear soil erosion and the location of trails. On the plane area of the Wadi Zeelim, the current stream bed truncates the Roman footpath (1), indicating the path predates the current riverbed configuration (Figure 5.3). It is worth noticing that in the Judean Desert, within areas that are no longer fluvially active, such as hillslopes and elevated planes, certain pedogenic and fluvial processes are minimal, at times allowing better preservation of archaeological remains. In contrast, active Wadie riverbeds in the Judean Desert can quickly incise and undercut the sedimentary accumulation due to the high surface runoff and the subsequently intense floodings events, as well as the decline in the levels of the Dead Sea (Lisker et al., 2010, Cohen and Laronne, 2005, Zituni et al., 2021). Similarly, on the hillslope area of the Zeelim Wadi some gullies and rills, or their outlets, overlie parts of Roman footpath (2), suggesting the latter predates the formers (Figure 5.3). Hence, these features imply a minimal recent use of the Roman footpath. The attribution of these trails to the different archaeological periods are based on surface finds and affiliated archaeological sites, rather than on absolute dating (Yekutieli, 2005, Davidovich, 2014). The latter is challenging outside archaeological sites both due to the limited datable sub-surface material in arid environments, as well as due to the interpretation of such materials as part of the early use of a footpath (Langgut et al., 2014, Nir et al., 2021). Therefore, we consider these two footpaths to be under long-term use during the Holocene, rather than proclaiming their absolute formation only for the specified archaeological periods.

Geomorphological and pedogenic effects

From a mechanical perspective, similar to pathways and footpaths in other regions, footpath in the Judean Desert tend to show higher penetration resistance and lower porosity than non-path controls (Sherman et al., 2019a, Nir et al., 2022). Due to the lower porosity and higher surface runoff, footpaths can promote different types of soil erosion (Buchwał and Rogowski, 2010b). Analyzing recreational trails, it has been documented that soil characteristics are effected by trampling and that erosion along the footpaths is promoted (Pounder, 1985, Fonseca Filho et al., 2018). In the Judean Desert, surface runoff causes gullies to initiate directly downslope from a footpath in both the Roman (2) and the EB (2) footpaths segments, located on slopes (Figure 5.2). Therefore footpaths, similar to pathways, and both unarmored and paved roads, promote gully erosion downslope from the used surface (Brandolini et al., 2006, Buchwał and Rogowski, 2010a, Salesa and Cerdà, 2020, Sidle et al., 2019, Sidle et al., 2004, Wagenbrenner

et al., 2015, Wimpey and Marion, 2010, Nyssen et al., 2002, Zgłobicki et al., 2021). Nir et al (2022) report that recent and long-termed used footpaths in sub-humid and temperate environments exhibited inhibited soil formation and that their use as footpaths results in microstructural evidence in the subsurface, i.e., lower porosity and higher pedogenic Fe oxides than in the non-path (Nir et al., 2022). However, while footpaths subsurface porosity in the temperate environment is relatively lower through a 3 cm depth, in the Judean Desert, footpaths showed distinct and consistent lower porosity only for the upper 0.1 cm (Figure 5.9). Both temperate and arid environments' footpath studies are of a preliminary and qualitative nature, examining different tools, and therefore sample sizes and depths are constrained. However, if the observed differences in footpath porosity ratios between temperate and arid environments are genuine, one explanation for that could be attributed to trampling on a wet surface in the more humid zones (Pietola et al., 2005, Nawaz et al., 2016) Nir et al 2022. The latter can result in higher compaction and lower porosity as opposed to the effect of trampling within a dry environment reported here. Interestingly, at 3 cm below surface, the lower porosity under footpaths re-emerges. The latter could be the result of soil formation activities or dust trapping in the non-path controls, forming aggregates with voids at a 3 cm depth, that do not occur under the footpaths (Figure 5.8). Depending on salinity, temperature and moisture, aggregates and soil crusts in lithosols and regolith soils can form. The typical biological agents responsible for soils crusts forming in the Judean desert are cyanobacteria, fungi, and lichens (Steinberger et al., 1999, Singer, 2007, Galun and Garty, 2001). As evident though micromorphology, footpath samples generally present lower amounts of aggregates which are also smaller in size than their respective control samples (figures 6 and 7), suggesting soil forming hindrance here, similar to the effect of footpaths in other climatic zones (Nir et al., 2022, Cole, 2004). Additionally, the light grey filamentous material (clacitic cementation), present in most of the non-path control samples but rarely under footpaths, is calcific bio-cementation, resulting from a combination of the regionally common micro-organisms, mosses, lichen and cyanobacteria (Wierzchos et al., 2006, Williams et al., 2012, Galun and Garty, 2001, Issa et al., 1999). Reduced bioturbation due to footpath formation and trampling were previously recorded under both subarctic and arid climates (Sherman et al., 2019a, Chenhao et al., 2019). However, in the long-term used trails studied (affiliated with the EBA and Roman period) the hindering of soil formation processes is not straight forward. Evidence of bio-cementation was recorded at one EBA attributed footpath sample, while aggregation was seen at one Roman and one EBA footpath samples (figures 5 and 6). However, the observed aggregates at the Roman footpath (1) sample were smaller and less developed than the aggregates at the non-path control,

suggesting lower soil formation stability i.e., regularly occurring humidity (Stoops, 2021, Lavee et al., 1996, Lavee et al., 1989). For the EB footpath (2), aggregation was evident at 5 cm depths implying the aggregates could be the results of surface formation prior to being used as a footpath and that these 5 cm incorporate the accumulation of the currant trail's surface. Alternately, in the case the EBA path was abandoned for several millennia, as suggested by routes used during later periods, the process involving water saturation and bacterial activity could have been re-established (Yekutieli, 2006, Davidovich, 2014, Cole, 1990). Both scenarios explaining the changes in aggregation should be taken cautiously as the stratigraphy of 5-10 cm evident from four micromorphological samples should not be over interpreted. The resulting micro-facies in the EBA footpath sample differ from those of the non-footpaths control, indicating a difference is still evident and distinguishable (figures 5-7). An important constrain on our understanding of past traila lies in the interpretation of abandoned ancient footpaths as opposed to currently used footpaths. It should be considered that less frequently used modern footpaths (the studied footpath is used daily during several seasons), may have similar features as long-term used abandoned footpaths. However, it has been shown that after two dozen events of footpath trampling, the fresh soil crust layers are destroyed (Cole, 1990). This implies that minimally used recent footpath should bare to some extent, similarities to the intensely used trails, if used concurrently.

Color changes

In the Judean Desert, one other interpreted effects of trampling is the abrasion of limestone pebbles, exposing its white-light colors, as evident by the positive correlation between the GB colors and Ca content (Figure 5.4). Both spectrometer measurements of the fine fractions as well as RGB values extracted from the UAV orthophotos, show lighter colors on the footpath than on non-path areas. In both scales, the highest degree of change lies in the blue band (Figure 5.8). This observation could result in 0-5% higher relative brightness or albedo values for the footpaths than for non-paths areas (Figure 5.8B). Such degree of albedo value changes is lower than that caused by vegetation cover for example. In the nearby Sinai arid peninsula, increased vegetation cover decreased the albedo values by 25% (Otterman and Tucker, 1985). For a different arid environment, it was suggested that a 2% increase in albedo values can correspond to ca. 2-3 deg Celsius decrease in surface temperature during spring (Zolotokrylin et al., 2020). Following this, the possible local cooling, resulting from footpaths distributed through the Judean Desert during several millennia, should be not be underestimated (Efrat, 1993). In the arid environment of the southern Levant, soil aggregates stability and crust biological activities

is controlled among other factors by temperature (Lavee et al., 1996). Therefore, higher albedo resulting in the cooling of footpaths surfaces, could be responsible for the observed pedogenic activities increasing bio-cementation and fine aggregates under long-term used footpaths, while they are absent from currently used footpath.

Methods evaluation

Four methods were used in this work in order to identify and assess the environmental effect of ancient and modern footpaths in arid context. It is evident that the sedimentary analysis (i.e., grain size, pH, EC, elemental) alone, has not produced valuable information that can differentiate footpaths from non-footpaths (e.g. supplementary Figure 5.2). However, this could be the result of the 5 cm bulk samples taken and therefore finer sampling strategy such as <1 cm intervals may produce valuable sedimentary data (Giesler and Lundström, 1993, Wells, 2010). Using micromorphology, a general trends of soil formation hindering under all footpaths compared with their controls was observed while archaeological footpaths in particular showed greater variability in this context and perhaps soil recuperation (figures 5-8). However, due to the variability between samples, a larger sample size and detailed spatial sampling are necessary to validate these trends (Croix et al., 2019). Image analysis has long been used in micromorphological context including attempts for assessing the degree of porosity (Arnay et al., 2021, Pires et al., 2009a, Rasa et al., 2012a). Using image analysis in open source R environment to evaluate subsurface porosity has produced a result showing significant reduction of porosity in footpaths samples compared with non-path controls at 0.1 cm below surface alone (Figure 5.9). In more humid environments the lower porosity reached 3cm below surface suggesting this tool could be useful for comparing between environments (Nir et al., 2022). Using UAV and laboratory analysis for assessing color differences between footpaths and non-footpaths (Figure 5.10) is very insightful in particular coupled with sedimentary analysis (Figure 5.4) that was helpful for understanding the process behind some of the differences (Chase et al., 2012). Therefore, using UAV and color analysis is useful for footpaths recognition while detailed micromorphological sampling may evaluate the type of formation and in the right context, depth and modern analogy, whether the path could be long termed used or abandoned.

5.7 Conclusion

In this study, we explored how footpath formation can impact local geomorphological and pedological processes. To this aim, we studied three footpaths in the arid environment of the

Judean Desert of variable temporal context, representing recent and long-term including archaeological use. The interstratification of the footpaths with geomorphological features, resulting for example from gully erosion or river incising, served us as indicators for the antiquity of a trail in concert wth the occurrence of archaeological remains (from different epochs). On the other hand, gullies initiating from footpaths bear witness of the local geomorphological impact of footpaths. Our analysis show a general trend of increased compactness, lower porosity, and brighter colors in the footpaths compared to their immediate surroundings and controls. For the high-resolution UAV data, footpaths have significantly higher albedo value than non-trail surrounding areas. From a temporal perspective, micromorphology was used to try and differentiate between intensively used recent trails and long-term used ones, for a given environment. However, as other processes are involved in crust and soil formations, this differentiation is not straight forward, even for arid environments where pedogenesis is limited when compared with humid zones. Further investigation using UAV and color recognition can be useful to explore the distribution of trails, particularly in arid limestone environment, and possibly quantify the albedo effect trails have on the landscape.

Acknowledgements

We would like to thank Moritz Nykamp and Philipp Hoelzmann from the laboratory for Physical Geography at the Freie Universität Berlin. Continues support was given by Jacob Hardt, Robert Busch and the PhD students and post docs of the Physical Geography working group at FU Berlin. Special thanks to Ruth Shahack Gross from Haifa University and Ariel Malinsky Buller of the Hebrew University of Jerusalem. Studienstiftung des Deutschen Volkes for personal funding during this research period.

Chapter 6

A geosocial interplay of trails and gullies

Nir, N., Knitter, D., Hardt, J. and Schütt, B., 2021.
Human movement and gully erosion: Investigating feedback mechanisms using Frequency Ratio and Least Cost Path analysis in Tigray, Ethiopia.
PloS one, 16(2), p.e0245248.
https://doi.org/10.1371/journal.pone.0245248

Abstract

The cost of human movement, whether expressed in time, effort, or distance, is a function of natural and human related variables. At the same time, human movement itself, whether on land, air or sea, causes environmental cost. We are looking into the long-term environmental relationship of this interplay. Gullies - linear landforms, which dissect the landscape - are considered to be a cost for human movement, as they can form unpassable barriers destroying present path networks. On the other hand, human movement creates pathways, which flatten the surface and decrease the water permeability potential. This process results in runoff generation and possibly gully erosion. Accordingly, the spatial relationship between pathways and gullies is investigated.

In the Tigray region of the Northern Ethiopian Highlands, gullies and pathways were mapped using remote sensing data. Frequency Ratio was used for assessing pathways as a variable affecting the location of gullies while Least Cost Paths were tested to evaluate the possible constraining impact gullies have on mobility. Based on these results, it is concluded that a positive feedback exists between the cost of human movement and gully erosion. We further discuss possible effects gullies may have had on trade, territory, and political affairs in Tigray. Consequently, we suggest that movement cost and gullying may not only hold strictly environmental or movement-related implications, but also socio-cultural ones.

6.1 Introduction

The history of human movement, whether as individuals or in groups, on a daily or migrational scale, is constrained or encouraged by its cost, i.e. stretch of way, and its difficulty, requirements and time (Barbosa-Filho et al. 2018). Decision making processes involving the cost of movement are based on several social, economic, and environmental factors (e.g. Featherstone 1997). The first two of these cost categories, the social and economic constraints on movement, are usually the result of direct human involvement, although at times they origin from natural factors (e.g. global raw materials distribution). In contrast, environmental costs of movement such as distance, climate and topography are not considered as a result of human activities. Investigations of both, natural and socio-economical aspects of cost have been in the focus of several disciplines with geography frequently taking the lead, as early as the 19th century, with 'laws of migration' addressing distance and growing urban areas while at the early 20th century distance and cost based on location of raw material became essential for productivity (Ravenstein 1885, Weber 1929). Later works looked into commute opportunities as a factor affecting employment in cities (e.g. Zipf 1946). Physical distance between individuals, societies and countries still holds great importance and relevance in a modern globalized economy (Ghemawat 2001). This is even more evident when we investigate historic and prehistoric societies (e.g. Liebermann et al. 1993).

Movement cost in historical perspective

In archaeology, various attempts have been made to evaluate the cost of movement: (a) Paleolithic hunter-gatherers groups research takes ethnographic mobility patterns, distribution of raw material, and availability of game into account (e.g. Ekshtain et al. 2017), while (b) movement cost in complex societies studies is more focused on trade and international relations (e.g. Harrower and D'Andrea 2014). These types of inquiries into human history would take topography, a presumably natural constrain, as a vital category in cost calculations (e.g. Tobler's hiking function, Uriarte Gonzalez's slope-dependant cost function, Herzog's metabolic cost function; Alberti 2019, Nakoinz & Knitter 2016). Using these topography-based cost theories to apply a Least Cost Path (LCP) calculation between two points, is at the heart of historical human movement investigation (Verhagen et al. 2019). While calculating cost of movement stream as a point of broken traffic have a considerable movement cost (Djurdjevac Conrad et al. 2018, Herzog 2010), Gully erosion, that has long been correlated with human activities (Nyssen et al. 2004), promotes the development of stream-like features with a valley and channel topography and resulting in a possible barrier-function to movement.

Gully erosion and pathways

Erosion is a natural process aiming at a levelling of relief reaching a dynamic equilibrium when environmental factors remain stable; extreme events can disturb this dynamic equilibrium (Nyssen et al. 2002). Settlement activities effect in a decrease of the thresholds for these erosional processes, resulting in accelerated erosion, so-called soil erosion (Nyssen et al. 2004). The resulting processes include removal, transport and deposition of sediments or soils by water with on-site effects by inter-rill, rill and gully erosion. Inter-rill erosion frequently results in sheet wash where thin layers of surface substrates are removed over larger areas (Verheijen et al. 2009). In contrast, rill erosion is caused by concentrated flows in small channels (depth < 30 cm; Gilley 2005). Gullies are also linear soil erosion features, having a minimum depth of 30 cm or a minimum cross-section area of 930 cmÇ and a minimum volume of 25-45 mÑ removed by ephemeral streams (Vandekerckhove et al. 1998, Martınez-Casasnovas et al. 2004, Schütt et al. 2005, Valentin et al. 2005); frequently, gullies are only few hundred meters in length with an upstream gully-head and downstream a seepage, mostly coinciding with fan accumulation at a break of slope (Nyssen et al. 2002, Poesen et al 2003). Gullies usually develop during one extreme rainfall event, generating surface runoff corresponding to a flash-flood. The global distribution of gullies is vast, with gullies occurring in all environments (Torri and Poesen 2014). Especially, bare surfaces, agricultural and pastoral practices are considered as favourable for gully erosion (Imeson and Kwaad 1980, Bennett et al. 2000). Highly erodible materials include loess, marls and sandy materials (Valentin et al. 2005).

Gullies have been investigated from several prisms, with a main focus on severe global soil loss problems and agricultural productivity (Poesen et al. 2003), but also for example as indicators for geomorphological activities on Mars (Christensen 2003). From a mechanical perspective, the threshold of the amount and form of surface runoff necessary to initiate gully erosion is determined by soil porosity and permeability, its shear strength and the size and slopes angles of a catchment area (Vandaele et al. 1996, Vandekerckhove et al. 1998, Bennett et al. 2000). These properties and occurrence of gullies have been correlated with geological, topographic, climatic and human induced variables (Valentin et al. 2005) and resulted in several studies that generated Gully Erosion Susceptibility Maps (GESM) for certain areas (e.g. Roy and Saha 2019, Arabameri et al. 2018). Notwithstanding, few recent investigations have looked into a possible enlargement of a runoff generating surface, resulting from paved and unpaved roads and animal trails (Nyssen et al. 2002, Schütt et al. 2005, Seutloali et al. 2016, Sidle et al. 2019 in press). These authors suggest that roads or pathways, resulting in compaction and thus reduced soil porosity and permeability, may be responsible for gully

volume changes as well as for the formation of new gullies. The experimental work by Ziegler and Giambelluca (2000) on erosion by runoff points out that road and pathway surfaces have significantly higher penetration resistance values than various types of fields; based on this observation it is concluded that footpaths can be the point of origin soil erosion. Hence, once the surface of a pathway is compacted and infiltration capacity is depleted it might be the starting point for gully erosion triggered by a extreme rainfall event (Seutloali et al. 2016). The gully might follow the pathway forming a holloway (Sidle et al. 2004) or in slopy terrain where footpaths tick up diagonal to the slope the gully develops nearly rectangular to the footpath where the concentrated runoff following the footpath overflowed its 'banks' (Schütt et al. 2005). While holloways have an important role in pathways and soil erosion dynamics, gullies are more noticeable landscape features, resulting in deep and at times long dissection of their surroundings (Nyssen et al. 2002, Sidle et al. 2019).

Movement cost and gully erosion

We consider that gullies, which are at least 2 m wide and deep and have steep flanks (box-shaped cross-profiles), are topographic obstacles that increase the cost of human movement. As the location of gullies is frequently determined by the location of pathways and roads, their occurrence is often associated with roads resulting from movement patterns of humans across the landscape. For assessing a possible positive feedback mechanism between gullies and the cost of human movement, we hypothesize that:

(1) Human movement, resulting in unpaved and paved pathways, promotes gully erosion.

(2) Gully erosion, resulting in box-shaped channels, is a barrier constraining oriented human movement.

Based on remote sensing data, the first hypothesis will be examined using Frequency Ratio (FR) index as a tool used to assess variables' importance in determining gullies location (Arabameri et al. 2018). The second hypothesis is tested by investigating path-length differences of randomly distributed Least Cost Paths (LCPs), assuming that longer paths resulting from the existence of gullies as uncrossable features. As study site four different spots from the Tigray region in the Ethiopian Highlands are selected, as it is an area well studied for both gully erosion as well for long-term human occupation and interregional movement is (e.g. Finneran 2007, Nyssen et al. 2004).

6.2 Study area

The Ethiopian region of Tigray comprises the northernmost part of the Ethiopian Highlands (Figure 6.1) with an area of more than 50,000 kmÇ and population nearing five million inhabitants (Billi 2015, Medhin 2011).

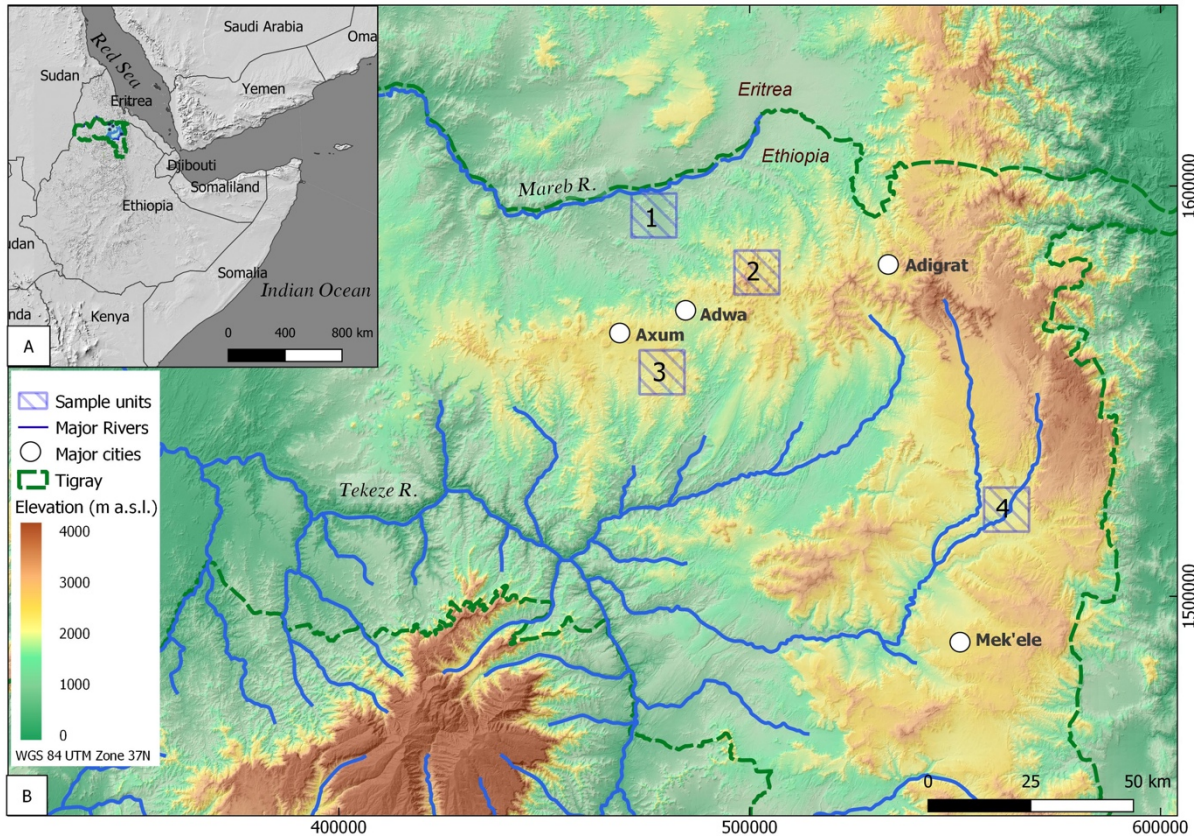

Figure 6.1. A: The Horn of Africa with the Tigray region of the Ethiopian Highlands marked in dash green line. B: The study area in central eastern Tigray. Numbered squares correspond to 10x10 km sample units: 1. Rama, 2. Yeha, 3. Daragà and 4. Wuqro. Sources: A: Natural Earth open source data available at naturalearthdata.com. B: color-coded hillshade map based on 30 m SRTM DEM provided by USGS earth explorer (USGS).

Environmental setting

The geological structure of Tigray comprises a variety of magmatic and sedimentary rocks with Late Proterozoic crystalline basement rocks being oldest. The Paleozoic Enticho Formation (Fm.), the Mesozoic Adigrat Fm. (terrestrial sandstones), and the Mesozoic (Jurassic) Antalo Fm. (limestone formed under shallow marine conditions) occur widespread (Beyth 1971). Oligocene volcanic activities of the Afar plume triggered large-scale emplacement of trap basalts (Hoffmann et al., 1997). Later volcanic activities in the Oligocene and Miocene resulted in plugs and domes, which pierce the modern surface (Natali et al., 2013). Several planation surfaces are the result of number of uplift phases triggered by tectonic movements of the Arabian-Nubian Shield. These are responsible for the stepped (locally termed “Amba”)

landscape of the region (Coltorti et al. 2007). Geomorphologically, the area can be subdivided into different landscape units: 1. cone shaped hills/mountains (volcanic plugs and domes), 2. flat to hilly areas of various sizes (plateaus and "Ambas") and 3. tectonically related depressions (grabens). Drainage of these features is dominated by small valleys, large ephemeral streams and few permanent streams with the Takeze river being the major one in central Tigray (Billi 2015). Gullies can be found in all of these geomorphological units (Gebremariam 2009).

The main perennial streams draining Tigray are tributary to the Gash (Mareb) River and the Nile River; in general, these perennial streams are deeply incised forming steep valleys. Present day morphodynamics in the area are dominated by slope wash, landslides and rockfalls. Today's climate in Tigray is tropical and driven by the monsoon. Yearly average daytime temperatures across Tigray vary from 20°C to 42 °C. Due to the influence of the monsoon three main seasons can be outlined: Rainy season corresponds to the monsoonal season and lasts from June to September (kremt), a dry cold season occurs from October to February (bega) and a pre-monsoonal warm period with little rainfall lasts from March until May (belg). Correspondingly, during the course of the year rainfall shows a bimodal distribution, composed of a smaller maximum from March to May and a larger maximum from July to October. During the main rainy season (kremt) rainfall appears within massive stormy events rather than gradual or persistent over time (Gebrehiwot 2013, Berhane et al. 2020). In eastern and central Tigray, which is in the focus of this study, mean annual precipitation during 1961-1990 varied between 500-800 mm (Harrower et al. 2020). Reconstructions of past climate suggest colder conditions, with a possible annual average increase by 7°C in the Ethiopian Highlands since Last Glacial Maximum (LGM) (Nyssen et al. 2004 and references therein). Based on sediments sequence in lake Tana, Lamb et al. (2007) interpreted three dry phases at 16,700, 15,100, 12,000 and one at 8,000 cal BP within a relatively more humid environment than current one. Bard et al. (2000) and Marshall et al. (2009) emphasize that since mid-Holocene (ca. 5,600 cal BP) the Ethiopian Highlands experienced a dry-humid-dry cycle, with several periods within this cycle resembling present day climate while Nyssen et al. (2004) conclude that current rainfall distribution pattern has existed during the same period.

Current vegetation in the area is composed of shrubs and savanna mix with Juniperus and Podocarpus mainly occurring along slopes. In 2005 about 0.2 % of the total Tigray area (~ 5 million ha) were covered by high woodlands and forests while about 43.2 % of the area were covered by low woodlands and shrublands (FAO Forest Department 2010). The nearly total absence of primary forests is assumed to be related to the intense and long lasting land use in

the whole Tigray area. Land use in Tigray follows millennia long traditions with grains being the major cultivated crop; today, agricultural areas of various types (e.g. Teff, fruit plantations, pastoral areas) occur area-wide (Medhin 2011). The main type of settlement are villages along the major roads with few of them being medium sized towns (up to 50,000 inhabitants). The only larger cities with administrative functions are Mekele, Adigrat and Aksum (Figure 1). During the past two decades a strong growth of urban areas occurred coinciding with road constructions. In the rural areas the construction of numerous micro-dams and the intensification of agricultural production took place (Aune et al. 1997, Medhin 2011). Multiple soil conservation measures are applied to prevent soil erosion, mainly using earth bunds, furrows and grassed lynchets (locally known as daget). Placing stone bunds and planting of trees and bushes to stabilize larger earth bunds are implemented since the early 1990ies (Dagnew et al. 2017, Frankl et al. 2013, Nyssen et al. 2000, Nyssen et al. 2002, Tebebu 2010).

Archaeology

While all over Ethiopia the Afar and Omo regions hold earliest evidences for genus homo and a central piece in the global human evolutionary puzzle, substantial archaeological findings in the Ethiopian Highlands and Tigray, only appear at the late Holocene with early chiefdoms and state formation (de la Torre et al. 2004, Finneran 2007, Fattovich 2012, Harrower et al. 2020, Villmoare et al. 2015). Furthermore, most recently, detailed surveys produced very few remains of stone age (ESA, MSA, LSA) material culture (Harrower and D'Andrea 2014). Intense archaeological research in Tigray has yet to produce clear cultural chronology during the middle to late Holocene phase. Among other reasons, this is attributed to vast variations in the material culture and what appears to be a very gradual and spatially diverse transition from foraging towards nomadism and to farming (Fattovich et al. 2001, Fattovich 2010). First evidences of hierarchies in the form of monumental temples appeared in the early 1st millennium BCE (Finneran 2007). However, it has been suggested that even later in time, there was no preference to a certain central place (Harrower and D'Andrea 2014). Architecture style and inscriptions brought the suggestion that this material culture originated in a mixed local and Arabian-peninsula originated elite, which some scholars name DM'T or 'Ethio-Sabean', indicating a cultural exchange with the kingdom of Saba around 700 BCE (Japp et al. 2011). However, the lack of evidence for a Sabean influence as well as they lack the prominent Sabean water harvesting technologies in the 1st millennium BCE sites in the Eritrean highlands ('Ancient Ona' culture) as well as at other sites in Tigray indicate more locally diversified and regional cultural practices (Curtis 2009, Harrower et al. 2020). During the first century BCE evidence of the kingdom of Aksum appeared which became the defining culture of Ethiopia's

history and which is famous for its massive steles (Finneran 2007). The Aksumite, based with their capital in the city of Aksum in central Tigray, governed the highlands for most of the first millennium CE. In addition to far reaching international trade, they formed some of the governing basis for the modern states of Ethiopia and Eritrea (Fattovich 2012).

The sample units

Four historically and environmentally representative sample units were chosen in order to investigate gully occurrence and indicators for human movement. It should be noted that even today, many people cross these areas on foot and no pedestrian bridges above these deep gullies were evident. Sample units were oriented around regions containing Ethio-Sabean or Aksumite archaeological sites - holding evidence of long-time human occupation. These sample units also represent a range of climatic, topographic and lithological characteristics in Tigray. To allow comparability between the sample units and due to calculation capacity limitations, a fixed plot area of 100 km2 was chosen for each of the four sample units.

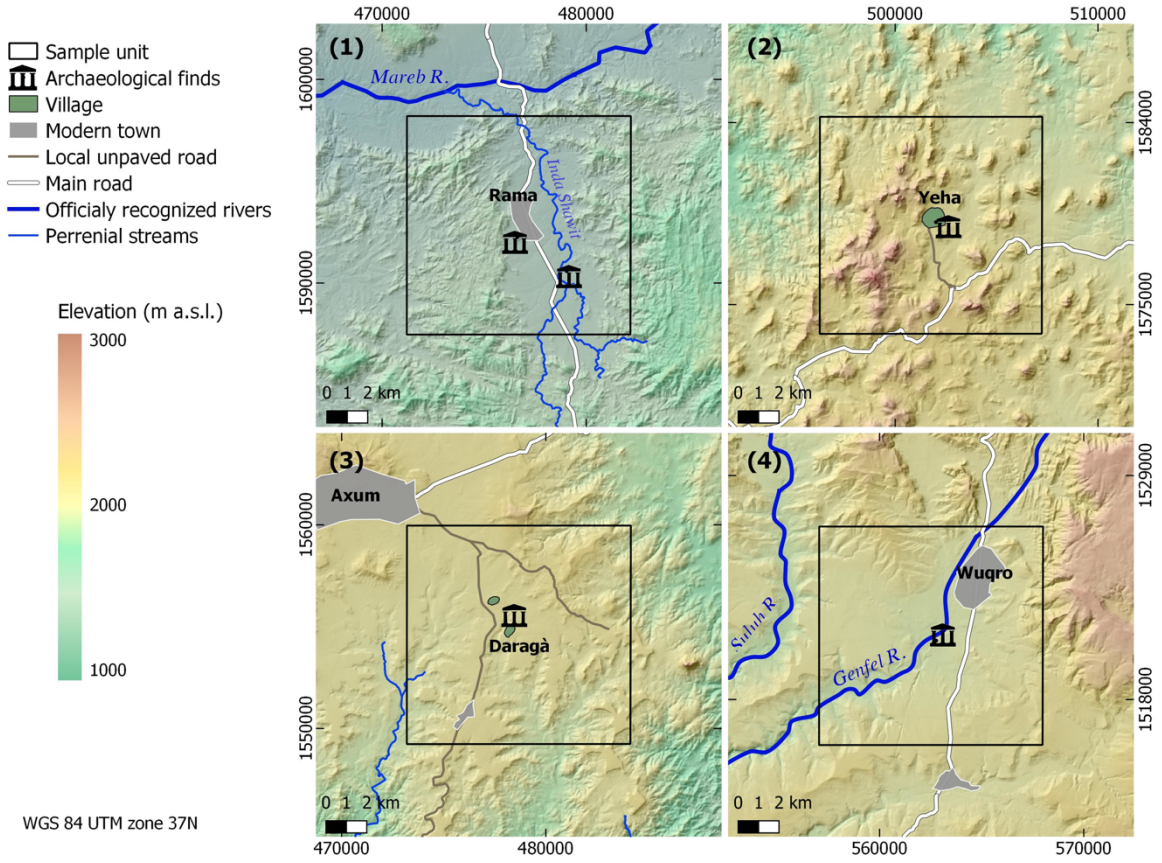

Figure 6.2. Topographic overview of the four sample units: Rama (1), Yeha (2), Daragà (3) and Wuqro (4). Color-coded hillshade maps based on 30 m SRTM DEM provided by USGS earth explorer [81-83].

Rama sample unit (1)

The Rama sample unit (#1 in Figure 2) is located in the Rama graben, which in the sample units covers a 2 km wide and approximately 10 km long area striking S-N. With an average elevation of 1300 m asl, the Rama sample unit is lower and warmer than the hills and ridges surrounding it. The graben is flanked by a hilly area with moderate rise to the west and rising ridges with steeper slopes and higher elevation differences to the east; to the south the graben structure disappears and shades off into the Ethiopian Highlands by a number of faults appearing as ridges with steep slopes. North of the graben lies the Mareb (Gash) River, flowing W-NW towards the Gash delta in Sudan and serving currently as the border river between Ethiopia and Eritrea. The lithology of the Rama sample unit is characterized by metasedimentary and metavolcanic Precambrian rocks (greywacke, sandstones) with granites and diorites as base rocks, exposed as flat and hilly granitoids units (Beyth 1972). Patchy occurrence of epidote, quartz and calcite veins are also common. Faults are diverse with SW-NE as the dominating direction (Gebremariam 2009). The Inda Shawit is a perennial river that drains the Rama graben to the north into the Mareb River. First and second order intermittent (mainly due to spring activity) to ephemeral channels drain the eastern and western graben flanks. Morphodynamics are characterized by intense soil erosion. Due to the high erosion intensity, with the exception of a fertile area on the floodplain of the Inda Shawit River, soils are highly degraded and locally the underlying bedrock is exposed. The area is intensively used for agriculture with only the patches with bare bedrock found uncultivated. Along the main channel citriculture and occasionally avocado plantations are alternating with the cultivation of various seasonal vegetables. Some slopes at the eastern and western graben flanks are terraced and planted with olive trees (olea welwitschii) and different grain crops including maize and sorghum as well as teff (Eragrostis tef) and finger millets (Aune et al. 1997, Medhin 2011). An unpaved road runs along the graben depression. At the centre of the Rama sample unit the modern town of Rama is located. Recent surveys of the area conducted by the German Archaeological Institute and of the Egyptian Museum Georg Steindorff of Leipzig University found graves and pottery attributed to the Aksumite period; attempts to uncover pre-Aksumite occupation are ongoing (Dietrich Raue personal communication, Pfeiffer et al. unpublished manuscript). Around these archaeological features the Rama sample unit was designed.

Yeha sample unit (2)

The Yeha sample unit (#2 in Figure 2) is located 10 km south-east of the Rama sample unit (Figure 1B). The most prominent geomorphological features are the cone-shaped hills and mountains reaching up to 2,400 m asl, forming the eastern extension of the so-called ‘Adwa

Mountains' (Machado 2015). Oligocene intrusive volcanic activities of the Afar plume formed phonolitic and trachytic plugs and domes that resemble the hilly-mountainous cone-shaped topography (Natali et al. 2013). Next to the volcanic rocks siltstones, sandstone (Adigrat sandstone) and metasedimentary rocks are abundant. A 500-1200 meters wide SW-NE oriented basin with several meters thick alluvial infills crosses the eastern part of the Yeha sample unit, being drained by a box-shaped channel with periodical runoff and several gullies formed in the alluvial infills draining directly into the box-shaped channel. Grassy mountain vegetation covers the uncultivated slopes while tillage areas occur in the flat areas of the basin infills and dominated by the cultivation of tef (Pietch 2017). An unpaved road connects the main road of central Tigray with the town of Yeha, which lies in the center of the Yeha sample unit. Archaeological evidences indicate almost three millennia long occupation of this area including a unique and well-known temple attributed to the Ethio-Sabean culture of the pre-Aksumite period (Japp et al. 2011).

Daragà sample unit (3)

The Daragà sample unit (#3 in Figure 2) is located 16 km south-west of the Yeha sample unit (2) and 2.5 km south of the modern city of Aksum . The landscape of the Daragà sample unit is composed of plains that are part of the Aksum plateau located in c. 2,000 m asl. Two perennial streams incised up to 100 m deep into the Aksum plateau drain the area. The plateau surface is resembled by Oligocene trap basalt and the sandstones of the Mesozoic Adigrat Formation (Hagos et al. 2010). Locally exposed bedrock as well as gullies are common indicating that soil erosion characterizes present morphodynamics. The valley floors are infilled by alluvial deposits in which the modern channel is slightly incised. The plateau area is predominantly used for tef cultivation while the alluvial plains are used as grazing areas for cattle. In the cultivated areas fields are split-off from each other by field stones piled up to small walls and frequently grown by cacti or endemic trees. Two unpaved roads or rather wide pathways cross the area along a N-S and NW-SE axis (Figure 2). The southern outskirts of Aksum expand south-eastwards along the northern edges of the Daragà sample unit, while few small villages occupy its central part including the hamlets of Hawelti and Melazo. In their surroundings, substantial archaeological findings were uncovered, including a temple attributed to the Ethio-Sabean culture (Contenson 1961, 1963; Leclant 1959).

Wuqro sample unit (4)

The Wuqro sample unit (#4 in Figure 2) is located 75 km south-east of Melazo and 82 km south-east of Yeha and lies about 40 km north of Tigray's capital Mekel'e. In the northern part of the Wuqro sample unit a local mountain range rises up to 2300 m asl with the slopes drained

to the south and the southwest by two valleys reaching the recipient in c. 1900 m asl. Geologically the unit belongs to the northern edge of the so-called 'Mekel'e outlier' composed of Paleozoic to Mesozoic dolomite-limestone (Asrat et al. 2010). An inverse fault crosses the area SW-NE and SE-NW trending normal faults appear in its southern part (Beyth 1972, Sembroni et al. 2017). The perennial Geba River drains the area following the major fault lines. Gullies are a prominent geomorphological feature along the slopes. The area is intensely cultivated by cropping maize, sorghum and tef. Occasionally fruit plantations occur along the valley floors. An asphalt road crosses the Wuqro sample unit in N-S direction connecting the cities of Mekel'e and Adigrat. The town of Wuqro lies in the centre of the Wuqro sample unit lies. About 300 m south of Wuqro a temple was excavated holding significant evidence of Ethio-Sabean material culture including a libation altar with a Sabaean inscription mentioning Yeha (Wolf and Nowotnick 2010).

Figure 6.3. A. Gully along pathway in the Rama sample unit (1), B. Initial gully head development perpendicular to a pathway in the Rama sample unit (1), C. Gully in the Yeha sample unit (2) with a small pathway descending into it, D. Gully in the Daragà sample unit (3).

6.3 Materials and methods

Data collection

Geomorphological features and gullies in the sample units were recorded during field work in October-November 2019. Sample unit (1) was extensively surveyed for in-depth measurements of gullies' profile parameters. Present day gullies, pathways, and roads were mapped at a 1:1000 m scale using satellite images provided by CNES/Airbus Maxar Technologies Map data @2020 as it appeared on Google Earth via Quick map service extension on QGIS version 3.4.5-Madeira (QGIS.org). A 30x30 m Digital Elevation Model (DEM) derived from Shuttle Radar Topography Mission (SRTM data, February 2000) was provided by United State Geological Survey (USGS) Earth Explorer (https://earthexplorer.usgs.gov).

Variables affecting gully erosion

The following categories have been shown in previous studies to influence gully erosion: elevation, aspect, plan curvature, slope angle, topographic wetness index (TWI), Normalized Difference Vegetation Index (NDVI), land use and land cover (LULC), lithology, soil type and distance from stream (Arabameri et al. 2018, Roy and Saha 2019, Martınez-Casasnovas 2004, Poesen et al. 2003). Except for lithology data for all categories was obtained through open access resources. Derivatives of the 30x30 m DEM were calculated using QGIS with GRASS (Geographic Resources Analysis Support System) GIS version 7.6 (GRASS Development Team) and SAGA (System for automated geoscientific analyses geographic information system) version 6.3 extensions. NDVI was calculated after Zhang et al. (2017) applying QGIS raster calculator for Sentinel-2 satellite imagery data (T37PDR, T37PER; 2020/06/25; https://scihub.copernicus.eu). Land use-land cover data were provided by the European Space Agency (ESA) Climate Change Initiative (CCI) based on Sentinel-2 data (http://2016africalandcover20m.esrin.esa.int/download.php; see supplementary table). Soil characters were obtained from the soil map of African continent (Dewitteet et al. 2013). Drainage network was obtained from the World Bank online water database (https://datacatalog.worldbank.org/dataset/ethiopia-rivers; produced by the Ethiopian Ministry of Water Resources). The parameter "distance from the stream" was calculated following Arabameri et al. (2018) and Roy and Saha (2019) using GDAL proximity raster extension for QGIS to generate 50 meters categories on a 250 meters total distance from the stream. The geological maps scale 1:250,000 of the area (ND 37-6, ND 37-7) were acquired from the Ethiopian Geological Survey in Addis Ababa and manually digitized. To receive information about the distribution of pathway and gully systems before the 1974-1991 Ethiopian Civil War and relocations going along pathways and roads were digitized from the USSR topographic maps generated in 1977 (1:200000; D37-13, D37-21, D37-28;

http://loadmap.net). Additionally, CORONA satellite images, conducted by US Central Intelligence Agency (KH4B, 1967; DS1102-2106DF072_c) were geocoded and pathways and gullies were mapped. All input layers were divided into categories and classes based on the natural distribution of the categories in the sample units with the intention that all areas would have at least 5 similar equally distributed intervals (Roy and Saha 2019). Input layers elevation, plan curvature, TWI, NDVI and slope angle were reclassified using 'class' and 'rcl.m' functions in R environment based on the evaluation of their natural distribution range using R software histogram 'hist' function (R Core team 2020). Analysing distances intervals of 25 m (for pathways) and 50 m (for roads and streams) were used following results and assessments of previous studies (Seutloali et al. 2016, Sidle et al. 2004, Zhang et al. 2019); this also incorporated a category of 'outside the range' following Roy and Saha (2019). Occasionally, additional edge intervals were formed to incorporate all results and to avoid loss of information. Slopes' aspects were categorized into eight intervals of intercardinal directions, additionally 'flat' areas lacking a distinct aspect were demarcated following Arabameri et al. (2018). Input layers for lithological units and soil characters have been categorized according to their natural features distributions. All non-pixel-based variables and all gullies were rasterized in QGIS environment (SAGA).

Frequency Ratio calculation

Frequency Ratio (FR) is a normalizing tool set to assess the relative frequency of gullies within each of the categories of the classified variables; it was calculated using R software (R Core team 2020). Based on pixels of each variable the following equation was applied (Eq. 1):

$$FR = \frac{(\frac{g}{C})}{(\frac{G}{S})} \qquad (1)$$

where g is the number of gully pixels for a class of a variable, C is the total number of pixels of that class, G is the total number of gully pixels within a sample unit and S the total pixels composing the sample unit (after Arabameri et al. 2018). If gullies are not at all affected by a given variable, a FR value of 1 is expected within all its classes. Any value >1, indicates a larger concentration of gullies in a class than an expected "equal", i.e. non-variable-related, distribution in the overall sample-unit. If a class's FR is < 1, gullies are relatively more abundant outside this class. Therefore, the further away the FR is of value 1, the higher the variable is rated in determining the location of gullies (Arabameri et al. 2018, Roy and Saha 2016).

Table 6.1. Classes distribution of the different natural, human and movement related variables tested for FR calculation of relative gully occurrences

Variables		Elevation * m a.s.l.	Slope	Aspect	TWI	P.curvature	NDVI	LULC	DFS [m]	DFR [m]	DFP [m]	DFPSM [m]	DFPCI [m]
Classes	1	1800-1900	0°-5°	Flat	5-7	(-100) - (-10)	(-0.2)-0.0751	Open water	0-50	0-50	0-25	0-50	0-25
	2	1900-2000	5°-10°	N	7-9	(-10) - (-3)	0.075-0.125	Built	50-100	50-100	25-50	50-100	25-50
	3	2000-2100	10°-15°	NE	9-11	(-3) - (-2)	0.125-0.175	Bare	100-150	100-150	50-75	100-150	50-75
	4	2100-2200	15°-20°	E	11-13	(-2) - (-1)	0.175-0.225	Sparse Veg.	150-200	150-200	75-100	150-200	75-100
	5	2200-2300	20°-25°	SE	13-15	(-1) - 0	0.225-0.275	Aquatic Veg.	200-250	200-250	100-125	200-250	100-125
	6	>2300	>25°	S	15-17.5	0 - 1	0.275-0.325	Cropland	>250	>250	>125	>250	>125
	7			SW		1 - 2	0.325-1	Grassland					
	8			W		2 - 9		Shrubs					
	9			NW		9 - 100		Tree cover					

TWI - Topographic Wetness Index, DFS - Distance From Stream, DFR - Distance From Road, DFP - Distance From Pathways, DFPSM - Distance From Pathways on Soviet Maps, DFPCI - Distance From Pathways on CORONA Images, NDVI - Normalized Difference Vegetation Index, LULC - Land Use Land Cover (as processed and described by the European Climate Change Initiative), P. Curvature - Plan Curvature with convex values represented as positive and concave values as negative. Notice variables lithology and soil type are missing as they were divided into classes according to the distribution within each sample unit based on soil and lithological maps.

*for Rama (1) elevation starts at 1100 m a.s.l and continues in similar 100 m intervals.

Cost of movement

The effects of gully formation on the development of the pathway network were assessed applying Least-Cost Path algorithms. Vectors of mapped gullies were transformed into 5 m wide pixels using 'Rasterize' function in QGIS environment (GDAL). In order for the gully pixels to be represented the DEM available in 30x30 m resolution was resampled into 5x5 m resolution using the 'resample' function in R environment ('raster' package) for both unmodified and modified (i.e. non-gully-added and gully added) layers. Applying a nearest neighbour resampling method makes sure to obtain reliable results for cost analysis (Gonçalves 2010, Dixon and Earls 2009, Gilbertson, et al. 2017, Rojas et al. 2008). The modified DEM

expressing gullies as obstacles to movement (corresponding to topographic walls of height 99,999) was generated using R (base and raster packages; R Team 2020).

Least-Cost Path (LCP) analysis is a well-established tool to compute a preferred movement route between two points and is mostly based on topographic features (e.g. Nakoinz & Knitter 2016, Paezet al. 2020). Before calculating LCPs, elevation differences in the resampled DEMs were transformed into a conductivity transition layer in R environment. Conductivity was based on the 'Wheeled' cost calculation (Eq. 2):

$$1/(1 + ((\text{abs}(x[adj]) * 100)/\text{critical slope})^2) \quad (2)$$

The x[adj] stands for slope angle as rise or descend for adjacent cells. Commonly used critical slope gradients are in the range of 8-16% (Alberti 2019). In the current work, a critical slope gradient of 12% was applied as a threshold, meaning that the paths are trying to avoid moving along slopes that have steeper inclinations than 12% (Alberti 2019).. The resulting conductivity transition layer stores the effort of movement from a source to a target pixel, applying Dijkstra's algorithm (Alberti 2019, Herzog 2014).. Target pixels are adjacent pixels that are defined by either a 4 (rook), 8 (queen), or 16 (knight) pixel neighbourhood, representing either horizontal, vertical or diagonal movement (Herzog 2016). This effort is represented as conductivity, i.e. the ease of crossing. Therefore, in the presented case, the conductivity results from a calculation that is determined by the slope gradient, applying the 12% threshold, between the source and target pixel. As the gully-representing values in the modified DEM are maximum 2 pixels wide, i.e., 2 squares in the transition layer, adjacency of 8 was chosen to minimize potentially topographic related 'jumping' over a gully pixel (Alberti 2019).. For the LCPs to cross as much of the sample unit's surface as possible, the units' northern, southern eastern and western edges were chosen as areas for goal and origin of the randomly generated LCPs. These edge areas were extracted in R using the 'Extent' function to select 1 km wide rectangular strips along the four edges of each sample unit (Alberti 2019). Following this, using the 'spsample' function ('sp' package), random goal and origin points were generated within these 1 km long and 10 km wide strips (Alberti 2019). Applying separate loops for north to south LCPs and east to west LCPs, this process was repeated 1000 times for each orientation and sample unit to obtain meaningful results (see supplementary material S file 2 for R code). A High-Performance

Computing cluster at Freie Universität Berlin was used to calculate the random LCPs.

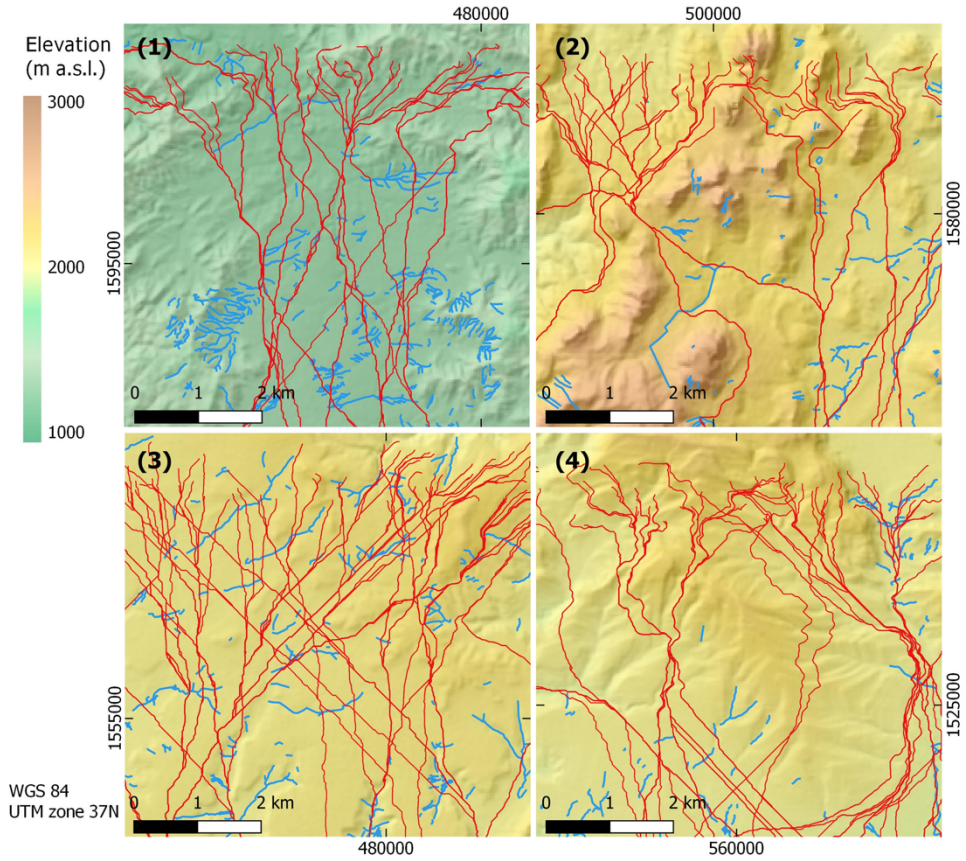

Figure 6.4. Gullies (blue lines) and randomly distributed least cost paths (red lines) within the four sample units: Rama (1), Yeha (2), Daragà (3) and Wuqro (4). Figures are showing the north-central section of each unit for comprehensible view of LCPs' starting points as well as the gullies' distribution in the landscape. Color-coded hillshade maps based on 30 m SRTM DEM provided by USGS earth explorer [81-83].

6.4 Results

Field observations

Gully erosion occurs across all landscape types of the four sample units. Gully networks including first, second and third order gully channels occur more frequently close to perennial or periodical streams while isolated gullies occur commonly in agricultural fields and along slopes. V-shaped gullies start predominantly mid-slope and frequently expose the local bedrock at their base. These usually reach the foot-slope and at times continue within the plains. In the plains, box-shaped gullies are the more typical form, though few v-shaped, usually narrower than the box shaped gullies, also occur. Where vegetation cover occurs, gullies are less frequent; this observation was especially made for the v-shaped gullies occurring along slopes. In the Wuqro sample unit (4) some gullies observed in upslope areas formed along fault lines. Gully distribution was not uniform across the sample units with the Rama (1) and Daragà (3)

sample units exhibiting the highest number of mapped gullies (Table 2). Regarding possible overall patterns, it is evident that gullies' lengths and locations vary between and within the sample units in both network and isolated forms. Many gullies exhibit a NW to SE direction. However, low mean resultant length values indicate a lack of unidirectional distribution pattern (Table 2). Some gullies are confined by valleys and seem to be predominantly shaped by topography, while others occur on the plains and along slopes (Figure 6.4). In the Daragà sample unit (3) the highest absolute number of holloways was recorded, composing 11% of its gullies, a ratio similar to the Wuqro (4) sample unit (Table 2).

Table 6.2. Distribution of gullies and holloways in the study area.

Sample Unit	Total number of gullies	Total length of gullies [m]	Gully Density [m²]*	Mean average**	Mean resultant length**	Total number of holloways	Holloways share in gullies [%]
1 Rama	880	163,775	4.2^{-6}	64.47°	0.112	8	0.9
2 Yeha	553	86,484	1.56^{-6}	107.29°	0.125	22	4
3 Daragà	905	199,230	3.37^{-6}	106.01°	0.182	107	11
4 Wuqro	368	77,733	1.48^{-6}	91.25°	0.311	41	11

*Gully density was calculated after mapping and transforming vectors into pixels ('Rasterize') for each sample unit. Following which, the amount of gully pixels was divided by the sum of all pixels of that sample unit [QGIS; 37,84,92].

** Mean average (degrees east of north) and mean resultant length where calculated using circular statistics ['circular' package; 87-89]. Mean resultant length is a precision evaluation between 0 and 1, where 0 indicates that the spread of gullies' orientations is wide (multidirectional) and 1 means that all gullies are oriented towards a single direction (unidirectional) [88-89].

Frequency Ratio (FR)

Different natural and human related variables with a possible effect on determining the location of gullies were systematically collected and each of these variables were sub-divided into their own classes (Table 1). Figure 6.5 incorporates the Frequency Ratio (FR) of all classes of a given variable, i.e., one box plot per variable. As each class holds one FR value (e.g. a certain lithological unit is a class with FR=2 while another unit composes another class with FR=1.2). Notwithstanding the asymmetric nature of FR, all classes of a given variable were plotted together to illustrate the spread of values and the distance from a 'non-affecting' FR value of 1. The distribution of gullies across the different sample units differs from a non-variable-

related FR of 1. Therefore, all variables are responsible for the location of gullies to various extents (Figure 6.5).

Due to the asymmetric nature of FR values, interpretation of deviations of the FR values from 1 could only be qualitatively and comparatively. Taking this limitation into account, it is evident that the four sample units show distinct FR value distributions which require a site-based analysis.

Among all variables, lithological characteristics dominate the location of gullies in the Rama (1) and Daragà (3) sample units. Topographic Wetness Index (TWI) is the most influential variable in the Yeha (2) and Wuqro (4) sample units. Slope gradient has little influence in the Daragà sample unit (3) while it has a relatively more dominant role in the Rama (1) and Yeha (2) sample units (Figure 6.5, supplementary material: S Table 1). For all sample units, the slope aspect exhibits only little influence on gully development, the same applies for the soil types. Some of the variables analysed, such as Land Use and Land Cover (LULC), show mainly FR values lower than 1, indicating that the amount of gully pixels in some classes is lower than expected from an equal distribution across space. However, the extent to which gullies are less likely to occur should not be over interpreted due to the asymmetric nature of FR. In the Wuqro sample unit (4), LULC has one class with a relatively higher FR value than the rest of the classes, indicating this class may have a more dominant role on determining the location of gullies (Figure 6.5). In general, movement related variables have weaker relationship with the occurrences of gullies than the non-movement related variables. However, random pixels equivalent to the number of gully pixels in each of the sample units were tested against the 'proximity to pathways' variable. This gives an estimation of the possible error size of a random distribution both for standard deviation and proximity to value 1. It is evident that movement related variables exceed the range of this distribution (Figure 6.5), indicating that the location of pathways and roads relates to the location of gullies. In the Rama (1), Yeha (2) and Wuqro (4) sample units, gullies are more likely to occur closer to pathways while in the Daragà sample unit (3), gullies are more likely to form outside the pathways' proximity range (25 meters). Proximity to roads has a relatively stronger correlation with the location of gullies than the proximity to pathways in the Rama (1) and Yeha (2) sample units - while in the Wuqro sample unit (4) gullies are less likely to occur in proximity to roads (Figure 6.5). For pathways based on USSR maps from 1977, gullies are more likely to occur closer to pathways in all sample units (Figure 6.5).

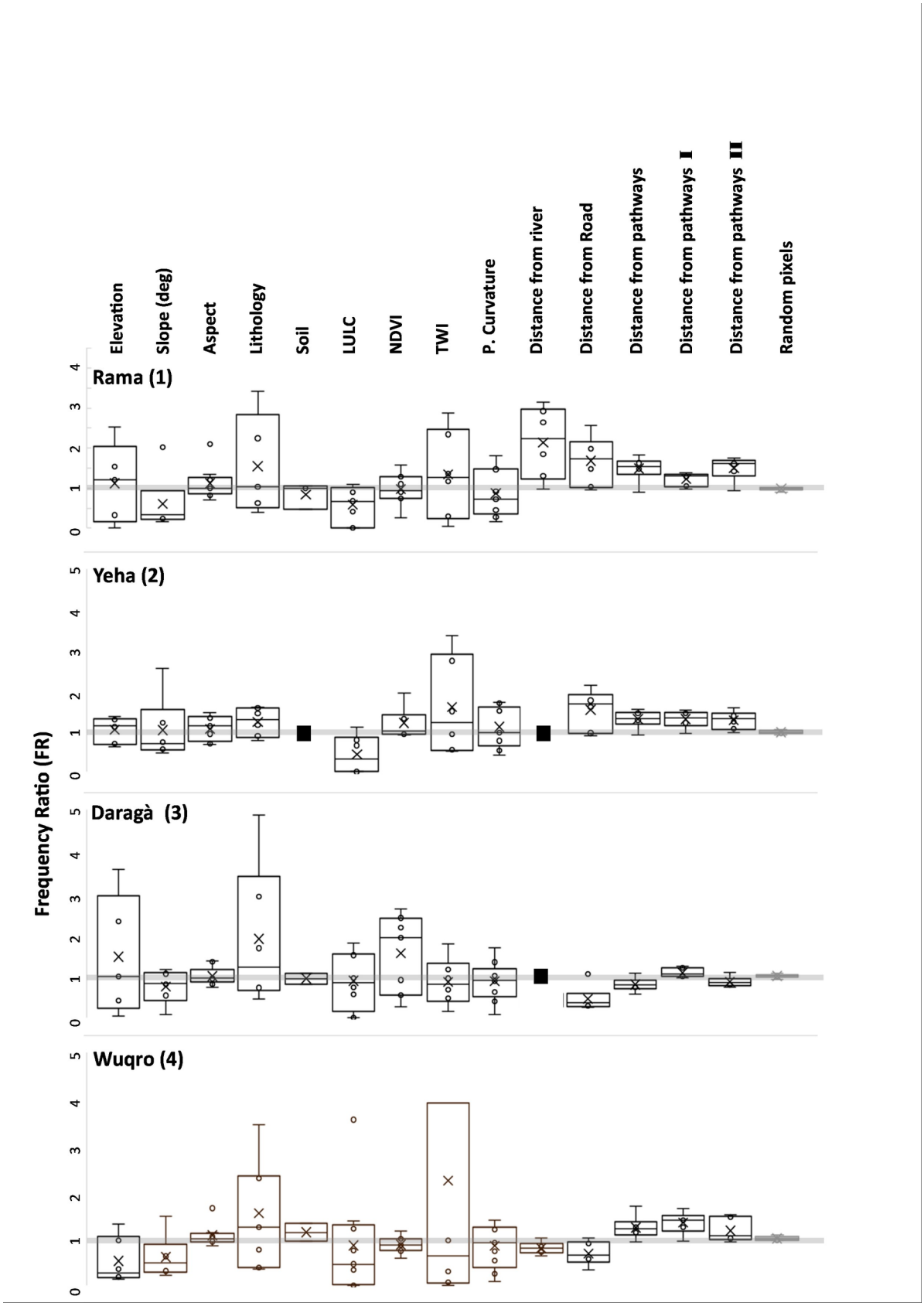

Figure 6.5. Frequency Ratio (FR) box plot diagrams of all classes within a given variable. Boxes represent 50% of FR distribution. Median is marked by a horizontal line while arithmetic mean marked by X. Circles represent the FR values whenever they were not used to generate the box plots borders itself. LULC - Land Use Land Cover,

NDVI - Normalized Difference Vegetation Index, TWI - Topographic Wetness Index, distance from pathways I – based on Soviet topographic maps, distance from pathways II – based on CORONA satellite images. Black squares are due to irrelevance of the variable for a given sample unit, i.e., one soil type at Yeha sample unite (2) or no officially mapped rivers in the vicinity of the sample units (2) and (3). Random pixels tested for their relative frequency in the 'distance from pathway' variable are marked in light grey at the right edge of the plot. For TWI in the Wuqro sample unit (4), highest FR is 10.4 and is not presented due to graphic limitations (see supplementary Table 1 for full results).

Least Cost Path Analysis

The randomly distributed Least Cost Paths cross gullies in multiple occasions as exhibited in the central-northern examples of the south to north LCP in all sample units (Figure 6.4). Changes in costs of movement, expressed here as changes in Least Cost Path lengths, are assessed after the implementation of high cost barriers at the location of gullies (Figure 6.6). Changed LCPs show a range of both increase as well as reduction in length from the unmodified LCP: The highest values reflect a 55% length increase compared to the unmodified DEM in the Daragà sample unit (3), following 34% increase in the Wuqro sample unit (4), 22% in the Rama sample unit (1) and a 17% increase in the Yeha (2) sample unit. In the Daragà sample unit (3), half of LCPs witnessed an increase of between 1.7-23.4%, while for the Rama (1), Wuqro (4) and Yeha (2) sample units, half of the LCPs were longer by 0.5-6%, 0.4-2.9% and -0.1-2.8% accordingly.

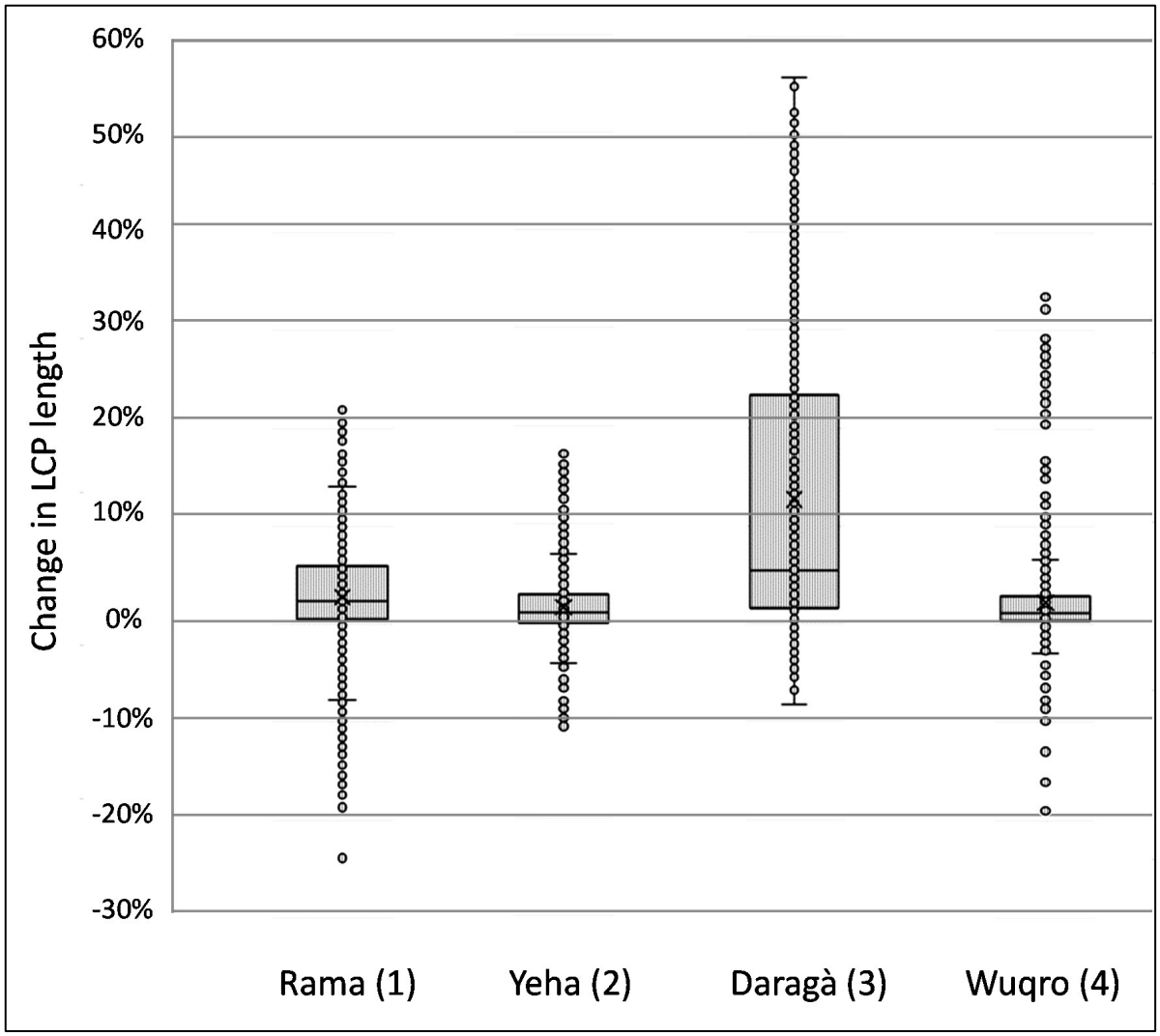

Figure 6.6. Changes in length of Least Cost Paths (LCPs) following the introduction of barriers along gully locations ('modified DEM'). Change is expressed by differences in the length of Least Cost Paths generated between two random points across the four sample units. The length difference (LCP without gullies as barriers / LCP with gullies as barriers) is expressed in percentage along the Y axis. Box plot representing 50% of changed LCPs (median). Mean marked by X while circles represent each changed LCP (n=2000 for each sample unit; See supplementary S Table 2 for full results).

Although most of the LCPs got longer when integrating gully barriers into the DEM, some LCPs exhibited even shorter paths after being 'blocked' by gullies (negative values in Figure 6.6). LCPs that became shorter account for 22% of the Daragà sample unit (3), 38% of the Rama sample unit (1), 25% of the Wuqro sample unit (4) and 55% of the LCPs in the Yeha sample unit (2). The most extreme path length shortening was witnessed in the Rama sample unit (1) with a maximum reduction of 24% of the path length compared to the unmodified DEM. In the Wuqro sample unit (4), maximum length reduction values is 19% while in the Yeha (2) and Daragà (3) sample units, the extreme values for LCPs length reduction were 11%

and 8% accordingly (Figure 6.6). After assessing the validity of the algorithm, it was evident that a topographic threshold, that was too high to cross before the introduction of gullies, has been considered as worth crossing due to the 'blocking' of other possible routes by the uncrossable gullies. This was due to either equal values in the cell's 'neighbourhood', causing the selection of cells whose cumulated length is not optimal (though their conductance is) or to a change in the transition matrix used as input for the shortest path algorithm.

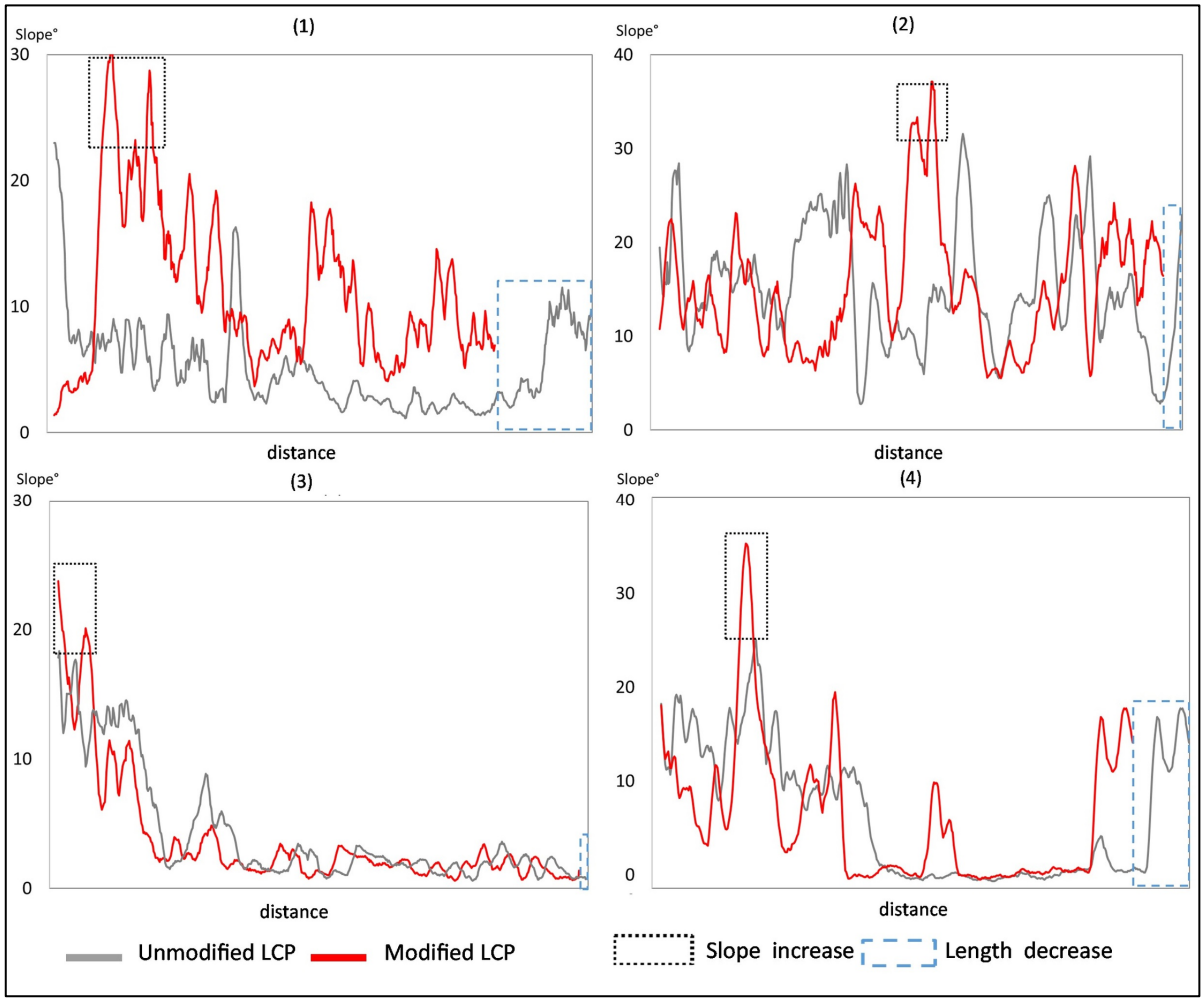

Figure 6.7. Comparison of slope values along Least Cost Paths (LCPs) based on the unmodified and modified DEM. Unmodified (original) LCPs appear as grey lines while modified LCPs appear as red lines. Selected for display were only the LCPs with the largest observed length reduction. Notice the black fine-dashed rectangles around the higher slope angles values of the LCP with gullies as barriers, as well as the dashed blue rectangles around the longer segments on the path-distance axis in the same modified LCP.

In order to understand the possible mechanism responsible for LCPs length shortening, LCPs of the extreme cases on the south to north LCPs axis, for each sample unit, both applied on the unmodified and the modified DEM, are presented along the slopes' gradients these LCPs cross. In all four sample units, the shorter S-N LCPs after gully blocking, also lead along steeper slopes than the unmodified LCP in at least one section of the pathway (Figures 7 and 8).

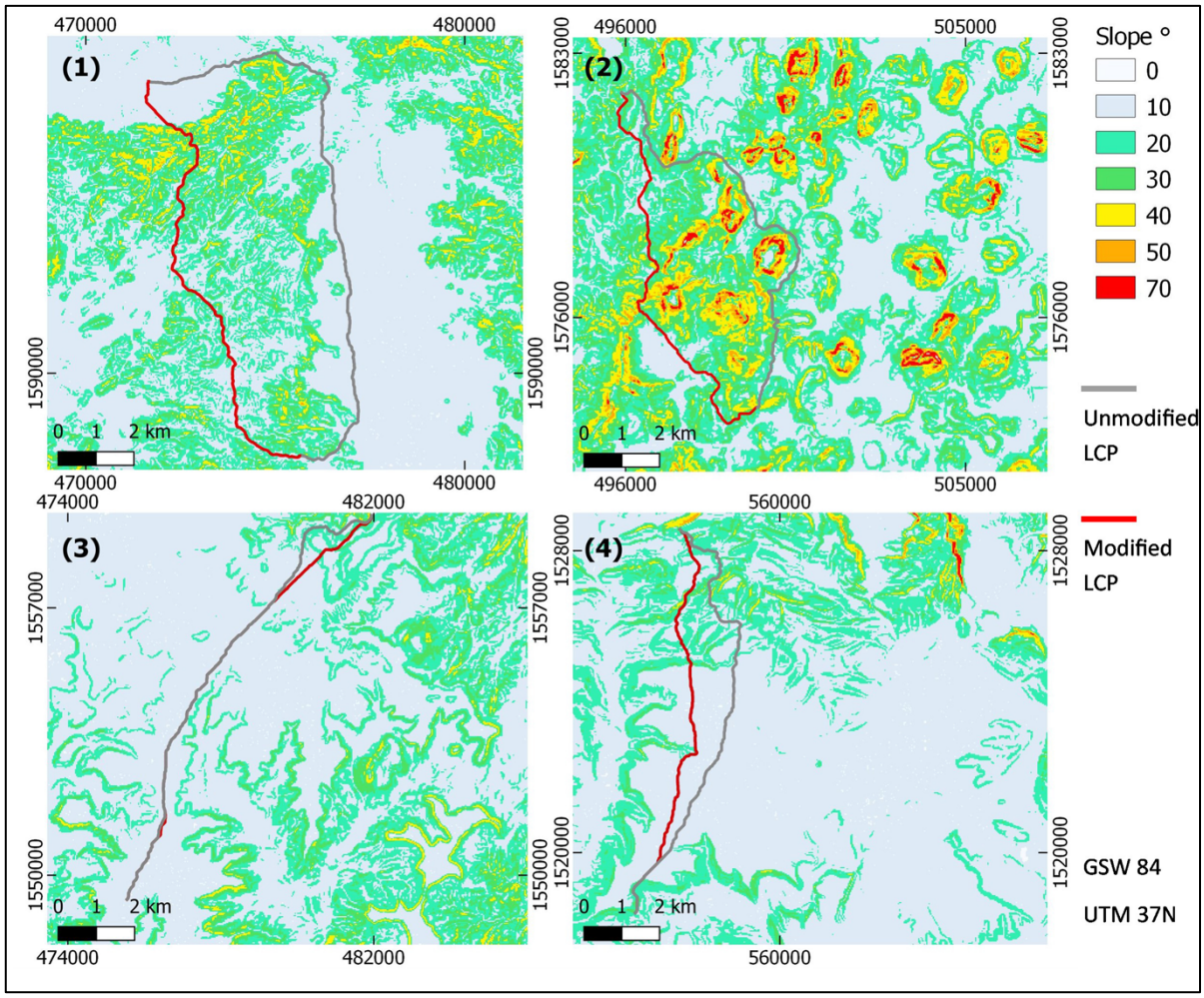

Figure 6.8. Spatial distribution of the Least Cost Paths (LCPs) with the largest observed length reduction presented in Figure 6.7. LCPs presented from north to south points. Unmodified LCPs appear as grey lines while modified LCPs appear as red lines. Numbers correspond to sample units. Notice areas with relatively higher slope angles. Slope maps based on 30 m SRTM DEM provided by USGS earth explorer [81-83].

6.5 Discussion

The effect of pathways and roads on gully erosion

The process of gully erosion and the corresponding distribution of gullies is controlled by a complex set of environmental and human induced factors (Arabameri et al. 2018). Addressing basic variables referred to by the literature was therefore the supporting basis to evaluate the relative possible influence of pathways and roads in the formation of gullies. For the four sample units analysed it has emerged that lithology and Topographic Wetness Index (TWI) are the most influential variables for the occurrence of gullies (Figure 4). Lithology incorporates all rock characters determined mainly by composing minerals and their interconnections. On the surface, these result in bedrock jointing and joint density, pore volume or typical weathering products which influence erosional processes (Mousazadeh and Salleh 2014). The other dominant variable, TWI, reflects a pixel's control on hydrologic processes as it includes the parameters slope and the upslope drainage tributary to the respective pixel (Beven and Kirkby 1979); consequently, high influence of TWI on gully development results from its high explanatory power on the pixel's relative moisture status (Buchanan et al. 2014). In order to evaluate the effect of pathways on the location of gullies, random pixels, equal to the number of pixels generated by gully mapping for each sample unit, were tested for their Frequency Ratio (FR) within the classes of the 'distance form pathways' variable. Results for actual gully pixels within the 'distances from pathways' variable goes well beyond these random pixels (Figure 4), proving that the location of gullies is related to the location of pathways. These gullies relate to pathways in different environments and topographies and are not strictly correlated to any other environmental character although a certain correlation with other environmental characters is probable. Results also show that the general effect of pathways and roads on the location of gullies is not as dominant as the effects of other environmental factors such as lithology, slope degree and elevation which are usually considered (Arabameri et al. 2018, Valentin et al. 2005). For the relationship between the occurrence of gullies and pathways the Daragà sample unit (3), however, shows mostly negative FR values, indicating that gullies are less likely to occur next to pathways (Figure 4). The same relationship is proven on the mappings of gullies and pathways based on the CORONA satellite images taken at the mid 1960ies, a time period before modern strong population growth and enlarging road network. An exceptional case builds the Daragà sample unit (3) where for the pathways mapped on the base on a USSR topographic maps, scale 1:200.000 published in the 1970ies a weak but positive relationship to the occurrence of today's gullies can be observed (Figure 4). Hence, more of the current gullies occur next to pathways known in the early 1970ies than they do next to modern pathways and roads. However, due to the coarse scale of the USSR topographic maps only a part of the existing pathways and roads might have been recorded, causing a bias

in the statistics based on these data. One reason for the negative relation between the occurrence of gullies and pathways might be due to the implementation of Soil and Water Conservation (SWC) measures in Tigray during the past decades (Nyssen et al. 2004). The SWC treatments in the study areas may have been more frequently implemented close to pathways and roads due to accessibility, producing a bias resulting in a negative relationship between pathways and gullies. Another reason for the negative relation between pathways and gullies may be especially in Daragà sample unit (3) due the occurrences of holloways, as holloways were neither considered in FR nor in LCP based on a demarcation problem: (1) Holloways are themselves pathways and hence could not be isolated from the movement variables, and (2) holloways in the sample units are usually only few decimetres deep and do not exceed a depth of 0.5 m and, therefore, do not form steep obstacles for movement necessary to be considered in the LCPs analysis. Pathways used for the FR calculation were mapped regardless of their possible holloway characters. In Daragà sample unit (3) the highest absolute number of holloways of all sample units was observed (Table 2). In consequence it has to be considered that in the landscape of the Daragà sample unit holloways - which serve both as pathways and shallow channels - are causing an increased "channel" density and, thus, effect that thresholds of concentrated runoff necessary to exceed to start gully erosion. This would result in a relatively low density of gullies around pathways turned holloways, compared to the other areas within the sample unit.

Results for Rama sample unit (1) are widely in agreement with a Gully Erosion Susceptibility Map (GESM) generated by applying a random forest machine learning classifier of similar environmental characters and human related variables in a small second order catchment within the Rama sample unit (1) (Busch 2020, unpublished Msc. thesis). The Gully Erosion Susceptibility Map suggests that elevation and aspect are the most relevant variables to predict the location of gully heads. In contrast, in the work at hand we identified for the Rama sample unit (1) that elevation and lithology are the most relevant factors followed by TWI and aspect influencing the development of gullies (Figure 4). Hence, both variables elevation and aspect, show high relevance to explain the natural distribution of gullies as documented on both Frequency Ratio as well as random forest classifier based GESM. However, the loading of some variables differs due to the relatively small size of the study area investigated by Busch (2020) with a total of 6.7 kmÇ with only little lithological differentiation, making lithology of low importance in determining the occurrences of gullies. Additionally, in contrast to the current work, while generating the GESM, the importance of Topographic Wetness Index TWI was lower than of other tested variables. This may be attributed to the TWI classes based on

natural breaks in the GESM (using ArcMap) rather than equal intervals (using R) applied in the current work. Beyond, in the GESM the movement related variable 'Proximity to pathways' was ranked between 6 and 8 out of total of 16 variables determining the location of gully heads, while produced by the FR calculation proximity to pathways for the Rama sample unit (1) was ranked 10 of 11 variables (excluding other movement related variables) (Figure 4, Busch 2020). This higher weighting of pathways as a variable in the GESM may be related to the, in average, different topographic character of the GESM study area than in the Rama sample unit (1) as introduced in the current sudy: the GESM study area is altogether hilly with more than 50% of slope angles at >5° while the Rama sample unit is composed largely of relatively flat surface <5° (Figure 2). Nyssen et al. (2002) observed for the Ethiopian Highlands, that the location of roads on a slope affects runoff generation and as a result the formation of gullies. In consequence, the in average steeper GESM study area (Busch 2020) than the Rama sample unit (1) would underlines the effect pathways hold on promoting gully erosion expressed in a higher weighting for this variable than that of the FR applied to the entire Rama sample unit (1).

The effect of gully erosion on human movement

The basic assumption behind the calculation of movement cost is that gullies form barriers to movement. Field observations made clear that most gullies encountered were at least 2-3 meters wide and 2-3 meters deep, while only few gullies are smaller in width and depth and, thus, crossable by humans (Figure 3). Notwithstanding, the geometry of gullies is highly variable along their course, perhaps to the extent some are crossable at certain points. While various of the available satellite images hold pixel sizes of 1 m x 1 m reliable mapping of gullies on this basis was difficult due to the poor ratio of the geometry of the forms to be mapped and the given image resolution, additionally impeded by low colour contrast of the images; reliable detection of gullies from satellite images was possible mainly when the gullies were deep enough and wider than 2-3 meters to generate visible shade. This observation is confirmed by comparison of satellite images with field data clearly showing that shallow gullies with less than 3 m width were undetectable in the available satellite images. This partial bias resulted in the fact that smaller, crossable gullies were unrecognizable while mapping from satellite images. Gullies. To further assure that mapped gullies for Least Cost Path (LCP) analysis where in fact at least 3 m wide, regular measurements of the width of the gullies were conducted using QGIS measure line while mapping the gullies based on satellite images. These frequent width validations showed additionally that most measured gullies are wider than 5 m.

Therefore, it is safe to assume that gullies mapped pose a barrier for movement during dry periods and even more so during heavy rains as it was observed that many gullies contain discharge. “Cost” in this study is presented as path length rather than calories or time to avoid assumptions on the type of mobility that occurred during recent Millennia, whether it was migration, trade or daily movement across Tigray or the Ethiopian Highlands (Verhagen et al. 2019).

Results of LCP analysis clearly point out the effect of the gullies on the LCPs modelled for crossing the respective sample units following a N-S axis. The extent of the elongation of a LCP is dependent upon the number of gullies has to cross forcing it to take a deviation. Density and amounts of gullies are higher in plains as occurring in Rama and Daragà sample units, than in well drained slopy areas such as in Yeha and most dominantly Wuqro sample units (Table 2, Figure 2). TWI is a variable related directly to drainage and is proven to be important for controlling the location of gullies (Figure 4). Therefore, the differences in gully density between the sample units can be explained by difference in flow dynamics. High drainage density in sample units (2) and (4) generates a decrease of peak flow in the respective concentrated surface runoff, causing that the threshold of surface runoff required for gully erosion is not reached (Torri and Poesen 2014, Vandekerckhove et al. 1998). In all sample units some Least Cost Paths lengthen by at least 15%, reaching an elongation of even 30% in Daragà sample unit (3), while median changes of LCPs lengths range between 1%-5% (Figure 5). These elongations of pathways are in general due to detours taken to avoid the barrier. An unexpected result is the observation that some of the modelled LCPs get curtailed due to the development of gullies. This dependency is explained by the occurrence of other topographic barriers that without the existence of gullies are avoided, but once the gullies appeared it gets costlier to cross the gully than the other topographic barrier (Figure 6) (Alberti 2019). This also implies that although shorter these changed pathways are usually more difficult due to lower topographic conductivity. In consequence it can be concluded that after gully development has started humans crossing the Ethiopian Highlands may have decided to take a steeper slope but shorter way due to gullies denying them crossing. Hence, it is our understanding that this unexpected anomaly should not be taken as a computing error but a result that may reflect real-life path planning.

While examining the differences between the lower medians and higher extreme values it should be considered that in the FR analysis it has been established that gullies occur often in proximity to pathways (Figure 4). Gullies, in this case obstacles for LCPs, are likelier to be around pathways and therefore paths people use in reality. For the random LCP analysis, the

more gullies a LCP encounters after gullies were introduced, the longer it became. This implies that LCPs which extended due to gullies crossing their original route may better reflect movement related realities than that of a median average value for all randomly generated LCPs. In consequence, we assume that in the Ethiopian Highlands a lengthening of LCPs due to the development of barriers resulting from gully erosion reliably amounts up to 15-30%. Moreover, median values take all values into account, including negative LCP values, the latter amounting to 11% to 30% of the values in the different sample units. As already discussed these values expressing shorter LCPs after the introduction of gullies as barriers usually coincide with a higher severity of the new pathway than the old one (Figure 6) and subsequently downplay our understanding of the change in LCPs by using strictly the median average results.

Gully erosion in the Ethiopian Highlands

The northern Ethiopian Highlands are part of the main African divide with Tekeze river draining into Nile river (Figure 1). The formation of the Ethiopian Highlands is part of the Tertiary formation of the Ethiopian–Yemen Plateau as well as Rift formation (Faccenna et al. 2019). Due to the strong relief the drainage network is deeply incised into the Ethiopian Highlands, forming the base level for erosion. Today, gullies are a permanent feature in the Ethiopian Highlands (Nyssen et al. 2004, Schütt et al. 2005). In order to understand for how long in history gullies have formed in the Ethiopian Highlands it can be assumed that the geological conditions were largely stable during settlement history. Paleo-environmental studies show that during much of the Holocene and in particular since mid-Holocene (ca. 5.6 cal kyr BP) climate in the Ethiopian Highlands was comparable to the current climate. Predominating climate since mid-Holocene had several semi-arid to dry-sub-humid phases with disperse vegetation cover under which gully erosion is more likely to take place (Bard et al. 2000, French et al 2009, Marshall et al. 2009, Nyssen et al. 2004, Pietch and Mechado 2014). Gullies can form under natural conditions especially considering disperse vegetation, slope gradient, and parent material (e.g. Panin et al 2009). However, their formation is accelerated under human impact on landscapes (Valentin et al. 2005). Gully erosion is initiated during heavy rainfall events when the shear stress at the parent material of a gully head is smaller than the shear stress caused by the running water (Valentin et al. 2005). In contrast, during moderate rainfall events runoff is not sufficient to transport the sediments to the outlet; in consequence, channels of gullies are characterized by alternating sections with strong channel bed accumulation and channel bed erosion. Resulting channel length-profiles show typical riffle-pools-sequences with decreasing frequency during channel development and concurrent formation of a concavity. Over time these processes result in a levelling of the gully topography

with a shape of older gullies characterized by flattened gully banks gullies, a flattened gully head and lower riffle-pool-frequency compared to a new gully (Leopold et al. 2020: 442-444, Vanwalleghem et al. 2005). In the Ethiopian Highlands various generations of gullies appear in parallel (Schütt et al. 2005, Nyssen et al. 2004, Pietch and Mechado 2014).

Based on the past climatic and environmental reconstructions and the tendency of gullies to develop under semi-arid to dry-sub humid climate, both older and more recent types of gullies in the Ethiopian Highlands may have been affected by pathways and in turn form obstacles for human movement (Figure 4, Figure 5). It is therefore highly probable that the proposed gullying-pathway mechanism occurred throughout much of human settlement history in the Ethiopian Highlands. Therefore, implications of the gully-pathway mechanism should be considered in archaeological and historical contexts (Pietsch and Machado 2014, Harrower et al. 2014, Samani et al. 2009).

Historical movement cost implications of gully erosion

Material culture shows that long distance exchanges are well dated into the 1st Millennium BC with the presence of Arabian architects, stonemasons and merchants in Tigray (Finneran 2007, Harrower and D'Andrea 2014, Japp et al. 2011). For the later Aksumite period (2nd century BCE-9th century CE), possible routes of exchanges and travel between Aksum and the port city of Adulis have been investigated using LCP analysis (Harrower and D'Andrea 2014). Results of the latter work generally support a 1st century CE documented account, the Periplus Maris Erythraei, suggesting an approximately eight-day travel time from Adulis to Aksum (Harrower and D'Andrea 2014). Considering a 15 % change of path lengths due to the development of gullies (Figure 5) and converting this into time units may imply in average 1.2 days of additional travel time during the 1st century CE. Additionally, most recent investigations on salt trade between the Ethiopian Highlands and locations across the Horn of Africa emphasizes the importance of inter-regional movement due to trade during the Aksumite period (Woldekiros 2019). Weighting up the effects of gully formation on the transport of goods depends on the way in which transport in the Ethiopian Highlands took place. Using packed animals such as donkeys has been suggested to take place in the Horn of Africa for the past 6000 years (Marshall 2007). While wheeled wagons were in partial use for 4000 years in Egypt and Mesopotamia and later vastly in ancient Rome (Rossi et al. 2016), whether due to lack of use or preservation bias, there are currently no archaeological evidence for wagon based good transportation in

Tigray during pre-Aksumite and Aksumite times (Fattovich 2010, Finneran 2007). Travelers through the Ethiopian Highlands most likely preferring packed animals for transportation because, at least before invention of sealed roads at the beginning of the 21st century, resistance for the use of simple wagons on the slopy and most likely badly maintained gravel roads was too high. In recent decades, the use of animal-drawn carts became more common in some parts of the Ethiopian Highlands mainly due to road modernization providing easier access to different areas (Kidanmariam 2000). The effect of gullies on transportation would slow both wheeled and animal packed goods transport, but would also highly vary between these two transport types. Moreover, as dominant features along and cutting through pathways, gullies may have affected decisions on which transportation is best to use in the dissected Ethiopian Highlands landscape. It has been suggested that in Ethiopia today, carts are able to carry up to ten times the load of that of pack-animals (Kidanmariam 2000). Since the Aksumite period until recently, ancient caravan activities using donkeys and camels as pack animal illustrate that crossing the Ethiopian Highlands is something large groups of humans did on a regular basis for millennia (Fattovich 2012, Woldekiros 2019),

While trade is dominant when considering the cost of movement, conveying wars - in particular since historical times - is deeply affected by the ability to quickly cross large terrains with full sized armies and in most cases with wheeled vehicles (Rossi et al. 2016). In the Ethiopian Highlands the Aksumite state, a millennium long political entity, had managed to remain independent despite nearby Nile based empires (Fattovich 2010). In modern African history, Ethiopians are proud to have avoided full scale colonisation. In 1896 the Italian army suffered a defeat in the battle of Adwa, a city located in Tigray (between Yeha (2) and Melazo (3) sample units). Later in 1935, using advanced military technology, the Italians managed to defeat the Ethiopian. However, may be due to complex topography and diverse ethnicity, the colonialist power never took hold of the county and suffered constant attacks by locals. In 1941 the allied forces led by the British defeated the Italians in the Horn of Africa and freed Ethiopia from Italian occupation. An important feature left from these five years of Italian rule are a network of roads across the Ethiopian Highlands which were constructed mainly to assist the occupation of Ethiopia (Bertazzini 2018, Milkias and Metaferia 2005). The millennium long Aksumite independence (1st millennium CE) despite more dominant rival neighbouring kingdoms, is due to a complexed set of natural, political and cultural reasons (Fatovich 2010, Finniran 2007), so does the failure of the Italian army to occupy the highlands in the late 19th century (González-Ruibal 2010). However, gullies, deterring large scale movement across the

Ethiopian Highlands should not be disregarded as a physical factor affecting these processes and events.

Additional social implications of gully erosion – an outlook

The dissection of the Ethiopian Highlands by gullies may have had an additional long-term effect on societies settling in the region. Based on archaeological evidences it is suggested that during the middle to late Holocene foragers groups co-existed in the Ethiopian Highlands alongside pastoral farmers (Fattovich 2010). Transition to complexed societies appeared in the Ethiopian Highlands, far later than in neighbouring today Egyptian and Sudanese territories, mostly along the Nile valley (Harrower and D'Andrea 2014). Since pre-Aksumite period the persistence of local traditions over external and multi-regional influences at least in Tigray lays evidence of a strong local culture (Fattovich 2012). From a socio-ecological perspective it has been argued that topography influences social structures by defining cultural boundaries through physical obstacles (Butzer 1982). It is also suggested that streams should be interpreted as natural properties as well as socio-cultural dimensions (Hussain and Floss 2016). Following these concepts, it is worth noting that both naturally occurring and human accelerated gullies may have influenced the landscape on a socio-evolutionary scale, contributing to more dissected Ethiopian Highlands with topographically bounded micro-environments. It is suggested that gullies of different age together with other topographic features, influenced the perception of territoriality. Such a dissected environment probably would impede external or multi-regional cultural trends and innovations to root (e.g. Kesler 2015, Zedeño 2016). This in turn would have encouraged more regional diversification, allowing different groups and practices to co-exist during the Holocene as well as strengthening the local over the regional as both are portrayed in the archaeological record.

6.6 Conclusions

Human movement and gully erosion are related to each other. Results of this study suggest that, for the Ethiopian Highlands, the more pathways develop, the more likely gullies are to occur in an area. If the cross profile of these gullies reaches dimensions of minimum 2 m depth and 2-3 m width, they obtain the characteristics of obstacles for movement of people. Consequently, humans will search for another pathway to continue moving and reach their destination while keeping the costs of movement as low as possible. This process will make their way longer when going around one or several topographical obstacles. When gullies result in deflection of pathways, this may lead to the creation of new gullies, subsequently forming a

feedback mechanism between the two. Moreover, former decisions for least cost pathways on the basis of given topography might be revised when new topographical obstacles develop, potentially resulting in the decision to include formerly avoided topographical barriers into the new pathway. This may possibly result in a shorter but more difficult pathway than the preceding one. In the Ethiopian Highlands, this relationship potentially impacted commerce and the exchange of goods, as well as large scale accessibility for military and other purposes. From a socio-cultural perspective, gullies may have contributed to a more diversified and sub-divided population in the Ethiopian Highlands, one that is less susceptible to external influences and trends as compared with nearby areas. As concepts of physical movement changed dramatically in recent decades, the gully-movement feedback mechanism in Tigray serves as an early example of the effect humans may have had on their natural environment.

Acknowledgements

Authority for Research and Conservation of Cultural Heritage (የቅርስ ባለስልጣን ተወካይ) of the Federal Democratic Republic of Ethiopia: Haileyesus Desta Ayalew, Tsegazeab Mezgebe and Haftum Birhane. We would like to express our deep sympathy for our partners in Tigray in hopes for a quick end to the current conflict. Universität Leipzig: Dietrich Raue; DAI: Iris Gerlach, Kristina Pfeiffer and Sarah Japp; Freie Universität Berlin: Fabian Becker, Sonja Bepita, Robert Busch, Vincent Haburaj, Wilhelm F. Hardt, Silvan Schmieg; MONREPOS: Ariel Malinsky-Buller; proofreading: Zack Rothbart; We would like to thank the editor and anonymous reviewers for their valuable comments; High-Performance Computing Cloud of Freie Universität Berlin.

d

Chapter 7

Synthesis: Footprints across time and space

Footpaths and unpaved roads have been created by most humans on this planet. This makes practically all of us active agents in the formation of this human landscape. The environmental imprint we make simply by walking can result in long-termed residues on the landscape. Some of these residues are expected and have in this work been qualitatively and semi-quantitively confirmed. Such is the case for the effect of footpath-trampling on porosity.

7.1. The mechanics of footpath trampling

Undisturbed micromorphological samples of footpath surfaces were taken in nine footpaths and a total of twelve locations: Three in eastern Germany, four in Tigray (Ethiopia), and five in the Judean Desert (Israel). Some common features are evident for all recreational (eastern Germany and the Judean Desert), agricultural (Tigray), and 'abandoned' i.e., historically used (the Judean Desert and Tigray) footpaths, of the different climatic zones and geological settings.

One striking and expected common feature to all is the reduction of pore space under footpath surfaces compared with their control samples. In the temperate zone under recreational use in eastern Germany, the differences between the three footpath samples and their controls appear to be the most convincing. In the smallest magnification, i.e., where the largest voids are detectable, the reduction of pores in footpaths compared with their control samples was significant for the entire 5 cm below the surface. In Tigray, one modern footpath was sampled from the surface and two likely historical (and incised) footpaths were sampled from ca. 5-10 cm below the surface to reflect the possible historical surface. There too, a similar reduction of porosity was evident while comparing multiple regional control samples to each corresponding footpath. In order to understand the process responsible for this observation, it is valuable to reflect on the type of voids and microstructure under footpath surfaces compared with those in the control samples. Footpath samples from temperate Berlin are generally with finer grains and a more massive microstructure, as opposed to the looser organization of the surfaces of their control samples, which serves as evidence of the effect of direct trampling pressure. In the urban park sample (Berlin) clays are oriented parallel on the border of the larger grains (speckled b-fabric), presumably also due to direct pressure from trampling. The latter clay compaction could also be responsible for increased clay content in the urban park footpath sample, making it browner than its grayer (sandier) control sample. Similarly, in the Ore

Mountains site, the footpath sample exhibits a massive microstructure of clayey-silty micromass as opposed to the granules-to-crumbs-microstructure of the control sample. Similarly, more massive microstructures are evident in the footpath samples from Tigray (Ethiopia) compared to the more bedded and open structures of the regional references. However, in the case of the Daraga footpath, which is a clayey to silty sample, no such pattern was observed.

Another structural feature distinguishing footpaths from their surroundings is the general pattern of the footpaths' sub-surfaces. The 5-10 cm below the surface of footpaths are rather of a sedimentary nature compared to the generally more pedogenically influenced control samples. For many footpath micromorphological samples, bedded and massive microstructures with clear contacts between them were evident as opposed to the more diffuse or bioturbated control samples. The latter observation was made for the footpath in the Ore Mountains forest, for a currently used and one likely historical footpath in Tigray, and for a currently used footpath in the Judean Desert.

The change in the types of voids also points to the effect of direct pressure. In eastern Germany, planes in the control samples are replaced by vughs in the corresponding footpath samples, i.e., the truncation of planes due to pressure. In the samples of Tigray, channels dominate the control samples in compared to footpath samples where they are relatively reduced. In the latter, planes are evident to a greater extent, indicating a more angular structure of the elongated voids due to pressure. In the Judean Desert, the microstructure of footpaths and control samples is generally massive to complex, i.e., it is difficult to distinguish between both. Additionally, a significant decrease in porosity in the three arid footpath samples compared with their control samples was limited to the upper 0.1 cm below the surface. Therefore, deeper and more structural effects of pressure due to trampling are documented for the samples originating from eastern Germany and Tigray than those observed in the samples from the Judean Desert. This difference may be caused by the severity of trampling is dependent on the humidity of the soil surface. However, other mechanisms responsible for the long-term effects of footpath formation could also explain these observations. One of these mechanisms is related to the interaction between the biological and mineralogical components of the soil.

7.2 The organic component

Similar to the decrease in porosity, the reduction of vegetation is an intuitively expected outcome of footpath forming processes that have been confirmed in this work. The effect of such reduction is best evident where vegetation is otherwise abundant. In the samples from the

temperate zone, especially within the forests of Berlin-Grunewald and the Ore mountains, soil horizons evident in the control samples are reduced under footpaths. Additionally, organic material composition is different between the footpath and control samples of temperate eastern Germany. In the Ore mountains forest, an O horizon dominated the control sample while it was either eroded or had not been developed in the footpath sample. This is likely due to the earlier mentioned lower porosity of the surface, hindering plant rooting and promoting surface overland flow that can erode any flora that may have managed to set root through the compacted footpath surface. In the forest of Berlin-Grunewald, a thin O horizon and an A horizon were evident in the control sample while large organic leaves and roots were evident only under the footpath surfaces. The process behind this is likely the forest litter that is trampled on and with the lower porosity, the supply of oxygen and water are limited causing the burial and fresh preservation of organic matter. In the sub-humid to semi-arid Ethiopian Highlands, no distinct difference in the organic components between footpaths and non-footpaths was observed. This supports the argument that where vegetation cover is low or where morpho dynamics are high, such a difference will be difficult to recognize. However, in the arid Judean Desert, the natural bioturbation and cement-forming activities of leaches and mosses seemed to be reduced or somewhat affected by the formation of footpaths. The reduction in biogenic activities in the desert was most striking in the currently used footpath sample, where a clear difference between the footpath and control samples was observed. However, the Roman period and Early Bronze Age footpath samples were too, exhibiting a change in bioturbation and bio-cementing to various degrees compared with their corresponding control samples. The process could be explained by the interference of typical desert soil crust formation by footpaths. The formation of soil crust and “desert pavement” requires stability and a degree of the fine fraction that is usually of aeolian or reworked aeolian origin. By trampling the soil crust, compacting the surfaces, and increasing surface overland flow, footpath formation mechanically removes and further hinders the stability needed for bioturbation and bio-cementing.

7.3 The inorganic component

Apart from Fe oxides, minerals observed under the footpaths were generally indistinguishable from those in the control samples (or for Tigray the regional references). Fe oxides were most visible as nodules or through more intense red and yellow colors of the micromass and were microscopically confirmed through OIL. Iron oxides were at times more dominant in the footpaths of the temperate and sub-humid zones, compared with their control samples. As Fe

oxides are closely related to pedogenesis processes, a further investigation of their abundance was conducted by Fe extraction using three different methods. Comparing the upper 5 cm of the soils (the surface), footpaths in both temperate and sub-humid zones had higher SRO Fe oxides compared with their controls. On the contrary, most of the footpath sub-surface (5-10 cm deep) samples, showed a higher abundance of SRO Fe oxides in the control samples than that in the footpaths. This difference could be explained by a process of water saturation on the surface of footpaths, i.e., puddles. After rain events, many of us have witnessed puddles forming on footpath surfaces but less so outside them, in cases of natural surroundings. This is likely due to the reduction of the pores which in turn promotes water stagnation. Fe is reduced and later Oxidized on the surfaces of footpaths generating more SRO pedogenic Fe oxides, while it is for the same reason lower in the sub-surface of footpaths. Such changes in the availability of mobile Fe on the soil surface can affect soil acidity. However, although such trends were observed for footpaths in the temperate zone, the difference in pH levels between footpaths and control samples was insignificant. Further effects of SRO Fe oxides abundance is on other properties of the soil (including C and N). This process is due to the elementary adsorption properties and the molecular surface of Fe oxides which can increase the abundance of several minerals and organic components and form a stable ternary phase with more than a dozen elements. Beyond these general trends, a phenomenon that is unique to urbanized areas is the higher amounts of Pb on footpath surfaces. This is either due to Pb pollution being better preserved under the compacted anoxic and dry footpath surfaces than in the better-drained control samples or to the lack of stable ternary phase of Pb with Fe oxides. As divers the effects on the sub-surface may be, much of the ecological fingerprints of footpaths are above the ground and off-site, i.e., as changes in the surface colors, local hydrological and geomorphological dynamics.

7.3. Surface colors

Following local observations, the hypothesis that the surfaces of trails in the Judean Desert are brighter than those of their surroundings was tested. Bulk sample analyses revealed that blue and green colors are more dominant in footpath samples than in the control samples while the red color was higher in control samples. This difference could be due to the bioturbation and cement-forming activities generating a darker and redder crust, which were observed to be more dominant off-site the footpaths than at the footpaths themselves. Another observation were the differences in brightness, as samples extracted from footpaths were brighter than the non-footpath control samples. Testing this hypothesis using UAV imagery produced similar

patterns. Reflection by radiation in the blue and green lights was higher at the surface of the three tested footpaths while reflection by radiation in the red light was also higher on the footpaths but to a lesser extent than for the other two colors. A calculation of the albedo values revealed a significantly higher albedo on the surfaces of footpaths than off-site the trails. The process likely responsible for a high albedo is a combination of three factors. First is the abrasion of the limestone by trampling that removes the patina from the gravel and pebbles. Second is the above-mentioned formation of soil crust and 'desert pavement' that has shown to have a thin layer of finer fraction, one that was correlated with Fe rather than calcium. The third reason is an artefact introduced by the method of UAV imagery where the larger boulders that are evident only outside the trails shadow their adjacent surfaces producing darker color values and lower albedo. The higher albedo values along the footpaths could promote a cooling effect on the microenvironment of the footpath itself..

7.4. Geomorphological dynamics and antiquity

Industrialization, deforestation, reforestation, and monoculture agriculture has resulted in vast changes of the central European landscape during recent centuries. The formation of these recent human landscapes challenges any attempt to attribute a specific geomorphological feature to one localized factor such as a footpath. Therefore, footpaths located in eastern Germany were excluded from examining of the geomorphological dynamics of trails. For the Judean Desert and the Ethiopian highlands, trails reveal three main types of interaction with linear soil erosion. Firstly, and the more commonly, is the initiation of gullies downslope from trails. Using Frequency Ration (FR) analysis, pathways have been shown to be a factor responsible for the location of gullies. Coupled with the observation that gullies are occurring directly downslope from trails following surface runoff that is promoted by path compaction, the FR analysis confirms that pathways are to some extent responsible to the occurrence of gullies. However, these trails were not as important of a factor as other commonly referred to inputs such as slope gradient, lithology, stream power index or elevation. Following the validation of this process, possible implication for both agricultural and recreational trails are to strengthen the ongoing attempts to redirect drainage along pathways, especially for paths running on hillslopes and on steep slope angels. For locating archaeological trails, gullies occurring downslope could be used as a tool to date pathways by applying OSL dating method using sediments accumulated on the fan of the gully. Additionally, while searching for acient pathways and recognizing a set of gullies that initiate along a slope line without any particular geomorphological reasoning, this could be possibly due to an older trail that is no longer

visible. After validating a possible occurrence of such a trail using UAV and/or on ground survey, the age of the footpath could similarly be evaluated using OSL dating method on the sedimentary outlets of the downslope occurring gullies.

A second type of linear soil erosion is the incision of the path itself. It has been shown in this work, that footpaths that are incised, usually follow the direction of the stream network while non incised footpaths do not. The likely process behind this observation is related to the basic formation of the streams, i.e., drainage is a function of the underlying geological structure, and an incised footpath could be described as a footpath turned stream. Additionally, footpaths that are incised, are less likely to have gullies generated downslope from their surface. The latter observation is due to the water runoff incising the path itself rather than forming overbank flow and initiating a gully downslope and perpendicular to the path. Consider the sedimentary yield, (destructive) water current energy, and cutback abilities of a gully that can reach a depth and width of several meters, as opposed to those of a 10-50 cm deep and 50-100 cm wide incised trail, the latter is likely to be more sustainable for the local geomorphological and hydrological dynamic then the former. Therefore, possible implementation of these combined observations could include a calculation of recreational and agricultural trails directions on slopy environments. Even the slight redirection of a path angel to make it more similar to the local stream network could potentially have hydrological results changing the course of water flow and incising the path itself.

A third type of interaction between trails and linear soil erosion is the cutting-off of the trail by gullies or streams. In the Judean Desert, the > 7-m truncation of the Roman-attributed trail by the active stream has been a clear tool for establishing the abandonment of this trail at least since the formation of the currently active riverbed. Therefore, in some cases geomorphology can serve as a legitimate dating method for human landscape features, similar to other relative chronologies. In Tigray, however, where morphodynamics during the past century have been very high, gullies have been seen truncating unpaved roads and footpaths in various environments. A methodological experiment was therefore conducted to assess the effect of deep gullies as a feature that blocks pathways completely and with it the ability of humans (and likely other animals) to move across the landscape. The experiment based on 8000 random Least Cost Paths (LCPs) which crossed a total of four 10x10-km sample units, which were recalculated following the implementation of the mapped gullies as barriers. The change that had occurred after the gullies were introduced led in some cases to a more than 30% increase

in a LCP length. The obvious explanation is that humans would have to walk longer to make the detour required to cross this obstacle, i.e., the gully. Surprisingly, in several cases the LCP became shorter following the introduction of gullies as berries. Several tests shown that the process behind this is the selection of a shorter but steeper rout that otherwise would have not been taken. Meaning the LCP might be shorter but one that would require more energy. Interestingly this decision by the algorithm could also reflect human decision-making process.

Taking all three types of geomorphological interactions into account, a socio-environmental process could be portrayed. We as humans have been and are still creating paths by our movement, promoting lower permeability, and generating surface runoff. Sometimes these contribute to the initiations of gullies downslope from the trail or to the incision of the path itself. When a gully is formed, its head can retreat and cutback on the very trail that contributed to its formation. Following this, humans would look for another path, a new one, sometimes prolonging their way in the course of doing so. After one or several rain events, a gully could be initiated downslope from the new trail, starting a similar cycle and resulting in a feedback mechanism between human movement and gully erosion. If we further consider deep gullies as barriers to human movement that are more than able to dissect the landscape, a different social interpretation could arise. On an historical scale, in areas with high morpho dynamics if agricultural practices of any type of land use changes including pathways promote more gully erosion, the latter can result in the community being more inclined to remain in their micro locality as they are repeatedly challenged by the appearance of gullies, contributing to a strong local culture as has been evident in the Ethiopian highlands. Another possibility is that these barriers would encourage the emergence of better technologies i.e., bridges, erosion protection measurements.

.5 A toolkit

Trying to examine the formation of trails as a widespread phenomenon across time and space in an experimental manner (rather than, for example, by a literature review) has proven to be both challenging and insightful. Such an investigation requires approaches of different scales and disciplines. Therefore, in order to understand the long-term ecological effects footpaths produce under different land uses and climatic zones, several tools have been adopted. Some of these tools have been more suitable than others. For compiling a toolkit to investigate footpaths in both archaeological and ecological contexts, the following tools are recommended:

1. Geomorphological mapping using UAV or high-resolution satellite imagery in a GIS environment and processing in R environments - taking linear soil erosion as indicators for the former location or effects of trails
2. Examining soil resistance using a penetrometer
3. Elemental analysis of subsurface sampled from different depths
4. Color analysis- analysing UAV images and applying field spectrometer on-site of soil surfaces or off-site to soil samples
5. Pedogenic Fe dissolution using Oxalic Acid for SRO Fe analysis (ICP)
6. Micromorphological vertical sampling of the surface or assumed historical surface
7. Micromorphological image analysis using an R environment to estimate soil porosity

Other methods looking at soil parameters, soil texture and soil mineral composition were useful, but they did not produce independent results that clearly differentiated footpath from non-footpath environments. Similarly, micromorphological observations and interpretations have been valuable as supportive evidence for the above-listed approaches and instruments.

7.6 Final notes

Pathways, and footpaths in particular, have been changing our landscapes under our very feet as well as above ground. The mechanics behind footpath trampling were studied using multiple methods to expose the resulting changes in the organic and inorganic components of soils, the surface colors of soils and the affected geomorphological and social dynamics (figure 7.1). These changes have been investigated in different continents under various climates and trail uses. The qualitative approach adopted in this work leaves a pathway for further quantitative research to follow, as well as several practical suggestions for possible archaeological and ecological implementations.

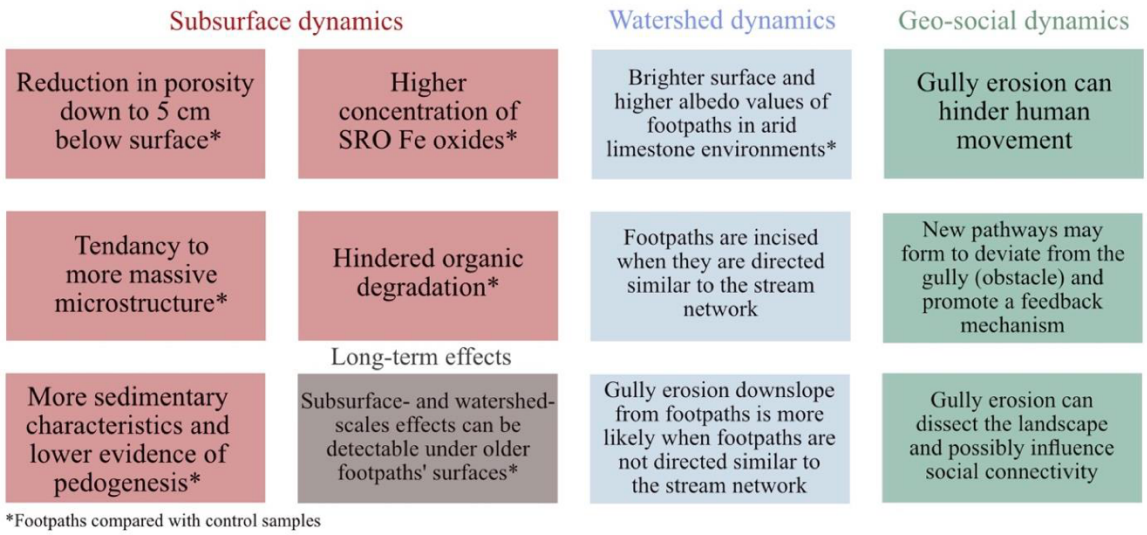

Figure 7.1 The thesis concluding chart incorporates the overall results and processual conclusions deriving from this research.

Chapter 8

8.1 Bibliography

Addisie, M. B., et al. (2018). Assessment of practices for controlling shallow valley-bottom gullies in the sub-humid Ethiopian highlands. Water 10(4): 389.

Agostinelli, C. and U. Lund (2013). R package 'circular': Circular Statistics (version 0.4-7). URL https://r-forge. r-project. org/projects/circular.

Aharoni, Y. and B. Rothenberg (1960). In the Foosteps of Kings and Rebels in the Judean desert. Massada, Tel Aviv.

Ahnert, F., et al. (1965). Fluvial Processes in Geomorphology. Geographical Review 55(3): 452.

Alberti, G. (2019). movecost: An R package for calculating accumulated slope-dependent anisotropic cost-surfaces and least-cost paths. SoftwareX 10: 100331.

Ambrose, S. H. (2001). Paleolithic technology and human evolution. Science 291(5509): 1748-1753.

Amiran, R. and O. Ilan (1978). Early Arad: the chalcolitic settlement and early bronze city.

Angus, I. (2015). When Did the Anthropocene Begin... and Why Does It Matter? Monthly Review 67(4): 1.

Arabameri, A., et al. (2020). Evaluation of Recent Advanced Soft Computing Techniques for Gully Erosion Susceptibility Mapping: A Comparative Study. Sensors 20: 2.

Arabameri, A., et al. (2019). Comparative assessment using boosted regression trees, binary logistic regression, frequency ratio and numerical risk factor for gully erosion susceptibility modelling. CATENA 183: 104223.

Arabameri, A., et al. (2018). GIS-based gully erosion susceptibility mapping: a comparison among three data-driven models and AHP knowledge-based technique. Environmental Earth Sciences 77(17).

Arnay, R., et al. (2021). Soil micromorphological image classification using deep learning: The porosity parameter. Applied Soft Computing 102: 107093.

Asfaha, T., et al. (2021). Status of cropping in the wider surroundings of Mekelle (Tigray, Ethiopia). an Asmi; Othman, N.; Zain, M. MdZ; Ab Wahid, M : A Study on Human Foot Pressure Behaviour and Balancing Characteristics 884: 1.

Ashkenazi, E., et al. (2021). Poplar trees in Israel's desert regions: Relicts of Roman and Byzantine settlement. Journal of Arid Environments 193: 104574.

Asmi, a., et al. (2020). A Study on Human Foot Pressure Behaviour and Balancing Characteristics. IOP Conference Series: Materials Science and Engineering 884(1): 012001.

Asrat, A., et al. (2003). Magma emplacement and mafic–felsic magma hybridization: structural evidence from the Pan-African Negash pluton, Northern Ethiopia. Journal of Structural Geology 25(9): 1451-1469.

Asscher, Y. and Y. Goren (2016). A Rapid On-Site Method for Micromorphological Block Impregnation and Thin Section Preparation. Geoarchaeology 31(4): 324-331.

Aune, J. B. and T. Berg (1997). Project Review of Rama Integrated Rural Development Programme. Ethiopia, Tigray.

Ayres, E., et al. (2008). Effects of human trampling on populations of soil fauna in the McMurdo Dry Valleys, Antarctica. In Conservation biology : the journal of the Society for Conservation Biology 22(6): 1544-1551.

Babel, U. (1975). Micromorphology of soil organic matter. Soil components, Springer: 369-473.

Bagheri, I., et al. (2012). Effect of Compaction on Physical and Micromorphological Properties of Forest Soils. American Journal of Plant Sciences 03(01): 159–163.

Bailey, G. N. and I. Davidson (1983). Site exploitation territories and topography: Two case studies from palaeolithic spain. Journal of Archaeological Science 10(2): 87-115.

Baker, V. R. (1996). Hypotheses and geomorphological reasoning. The scientific nature of geomorphology: 57-85.

Baker, V. R. and C. R. Twidale (1991). The reenchantment of geomorphology. Geomorphology 4(2): 73-100.

Ballantyne, M. and C. M. Pickering (2015). The impacts of trail infrastructure on vegetation and soils: Current literature and future directions. Journal of Environmental Management 164: 53-64.

Balter, M. (2010). The tangled roots of agriculture, American Association for the Advancement of Science.

Bar-Adon, P. and Z. Greenhut (1989). Excavations in the Judean Desert. 'Atiqot: Hebrew Series/8-*1 :עתיקות: סידרה עברית*.

Bar-Yosef, O. (1986). The walls of Jericho: an alternative interpretation. Current Anthropology 27(2): 157-162.

Barbosa, H., et al. (2018). Human mobility: Models and applications. Physics Reports 734: 1-74.

Barbosa, H., et al. (2018). Human mobility: Models and applications. Physics Reports 734: 1-74.

Bard, K. A., et al. (2000). The environmental history of Tigray (Northern Ethiopia) in the Middle and Late Holocene: a preliminary outline. African Archaeological Review 17(2): 65-86.

Barros, A. and C. M. Pickering (2015). Impacts of experimental trampling by hikers and pack animals on a high-altitude alpine sedge meadow in the Andes. Plant Ecology & Diversity 8(2): 265-276.

Bartkowiak, A., et al. (2017). Evaluation of the content of Zn, Cu, Ni and Pb as well as the enzymatic activity of forest soils exposed to the effect of road traffic pollution. Environmental Science and Pollution Research 24(30): 23893–23902.

Batey, T. (2009). Soil compaction and soil management--a review. In Soil Use and Management 25(4): 335-345.

Baumann, C., et al. (2020). Fox dietary ecology as a tracer of human impact on Pleistocene ecosystems. PloS one 15(7): e0235692.

Beard, C. A. (1929). The Duk-Duks. By Elizabeth Ann Weber. (Chicago: University of Chicago Press. 1929. Pp. xix, 142.) - Civic Training in Soviet Russia, By Samuel N. Harper. (Chicago: University of Chicago Press. 1929. Pp. xvii, 401.) - Great Britain: A Study of Civic Loyalty. By John M. Gaus. (Chicago: University of Chicago Press. 1929. Pp. xxi, 329). American Political Science Review 23(4): 1005-1007.

Belachew, P. H. D. (2020). Hydrological Processes and Control of Gully Erosion in a Watershed in the Sub Humid Highlands of Ethiopia.

Bell, M. and J. Leary (2020). Pathways to past ways: a positive approach to routeways and mobility. Antiquity: 1349–1359.

Bennett, S. J., et al. (2000). Characteristics of actively eroding ephemeral gullies in an experimental channel. Transactions of the ASAE 43(3): 641.

Bennett, S. J., et al. (2000). Characteristics of actively eroding gullies in an experimental channel. Transactions of the ASAE 43: 3.

Bent, J. T. (1893). The ancient trade route across Ethiopia. The Geographical Journal 2(2): 140–146.

Berhane, A., et al. (2020). Trends in extreme temperature and rainfall indices in the semi-arid areas of Western Tigray, Ethiopia. Environmental Systems Research 9(1).

Berkofsky, L. (1976). The effect of variable surface albedo on the atmospheric circulation in desert regions. Journal of Applied Meteorology and Climatology 15(11): 1139-1144.

Berlin, G. ATKIS DGM 1, Digital terrain model of Berlin: dl-de/by-2-0. from https://www.stadtentwicklung.berlin.de/geoinformation.

Berna, F., et al. (2007). Sediments exposed to high temperatures: reconstructing pyrotechnological processes in Late Bronze and Iron Age Strata at Tel Dor (Israel). Journal of Archaeological Science 34(3): 358–373.

Bernhardt-Römermann, M., et al. (2011). Functional traits and local environment predict vegetation responses to disturbance: a pan-European multi-site experiment. Journal of Ecology 99(3): 777–787. Journal of Ecology 2011.99:777-787

Bertazzini, M. C. (2018). The long-term impact of Italian colonial roads in the Horn of Africa. 1935-2000.

Bertazzini, M. C. (2021). The long-term impact of Italian colonial roads in the Horn of Africa, 1935–2015. Journal of Economic Geography 22(1): 181-214.

Beven, K. J. and M. J. Kirkby (1979). A physically based, variable contributing area model of basin hydrology / Un modèle à base physique de zone d'appel variable de l'hydrologie du bassin versant. Hydrological Sciences Bulletin 24(1): 43-69.

Beyth, M. (1971). The geology of central and western Tigray. Unpublished Report. A. A. Eigs. P. ed., 2015. Landscapes and landforms of Ethiopia. Springer, Billi.

Beyth, M. (1972). The geology of central and western Tigre, Ethiopia. Unpublished Ph. D. dissertation, University of Bonn, Germany.

Bigham, J. M., et al. (2002). Iron oxides. Soil mineralogy with environmental applications 7: 323–366.

Billi, P. (2015). Geomorphological Landscapes of Ethiopia. World Geomorphological Landscapes, Springer Netherlands: 3-32.

Binford, L. R., et al. (1985). Taphonomy at a distance: Zhoukoudian, the cave home of Beijing Man?[and comments and reply]. Current Anthropology 26(4): 413-442.

Birkeland, P. W. (1984). Soils and geomorphology, Oxford university press.

Bivand, R. S., et al. (2013). Classes for Spatial Data in R. Applied Spatial Data Analysis with R, Springer New York: 21-57.

Blum, P. (1997). Physical properties handbook: a guide to the shipboard measurement of physical properties of deep-sea cores.

Blumfield, T. J., et al. (2005). Mineral nitrogen dynamics following soil compaction and cultivation during hoop pine plantation establishment. Forest Ecology and Management 204(1): 131–137.

Boardman, J. (2013). The hydrological role of `sunken lanes' with respect to sediment mobilization and delivery to watercourses with particular reference to West Sussex, southern England.

Bresson, L. J. S. Sediments. M.; Zambaux, C. (1990) Micromorphological study of compaction induced by mechanical stress for a Dystrochreptic Fragiudalf. In Developments in soil science, vol. 19 , pp. 33--40, Elsevier: 1636-1644.

Boardman, J. (2022). Footpath erosion: assessment, extent and impacts with especial reference to the UK. Geography 107(2): 60-69.

Boardman, J. (2022). Sunken lanes in southern England: A review. Proceedings of the Geologists' Association.

Boaretto, E. (2009). Dating materials in good archaeological contexts: the next challenge for radiocarbon analysis. Radiocarbon 51(1): 275-281.

Bocco, G. (1991). Gully erosion: processes and models. Progress in physical geography 15(4): 392-406.

Boelhouwers, J. and T. Scheepers (2004). The role of antelope trampling on scarp erosion in a hyper-arid environment, Skeleton Coast, Namibia. Journal of Arid Environments 58(4): 545-557.

Borrelli, P., et al. (2017). An assessment of the global impact of 21st century land use change on soil erosion. Nature communications 8(1): 1–13.

Botta, G. F., et al. (2020). Effect of cattle trampling and farm machinery traffic on soil compaction of an Entic Haplustoll in a semiarid region of Argentina. Agronomy Research 18(S2): 1163–1176.

Brandolini, P., et al. (2006). Geomorphological hazard and tourist vulnerability along Portofino Park trails (Italy). Natural hazards and Earth system sciences 6(4): 563-571.

Breitbarth, A., et al. (2019). Measurement accuracy and dependence on external influences of the iPhone X TrueDepth sensor. Photonics and Education in Measurement Science 2019, SPIE.

Bresson, L. M. and C. Zambaux (1990). Micromorphological study of compaction induced by mechanical stress for a Dystrochreptic Fragiudalf. Developments in soil science, Elsevier. 19: 33–40.

Breton, J.-F. (2011). Relations between Ethiopia and South Arabia: problems of architecture. Annales d'Ethiopie 26(1): 53–77.

Brewer, R. and J. Sleeman (1960). Soil structure and fabric: their definition and description. Journal of Soil Science 11(1): 172-185.

Buchanan, B. P., et al. (2014). Evaluating topographic wetness indices across central New York agricultural landscapes. Hydrology and Earth System Sciences 18(8): 3279-3299.

Buchwa, A. and J. Fidelus (2008). The development of erosive and denudational landforms on footpaths sections in the Babia G□ra Massif and the Western Tatras. Geomorphologia Slovaca et Bohemica 2: 14-24.

Buchwał, A. and M. Rogowski (2010). The methods of preventing trail erosion on the examples of intensively used footpaths in the Tatra and the Babia Góra National Parks. Geomorphologia Slovaca et Bohemica 10(1): 7-15.

Busch, R. (2020). Gully-susceptibility model, determining the human influence on the local landscape in northern Tigray, Ethiopia.

Busch, R., et al. (2021). Modeling gully erosion susceptibility to evaluate human impact on local landscape dynamics in Tigray, Ethiopia. Remote Sensing 13(7).

Butzer, K. W. (1982). Archaeology as human ecology: method and theory for a contextual approach, Cambridge University Press.

Butzer, K. W. (2005). Environmental history in the Mediterranean world: cross-disciplinary investigation of cause-and-effect for degradation and soil erosion. Journal of Archaeological Science 32(12): 1773–1800.

Butzer, K. W. and G. H. Endfield (2012). Critical perspectives on historical collapse. Proceedings of the National Academy of Sciences of the United States of America 109(10): 3628–3631.

Calvet, M., et al. (2021). Denudation history and palaeogeography of the Pyrenees and their peripheral basins: an 84-million-year geomorphological perspective. Earth-Science Reviews 215: 103436.

Cao, C., et al. (2018). Measuring landscape albedo using unmanned aerial vehicles. Remote Sensing 10(11): 1812.

Cao, L., et al. (2021). Variations in rill morphology on unpaved road surfaces and their controlling factors. Earth Surface Processes and Landforms.

Caraman, P. (1985). The Lost Empire: The Story of the Jesuits in Ethiopia, 1555-1634, Sidgwick & Jackson London.

Carleton, W. C. and M. Collard (2020). Recent major themes and research areas in the study of human-environment interaction in prehistory. Environmental Archaeology 25(1): 114-130.

Certini, G. and R. Scalenghe (2022). The crucial interactions between climate and soil. Science of The Total Environment: 159169.

Charbonnier, M.-C. and C. Cammas (2018). Characterization of Gallo-Roman roads in northern France using micromorphological methods. Quaternary International 483: 194-210.

Chase, A. F., et al. (2012). Geospatial revolution and remote sensing LiDAR in Mesoamerican archaeology. Proceedings of the National Academy of Sciences 109(32): 12916-12921.

Chen, C., et al. (2020). Iron-mediated organic matter decomposition in humid soils can counteract protection. Nature communications 11(1): 1–13.

Chenhao, X., et al. (2019). Response and Simulation of Vegetation in Desert Scenic Spot to Tourists' Trampling Disturbance. Cross-Cultural Communication 15(4): 15-24.

Cherry, J. F., et al. (1991). Landscape archaeology as long-term history. Nothern Keos in the Cycladic Islands. Los Angeles: Institute of Archaeology, University of California.

Christensen, P. R. (2003). Formation of recent martian gullies through melting of extensive water-rich snow deposits. Nature 422(6927): 45-48.

Clapham, C. (2019). The Political Economy of Ethiopia from the Imperial Period to the Present. The Oxford Handbook of the Ethiopian Economy, Oxford University Press: 32-47.

Clark, J. S., et al. (2009). Soil microbial community response to drought and precipitation variability in the Chihuahuan Desert. Microbial ecology 57(2): 248-260.

Clevis, Q., et al. (2006). Geoarchaeological simulation of meandering river deposits and settlement distributions: A three-dimensional approach. Geoarchaeology: An International Journal 21(8): 843-874.

Cohen, H. and J. B. Laronne (2005). High rates of sediment transport by flashfloods in the Southern Judean Desert, Israel. Hydrological Processes: An International Journal 19(8): 1687-1702.

Cole, D. N. (1990). Trampling disturbance and recovery of cryptogamic soil crusts in Grand Canyon National Park. The Great Basin Naturalist: 321-325.

Cole, D. N. (2004). Impacts of hiking and camping on soils and vegetation: a review. Environmental impacts of ecotourism 41: 60.

Coleman, D. C., et al. (2017). Fundamentals of soil ecology, Academic press.

Collins, K. t. and A. McGown (1974). The form and function of microfabric features in a variety of natural soils. Geotechnique 24(2): 223-254.

Coltorti, M., et al. (2007). Planation surfaces in Northern Ethiopia. Geomorphology 89(3-4): 287-296.

Connan, J., et al. (1992). Molecular archaeology: Export of Dead Sea asphalt to Canaan and Egypt in the Chalcolithic-Early Bronze Age (4th-3rd millennium BC). Geochimica et Cosmochimica Acta 56(7): 2743-2759.

Conrad, O., et al. (2015). System for Automated Geoscientific Analyses (SAGA) v. 2.1.4. Geoscientific Model Development 8(7): 1991-2007.

Contenson, H. d. (1961). Les fouilles \`a Haoulti-Melazo en 1958. In Annales d' \'E thiopie (1: 39-60.

Contenson, H. d. (1963). Les fouilles de Haoulti en 1959 - Rapport pr□liminaire. Annales 39: 41-86.

Contenson, H. d. (1981). Pre-aksumite culture. UNESCO general history of Africa 2: 341–361.

Coop, G., et al. (2009). The role of geography in human adaptation. PLoS genetics 5(6): e1000500.

Coulon, E. and A. Bruand (1989). Effects of compaction on the pore space geometry in sandy soils. Soil and Tillage Research 15(1-2): 137–151.

Courty, M. A., et al. (1989). Soils and micromorphology in archaeology. Cambridge: Cambridge.

Coward, E. K., et al. (2017). Iron-mediated mineralogical control of organic matter accumulation in tropical soils. Geoderma 306: 206–216.

Crandell, O. (2020). A probabilistic method for Least Cost Path calculation. Peer Community in Archaeology 1: 100005.

Crawford, O. G. S. (2019). Ethiopian Itineraries Circa 1400-1524: Including Those Collected by Alessandro Zorzi at Venice in the Years 1519-24, Routledge.

Croft, D. B. (2019). Walking in Each Other's Footsteps: Do Animal Trail Makers Confer Resilience against Trampling Tourists? Environments 6(7): 83.

Croix, S., et al. (2019). Single context, metacontext, and high definition archaeology: Integrating new standards of stratigraphic excavation and recording. Journal of Archaeological Method and Theory 26(4): 1591-1631.

Curtis, M. C. (2009). Relating the Ancient Ona Culture to the Wider Northern Horn: Discerning Patterns and Problems in the Archaeology of the First Millennium BC. African Archaeological Review 26(4): 327-350.

d'Oleire-Oltmanns, S., et al. (2012). Unmanned aerial vehicle (UAV) for monitoring soil erosion in Morocco. Remote Sensing 4(11): 3390-3416.

Dagnew, D. C., et al. (2017). Effects of land use on catchment runoff and soil loss in the sub-humid Ethiopian highlands. Ecohydrology & Hydrobiology 17(4): 274-282.

Dagnew, D. C., et al. (2015). Impact of conservation practices on runoff and soil loss in the sub-humid Ethiopian Highlands: The Debre Mawi watershed. In Journal of Hydrology and Hydromechanics 63 ,(3): 210-219.

Dagnew, D. C., et al. (2015). Impact of conservation practices on runoff and soil loss in the sub-humid Ethiopian Highlands: The Debre Mawi watershed. Journal of Hydrology and Hydromechanics 63(3): 210–219.

Dalrymple, J. (1958). The application of soil micromorphology to fossil soils and other deposits from archaeological sites. Journal of Soil Science 9(2): 199-209.

David, L., et al. (2011). Geological and geomorphological problems caused by transportation and industry. Open Geosciences 3(3): 271–286.

Davidovich, U. (2013). The Chalcolithic-Early Bronze Age Transition: A View from the Judean Desert Caves, Southern Levant. Paléorient: 125-138.

Davidovich, U. (2014). The Judean Desert during the Chalcolithic, Bronze and Iron Ages (sixth–first millennia BCE): desert and sown relations in light of activity patterns in a defined desert environment. Unpublished PhD dissertation, The Hebrew University.

Davison, W. (1993). Iron and manganese in lakes. Earth-Science Reviews 34(2): 119–163.

de Contenson, H. (1961). Les fouilles à Haoulti-Melazo en 1958. Annales d'Ethiopie 4(1): 39-60.

de Contenson, H. (1963). Les fouilles de Haoulti en 1959. — Rapport préliminaire. Annales d'Ethiopie 5(1): 41-86.

de Gruchy, M. and E. Cunliffe (2020). How the Hollow Ways Got Their Form and Kept Them: 5000 Years of Hollow Ways at Tell Al-Hawa. New Agendas in Remote Sensing and Landscape Archaeology in the Near East: 124.

de la Torre, I. (2004). Omo Revisited. Current Anthropology 45(4): 439-465.

de Mendoza, L. H. and W. A. Jester (1978). Obsidian sources in Guatemala: a regional approach. American Antiquity 43(3): 424-435.

Descheemaeker, K., et al. (2006). Runoff on slopes with restoring vegetation: a case study from the Tigray highlands, Ethiopia. Journal of Hydrology 331(1-2): 219–241.

Devos, Y., et al. (2022). Understanding the formation of buried urban Anthrosols and Technosols: An integrated soil micromorphological and phytolith study of the Dark Earth on the Mundaneum site (Mons, Belgium). CATENA 215: 106322.

Dewitte, O., et al. (2013). Harmonisation of the soil map of Africa at the continental scale. Geoderma 211-212: 138-153.

Dias Junior, M. d. S., et al. (2008). Assessment of the soil compaction of two ultisols caused by logging operations. Revista Brasileira de Ciência do Solo 32(6): 2245–2253.

Dijkstra, E. W. (1959). A note on two problems in connexion with graphs. Numerische Mathematik 1(1): 269-271.

Dixon, B. and J. Earls (2009). Resample or not? :) Effects of resolution of DEMs in watershed modeling. Hydrological Processes: An International Journal 23(12): 1714-1724.

Djurdjevac Conrad, N., et al. (2018). Human mobility and innovation spreading in ancient times: a stochastic agent-based simulation approach. EPJ Data Science 7(1).

Dotterweich, M. (2005). High-resolution reconstruction of a 1300 year old gully system in northern Bavaria, Germany: a basis for modelling long-term human-induced landscape evolution. The Holocene 15(7): 994-1005.

Dotterweich, M., et al. (2012). High resolution gully erosion and sedimentation processes, and land use changes since the Bronze Age and future trajectories in the Kazimierz Dolny area (Nałęczów Plateau, SE-Poland). CATENA 95: 50-62.

Doyle, M. O. and M. L. Otte (1997). Organism-induced accumulation of iron, zinc and arsenic in wetland soils. Environmental Pollution 96(1): 1–11.

Drauschke, T., et al. (2015). CO2-emissions from a short rotation forestry and a spruce forest site in the Erzgebirge, Germany. ББК 28.081+ 20.1 П 78: 158.

Dregne, H. E. (2011). Soils of arid regions, Elsevier.

Duncan, N. A., et al. (2021). Pre-Columbian fire management and control of climate-driven floodwaters over 3,500 years in southwestern Amazonia. Proceedings of the National Academy of Sciences 118(40): e2022206118.

Efrat, E. (1993). Human ecology and the albedo effect in an arid environment. Human Ecology 21(3): 281-293.

Eichhorn, B., et al. (2005). Desert roads and transport vessels from Late Roman-Coptic times in the Eastern Sahara. Journal of African Archaeology 3(2): 213-229.

Eisenreich, A., et al. (2021). Circular Project Selection: How Companies Can Evaluate Circular Innovation Projects. Sustainability 13(22): 12407.

Eissmann, L. (2002). Quaternary geology of eastern Germany (Saxony, Saxon–Anhalt, south Brandenburg, Thüringia), type area of the Elsterian and Saalian stages in Europe. Quaternary Science Reviews 21(11): 1275-1346.

Ekshtain, R., et al. (2016). Local and Nonlocal Procurement of Raw Material in Amud Cave, Israel: The Complex Mobility of Late Middle Paleolithic Groups. Geoarchaeology 32(2): 189-214.

Ekshtain, R., et al. (2017). Local and nonlocal procurement of raw material in Amud Cave, Israel: the complex mobility of late Middle Paleolithic groups. Geoarchaeology 32(2): 189-214.

Eldridge, D. J. (1998). Trampling of microphytic crusts on calcareous soils, and its impact on erosion under rain-impacted flow. CATENA 33(3-4): 221–239.

Escadafal, R., et al. (1989). Munsell soil color and soil reflectance in the visible spectral bands of Landsat MSS and TM data. Remote Sensing of Environment 27(1): 37-46.

Eshel, H. (2003). Documents of the First Jewish Revolt from the Judean desert, Routledge.

Ethiopia, C. S. A. (2013). Satistical Data Tigray, Open Data for Africa.

Etten, J. V. (2017). R package gdistance: distances and routes on geographical grids. FAO Forest Department 2010.

Faccenna, C., et al. (2019). Role of dynamic topography in sustaining the Nile River over 30 million years. Nature Geoscience 12(12): 1012-1017.

Fairbairn, A. S., et al. (2006). Pleistocene occupation of New Guinea's highland and subalpine environments. World Archaeology 38(3): 371-386.

Falk, J. H. and J. D. Balling (2010). Evolutionary influence on human landscape preference. Environment and behavior 42(4): 479-493.

Fanning, P. C., et al. (2009). The surface archaeological record in arid Australia: geomorphic controls on preservation, exposure, and visibility. Geoarchaeology: An International Journal 24(2): 121-146.

Fattovich, R. (2009). Reconsidering Yeha, c. 800–400 BC. African Archaeological Review 26(4): 275-290.

Fattovich, R. (2010). The development of ancient states in the northern Horn of Africa, c. 3000 BC--AD 1000: an archaeological outline. In Journal of World Prehistory 23(3): 145-175.

Fattovich, R. (2010). The development of ancient states in the northern Horn of Africa, c. 3000 BC-AD 1000: an archaeological outline. Journal of World Prehistory 23(3): 145-175.

Fattovich, R. (2012). The northern Horn of Africa in the first millennium BCE: Local traditions and external connections. Rassegna di Studi Etiopici 4: 1-60.

Fattovich, R. and K. A. Bard (2001). The Proto-Aksumite Period: An Overview. Annales d'Ethiopie 17(1): 3-24.

Featherstone, M. (2018). Travel, Migration, and Images of Social Life. Global History and Migrations, Routledge: 239-277.

Fikire, A. H. and M. B. Zegeye (2021). Determinants of Multiple Agricultural Technology Adoption: Evidence from Rural Amhara Region, Ethiopia, MDPI AG.

Finneran, N. (2007). The Archaeology of Ethiopia, Routledge.

FitzPatrick, E. A. (1984). The micromorphology of soils. Micromorphology of soils, Springer: 331-357.

Flückiger, M., et al. (2022). Roman transport network connectivity and economic integration. The Review of Economic Studies 89(2): 774-810.

Foley, R. A. and M. M. Lahr (2015). Lithic landscapes: Early human impact from stone tool production on the central Saharan environment. PloS one 10(3): e0116482.

Fonseca Filho, R. E., et al. (2018). Pedological aspects as environmental quality indicators of a touristic trail in the Serra do Cipó National Park/MG. REM-International Engineering Journal 71: 543-551.

Frank, F. (1934). Aus der'Araba. I. Reiseberichte. Zeitschrift des Deutschen Palästina-Vereins (1878-1945)(H. 3/4): 191-280.

Frankl, A., et al. (2013). Quantifying long-term changes in gully networks and volumes in dryland environments: The case of Northern Ethiopia. Geomorphology 201: 254-263.

Frei, E. and M. G. Cline (1949). Profile studies of normal soils of New York: II Micromorpholigical studies of the grey brown podzolic soil sequence. Soil Science 68(4): 333-344.

French, C., et al. (2009). New geoarchaeological investigations of the valley systems in the Aksum area of northern Ethiopia. CATENA 78(3): 218-233.

Friesem, D. E., et al. (2020). Variability and complexity in calcite-based plaster production: A case study from a Pre-Pottery Neolithic B infant burial at Tel Ro'im West and its implications to mortuary practices in the Southern Levant. Journal of Archaeological Science 113: 105048.

Galun, M. and J. Garty (2001). Biological soil crusts of the Middle East. Biological soil crusts: Structure, function, and management, Springer: 95-106.

García, J.-L., et al. (2021). A composite 10Be, IR-50 and 14C chronology of the pre-LGM full ice extent of the western Patagonian Ice Sheet in the Isla de Chiloé, south Chile (42ºS. E&G-Quaternary Science Journal 70(1).

Garfunkel, Z. and Z. Ben-Avraham (1996). The structure of the Dead Sea basin. Tectonophysics 266(1-4): 155-176.

Gebrehiwot, T. and A. van der Veen (2013). Assessing the evidence of climate variability in the northern part of Ethiopia. Journal of Development and Agricultural Economics 5(3): 104–119.

Gebremariam, S. (2009). Nature and characteristics of metasedimentary rock hosted gold and base metal mineralization in the Workamba area, central Tigray, northern Ethiopia, lmu.

Geeter, S. d., et al. (2020). Does the topographic threshold concept explain the initiation points of sunken lanes in the European loess belt? CATENA 192: 104586.

Geo, S. N. D. terrain model of Saxony. dl-de/by-2-0, Staatsbetrieb Geobasisinformation und Vermessung Sachsen. Available online at.

Geoportal Berlin: Atkis, D. G. M. Digital terrain model of Berlin. dl-de/by-2-0, Available online at.

Gerasimova, M. I. and N. V. Savitskaya (2020). Micromorphological Interpretation of Natural and Anthropogenic Evolution of Soils in Bykovo Lacustrine-Alluvial Section of the Moskva River Floodplain. Eurasian Soil Science 53(7): 950–959.

Ghemawat, P. (2001). Distance still matters. Harvard business review 79(8): 137-147.

Gholizadeh, A., et al. (2020). Spectroscopic measurements and imaging of soil colour for field scale estimation of soil organic carbon. Geoderma 357: 113972.

Gibling, M. R. (2018). River systems and the anthropocene: A late pleistocene and Holocene timeline for human influence. Quaternary 1(3): 21.

Gibson, K. R. (2002). Evolution of human intelligence: The roles of brain size and mental construction. Brain, behavior and evolution 59(1-2): 10-20.

Giesler, R. and U. Lundström (1993). Soil solution chemistry: effects of bulking soil samples. Soil Science Society of America Journal 57(5): 1283-1288.

Gilbertson, J. K., et al. (2017). Effect of pan-sharpening multi-temporal Landsat 8 imagery for crop type differentiation using different classification techniques. Computers and Electronics in Agriculture 134: 151-159.

Gilley, J. E. (2005). Encyclopaedia of Soils In The Environment: Vol.-IV. U.K., Elsevier Ltd.

Gnanadass, E. and A. Y. Sanders (2018). Gender Still Matters in Distance Education. Handbook of Distance Education, Routledge: 79-91.

Goldberg, P. (2000). Micromorphology and site formation at Die Kelders cave I, South Africa. Journal of Human Evolution 38(1): 43-90.

Goldberg, P. (2018). Micromorphology. The Encyclopedia of Archaeological Sciences: 1–4.

Goldberg, P. and F. Berna (2010). Micromorphology and context. Quaternary International 214(1-2): 56–62.

Goldberg, P. and R. Macphail (2008). Practical and theoretical geoarchaeology, Blackwell publishing Oxford.

Goldfus, H., et al. (2016). The significance of geomorphological and soil formation research for understanding the unfinished Roman ramp at Masada. CATENA 146: 73-87.

Gonçalves, A. B. (2010). An extension of GIS-based least-cost path modelling to the location of wide paths. International Journal of Geographical Information Science 24(7): 983-996.

González-Ruibal, A. (2010). Fascist Colonialism: The Archaeology of Italian Outposts in Western Ethiopia (1936–41). International Journal of Historical Archaeology 14(4): 547-574.

Gonzalves, A. B. (2010). An extension of GIS-based least-cost path modelling to the location of wide paths. International Journal of Geographical Information Science 24(7): 983-996.

Goudie, A. G. (2004). Encyclopedia of geomorphology, Psychology Press.

Gowen, K. M. and T. S. de Smet (2020). Testing least cost path (LCP) models for travel time and kilocalorie expenditure: Implications for landscape genomics. PloS one 15(9): e0239387-e0239387.

Greenbaum, N., et al. (2014). The stratigraphy and paleogeography of the Middle Paleolithic open-air site of 'Ein Qashish, Northern Israel. Quaternary International 331: 203-215.

Guazzini, F. (2012). Paulos Milkias and Getachew Metaferia (edited by): The Battle of Adwa. Reflections on Ethiopia's Historic Victory against European Colonialism. Aethiopica 11: 287-291.

Guimarães, D. V., et al. (2013). Soil organic matter pools and carbon fractions in soil under different land uses. Soil and Tillage Research 126: 177–182.

Gutiérrez-Rodríguez, M., et al. (2022). Microstratigraphic analysis of the main Roman road in Hispania: the Via Augusta where it passes through the Ianus Augustus (Mengíbar, Spain). Archaeological and Anthropological Sciences 14(8): 1-32.

Haburaj, V., et al. (2020). Coupling spectral imaging and laboratory analyses to digitally map sediment parameters and stratigraphic layers in Yeha, Ethiopia. PloS one 15(9): e0238894-e0238894.

Hagos, M., et al. (2010). Geochemical characteristics of the alkaline basalts and the phonolite - trachyte plugs of the Aksum area, Northern Ethiopia. Austrian Journal of Earth Sciences 103: 153-170.

Hagos, M., et al. (2010). Geology, Petrology, and Geochemistry of the Basaltic Rocks of the Axum Area, Northern Ethiopia. Topics in Igneous Petrology, Springer Netherlands: 69-93.

Hajdas, I., et al. (2021). Radiocarbon dating. Nature Reviews Methods Primers 1(1): 1-26.

Haliva-Cohen, A., et al. (2012). Sources and transport routes of fine detritus material to the Late Quaternary Dead Sea basin. Quaternary Science Reviews 50: 55-70.

Hallett, S., et al. (2013). Harmonisation of the soil map of Africa at the continental scale. Geoderma 211: 138-153.

Hamza, M. A. and W. K. Anderson (2005). Soil compaction in cropping systems: A review of the nature, causes and possible solutions. Soil and Tillage Research 82(2): 121–145.

Harden, C. P. (1992). Incorporating roads and footpaths in watershed-scale hydrologic and soil erosion models. Physical Geography 13(4): 368–385.

Harden, C. P., et al. (2014). Understanding human–landscape interactions in the Anthropocene. Environmental management 53(1): 4-13.

Hardt, J., et al. (2023). Palaeoenvironmental research at Hawelti-Melazo (Tigray, northern Ethiopia) – insights from sedimentological and geomorphological analyses. E&G Quaternary Science Journal.

Hardt, J., et al. (2023). Understanding historical pathways In Tigray using travelers reports and least cost path analysis. The Cartographic Journal.

Harel, M. (1967). Israelite and Roman roads in the Judean desert. Israel Exploration Journal: 18-26.

Harrower, M. J. and A. C. D'Andrea (2014). Landscapes of State Formation: Geospatial Analysis of Aksumite Settlement Patterns (Ethiopia). African Archaeological Review 31(3): 513-541.

Harrower, M. J., et al. (2020). Water, Geography, and Aksumite Civilization: The Southern Red Sea Archaeological Histories (SRSAH) Project Survey (2009--2016) ,. In Afr Archaeol Rev, pp: 1-17.

Henshilwood, C. S., et al. (2001). Blombos Cave, southern Cape, South Africa: preliminary report on the 1992–1999 excavations of the Middle Stone Age levels. Journal of Archaeological Science 28(4): 421-448.

Henze, P. B. (2000). Medieval Ethiopia. Layers of Time, Palgrave Macmillan US: 44-82.

Herbin, T., et al. (2011). The effects of dairy cow weight on selected soil physical properties indicative of compaction. In Soil Use and Management 27(1): 36-44.

Herzog, I. (2010). April. Theory and practice of cost functions. Fusion of Cultures, European Upper Paleolithic river systems and their role as features of spatial organization. Journal of Archaeological Method and Theory 23(4) pp.1162-1218: 431-434.

Herzog, I. (2010). Theory and practice of cost functions. Fusion of cultures. Proceedings of the 38th annual conference on computer applications and quantitative methods in archaeology, Granada, Spain.

Herzog, I. (2014). A review of case studies in archaeological least-cost analysis. Archeologia e Calcolatori 25: 223-239.

Herzog, I. (2016). The potential and limits of optimal path analysis. Computational approaches to archaeological spaces, Routledge: 187-220.

Herzog, I. (2017). Reconstructing pre-industrial long distance roads in a hilly region in Germany, Based on Historical and Archaeological Data. Studies in Digital Heritage 1(2): 642-660.

Herzog, I. (2021). Issues in Replication and Stability of Least-cost Path Calculations. Studies in Digital Heritage 5(2): 131-155.

Hijmans, R. (2020). raster: Geographic Data Analysis and Modeling (R package version 3.3-13)[Computer software]. Retrieved form https://CRAN. R-project. org/package= raster.

Hirschfeld, Y. (2006). The archaeology of the Dead Sea valley in the Late Hellenistic and Early Roman periods. SPECIAL PAPERS-GEOLOGICAL SOCIETY OF AMERICA 401: 215.

Hoelzmann, P., et al. (2017). A new device to mount portable energy-dispersive X-ray fluorescence spectrometers (p-ED-XRF) for semi-continuous analyses of split (sediment) cores and solid samples. In Geoscientific Instrumentation, Methods and Data Systems 6(1): 93-101.

Hofmann, C., et al. (1997). Timing of the Ethiopian flood basalt event and implications for plume birth and global change. Nature 389(6653): 838-841.

Holzapfel, C. (2014). Deserts Encyclopedia of ecology. S. E. Jorgensen and B. Fath, Newnes: 879.

Hussain, S. T. and H. Floss (2016). Streams as Entanglement of Nature and Culture: European Upper Paleolithic River Systems and Their Role as Features of Spatial Organization. Journal of archaeological method and theory 23(4): 1162-1218.

Imeson, A. and F. Kwaad (1980). Gully types and gully prediction. Geografisch Tijdschrift 14(5): 430-441.

Imeson, A. C. and F. J. P. M. Kwaad (1980). Gully types and gully prediction. Geografisch Tijdschrift 14(5): 430-441.

Iraj, B., et al. (2011). Effect of compaction on physical and micromorphological properties of forest soils, In AJPS 2012.

Isler, K. and C. P. van Schaik (2012). Allomaternal care, life history and brain size evolution in mammals. Journal of Human Evolution 63(1): 52-63.

Issa, O. M., et al. (1999). Morphology and microstructure of microbiotic soil crusts on a tiger bush sequence (Niger, Sahel). CATENA 37(1-2): 175-196.

Itkin, D., et al. (2018). Pedology of archaeological soils in tells of the Judean foothills, Israel. CATENA 168: 47-61.

Jackson, J. B. (1984). Discovering the vernacular landscape, Yale University Press.

Jackson, J. B. (1994). A sense of place, a sense of time, Yale University Press.

Jammalamadaka, S. R. and A. SenGupta (2001). Topics in Circular Statistics, WORLD SCIENTIFIC.

Japp, S., et al. (2011). Yeha and Hawelti: cultural contacts between Saba? and D?MT-New research by the Proceedings of the Seminar for Arabian Studies Archaeopress: 145-160.

Jarman, C. L., et al. (2017). Diet of the prehistoric population of Rapa Nui (Easter Island, Chile) shows environmental adaptation and resilience. American journal of physical anthropology 164(2): 343-361.

Jarmer, T. and M. Shoshany (2016). Relationships between soil spectral and chemical properties along a climatic gradient in the Judean desert. Arid Land Research and Management 30(2): 123-137.

Jarvis, A., et al. (2008). Hole-filled SRTM for the globe Version 4. available from the CGIAR-CSI SRTM 90m Database (http://srtm. csi. cgiar. org) 15: 25–54.

Jim, C. Y. (1993). Soil Compaction as a Constraint to Tree Growth in Tropical & Subtropical Urban Habitats. Environmental Conservation 20(1): 35–49.
Environmental Conservation

Johnson, D. B. (1977). Efficient algorithms for shortest paths in sparse networks. Journal of the ACM (JACM) 24(1): 1-13.

Junge, A., et al. (2021). Construction and use of rock-cut cisterns: a chronological OSL approach in the arid Negev Highlands, Israel. Archaeological and Anthropological Sciences 13(9): 1-21.

Kaiser, K., et al. (2002). Stabilization of organic matter by soil minerals---investigations of density and particle-size fractions from two acid forest soils. In Journal of Plant Nutrition and Soil Science 165(4): 451-459.

Kapeliuk, O. (2014). Rassegna di Studi Etiopici. Nuova Serie, Vol. III. Aethiopica 16: 247-252.

Kappelman, J. (1996). The evolution of body mass and relative brain size in fossil hominids. Journal of Human Evolution 30(3): 243-276.

Karkanas, P. and A. Van de Moortel (2014). Micromorphological analysis of sediments at the Bronze Age site of Mitrou, central Greece: patterns of floor construction and maintenance. Journal of Archaeological Science 43: 198-213.

Kawahigashi, M., et al. (2006). Sorption of dissolved organic matter by mineral soils of the Siberian forest tundra. Global Change Biology 12(10): 1868–1877.

Kay, A. M. and M. J. Liddle (1989). Impact of human trampling in different zones of a coral reef flat. Environmental management 13(4): 509-520.

Kendal, J., et al. (2011). Human niche construction in interdisciplinary focus. Philosophical Transactions of the Royal Society B: Biological Sciences 366(1566): 785-792.

Kesler, D. C. and R. S. Walker (2015). Geographic distribution of isolated indigenous societies in Amazonia and the efficacy of indigenous territories. PloS one 10(5): e0125113-e0125113.

Kidanmariam, G. (2000). The use of donkeys for transport in Amhara Region, Ethiopia.

Kropek, J. P. Starkey and D. Fielding. Z. and Nyssen, J., 2019. Historical aerial and terrestrial photographs for the investigation of mass movement dynamics in the Ethiopian Highlands. Land Degradation & Development, 30(5), pp.483-493.

Kilbride, C., et al. (2006). A comparison of Cu, Pb, As, Cd, Zn, Fe, Ni and Mn determined by acid extraction/ICP--OES and ex situ field portable X-ray fluorescence analyses. In Environmental Pollution 143(1): 16-23.

Kirchner, A., et al. (2020). Spatial analysis of hollow ways in the Hildesheimer Wald Mountains (Lower Saxony, Germany) as a model for mountainous regions of Central Europe. Erdkunde(H. 1): 1-14.

Kirsten, F., et al. (2021). Early Holocene aeolian sediments in southwestern Crete− preliminary results. In Mediterranean Geoscience Reviews, pp: 1-19.

Kissling, M., et al. (2009). Short-term and long-term effects of human trampling on above-ground vegetation, soil density, soil organic matter and soil microbial processes in suburban beech forests. Applied Soil Ecology 42(3): 303–314.

Konka, B., et al. (2012). Shear Zone-Hosted Base Metal Mineralization near Abraha Weatsebaha-Adidesta and Hawzein, Tigray Region, Northern Ethiopia. Momona Ethiopian Journal of Science 4(1): 3.

Kooistra, M. J. and N. K. Tovey (1994). Effects of Compaction on Soil Microstructure. Soil Compaction in Crop Production, Elsevier. 11: 91–111.

Kopittke, P. M., et al. (2019). Soil and the intensification of agriculture for global food security. Environment international 132: 105078.

Kozlowski, T. T. (1999). Soil Compaction and Growth of Woody Plants. Scandinavian Journal of Forest Research 14(6): 596–619.

Krieger, G., et al. (2007). TanDEM-X: A satellite formation for high-resolution SAR interferometry. IEEE Transactions on Geoscience and Remote Sensing 45(11): 3317-3341.

Kubïena, W. L. (1939). Micropedology. Soil Science 47(2): 163.

Kumar, R. and M. Tao (1975). Multiple forms of casein kinase from rabbit erythrocytes. Biochimica et biophysica acta 410(1): 87–98.

Lamb, H. F., et al. (2007). Late Pleistocene desiccation of Lake Tana, source of the Blue Nile. Quaternary Science Reviews 26(3-4): 287-299.

Langgut, D., et al. (2014). Dead Sea pollen record and history of human activity in the Judean Highlands (Israel) from the Intermediate Bronze into the Iron Ages (~ 2500–500 BCE). Palynology 38(2): 280-302.

Lannoeye, W., et al. (2016). The use of SfM-photogrammetry to quantify and understand gully degradation at the temporal scale of rainfall events: an example from the Ethiopian drylands. Physical Geography 37(6): 430-451.

Larramendy, M. L. and S. Soloneski (2019). Pesticides: Use and Misuse and Their Impact in the Environment, BoD–Books on Demand.

Laurance, S. G. (2004). Landscape connectivity and biological corridors. Agroforestry and biodiversity conservation in tropical landscapes 1: 50-63.

Lavee, H., et al. (1996). Aggregate stability dynamics as affected by soil temperature and moisture regimes. Geografiska Annaler: Series A, Physical Geography 78(1): 73-82.

Lavee, H., et al. (1989). Pedogenic indicators of subsurface flow on Judean Desert hillslopes. Earth Surface Processes and Landforms 14(6): 545-555.

Leclant, J. (1959). Haoulti-Melazo (1955-1956). Annales d'Ethiopie 3(1): 43-82.

Leclant, J. (1959). Les fouilles à Axoum en 1955-1956. Rapport préliminaire. Annales d'Ethiopie 3(1): 3–23.

Lee, M.-J., et al. (2012). Application of frequency ratio model and validation for predictive flooded area susceptibility mapping using GIS. 2012 IEEE International Geoscience and Remote Sensing Symposium, IEEE.

Lei, S. A. (2004). Soil compaction from human trampling, biking, and off-road motor vehicle activity in a blackbrush (Coleogyne ramosissima) shrubland. Western North American Naturalist: 125–130.

Leopold, L. B., et al. (2020). Fluvial processes in geomorphology, Courier Dover Publications.

Lewis, S. L. and M. A. Maslin (2015). Defining the anthropocene. Nature 519(7542): 171-180.

Liddle, M. J. (1975). A selective review of the ecological effects of human trampling on natural ecosystems. Biological Conservation 7(1): 17-36.

Lieberman, D. E., et al. (1993). The Rise and Fall of Seasonal Mobility among Hunter-Gatherers: The Case of the Southern Levant [and Comments and Replies]. Current Anthropology 34(5): 599-631.

Lisker, S., et al. (2010). Late Neogene rift valley fill sediments preserved in caves of the Dead Sea Fault Escarpment (Israel): palaeogeographic and morphotectonic implications. Sedimentology 57(2): 429-445.

Livingstone, I. and A. Warren (1996). Aeolian geomorphology: an introduction, Addison Wesley Longman Ltd.

Llobera, M. and T. J. Sluckin (2007). Zigzagging: Theoretical insights on climbing strategies. Journal of Theoretical Biology 249(2): 206-217.

Loor, I. and J. Evans (2021). Understanding the value and vulnerability of informal infrastructures: Footpaths in Quito. Journal of Transport Geography 94: 103112.

Lull, H. W. (1959). Soil compaction on forest and range lands, Forest Service, US Department of Agriculture.

Machado, M. J. (2015). Geomorphology of the Adwa District. World Geomorphological Landscapes, Springer Netherlands: 163-178.

Mackay, A., et al. (2022). Reconstructing Middle Stone Age mobility patterns from raw material transfers in South Africa's Still Bay (77–70 ka) technocomplex. Archaeological and Anthropological Sciences 14(1): 1-16.

Malinsky-Buller, A., et al. (2021). Short-term occupations at high elevation during the Middle Paleolithic at Kalavan 2 (Republic of Armenia). PloS one 16(2): e0245700.

Marniemi, J. and M. G. Parkki (1975). Radiochemical assay of glutathione S-epoxide transferase and its enhancement by phenobarbital in rat liver in vivo. Biochemical pharmacology 24(17): 1569–1572.

Marples, D. R. (2018). Nuclear Power in the Former USSR: Historical and Contemporary Perspectives. Nuclear Energy and Security in the Former Soviet Union, Routledge: 19-44.

Marshall, F. (2007). African pastoral perspectives on domestication of the donkey: a first synthesis. Rethinking agriculture: archaeological and ethnoarchaeological perspectives, pp: 371-407.

Marshall, M. H., et al. (2009). Climatic change in northern Ethiopia during the past 17,000 years: A diatom and stable isotope record from Lake Ashenge. Palaeogeography, Palaeoclimatology, Palaeoecology 279(1-2): 114-127.

Martinez-Casasnovas, J. A., et al. (2004). Assessment of sidewall erosion in large gullies using multi-temporal DEMs and logistic regression analysis. Geomorphology 58(1-4): 305-321.

Mascher, M., et al. (2016). Genomic analysis of 6,000-year-old cultivated grain illuminates the domestication history of barley. Nature Genetics 48(9): 1089-1093.

Massilani, D., et al. (2022). Microstratigraphic preservation of ancient faunal and hominin DNA in Pleistocene cave sediments. Proceedings of the National Academy of Sciences 119(1): e2113666118.

Mattivi, P., et al. (2019). TWI computation: a comparison of different open source GISs. Open Geospatial Data, Software and Standards 4(1).

Mazar, B., et al. (1966). En-Gedi, The First and Second Seasons of Excavations, 1961-1962 ('A tiqot [ES] 5). English Series 5.

McKeever, S. (2011). Optically stimulated luminescence: a brief overview. Radiation Measurements 46(12): 1336-1341.

McLean, A. and X. Rubio-Campillo (2022). Beyond Least Cost Paths: Circuit theory, maritime mobility and patterns of urbanism in the Roman Adriatic. Journal of Archaeological Science 138: 105534.

McLennan, S. M. (1995). Sediments and soils: Chemistry and abundances. Rock physics and phase relations, A handbook of physical constants, AGU Reference Shelf 3: 8-19.

Medhin, G. (2011). Livelihood zones analysis: a tool for planning agricultural water management investments, Ethiopia. Food and Agriculture Organization of the United Nations (FAO).

Menzies, J. and J. J. M. Meer (2018). Micromorphology and Microsedimentology of Glacial Sediments. Past Glacial Environments, Elsevier: 753–806.

Merryman Boncori, J. (2016). Caveats Concerning the Use of SRTM DEM Version 4.1 (CGIAR-CSI). Remote Sensing 8(10): 793.

Mikutta, R., et al. (2006). Stabilization of soil organic matter: association with minerals or chemical recalcitrance? Biogeochemistry 77(1): 25–56.

Milkias, P. and G. Metaferia (2005). The Battle of Adwa: Reflections on Ethiopia's historic victory against European colonialism, Algora Publishing.

Miller, B. A. and J. Juilleret (2020). The colluvium and alluvium problem: Historical review and current state of definitions. Earth-Science Reviews 209: 103316.

Miller, C. E., et al. (2010). Dumping, sweeping and trampling: experimental micromorphological analysis of anthropogenically modified combustion features.

Moran, E. F. (2018). Human Adaptability an Introduction to Ecological Anthropology: An Introduction to Ecological Anthropology, Routledge.

Morrocco, S. M. and C. K. Ballantyne (2008). Footpath morphology and terrain sensitivity on high plateaux: the Mamore Mountains, Western Highlands of Scotland. Earth Surface Processes and Landforms: The Journal of the British Geomorphological Research Group 33(1): 40-54.

Mousazadeh, F. and K. O. Salleh (2014). The Influence of Lithology and Soil on the Occurrence and Expansion of Gully Erosion, Toroud Basin – Iran. Procedia - Social and Behavioral Sciences 120: 749-756.

Muehlbauer, M. (2021). From Stone to Dust: The Life of the Kufic-Inscribed Frieze of Wuqro Cherqos in Tigray, Ethiopia. Muqarnas Online 38(1): 1-34.

Mussi, M., et al. (2021). After the emergence of the Acheulean at Melka Kunture (Upper Awash, Ethiopia): From Gombore IB (1.6 Ma) to Gombore Iγ (1.4 Ma), Gombore Iδ (1.3 Ma) and Gombore II OAM Test Pit C (1.2 Ma). Quaternary International.

Nakoinz, O. and D. Knitter (2016). Modelling Human Behaviour in Landscapes. Quantitative Archaeology and Archaeological Modelling, Springer International Publishing.

Natali, C., et al. (2013). The Aksum-Adwa basalt-trachyte complex: a late magmatic activity at the periphery of the Afar plume. Contributions to Mineralogy and Petrology 166: 351-370.

Nawaz, M. F. and Bourri (2016). Early detection of the effects of compaction in forested soils: evidence from selective extraction techniques. In J Soils Sediments 16(9): 2223-2233.

Nawaz, M. F., et al. (2013). Soil compaction impact and modelling. A review. Agronomy for sustainable development 33(2): 291–309.

Nazari Samani, A., et al. (2009). Geomorphic threshold conditions for gully erosion in Southwestern Iran (Boushehr-Samal watershed). Journal of Asian Earth Sciences 35(2): 180-189.

Neve, S. d. and G. Hofman (2000). Influence of soil compaction on carbon and nitrogen mineralization of soil organic matter and crop residues. Biology and Fertility of Soils 30(5-6): 544–549.

Nicosia, C. and G. Stoops (2017). Archaeological soil and sediment micromorphology, John Wiley & Sons.

Nigussie, T., et al. (2017). Feasibility study for power generation using off- grid energy system from micro hydro-PV-diesel generator-battery for rural area of Ethiopia: The case of Melkey Hera village, Western Ethiopia. AIMS Energy 5(4): 667-690.

Nir, N., et al. (submitted manuscript). The environmental footprint of Holocene societies: a multi-temporal study of footpaths in the Judean Desert, Israel.

Nir, N., et al. (2021). Human movement and gully erosion: Investigating feedback mechanisms using Frequency Ratio and Least Cost Path analysis in Tigray, Ethiopia. In PloS one 16: 2.

Nir, N., et al. (2022). Footpaths: Pedogenic and geomorphological long-term effects of human trampling. CATENA 215: 106312.

Nykamp, M., et al. (2020). Late Holocene geomorphodynamics in the vicinity of G o bekli Tepe, SE Turkey. In CATENA 195.

Nykamp, M., et al. (2020). Late Holocene geomorphodynamics in the vicinity of Göbekli Tepe, SE Turkey. CATENA 195: 104759.

Nyssen, J., et al. (2017). Geographical determinants of inorganic fertiliser sales and of resale prices in north Ethiopia. Agriculture, Ecosystems & Environment 249: 256-268.

Nyssen, J., et al. (2020). Exploration of a medieval African map (Aksum, Ethiopia)--How do historical maps fit with topography? In : Liber Amicorum: Philippe De Maeyer In Kaart: University Press, pp: 165-178.

Nyssen, J., et al. (2000). Soil and water conservation in Tigray (Northern Ethiopia): the traditional dagat technique and its integration with introduced techniques. Land Degradation & Development 11(3): 199-208.

Nyssen, J., et al. (2000). Tillage erosion on slopes with soil conservation structures in the Ethiopian highlands. Soil and Tillage Research 57(3): 115–127.

Nyssen, J., et al. (2004). Human impact on the environment in the Ethiopian and Eritrean highlands---a state of the art. In Earth-Science Reviews 64(3-4): 273-320.

Nyssen, J., et al. (2002). Impact of road building on gully erosion risk: a case study from the Northern Ethiopian Highlands. In Earth Surf 27(12): 1267-1283.

Nyssen, J., et al. (2005). Rainfall erosivity and variability in the Northern Ethiopian Highlands. Journal of Hydrology 311(1-4): 172–187.

Olson, G. W. (1984). Soil profile descriptions. Field Guide to Soils and the Environment Applications of Soil Surveys. Dordrecht, Springer Netherlands: 3-9.

Otterman, J. and C. Tucker (1985). Satellite measurements of surface albedo and temperatures in semi-desert. Journal of Applied Meteorology and Climatology 24(3): 228-235.

Páez, A., et al. (2020). Comparing distance, time, and metabolic energy cost functions for walking accessibility in infrastructure-poor regions. Journal of Transport Geography 82: 102564.

Panagos, P., et al. (2011). European digital archive on soil maps (EuDASM): preserving important soil data for public free access. International Journal of Digital Earth 4(5): 434-443.

Panarello, A., et al. (2017). Walking along the oldest human fossil pathway (Roccamonfina volcano, Central Italy)? Journal of Archaeological Science: Reports 13: 476-490.

Panin, A. V., et al. (2009). Long-term development of Holocene and Pleistocene gullies in the Protva River basin, Central Russia. Geomorphology 108(1-2): 71-91.

Pawłowska, K. and L.-M. Shillito (2022). An Integrated Zooarchaeological and Micromorphological Perspective on Midden Taphonomy at Late Neolithic Çatalhöyük. Open Archaeology 8(1): 436-459.

Pearce, D. W., et al. (1990). Economics of natural resources and the environment, Johns Hopkins University Press.

Petschko, H., et al. (2022). Sunken Roads and Palaeosols in Loess Areas in Lower Austria: Landform Development and Cultural Importance. Landscapes and Landforms of Austria, Springer: 179-191.

Pfeiffer, K. and I. Gerlach (2020). Rama, Ethiopia (Tigray). Routes of Interaction–New Research in the Rama Valley. e-Forschungsberichte: § 1–7-§ 1–7.

Phillips, J. D., et al. (2021). Fine sediment storage in an eroding forest trail system. Physical Geography 42(1): 50-72.

Phillipson, D. W. (2012). Foundations of an African Civilisation: Aksum & the Northern Horn, 1000 BC-1300 AD, Boydell & Brewer Ltd.

Pietola, L., et al. (2005). Effects of trampling by cattle on the hydraulic and mechanical properties of soil. Soil and Tillage Research 82(1): 99–108.

Pietsch, D. and P. Kühn (2017). Buried soils in the context of geoarchaeological research—two examples from Germany and Ethiopia. Archaeological and Anthropological Sciences 9(8): 1571–1583.

Pietsch, D. and M. J. Machado (2014). Colluvial deposits - proxies for climate change and cultural chronology. A case study from Tigray, Ethiopia. Zeitschrift für Geomorphologie, Supplementary Issues 58(1): 119-136.

Pires, L. F., et al. (2009). Pore system changes of damaged Brazilian oxisols and nitosols induced by wet-dry cycles as seen in 2-D micromorphologic image analysis. Anais da Academia Brasileira de Ciências 81(1): 151–161.

Plummer, S., et al. (2017). The ESA Climate Change Initiative (CCI): A European contribution to the generation of the Global Climate Observing System. Remote Sensing of Environment 203: 2-8.

Poesen, J., et al. (2003). Gully erosion and environmental change: importance and research needs. CATENA 50(2-4): 91–133.

Poudyal, C. P., et al. (2010). Landslide susceptibility maps comparing frequency ratio and artificial neural networks: a case study from the Nepal Himalaya. Environmental Earth Sciences 61(5): 1049-1064.

Pounder, E. (1985). The effects of footpath development on vegetation at the Okstindan Research Station in Arctic Norway. Biological Conservation 34(3): 273-288.

QGIS.org (2021). QGIS Geographic Information System: QGIS Association; 2021.

Qin, C.-Z. and L.-J. Zhu (2020). GDAL/OGR and Geospatial Data IO Libraries. Geographic Information Science & Technology Body of Knowledge 2020(Q4).

R Core Team, R. (2013). R: A language and environment for statistical computing.

Raccidi, M. (2013). Wagons on the move: The study of wagons through landscape archaeology. Quaternary International 312: 12–26.

Rahmati, O., et al. (2016). Gully erosion susceptibility mapping: the role of GIS-based bivariate statistical models and their comparison. Natural Hazards 82(2): 1231-1258.

Rasa, K., et al. (2012). Structure and pore system in differently managed clayey surface soil as described by micromorphology and image analysis. Geoderma 173-174: 10–18.

Rast, W. (2001). Early Bronze Age State Formation in the Southeast Dead Sea Plain, Jordan. Studies in the Archaeology of Israel and Neighboring Lands in Memory of Douglas L. Esse: 519-533.

Ravenstein, E. G. (1885). The Laws of Migration. Journal of the Statistical Society of London 48(2): 167.

Rees, W. G. (2004). Least-cost paths in mountainous terrain. Computers & Geosciences 30(3): 203-209.

Rentzel, P., et al. (2017). Trampling, poaching and the effect of traffic. In Archaeological soil and sediment micromorphology 68(12): 1822-1830.

Roberts, P. and M. Petraglia (2015). Pleistocene rainforests: barriers or attractive environments for early human foragers? World Archaeology 47(5): 718-739.

Rodgers, M. M. (1988). Dynamic biomechanics of the normal foot and ankle during walking and running. Physical therapy 68(12): 1822–1830.

Rodway-Dyer, S. and N. Ellis (2018). Combining remote sensing and on-site monitoring methods to investigate footpath erosion within a popular recreational heathland environment. Journal of Environmental Management 215: 68-78.

Rodway-Dyer, S. and D. Walling (2010). The use of 137Cs to establish longer-term soil erosion rates on footpaths in the UK. Journal of Environmental Management 91(10): 1952-1962.

Rogers, D. F. and S. D. Rogers (1985). A Raster Display Graphics Package for Education. Computer Graphics, Springer Japan: 123-138.

Rogers, S. R., et al. (2014). Least cost path analysis for predicting glacial archaeological site potential in central Europe. Across space and time 261.

Rojas, R., et al. (2008). Grid Scale Effects on Watershed Soil Erosion Models. Journal of Hydrologic Engineering 13(9): 793-802.

Roovers, P., et al. (2004). Experimental trampling and vegetation recovery in some forest and heathland communities. Applied Vegetation Science 7(1): 111–118.

Rosenberg, N. J. (1964). Response of plants to the physical effects of soil compaction. Advances in Agronomy 16: 181-196.

Rossel, S., et al. (2008). Domestication of the donkey: Timing, processes, and indicators. Proceedings of the National Academy of Sciences 105(10): 3715-3720.

Rossi, A. M., et al. (2008). Bulk density determination by automated three-dimensional laser scanning. Soil Science Society of America Journal 72(6): 1591-1593.

Rossi, C., et al. (2015). Ancient road transport devices: Developments from the Bronze Age to the Roman Empire. Frontiers of Mechanical Engineering 11(1): 12-25.

Rossi, C., et al. (2016). Ancient road transport devices: Developments from the Bronze Age to the Roman Empire. Frontiers of Mechanical Engineering 11(1): 12-25.

Rothenberg, B. (1970). An archaeological survey of South Sinai: first season 1967/1968, preliminary report. Palestine Exploration Quarterly 102(1): 4-29.

Roy, J. and D. S. Saha (2019). GIS-based Gully Erosion Susceptibility Evaluation Using Frequency Ratio, Cosine Amplitude and Logistic Regression Ensembled with fuzzy logic in Hinglo River Basin, India. Remote Sensing Applications: Society and Environment 15: 100247.

Ryan, J. C., et al. (2017). Derivation of high spatial resolution albedo from UAV digital imagery: application over the Greenland Ice Sheet. Frontiers in Earth Science 5: 40.

Salesa, D. and A. Cerdà (2020). Soil erosion on mountain trails as a consequence of recreational activities. A comprehensive review of the scientific literature. Journal of Environmental Management 271: 110990.

Samani, A. N., et al. (2009). Geomorphic threshold conditions for gully erosion in Southwestern Iran (Boushehr-Samal watershed). Journal of Asian Earth Sciences 35(2): 180-189.

Schild, A. (2016). Archaeological Least Cost Path Modeling: A Behavioral Study of Middle Bronze Age Merchant Travel Routes Across the Amanus Mountains, Turkey, University of Southern California.

Schmidt, P. R. (2002). The'Ona'culture of greater Asmara: Archaeology's liberation of Eritrea's ancient history from colonial paradigms. Journal of Eritrean Studies (Asmara) 1(1): 29–58.

Schuett, B., et al. (2005). Soil erosion processes and landscape sensitivity in the Ethiopian Highlands. Prasad. A. H and O. a. K. Sustainable management of water resources, Challenges and Prospects. Nairobi p: 177-203.

Schulten, A., et al. (1933). Masada die Burg des Herodes und die römischen Lager mit einem Anhang: Beth-Ter. Zeitschrift des Deutschen Palästina-Vereins (1878-1945)(H. 1/3): 1-185.

Schumm, S. A. (1979). Geomorphic thresholds: the concept and its applications. Transactions of the Institute of British Geographers: 485-515.

Schütt, B., et al. (2005). Soil erosion processes and landscape sensitivity in the Ethiopian Highlands. Sustainable management of water resources: Challenges and Prospects. Nairobi: 177-203.

Seifert, T. and L. Baumann (1994). On the metallogeny of the Central Erzgebirge anticlinal area (Marienberg district), Saxony, Germany. Monogr. Series on Mineral Deposits 31: 169–190.

Seifried, R. M. and C. A. Gardner (2019). Reconstructing historical journeys with least-cost analysis: Colonel William Leake in the Mani Peninsula, Greece. Journal of Archaeological Science: Reports 24: 391-411.

Sembroni, A., et al. (2017). Geology of the Tekeze River basin (Northern Ethiopia). Journal of Maps 13(2): 621-631.

Senanayake, S., et al. (2020). Assessing Soil Erosion Hazards Using Land-Use Change and Landslide Frequency Ratio Method: A Case Study of Sabaragamuwa Province, Sri Lanka. Remote Sensing 12(9): 1483.

Seutloali, K. E., et al. (2015). An assessment of gully erosion along major armoured roads in south-eastern region of South Africa: a remote sensing and GIS approach. Geocarto International 31(2): 225-239.

Seutloali, K. E., et al. (2016). An assessment of gully erosion along major armoured roads in south-eastern region of South Africa: a remote sensing and GIS approach. Geocarto International 31(2): 225–239.

Shah, A. N., et al. (2017). Soil compaction effects on soil health and cropproductivity: an overview. Environmental Science and Pollution Research 24(11): 10056–10067.

Shahack-Gross, R. (2017). Archaeological formation theory and geoarchaeology: State-of-the-art in 2016. Journal of Archaeological Science 79: 36-43.

Shahack-Gross, R., et al. (2003). Geo-ethnoarchaeology of pastoral sites: the identification of livestock enclosures in abandoned Maasai settlements. Journal of Archaeological Science 30(4): 439–459.

Shea, J. J. (2016). Stone tools in human evolution: behavioral differences among technological primates, Cambridge University Press.

Sherman, C., et al. (2019). The effect of human trampling activity on a soil microbial community at the Oulanka Natural Reserve, Finland. Applied Soil Ecology 135: 104–112.

Shipitalo, M. J., et al. (2004). Interaction of earthworm burrows and cracks in a clayey, subsurface-drained, soil. Applied Soil Ecology 26(3): 209–217.

Sidle, R. C., et al. (2019). January. Evidence of how roads and trails contribute to gully erosion in drylands. In Geophysical Research Abstracts (Vol. 21).

Sidle, R. C., et al. (2018). Hydrogeomorphic processes affecting dryland gully erosion: Implications for modelling. Progress in Physical Geography: Earth and Environment 43(1): 46-64.

Sidle, R. C., et al. (2004). Sediment pathways in a tropical forest: effects of logging roads and skid trails. Hydrological Processes 18(4): 703-720.

Sidle, R. C., et al. (2006). Erosion processes in steep terrain—Truths, myths, and uncertainties related to forest management in Southeast Asia. Forest Ecology and Management 224(1-2): 199-225.

Silva, S. R., et al. (2011). Effect of compaction on microbial activity and carbon and nitrogen transformations in two oxisols with different mineralogy. Revista Brasileira de Ciência do Solo 35(4): 1141–1149.

Sime, G. and J. B. Anne (2019). Rural livelihood vulnerabilities, coping strategies and outcomes: A case study in central rift valley of Ethiopia. African Journal of Food Agriculture Nutrition and Development 19(03): 14602-14621.

Simini, F. and M. Tomasini (2018). Human mobility: Models and applications. Physics Reports 734: 1-74.

Simpson, F. (1952). New Place: The Only Representation of Shakespeare's House From an Unpublished Manuscript. Shakespeare Survey, Cambridge University Press: 55-57.

Singer, A. (2007). The soils of Israel, Springer Science & Business Media.

Singer, A., et al. (2003). Dust deposition over the Dead Sea. Journal of Arid Environments 53(1): 41-59.

Six, J., et al. (2004). A history of research on the link between (micro) aggregates, soil biota, and soil organic matter dynamics. Soil and Tillage Research 79(1): 7–31.

Smerdon, E. T. and R. P. Beasley (1959). The tractive force theory applied to stability of open channels in cohesive soils, University of Missouri, College of Agriculture, Agricultural Experiment Station.

Smidt, W. G. C. and M. M. Haggag Rashidy (2012). Another Arabic Inscription from the Eastern Tigrayan Trade Route (III): The malik al-Ḥabaša in Negaš. Northeast African Journal of Social Sciences and Humanities 2: 123–130.

Smith, B. D. and M. A. Zeder (2013). The onset of the Anthropocene. Anthropocene 4: 8-13.

Smith, V. L. (1968). Economics of production from natural resources. The American Economic Review 58(3): 409-431.

Snead, J., et al. (2009). Making human space: the archaeology of trails. and roads, paths.

Snead, J. E. (2006). Trails of Tradition: Archaeology, Landscape, and Movement. Proceedings of the Landscapes of Movement Symposium, University of Pennsylvania Museum, Philadelphia, PA, USA.

Snead, J. E., et al. (2011). Landscapes of movement: trails, paths, and roads in anthropological perspective, University of Pennsylvania Press.

Soane, B. and C. Van Ouwerkerk (1994). Soil compaction problems in world agriculture. Developments in agricultural engineering, Elsevier. 11: 1-21.

Song, X., et al. (2022). Towards a better understanding of the role of Fe cycling in soil for carbon stabilization and degradation. Carbon Research 1(1): 1-16.

Staff, S. (1999). Soil Taxonomy: A basic system of soil classification for making and interpreting soil surveys, 2nd edn, Handbook No. 436. Washington DC: US Department of Agriculture. Natural Resources Conservation Service: 869.

Staff, S. S. (1999). Soil Taxonomy. Agricultural Handbook 436, United States Department of Agriculture Washington DC.

Stahlschmidt, M. C., et al. (2018). Geoarchaeological Investigation of Site Formation and Depositional Environments at the Middle Palaeolithic Open-Air Site of 'Ein Qashish, Israel. Journal of Paleolithic Archaeology 1(1): 32-53.

Steegen, a., et al. (2000). Sediment export by water from an agricultural catchment in the Loam Belt of central Belgium. Geomorphology 33(1-2): 25–36.

Steffen, W., et al. (2018). Trajectories of the Earth System in the Anthropocene. Proceedings of the National Academy of Sciences 115(33): 8252-8259.

Stein, M., et al. (2007). Late Quaternary changes in desert dust inputs to the Red Sea and Gulf of Aden from 87Sr/86Sr ratios in deep-sea cores. Earth and Planetary Science Letters 261(1-2): 104-119.

Steinberger, Y., et al. (1999). Soil carbohydrates along a topoclimatic gradient in a Judean desert ecosystem. Land Degradation & Development 10(6): 523-530.

Steinberger, Y., et al. (1999). Phospholipid fatty acid profiles as indicators for the microbial community structure in soils along a climatic transect in the Judean Desert. Biology and Fertility of Soils 28(3): 292-300.

Stiner, M. C., et al. (2001). Bone preservation in Hayonim Cave (Israel): a macroscopic and mineralogical study. Journal of Archaeological Science 28(6): 643-659.

Stoops, G. (2021). Guidelines for analysis and description of soil and regolith thin sections, John Wiley & Sons.

Storozum, M. J., et al. (2021). The influence of ancient herders on soil development at Luxmanda, Mbulu Plateau, Tanzania. CATENA 204: 105376.

Strahler, A. N. (1952). Dynamic basis of geomorphology. Geological society of america bulletin 63(9): 923-938.

Studlar, S. M. (1980). Trampling effects on bryophytes: trail surveys and experiments. Bryologist: 301-313.

Stumm, W. and B. Sulzberger (1992). The cycling of iron in natural environments: considerations based on laboratory studies of heterogeneous redox processes. Geochimica et Cosmochimica Acta 56(8): 3233–3257.

Summerhayes, G. (2017). Archaeological Research at Caution Bay, Papua New Guinea: Cultural, Linguistic and Environmental Setting Edited by T. Richards, B. David, K. Aplin and I. McNiven

Caution Bay Studies in Archaeology 1, Archaeopress Archaeology 297 Archaeopress, Oxford, 2016. Archaeology in Oceania 53(1): 75-76.

Sun, L., et al. (2013). A review on rill erosion process and its influencing factors. Chinese geographical science 23(4): 389-402.

Sutherland, R., et al. (2001). Hydrophysical degradation associated with hiking-trail use: a case study of Hawai'iloa Ridge Trail, O'ahu, Hawai'i. Land Degradation & Development 12(1): 71-86.

Tarolli, P., et al. (2019). From features to fingerprints: A general diagnostic framework for anthropogenic geomorphology. Progress in Physical Geography: Earth and Environment 43(1): 95-128.

Team, R. C. (2020). R: A Language and Environment for Statistical Computing (Vienna. Austria, R Foundation for Statistical Computing.

Tebebu, T. Y., et al. (2010). Surface and subsurface flow effect on permanent gully formation and upland erosion near Lake Tana in the northern highlands of Ethiopia. Hydrology and Earth System Sciences 14(11): 2207-2217.

Tejedo, P., et al. (2016). Assessing environmental conditions of Antarctic footpaths to support management decisions. Journal of Environmental Management 177: 320-330.

Thiemann, S., et al. (2005). Assessment of erosion and soil erosion processes–a case study from the Northern Ethiopian Highland. FWU Water Resour. Publ 3: 173–185.

Thomas, C. D., et al. (2004). Extinction risk from climate change. Nature 427(6970): 145-148.

Tichomirowa, M., et al. (2019). Dating multiply overprinted granites: The effect of protracted magmatism and fluid flow on dating systems (zircon U-Pb: SHRIMP/SIMS, LA-ICP-MS, CA-ID-TIMS; and Rb–Sr, Ar–Ar)–Granites from the Western Erzgebirge (Bohemian Massif, Germany). Chemical Geology 519: 11–38.

Tobler, W. (1993). Three presentations on geographical analysis and modeling, Citeseer.

Tomczyk, A. M. and M. Ewertowski (2013). Quantifying short-term surface changes on recreational trails: The use of topographic surveys and ‘digital elevation models of differences’(DODs). Geomorphology 183: 58-72.

Torri, D. and J. Poesen (2014). A review of topographic threshold conditions for gully head development in different environments. Earth-Science Reviews 130: 73-85.

Tsokas, G. N., et al. (2009). Tracing a major Roman road in the area of ancient Helike by resistivity tomography. Archaeological Prospection 16(4): 251-266.

Tuomi, M., et al. (2021). Stomping in silence: Conceptualizing trampling effects on soils in polar tundra. Functional Ecology 35(2): 306-317.

Ullah, I. I. (2011). A GIS method for assessing the zone of human-environmental impact around archaeological sites: a test case from the Late Neolithic of Wadi Ziqlâb, Jordan. Journal of Archaeological Science 38(3): 623-632.

Ullman, M., et al. (2023). Formation Processes and Spatial Patterning in a Late Prehistoric Cave in Northern Israel, Informed by Slam-Based Lidar. Informed by Slam-Based Lidar.

Umweltamt Steglitz-Zehlendorf von, B. (2016). Wasserbuch Steglitz-Zehlendorf (Memento des Originals vom 13. Januar 2016.

Ur, J. (2003). CORONA satellite photography and ancient road networks: A northern Mesopotamian case study. Antiquity 77(295): 102-115.

USGS (2019). United States Geological Survey (USGS) Earth Explorer, Available online at https://earthexplorer.usgs.gov.

Valentin, C., et al. (2005). Gully erosion: Impacts, factors and control. CATENA 63(2-3): 132–153.

van Andel, T. H., et al. (1990). Land Use and Soil Erosion in Prehistoric and Historical Greece. Journal of Field Archaeology 17(4): 379–396.

van Etten, J. (2017). *R* Package: Distances and Routes on Geographical Grids. Journal of Statistical Software 76(13).

Vandaele, K., et al. (1996). Geomorphic threshold conditions for ephemeral gully incision. Geomorphology 16(2): 161–173.

Vandekerckhove, L., Poesen, J., Wijdenes, D.O. and T. De Figueiredo (1998). Topographical thresholds for ephemeral gully initiation in intensively cultivated areas of the Mediterranean. CATENA 33(3-4): 271–292.

Vanwalleghem, T., et al. (2005). Reconstructing rainfall and land-use conditions leading to the development of old gullies. The Holocene 15(3): 378-386.

Verhagen, P., et al. (2019). Modelling of Pathways and Movement Networks in Archaeology: An Overview of Current Approaches. Computational Social Sciences, Springer International Publishing: 217-249.

Verheijen, F. G., Jones, R.J., Rickson, R.J. and C. J. Smith (2009). Tolerable versus actual soil erosion rates in Europe. Europe. Earth-Science Reviews 94(1-4): 23–38.

Verrecchia, E. P. and L. Trombino (2021). The Future of Soil Micromorphology. A Visual Atlas for Soil Micromorphologists, Springer: Nature 151-155.

Villmoare, B., et al. (2015). Early *Homo* at 2.8 Ma from Ledi-Geraru, Afar, Ethiopia. Science 347(6228): 1352-1355.

Vita-Finzi, C., et al. (1970). Prehistoric Economy in the Mount Carmel Area of Palestine: Site Catchment Analysis. Proceedings of the Prehistoric Society 36: 1-37.

Wadley, L. (2013). Recognizing complex cognition through innovative technology in Stone Age and Palaeolithic sites. Cambridge Archaeological Journal 23(2): 163-183.

Wagenbrenner, J. W., et al. (2015). Effects of post-fire salvage logging and a skid trail treatment on ground cover, soils, and sediment production in the interior western United States. Forest Ecology and Management 335: 176-193.

Walker, R. and L. Craighead (1997). Analyzing wildlife movement corridors in Montana using GIS. Proceedings of the 1997 ESRI user conference, Redlands, USA.

Wang, D., et al. (2020). Long-term impacts of soil compaction and cultivation on soil carbon and nitrogen pools, foliar δ13C and δ15N as well as tree growth in a hoop pine plantation of subtropical Australia. Journal of Soils and Sediments 20(7): 2829–2842.

Wang, D., et al. (2021). Mosaic desert pavement influences water infiltration and vegetation distribution on fluvial fan surfaces. Hydrological Processes 35(9): e14373.

Wang, Z., et al. (2016). Early spring post-fire snow albedo dynamics in high latitude boreal forests using Landsat-8 OLI data. Remote Sensing of Environment 185: 71-83.

Ward-Perkins, J. B. (1962). Etruscan towns, Roman roads and medieval villages: the historical geography of southern Etruria. The Geographical Journal 128(4): 389-404.

Waters, C. N., et al. (2016). The Anthropocene is functionally and stratigraphically distinct from the Holocene. Science 351(6269): aad2622.

Waters, M. R. (1988). The impact of fluvial processes and landscape evolution on archaeological sites and settlement patterns along the San Xavier reach of the Santa Cruz River, Arizona. Geoarchaeology 3(3): 205-219.

Watson, A. (1984). Paths and people in the Cairngorms. Scottish Geographical Magazine 100(3): 151-160.

Weaver, T. and D. Dale (1978). Trampling effects of hikers, motorcycles and horses in meadows and forests. Journal of Applied Ecology: 451-457.

Weber, A. (1929). Theory of the Location of Industries. Chicago, University of Press.

Weber, A. and C. J. Friedrich (1929). Alfred Weber's theory of the location of industries.

Weber, M., et al. (2018). Mathematical Modeling of the Spreading of Innovations in the Ancient World. eTopoi. Journal for Ancient Studies 7: 1-32.

webmineral.com. Minerals Arranged by X-Ray Powder Diffraction. from http://webmineral.com/MySQL/xray.php#.YU8nm0gYBaQ.

Wei (2016). Preliminary characterization of pottery by cathodoluminescence and SEM--EDX analyses: an example from the Yeha region (Ethiopia). In Archaeometry 58(2): 239-254.

Weiß, C., et al. (2016). Preliminary characterization of pottery by cathodoluminescence and SEM–EDX analyses: an example from the Yeha region (Ethiopia). Archaeometry 58(2): 239–254.

Wells, E. C. (2010). Sampling design and inferential bias in archaeological soil chemistry. Journal of Archaeological Method and Theory 17(3): 209-230.

Werner, B. T. and D. E. Mcnamara (2007). Dynamics of coupled human-landscape systems. Geomorphology 91(3-4): 393-407.

Wessolek, G., et al. (2008). Percolation characteristics of a water-repellent sandy forest soil. In European Journal of Soil Science 59(1): 14-23.

Wieder, M. and H. Lavee (1990). Micromorphological characteristics induced by subsurface water flow in the Judean desert. Developments in soil science, Elsevier. 19: 235-243.

Wierzchos, J., et al. (2006). Micromorphological characterization and lithification of microbial mats from the Ebro Delta (Spain). International Microbiology, 2006, vol. 9, núm. 4, p. 289-296.

Wikiloc (2022). Lower Nahal Zeelim. Best Trails in Israel. Retrieved 03.02.2022, 2022, from https://de.wikiloc.com/routen-wandern/lower-nahal-zeelim-21014675.

Wilkinson, T. J. (1993). Linear hollows in the Jazira, upper Mesopotamia. Antiquity 67(256): 548-562.

Wilkinson, T. J., et al. (2010). The geoarchaeology of route systems in northern Syria. Geoarchaeology 25(6): 745-771.

Wilkinson, T. J., et al. (2015). Hydraulic landscapes in Mesopotamia: The role of human niche construction. Water History 7(4): 397-418.

Williams, A. J., et al. (2012). Biological soil crusts in the Mojave Desert, USA: micromorphology and pedogenesis. Soil Science Society of America Journal 76(5): 1685-1695.

Wimpey, J. F. and J. L. Marion (2010). The influence of use, environmental and managerial factors on the width of recreational trails. Journal of Environmental Management 91(10): 2028–2037.

Winterhalder, B. (1981). Foraging strategies in the boreal forest: an analysis of Cree hunting and gathering.

Woldekiros, H. S. (2019). The Route Most Traveled: The Afar Salt Trail, North Ethiopia Chungará (Arica ahead): 0-0.

Woldekiros, H. S. (2019). The route most travelled: The Afar salt trail, North Ethiopia. Chungara 51(1): 95-110.

Wolf, P. and U. Nowotnick (2010). The Almaqah temple of Meqaber Ga?ewa near Wuqro (Tigray, Ethiopia). Proceedings of the Seminar for Arabian Studies 367-380.

Wood, Y., et al. (2005). Surface control of desert pavement pedologic process and landscape function, Cima Volcanic field, Mojave Desert, California. CATENA 59(2): 205-230.

Yadin, Y. (1965). The Excavation of Masada—1963/64: Preliminary Report. Israel Exploration Journal: 1-120.

Yadin, Y. (1966). Masada: Herod's fortress and the Zealots' last stand.

Yaşar Korkanç, S. (2014). Impacts of recreational human trampling on selected soil and vegetation properties of Aladag Natural Park, Turkey. CATENA 113: 219–225.

Yekutieli, Y. (2004). The desert, the sown and the Egyptian colony. Ägypten und Levante/Egypt and the Levant: 163-171.

Yekutieli, Y. (2005). Landscape of Control. Ancient near eastern studies 41(0): 5-37.

Yekutieli, Y. (2006). Is somebody watching you? Ancient surveillance systems in the southern Judean Desert. Journal of Mediterranean Archaeology 19(1): 65.

Yekutieli, Y. (2009). The Har Hemar site: a northern outpost on the desert margin? Tel Aviv 36(2): 218-240.

YLI-HALLA, M., et al. (2009). Evidence for the formation of Luvisols/Alfisols as a response to coupled pedogenic and anthropogenic influences in a clay soil in Finland. Agricultural and Food Science 18(3-4): 388–401.

Yukihara, E. G. and S. W. McKeever (2011). Optically stimulated luminescence: fundamentals and applications, John Wiley & Sons.

Zachar, D. (2011). Soil erosion, Elsevier.

Zádorová, T. and V.Ení žek (2018). Formation, morphology and classification of colluvial soils: a review. European Journal of Soil Science 69(4): 577-591.

Zedeno, M. (2016). The Archaeology Of Territory. Handbook of landscape archaeology: 210-217.

Zedeño, M. N. and R. W. Stoffle (2003). Tracking the role of pathways in the evolution of a human landscape: the St Croix riverway in ethnohistorical perspective. The Colonization of Unfamiliar Landscapes, Routledge: 83-85.

Zgłobicki, W., et al. (2021). Sunken lanes-Development and functions in landscapes. Earth-Science Reviews: 103757.

Zhang, T., et al. (2017). Band selection in sentinel-2 satellite for agriculture applications. 2017 23rd International Conference on Automation and Computing (ICAC), IEEE.

Zhang, Y., et al. (2019). Rill and gully erosion on unpaved roads under heavy rainfall in agricultural watersheds on China's Loess Plateau. Agriculture, Ecosystems & Environment 284.

Ziegler, A. D., et al. (2000). Runoff generation and sediment production on unpaved roads, footpaths and agricultural land surfaces in northern Thailand. Earth Surface Processes and Landforms 25(5): 519-534.

Ziegler, A. D., et al. (2001). Acceleration of Horton overland flow and erosion by footpaths in an upland agricultural watershed in northern Thailand. Geomorphology 41(4): 249–262.

Zipf, G. K. (1946). The P 1 P 2 D Hypothesis: On the Intercity Movement of Persons. American Sociological Review 11(6): 677.

Zituni, R., et al. (2021). Magnitude, frequency and hazard assessment of the largest floods in steep, mountainous bedrock channels of the Southern Judean Desert, Israel. Journal of Hydrology: Regional Studies 37: 100886.

Zolotokrylin, A. N., et al. (2020). Local climatically-driven changes of albedo and surface temperatures in the Sonoran Desert. Journal of Arid Environments 178: 104147.

8.2 Supplementary materials

Supplementary materials chapter 4

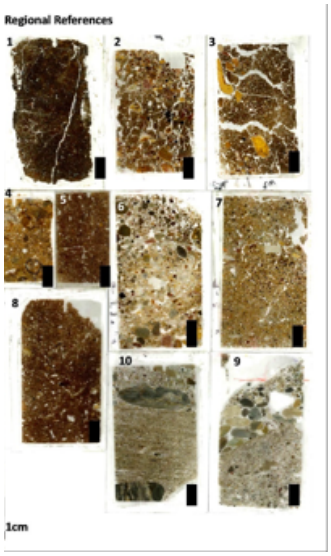

Supplementary Fig. 1. Regional reference sample slides. Black bar corresponds to 1 cm.

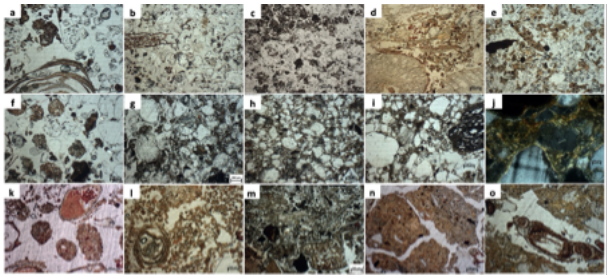

Supplementary Fig. 2. G1 control, surface (a) and subsurface (b). G1 footpath, surface (c), and subsurface (d and e). G2 control surface (f) and subsurface (g). G2 footpath surface (h), and subsurface (I and j). G2 control surface (k) and subsurface (l). G2 footpath surface (sample M), and subsurface (n and o). All images are taken in PPL apart from j that is taken in XPL.

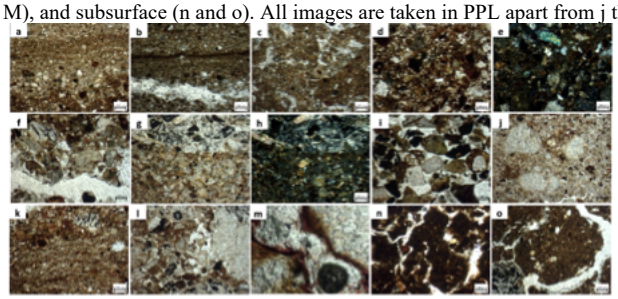

Supplementary Fig. 3. Rama incised footpath surface (a) and subsurface (b). Yeha incised footpath (sample Y), 6 cm (c,d), 8 cm (f,e), 12 cm (g and h) and 15 cm (i) below surface. Yeha incised footpath margins (sample Y*), 1 cm (j), 3 cm (k) and 6 cm (l and m) below surface. Melazo incised footpath (sample M), 7 cm (n) and 11 cm (o) below surface. All images were taken in PPL apart from e and h that were taken in XPL.

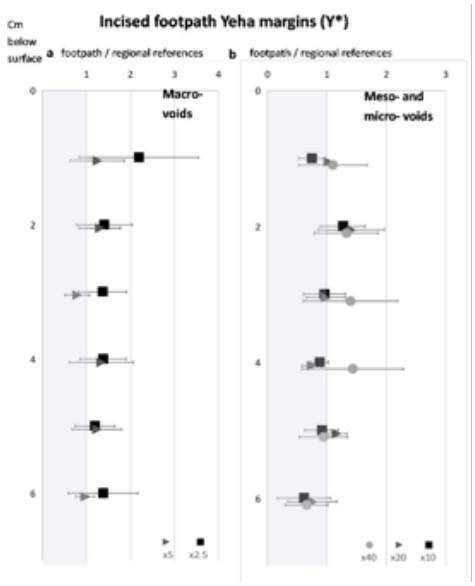

Supplementary Fig. 4. Relative differences in porosity ('imager' package in R environment). a-b. Between incised footpath Yeha margins (sample Y*) and regional reference samples (n=5).

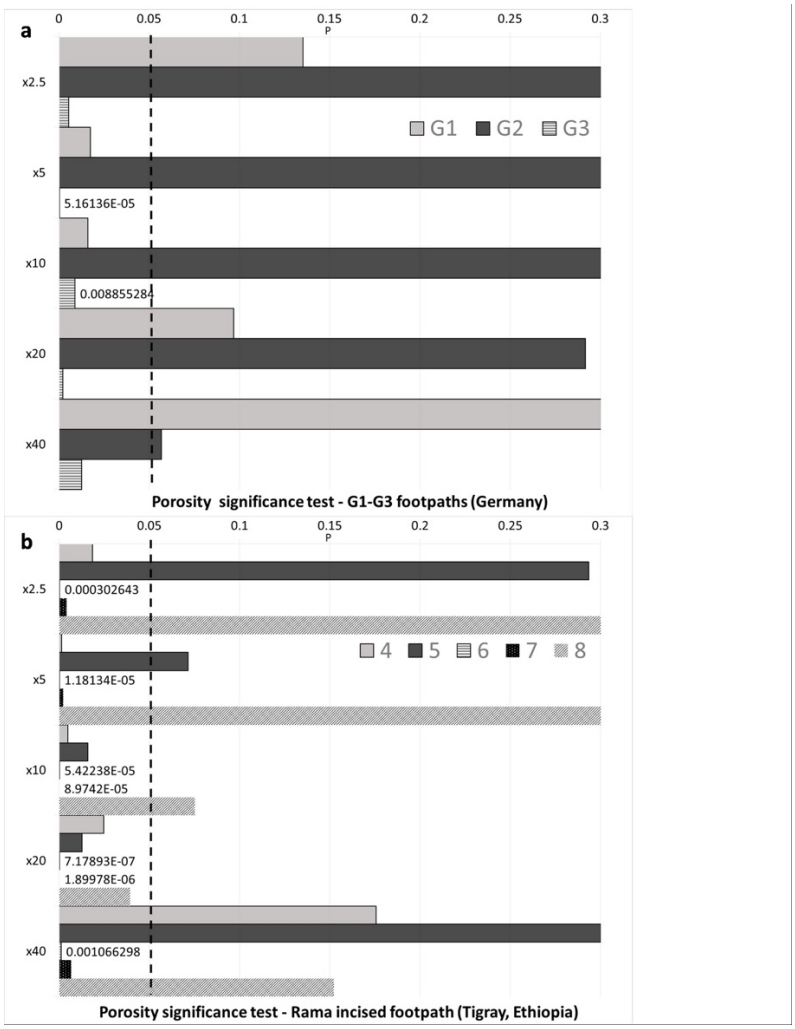

Supplementary Fig. 5. Significance tests (T test), comparing porosity in footpath samples with control samples (for footpaths located in Germany) and regional reference samples (for Rama footpath in Tigray). The test takes the entire upper 5 cm of the footpath samples into account. a. The three footpaths from Germany (samples G1F-G3F) tested against their control samples (samples G1C-G3C). b. The (currently used) incised footpath (sample R) from Tigray tested against five regional reference samples (samples 4-8). The five objective lens sizes (y axis) are aimed at detecting macro (x2.5, x5), meso (x10) and micro (x20, x40) voids. Values left of the dotted lines show significantly lower porosity in the footpath than in associated control or regional reference sample for a given objective lens.

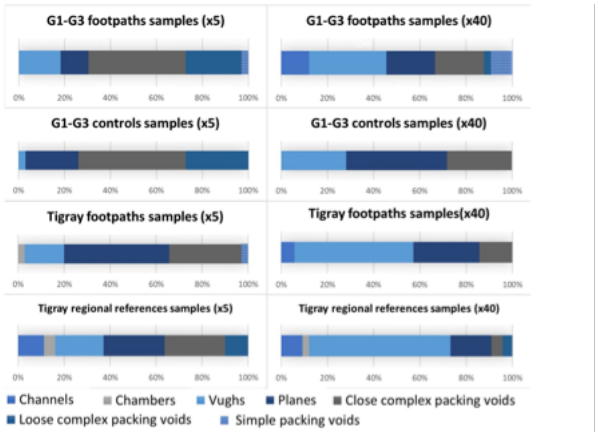

Supplementary Fig. 6. Differences in void types for the objective lenses x5 and x40 divided into sampling groups of (1) footpath and control samples originating from Germany (n=65 for each objective lens step) and (2) footpath and regional reference samples originating from Tigray (n=100 for each objective lens step).

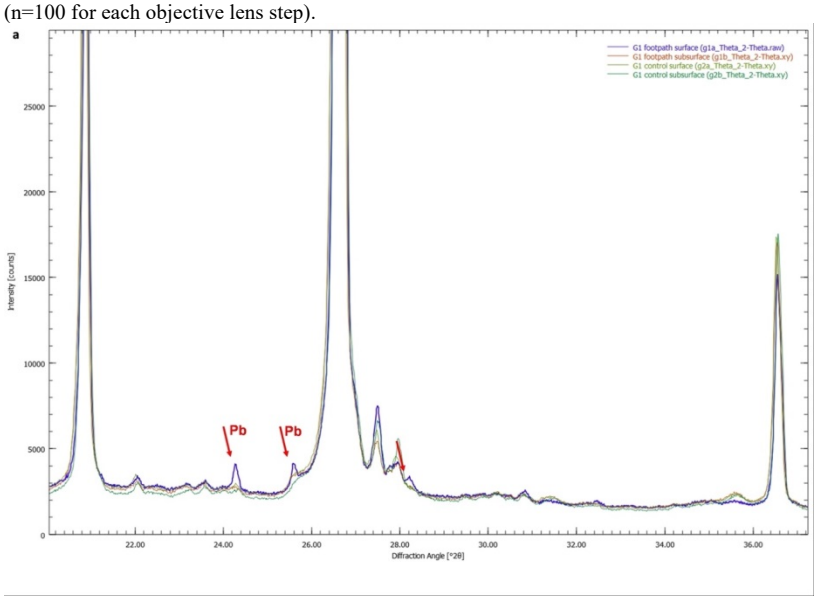

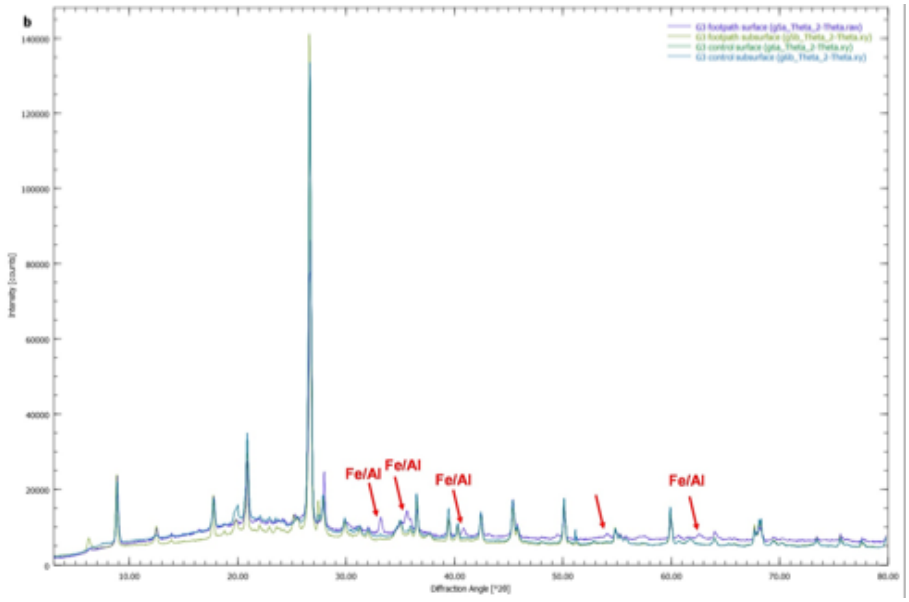

Supplementary Fig. 7. X-Ray Diffraction (XRD) spectra of footpaths G1 (7a) and G3 (7b), located in the sandy forest west of Berlin and the fine grained Ore mountains accordingly, both of a temperate climatic zone (n=4 for each). Arrows pointing at peaks attributed to Pb (Fig 7a) or Fe/Al oxides (Fig 7b) that are evident in the footpath surface sample but not in the control sample or the subsurface of the path.

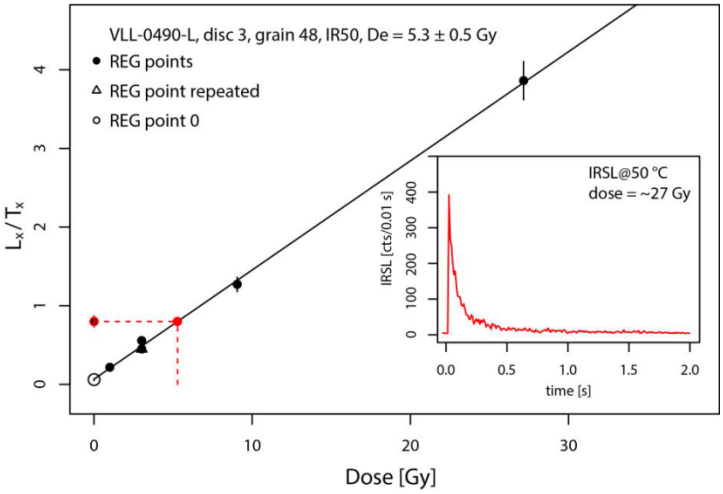

Supplementary Fig. 8. Representative dose response curve and decay curve for a single feldpsar grain of sample VLL-0490-L. Plots generated using the R-luminescence package of Kreutzer et al. (2012).

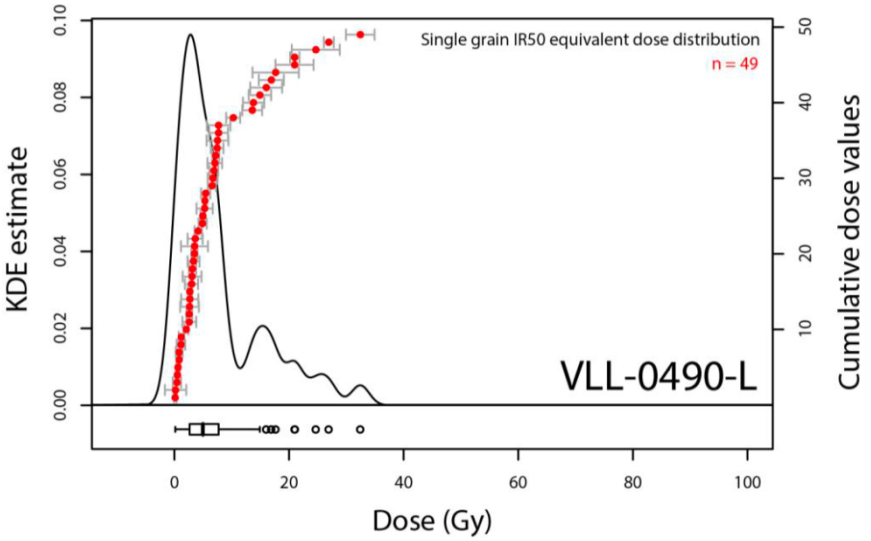

Supplementary Fig. 9. Single grain equivalent dose distribution for sample VLL-0490-L showing the equivalent doses as well as a box plot and a KDE estimate plot. Plot generated using the R-luminescence package of Kreutzer et al. (2012).

Supplementary Table 1. grain size distribution for samples from currently used footpaths in Germany

Sample\mm	>2mm	1-2mm	<1mm	>mm 2%	1-2mm %	<1mm %
G1 F 0-3.5	3.12	1.58	33.8	8.1038961	4.1038961	87.7922078
G1 F 3.5-	4.34	1.2	43.66	8.82113821	2.43902439	88.7398374
G1 C 0-1.5	3.12	2.4	39.62	6.91182986	5.3167922	87.7713779
G1 C 1.5-	1.58	2	116.16	1.31952564	1.67028562	97.0101887
G2 F 0-6	12.64	7.29	54.93	16.8848517	9.73817793	73.3769703
G2 F 6-	6.11	9.59	62.73	7.79038633	12.227464	79.9821497
G2 C 0-6	5.05	2.63	28.98	13.7752319	7.17403164	79.0507365
G2 C 6-	3.99	2.66	34.7	9.64933495	6.43288996	83.9177751
G3 F 0-7-	47.92	14.31	71.87	35.7345265	10.6711409	53.5943326
G3 F 7-15	24.21	3.69	27.39	43.7873033	6.67390125	49.5387954
G3 C 0-8	5.97	3.17	16.82	22.9969183	12.211094	64.7919877
G3 C 8-13	38.61	8.11	35.46	46.9822341	9.86858116	43.1491847

Supplementary Table 2. Locations and depths of the regional references

Regional reference sample	Location	Type	Depth below surface
1	c. 110 m northeast of the Melazo archaeological site	Natural gully exposure	80 cm
2			65 cm
3			70 cm
4	c. 1 km south of the Yeha archaeological site	Natural gully exposure	270 cm
5			310 cm
6	c. 360 m northwest of the Melazo archaeological site	Natural gully exposure	70 cm
7			120 cm
8	c. 2 km east of the Rama incised footpath.	Natural gully exposure	290 cm

9	c. 150 m north of the Rama incised footpath.	Gully fan deposits	5-13 cm
10			13-20 cm
11	c. 2 m south of the Yeha incised footpath	Natural gully exposure	5-10 cm

Supplementary Table 3. Micromorphological description of footpath and control samples from Germany (samples G1-G3) and incised footpaths from Tigray, Ethiopia (samples R, Y, Y* and M). See supplementary Figs. 2 and 3 for illustration.

Site	Type	Depth	Inorganic constituents	Micro-structure	Voids	c/f related distrib.	Organic residues, pedofeatures and b-fabric
G1	Control sample G1C	Surface	Medium to coarse sand sized subangular quartz	Single grain to crumb	Complex packing voids, vughs	Monic to enaulic	Gravel sized plant organ and tissue residues, humified plant residues impregnated with Fe oxides, undifferentiated b-fabric
		Sub-surface	Medium to coarse sand sized subangular quartz	Crumb	Complex packing voids, vughs	Enaulic	Very few 0.5 mm long and 0.2 mm thick elongated plant organ and tissue residues, few humified plants and cells residues and typic Fe oxide nodules, undifferentiated b-fabric
	Footpath G1F	Surface	Fine to medium sand sized subrounded quartz	Massive and crumb	Complex packing voids	Porphyric, Enaulic	Plant tissue and humified plant residues sometimes impregnated with Fe oxides, undifferentiated b-fabric
		Sub-surface	Few fine to medium sand sized subrounded quartz	Granules to crumb	Complex packing voids, vughs	Enaulic, Porphyric	Amorphous organic fine material impregnated with Fe oxides, gravel sized plant tissue residues. Few spherese organic excrements and sand sized, angular to sub rounded and digitate, dark Fe nodules, undifferentiated b-fabric
G2	Control sample G2C	Surface	Medium to coarse sand sized sub rounded quartz	Granules to crumb	Complex packing voids	Enaulic	Sand sized pellets and plant tissues crumbs. Humified plant residues are impregnated with Fe oxides, undifferentiated b-fabric
		Sub-surface	Very fine to medium sand sized sub rounded quartz. Micromass: quartz silts and clays	Massive and crumb	Complex packing voids, vughs	Enaulic, porphyric	Few humified plant residues with amorphous organic staining and humified plant organ residues. Polymorphic amorphous organic fine material, undifferentiated b-fabric
	Footpath G2F	Surface	Medium to fine sand sized sub rounded and subangular quartz and feldspar. Micromass: silt and clay	Massive	channels, planes	Porphyric	Humified plant and cell residues and Mn typic mammillate nodules, undifferentiated b-fabric
		Sub-surface	Fine and coarse sand sized sub rounded quartz and feldspar. Micromass: quartz silt and clay	Massive	Complex packing voids	Porphyric	C. 1 mm sized humified or charred plant organ residues, granostriated and speckled b-fabric
G3	Control sample G2C	Surface	Sand sized clay aggregates	Granules to crumb	Complex packing voids	Enaulic	Amorphous organic fine material and Al/Fe oxides. Undifferentiated b-fabric
		Sub-surface	Micromass: clay	Massive to crumb	Complex packing voids. vughs, chambers	Enaulic, porphyric	Large plant organ residues (c. 500um diameter) and finer (fine sand size)

							humified plant residues, undifferentiated b-fabric
	Footpath G3F	Surface	Subangular sand to gravel sized minerals and rock fragments	Massive	complex packing voids, planes	Porphyric	Polymorphic amorphous organic fine material visible as crumb aggregates, plant organ residues and Al and Fe oxides. Undifferentiated b-fabric
		Sub-surface	Subangular sand to gravel sized minerals and rock fragments	Subangular blocky	Planes, channels, vughs	Porphyric	Typic Fe oxide nodules and plant organ residues are evident within planes and channels, undifferentiated b-fabric
Rama		Surface	Silt and fine sands of quartz, clay	Bedded-massive	complex packing voids, vughs, horizontal planes	Porphyric	Silty layers (>200 µm) with fine sand alternating with clayey layers that are impregnated with Fe oxides. In addition, there are thin (c. 70 µm) layers of clay with Fe oxides impregnation. Typic Fe oxide nodules, undifferentiated b-fabric
		Sub-surface	Silt and fine sand of quartz, clay	Massive to vermicular	Vughs, planes, channels	Porphyric	Weakly developed peds and typic Fe oxide nodules, speckled b-fabric
Yeha		6-8 cm	Fine sand subrounded to subangular quartz and few olivine Micromass: mica and quartz silt	Crumb to massive	Vughs, channels	Porphyric to enaulic	Typic Fe oxide nodules, Fe impregnated, undifferentiated b-fabric
		8-10cm	Fine to medium sand size subangular quartz, feldspar, micas and rock fragments Micromass: mica and quartz silt and clays	Crumb to massive	Vughs, planes	Porphyric to enaulic	Fe impregnated clay, horizontal semi accommodating plane (100-500 µm wide) at the contact to upper layer (8 cm), undifferentiated b-fabric
		10-13 cm	Fine sand sized and subangular quartz, mica and amphibole. Micromass: mica and quartz silt	Massive	Vughs, planes	Porphyric	Typic Fe oxide nodules undifferentiated b-fabric, calcitic construction material
		13-18	Medium to coarse sand sized, subangular to subrounded rock fragments and quartz grains	Massive	Complex packing voids	Enaulic to monic	Homogenous and grain-supported. Fe oxide nodules and impregnation of clayey-silty aggregates, undifferentiated b-fabric
Yeha margins		1-7 cm	Fine to coarse sand size, subrounded rock fragments, feldspar and quartz. Micromass: silty clay	bedded – massive, crumb	Complex packing voids, planes, vughs	Porphyric to enaulic	Bedding of alternating silts and clays layers at 7cm below surface grains are also coated with amorphous clay and Fe oxides, undifferentiated b-fabric, some units are massive and compacted
Melazo		6-12 cm	Few fine sand sized subangular minerals and basalt fragments. Micromass: clay	Subangular blocky	Channels, planes, vughs	Porphyric	Fe impregnation, limpid to speckled aspect, poro-striated b-fabric

Supplementary Table 4. The % of void types for each sample for the four objective lenses in 1cm intervals.

		channels-vesicles %	Chambers %	Vughs %	Planes %	close complex pack %	loose complex%	simple pack %
Macro-voids	G1 Footpath	0	0	9.1	0	63.636	27.273	0
	G1 control	0	0	0	0	54.545	36.364	9.0909
	G2 Footpath	0	0	45	36.36364	9.0909	9.0909	0
	G2 Control	0	0	9.1	9.090909	81.818	0	0
	G3 Footpath	0	0	0	60	40	0	0
	G3Control	0	0	0	0	18.182	81.818	0
	Yeha 6-13	0	0	43	42.85714	14.286	0	0
	Yeha 13-20	0	0	0	0	85.714	0	14.286
	Yeha margins	0	0	14	28.57143	57.143	0	0
	Melazo	0	14	0	85.71429	0	0	0
	Rama	0	0	29	71.42857	0	0	0
	RR 1	43	14	14	28.57143	0	0	0
	RR 2	0	14	0	85.71429	0	0	0
	RR 3	14	0	14	71.42857	0	0	0
	RR 4	0	20	60	0	20	0	0
	RR 5	40	0	20	20	20	0	0
	RR 6	0	0	14	14.28571	28.571	42.857	0
	RR 7	0	0	17	16.66667	66.667	0	0
	RR 8	14	0	71	14.28571	0	0	0
	RR 9	0	0	0	0	42.857	57.143	0
	RR 10	0	0	0	14.28571	85.714	0	0
		channels-vesicles %	chambers	vughs	planes	close complex pack	loose cmplex	close simple pak
Meso-voids	G1 Footpath	18	0	0	9.090909	54.545	18.182	0
	G1 control	9.1	0	0	0	45.455	36.364	9.0909
	G2 Footpath	9.1	9.1	36	36.36364	9.0909	0	0
	G2 Control	0	0	18	27.27273	54.545	0	0
	G3 Footpath	0	0	20	40	40	0	0
	G3Control	0	0	9.1	0	54.545	27.273	9.0909
	Yeha 6-13	0	0	14	85.71429	0	0	0
	Yeha 13-20	0	0	29	28.57143	42.857	0	0
	Yeha margins	14	14	29	0	28.571	14.286	0
	Melazo	29	14	14	42.85714	0	0	0
	Rama	0	0	43	57.14286	0	0	0
	RR 1	14	29	14	42.85714	0	0	0
	RR 2	29	14	43	14.28571	0	0	0
	RR 3	0	0	71	28.57143	0	0	0
	RR 4	0	20	40	20	20	0	0
	RR 5	40	60	0	0	0	0	0
	RR 6	0	0	14	57.14286	0	28.571	0
	RR 7	0	0	29	14.28571	57.143	0	0
	RR 8	0	43	57	0	0	0	0
	RR 9	0	0	0	57.14286	42.857	0	0
	RR 10	0	0	29	14.28571	57.143	0	0
		channels-ves	chambers	vughs	planes	close complex pack	loose cmplex	close simple pak
Meso1-voids	G1 Footpath	18	0	9.1	27.27273	45.455	0	0
	G1 control	18	0	9.1	0	45.455	9.0909	18.182
	G2 Footpath	0	0	36	63.63636	0	0	0
	G2 Control	0	0	0	72.72727	27.273	0	0
	G3 Footpath	10	0	30	30	30	0	0
	G3Control	0	0	18	9.090909	45.455	27.273	0
	Yeha 6-13	0	0	29	71.42857	0	0	0
	Yeha 13-20	0	0	29	57.14286	14.286	0	0

	Yeha margins	14	14	14	0	42.857	14.286	0
	Melazo	14	0	71	14.28571	0	0	0
	Rama	14	0	43	42.85714	0	0	0
	RR 1	29	14	29	28.57143	0	0	0
	RR 2	29	0	43	28.57143	0	0	0
	RR 3	14	0	43	42.85714	0	0	0
	RR 4	0	0	80	0	20	0	0
	RR 5	20	40	40	0	0	0	0
	RR 6	0	0	43	28.57143	0	28.571	0
	RR 7	0	0	71	14.28571	14.286	0	0
	RR 8	0	14	71	14.28571	0	0	0
	RR 9	0	0	0	28.57143	71.429	0	0
	RR 10	0	0	14	42.85714	42.857	0	0
		channels-ves	chambers	vughs	planes	close complex pack	loose cmplex	close simple pak
Micro-voids	G1 Footpath	9.1	0	55	9.090909	27.273	0	0
	G1 control	18	0	18	0	36.364	9.0909	18.182
	G2 Footpath	9.1	0	27	54.54545	0	0	9.0909
	G2 Control	0	0	27	63.63636	9.0909	0	0
	G3 Footpath	0	0	30	40	30	0	0
	G3Control	0	0	27	27.27273	45.455	0	0
	Yeha 6-13	0	0	29	57.14286	14.286	0	0
	Yeha 13-20	0	0	57	28.57143	14.286	0	0
	Yeha margins	0	0	43	14.28571	42.857	0	0
	Melazo	29	0	43	28.57143	0	0	0
	Rama	0	0	86	14.28571	0	0	0
	RR 1	0	14	86	0	0	0	0
	RR 2	29	0	71	0	0	0	0
	RR 3	29	14	43	14.28571	0	0	0
	RR 4	0	0	60	20	20	0	0
	RR 5	20	0	80	0	0	0	0
	RR 6	0	0	43	14.28571	0	42.857	0
	RR 7	14	0	71	14.28571	0	0	0
	RR 8	0	0	71	28.57143	0	0	0
	RR 9	0	0	57	28.57143	14.286	0	0
	RR 10	0	0	29	57.14286	14.286	0	0

Supplementary Table 5. XRF Fe, TOC and Fe extraction methods for the footpath samples originating from Germany and Tigray, Ethiopia

	Total Fe XRF	**Fe (ug/g)**	**/XRF**	**RDS**	**Al 396.153 (ug/g)**	**RDS**
G1sFsurface	4746	**268.000**	0.056	1.0%	23.198	3.0%
G1F subsurface	5252.86	206.812	0.039	1.2%	95.102	2.1%
G2 surface	4062.29	232.737	0.057	2.2%	100.583	0.4%
G2b subsurface	3555.64	259.353	0.073	1.2%	102.857	1.2%
G3 surface	14365.52	704.533	0.049	2.9%	281.289	0.6%
G3b subsurface	16733.11	477.457	0.029	3.3%	264.410	0.3%
G4 surface	13493.26	609.305	0.045	1.5%	259.722	1.3%
G4b subsurface	7631.29	711.557	0.093	1.2%	330.975	0.3%
G5 surface	101603.41	2733.443	0.027	0.1%	2025.110	1.9%
G5b subsurface	67029.79	3227.610	0.048	1.4%	2726.583	0.8%
G6 surface	36804.14	961.181	0.026	2.1%	242.501	0.3%
G6b subsurface	51648.28	5893.591	0.114	2.4%	1010.120	0.6%
Yeha Y 0-13	140655.92	1480.537	0.011	3.2%	1845.771	1.2%
Y6b 13-18	140163.84	1198.086	0.009	1.7%	1289.785	0.6%

Yeha Y*	95117.27	483.014	0.005	0.8%	794.358	1.0%
RR11	85949.93	412.368	0.005	3.0%	404.682	0.5%
Melazo	105604.23	970.107	0.009	0.6%	1550.767	1.1%
RR6 (subsurface)	92775.3	740.885	0.008	1.1%	1050.789	0.9%
DPG2-2	108424.72	373.361	0.003	2.4%	366.323	1.0%
Rama surface	92148.8	788.134	0.009	0.4%	716.989	0.4%
RR9	25275.05	195.002	0.008	1.6%	270.065	0.7%
	Organic Carbon/TC	**Fe (ug/g)**	**/XRF**	**RSDs**	**Al (ug/g)**	RSDs
G1sFsurface	8.6797297	334.151	0.070	3.1%	214.268	1.2%
G1F subsurface	5.5186567	325.058	0.062	0.7%	192.187	0.4%
G2 surface	6.9333333	309.558	0.076	1.5%	175.750	1.4%
G2b subsurface	2.8935733	345.795	0.097	1.8%	164.513	0.7%
G3 surface	2.3972621	793.078	0.055	1.6%	134.826	1.3%
G3b subsurface	1.597861	474.878	0.028	4.0%	105.250	1.0%
G4 surface	2.8549801	698.379	0.052	1.3%	220.744	0.0%
G4b subsurface	8.6850606	569.444	0.075	2.3%	143.403	1.1%
G5 surface	14.043478	3041.038	0.030	1.6%	3421.925	2.3%
G5b subsurface	9.930759	4178.694	0.062	1.7%	#####	1.7%
G6 surface	39.019737	1879.273	0.051	0.5%	818.796	0.4%
G6b subsurface	24.930114	9370.689	0.181	3.5%	#####	0.7%
Yeha Y 0-13	0.7187105	611.689	0.004	3.1%	1055.202	1.6%
Y6b 13-18	0.4102886	643.834	0.005	3.2%	1119.313	1.5%
Yeha Y*	0.975	520.785	0.005	2.5%	1338.914	0.6%
RR11	1.0433766	239.735	0.003	2.6%	136.456	1.1%
Melazo	1.3472527	575.166	0.005	2.1%	696.809	0.6%
RR6 (subsurface)	1.2638132	371.820	0.004	2.6%	403.819	1.1%
DPG2-2	0.2655928	334.017	0.003	1.0%	624.558	1.1%
Rama surface	16.915803	733.021	0.008	1.2%	877.855	1.2%
RR9	0.3694737	677.064	0.027	2.6%	925.704	1.3%
		Fe (ug/g)	**/XRF**	**RSDs**	**Al (ug/g)**	**RDS**
G1sF surface		203.780	0.043	2.5%	152.855	0.5%
G1F subsurface		382.193	0.073	0.2%	249.778	1.2%
G2 surface		261.930	0.064	2.5%	180.400	1.1%
G2b subsurface		359.021	0.101	3.2%	203.193	0.9%
G3 surface		604.210	0.042	3.2%	132.272	1.5%
G3b subsurface		425.775	0.025	0.4%	116.036	0.4%
G4 surface		496.431	0.037	3.0%	199.697	0.2%
G4b subsurface		497.676	0.065	2.3%	168.000	0.6%
G5 surface		3232.488	0.032	1.1%	3439.741	0.9%
G5b subsurface		6499.029	0.097	2.0%	#####	2.1%
G6 surface		1391.709	0.038	3.8%	634.417	0.9%
G6b subsurface		9222.506	0.179	1.9%	1861.084	0.9%
Yeha Y 0-13		261.102	0.002	2.7%	482.470	0.6%
Y6b 13-18		276.398	0.002	2.0%	507.870	1.5%
Yeha Y*		219.983	0.002	1.8%	619.245	0.8%
RR11		109.732	0.001	5.8%	149.441	1.0%
Melazo		505.320	0.005	1.0%	466.152	1.4%
RR6 (subsurface)		187.759	0.002	0.5%	168.612	0.3%
DPG2-2		149.595	0.001	4.6%	224.278	0.3%
Rama surface		375.067	0.004	1.5%	430.841	0.6%
RR9		276.105	0.011	2.3%	383.105	0.6%

Supplementary Table 6. Characteristics and topographic positions of the sampled incised footpaths in central Tigray

Incised footpath	Length (m)	Surface area (m²)	Footpath Median Slope°	Footpath Mean slope ° **	Footpath Mean slope SD	Watershed median slope deg	Watershed mean slope°	Watershed mean slope° SD
Rama	2191	11449	2.6	4.3	4.1	6.5	9.9	8.8
Yeha^	3185	19138	9.9	10.3	5.9	16.6	17.5	9.9
Melazo	2654	18781	2.3	2.4	2.0	3.3	4.3	3.4

^Yeha incised footpath refers to the well-connected segments of this footpath close to the sampling area only and not the identified continuation of it to the north ** averaged values along the line features of the incised footpaths

Supplementary Table 7. Gullies in the vicinity of non-incised and incised footpaths

	Gully heads in 5 m distance to footpath	Gully heads in 5 m distance to footpath per 100 m of footpath
Non-incised footpaths	57	0.195
Incised footpaths	5	0.089

Supplementary Table 8. Summary of luminescence data

Sample lab code	Sample field code	238Ur (Bq/Kg)	232Th (Bq/Kg)	40K (Bq/Kg)	Depth (m)	Fs ir50 De (Gy) [1]	Dose rate (Gy/Ka) [2]	IR50 age (ka) fade d [3]	IR50 (ka) fading corrected [4]
VLL 0490-L	MM3-OSL4	17.1 ±1.5	15.2_±1.1	329_±20	0.25	2.99_±0.18	2.47_±0.18	1.2_±0.1	1.5_±0.2

1 Calculated using the bootstrapped MAM-3 (Galbraith et al. 1999, Cunningham & Wallinga 2012).
2 Overall feldspar doserate.
3 Age calculated using the software ADELE (Kulig 2005).
4 Corrected for fading according to the method of Huntley & Lamothe (2001) using the R Luminescence package (Kreutzer et al. 2012).

Supplementary Text 1. Regional reference samples descriptions
Regional reference sample 8 was sampled from a natural gully exposure ca. 600 m south-east of a segment of the Rama footpath and ca. 2.4 km east of the footpath's sampling location. This reference sample was taken from a compacted silty deposit containing occasional pebbles, at a depth of 290 cm below surface. Regional reference samples 9-10 were consecutively (vertically) sampled at a gully fan, located ca. 90 m northwest of a section of the Rama incised footpath and ca. 1.5 km west of the footpath's sampling location. The layer sampled in regional reference sample 9 contains silty sands and gravels a depth of 20-25 cm below surface while regional reference sample 10 contains silty sand at a depth of ca. 25-35 cm below surface.
Regional reference sample 4 was sampled from a natural exposure 1.2 km south of the archaeological site of Yeha. The sample was extracted from a layer contacting fine sand, silts and gravels with pebbles (2-15 cm) layered in ca. 5-15 cm intervals, a at depth of 270 cm below surface. Regional reference sample 5 was sampled on the same exposure, ca. 70 m south of regional reference sample 4, from a homogeneous silty layer at a depth of 310 cm below surface.
The regional reference sample 1 was extracted ca. 110 m north-east of the Melazo archaeological site, from a natural gully exposure of heavily compacted massive, dark reddish to grey, silty clay deposits at ca. 80 cm below surface. Regional reference samples 2-3 were extracted 2 meters east of regional reference sample 1, within a similar grey clayey groundmass exhibiting here lamination of sub angular (1-3 cm sized) gravels and a mix of clay and sand, at 60-75 cm below surface. Regional reference sample 6 was taken ca. 360 m north-west of the archaeological site, at a gully exposed profile composed of sandy silt, gravels and sub angular stones at a depth of 70 cm below surface. Reference sample 7 was extracted at a depth of 120 cm below surface within the same exposure as reference sample 6. The sampled layer of reference sample 7 included Intercalations of bedded stones and gravels in a sandy matrix.

Supplementary Text 2. Carbon Dating ^{14}C
Soil organic carbon from five bulk samples of micromorphological regional references and under footpath surfaces were dated. AMS ^{14}C dating was performed at the Foundation of the A. Mickiewicz University ul. Rubież 46, 61-612 Poznań, Poland - Poznań Radiocarbon Laboratory using "Compact Carbon AMS" machine produced by NEC, and the self-designed lines for graphite production from natural samples. The published procedure is available at Goslar et al (2004) and at https://radiocarbon.pl/en/ams-laboratory/. Preliminary ^{14}C investigation of the upper 30cm of the Yeha footpath main sampling location, using two bulk samples for carbon dating, gave 215 years BP at 3-7 cm below surface and 1285 years BP at 17-20 cm below surface. Suggesting accumulation or at least the formation of the organic carbon, took place throughout the last millennium, excluding possible old wood effect. This generally supports a long term accumulation of the sediments, while micromorphology reflects the use of the dated location at these depths as a footpath and a stream (also related to footpath incision) . In the Daraga footpath, only one ^{14}C value could be extracted at 12 cm below surface giving the date of 995 years BP. As this is only one value, it is not to be over interpreted, however if this reflects sedimentation rather than soil formation, it generally supports a similar timing of the deposition as the Yeha sample. At the Daraga regional reference profile, samples were fated to 1600 and 1530 years BP at 70 and 180 cm below surface accordingly, indicating possibly slower accumulation for non-footpath areas but this should be taken cautiously considering the problematic nature of dating amorphas organic carbon. Samples have a max error of -+35 years.

References
Goslar, T., Czernik, J. and Goslar, E., 2004. Low-energy 14C AMS in Poznań radiocarbon laboratory, Poland. Nuclear instruments and methods in physics research section B: Beam Interactions with Materials and Atoms, 223, pp.5-11.

Supplementary text 3: Luminescence dating (Corresponding author for this supplement: C. Lüthgens, christopher.luethgens@boku.ac.at)
Introduction
This supplementary text provides detailed information on the luminescence methods, experimental setup, data evaluation and age calculation used in this study. The methodological approach was successfully applied in previous studies, which will be referenced below in order to keep this document as concise as possible. For the interpretation of the luminescence age, please see the main text of the publication. All analyses described in the supplement were conducted at the Vienna Laboratory for Luminescence dating (VLL), at the Institute of Applied Geology,

University of Natural Resources and Life Sciences, Vienna. In general, luminescence dating techniques enable the determination of depositional ages for sediments. During light exposure (transport) of quartz and feldspar grains in nature, the latent luminescence signal is depleted (zeroed or optically bleached), while after burial, the mineral grains act as natural dosimeters accumulating energy (equivalent dose) imparted from naturally occurring radionuclides and cosmic radiation over time (dose rate). A luminescence age can be calculated according to the general age equation

age = equivalent dose (Gy) / dose rate (Gy/a).

For detailed information the background of luminescence dating, please see the following overview papers: Preusser et al. (2008), Rhodes (2011), Wintle (2008).

Sample preparation and initial tests

Given the challenging sampling situation in the field, only one sample could be taken for luminescence dating purposes by driving a stainless steel cylinder into the freshly cleaned sediment face. An additional sample from the bulk sediments surrounding the sampling sport was taken for radionuclide analysis. The luminescence sample was packed light-tight and transported to the VLL. At the VLL, all sample preparation was conducted under subdued red light conditions according to a standard procedure described in detail in Lüthgens et al (2017) and Rades et al. (2018). The quartz and potassium-rich feldspar separates obtained in the grain size of 200- 250 µm were subsequently tested for their basic luminescence properties, and unfortunately, quartz revealed poor qualities (dim signals and slow signal decay indicating the lack of a dominant fast component in the quartz signal required for dating). Because of that, all subsequent luminescence analyses were conducted using feldspar as a dosimeter.

The bulk sample for radionuclide analysis using low-level, high-resolution gamma spectrometry was dried and stored in a sealed Petri-dish (~60g dry weight) for at least a month to re-establish secondary Rn (Radon) equilibrium before measurement.

Experimental setup quality tests

Determination of the equivalent dose

Given the nature of the sampled sediments, the short transport distances minimize the chance for sufficient light exposure (to ensure complete bleaching) of the mineral grains during transport. In such cases, incomplete bleaching of the luminescence signal of sediments prior to subsequent burial may occur, which leads to age overestimation if not detected and corrected for. To reliably detect potential incomplete bleaching in the sample under investigation, a single-grain regenerative dose protocol (eliminating averaging effects if aliquots with multiple grains were used, Reimann et al. 2012) for the best bleachable feldspar luminescence signal (Blomdin et al. 2012) stimulated at a temperature of 50°C (IR50) was used for dating. This protocol was previously successfully applied at the VLL in different studies (protocol described in detail in e.g. Gómez et al. 2022, Kurečić et al. 2021, Garcia et al. 2021, Garcia et al. 2019 and the respective supplementary documents).

All measurements were conducted in the VLL using a Risø DA-20 automated luminescence reader system equipped with a dual laser single grain system (Bøtter-Jensen et al. 2000, 2003, 2010). An 830 nm infrared laser was used for stimulation of the luminescence signals, which were detected through a LOT/Oriel D410/30 optical interference filter, selecting the K-feldspar emission at 410 nm (Krbetschek et al. 1997). A dose recovery test revealed an excellent recovery ratio in agreement with unity within error and a minimal spread in the data as expressed by an overdispersion value of only ~5%. Supplementary Fig. 8 shows a representative dose response and decay curve for the IR50 signal, demonstrating the feldspar luminescence properties.

Whenever feldspar is used, the effects of fading (a thermal signal loss over time, Wintle 1973) must be taken into account and must be corrected for. Fading experiments according to Auclair et al. (2003) yielded a g-value of 2.8 ±0.2 for the sample. Fading correction was later conducted using this g-value in the R-luminescence package (Kreutzer et al. 2012) using the approach of Huntley & Lamothe (2001).

Determination of the dose rate

The overall dose rate consist of the contribution of ionising radiation from cosmic radiation, internal radiation from 40K within the potassium-rich feldspar grains, and external radiation from the decay of naturally occurring radionuclides (238U and 232Th decay chains, as well as 40K). The latter was determined by high-resolution, low-level gamma spectrometry at the VLL on a Baltic Scientific Instruments (BSI) high purity Germanium (HPGe) p-type detector (~52% efficiency). The external dose rate was calculated using the conversion factors of Adamiec & Aitken (1998) and the β-attenuation factors of Mejdahl (1979), additionally taking an average water content of 15 ±5 % since burial and an average alpha efficiency (a-value) of 0.08 ±0.02 into account. For the calculation of the internal doserate, a potassium content of 12.5 ±0.5% following Huntley & Baril (1997) was used. The contribution from cosmic radiation was calculated according to Prescott & Stephan (1982) and Prescott & Hutton (1994), with respect to the geographical position of the sampling spot (longitude, latitude, and altitude), the depth below surface, as well as the average density of the sediment overburden, and including an uncertainty of 10% on the cosmic dose rate. All dose rate and age calculations were conducted using the software ADELE (Kulig 2005).

Results

After application of the rejection criteria derived from the dose recovery experiment (recycling <20%, recuperation <20% of the natural signal, test dose error <20%, and signal >3σ above background), 49 equivalent dose values were determined for the sample (Supplementary Fig. 9). The equivalent dose distribution is clearly skewed towards higher values, which is a strong indicator for incomplete bleaching to be present in the sample, which is also represented in an overdispersion value (calculated using the central age model (CAM) of Galbraith et al. 1999) of 77±11%. Therefore, the calculation of an average equivalent dose was done using the three-parameter minimum age model (MAM-3) of Galbraith et al. (1999). For the MAM, a threshold for the σb (overdispersion) parameter must be defined, representing the minimum spread expected for a well bleached sample. Because such a sample is not available in this study, an uncertainty for the σb parameter must be included in the calculations, which can be achieved by using the bootstrapped version of the MAM (Cunningham & Wallinga 2012). Here we used 0.2 ±0.1 σb as a threshold. The results of all measurements and calculations, including age calculation and fading correction are provided in Supplementary Table 8. Only the fading corrected age (marked in bold in Supplementary Table 8) should be used for subsequent interpretation.

Reliability of the data

Despite the fact that only a single luminescence age could be determined in this study (because only one sample could be taken), the age is in general agreement with the lower and of the age range determined by radiocarbon dating (see main text of this publication). By following the luminescence dating approach described above, it was possible to identify and correct for the effects of incomplete bleaching in the sample. Despite the fact that most of the grains of the sample that actually emitted a significant luminescence signal showed favourable luminescence properties (Supplementary Fig. 8), only a very low percentage of grains emitted a significant luminescence signal at all. Only about 2.5 % of the grains passed all rejection criteria (49 out of 2000 grains measured, an exceptionally low value for feldspar single grains), resulting in a rather small population. However, the shape of the dose distribution allows for a reliable statistical evaluation. The analysis of additional samples in future studies could further corroborate the dating result presented here. For a broader discussion of general sources for uncertainty in single grain feldspar dating, please see Garcia et al. (2019, supplementary material).

References

Adamiec, G., Aitken, M., 1998. Dose-rate conversion factors: update. Ancient TL 16, 37-50.

Auclair, M., Lamothe, M., Huot, S., 2003. Measurement of anomalous fading for feldspar IRSL using SAR. Radiation Measurements 37, 487-492.

Blomdin, R., Murray, A., Thomsen, K., Buylaert, J.-P., Sohbati, R., Jansson, K., Alexanderson, H., 2012. Timing of the deglaciation in southern Patagonia: Testing the applicability of K-Feldspar IRSL. Quaternary Geochronology 10, 264-272.
Bøtter-Jensen, L., Andersen, C., Duller, G., Murray, A., 2003. Developments in radiation, stimulation and observation facilities in luminescence measurements. Radiation Measurements 37, 535-541.
Bøtter-Jensen, L., Bulur, E., Duller, G., Murray, A., 2000. Advances in luminescence instrument systems. Radiation Measurements 32, 523-528.
Bøtter-Jensen, L., Thomsen, K., Jain, M. (2010): Review of optically stimulated luminescence (OSL) instrumental developments for retrospective dosimetry. Radiation Measurements 45(3-6), 253-257.
Cunningham, A., Wallinga, J., 2012. Realizing the potential of fluvial archives using robust OSL chronologies. Quaternary Geochronology 12, 98-106.
Garcia, J.-L., Binnie, S., Hein, A., Lüthgens, C., Rodés, A., Vega, R. (2021): A composite 10Be, IR-50 and 14C chronology of the pre-Last Glacial Maximum (LGM) full ice extent of the western Patagonian Ice Sheet on the Isla de Chiloé, south Chile (42° S). E&G Quaternary Science Journal 70, 105-128.
Garcia, J., Maldonado, A., de Porras, M., Nuevo Delaunay, A., Reyes, O., Ebensperger, C., Binnie, S., Lüthgens, C., Méndez, C. (2019): Early deglaciation and paleolake history of Río Cisnes Glacier, Patagonian Ice Sheet (44°S). Quaternary Research 91, 194-217.
Galbraith, R., Roberts, R., Laslett, G., Yoshida, H., Olley, J., 1999. Optical dating of single and multiple grains of Quartz from Jinmium rock shelter, northern Australia: Part I, experimental design and statistical models. Archaeometry 41, 339-364.
Gómez, G.A., García, J.-L., Villagrán, C., Lüthgens, C., Abarzúa, A.M. (2022): Vegetation, glacier, and climate changes before the global last glacial maximum in the Isla Grande de Chiloé, southern Chile (42° S). Quaternary Science Reviews 276, 107301.
Huntley, D., Baril, M., 1997. The K content of the K-feldspars being measured in optical and thermoluminescence dating. Ancient TL 15, 11-13.
Huntley, D., Lamothe, M., 2001. Ubiquity of anomalous fading in K-feldspars and the measurement and correction for it in optical dating. Canadian Journal of Earth Sciences 38, 1093-1106.
Krbetschek, M., Götze, J., Dietrich, A., Trautmann, T., 1997. Spectral information from minerals relevant for luminescence dating. Radiation Measurements 27, 695-748.
Kreutzer, S., Schmidt, C., Fuchs, M., Dietze, M., Fuchs, M., 2012. Introducing an R package for luminescence dating analysis. Ancient TL 30, 1-8.
Kulig G., 2005. Erstellung einer Auswertesoftware zur Altersbestimmung mittels Lumineszenzverfahren unter spezieller Berücksichtigung des Einflusses radioaktiver Ungleichgewichte in der 238U-Zerfallsreihe. 35 p., B.Sc. thesis, Freiberg (Technische Universität Bergakademie Freiberg).
Kurečić, T., Bočić, N., Wacha, L., Bakrač, K., Grizel, A., Tresić, D.T. Pavičić, Lüthgens, C., Sironić, A., Radović, S., Redovniković, L., Fiebig, M. (2021): Changes in Cave Sedimentation Mechanisms During the Late Quaternary: An Example From the Lower Cerovačka Cave, Croatia. Frontiers in Earth Science 9, 672229.
Lüthgens, C., Neuhuber, S., Grupe, S., Payer, T., Peresson, M., Fiebig, M., 2017. Geochronological investigations using a combination of luminescence and cosmogenic nuclide burial dating of drill cores from the Vienna Basin. Zeitschrift der Deutschen Gesellschaft für Geowissenschaften 168, 115-140.
Mejdahl, V., 1979. Thermoluminescence dating: beta attenuation in quartz grains. Achaeometry 21, 61-73.
Preusser, F., Degering, D., Fuchs, M., Hilgers, A., Kadereit, A., Klasen, N., Krbetschek, M., Richter, D. & Spencer, J., 2008. Luminescence dating: basics, methods and applications. E&G Quaternary Science Journal, 57, 95-149.
Prescott, J., Hutton J., 1994. Cosmic ray distributions to dose rates for luminescence and ESR dating: large depths and long-term variations. Radiation Measurements 23, 497-500.
Prescott, J., Stephan, L., 1982. The contribution of cosmic radiation to the environmental dose for thermoluminescent dating - Latitude, altitude and depth dependencies. PACT 6, 17-25.
Rades, E., Fiebig, M., Lüthgens, C., 2018. Luminescence dating of the Rissian type section in southern Germany as a base for correlation. Quaternary International, in press, corrected proof.
Reimann, T., Thomsen, K., Jain, M., Murray, A., Frechen, M., 2012, Single-grain dating of young sediments using the pIRIR signal from feldspar. Quaternary Geochronology 11, 28-41.
Rhodes, E., 2011. Optically Stimulated Luminescence Dating of Sediments over the Past 200,000 Annual Review of Earth and Planetary Sciences 39, 461-488.
Wintle, A., 1973. Anomalous Fading of Thermo-luminescence in Mineral Samples. Nature 245, 143-144.
Wintle, A., 2008. Luminescence dating: where it has been and where it is going. Boreas 37, 471-482.

Supplementary R script.

Paired t-test differences; (R package -stat) – Red: t = -3.3673, df = 29, p-value = 0.002156, Green t = 4.5335, df = 29, p-value = 9.255e-05. Blue t = 2.9181, df = 29, p-value = 0.006739, Brightness t = 2.3503, df = 29, p-value = 0.02577. Wilcoxon signed rank test for greater than type of difference revealed that the red color band is significantly higher in the control samples (V = 370, p-value = 0.001872) while green, blue and brightness measurements are significantly higher in footpaths samples (Green p-value:5.529e-05; Blue p-value: 0.004651; Brightness: p-value = 0.02997).

Supplementary script 1

Color

```
rm(list = ls())

setwd("/Users/nn/Downloads/desert footpaths/color")

setwd("E:/phd/desert footpaths/color")




##########################allsamplesallcolorstriplicates
##controls
r<-read.csv2("all_r.csv")
g<-read.csv2("all_g.csv")
b<-read.csv2("all_b.csv")


unlst.r<-unlist(r)
unlst.g<-unlist(g)
unlst.b<-unlist(b)


set.seed(9991)
r_all<-unlst.r
g_all<-unlst.g
b_all<-unlst.b
df_all<-data.frame(r_all,g_all,b_all)

image(1:nrow(df_all),1,as.matrix(1:nrow(df_all)),col=rgb(df_all$r_all,df_all$g_all,df_all$b_all),xlab="",ylab="",xaxt="n",yaxt="n",bty="n")

df_all

controls<-read.csv2("control_surfaces_col.csv")
footpaths<-read.csv2("footpath_surfaces_col.csv")
brightness<-read.csv2("bright.all.csv")
brightness.s<-read.csv2("bright.surface.csv")

brightness.s_df<-data.frame(brightness.s)

brightness.s_df$b1[1:10]
brightness.s_df$b1[11:20]
footpath.brightness<-c(brightness.s_df$b1[1:10],brightness.s$b2[1:10],brightness.s_df$b3[1:10])
control.brightess<-c(brightness.s_df$b1[11:20],brightness.s$b2[11:20],brightness.s_df$b3[11:20])


#footpath

unlst.rf<-unlist(footpaths$r)
unlst.gf<-unlist(footpaths$g)
unlst.bf<-unlist(footpaths$b)
unlst.brigghtness<-unlist(footpath.brightness)


set.seed(9991)
R<-unlst.rf
G<-unlst.gf
B<-unlst.bf
R.r<-R/(R+G+B)
```

```
G.r<-G/(R+G+B)
B.r<-B/(R+G+B)

Brightness<-unlst.brigghtness
str(B)
str(Br)

dff<-data.frame(R.r,G.r,B.r,Brightness)
dff
image(1:nrow(dff),1,as.matrix(1:nrow(dff)),col=rgb(dff$R,dff$G,dff$B,dff$Br),xlab="",ylab="",xaxt="n",yaxt="n",bty="n")

#control

unlst.rc<-unlist(controls$r)
unlst.gc<-unlist(controls$g)
unlst.bc<-unlist(controls$b)
unlst.brigghtness.c<-unlist(control.brightess)

set.seed(9991)
Rc<-unlst.rc
Gc<-unlst.gc
Bc<-unlst.bc
Brc<-unlst.brigghtness.c

R.c.r<-Rc/(Rc+Gc+Bc)
G.c.r<-Gc/(Rc+Gc+Bc)
B.c.r<-Bc/(Rc+Gc+Bc)

dfc<-data.frame(R.c.r,G.c.r,B.c.r,Brc)
dfc
image(1:nrow(dfc),1,as.matrix(1:nrow(dfc)),col=rgb(dfc$x1,dfc$x2,dfc$x3),xlab="",ylab="",xaxt="n",yaxt="n",bty="n")



############ploting the ratios
boxplot(log(dff/dfc), ylab="Log [footpath surfaces / control surfaces]")
abline(h=c(0), col="grey61",lwd=1)

R.c.r
R.r
############testing significance
t.test(dff$R.r,dfc$R.c.r, paired = TRUE)
t.test(dff$G.r,dfc$G.c.r, paired = TRUE)
t.test(dff$B.r,dfc$B.c.r, paired = TRUE)
t.test(dff$Brightness,dfc$Brc, paired = TRUE)

wilcox.test(dfc$R.c.r,dff$R.r, alternative="greater", paired=TRUE)
wilcox.test(dff$G.r,dfc$G.c.r, alternative="greater", paired=TRUE)
wilcox.test(dff$B.r,dfc$B.c.r, alternative="greater", paired=TRUE)
wilcox.test(dff$Brightness,dfc$Brc,alternative="greater", paired=TRUE)
plot(dfc$G.c.r/dff$G.r,dfc$Brc/dff$Brightness)
cor(dff,dfc)

############################blast from the past




#control
rc<-read.csv("rc.csv")
gc<-read.csv("gc.csv")
bc<-read.csv("bc.csv")
allcol<-read.csv("allcol.csv")


unlst.rc<-unlist(rc)
unlst.gc<-unlist(gc)
unlst.bc<-unlist(bc)
```

```
set.seed(9991)
x1<-unlst.rc
x2<-unlst.gc
x3<-unlst.bc
dfc<-data.frame(x1,x2,x3)
dfc
image(1:nrow(dfc),1,as.matrix(1:nrow(dfc)),col=rgb(dfc$x1,dfc$x2,dfc$x3),xlab="",ylab="",xaxt="n",yaxt="n",bty="n")

#footpath

rf<-read.csv("rf.csv")
gf<-read.csv("gf.csv")
bf<-read.csv("bf.csv")

unlst.rf<-unlist(rf)
unlst.gf<-unlist(gf)
unlst.bf<-unlist(bf)



set.seed(9991)
x1<-unlst.rf
x2<-unlst.gf
x3<-unlst.bf
dff<-data.frame(x1,x2,x3)
dff
image(1:nrow(dff),1,as.matrix(1:nrow(dff)),col=rgb(dff$x1,dff$x2,dff$x3),xlab="",ylab="",xaxt="n",yaxt="n",bty="n")


dff/dfc
#############################################################################################
rm(list = ls())

colorfootpath<-read.csv2("colorfootpaths.csv")
colorcontrols<- read.csv2("colorcontrols.csv")
u.cc<-unlist(colorcontrols)
u.cf<-unlist(colorfootpath)
clc<-data.frame(u.cc)
clf<-data.frame(u.cf)

plot(dff$Brightness,dfc$Brc)
colors <- rgb(red,green,blue)

cor.test(dff$Brightness,dfc$Brc)

print(dff)

dff/dfc

col
rect(  rep((0:(col- 1)/col),line) ,  sort(rep((0:(line - 1)/line),col),decreasing=T)   ,   rep((1:col/col),line) ,
sort(rep((1:line/line),col),decreasing=T),  border = "light gray" , col=colors)

rgbtest<-rgb(unlst.r,unlst.g,unlst.b)

write.csv2(rgbtest,"rgbtest.csv")

UAV Colors

install.packages("raster", type = "mac.binary")
install.packages("Rcpp")
install.packages("terra")
install.packages("rgdal")
install.packages("gdistance")
install.packages("ggplot2")

library(st)
library(sf)
library(rgdal)
library(raster)
library(gdistance)
```

```
library(ggplot2)


#upload rasters of orthophotos of Red band
NZ_band_1<-raster::raster("NZ_band_1.tif")
NZ_band_2<-raster::raster("NZ_band_2.tif")
NZ_band_3<-raster::raster("NZ_band_3.tif")
getwd()
Demnz<-raster::raster("nahal.zohar.dem.tif")
sdemnz<-slopeAspect(Demnz,filename = "slopeaspectnz.tif", out = c("slope"))
#upload footpaths and controls

####################NZM



#upload footpaths and controls

#NZM footpath
NZM_alongpath_0_1<- st_read("NZM_alongpath_0_1.gpkg")
NZM_alongpath_0_2<- st_read("NZM_alongpath_0_2.gpkg")
NZM_alongpath_0_3<- st_read("NZM_alongpath_0_3.gpkg")
NZM_alongpath_.1_1<- st_read("NZM_alongpath_-1_1.gpkg")
NZM_alongpath_.1_2<- st_read("NZM_alongpath_-1_2.gpkg")
NZM_alongpath_.1_3<- st_read("NZM_alongpath_-1_3.gpkg")
NZM_alongpath_..1_1<- st_read("NZM_alongpath_1_1.gpkg")
NZM_alongpath_..1_2<- st_read("NZM_alongpath_1_2.gpkg")
NZM_alongpath_..1_3<- st_read("NZM_alongpath_1_3.gpkg")
########new lines
NZM_alongpath_0_1<- st_read("NZ_M_alongpath_0_1.shp")
NZM_alongpath_0_2<- st_read("NZ_M_alongpath_0_2.shp")
NZM_alongpath_0_3<- st_read("NZ_M_alongpath_0_3.shp")
NZM_alongpath_.1_1<- st_read("NZ_M_alongpath_-1_1.shp")
NZM_alongpath_.1_2<- st_read("NZ_M_alongpath_-1_2.shp")
NZM_alongpath_.1_3<- st_read("NZ_M_alongpath_-1_3.shp")
NZM_alongpath_..1_1<- st_read("NZ_M_alongpath_1_1.shp")
NZM_alongpath_..1_2<- st_read("NZ_M_alongpath_1_2.shp")
NZM_alongpath_..1_3<- st_read("NZ_M_alongpath_1_3.shp")

rm(NZM_band_1_alongpath_..1_2,NZM_alongpath_..1_2)
#band 1
NZM_band_1_alongpath_0_1<-raster::extract(NZ_band_1,NZM_alongpath_0_1, along = TRUE,cellnumbers = FALSE)
NZM_band_1_alongpath_0_2<-raster::extract(NZ_band_1,NZM_alongpath_0_2, along = TRUE,cellnumbers = FALSE)
NZM_band_1_alongpath_0_3<-raster::extract(NZ_band_1,NZM_alongpath_0_3, along = TRUE,cellnumbers = FALSE)
NZM_band_1_alongpath_.1_1<-raster::extract(NZ_band_1,NZM_alongpath_.1_1, along = TRUE,cellnumbers = FALSE)
NZM_band_1_alongpath_.1_2<-raster::extract(NZ_band_1,NZM_alongpath_.1_2, along = TRUE,cellnumbers = FALSE)
NZM_band_1_alongpath_.1_3<-raster::extract(NZ_band_1,NZM_alongpath_.1_3, along = TRUE,cellnumbers = FALSE)
NZM_band_1_alongpath_..1_1<-raster::extract(NZ_band_1,NZM_alongpath_..1_1, along = TRUE,cellnumbers = FALSE)
NZM_band_1_alongpath_..1_2<-raster::extract(NZ_band_1,NZM_alongpath_..1_2, along = TRUE,cellnumbers = FALSE)
NZM_band_1_alongpath_..1_3<-raster::extract(NZ_band_1,NZM_alongpath_..1_3, along = TRUE,cellnumbers = FALSE)


NZM_band_1_alongpath_0_1_ul<-unlist(NZM_band_1_alongpath_0_1)
NZM_band_1_alongpath_0_1_ul_sum<-sum(NZM_band_1_alongpath_0_1_ul)
NZM_band_1_alongpath_0_1_ul_mean<-mean(NZM_band_1_alongpath_0_1_ul)
NZM_band_1_alongpath_0_1_ul_sd<-sd(NZM_band_1_alongpath_0_1_ul)
NZM_band_1_alongpath_0_2_ul<-unlist(NZM_band_1_alongpath_0_2)
NZM_band_1_alongpath_0_2_ul_sum<-sum(NZM_band_1_alongpath_0_2_ul)
NZM_band_1_alongpath_0_2_ul_mean<-mean(NZM_band_1_alongpath_0_2_ul)
NZM_band_1_alongpath_0_2_ul_sd<-sd(NZM_band_1_alongpath_0_2_ul)
NZM_band_1_alongpath_0_3_ul<-unlist(NZM_band_1_alongpath_0_3)
NZM_band_1_alongpath_0_3_ul_sum<-sum(NZM_band_1_alongpath_0_3_ul)
NZM_band_1_alongpath_0_3_ul_mean<-mean(NZM_band_1_alongpath_0_3_ul)
NZM_band_1_alongpath_0_3_ul_sd<-sd(NZM_band_1_alongpath_0_3_ul)
NZM_band_1_alongpath_.1_1_ul<-unlist(NZM_band_1_alongpath_.1_1)
NZM_band_1_alongpath_.1_1_ul_sum<-sum(NZM_band_1_alongpath_.1_1_ul)
NZM_band_1_alongpath_.1_1_ul_mean<-mean(NZM_band_1_alongpath_.1_1_ul)
NZM_band_1_alongpath_.1_1_ul_sd<-sd(NZM_band_1_alongpath_.1_1_ul)
NZM_band_1_alongpath_.1_2_ul<-unlist(NZM_band_1_alongpath_.1_2)
NZM_band_1_alongpath_.1_2_ul_sum<-sum(NZM_band_1_alongpath_.1_2_ul)
NZM_band_1_alongpath_.1_2_ul_mean<-mean(NZM_band_1_alongpath_.1_2_ul)
```

```
NZM_band_1_alongpath_.1_2_ul_sd<-sd(NZM_band_1_alongpath_.1_2_ul)
NZM_band_1_alongpath_.1_3_ul<-unlist(NZM_band_1_alongpath_.1_3)
NZM_band_1_alongpath_.1_3_ul_sum<-sum(NZM_band_1_alongpath_.1_3_ul)
NZM_band_1_alongpath_.1_3_ul_mean<-mean(NZM_band_1_alongpath_.1_3_ul)
NZM_band_1_alongpath_.1_3_ul_sd<-sd(NZM_band_1_alongpath_.1_3_ul)
NZM_band_1_alongpath_..1_1_ul<-unlist(NZM_band_1_alongpath_..1_1)
NZM_band_1_alongpath_..1_1_ul_sum<-sum(NZM_band_1_alongpath_..1_1_ul)
NZM_band_1_alongpath_..1_1_ul_mean<-mean(NZM_band_1_alongpath_..1_1_ul)
NZM_band_1_alongpath_..1_1_ul_sd<-sd(NZM_band_1_alongpath_..1_1_ul)
NZM_band_1_alongpath_..1_2_ul<-unlist(NZM_band_1_alongpath_..1_2)
NZM_band_1_alongpath_..1_2_ul_sum<-sum(NZM_band_1_alongpath_..1_2_ul)
NZM_band_1_alongpath_..1_2_ul_mean<-mean(NZM_band_1_alongpath_..1_2_ul)
NZM_band_1_alongpath_..1_2_ul_sd<-sd(NZM_band_1_alongpath_..1_2_ul)
NZM_band_1_alongpath_..1_3_ul<-unlist(NZM_band_1_alongpath_..1_3)
NZM_band_1_alongpath_..1_3_ul_sum<-sum(NZM_band_1_alongpath_..1_3_ul)
NZM_band_1_alongpath_..1_3_ul_mean<-mean(NZM_band_1_alongpath_..1_3_ul)
NZM_band_1_alongpath_..1_3_ul_sd<-sd(NZM_band_1_alongpath_..1_3_ul)



#band 2
NZM_band_2_alongpath_0_1<-raster::extract(NZ_band_2,NZM_alongpath_0_1, along = TRUE,cellnumbers = FALSE)
NZM_band_2_alongpath_0_2<-raster::extract(NZ_band_2,NZM_alongpath_0_2, along = TRUE,cellnumbers = FALSE)
NZM_band_2_alongpath_0_3<-raster::extract(NZ_band_2,NZM_alongpath_0_3, along = TRUE,cellnumbers = FALSE)
NZM_band_2_alongpath_.1_1<-raster::extract(NZ_band_2,NZM_alongpath_.1_1, along = TRUE,cellnumbers = FALSE)
NZM_band_2_alongpath_.1_2<-raster::extract(NZ_band_2,NZM_alongpath_.1_2, along = TRUE,cellnumbers = FALSE)
NZM_band_2_alongpath_.1_3<-raster::extract(NZ_band_2,NZM_alongpath_.1_3, along = TRUE,cellnumbers = FALSE)
NZM_band_2_alongpath_..1_1<-raster::extract(NZ_band_2,NZM_alongpath_..1_1, along = TRUE,cellnumbers = FALSE)
NZM_band_2_alongpath_..1_2<-raster::extract(NZ_band_2,NZM_alongpath_..1_2, along = TRUE,cellnumbers = FALSE)
NZM_band_2_alongpath_..1_3<-raster::extract(NZ_band_2,NZM_alongpath_..1_3, along = TRUE,cellnumbers = FALSE)


NZM_band_2_alongpath_0_1_ul<-unlist(NZM_band_2_alongpath_0_1)
NZM_band_2_alongpath_0_1_ul_sum<-sum(NZM_band_2_alongpath_0_1_ul)
NZM_band_2_alongpath_0_1_ul_mean<-mean(NZM_band_2_alongpath_0_1_ul)
NZM_band_2_alongpath_0_1_ul_sd<-sd(NZM_band_2_alongpath_0_1_ul)
NZM_band_2_alongpath_0_2_ul<-unlist(NZM_band_2_alongpath_0_2)
NZM_band_2_alongpath_0_2_ul_sum<-sum(NZM_band_2_alongpath_0_2_ul)
NZM_band_2_alongpath_0_2_ul_mean<-mean(NZM_band_2_alongpath_0_2_ul)
NZM_band_2_alongpath_0_2_ul_sd<-sd(NZM_band_2_alongpath_0_2_ul)
NZM_band_2_alongpath_0_3_ul<-unlist(NZM_band_2_alongpath_0_3)
NZM_band_2_alongpath_0_3_ul_sum<-sum(NZM_band_2_alongpath_0_3_ul)
NZM_band_2_alongpath_0_3_ul_mean<-mean(NZM_band_2_alongpath_0_3_ul)
NZM_band_2_alongpath_0_3_ul_sd<-sd(NZM_band_2_alongpath_0_3_ul)
NZM_band_2_alongpath_.1_1_ul<-unlist(NZM_band_2_alongpath_.1_1)
NZM_band_2_alongpath_.1_1_ul_sum<-sum(NZM_band_2_alongpath_.1_1_ul)
NZM_band_2_alongpath_.1_1_ul_mean<-mean(NZM_band_2_alongpath_.1_1_ul)
NZM_band_2_alongpath_.1_1_ul_sd<-sd(NZM_band_2_alongpath_.1_1_ul)
NZM_band_2_alongpath_.1_2_ul<-unlist(NZM_band_2_alongpath_.1_2)
NZM_band_2_alongpath_.1_2_ul_sum<-sum(NZM_band_2_alongpath_.1_2_ul)
NZM_band_2_alongpath_.1_2_ul_mean<-mean(NZM_band_2_alongpath_.1_2_ul)
NZM_band_2_alongpath_.1_2_ul_sd<-sd(NZM_band_2_alongpath_.1_2_ul)
NZM_band_2_alongpath_.1_3_ul<-unlist(NZM_band_2_alongpath_.1_3)
NZM_band_2_alongpath_.1_3_ul_sum<-sum(NZM_band_2_alongpath_.1_3_ul)
NZM_band_2_alongpath_.1_3_ul_mean<-mean(NZM_band_2_alongpath_.1_3_ul)
NZM_band_2_alongpath_.1_3_ul_sd<-sd(NZM_band_2_alongpath_.1_3_ul)
NZM_band_2_alongpath_..1_1_ul<-unlist(NZM_band_2_alongpath_..1_1)
NZM_band_2_alongpath_..1_1_ul_sum<-sum(NZM_band_2_alongpath_..1_1_ul)
NZM_band_2_alongpath_..1_1_ul_mean<-mean(NZM_band_2_alongpath_..1_1_ul)
NZM_band_2_alongpath_..1_1_ul_sd<-sd(NZM_band_2_alongpath_..1_1_ul)
NZM_band_2_alongpath_..1_2_ul<-unlist(NZM_band_2_alongpath_..1_2)
NZM_band_2_alongpath_..1_2_ul_sum<-sum(NZM_band_2_alongpath_..1_2_ul)
NZM_band_2_alongpath_..1_2_ul_mean<-mean(NZM_band_2_alongpath_..1_2_ul)
NZM_band_2_alongpath_..1_2_ul_sd<-sd(NZM_band_2_alongpath_..1_2_ul)
NZM_band_2_alongpath_..1_3_ul<-unlist(NZM_band_2_alongpath_..1_3)
NZM_band_2_alongpath_..1_3_ul_sum<-sum(NZM_band_2_alongpath_..1_3_ul)
NZM_band_2_alongpath_..1_3_ul_mean<-mean(NZM_band_2_alongpath_..1_3_ul)
NZM_band_2_alongpath_..1_3_ul_sd<-sd(NZM_band_2_alongpath_..1_3_ul)


#band 3
```

```
NZM_band_3_alongpath_0_1<-raster::extract(NZ_band_3,NZM_alongpath_0_1, along = TRUE,cellnumbers = FALSE)
NZM_band_3_alongpath_0_2<-raster::extract(NZ_band_3,NZM_alongpath_0_2, along = TRUE,cellnumbers = FALSE)
NZM_band_3_alongpath_0_3<-raster::extract(NZ_band_3,NZM_alongpath_0_3, along = TRUE,cellnumbers = FALSE)
NZM_band_3_alongpath_.1_1<-raster::extract(NZ_band_3,NZM_alongpath_.1_1, along = TRUE,cellnumbers = FALSE)
NZM_band_3_alongpath_.1_2<-raster::extract(NZ_band_3,NZM_alongpath_.1_2, along = TRUE,cellnumbers = FALSE)
NZM_band_3_alongpath_.1_3<-raster::extract(NZ_band_3,NZM_alongpath_.1_3, along = TRUE,cellnumbers = FALSE)
NZM_band_3_alongpath_..1_1<-raster::extract(NZ_band_3,NZM_alongpath_..1_1, along = TRUE,cellnumbers = FALSE)
NZM_band_3_alongpath_..1_2<-raster::extract(NZ_band_3,NZM_alongpath_..1_2, along = TRUE,cellnumbers = FALSE)
NZM_band_3_alongpath_..1_3<-raster::extract(NZ_band_3,NZM_alongpath_..1_3, along = TRUE,cellnumbers = FALSE)


NZM_band_3_alongpath_0_1_ul<-unlist(NZM_band_3_alongpath_0_1)
NZM_band_3_alongpath_0_1_ul_sum<-sum(NZM_band_3_alongpath_0_1_ul)
NZM_band_3_alongpath_0_1_ul_mean<-mean(NZM_band_3_alongpath_0_1_ul)
NZM_band_3_alongpath_0_1_ul_sd<-sd(NZM_band_3_alongpath_0_1_ul)
NZM_band_3_alongpath_0_2_ul<-unlist(NZM_band_3_alongpath_0_2)
NZM_band_3_alongpath_0_2_ul_sum<-sum(NZM_band_3_alongpath_0_2_ul)
NZM_band_3_alongpath_0_2_ul_mean<-mean(NZM_band_3_alongpath_0_2_ul)
NZM_band_3_alongpath_0_2_ul_sd<-sd(NZM_band_3_alongpath_0_2_ul)
NZM_band_3_alongpath_0_3_ul<-unlist(NZM_band_3_alongpath_0_3)
NZM_band_3_alongpath_0_3_ul_sum<-sum(NZM_band_3_alongpath_0_3_ul)
NZM_band_3_alongpath_0_3_ul_mean<-mean(NZM_band_3_alongpath_0_3_ul)
NZM_band_3_alongpath_0_3_ul_sd<-sd(NZM_band_3_alongpath_0_3_ul)
NZM_band_3_alongpath_.1_1_ul<-unlist(NZM_band_3_alongpath_.1_1)
NZM_band_3_alongpath_.1_1_ul_sum<-sum(NZM_band_3_alongpath_.1_1_ul)
NZM_band_3_alongpath_.1_1_ul_mean<-mean(NZM_band_3_alongpath_.1_1_ul)
NZM_band_3_alongpath_.1_1_ul_sd<-sd(NZM_band_3_alongpath_.1_1_ul)
NZM_band_3_alongpath_.1_2_ul<-unlist(NZM_band_3_alongpath_.1_2)
NZM_band_3_alongpath_.1_2_ul_sum<-sum(NZM_band_3_alongpath_.1_2_ul)
NZM_band_3_alongpath_.1_2_ul_mean<-mean(NZM_band_3_alongpath_.1_2_ul)
NZM_band_3_alongpath_.1_2_ul_sd<-sd(NZM_band_3_alongpath_.1_2_ul)
NZM_band_3_alongpath_.1_3_ul<-unlist(NZM_band_3_alongpath_.1_3)
NZM_band_3_alongpath_.1_3_ul_sum<-sum(NZM_band_3_alongpath_.1_3_ul)
NZM_band_3_alongpath_.1_3_ul_mean<-mean(NZM_band_3_alongpath_.1_3_ul)
NZM_band_3_alongpath_.1_3_ul_sd<-sd(NZM_band_3_alongpath_.1_3_ul)
NZM_band_3_alongpath_..1_1_ul<-unlist(NZM_band_3_alongpath_..1_1)
NZM_band_3_alongpath_..1_1_ul_sum<-sum(NZM_band_3_alongpath_..1_1_ul)
NZM_band_3_alongpath_..1_1_ul_mean<-mean(NZM_band_3_alongpath_..1_1_ul)
NZM_band_3_alongpath_..1_1_ul_sd<-sd(NZM_band_3_alongpath_..1_1_ul)
NZM_band_3_alongpath_..1_2_ul<-unlist(NZM_band_3_alongpath_..1_2)
NZM_band_3_alongpath_..1_2_ul_sum<-sum(NZM_band_3_alongpath_..1_2_ul)
NZM_band_3_alongpath_..1_2_ul_mean<-mean(NZM_band_3_alongpath_..1_2_ul)
NZM_band_3_alongpath_..1_2_ul_sd<-sd(NZM_band_3_alongpath_..1_2_ul)
NZM_band_3_alongpath_..1_3_ul<-unlist(NZM_band_3_alongpath_..1_3)
NZM_band_3_alongpath_..1_3_ul_sum<-sum(NZM_band_3_alongpath_..1_3_ul)
NZM_band_3_alongpath_..1_3_ul_mean<-mean(NZM_band_3_alongpath_..1_3_ul)
NZM_band_3_alongpath_..1_3_ul_sd<-sd(NZM_band_3_alongpath_..1_3_ul)


NZM_bands_values<-list(NZM_band_1_alongpath_0_1_ul_sum,NZM_band_1_alongpath_0_2_ul_sum,
            NZM_band_1_alongpath_0_3_ul_sum,NZM_band_1_alongpath_.1_1_ul_sum,
            NZM_band_1_alongpath_.1_2_ul_sum,NZM_band_1_alongpath_.1_3_ul_sum,
            NZM_band_1_alongpath_..1_1_ul_sum, NZM_band_1_alongpath_..1_2_ul_sum,
            NZM_band_1_alongpath_..1_3_ul_sum, NZM_band_2_alongpath_0_1_ul_sum,
            NZM_band_2_alongpath_0_2_ul_sum, NZM_band_2_alongpath_0_3_ul_sum,
            NZM_band_2_alongpath_.1_1_ul_sum, NZM_band_2_alongpath_.1_2_ul_sum,
            NZM_band_2_alongpath_.1_3_ul_sum, NZM_band_2_alongpath_..1_1_ul_sum,
            NZM_band_2_alongpath_..1_2_ul_sum, NZM_band_2_alongpath_..1_3_ul_sum,
            NZM_band_3_alongpath_0_1_ul_sum, NZM_band_3_alongpath_0_2_ul_sum,
            NZM_band_3_alongpath_0_3_ul_sum, NZM_band_3_alongpath_.1_1_ul_sum,
            NZM_band_3_alongpath_.1_2_ul_sum, NZM_band_3_alongpath_.1_3_ul_sum,
            NZM_band_3_alongpath_..1_1_ul_sum, NZM_band_3_alongpath_..1_2_ul_sum,
            NZM_band_3_alongpath_..1_3_ul_sum)
NZM_bands_values_unlisted<-unlist(NZM_bands_values)

NZM_bands_mean_values<-list(NZM_band_1_alongpath_0_1_ul_mean,NZM_band_1_alongpath_0_2_ul_mean,
              NZM_band_1_alongpath_0_3_ul_mean,NZM_band_1_alongpath_.1_1_ul_mean,
              NZM_band_1_alongpath_.1_2_ul_mean,NZM_band_1_alongpath_.1_3_ul_mean,
              NZM_band_1_alongpath_..1_1_ul_mean, NZM_band_1_alongpath_..1_2_ul_mean,
              NZM_band_1_alongpath_..1_3_ul_mean, NZM_band_2_alongpath_0_1_ul_mean,
```

```
                NZM_band_2_alongpath_0_2_ul_mean, NZM_band_2_alongpath_0_3_ul_mean,
                NZM_band_2_alongpath_.1_1_ul_mean, NZM_band_2_alongpath_.1_2_ul_mean,
                NZM_band_2_alongpath_.1_3_ul_mean, NZM_band_2_alongpath_..1_1_ul_mean,
                NZM_band_2_alongpath_..1_2_ul_mean, NZM_band_2_alongpath_..1_3_ul_mean,
                NZM_band_3_alongpath_0_1_ul_mean, NZM_band_3_alongpath_0_2_ul_mean,
                NZM_band_3_alongpath_0_3_ul_mean, NZM_band_3_alongpath_.1_1_ul_mean,
                NZM_band_3_alongpath_.1_2_ul_mean, NZM_band_3_alongpath_.1_3_ul_mean,
                NZM_band_3_alongpath_..1_1_ul_mean, NZM_band_3_alongpath_..1_2_ul_mean,
                NZM_band_3_alongpath_..1_3_ul_mean)
NZM_bands_mean_values_unlisted<-unlist(NZM_bands_mean_values)

NZM_bands_sd_values<-list(NZM_band_1_alongpath_0_1_ul_sd,NZM_band_1_alongpath_0_2_ul_sd,
                NZM_band_1_alongpath_0_3_ul_sd,NZM_band_1_alongpath_.1_1_ul_sd,
                NZM_band_1_alongpath_.1_2_ul_sd,NZM_band_1_alongpath_.1_3_ul_sd,
                NZM_band_1_alongpath_..1_1_ul_sd, NZM_band_1_alongpath_..1_2_ul_sd,
                NZM_band_1_alongpath_..1_3_ul_sd, NZM_band_2_alongpath_0_1_ul_sd,
                NZM_band_2_alongpath_0_2_ul_sd, NZM_band_2_alongpath_0_3_ul_sd,
                NZM_band_2_alongpath_.1_1_ul_sd, NZM_band_2_alongpath_.1_2_ul_sd,
                NZM_band_2_alongpath_.1_3_ul_sd, NZM_band_2_alongpath_..1_1_ul_sd,
                NZM_band_2_alongpath_..1_2_ul_sd, NZM_band_2_alongpath_..1_3_ul_sd,
                NZM_band_3_alongpath_0_1_ul_sd, NZM_band_3_alongpath_0_2_ul_sd,
                NZM_band_3_alongpath_0_3_ul_sd, NZM_band_3_alongpath_.1_1_ul_sd,
                NZM_band_3_alongpath_.1_2_ul_sd, NZM_band_3_alongpath_.1_3_ul_sd,
                NZM_band_3_alongpath_..1_1_ul_sd, NZM_band_3_alongpath_..1_2_ul_sd,
                NZM_band_3_alongpath_..1_3_ul_sd)
NZM_bands_sd_values_unlisted<-unlist(NZM_bands_sd_values)



write.csv2(c(NZM_bands_values_unlisted,NZM_bands_mean_values_unlisted,NZM_bands_sd_values_unlisted),"NZM_bands_values.csv")


#NZ footpath
NZ_alongpath_0_1<- st_read("NZ_alongpath_0_1.gpkg")
NZ_alongpath_0_2<- st_read("NZ_alongpath_0_2.gpkg")
NZ_alongpath_0_3<- st_read("NZ_alongpath_0_3.gpkg")
NZ_alongpath_.1_1<- st_read("NZ_alongpath_-1_1.gpkg")
NZ_alongpath_.1_2<- st_read("NZ_alongpath_-1_2.gpkg")
NZ_alongpath_.1_3<- st_read("NZ_alongpath_-1_3.gpkg")
NZ_alongpath_..1_1<- st_read("NZ_alongpath_1_1.gpkg")
NZ_alongpath_..1_2<- st_read("NZ_alongpath_1_2.gpkg")
NZ_alongpath_..1_3<- st_read("NZ_alongpath_1_3.gpkg")



#band 1
NZ_band_1_alongpath_0_1<-raster::extract(NZ_band_1,NZ_alongpath_0_1, along = TRUE,cellnumbers = FALSE)
NZ_band_1_alongpath_0_2<-raster::extract(NZ_band_1,NZ_alongpath_0_2, along = TRUE,cellnumbers = FALSE)
NZ_band_1_alongpath_0_3<-raster::extract(NZ_band_1,NZ_alongpath_0_3, along = TRUE,cellnumbers = FALSE)
NZ_band_1_alongpath_.1_1<-raster::extract(NZ_band_1,NZ_alongpath_.1_1, along = TRUE,cellnumbers = FALSE)
NZ_band_1_alongpath_.1_2<-raster::extract(NZ_band_1,NZ_alongpath_.1_2, along = TRUE,cellnumbers = FALSE)
NZ_band_1_alongpath_.1_3<-raster::extract(NZ_band_1,NZ_alongpath_.1_3, along = TRUE,cellnumbers = FALSE)
NZ_band_1_alongpath_..1_1<-raster::extract(NZ_band_1,NZ_alongpath_..1_1, along = TRUE,cellnumbers = FALSE)
NZ_band_1_alongpath_..1_2<-raster::extract(NZ_band_1,NZ_alongpath_..1_2, along = TRUE,cellnumbers = FALSE)
NZ_band_1_alongpath_..1_3<-raster::extract(NZ_band_1,NZ_alongpath_..1_3, along = TRUE,cellnumbers = FALSE)


NZ_band_1_alongpath_0_1_ul<-unlist(NZ_band_1_alongpath_0_1)
NZ_band_1_alongpath_0_1_ul_sum<-sum(NZ_band_1_alongpath_0_1_ul)
NZ_band_1_alongpath_0_1_ul_mean<-mean(NZ_band_1_alongpath_0_1_ul)
NZ_band_1_alongpath_0_1_ul_sd<-sd(NZ_band_1_alongpath_0_1_ul)
NZ_band_1_alongpath_0_2_ul<-unlist(NZ_band_1_alongpath_0_2)
NZ_band_1_alongpath_0_2_ul_sum<-sum(NZ_band_1_alongpath_0_2_ul)
NZ_band_1_alongpath_0_2_ul_mean<-mean(NZ_band_1_alongpath_0_2_ul)
NZ_band_1_alongpath_0_2_ul_sd<-sd(NZ_band_1_alongpath_0_2_ul)
NZ_band_1_alongpath_0_3_ul<-unlist(NZ_band_1_alongpath_0_3)
NZ_band_1_alongpath_0_3_ul_sum<-sum(NZ_band_1_alongpath_0_3_ul)
NZ_band_1_alongpath_0_3_ul_mean<-mean(NZ_band_1_alongpath_0_3_ul)
NZ_band_1_alongpath_0_3_ul_sd<-sd(NZ_band_1_alongpath_0_3_ul)
NZ_band_1_alongpath_.1_1_ul<-unlist(NZ_band_1_alongpath_.1_1)
```

```
NZ_band_1_alongpath_.1_1_ul_sum<-sum(NZ_band_1_alongpath_.1_1_ul)
NZ_band_1_alongpath_.1_1_ul_mean<-mean(NZ_band_1_alongpath_.1_1_ul)
NZ_band_1_alongpath_.1_1_ul_sd<-sd(NZ_band_1_alongpath_.1_1_ul)
NZ_band_1_alongpath_.1_2_ul<-unlist(NZ_band_1_alongpath_.1_2)
NZ_band_1_alongpath_.1_2_ul_sum<-sum(NZ_band_1_alongpath_.1_2_ul)
NZ_band_1_alongpath_.1_2_ul_mean<-mean(NZ_band_1_alongpath_.1_2_ul)
NZ_band_1_alongpath_.1_2_ul_sd<-sd(NZ_band_1_alongpath_.1_2_ul)
NZ_band_1_alongpath_.1_3_ul<-unlist(NZ_band_1_alongpath_.1_3)
NZ_band_1_alongpath_.1_3_ul_sum<-sum(NZ_band_1_alongpath_.1_3_ul)
NZ_band_1_alongpath_.1_3_ul_mean<-mean(NZ_band_1_alongpath_.1_3_ul)
NZ_band_1_alongpath_.1_3_ul_sd<-sd(NZ_band_1_alongpath_.1_3_ul)
NZ_band_1_alongpath_..1_1_ul<-unlist(NZ_band_1_alongpath_..1_1)
NZ_band_1_alongpath_..1_1_ul_sum<-sum(NZ_band_1_alongpath_..1_1_ul)
NZ_band_1_alongpath_..1_1_ul_mean<-mean(NZ_band_1_alongpath_..1_1_ul)
NZ_band_1_alongpath_..1_1_ul_sd<-sd(NZ_band_1_alongpath_..1_1_ul)
NZ_band_1_alongpath_..1_2_ul<-unlist(NZ_band_1_alongpath_..1_2)
NZ_band_1_alongpath_..1_2_ul_sum<-sum(NZ_band_1_alongpath_..1_2_ul)
NZ_band_1_alongpath_..1_2_ul_mean<-mean(NZ_band_1_alongpath_..1_2_ul)
NZ_band_1_alongpath_..1_2_ul_sd<-sd(NZ_band_1_alongpath_..1_2_ul)
NZ_band_1_alongpath_..1_3_ul<-unlist(NZ_band_1_alongpath_..1_3)
NZ_band_1_alongpath_..1_3_ul_sum<-sum(NZ_band_1_alongpath_..1_3_ul)
NZ_band_1_alongpath_..1_3_ul_mean<-mean(NZ_band_1_alongpath_..1_3_ul)
NZ_band_1_alongpath_..1_3_ul_sd<-sd(NZ_band_1_alongpath_..1_3_ul)

#band 2
NZ_band_2_alongpath_0_1<-raster::extract(NZ_band_2,NZ_alongpath_0_1, along = TRUE,cellnumbers = FALSE)
NZ_band_2_alongpath_0_2<-raster::extract(NZ_band_2,NZ_alongpath_0_2, along = TRUE,cellnumbers = FALSE)
NZ_band_2_alongpath_0_3<-raster::extract(NZ_band_2,NZ_alongpath_0_3, along = TRUE,cellnumbers = FALSE)
NZ_band_2_alongpath_.1_1<-raster::extract(NZ_band_2,NZ_alongpath_.1_1, along = TRUE,cellnumbers = FALSE)
NZ_band_2_alongpath_.1_2<-raster::extract(NZ_band_2,NZ_alongpath_.1_2, along = TRUE,cellnumbers = FALSE)
NZ_band_2_alongpath_.1_3<-raster::extract(NZ_band_2,NZ_alongpath_.1_3, along = TRUE,cellnumbers = FALSE)
NZ_band_2_alongpath_..1_1<-raster::extract(NZ_band_2,NZ_alongpath_..1_1, along = TRUE,cellnumbers = FALSE)
NZ_band_2_alongpath_..1_2<-raster::extract(NZ_band_2,NZ_alongpath_..1_2, along = TRUE,cellnumbers = FALSE)
NZ_band_2_alongpath_..1_3<-raster::extract(NZ_band_2,NZ_alongpath_..1_3, along = TRUE,cellnumbers = FALSE)


NZ_band_2_alongpath_0_1_ul<-unlist(NZ_band_2_alongpath_0_1)
NZ_band_2_alongpath_0_1_ul_sum<-sum(NZ_band_2_alongpath_0_1_ul)
NZ_band_2_alongpath_0_1_ul_mean<-mean(NZ_band_2_alongpath_0_1_ul)
NZ_band_2_alongpath_0_1_ul_sd<-sd(NZ_band_2_alongpath_0_1_ul)
NZ_band_2_alongpath_0_2_ul<-unlist(NZ_band_2_alongpath_0_1)
NZ_band_2_alongpath_0_2_ul_sum<-sum(NZ_band_2_alongpath_0_2_ul)
NZ_band_2_alongpath_0_2_ul_mean<-mean(NZ_band_2_alongpath_0_2_ul)
NZ_band_2_alongpath_0_2_ul_sd<-sd(NZ_band_2_alongpath_0_2_ul)
NZ_band_2_alongpath_0_3_ul<-unlist(NZ_band_2_alongpath_0_3)
NZ_band_2_alongpath_0_3_ul_sum<-sum(NZ_band_2_alongpath_0_3_ul)
NZ_band_2_alongpath_0_3_ul_mean<-mean(NZ_band_2_alongpath_0_3_ul)
NZ_band_2_alongpath_0_3_ul_sd<-sd(NZ_band_2_alongpath_0_3_ul)
NZ_band_2_alongpath_.1_1_ul<-unlist(NZ_band_2_alongpath_.1_1)
NZ_band_2_alongpath_.1_1_ul_sum<-sum(NZ_band_2_alongpath_.1_1_ul)
NZ_band_2_alongpath_.1_1_ul_mean<-mean(NZ_band_2_alongpath_.1_1_ul)
NZ_band_2_alongpath_.1_1_ul_sd<-sd(NZ_band_2_alongpath_.1_1_ul)
NZ_band_2_alongpath_.1_2_ul<-unlist(NZ_band_2_alongpath_.1_2)
NZ_band_2_alongpath_.1_2_ul_sum<-sum(NZ_band_2_alongpath_.1_2_ul)
NZ_band_2_alongpath_.1_2_ul_mean<-mean(NZ_band_2_alongpath_.1_2_ul)
NZ_band_2_alongpath_.1_2_ul_sd<-sd(NZ_band_2_alongpath_.1_2_ul)
NZ_band_2_alongpath_.1_3_ul<-unlist(NZ_band_2_alongpath_.1_3)
NZ_band_2_alongpath_.1_3_ul_sum<-sum(NZ_band_2_alongpath_.1_3_ul)
NZ_band_2_alongpath_.1_3_ul_mean<-mean(NZ_band_2_alongpath_.1_3_ul)
NZ_band_2_alongpath_.1_3_ul_sd<-sd(NZ_band_2_alongpath_.1_3_ul)
NZ_band_2_alongpath_..1_1_ul<-unlist(NZ_band_2_alongpath_..1_1)
NZ_band_2_alongpath_..1_1_ul_sum<-sum(NZ_band_2_alongpath_..1_1_ul)
NZ_band_2_alongpath_..1_1_ul_mean<-mean(NZ_band_2_alongpath_..1_1_ul)
NZ_band_2_alongpath_..1_1_ul_sd<-sd(NZ_band_2_alongpath_..1_1_ul)
NZ_band_2_alongpath_..1_2_ul<-unlist(NZ_band_2_alongpath_..1_2)
NZ_band_2_alongpath_..1_2_ul_sum<-sum(NZ_band_2_alongpath_..1_2_ul)
NZ_band_2_alongpath_..1_2_ul_mean<-mean(NZ_band_2_alongpath_..1_2_ul)
NZ_band_2_alongpath_..1_2_ul_sd<-sd(NZ_band_2_alongpath_..1_2_ul)
NZ_band_2_alongpath_..1_3_ul<-unlist(NZ_band_2_alongpath_..1_3)
NZ_band_2_alongpath_..1_3_ul_sum<-sum(NZ_band_2_alongpath_..1_3_ul)
NZ_band_2_alongpath_..1_3_ul_mean<-mean(NZ_band_2_alongpath_..1_3_ul)
```

```
NZ_band_2_alongpath_..1_3_ul_sd<-sd(NZ_band_2_alongpath_..1_3_ul)


#band 3

NZ_band_3_alongpath_0_1<-raster::extract(NZ_band_3,NZ_alongpath_0_1, along = TRUE,cellnumbers = FALSE)
NZ_band_3_alongpath_0_2<-raster::extract(NZ_band_3,NZ_alongpath_0_2, along = TRUE,cellnumbers = FALSE)
NZ_band_3_alongpath_0_3<-raster::extract(NZ_band_3,NZ_alongpath_0_3, along = TRUE,cellnumbers = FALSE)
NZ_band_3_alongpath_.1_1<-raster::extract(NZ_band_3,NZ_alongpath_.1_1, along = TRUE,cellnumbers = FALSE)
NZ_band_3_alongpath_.1_2<-raster::extract(NZ_band_3,NZ_alongpath_.1_2, along = TRUE,cellnumbers = FALSE)
NZ_band_3_alongpath_.1_3<-raster::extract(NZ_band_3,NZ_alongpath_.1_3, along = TRUE,cellnumbers = FALSE)
NZ_band_3_alongpath_..1_1<-raster::extract(NZ_band_3,NZ_alongpath_..1_1, along = TRUE,cellnumbers = FALSE)
NZ_band_3_alongpath_..1_2<-raster::extract(NZ_band_3,NZ_alongpath_..1_2, along = TRUE,cellnumbers = FALSE)
NZ_band_3_alongpath_..1_3<-raster::extract(NZ_band_3,NZ_alongpath_..1_3, along = TRUE,cellnumbers = FALSE)



NZ_band_3_alongpath_0_1_ul<-unlist(NZ_band_3_alongpath_0_1)
NZ_band_3_alongpath_0_1_ul_sum<-sum(NZ_band_3_alongpath_0_1_ul)
NZ_band_3_alongpath_0_1_ul_mean<-mean(NZ_band_3_alongpath_0_1_ul)
NZ_band_3_alongpath_0_1_ul_sd<-sd(NZ_band_3_alongpath_0_1_ul)
NZ_band_3_alongpath_0_2_ul<-unlist(NZ_band_3_alongpath_0_1)
NZ_band_3_alongpath_0_2_ul_sum<-sum(NZ_band_3_alongpath_0_2_ul)
NZ_band_3_alongpath_0_2_ul_mean<-mean(NZ_band_3_alongpath_0_2_ul)
NZ_band_3_alongpath_0_2_ul_sd<-sd(NZ_band_3_alongpath_0_2_ul)
NZ_band_3_alongpath_0_3_ul<-unlist(NZ_band_3_alongpath_0_3)
NZ_band_3_alongpath_0_3_ul_sum<-sum(NZ_band_3_alongpath_0_3_ul)
NZ_band_3_alongpath_0_3_ul_mean<-mean(NZ_band_3_alongpath_0_3_ul)
NZ_band_3_alongpath_0_3_ul_sd<-sd(NZ_band_3_alongpath_0_3_ul)
NZ_band_3_alongpath_.1_1_ul<-unlist(NZ_band_3_alongpath_.1_1)
NZ_band_3_alongpath_.1_1_ul_sum<-sum(NZ_band_3_alongpath_.1_1_ul)
NZ_band_3_alongpath_.1_1_ul_mean<-mean(NZ_band_3_alongpath_.1_1_ul)
NZ_band_3_alongpath_.1_1_ul_sd<-sd(NZ_band_3_alongpath_.1_1_ul)
NZ_band_3_alongpath_.1_2_ul<-unlist(NZ_band_3_alongpath_.1_2)
NZ_band_3_alongpath_.1_2_ul_sum<-sum(NZ_band_3_alongpath_.1_2_ul)
NZ_band_3_alongpath_.1_2_ul_mean<-mean(NZ_band_3_alongpath_.1_2_ul)
NZ_band_3_alongpath_.1_2_ul_sd<-sd(NZ_band_3_alongpath_.1_2_ul)
NZ_band_3_alongpath_.1_3_ul<-unlist(NZ_band_3_alongpath_.1_3)
NZ_band_3_alongpath_.1_3_ul_sum<-sum(NZ_band_3_alongpath_.1_3_ul)
NZ_band_3_alongpath_.1_3_ul_mean<-mean(NZ_band_3_alongpath_.1_3_ul)
NZ_band_3_alongpath_.1_3_ul_sd<-sd(NZ_band_3_alongpath_.1_3_ul)
NZ_band_3_alongpath_..1_1_ul<-unlist(NZ_band_3_alongpath_..1_1)
NZ_band_3_alongpath_..1_1_ul_sum<-sum(NZ_band_3_alongpath_..1_1_ul)
NZ_band_3_alongpath_..1_1_ul_mean<-mean(NZ_band_3_alongpath_..1_1_ul)
NZ_band_3_alongpath_..1_1_ul_sd<-sd(NZ_band_3_alongpath_..1_1_ul)
NZ_band_3_alongpath_..1_2_ul<-unlist(NZ_band_3_alongpath_..1_2)
NZ_band_3_alongpath_..1_2_ul_sum<-sum(NZ_band_3_alongpath_..1_2_ul)
NZ_band_3_alongpath_..1_2_ul_mean<-mean(NZ_band_3_alongpath_..1_2_ul)
NZ_band_3_alongpath_..1_2_ul_sd<-sd(NZ_band_3_alongpath_..1_2_ul)
NZ_band_3_alongpath_..1_3_ul<-unlist(NZ_band_3_alongpath_..1_3)
NZ_band_3_alongpath_..1_3_ul_sum<-sum(NZ_band_3_alongpath_..1_3_ul)
NZ_band_3_alongpath_..1_3_ul_mean<-mean(NZ_band_3_alongpath_..1_3_ul)
NZ_band_3_alongpath_..1_3_ul_sd<-sd(NZ_band_3_alongpath_..1_3_ul)

##########################################

NZ_bands_values<-list(NZ_band_1_alongpath_0_1_ul_sum,NZ_band_1_alongpath_0_2_ul_sum,
                      NZ_band_1_alongpath_0_3_ul_sum,NZ_band_1_alongpath_.1_1_ul_sum,
                      NZ_band_1_alongpath_.1_2_ul_sum,NZ_band_1_alongpath_.1_3_ul_sum,
                      NZ_band_1_alongpath_..1_1_ul_sum, NZ_band_1_alongpath_..1_2_ul_sum,
                      NZ_band_1_alongpath_..1_3_ul_sum, NZ_band_2_alongpath_0_1_ul_sum,
                      NZ_band_2_alongpath_0_2_ul_sum, NZ_band_2_alongpath_0_3_ul_sum,
                      NZ_band_2_alongpath_.1_1_ul_sum, NZ_band_2_alongpath_.1_2_ul_sum,
                      NZ_band_2_alongpath_.1_3_ul_sum, NZ_band_2_alongpath_..1_1_ul_sum,
                      NZ_band_2_alongpath_..1_2_ul_sum, NZ_band_2_alongpath_..1_3_ul_sum,
                      NZ_band_3_alongpath_0_1_ul_sum, NZ_band_3_alongpath_0_2_ul_sum,
                      NZ_band_3_alongpath_0_3_ul_sum, NZ_band_3_alongpath_.1_1_ul_sum,
                      NZ_band_3_alongpath_.1_2_ul_sum, NZ_band_3_alongpath_.1_3_ul_sum,
                      NZ_band_3_alongpath_..1_1_ul_sum, NZ_band_3_alongpath_..1_2_ul_sum,
                      NZ_band_3_alongpath_..1_3_ul_sum)
NZ_bands_values_unlisted<-unlist(NZ_bands_values)
```

```
NZ_bands_mean_values<-list(NZ_band_1_alongpath_0_1_ul_mean,NZ_band_1_alongpath_0_2_ul_mean,
                NZ_band_1_alongpath_0_3_ul_mean,NZ_band_1_alongpath_.1_1_ul_mean,
                NZ_band_1_alongpath_.1_2_ul_mean,NZ_band_1_alongpath_.1_3_ul_mean,
                NZ_band_1_alongpath_..1_1_ul_mean, NZ_band_1_alongpath_..1_2_ul_mean,
                NZ_band_1_alongpath_..1_3_ul_mean, NZ_band_2_alongpath_0_1_ul_mean,
                NZ_band_2_alongpath_0_2_ul_mean, NZ_band_2_alongpath_0_3_ul_mean,
                NZ_band_2_alongpath_.1_1_ul_mean, NZ_band_2_alongpath_.1_2_ul_mean,
                NZ_band_2_alongpath_.1_3_ul_mean, NZ_band_2_alongpath_..1_1_ul_mean,
                NZ_band_2_alongpath_..1_2_ul_mean, NZ_band_2_alongpath_..1_3_ul_mean,
                NZ_band_3_alongpath_0_1_ul_mean, NZ_band_3_alongpath_0_2_ul_mean,
                NZ_band_3_alongpath_0_3_ul_mean, NZ_band_3_alongpath_.1_1_ul_mean,
                NZ_band_3_alongpath_.1_2_ul_mean, NZ_band_3_alongpath_.1_3_ul_mean,
                NZ_band_3_alongpath_..1_1_ul_mean, NZ_band_3_alongpath_..1_2_ul_mean,
                NZ_band_3_alongpath_..1_3_ul_mean)
NZ_bands_mean_values_unlisted<-unlist(NZ_bands_mean_values)

NZ_bands_sd_values<-list(NZ_band_1_alongpath_0_1_ul_sd,NZ_band_1_alongpath_0_2_ul_sd,
                NZ_band_1_alongpath_0_3_ul_sd,NZ_band_1_alongpath_.1_1_ul_sd,
                NZ_band_1_alongpath_.1_2_ul_sd,NZ_band_1_alongpath_.1_3_ul_sd,
                NZ_band_1_alongpath_..1_1_ul_sd, NZ_band_1_alongpath_..1_2_ul_sd,
                NZ_band_1_alongpath_..1_3_ul_sd, NZ_band_2_alongpath_0_1_ul_sd,
                NZ_band_2_alongpath_0_2_ul_sd, NZ_band_2_alongpath_0_3_ul_sd,
                NZ_band_2_alongpath_.1_1_ul_sd, NZ_band_2_alongpath_.1_2_ul_sd,
                NZ_band_2_alongpath_.1_3_ul_sd, NZ_band_2_alongpath_..1_1_ul_sd,
                NZ_band_2_alongpath_..1_2_ul_sd, NZ_band_2_alongpath_..1_3_ul_sd,
                NZ_band_3_alongpath_0_1_ul_sd, NZ_band_3_alongpath_0_2_ul_sd,
                NZ_band_3_alongpath_0_3_ul_sd, NZ_band_3_alongpath_.1_1_ul_sd,
                NZ_band_3_alongpath_.1_2_ul_sd, NZ_band_3_alongpath_.1_3_ul_sd,
                NZ_band_3_alongpath_..1_1_ul_sd, NZ_band_3_alongpath_..1_2_ul_sd,
                NZ_band_3_alongpath_..1_3_ul_sd)
NZ_bands_sd_values_unlisted<-unlist(NZ_bands_sd_values)



write.csv2(c(NZ_bands_values_unlisted,NZ_bands_mean_values_unlisted,NZ_bands_sd_values_unlisted),"NZ_bands_values.csv")



#######################Zeelim Slope Footpath Roman



#upload rasters of orthophotos of bands
ZS_band_1<-raster::raster("ZS_band_1.tif")
ZS_band_2<-raster::raster("ZS_band_2.tif")
ZS_band_3<-raster::raster("ZS_band_3.tif")


#upload footpaths and controls

#ZS footpath
ZS_alongpath_0_1<- st_read("ZS_alongpath_0_1.gpkg")
ZS_alongpath_0_2<- st_read("ZS_alongpath_0_2.gpkg")
ZS_alongpath_0_3<- st_read("ZS_alongpath_0_3.gpkg")
ZS_alongpath_.1_1<- st_read("ZS_alongpath_-1_1.gpkg")
ZS_alongpath_.1_2<- st_read("ZS_alongpath_-1_2.gpkg")
ZS_alongpath_.1_3<- st_read("ZS_alongpath_-1_3.gpkg")
ZS_alongpath_..1_1<- st_read("ZS_alongpath_1_1.gpkg")
ZS_alongpath_..1_2<- st_read("ZS_alongpath_1_2.gpkg")
ZS_alongpath_..1_3<- st_read("ZS_alongpath_1_3.gpkg")


#band 1
ZS_band_1_alongpath_0_1<-raster::extract(ZS_band_1,ZS_alongpath_0_1, along = TRUE,cellnumbers = FALSE)
ZS_band_1_alongpath_0_2<-raster::extract(ZS_band_1,ZS_alongpath_0_2, along = TRUE,cellnumbers = FALSE)
ZS_band_1_alongpath_0_3<-raster::extract(ZS_band_1,ZS_alongpath_0_3, along = TRUE,cellnumbers = FALSE)
ZS_band_1_alongpath_.1_1<-raster::extract(ZS_band_1,ZS_alongpath_.1_1, along = TRUE,cellnumbers = FALSE)
ZS_band_1_alongpath_.1_2<-raster::extract(ZS_band_1,ZS_alongpath_.1_2, along = TRUE,cellnumbers = FALSE)
ZS_band_1_alongpath_.1_3<-raster::extract(ZS_band_1,ZS_alongpath_.1_3, along = TRUE,cellnumbers = FALSE)
ZS_band_1_alongpath_..1_1<-raster::extract(ZS_band_1,ZS_alongpath_..1_1, along = TRUE,cellnumbers = FALSE)
```

```
ZS_band_1_alongpath_..1_2<-raster::extract(ZS_band_1,ZS_alongpath_..1_2, along = TRUE,cellnumbers = FALSE)
ZS_band_1_alongpath_..1_3<-raster::extract(ZS_band_1,ZS_alongpath_..1_3, along = TRUE,cellnumbers = FALSE)

ZS_band_1_alongpath_0_1_ul<-unlist(ZS_band_1_alongpath_0_1)
ZS_band_1_alongpath_0_1_ul_sum<-sum(ZS_band_1_alongpath_0_1_ul)
ZS_band_1_alongpath_0_1_ul_mean<-mean(ZS_band_1_alongpath_0_1_ul)
ZS_band_1_alongpath_0_1_ul_sd<-sd(ZS_band_1_alongpath_0_1_ul)
ZS_band_1_alongpath_0_2_ul<-unlist(ZS_band_1_alongpath_0_2)
ZS_band_1_alongpath_0_2_ul_sum<-sum(ZS_band_1_alongpath_0_2_ul)
ZS_band_1_alongpath_0_2_ul_mean<-mean(ZS_band_1_alongpath_0_2_ul)
ZS_band_1_alongpath_0_2_ul_sd<-sd(ZS_band_1_alongpath_0_2_ul)
ZS_band_1_alongpath_0_3_ul<-unlist(ZS_band_1_alongpath_0_3)
ZS_band_1_alongpath_0_3_ul_sum<-sum(ZS_band_1_alongpath_0_3_ul)
ZS_band_1_alongpath_0_3_ul_mean<-mean(ZS_band_1_alongpath_0_3_ul)
ZS_band_1_alongpath_0_3_ul_sd<-sd(ZS_band_1_alongpath_0_3_ul)
ZS_band_1_alongpath_.1_1_ul<-unlist(ZS_band_1_alongpath_.1_1)
ZS_band_1_alongpath_.1_1_ul_sum<-sum(ZS_band_1_alongpath_.1_1_ul)
ZS_band_1_alongpath_.1_1_ul_mean<-mean(ZS_band_1_alongpath_.1_1_ul)
ZS_band_1_alongpath_.1_1_ul_sd<-sd(ZS_band_1_alongpath_.1_1_ul)
ZS_band_1_alongpath_.1_2_ul<-unlist(ZS_band_1_alongpath_.1_2)
ZS_band_1_alongpath_.1_2_ul_sum<-sum(ZS_band_1_alongpath_.1_2_ul)
ZS_band_1_alongpath_.1_2_ul_mean<-mean(ZS_band_1_alongpath_.1_2_ul)
ZS_band_1_alongpath_.1_2_ul_sd<-sd(ZS_band_1_alongpath_.1_2_ul)
ZS_band_1_alongpath_.1_3_ul<-unlist(ZS_band_1_alongpath_.1_3)
ZS_band_1_alongpath_.1_3_ul_sum<-sum(ZS_band_1_alongpath_.1_3_ul)
ZS_band_1_alongpath_.1_3_ul_mean<-mean(ZS_band_1_alongpath_.1_3_ul)
ZS_band_1_alongpath_.1_3_ul_sd<-sd(ZS_band_1_alongpath_.1_3_ul)
ZS_band_1_alongpath_..1_1_ul<-unlist(ZS_band_1_alongpath_..1_1)
ZS_band_1_alongpath_..1_1_ul_sum<-sum(ZS_band_1_alongpath_..1_1_ul)
ZS_band_1_alongpath_..1_1_ul_mean<-mean(ZS_band_1_alongpath_..1_1_ul)
ZS_band_1_alongpath_..1_1_ul_sd<-sd(ZS_band_1_alongpath_..1_1_ul)
ZS_band_1_alongpath_..1_2_ul<-unlist(ZS_band_1_alongpath_..1_2)
ZS_band_1_alongpath_..1_2_ul_sum<-sum(ZS_band_1_alongpath_..1_2_ul)
ZS_band_1_alongpath_..1_2_ul_mean<-mean(ZS_band_1_alongpath_..1_2_ul)
ZS_band_1_alongpath_..1_2_ul_sd<-sd(ZS_band_1_alongpath_..1_2_ul)
ZS_band_1_alongpath_..1_3_ul<-unlist(ZS_band_1_alongpath_..1_3)
ZS_band_1_alongpath_..1_3_ul_sum<-sum(ZS_band_1_alongpath_..1_3_ul)
ZS_band_1_alongpath_..1_3_ul_mean<-mean(ZS_band_1_alongpath_..1_3_ul)
ZS_band_1_alongpath_..1_3_ul_sd<-sd(ZS_band_1_alongpath_..1_3_ul)

#band 2
ZS_band_2_alongpath_0_1<-raster::extract(ZS_band_2,ZS_alongpath_0_1, along = TRUE,cellnumbers = FALSE)
ZS_band_2_alongpath_0_2<-raster::extract(ZS_band_2,ZS_alongpath_0_2, along = TRUE,cellnumbers = FALSE)
ZS_band_2_alongpath_0_3<-raster::extract(ZS_band_2,ZS_alongpath_0_3, along = TRUE,cellnumbers = FALSE)
ZS_band_2_alongpath_.1_1<-raster::extract(ZS_band_2,ZS_alongpath_.1_1, along = TRUE,cellnumbers = FALSE)
ZS_band_2_alongpath_.1_2<-raster::extract(ZS_band_2,ZS_alongpath_.1_2, along = TRUE,cellnumbers = FALSE)
ZS_band_2_alongpath_.1_3<-raster::extract(ZS_band_2,ZS_alongpath_.1_3, along = TRUE,cellnumbers = FALSE)
ZS_band_2_alongpath_..1_1<-raster::extract(ZS_band_2,ZS_alongpath_..1_1, along = TRUE,cellnumbers = FALSE)
ZS_band_2_alongpath_..1_2<-raster::extract(ZS_band_2,ZS_alongpath_..1_2, along = TRUE,cellnumbers = FALSE)
ZS_band_2_alongpath_..1_3<-raster::extract(ZS_band_2,ZS_alongpath_..1_3, along = TRUE,cellnumbers = FALSE)


ZS_band_2_alongpath_0_1_ul<-unlist(ZS_band_2_alongpath_0_1)
ZS_band_2_alongpath_0_1_ul_sum<-sum(ZS_band_2_alongpath_0_1_ul)
ZS_band_2_alongpath_0_1_ul_mean<-mean(ZS_band_2_alongpath_0_1_ul)
ZS_band_2_alongpath_0_1_ul_sd<-sd(ZS_band_2_alongpath_0_1_ul)
ZS_band_2_alongpath_0_2_ul<-unlist(ZS_band_2_alongpath_0_1)
ZS_band_2_alongpath_0_2_ul_sum<-sum(ZS_band_2_alongpath_0_2_ul)
ZS_band_2_alongpath_0_2_ul_mean<-mean(ZS_band_2_alongpath_0_2_ul)
ZS_band_2_alongpath_0_2_ul_sd<-sd(ZS_band_2_alongpath_0_2_ul)
ZS_band_2_alongpath_0_3_ul<-unlist(ZS_band_2_alongpath_0_3)
ZS_band_2_alongpath_0_3_ul_sum<-sum(ZS_band_2_alongpath_0_3_ul)
ZS_band_2_alongpath_0_3_ul_mean<-mean(ZS_band_2_alongpath_0_3_ul)
ZS_band_2_alongpath_0_3_ul_sd<-sd(ZS_band_2_alongpath_0_3_ul)
ZS_band_2_alongpath_.1_1_ul<-unlist(ZS_band_2_alongpath_.1_1)
ZS_band_2_alongpath_.1_1_ul_sum<-sum(ZS_band_2_alongpath_.1_1_ul)
ZS_band_2_alongpath_.1_1_ul_mean<-mean(ZS_band_2_alongpath_.1_1_ul)
ZS_band_2_alongpath_.1_1_ul_sd<-sd(ZS_band_2_alongpath_.1_1_ul)
ZS_band_2_alongpath_.1_2_ul<-unlist(ZS_band_2_alongpath_.1_2)
ZS_band_2_alongpath_.1_2_ul_sum<-sum(ZS_band_2_alongpath_.1_2_ul)
ZS_band_2_alongpath_.1_2_ul_mean<-mean(ZS_band_2_alongpath_.1_2_ul)
```

```
ZS_band_2_alongpath_.1_2_ul_sd<-sd(ZS_band_2_alongpath_.1_2_ul)
ZS_band_2_alongpath_.1_3_ul<-unlist(ZS_band_2_alongpath_.1_3)
ZS_band_2_alongpath_.1_3_ul_sum<-sum(ZS_band_2_alongpath_.1_3_ul)
ZS_band_2_alongpath_.1_3_ul_mean<-mean(ZS_band_2_alongpath_.1_3_ul)
ZS_band_2_alongpath_.1_3_ul_sd<-sd(ZS_band_2_alongpath_.1_3_ul)
ZS_band_2_alongpath_..1_1_ul<-unlist(ZS_band_2_alongpath_..1_1)
ZS_band_2_alongpath_..1_1_ul_sum<-sum(ZS_band_2_alongpath_..1_1_ul)
ZS_band_2_alongpath_..1_1_ul_mean<-mean(ZS_band_2_alongpath_..1_1_ul)
ZS_band_2_alongpath_..1_1_ul_sd<-sd(ZS_band_2_alongpath_..1_1_ul)
ZS_band_2_alongpath_..1_2_ul<-unlist(ZS_band_2_alongpath_..1_2)
ZS_band_2_alongpath_..1_2_ul_sum<-sum(ZS_band_2_alongpath_..1_2_ul)
ZS_band_2_alongpath_..1_2_ul_mean<-mean(ZS_band_2_alongpath_..1_2_ul)
ZS_band_2_alongpath_..1_2_ul_sd<-sd(ZS_band_2_alongpath_..1_2_ul)
ZS_band_2_alongpath_..1_3_ul<-unlist(ZS_band_2_alongpath_..1_3)
ZS_band_2_alongpath_..1_3_ul_sum<-sum(ZS_band_2_alongpath_..1_3_ul)
ZS_band_2_alongpath_..1_3_ul_mean<-mean(ZS_band_2_alongpath_..1_3_ul)
ZS_band_2_alongpath_..1_3_ul_sd<-sd(ZS_band_2_alongpath_..1_3_ul)


#band 3

ZS_band_3_alongpath_0_1<-raster::extract(ZS_band_3,ZS_alongpath_0_1, along = TRUE,cellnumbers = FALSE)
ZS_band_3_alongpath_0_2<-raster::extract(ZS_band_3,ZS_alongpath_0_2, along = TRUE,cellnumbers = FALSE)
ZS_band_3_alongpath_0_3<-raster::extract(ZS_band_3,ZS_alongpath_0_3, along = TRUE,cellnumbers = FALSE)
ZS_band_3_alongpath_.1_1<-raster::extract(ZS_band_3,ZS_alongpath_.1_1, along = TRUE,cellnumbers = FALSE)
ZS_band_3_alongpath_.1_2<-raster::extract(ZS_band_3,ZS_alongpath_.1_2, along = TRUE,cellnumbers = FALSE)
ZS_band_3_alongpath_.1_3<-raster::extract(ZS_band_3,ZS_alongpath_.1_3, along = TRUE,cellnumbers = FALSE)
ZS_band_3_alongpath_..1_1<-raster::extract(ZS_band_3,ZS_alongpath_..1_1, along = TRUE,cellnumbers = FALSE)
ZS_band_3_alongpath_..1_2<-raster::extract(ZS_band_3,ZS_alongpath_..1_2, along = TRUE,cellnumbers = FALSE)
ZS_band_3_alongpath_..1_3<-raster::extract(ZS_band_3,ZS_alongpath_..1_3, along = TRUE,cellnumbers = FALSE)



ZS_band_3_alongpath_0_1_ul<-unlist(ZS_band_3_alongpath_0_1)
ZS_band_3_alongpath_0_1_ul_sum<-sum(ZS_band_3_alongpath_0_1_ul)
ZS_band_3_alongpath_0_1_ul_mean<-mean(ZS_band_3_alongpath_0_1_ul)
ZS_band_3_alongpath_0_1_ul_sd<-sd(ZS_band_3_alongpath_0_1_ul)
ZS_band_3_alongpath_0_2_ul<-unlist(ZS_band_3_alongpath_0_1)
ZS_band_3_alongpath_0_2_ul_sum<-sum(ZS_band_3_alongpath_0_2_ul)
ZS_band_3_alongpath_0_2_ul_mean<-mean(ZS_band_3_alongpath_0_2_ul)
ZS_band_3_alongpath_0_2_ul_sd<-sd(ZS_band_3_alongpath_0_2_ul)
ZS_band_3_alongpath_0_3_ul<-unlist(ZS_band_3_alongpath_0_3)
ZS_band_3_alongpath_0_3_ul_sum<-sum(ZS_band_3_alongpath_0_3_ul)
ZS_band_3_alongpath_0_3_ul_mean<-mean(ZS_band_3_alongpath_0_3_ul)
ZS_band_3_alongpath_0_3_ul_sd<-sd(ZS_band_3_alongpath_0_3_ul)
ZS_band_3_alongpath_.1_1_ul<-unlist(ZS_band_3_alongpath_.1_1)
ZS_band_3_alongpath_.1_1_ul_sum<-sum(ZS_band_3_alongpath_.1_1_ul)
ZS_band_3_alongpath_.1_1_ul_mean<-mean(ZS_band_3_alongpath_.1_1_ul)
ZS_band_3_alongpath_.1_1_ul_sd<-sd(ZS_band_3_alongpath_.1_1_ul)
ZS_band_3_alongpath_.1_2_ul<-unlist(ZS_band_3_alongpath_.1_2)
ZS_band_3_alongpath_.1_2_ul_sum<-sum(ZS_band_3_alongpath_.1_2_ul)
ZS_band_3_alongpath_.1_2_ul_mean<-mean(ZS_band_3_alongpath_.1_2_ul)
ZS_band_3_alongpath_.1_2_ul_sd<-sd(ZS_band_3_alongpath_.1_2_ul)
ZS_band_3_alongpath_.1_3_ul<-unlist(ZS_band_3_alongpath_.1_3)
ZS_band_3_alongpath_.1_3_ul_sum<-sum(ZS_band_3_alongpath_.1_3_ul)
ZS_band_3_alongpath_.1_3_ul_mean<-mean(ZS_band_3_alongpath_.1_3_ul)
ZS_band_3_alongpath_.1_3_ul_sd<-sd(ZS_band_3_alongpath_.1_3_ul)
ZS_band_3_alongpath_..1_1_ul<-unlist(ZS_band_3_alongpath_..1_1)
ZS_band_3_alongpath_..1_1_ul_sum<-sum(ZS_band_3_alongpath_..1_1_ul)
ZS_band_3_alongpath_..1_1_ul_mean<-mean(ZS_band_3_alongpath_..1_1_ul)
ZS_band_3_alongpath_..1_1_ul_sd<-sd(ZS_band_3_alongpath_..1_1_ul)
ZS_band_3_alongpath_..1_2_ul<-unlist(ZS_band_3_alongpath_..1_2)
ZS_band_3_alongpath_..1_2_ul_sum<-sum(ZS_band_3_alongpath_..1_2_ul)
ZS_band_3_alongpath_..1_2_ul_mean<-mean(ZS_band_3_alongpath_..1_2_ul)
ZS_band_3_alongpath_..1_2_ul_sd<-sd(ZS_band_3_alongpath_..1_2_ul)
ZS_band_3_alongpath_..1_3_ul<-unlist(ZS_band_3_alongpath_..1_3)
ZS_band_3_alongpath_..1_3_ul_sum<-sum(ZS_band_3_alongpath_..1_3_ul)
ZS_band_3_alongpath_..1_3_ul_mean<-mean(ZS_band_3_alongpath_..1_3_ul)
ZS_band_3_alongpath_..1_3_ul_sd<-sd(ZS_band_3_alongpath_..1_3_ul)

##########################################
```

```
ZS_bands_values<-list(ZS_band_1_alongpath_0_1_ul_sum,ZS_band_1_alongpath_0_2_ul_sum,
              ZS_band_1_alongpath_0_3_ul_sum,ZS_band_1_alongpath_.1_1_ul_sum,
              ZS_band_1_alongpath_.1_2_ul_sum,ZS_band_1_alongpath_.1_3_ul_sum,
              ZS_band_1_alongpath_..1_1_ul_sum, ZS_band_1_alongpath_..1_2_ul_sum,
              ZS_band_1_alongpath_..1_3_ul_sum, ZS_band_2_alongpath_0_1_ul_sum,
              ZS_band_2_alongpath_0_2_ul_sum, ZS_band_2_alongpath_0_3_ul_sum,
              ZS_band_2_alongpath_.1_1_ul_sum, ZS_band_2_alongpath_.1_2_ul_sum,
              ZS_band_2_alongpath_.1_3_ul_sum, ZS_band_2_alongpath_..1_1_ul_sum,
              ZS_band_2_alongpath_..1_2_ul_sum, ZS_band_2_alongpath_..1_3_ul_sum,
              ZS_band_3_alongpath_0_1_ul_sum, ZS_band_3_alongpath_0_2_ul_sum,
              ZS_band_3_alongpath_0_3_ul_sum, ZS_band_3_alongpath_.1_1_ul_sum,
              ZS_band_3_alongpath_.1_2_ul_sum, ZS_band_3_alongpath_.1_3_ul_sum,
              ZS_band_3_alongpath_..1_1_ul_sum, ZS_band_3_alongpath_..1_2_ul_sum,
              ZS_band_3_alongpath_..1_3_ul_sum)
ZS_bands_values_unlisted<-unlist(ZS_bands_values)

ZS_bands_mean_values<-list(ZS_band_1_alongpath_0_1_ul_mean,ZS_band_1_alongpath_0_2_ul_mean,
                ZS_band_1_alongpath_0_3_ul_mean,ZS_band_1_alongpath_.1_1_ul_mean,
                ZS_band_1_alongpath_.1_2_ul_mean,ZS_band_1_alongpath_.1_3_ul_mean,
                ZS_band_1_alongpath_..1_1_ul_mean, ZS_band_1_alongpath_..1_2_ul_mean,
                ZS_band_1_alongpath_..1_3_ul_mean, ZS_band_2_alongpath_0_1_ul_mean,
                ZS_band_2_alongpath_0_2_ul_mean, ZS_band_2_alongpath_0_3_ul_mean,
                ZS_band_2_alongpath_.1_1_ul_mean, ZS_band_2_alongpath_.1_2_ul_mean,
                ZS_band_2_alongpath_.1_3_ul_mean, ZS_band_2_alongpath_..1_1_ul_mean,
                ZS_band_2_alongpath_..1_2_ul_mean, ZS_band_2_alongpath_..1_3_ul_mean,
                ZS_band_3_alongpath_0_1_ul_mean, ZS_band_3_alongpath_0_2_ul_mean,
                ZS_band_3_alongpath_0_3_ul_mean, ZS_band_3_alongpath_.1_1_ul_mean,
                ZS_band_3_alongpath_.1_2_ul_mean, ZS_band_3_alongpath_.1_3_ul_mean,
                ZS_band_3_alongpath_..1_1_ul_mean, ZS_band_3_alongpath_..1_2_ul_mean,
                ZS_band_3_alongpath_..1_3_ul_mean)
ZS_bands_mean_values_unlisted<-unlist(ZS_bands_mean_values)

ZS_bands_sd_values<-list(ZS_band_1_alongpath_0_1_ul_sd,ZS_band_1_alongpath_0_2_ul_sd,
              ZS_band_1_alongpath_0_3_ul_sd,ZS_band_1_alongpath_.1_1_ul_sd,
              ZS_band_1_alongpath_.1_2_ul_sd,ZS_band_1_alongpath_.1_3_ul_sd,
              ZS_band_1_alongpath_..1_1_ul_sd, ZS_band_1_alongpath_..1_2_ul_sd,
              ZS_band_1_alongpath_..1_3_ul_sd, ZS_band_2_alongpath_0_1_ul_sd,
              ZS_band_2_alongpath_0_2_ul_sd, ZS_band_2_alongpath_0_3_ul_sd,
              ZS_band_2_alongpath_.1_1_ul_sd, ZS_band_2_alongpath_.1_2_ul_sd,
              ZS_band_2_alongpath_.1_3_ul_sd, ZS_band_2_alongpath_..1_1_ul_sd,
              ZS_band_2_alongpath_..1_2_ul_sd, ZS_band_2_alongpath_..1_3_ul_sd,
              ZS_band_3_alongpath_0_1_ul_sd, ZS_band_3_alongpath_0_2_ul_sd,
              ZS_band_3_alongpath_0_3_ul_sd, ZS_band_3_alongpath_.1_1_ul_sd,
              ZS_band_3_alongpath_.1_2_ul_sd, ZS_band_3_alongpath_.1_3_ul_sd,
              ZS_band_3_alongpath_..1_1_ul_sd, ZS_band_3_alongpath_..1_2_ul_sd,
              ZS_band_3_alongpath_..1_3_ul_sd)
ZS_bands_sd_values_unlisted<-unlist(ZS_bands_sd_values)



write.csv2(c(ZS_bands_values_unlisted,ZS_bands_mean_values_unlisted,ZS_bands_sd_values_unlisted),"ZS_bands_values.csv")


########################################Zeelim Plane Roman

#upload rasters of orthophotos of bands
ZP_band_1<-raster::raster("ZP_band_1.tif")
ZP_band_2<-raster::raster("ZP_band_2.tif")
ZP_band_3<-raster::raster("ZP_band_3.tif")


#upload footpaths and controls

#ZP footpath
ZP_alongpath_0_1<- st_read("ZP_alongpath_0_1.gpkg")
ZP_alongpath_0_2<- st_read("ZP_alongpath_0_2.gpkg")
ZP_alongpath_0_3<- st_read("ZP_alongpath_0_3.gpkg")
ZP_alongpath_.1_1<- st_read("ZP_alongpath_-1_1.gpkg")
ZP_alongpath_.1_2<- st_read("ZP_alongpath_-1_2.gpkg")
ZP_alongpath_.1_3<- st_read("ZP_alongpath_-1_3.gpkg")
```

```
ZP_alongpath_..1_1<- st_read("ZP_alongpath_1_1.gpkg")
ZP_alongpath_..1_2<- st_read("ZP_alongpath_1_2.gpkg")
ZP_alongpath_..1_3<- st_read("ZP_alongpath_1_3.gpkg")


#band 1
ZP_band_1_alongpath_0_1<-raster::extract(ZP_band_1,ZP_alongpath_0_1, along = TRUE,cellnumbers = FALSE)
ZP_band_1_alongpath_0_2<-raster::extract(ZP_band_1,ZP_alongpath_0_2, along = TRUE,cellnumbers = FALSE)
ZP_band_1_alongpath_0_3<-raster::extract(ZP_band_1,ZP_alongpath_0_3, along = TRUE,cellnumbers = FALSE)
ZP_band_1_alongpath_.1_1<-raster::extract(ZP_band_1,ZP_alongpath_.1_1, along = TRUE,cellnumbers = FALSE)
ZP_band_1_alongpath_.1_2<-raster::extract(ZP_band_1,ZP_alongpath_.1_2, along = TRUE,cellnumbers = FALSE)
ZP_band_1_alongpath_.1_3<-raster::extract(ZP_band_1,ZP_alongpath_.1_3, along = TRUE,cellnumbers = FALSE)
ZP_band_1_alongpath_..1_1<-raster::extract(ZP_band_1,ZP_alongpath_..1_1, along = TRUE,cellnumbers = FALSE)
ZP_band_1_alongpath_..1_2<-raster::extract(ZP_band_1,ZP_alongpath_..1_2, along = TRUE,cellnumbers = FALSE)
ZP_band_1_alongpath_..1_3<-raster::extract(ZP_band_1,ZP_alongpath_..1_3, along = TRUE,cellnumbers = FALSE)

ZP_band_1_alongpath_0_1_ul<-unlist(ZP_band_1_alongpath_0_1)
ZP_band_1_alongpath_0_1_ul_sum<-sum(ZP_band_1_alongpath_0_1_ul)
ZP_band_1_alongpath_0_1_ul_mean<-mean(ZP_band_1_alongpath_0_1_ul)
ZP_band_1_alongpath_0_1_ul_sd<-sd(ZP_band_1_alongpath_0_1_ul)
ZP_band_1_alongpath_0_2_ul<-unlist(ZP_band_1_alongpath_0_2)
ZP_band_1_alongpath_0_2_ul_sum<-sum(ZP_band_1_alongpath_0_2_ul)
ZP_band_1_alongpath_0_2_ul_mean<-mean(ZP_band_1_alongpath_0_2_ul)
ZP_band_1_alongpath_0_2_ul_sd<-sd(ZP_band_1_alongpath_0_2_ul)
ZP_band_1_alongpath_0_3_ul<-unlist(ZP_band_1_alongpath_0_3)
ZP_band_1_alongpath_0_3_ul_sum<-sum(ZP_band_1_alongpath_0_3_ul)
ZP_band_1_alongpath_0_3_ul_mean<-mean(ZP_band_1_alongpath_0_3_ul)
ZP_band_1_alongpath_0_3_ul_sd<-sd(ZP_band_1_alongpath_0_3_ul)
ZP_band_1_alongpath_.1_1_ul<-unlist(ZP_band_1_alongpath_.1_1)
ZP_band_1_alongpath_.1_1_ul_sum<-sum(ZP_band_1_alongpath_.1_1_ul)
ZP_band_1_alongpath_.1_1_ul_mean<-mean(ZP_band_1_alongpath_.1_1_ul)
ZP_band_1_alongpath_.1_1_ul_sd<-sd(ZP_band_1_alongpath_.1_1_ul)
ZP_band_1_alongpath_.1_2_ul<-unlist(ZP_band_1_alongpath_.1_2)
ZP_band_1_alongpath_.1_2_ul_sum<-sum(ZP_band_1_alongpath_.1_2_ul)
ZP_band_1_alongpath_.1_2_ul_mean<-mean(ZP_band_1_alongpath_.1_2_ul)
ZP_band_1_alongpath_.1_2_ul_sd<-sd(ZP_band_1_alongpath_.1_2_ul)
ZP_band_1_alongpath_.1_3_ul<-unlist(ZP_band_1_alongpath_.1_3)
ZP_band_1_alongpath_.1_3_ul_sum<-sum(ZP_band_1_alongpath_.1_3_ul)
ZP_band_1_alongpath_.1_3_ul_mean<-mean(ZP_band_1_alongpath_.1_3_ul)
ZP_band_1_alongpath_.1_3_ul_sd<-sd(ZP_band_1_alongpath_.1_3_ul)
ZP_band_1_alongpath_..1_1_ul<-unlist(ZP_band_1_alongpath_..1_1)
ZP_band_1_alongpath_..1_1_ul_sum<-sum(ZP_band_1_alongpath_..1_1_ul)
ZP_band_1_alongpath_..1_1_ul_mean<-mean(ZP_band_1_alongpath_..1_1_ul)
ZP_band_1_alongpath_..1_1_ul_sd<-sd(ZP_band_1_alongpath_..1_1_ul)
ZP_band_1_alongpath_..1_2_ul<-unlist(ZP_band_1_alongpath_..1_2)
ZP_band_1_alongpath_..1_2_ul_sum<-sum(ZP_band_1_alongpath_..1_2_ul)
ZP_band_1_alongpath_..1_2_ul_mean<-mean(ZP_band_1_alongpath_..1_2_ul)
ZP_band_1_alongpath_..1_2_ul_sd<-sd(ZP_band_1_alongpath_..1_2_ul)
ZP_band_1_alongpath_..1_3_ul<-unlist(ZP_band_1_alongpath_..1_3)
ZP_band_1_alongpath_..1_3_ul_sum<-sum(ZP_band_1_alongpath_..1_3_ul)
ZP_band_1_alongpath_..1_3_ul_mean<-mean(ZP_band_1_alongpath_..1_3_ul)
ZP_band_1_alongpath_..1_3_ul_sd<-sd(ZP_band_1_alongpath_..1_3_ul)

#band 2
ZP_band_2_alongpath_0_1<-raster::extract(ZP_band_2,ZP_alongpath_0_1, along = TRUE,cellnumbers = FALSE)
ZP_band_2_alongpath_0_2<-raster::extract(ZP_band_2,ZP_alongpath_0_2, along = TRUE,cellnumbers = FALSE)
ZP_band_2_alongpath_0_3<-raster::extract(ZP_band_2,ZP_alongpath_0_3, along = TRUE,cellnumbers = FALSE)
ZP_band_2_alongpath_.1_1<-raster::extract(ZP_band_2,ZP_alongpath_.1_1, along = TRUE,cellnumbers = FALSE)
ZP_band_2_alongpath_.1_2<-raster::extract(ZP_band_2,ZP_alongpath_.1_2, along = TRUE,cellnumbers = FALSE)
ZP_band_2_alongpath_.1_3<-raster::extract(ZP_band_2,ZP_alongpath_.1_3, along = TRUE,cellnumbers = FALSE)
ZP_band_2_alongpath_..1_1<-raster::extract(ZP_band_2,ZP_alongpath_..1_1, along = TRUE,cellnumbers = FALSE)
ZP_band_2_alongpath_..1_2<-raster::extract(ZP_band_2,ZP_alongpath_..1_2, along = TRUE,cellnumbers = FALSE)
ZP_band_2_alongpath_..1_3<-raster::extract(ZP_band_2,ZP_alongpath_..1_3, along = TRUE,cellnumbers = FALSE)

ZP_band_2_alongpath_0_1_ul<-unlist(ZP_band_2_alongpath_0_1)
ZP_band_2_alongpath_0_1_ul_sum<-sum(ZP_band_2_alongpath_0_1_ul)
ZP_band_2_alongpath_0_1_ul_mean<-mean(ZP_band_2_alongpath_0_1_ul)
ZP_band_2_alongpath_0_1_ul_sd<-sd(ZP_band_2_alongpath_0_1_ul)
ZP_band_2_alongpath_0_2_ul<-unlist(ZP_band_2_alongpath_0_1)
ZP_band_2_alongpath_0_2_ul_sum<-sum(ZP_band_2_alongpath_0_2_ul)
ZP_band_2_alongpath_0_2_ul_mean<-mean(ZP_band_2_alongpath_0_2_ul)
```

```
ZP_band_2_alongpath_0_2_ul_sd<-sd(ZP_band_2_alongpath_0_2_ul)
ZP_band_2_alongpath_0_3_ul<-unlist(ZP_band_2_alongpath_0_3)
ZP_band_2_alongpath_0_3_ul_sum<-sum(ZP_band_2_alongpath_0_3_ul)
ZP_band_2_alongpath_0_3_ul_mean<-mean(ZP_band_2_alongpath_0_3_ul)
ZP_band_2_alongpath_0_3_ul_sd<-sd(ZP_band_2_alongpath_0_3_ul)
ZP_band_2_alongpath_.1_1_ul<-unlist(ZP_band_2_alongpath_.1_1)
ZP_band_2_alongpath_.1_1_ul_sum<-sum(ZP_band_2_alongpath_.1_1_ul)
ZP_band_2_alongpath_.1_1_ul_mean<-mean(ZP_band_2_alongpath_.1_1_ul)
ZP_band_2_alongpath_.1_1_ul_sd<-sd(ZP_band_2_alongpath_.1_1_ul)
ZP_band_2_alongpath_.1_2_ul<-unlist(ZP_band_2_alongpath_.1_2)
ZP_band_2_alongpath_.1_2_ul_sum<-sum(ZP_band_2_alongpath_.1_2_ul)
ZP_band_2_alongpath_.1_2_ul_mean<-mean(ZP_band_2_alongpath_.1_2_ul)
ZP_band_2_alongpath_.1_2_ul_sd<-sd(ZP_band_2_alongpath_.1_2_ul)
ZP_band_2_alongpath_.1_3_ul<-unlist(ZP_band_2_alongpath_.1_3)
ZP_band_2_alongpath_.1_3_ul_sum<-sum(ZP_band_2_alongpath_.1_3_ul)
ZP_band_2_alongpath_.1_3_ul_mean<-mean(ZP_band_2_alongpath_.1_3_ul)
ZP_band_2_alongpath_.1_3_ul_sd<-sd(ZP_band_2_alongpath_.1_3_ul)
ZP_band_2_alongpath_..1_1_ul<-unlist(ZP_band_2_alongpath_..1_1)
ZP_band_2_alongpath_..1_1_ul_sum<-sum(ZP_band_2_alongpath_..1_1_ul)
ZP_band_2_alongpath_..1_1_ul_mean<-mean(ZP_band_2_alongpath_..1_1_ul)
ZP_band_2_alongpath_..1_1_ul_sd<-sd(ZP_band_2_alongpath_..1_1_ul)
ZP_band_2_alongpath_..1_2_ul<-unlist(ZP_band_2_alongpath_..1_2)
ZP_band_2_alongpath_..1_2_ul_sum<-sum(ZP_band_2_alongpath_..1_2_ul)
ZP_band_2_alongpath_..1_2_ul_mean<-mean(ZP_band_2_alongpath_..1_2_ul)
ZP_band_2_alongpath_..1_2_ul_sd<-sd(ZP_band_2_alongpath_..1_2_ul)
ZP_band_2_alongpath_..1_3_ul<-unlist(ZP_band_2_alongpath_..1_3)
ZP_band_2_alongpath_..1_3_ul_sum<-sum(ZP_band_2_alongpath_..1_3_ul)
ZP_band_2_alongpath_..1_3_ul_mean<-mean(ZP_band_2_alongpath_..1_3_ul)
ZP_band_2_alongpath_..1_3_ul_sd<-sd(ZP_band_2_alongpath_..1_3_ul)
```

#band 3

```
ZP_band_3_alongpath_0_1<-raster::extract(ZP_band_3,ZP_alongpath_0_1, along = TRUE,cellnumbers = FALSE)
ZP_band_3_alongpath_0_2<-raster::extract(ZP_band_3,ZP_alongpath_0_2, along = TRUE,cellnumbers = FALSE)
ZP_band_3_alongpath_0_3<-raster::extract(ZP_band_3,ZP_alongpath_0_3, along = TRUE,cellnumbers = FALSE)
ZP_band_3_alongpath_.1_1<-raster::extract(ZP_band_3,ZP_alongpath_.1_1, along = TRUE,cellnumbers = FALSE)
ZP_band_3_alongpath_.1_2<-raster::extract(ZP_band_3,ZP_alongpath_.1_2, along = TRUE,cellnumbers = FALSE)
ZP_band_3_alongpath_.1_3<-raster::extract(ZP_band_3,ZP_alongpath_.1_3, along = TRUE,cellnumbers = FALSE)
ZP_band_3_alongpath_..1_1<-raster::extract(ZP_band_3,ZP_alongpath_..1_1, along = TRUE,cellnumbers = FALSE)
ZP_band_3_alongpath_..1_2<-raster::extract(ZP_band_3,ZP_alongpath_..1_2, along = TRUE,cellnumbers = FALSE)
ZP_band_3_alongpath_..1_3<-raster::extract(ZP_band_3,ZP_alongpath_..1_3, along = TRUE,cellnumbers = FALSE)
```

```
ZP_band_3_alongpath_0_1_ul<-unlist(ZP_band_3_alongpath_0_1)
ZP_band_3_alongpath_0_1_ul_sum<-sum(ZP_band_3_alongpath_0_1_ul)
ZP_band_3_alongpath_0_1_ul_mean<-mean(ZP_band_3_alongpath_0_1_ul)
ZP_band_3_alongpath_0_1_ul_sd<-sd(ZP_band_3_alongpath_0_1_ul)
ZP_band_3_alongpath_0_2_ul<-unlist(ZP_band_3_alongpath_0_1)
ZP_band_3_alongpath_0_2_ul_sum<-sum(ZP_band_3_alongpath_0_2_ul)
ZP_band_3_alongpath_0_2_ul_mean<-mean(ZP_band_3_alongpath_0_2_ul)
ZP_band_3_alongpath_0_2_ul_sd<-sd(ZP_band_3_alongpath_0_2_ul)
ZP_band_3_alongpath_0_3_ul<-unlist(ZP_band_3_alongpath_0_3)
ZP_band_3_alongpath_0_3_ul_sum<-sum(ZP_band_3_alongpath_0_3_ul)
ZP_band_3_alongpath_0_3_ul_mean<-mean(ZP_band_3_alongpath_0_3_ul)
ZP_band_3_alongpath_0_3_ul_sd<-sd(ZP_band_3_alongpath_0_3_ul)
ZP_band_3_alongpath_.1_1_ul<-unlist(ZP_band_3_alongpath_.1_1)
ZP_band_3_alongpath_.1_1_ul_sum<-sum(ZP_band_3_alongpath_.1_1_ul)
ZP_band_3_alongpath_.1_1_ul_mean<-mean(ZP_band_3_alongpath_.1_1_ul)
ZP_band_3_alongpath_.1_1_ul_sd<-sd(ZP_band_3_alongpath_.1_1_ul)
ZP_band_3_alongpath_.1_2_ul<-unlist(ZP_band_3_alongpath_.1_2)
ZP_band_3_alongpath_.1_2_ul_sum<-sum(ZP_band_3_alongpath_.1_2_ul)
ZP_band_3_alongpath_.1_2_ul_mean<-mean(ZP_band_3_alongpath_.1_2_ul)
ZP_band_3_alongpath_.1_2_ul_sd<-sd(ZP_band_3_alongpath_.1_2_ul)
ZP_band_3_alongpath_.1_3_ul<-unlist(ZP_band_3_alongpath_.1_3)
ZP_band_3_alongpath_.1_3_ul_sum<-sum(ZP_band_3_alongpath_.1_3_ul)
ZP_band_3_alongpath_.1_3_ul_mean<-mean(ZP_band_3_alongpath_.1_3_ul)
ZP_band_3_alongpath_.1_3_ul_sd<-sd(ZP_band_3_alongpath_.1_3_ul)
ZP_band_3_alongpath_..1_1_ul<-unlist(ZP_band_3_alongpath_..1_1)
ZP_band_3_alongpath_..1_1_ul_sum<-sum(ZP_band_3_alongpath_..1_1_ul)
```

```
ZP_band_3_alongpath_..1_1_ul_mean<-mean(ZP_band_3_alongpath_..1_1_ul)
ZP_band_3_alongpath_..1_1_ul_sd<-sd(ZP_band_3_alongpath_..1_1_ul)
ZP_band_3_alongpath_..1_2_ul<-unlist(ZP_band_3_alongpath_..1_2)
ZP_band_3_alongpath_..1_2_ul_sum<-sum(ZP_band_3_alongpath_..1_2_ul)
ZP_band_3_alongpath_..1_2_ul_mean<-mean(ZP_band_3_alongpath_..1_2_ul)
ZP_band_3_alongpath_..1_2_ul_sd<-sd(ZP_band_3_alongpath_..1_2_ul)
ZP_band_3_alongpath_..1_3_ul<-unlist(ZP_band_3_alongpath_..1_3)
ZP_band_3_alongpath_..1_3_ul_sum<-sum(ZP_band_3_alongpath_..1_3_ul)
ZP_band_3_alongpath_..1_3_ul_mean<-mean(ZP_band_3_alongpath_..1_3_ul)
ZP_band_3_alongpath_..1_3_ul_sd<-sd(ZP_band_3_alongpath_..1_3_ul)

##########################################

ZP_bands_values<-list(ZP_band_1_alongpath_0_1_ul_sum,ZP_band_1_alongpath_0_2_ul_sum,
            ZP_band_1_alongpath_0_3_ul_sum,ZP_band_1_alongpath_.1_1_ul_sum,
            ZP_band_1_alongpath_.1_2_ul_sum,ZP_band_1_alongpath_.1_3_ul_sum,
            ZP_band_1_alongpath_..1_1_ul_sum, ZP_band_1_alongpath_..1_2_ul_sum,
            ZP_band_1_alongpath_..1_3_ul_sum, ZP_band_2_alongpath_0_1_ul_sum,
            ZP_band_2_alongpath_0_2_ul_sum, ZP_band_2_alongpath_0_3_ul_sum,
            ZP_band_2_alongpath_.1_1_ul_sum, ZP_band_2_alongpath_.1_2_ul_sum,
            ZP_band_2_alongpath_.1_3_ul_sum, ZP_band_2_alongpath_..1_1_ul_sum,
            ZP_band_2_alongpath_..1_2_ul_sum, ZP_band_2_alongpath_..1_3_ul_sum,
            ZP_band_3_alongpath_0_1_ul_sum, ZP_band_3_alongpath_0_2_ul_sum,
            ZP_band_3_alongpath_0_3_ul_sum, ZP_band_3_alongpath_.1_1_ul_sum,
            ZP_band_3_alongpath_.1_2_ul_sum, ZP_band_3_alongpath_.1_3_ul_sum,
            ZP_band_3_alongpath_..1_1_ul_sum, ZP_band_3_alongpath_..1_2_ul_sum,
            ZP_band_3_alongpath_..1_3_ul_sum)
ZP_bands_values_unlisted<-unlist(ZP_bands_values)

ZP_bands_mean_values<-list(ZP_band_1_alongpath_0_1_ul_mean,ZP_band_1_alongpath_0_2_ul_mean,
              ZP_band_1_alongpath_0_3_ul_mean,ZP_band_1_alongpath_.1_1_ul_mean,
              ZP_band_1_alongpath_.1_2_ul_mean,ZP_band_1_alongpath_.1_3_ul_mean,
              ZP_band_1_alongpath_..1_1_ul_mean, ZP_band_1_alongpath_..1_2_ul_mean,
              ZP_band_1_alongpath_..1_3_ul_mean, ZP_band_2_alongpath_0_1_ul_mean,
              ZP_band_2_alongpath_0_2_ul_mean, ZP_band_2_alongpath_0_3_ul_mean,
              ZP_band_2_alongpath_.1_1_ul_mean, ZP_band_2_alongpath_.1_2_ul_mean,
              ZP_band_2_alongpath_.1_3_ul_mean, ZP_band_2_alongpath_..1_1_ul_mean,
              ZP_band_2_alongpath_..1_2_ul_mean, ZP_band_2_alongpath_..1_3_ul_mean,
              ZP_band_3_alongpath_0_1_ul_mean, ZP_band_3_alongpath_0_2_ul_mean,
              ZP_band_3_alongpath_0_3_ul_mean, ZP_band_3_alongpath_.1_1_ul_mean,
              ZP_band_3_alongpath_.1_2_ul_mean, ZP_band_3_alongpath_.1_3_ul_mean,
              ZP_band_3_alongpath_..1_1_ul_mean, ZP_band_3_alongpath_..1_2_ul_mean,
              ZP_band_3_alongpath_..1_3_ul_mean)
ZP_bands_mean_values_unlisted<-unlist(ZP_bands_mean_values)

ZP_bands_sd_values<-list(ZP_band_1_alongpath_0_1_ul_sd,ZP_band_1_alongpath_0_2_ul_sd,
            ZP_band_1_alongpath_0_3_ul_sd,ZP_band_1_alongpath_.1_1_ul_sd,
            ZP_band_1_alongpath_.1_2_ul_sd,ZP_band_1_alongpath_.1_3_ul_sd,
            ZP_band_1_alongpath_..1_1_ul_sd, ZP_band_1_alongpath_..1_2_ul_sd,
            ZP_band_1_alongpath_..1_3_ul_sd, ZP_band_2_alongpath_0_1_ul_sd,
            ZP_band_2_alongpath_0_2_ul_sd, ZP_band_2_alongpath_0_3_ul_sd,
            ZP_band_2_alongpath_.1_1_ul_sd, ZP_band_2_alongpath_.1_2_ul_sd,
            ZP_band_2_alongpath_.1_3_ul_sd, ZP_band_2_alongpath_..1_1_ul_sd,
            ZP_band_2_alongpath_..1_2_ul_sd, ZP_band_2_alongpath_..1_3_ul_sd,
            ZP_band_3_alongpath_0_1_ul_sd, ZP_band_3_alongpath_0_2_ul_sd,
            ZP_band_3_alongpath_0_3_ul_sd, ZP_band_3_alongpath_.1_1_ul_sd,
            ZP_band_3_alongpath_.1_2_ul_sd, ZP_band_3_alongpath_.1_3_ul_sd,
            ZP_band_3_alongpath_..1_1_ul_sd, ZP_band_3_alongpath_..1_2_ul_sd,
            ZP_band_3_alongpath_..1_3_ul_sd)
ZP_bands_sd_values_unlisted<-unlist(ZP_bands_sd_values)

write.csv2(c(ZP_bands_values_unlisted,ZP_bands_mean_values_unlisted,ZP_bands_sd_values_unlisted),"ZP_bands_values.csv")
col_val<-read.csv2("uav_cols.csv")

nzm_p_r<-median(col_val$ebmp[1:3])
nzm_p_g<-median(col_val$ebmp[4:6])
nzm_p_b<-median(col_val$ebmp[7:9])
nzm_a_r<-median(col_val$ebma[1:3])
nzm_a_g<-median(col_val$ebma[4:6])
nzm_a_b<-median(col_val$ebma[7:9])
nzm_b_r<-median(col_val$ebmb[1:3])
```

```
nzm_b_g<-median(col_val$ebmb[4:6])
nzm_b_b<-median(col_val$ebmb[7:9])
eb_p_r<-median(col_val$ebp[1:3])
eb_p_g<-median(col_val$ebp[4:6])
eb_p_b<-median(col_val$ebp[7:9])
eb_a_r<-median(col_val$eba[1:3])
eb_a_g<-median(col_val$eba[4:6])
eb_a_b<-median(col_val$eba[7:9])
eb_b_r<-median(col_val$ebb[1:3])
eb_b_g<-median(col_val$ebb[4:6])
eb_b_b<-median(col_val$ebb[7:9])
zs_p_r<-median(col_val$zsp[1:3])
zs_p_g<-median(col_val$zsp[4:6])
zs_p_b<-median(col_val$zsp[7:9])
zs_a_r<-median(col_val$zsa[1:3])
zs_a_g<-median(col_val$zsa[4:6])
zs_a_b<-median(col_val$zsa[7:9])
zs_b_r<-median(col_val$zsb[1:3])
zs_b_g<-median(col_val$zsb[4:6])
zs_b_b<-median(col_val$zsb[7:9])
zp_p_r<-median(col_val$zpp[1:3])
zp_p_g<-median(col_val$zpp[4:6])
zp_p_b<-median(col_val$zpp[7:9])
zp_a_r<-median(col_val$zpa[1:3])
zp_a_g<-median(col_val$zpa[4:6])
zp_a_b<-median(col_val$zpa[7:9])
zp_b_r<-median(col_val$zpb[1:3])
zp_b_g<-median(col_val$zpb[4:6])
zp_b_b<-median(col_val$zpb[7:9])

############################dividing path ba the values above and below and log

nzm_f_ab_r<-log(nzm_p_r/nzm_a_r)
nzm_f_ab_g<-log(nzm_p_g/nzm_a_g)
nzm_f_ab_b<-log(nzm_p_b/nzm_a_b)
nzm_f_bl_r<-log(nzm_p_r/nzm_b_r)
nzm_f_bl_g<-log(nzm_p_g/nzm_b_g)
nzm_f_bl_b<-log(nzm_p_b/nzm_b_b)
nzm_r<-c(nzm_f_ab_r,nzm_f_bl_r)
nzm_g<-c(nzm_f_ab_g,nzm_f_bl_g)
nzm_b<-c(nzm_f_ab_b,nzm_f_bl_b)

eb_f_ab_r<-log(eb_p_r/eb_a_r)
eb_f_ab_g<-log(eb_p_g/eb_a_g)
eb_f_ab_b<-log(eb_p_b/eb_a_b)
eb_f_bl_r<-log(eb_p_r/eb_b_r)
eb_f_bl_g<-log(eb_p_g/eb_b_g)
eb_f_bl_b<-log(eb_p_b/eb_b_b)
eb_r<-c(eb_f_ab_r,eb_f_bl_r)
eb_g<-c(eb_f_ab_g,eb_f_bl_g)
eb_b<-c(eb_f_ab_b,eb_f_bl_b)

zs_f_ab_r<-log(zs_p_r/zs_a_r)
zs_f_ab_g<-log(zs_p_g/zs_a_g)
zs_f_ab_b<-log(zs_p_b/zs_a_b)
zs_f_bl_r<-log(zs_p_r/zs_b_r)
zs_f_bl_g<-log(zs_p_g/zs_b_g)
zs_f_bl_b<-log(zs_p_b/zs_b_b)

zs_r<-c(zs_f_ab_r,zs_f_bl_r)
zs_g<-c(zs_f_ab_g,zs_f_bl_g)
zs_b<-c(zs_f_ab_b,zs_f_bl_b)

zp_f_ab_r<-log(zp_p_r/zp_a_r)


zp_f_ab_g<-log(zp_p_g/zp_a_g)
zp_f_ab_b<-log(zp_p_b/zp_a_b)
zp_f_bl_r<-log(zp_p_r/zp_b_r)
zp_f_bl_g<-log(zp_p_g/zp_b_g)
zp_f_bl_b<-log(zp_p_b/zp_b_b)
```

```
##############listing the above and below ratios together
zp_r<-c(zp_f_ab_r,zp_f_bl_r)
zp_g<-c(zp_f_ab_g,zp_f_bl_g)
zp_b<-c(zp_f_ab_b,zp_f_bl_b)
set.seed(9991)

#################combining the bands ratios of the three paths
R<-c(eb_r,zs_r,zp_r)
G<-c(eb_g,zs_g,zp_g)
B<-c(eb_b,zs_b,zp_b)

O.R<-
  Albedo<-albedo_ratio
dfAf<-data.frame(R,G,B,Albedo)

####################ploting the ratios

boxplot(dfAf,ylab="Log [footpath surfaces / control surfaces] UAV")

boxplot(nzm_r, nzm_g, nzm_b,eb_r,eb_g,eb_b,zs_r,zs_g,zs_b,zp_r,zp_g,zp_b)

abline(h=c(0), col="black",lwd=1)


nzm_p_r_c<-c(col_val$ebmp[1:3])
nzm_p_g_c<-c(col_val$ebmp[4:6])
nzm_p_b_c<-c(col_val$ebmp[7:9])
nzm_a_r_c<-c(col_val$ebma[1:3])
nzm_a_g_c<-c(col_val$ebma[4:6])
nzm_a_b_c<-c(col_val$ebma[7:9])
nzm_b_r_c<-c(col_val$ebmb[1:3])
nzm_b_g_c<-c(col_val$ebmb[4:6])
nzm_b_b_c<-c(col_val$ebb[7:9])
eb_p_r_c<-c(col_val$ebp[1:3])
eb_p_g_c<-c(col_val$ebp[4:6])
eb_p_b_c<-c(col_val$ebp[7:9])
eb_a_r_c<-c(col_val$eba[1:3])
eb_a_g_c<-c(col_val$eba[4:6])
eb_a_b_c<-c(col_val$eba[7:9])
eb_b_r_c<-c(col_val$ebb[1:3])
eb_b_g_c<-c(col_val$ebb[4:6])
eb_b_b_c<-c(col_val$ebb[7:9])
zs_p_r_c<-c(col_val$zsp[1:3])
zs_p_g_c<-c(col_val$zsp[4:6])
zs_p_b_c<-c(col_val$zsp[7:9])
zs_a_r_c<-c(col_val$zsa[1:3])
zs_a_g_c<-c(col_val$zsa[4:6])
zs_a_b_c<-c(col_val$zsa[7:9])
zs_b_r_c<-c(col_val$zsb[1:3])
zs_b_g_c<-c(col_val$zsb[4:6])
zs_b_b_c<-c(col_val$zsb[7:9])
zp_p_r_c<-c(col_val$zpp[1:3])
zp_p_g_c<-c(col_val$zpp[4:6])
zp_p_b_c<-c(col_val$zpp[7:9])
zp_a_r_c<-c(col_val$zpa[1:3])
zp_a_g_c<-c(col_val$zpa[4:6])
zp_a_b_c<-c(col_val$zpa[7:9])
zp_b_r_c<-c(col_val$zpb[1:3])
zp_b_g_c<-c(col_val$zpb[4:6])
zp_b_b_c<-c(col_val$zpb[7:9])

#########colecting
nzm_control_r<-c(nzm_a_r_c,nzm_b_r_c)
nzm_control_g<-c(nzm_a_g_c,nzm_b_g_c)
nzm_control_b<-c(nzm_a_b_c,nzm_b_b_c)
eb_control_r<-c(eb_a_r_c,eb_b_r_c)
eb_control_g<-c(eb_a_g_c,eb_b_g_c)
eb_control_b<-c(eb_a_b_c,eb_b_b_c)
zs_control_r<-c(zs_a_r_c,zs_b_r_c)
zs_control_g<-c(zs_a_g_c,zs_b_g_c)
```

```
zs_control_b<-c(zs_a_b_c,zs_b_b_c)
zp_control_r<-c(zp_a_r_c,zp_b_r_c)
zp_control_g<-c(zp_a_g_c,zp_b_g_c)
zp_control_b<-c(zp_a_b_c,zp_b_b_c)

nzm_tr<-t.test(nzm_p_r_c,nzm_control_r)
nzm_tg<-t.test(nzm_p_g_c,nzm_control_g)
nzm_tb<-t.test(nzm_p_b_c,nzm_control_b)
eb_tr<-t.test(eb_p_r_c,eb_control_r)
eb_tg<-t.test(eb_p_g_c,eb_control_g)
eb_tb<-t.test(eb_p_b_c,eb_control_b)
zs_tr<-t.test(zs_p_r_c,zs_control_r)
zs_tg<-t.test(zs_p_g_c,zs_control_g)
zs_tb<-t.test(zs_p_b_c,zs_control_b)
zp_tr<-t.test(zp_p_r_c,zp_control_r)
zp_tg<-t.test(zp_p_g_c,zp_control_g)
zp_tb<-t.test(zp_p_b_c,zp_control_b)



####################albedo###############
albedo_zs_f <- ((0.5621*ZS_band_1_alongpath_0_1_ul_sum) + (0.1479*ZS_band_2_alongpath_0_1_ul_sum) +
          (0.2512*ZS_band_3_alongpath_0_1_ul_sum) - 0.0015)

albedo_zs_c <- (0.5621*ZS_band_1_alongpath_.1_1_ul_sum) + (0.1479*ZS_band_2_alongpath_.1_1_ul_sum) +
 (0.2512*ZS_band_3_alongpath_.1_1_ul_sum) - 0.0015
albedo_zs_c. <- (0.5621*ZS_band_1_alongpath_..1_1_ul_sum) + (0.1479*ZS_band_2_alongpath_..1_1_ul_sum) +
 (0.2512*ZS_band_3_alongpath_..1_1_ul_sum) - 0.0015

albedo_zp_f <- (0.5621*ZP_band_1_alongpath_0_1_ul_sum) + (0.1479*ZP_band_2_alongpath_0_1_ul_sum) +
 (0.2512*ZP_band_3_alongpath_0_1_ul_sum) - 0.0015
albedo_zp_c <- (0.5621*ZP_band_1_alongpath_.1_1_ul_sum) + (0.1479*ZP_band_2_alongpath_.1_1_ul_sum) +
 (0.2512*ZP_band_3_alongpath_.1_1_ul_sum) - 0.0015
albedo_zp_c. <- (0.5621*ZP_band_1_alongpath_..1_1_ul_sum) + (0.1479*ZP_band_2_alongpath_..1_1_ul_sum) +
 (0.2512*ZP_band_3_alongpath_..1_1_ul_sum) - 0.0015

albedo_nz_f <- (0.5621*NZ_band_1_alongpath_0_1_ul_sum) + (0.1479*NZ_band_2_alongpath_0_1_ul_sum) +
 (0.2512*NZ_band_3_alongpath_0_1_ul_sum) - 0.0015
albedo_nz_c <- (0.5621*NZ_band_1_alongpath_.1_1_ul_sum) + (0.1479*NZ_band_2_alongpath_.1_1_ul_sum) +
 (0.2512*NZ_band_3_alongpath_.1_1_ul_sum) - 0.0015
albedo_nz_c. <- (0.5621*NZ_band_1_alongpath_..1_1_ul_sum) + (0.1479*NZ_band_2_alongpath_..1_1_ul_sum) +
 (0.2512*NZ_band_3_alongpath_..1_1_ul_sum) - 0.0015

albedo_nzm_f <- (0.5621*NZM_band_1_alongpath_0_1_ul_sum) + (0.1479*NZM_band_2_alongpath_0_1_ul_sum) +
 (0.2512*NZM_band_3_alongpath_0_1_ul_sum) - 0.0015
albedo_nzm_c <- (0.5621*NZM_band_1_alongpath_.1_1_ul_sum) + (0.1479*NZM_band_2_alongpath_.1_1_ul_sum) +
 (0.2512*NZM_band_3_alongpath_.1_1_ul_sum) - 0.0015
albedo_nzm_c. <- (0.5621*NZM_band_1_alongpath_..1_1_ul_sum) + (0.1479*NZM_band_2_alongpath_..1_1_ul_sum) +
 (0.2512*NZM_band_3_alongpath_..1_1_ul_sum) - 0.0015

albedo_zs_f_all <- ((0.5621*(ZS_band_1_alongpath_0_1_ul/255)) + (0.1479*(ZS_band_2_alongpath_0_1_ul/255)) +
            (0.2512*(ZS_band_3_alongpath_0_1_ul/255)) - 0.0015)/(0.5621+0.1479+0.2512)

plot(albedo_zs_f_all)

albedo_zs_c_all <- (0.5621*ZS_band_1_alongpath_.1_1_ul) + (0.1479*ZS_band_2_alongpath_.1_1_ul) +
 (0.2512*ZS_band_3_alongpath_.1_1_ul) - 0.0015
albedo_zs_c_all. <- (0.5621*ZS_band_1_alongpath_..1_1_ul) + (0.1479*ZS_band_2_alongpath_..1_1_ul) +
 (0.2512*ZS_band_3_alongpath_..1_1_ul) - 0.0015

albedo_zp_f_all <- (0.5621*ZP_band_1_alongpath_0_1_ul) + (0.1479*ZP_band_2_alongpath_0_1_ul) +
 (0.2512*ZP_band_3_alongpath_0_1_ul) - 0.0015
albedo_zp_c_all <- (0.5621*ZP_band_1_alongpath_.1_1_ul) + (0.1479*ZP_band_2_alongpath_.1_1_ul) +
 (0.2512*ZP_band_3_alongpath_.1_1_ul) - 0.0015
albedo_zp_c_all. <- (0.5621*ZP_band_1_alongpath_..1_1_ul) + (0.1479*ZP_band_2_alongpath_..1_1_ul) +
 (0.2512*ZP_band_3_alongpath_..1_1_ul) - 0.0015


albedo_nz_f_all <- (0.5621*NZ_band_1_alongpath_0_1_ul) + (0.1479*NZ_band_2_alongpath_0_1_ul) +
 (0.2512*NZ_band_3_alongpath_0_1_ul) - 0.0015
```

```
albedo_nz_c_all <- (0.5621*NZ_band_1_alongpath_.1_1_ul) + (0.1479*NZ_band_2_alongpath_.1_1_ul) +
  (0.2512*NZ_band_3_alongpath_.1_1_ul) - 0.0015
albedo_nz_c_all. <- (0.5621*NZ_band_1_alongpath_..1_1_ul) + (0.1479*NZ_band_2_alongpath_..1_1_ul) +
  (0.2512*NZ_band_3_alongpath_..1_1_ul) - 0.0015


albedo_nzm_f_all <- (0.5621*NZM_band_1_alongpath_0_1_ul) + (0.1479*NZM_band_2_alongpath_0_1_ul) +
  (0.2512*NZM_band_3_alongpath_0_1_ul) - 0.0015
albedo_nzm_c_all <- (0.5621*NZM_band_1_alongpath_.1_1_ul) + (0.1479*NZM_band_2_alongpath_.1_1_ul) +
  (0.2512*NZM_band_3_alongpath_.1_1_ul) - 0.0015
albedo_nzm_c_all. <- (0.5621*NZM_band_1_alongpath_..1_1_ul) + (0.1479*NZM_band_2_alongpath_..1_1_ul) +
  (0.2512*NZM_band_3_alongpath_..1_1_ul) - 0.0015



plot(x,y, color=factor(group))


group <- ifelse(albedo_nz_f_all, "Group 1",
          ifelse(albedo_nz_c_all, "Group 2",
              ifelse(albedo_nz_c_all., "Group 3")))


adpoint(albedo_nz_c_all/255, add=TRUE)

boxplot(c(albedo_nz_f,albedo_zp_f,albedo_zs_f),c(albedo_nz_c,albedo_zp_c,albedo_zs_c))

albedo_ratio_no_log<-c((albedo_nz_f/albedo_nz_c),(albedo_nz_f/albedo_nz_c.),
                (albedo_zp_f/albedo_zp_c) ,(albedo_zp_f/albedo_zp_c.),
                (albedo_zs_f/albedo_zs_c), (albedo_zs_f/albedo_zs_c.))


mean((100*albedo_ratio_no_log)-100)

albedo_ratio<-log(c((albedo_nz_f/albedo_nz_c),(albedo_nz_f/albedo_nz_c.),
              (albedo_zp_f/albedo_zp_c) ,(albedo_zp_f/albedo_zp_c.),
              (albedo_zs_f/albedo_zs_c), (albedo_zs_f/albedo_zs_c.),
              (albedo_nzm_f/albedo_nz_c),(albedo_nz_f/albedo_nzm_c.)))

boxplot(albedo_ratio,ylab="Log [footpath surfaces / control surfaces]", xlab="Albedo")

abline(h=c(0), col="black",lwd=1)

t.test(albedo_nz_f_all,c(albedo_nz_c_all,albedo_nz_c_all.))
t.test(albedo_nzm_f_all,c(albedo_nzm_c_all,albedo_nzm_c_all.))
t.test(albedo_zs_f_all*255,albedo_zs_c_all)
t.test(albedo_zp_f_all,albedo_zp_c_all)


plot(albedo_zp_c_all/255,lty=3,lwd=2,col="forestgreen", type='l')

albedo_zs_c_all
lines(albedo_nz_c_all/255,lty=3,lwd=2,col="forestgreen")
lines(albedo_nz_c_all./255,lty=3,lwd=2,col="forestgreen")
lines(albedo_nz_f_all/255,lty=3,lwd=2,col="blue")

lines(albedo_zs_c_all/255,lty=3,lwd=2,col="forestgreen")
lines(albedo_zs_c_all./255,lty=3,lwd=2,col="green")
lines(albedo_zs_f_all/255,lty=3,lwd=2,col="blue")

lines(albedo_zp_c_all/255,lty=3,lwd=2,col="forestgreen")
lines(albedo_zp_c_all./255,lty=3,lwd=2,col="green")
lines(albedo_zp_f_all/255,lty=3,lwd=2,col="blue")

mean(albedo_zs_f_all/255)
sd(albedo_zs_f_all/255)


######################################### plot
```

```
####################################dem

#dem extract

Demnz_alongpath_0_1<-raster::extract(Demnz,NZ_alongpath_0_1, along = TRUE,cellnumbers = FALSE)
Demnz_alongpath_0_2<-raster::extract(Demnz,NZ_alongpath_0_2, along = TRUE,cellnumbers = FALSE)
Demnz_alongpath_0_3<-raster::extract(Demnz,NZ_alongpath_0_3, along = TRUE,cellnumbers = FALSE)
Demnz_alongpath_.1_1<-raster::extract(Demnz,NZ_alongpath_.1_1, along = TRUE,cellnumbers = FALSE)
Demnz_alongpath_.1_2<-raster::extract(Demnz,NZ_alongpath_.1_2, along = TRUE,cellnumbers = FALSE)
Demnz_alongpath_.1_3<-raster::extract(Demnz,NZ_alongpath_.1_3, along = TRUE,cellnumbers = FALSE)
Demnz_alongpath_..1_1<-raster::extract(Demnz,NZ_alongpath_..1_1, along = TRUE,cellnumbers = FALSE)
Demnz_alongpath_..1_2<-raster::extract(Demnz,NZ_alongpath_..1_2, along = TRUE,cellnumbers = FALSE)
Demnz_alongpath_..1_3<-raster::extract(Demnz,NZ_alongpath_..1_3, along = TRUE,cellnumbers = FALSE)


Demnz_alongpath_0_1_ul<-unlist(Demnz_alongpath_0_1)
Demnz_alongpath_0_1_ul_sum<-sum(Demnz_alongpath_0_1_ul)
Demnz_alongpath_0_1_ul_mean<-mean(Demnz_alongpath_0_1_ul)
Demnz_alongpath_0_1_ul_sd<-sd(Demnz_alongpath_0_1_ul)
Demnz_alongpath_0_2_ul<-unlist(Demnz_alongpath_0_2)
Demnz_alongpath_0_2_ul_sum<-sum(Demnz_alongpath_0_2_ul)
Demnz_alongpath_0_2_ul_mean<-mean(Demnz_alongpath_0_2_ul)
Demnz_alongpath_0_2_ul_sd<-sd(Demnz_alongpath_0_2_ul)
Demnz_alongpath_0_3_ul<-unlist(Demnz_alongpath_0_3)
Demnz_alongpath_0_3_ul_sum<-sum(Demnz_alongpath_0_3_ul)
Demnz_alongpath_0_3_ul_mean<-mean(Demnz_alongpath_0_3_ul)
Demnz_alongpath_0_3_ul_sd<-sd(Demnz_alongpath_0_3_ul)
Demnz_alongpath_.1_1_ul<-unlist(Demnz_alongpath_.1_1)
Demnz_alongpath_.1_1_ul_sum<-sum(Demnz_alongpath_.1_1_ul)
Demnz_alongpath_.1_1_ul_mean<-mean(Demnz_alongpath_.1_1_ul)
Demnz_alongpath_.1_1_ul_sd<-sd(Demnz_alongpath_.1_1_ul)
Demnz_alongpath_.1_2_ul<-unlist(Demnz_alongpath_.1_2)
Demnz_alongpath_.1_2_ul_sum<-sum(Demnz_alongpath_.1_2_ul)
Demnz_alongpath_.1_2_ul_mean<-mean(Demnz_alongpath_.1_2_ul)
Demnz_alongpath_.1_2_ul_sd<-sd(Demnz_alongpath_.1_2_ul)
Demnz_alongpath_.1_3_ul<-unlist(Demnz_alongpath_.1_3)
Demnz_alongpath_.1_3_ul_sum<-sum(Demnz_alongpath_.1_3_ul)
Demnz_alongpath_.1_3_ul_mean<-mean(Demnz_alongpath_.1_3_ul)
Demnz_alongpath_.1_3_ul_sd<-sd(Demnz_alongpath_.1_3_ul)
Demnz_alongpath_..1_1_ul<-unlist(Demnz_alongpath_..1_1)
Demnz_alongpath_..1_1_ul_sum<-sum(Demnz_alongpath_..1_1_ul)
Demnz_alongpath_..1_1_ul_mean<-mean(Demnz_alongpath_..1_1_ul)
Demnz_alongpath_..1_1_ul_sd<-sd(Demnz_alongpath_..1_1_ul)
Demnz_alongpath_..1_2_ul<-unlist(Demnz_alongpath_..1_2)
Demnz_alongpath_..1_2_ul_sum<-sum(Demnz_alongpath_..1_2_ul)
Demnz_alongpath_..1_2_ul_mean<-mean(Demnz_alongpath_..1_2_ul)
Demnz_alongpath_..1_2_ul_sd<-sd(Demnz_alongpath_..1_2_ul)
Demnz_alongpath_..1_3_ul<-unlist(Demnz_alongpath_..1_3)
Demnz_alongpath_..1_3_ul_sum<-sum(Demnz_alongpath_..1_3_ul)
Demnz_alongpath_..1_3_ul_mean<-mean(Demnz_alongpath_..1_3_ul)
Demnz_alongpath_..1_3_ul_sd<-sd(Demnz_alongpath_..1_3_ul)

Voids analysis
########################
 setwd("E:/phd/desert footpaths/micromorphology/desert computed")
setwd("/Users/nn/Downloads/desert footpaths/micromorphology")

library(imager)
path<-"/Users/nn/Downloads/desert footpaths/micromorphology/desert computed"
photos <- list.files(
  path = path,
  recursive = TRUE,
  full.names = TRUE)

#spliting the lists
ppl_choice<-seq(1,length(photos),2)
xpl_choice<-seq(2,length(photos),2)

ppla<-list(photos[ppl_choice])
xpla<-list(photos[xpl_choice])
ppl<-unlist(ppla)
```

```
xpl<-unlist(xpla)

voids_ratio<-c()

## the loop:
for (i in 1:180) {
  ppl_i<-jpeg::readJPEG(ppl[i])
  cimg_ppl<-as.cimg(ppl_i)
  grey_ppl<-grayscale(cimg_ppl)

  xpl_i<-jpeg::readJPEG(xpl[i])
  cimg_xpl<-as.cimg(xpl_i)
  grey_xpl<-grayscale(cimg_xpl)
   #correct quartz using the xpl
  corrected<-grey_ppl-grey_xpl

  #bw for corrected image
  bw<-threshold(corrected, thr = "auto", approx = TRUE, adjust = 1.2)

  #binary: voids are white=1
  binary<-as.numeric(bw)

  #void ratio for binary: 1 pixels / total pixels
  voids_ratio [i]<-sum(binary)/length(binary)
}
write.csv(voids_ratio,"voids_ratio_2.5.csv")
print(voids_ratio)
unlist(voids_ratio)
list(voids_ratio)
write.csv2(voids_ratio, "voidsratio.csv")
# voids_ratio: white is 1 => more voids is higher ration (closer to 1)
Correlation
library(corrplot)
library(correlation)
library(Hmisc)
### Input Files
all.samples.nlog<-read.csv2("all.samples.1..csv")
all.surfaces.nlog<-read.csv2("all.surfaces.rgb.1.csv")
all.samples<-log(all.samples.nlog)
all.surfaces<-log(all.surfaces.nlog)
p.all.samples <- Hmisc::rcorr(as.matrix(all.samples)) # rcorr() accepts matrices only
p.all.surfaces <- Hmisc::rcorr(as.matrix(all.surfaces)) # rcorr() accepts matrices only
### plotting
test.p.allsamples = corrplot::cor.mtest(p.all.samples$r, conf.level = 0.99)
corrplot::corrplot((cor(all.samples)), p.mat = test.p.allsamples$p,
      method = 'color', col.lim = c(-1, 1),diag = FALSE, type = 'upper',
      sig.level = 0.05, pch.cex = 0.9, is.corr=TRUE,
      insig = 'pch', pch.col = 'grey20', order = 'original',
      title = 'All samples n = 50')
test.p.allsurfaces = corrplot::cor.mtest(p.all.surfaces$r, conf.level = 0.99)
corrplot::corrplot(p.all.surfaces$r, p.mat = test.p.allsurfaces$p, method = 'color', diag = FALSE, type = 'upper',
      sig.level = 0.01, pch.cex = 0.9,tl.cex = 1,
      insig = 'pch', pch.col = 'grey20', order = 'original',
      title = 'All surface samples n = 20')
```

Chapter 6 Supplementary

R script 1.

Frequency Ratio (FR) calculation

R script for all reclassified variables (elevation, slope aspect, slope angle, TWI, P.curvature, NDVI, DFS, DFR,DRP ,DFPSM , SFPCI) and non-reclassified (LULC, lithology, soil).

 ## For LULC the natural break alone was used while for lithology and soil types, classifications were based on the spatial units in the according maps

The script uses elevation as an example. Based on data in table 1, this could be applied to all other variables
library(raster)

```
## Loading the 5 m x 5 m DEMs
Elevation_ sample_unit_1<-raster("elevation_ sample_unit_1.tif")
Elevation_ sample_unit_2<-raster("elevation_ sample_unit_2.tif")
Elevation_ sample_unit_3<-raster("elevation_ sample_unit_3.tif")
Elevation_ sample_unit_4<-raster("elevation_ sample_unit_4.tif")

## Loading the gullies and matching them with the DEMs' rows and columns for later calculations
Gullies_ sample_unit_1<-resample(raster("gullies_ sample_unit_1.tif"),raster("elevation_ sample_unit_1.tif"),method="ngb")
Gullies_ sample_unit_2<-resample(raster("gullies_ sample_unit_2.tif"),raster("elevation_ sample_unit_2.tif"),method="ngb")
Gullies_ sample_unit_3<-resample(raster("gullies_ sample_unit_3.tif"),raster("elevation_ sample_unit_2.tif"),method="ngb")
Gullies_ sample_unit_4<-resample(raster("gullies_ sample_unit_4.tif"),raster("elevation_ sample_unit_2.tif"),method="ngb")

## Evaluating the natural distribution of the elevation in the sample units
hist(Elevation_ sample_unit_1)
hist(Elevation_ sample_unit_2)
hist(Elevation_ sample_unit_3)
hist(Elevation_ sample_unit_4)

## Reclassify in same size categories according to the common natural distribution of the sample units for generating similar data sets
(elevation, slope aspect, slope angle, TWI, P.curvature, NDVI).
class <- c(1800, 1900, 1,
        1900, 2000, 2,
        2000, 2100, 3,
        2100, 2200, 4,
        2200, 2300, 5,
        2300, 2900, 6)

 ## For variable elevation only: Sample unit 1 which is different in elevation has a different classification. All other reclassified variables in
all sample units were sub-categorized together.

class <- c(1100, 1200, 1,
        1200, 1300, 2,
        1300, 1400, 3,
        1400, 1500, 4,
        1500, 1600, 5,
        1600, 2300, 6)

## Reclassification for all distance-based variables (rivers, roads, pathways, soviet mapped pathways, CORONA image based mapped
pathways). The following example is in the case of streams and roads (distance in meters)
 class <- c( 0, 50, 1,
         50, 100, 2,
         100, 150, 3,
         150, 200, 4,
         200, 250, 5,
         250, 50000, 6)

 ## For all reclassified variables: Reshape the object into a matrix with columns and rows
 rcl.sl <- matrix(class,
            ncol=3,
            byrow=TRUE)

## For all reclassified variables: Reclassify the variable using the reclass object - rcl.m
Elevation_reclas_sample_unit_1 <- reclassify(Elevation_ sample_unit_1,  rcl.sl)
Elevation_reclas_sample_unit_1[Elevation_reclas_sample_unit_1[]==-1] <- NA
Elevation_reclas_sample_unit_2 <- reclassify(Elevation_ sample_unit_2,  rcl.sl)
Elevation_reclas_sample_unit_2[Elevation_reclas_sample_unit_2[]==-1] <- NA
Elevation_reclas_sample_unit_3 <- reclassify(Elevation_ sample_unit_3,  rcl.sl)
Elevation_reclas_sample_unit_3[Elevation_reclas_sample_unit_3[]==-1] <- NA
Elevation_reclas_sample_unit_4 <- reclassify(Elevation_ sample_unit_4,  rcl.sl)
Elevation_reclas_sample_unit_4[Elevation_reclas_sample_unit_4[]==-1] <- NA

## For all variables: Calculation of overlap - gullies pixels for each variable
Elevation_Gullies_sample_unit_<-Elevation_reclas_sample_unit_1* Gullies_ sample_unit_1
Elevation_Gullies_sample_unit_2<-Elevation_reclas_sample_unit_2* Gullies_ sample_unit_2
Elevation_Gullies_sample_unit_3<-Elevation_reclas_sample_unit_3* Gullies_ sample_unit_2
Elevation_Gullies_sample_unit_4<-Elevation_reclas_sample_unit_4* Gullies_ sample_unit_2

### Exporting spatial data for documentation
writeRaster(Elevation_Gullies_ sample_unit,"Elevation_Gullies_ sample_unit.tif",overwrite=TRUE)
```

```
## FR calculation

## Gully and variable pixel overlap = g
tmp1 <- hist(Elevation_Gullies_sample_unit, density = NULL, axes = TRUE, plot = TRUE)

## variable pixel = C
tmp2 <- hist(Elevation_reclas_sample_unit_2,
                density = NULL, col = "red",
                main = paste(" elevation in the  sample_unit_2"),
                xlab = "Elevations", ylab="Gullies (in Pixel frequency)",
                axes = TRUE, plot = TRUE)

## Output total gully pixels  = G
tmp3 <- hist(Gullies_sample_unit_2,
     density = NULL, col = "red",
     main = paste("Gullies by elevation in the  sample_unit_2"), xlab = "Elevations", ylab="Gullies (in Pixel frequency)",
     axes = TRUE, plot = TRUE)
## Output sample unit pixel  = S
tmp4  <-hist(Elevation_sample_unit_2,plot=FALSE)

## Producing data frames
g.df<-data.frame(counts=tmp1$counts)
C.df<-data.frame(counts=tmp2$counts)
G.df<-data.frame(counts=tmp3$counts)
S.df<-data.frame(counts=tmp4$counts)

## Retrieving the relevant numbers from each data frame
names(g.df)[names(g.df) == "counts"] <- "gullies"
names(C.df)[names(C.df) == "counts"] <- "category"

G<-sum(G.df)
S<-sum(S.df)

g.df[g.df[]==0] <-NA
C.df[C.df[]==0] <-NA

g<-na.omit(g.df)
C<-na.omit(C.df)

## Binding the four elements into one object
FR_data<-cbind(g,C,G,S)

## Calculating the Frequency Ratios of the classes for a given variable
FR_data_Elevation_sample_unit<-(FR_data$gullies/FR_data$category)/(FR_data$G/FR_data$S)
## Export the data
write.csv(FR_data_Elevation_sample_unit," FR_data_Elevation_sample_unit.csv")


R script 2.

## Least Cost Path Analysis

library(raster)
library(gdistance)
library(rgdal)

## general
altDiff <- function(x){x[2] - x[1]}


## wheel critical slope cost function; the slope is requested as rise/run by the cost function;
## sl.crit (=critical slope, in percent) is "the transition where switchbacks become more effective than direct uphill or downhill paths" and
typically is in the range 8-16
sl.crit <- 12


## DEM
dem <- raster("./sample_unit_DEM_res.tif")
hd <- transition(dem, altDiff, 8, symm=FALSE)
slope <- geoCorrection(hd)
adj <- adjacent(dem, cells=1:ncell(dem), pairs=TRUE, directions = 8)
```

```
speed <- slope

## wheel critical slope
speed[adj] <- 1 / (1 + ((abs(slope[adj])*100) / sl.crit)^2)
Conductance <- geoCorrection(speed)

## Gullies as barriers
gullies_raw <- raster("./sample_unit_gullies_res.tif")
dem_gullies <- dem
dem_gullies[gullies_raw] <- 99999

hd2 <- transition(dem_gullies, altDiff, 8, symm=FALSE)
slope2 <- geoCorrection(hd2)
adj2 <- adjacent(dem_gullies, cells=1:ncell(dem_gullies), pairs=TRUE, directions = 8)
speed2 <- slope2

## wheel critical slope
speed2[adj2] <- 1 / (1 + ((abs(slope2[adj2])*100) / sl.crit)^2)
Conductance_gullies <- geoCorrection(speed2)

## Areas for random points
N_R<- extent(dem)
N_R[3] <- N_R[4] - 1000
S_R<- extent(dem)
S_R[4] <- S_R[3] + 1000
poly_sample_unit_N<-as(N_R, "SpatialPolygons")
poly_sample_unit_S<-as(S_R, "SpatialPolygons")

##Raster Values
sample_unit_ng_con<-raster(Conductance)
sample_unit_g_con<-raster(Conductance_gullies)


## results files
my_results <- c()
my_length_ng  <- c()
my_length_g <- c()
my_conduc_results_mean_ng  <- c()
my_conduc_results_mean_g  <- c()

my_conduc_results_median_ng  <- c()
my_conduc_results_median_g  <- c()


## the loop:
for (i in 1:1000) {
   origin <- spsample(poly_sample_unit_N[1,], 1, type = 'random')
  goal <- spsample(poly_sample_unit_S[1,], 1, type='random')
   sample_unit_ng_lcp <- shortestPath(Conductance, origin, goal,
                          output="SpatialLines")
   sample_unit_g_lcp <- shortestPath(Conductance_gullies, origin, goal,
                         output="SpatialLines")

## Extract the lines
 sample_unit_ng <- SpatialLinesDataFrame(sample_unit_ng_lcp, data.frame(id=1:length(sample_unit_ng_lcp)))
 sample_unit_g <- SpatialLinesDataFrame(sample_unit_g_lcp, data.frame(id=1:length(sample_unit_g_lcp)))
   dir.create("ng")
 dir.create("g")
 writeOGR(sample_unit_ng, dsn=paste0("ng/","lcp_ng_",i,".gpkg"), layer = "new_ng",
        driver = "GPKG")
 writeOGR(sample_unit_g, dsn=paste0("g/","lcp_g_",i,".gpkg"), layer = "new_g",
        driver = "GPKG")
   ngl<-SpatialLinesLengths(sample_unit_ng)
 gl<-SpatialLinesLengths(sample_unit_g)
   my_length_ng [i] <-ngl
 my_length_g [i] <-gl
   a<-((1-(ngl[1]/gl[1]))*100)
   my_results [i] <-a


 ## Extracting conductivity data
```

```
 sample_unit_extract_ng<-extract(sample_unit_ng_con,sample_unit_ng, along = TRUE,
                         cellnumbers = FALSE)
 sample_unit_extract_g<-extract(sample_unit_g_con,sample_unit_g, along = TRUE,
                        cellnumbers = FALSE)
   a1<-mean.default(unlist(sample_unit_extract_ng))
 a2<-mean.default(unlist(sample_unit_extract_g))
 my_conduc_results_mean_ng [i] <- a1
 my_conduc_results_mean_g [i] <- a2
b1<-median(unlist(sample_unit_extract_ng))
b2<-median(unlist(sample_unit_extract_g))
   my_conduc_results_median_ng [i] <- b1
 my_conduc_results_median_g [i] <- b2}

## Writing the output file
total<-data.frame(calculation=my_results, length_ng=my_length_ng, length_g=my_length_g,
cond_mean_ng=my_conduc_results_mean_ng,
             cond_mean_g=my_conduc_results_mean_g, cond_med_ng=my_conduc_results_median_ng,
cond_med_g=my_conduc_results_median_g)
write.csv(total,"sample_unit__LCP_total_data.csv")



##East to west LCPs calculations differs in:

## Areas for random points
E_R<- extent(dem)
E_R[1] <- E_R[2] - 1000
W_R<- extent(dem)
W_R[2] <- W_R[1] + 1000
poly_sample_unit_E<-as(E_R, "SpatialPolygons")
poly_sample_unit_W<-as(W_R, "SpatialPolygons")

## the loop:
for (i in 1:1000) {
   origin <- spsample(poly_sample_unit_E[1,], 1, type = 'random')
  goal <- spsample(poly_sample_unit_W[1,], 1, type='random')
   sample_unit_ng_lcp <- shortestPath(Conductance, origin, goal,
                             output="SpatialLines")
   sample_unit_g_lcp <- shortestPath(Conductance_gullies, origin, goal,
HW2<-readOGR("HW2.gpkg")
HW3<-readOGR("HW3.gpkg")

#watershed
HWareas<-readOGR("holloways.gpkg")
HW1area<-readOGR("HWa1.gpkg")
HW2area<-readOGR("HWa2.gpkg")
HW3area<-readOGR("HWa3.gpkg")

#footpaths and holloways rama
r.fps<-readOGR("r.fps.gpkg")
r.hws<-readOGR("r.hws.gpkg")
gullies<-readOGR("
```

	Rama sample unite (1) N-S					Yeha sample unite (2) N-S				
	UM L	M L	UM C	M C	L Ch %	UM L	M L	UM C	M C	L Ch %
1	12849.11	13141.36	0.092	0.094	2.2239	13159.65	13956.21	0.114	0.12	5.7076
2	12565.03	12667.16	0.092	0.094	0.8063	15876.61	15953.8	0.103	0.108	0.4839
3	12547.18	13332.49	0.094	0.1	5.8902	11777.86	13001.78	0.1	0.084	9.4135
4	12223.19	12938.29	0.095	0.102	5.527	13168.58	13219.5	0.079	0.078	0.3852
5	13671.36	13962.91	0.096	0.096	2.088	12013.81	12013.4	0.088	0.096	-0.0035
6	13285.3	13387.43	0.096	0.098	0.7629	14360.9	14325.04	0.083	0.084	-0.2503
7	13645	13969.98	0.096	0.097	2.3262	15906.58	15897.29	0.099	0.103	-0.0584
8	11801.06	12081.6	0.097	0.104	2.322	11316.28	11241.8	0.106	0.106	-0.6625
9	12150.97	13012.05	0.097	0.108	6.6175	15917.04	16398.93	0.119	0.114	2.9385
10	12695.92	13026.13	0.098	0.1	2.535	11329.53	11881.61	0.122	0.121	4.6465
11	12524.97	13501.1	0.098	0.109	7.2301	11221.32	11383.36	0.123	0.122	1.4235
12	13525.33	13400.48	0.099	0.099	-0.9317	13039.84	13149.46	0.117	0.122	0.8336
13	12095.71	11917.69	0.1	0.095	-1.4938	11984.19	11984.19	0.077	0.077	0
14	11967.07	11920.5	0.1	0.1	-0.3907	12880.13	13389.09	0.127	0.121	3.8013
15	13114.06	13015.77	0.1	0.101	-0.7551	12011.62	12119.11	0.073	0.084	0.8869
16	12439.77	12393.2	0.1	0.1	-0.3758	11400.57	12888.28	0.111	0.109	11.543
17	13305.75	13217.46	0.1	0.1	-0.6679	11509.43	12505.53	0.069	0.072	7.9653
18	12371.21	12213.73	0.1	0.102	-1.2894	10003.25	10193.76	0.128	0.128	1.8688
19	13033.75	13493.41	0.1	0.105	3.4065	11225.81	11208.74	0.093	0.09	-0.1523
20	11727.15	11787.06	0.1	0.101	0.5083	13076.78	13861.55	0.075	0.08	5.6615
21	12334.5	12287.93	0.1	0.1	-0.379	13023.75	13137.51	0.109	0.114	0.8659
22	13306.33	13978.29	0.1	0.099	4.8072	12344.34	12446.39	0.108	0.113	0.8199
23	12583.82	12537.26	0.1	0.101	-0.3714	10949.28	11437.15	0.131	0.127	4.2656
24	12320.62	12716.72	0.1	0.107	3.1148	11993.54	11979.11	0.084	0.084	-0.1205
25	13119.17	13340.38	0.1	0.103	1.6582	12070.54	12175.52	0.1	0.106	0.8622
26	13889.52	14040.18	0.1	0.098	1.0731	11539.22	11641.27	0.11	0.116	0.8766
27	12583.56	12546.69	0.1	0.102	-0.2938	15025.33	15131.52	0.107	0.112	0.7018
28	12821.95	12157.9	0.101	0.098	-5.4619	13289.14	13272.49	0.092	0.093	-0.1255
29	13939.45	13851.16	0.101	0.101	-0.6374	9589.615	9784.798	0.122	0.12	1.9948
30	12716.36	12770.09	0.101	0.095	0.4207	13784.85	14201.04	0.068	0.071	2.9307
31	12740.6	12757.97	0.101	0.101	0.1361	15244.6	15675.84	0.099	0.106	2.751
32	13830.39	13705.54	0.101	0.101	-0.911	15967.75	16474.29	0.112	0.11	3.0747
33	12727.93	12960.69	0.101	0.101	1.7959	14643.62	14623.62	0.083	0.081	-0.1368

34	13147.32	13549.03	0.101	0.101	2.9649	12109.22	12095.29	0.097	0.101	-0.1152
35	13346.4	13999.57	0.101	0.105	4.6657	12159.12	12142.13	0.08	0.088	-0.1399
36	12836.04	12981.48	0.101	0.101	1.1204	13001.6	13447.4	0.098	0.107	3.3152
37	13426.89	13930.06	0.101	0.1	3.6121	16005.21	16561.74	0.121	0.117	3.3604
38	12852.19	12826.3	0.101	0.097	-0.2019	12148.47	12361.44	0.109	0.109	1.7228
39	13693.94	14758.41	0.101	0.101	7.2126	15594.34	15783.42	0.112	0.114	1.198
40	12433.14	12412.43	0.101	0.102	-0.1669	10621.9	10493.83	0.108	0.115	-1.2205
41	12658.52	12972.49	0.102	0.109	2.4203	11183.21	11943.27	0.12	0.12	6.3638
42	12769.62	12871.72	0.102	0.098	0.7932	15519.87	15897.27	0.1	0.106	2.374
43	13418.14	13007.01	0.102	0.097	-3.1608	12688.21	12689.93	0.102	0.104	0.0135
44	12561.95	12926.42	0.102	0.109	2.8196	12094.28	12447.16	0.1	0.109	2.835
45	13796.13	13444	0.102	0.098	-2.6193	10017.62	10350.42	0.131	0.123	3.2154
46	12841.63	12955.86	0.102	0.101	0.8817	17518.28	17575.23	0.11	0.111	0.324
47	13323.97	13645.1	0.102	0.102	2.3534	16113.06	16082.56	0.101	0.105	-0.1897
48	11981	12111.92	0.102	0.105	1.0809	12245.68	13400.24	0.073	0.081	8.616

49	11402.34	12109.56	0.146	0.143	5.8402	13038.16	13189.46	0.124	0.123	1.1471
50	11975.09	11979.23	0.143	0.143	0.0346	16754.33	16864.42	0.127	0.127	0.6528
51	13739.38	13432.18	0.106	0.113	-2.287	14630.74	14891.12	0.131	0.13	1.7486
52	10829.21	11179.45	0.137	0.132	3.1329	12484.97	12894.41	0.12	0.123	3.1754
53	11316.38	11761.85	0.136	0.14	3.7875	10565.53	11541.74	0.135	0.138	8.4581
54	12605.7	12683.86	0.112	0.12	0.6162	10275.28	11509.92	0.133	0.134	10.727
55	11712.63	12239.37	0.108	0.121	4.3037	12205.11	12304.61	0.125	0.12	0.8086
56	14425.88	14839.52	0.131	0.136	2.7874	13322.31	13409.97	0.116	0.113	0.6537
57	12260.31	12922.56	0.148	0.148	5.1248	12584.81	12597.12	0.126	0.123	0.0977
58	10787.73	12123.28	0.136	0.133	11.016	13527.68	13429.69	0.123	0.121	-0.73
59	11700.52	11927.17	0.117	0.12	1.9003	13007.51	13142.25	0.12	0.12	1.0252
60	11626.59	12544.32	0.134	0.132	7.3159	11970.33	12423.47	0.126	0.126	3.6474
61	12444.08	14674.29	0.14	0.145	15.198	13423.97	13527.11	0.116	0.119	0.7624
62	13872.46	14049.53	0.134	0.13	1.2603	14555.29	15808.06	0.131	0.131	7.9249
63	10895.28	11334.72	0.13	0.125	3.877	11980.71	11962.93	0.123	0.121	-0.149
64	13054.08	16030.9	0.112	0.109	18.569	11358.07	11492.8	0.129	0.129	1.1723
65	14982.35	14971.68	0.127	0.135	-0.071	14272.62	15678.74	0.126	0.129	8.9683
66	12807.93	12765.8	0.142	0.142	-0.33	12584.73	12775.77	0.123	0.122	1.4953
67	11358.24	11712.17	0.138	0.135	3.0219	11382.62	11447.68	0.123	0.124	0.5683
68	13220.34	13224.48	0.138	0.139	0.0313	12953.91	13092.78	0.121	0.12	1.0607
69	10745.77	10903.67	0.147	0.147	1.4482	15211.93	15453.53	0.124	0.123	1.5634
70	10300.14	10581.1	0.147	0.145	2.6552	12092.15	12210.35	0.124	0.124	0.968
71	11517.23	11556.23	0.144	0.144	0.3374	11461.27	11777.87	0.131	0.127	2.6881
72	10792.94	11099.96	0.149	0.146	2.766	13478.66	13253.13	0.114	0.113	-1.702
73	12279.33	13808.69	0.128	0.124	11.075	13022.12	13293.63	0.134	0.135	2.0424
74	11671.34	12192	0.145	0.146	4.2705	12152.27	12270.47	0.123	0.123	0.9633
75	13513.1	13596.78	0.133	0.14	0.6154	11399.12	12006.14	0.128	0.131	5.0559
76	10828.61	11201.7	0.146	0.145	3.3306	10846.61	11016.52	0.138	0.139	1.5424
77	10937.64	11037.05	0.141	0.144	0.9007	11205.57	12908.23	0.139	0.137	13.19
78	11056.22	11382.74	0.126	0.127	2.8685	13782.21	12889.92	0.115	0.117	-6.922
79	12968.25	13170.68	0.136	0.134	1.5369	13326.32	13401.76	0.119	0.121	0.5629
80	11956.29	11956.29	0.139	0.139	0	11564	11537.93	0.121	0.119	-0.226
81	11245.73	11534.97	0.146	0.144	2.5075	11801.95	12015.21	0.129	0.127	1.7749
82	13309.85	13371.9	0.131	0.137	0.464	13450.22	13546.49	0.123	0.125	0.7107
83	11795.14	13704.67	0.143	0.148	13.933	10924.04	11166.29	0.122	0.126	2.1695
84	13872.82	13889.39	0.134	0.133	0.1193	13749.74	13824.6	0.12	0.116	0.5414
85	12008.75	13628.25	0.143	0.146	11.883	12936.09	12975.59	0.128	0.127	0.3044
86	11705.37	13989.79	0.124	0.142	16.329	12731.37	12890.96	0.118	0.119	1.238

87	12847.66	14048.2	0.121	0.114	8.5459	11816.14	11569.16	0.123	0.122	-2.135
88	12918.85	14529.01	0.122	0.111	11.082	12877.32	12794.89	0.123	0.121	-0.644
89	14560.31	14917.5	0.13	0.126	2.3945	13386.86	13582.64	0.138	0.137	1.4413
90	12204.77	13127.75	0.125	0.128	7.0308	11269.4	11408.28	0.128	0.127	1.2173
91	12357.1	13264.13	0.129	0.139	6.8383	11821.24	11931.24	0.135	0.133	0.9219
92	11447.55	11658.51	0.132	0.13	1.8094	13043.91	13208.43	0.122	0.119	1.2456
93	12178.29	12386.66	0.137	0.141	1.6822	12440.2	12770.24	0.131	0.129	2.5844
94	12051.88	14247.34	0.125	0.137	15.41	12030.05	12474.07	0.135	0.12	3.5595
95	14635.13	14756.85	0.134	0.137	0.8248	11957.74	12060.67	0.127	0.123	0.8534
96	14901.31	14625.99	0.132	0.14	-1.882	12875.65	13305.39	0.126	0.125	3.2298
97	11666.9	14726.04	0.131	0.144	20.774	12089.66	12077.23	0.12	0.12	-0.103
98	17259.56	17797.04	0.125	0.12	3.0201	11011.31	11123.65	0.133	0.133	1.0099
99	11173.68	11857.65	0.146	0.146	5.7682	12346.06	12390.58	0.12	0.12	0.3593
100	12429.84	12455.91	0.142	0.143	0.2093	13614.51	13769.24	0.125	0.119	1.1237
101	12962.21	15056.64	0.133	0.136	13.91	12985.62	13217.58	0.115	0.122	1.7549
102	13340.47	13231.77	0.137	0.136	-0.822	14777.25	15131.69	0.122	0.123	2.3423
103	13691.25	13213.21	0.136	0.139	-3.618	11575.58	12316.88	0.129	0.129	6.0186
104	11845.79	12422.23	0.112	0.121	4.6404	14987.72	15324.49	0.134	0.129	2.1976
105	12430.94	12639.01	0.112	0.123	1.6463	12576.4	12675.48	0.127	0.12	0.7817
106	12465.73	13036.6	0.136	0.137	4.379	10585.68	11868.37	0.135	0.134	10.808
107	11682.33	12359.23	0.135	0.134	5.4769	16249.54	16741.01	0.132	0.129	2.9357
108	11554.3	11868.6	0.146	0.145	2.6482	11082.94	11058.08	0.12	0.12	-0.225
109	13021.55	13389.97	0.127	0.138	2.7515	13252.76	13443.8	0.124	0.123	1.421
110	11740.26	13319.46	0.115	0.115	11.856	12058.02	12157.51	0.125	0.12	0.8184
111	11805.25	12481.89	0.123	0.118	5.421	11393	11624.33	0.138	0.141	1.9901
112	14724.97	15115.73	0.122	0.128	2.5851	12960.87	13115.6	0.125	0.119	1.1797
113	11947.72	11951.86	0.141	0.141	0.0347	11615.96	11668.6	0.119	0.119	0.4511
114	15176.61	15743.8	0.132	0.126	3.6026	12366.28	12781.96	0.128	0.121	3.2521
115	12166.4	13623.64	0.122	0.125	10.696	10951.39	12070.08	0.123	0.122	9.2683
116	12874.82	14404.94	0.127	0.134	10.622	13125.77	13329.74	0.129	0.128	1.5302
117	11949.47	12234.06	0.141	0.14	2.3262	11206.17	11244.66	0.132	0.131	0.3423
118	12372.65	12817.45	0.145	0.147	3.4703	11356.17	11766.53	0.123	0.127	3.4876
119	13320.33	13188.08	0.114	0.121	-1.003	12551.12	13165.11	0.127	0.127	4.6637
120	11621.02	11623.95	0.146	0.146	0.0252	12426.96	13234.92	0.125	0.125	6.1047

121	13131.14	13129.42	0.142	0.142	-0.013	11707.98	11810.91	0.121	0.117	0.8715
122	13425.1	14829.12	0.118	0.123	9.468	11905.17	12013.46	0.121	0.123	0.9014
123	12478.99	12613.42	0.111	0.117	1.0658	15129.35	16402.41	0.127	0.128	7.7615
124	13789.24	14216.81	0.136	0.133	3.0075	12155.81	12489.58	0.135	0.137	2.6723
125	11920.04	12623.25	0.131	0.122	5.5707	10638.71	10791.97	0.13	0.129	1.4201
126	11325.1	12078.9	0.123	0.123	6.2406	11660.81	12466.59	0.133	0.133	6.4635
127	12846.17	17625.08	0.138	0.132	27.114	12584.99	12864.61	0.132	0.136	2.1736
128	13596.67	15330.81	0.138	0.132	11.311	12996.07	13200.04	0.129	0.127	1.5452
129	15805.8	15996.69	0.123	0.129	1.1933	10741.55	11783.49	0.125	0.121	8.8424
130	11991.56	11964.28	0.143	0.142	-0.228	12421.53	12648.52	0.133	0.132	1.7946
131	14084.31	14480.43	0.119	0.125	2.7355	11099.77	11164.83	0.124	0.124	0.5827
132	11391.96	11836.26	0.148	0.149	3.7537	14012.06	14073.77	0.12	0.124	0.4385
133	11809.92	12676.11	0.145	0.146	6.8332	11943.83	11996.46	0.121	0.121	0.4388
134	15333.39	15694.4	0.129	0.127	2.3002	12531.41	12371.59	0.122	0.117	-1.292
135	12278.31	12290.74	0.145	0.145	0.1011	11223.12	11380.52	0.13	0.131	1.3831
136	12093.58	12250.99	0.146	0.146	1.2848	12142.13	12116.07	0.124	0.122	-0.215
137	11394.18	13072	0.144	0.149	12.835	11734.85	11708.79	0.126	0.124	-0.223
138	11879.15	16237.85	0.133	0.136	26.843	11666	11865.82	0.128	0.128	1.6841
139	14926.35	14425.77	0.107	0.111	-3.47	11452.91	11867.59	0.132	0.13	3.4942
140	11915.51	12344.66	0.142	0.14	3.4764	11035.73	11051.59	0.124	0.125	0.1435
141	12556.27	12810.03	0.133	0.135	1.981	13462.76	13562.26	0.121	0.117	0.7336
142	14116.02	13683.05	0.117	0.121	-3.164	15222.88	16329.29	0.137	0.143	6.7756
143	10843.85	11633.51	0.124	0.126	6.7878	13719.96	13621.97	0.123	0.122	-0.719
144	13330.65	15596.29	0.121	0.114	14.527	14156.1	14356.48	0.128	0.125	1.3958
145	11711.38	13684.76	0.143	0.148	14.42	10874.44	11492.8	0.131	0.13	5.3804
146	13546.04	16251.35	0.119	0.124	16.647	15547.64	15647.23	0.129	0.126	0.6364
147	13157.64	13343.29	0.116	0.127	1.3913	12880.77	13071.81	0.127	0.126	1.4615
148	11317.83	13765.95	0.143	0.147	17.784	13923.57	14039.01	0.122	0.121	0.8223
149	11428.47	11928.34	0.128	0.124	4.1906	10666.02	10553.98	0.122	0.116	-1.062
150	12267.67	12283.53	0.142	0.141	0.1291	15143.02	16084.37	0.125	0.128	5.8526
151	11900.19	12664.19	0.137	0.131	6.0328	11437.05	11502.11	0.122	0.123	0.5656
152	11515.78	11739.96	0.145	0.144	1.9095	12592.65	12963.79	0.124	0.122	2.8629
153	11674.27	12014.43	0.147	0.145	2.8312	15351.48	15273.28	0.116	0.119	-0.512
154	15384.08	15388.22	0.129	0.13	0.0269	11037.46	11676.52	0.139	0.138	5.4731

155	11643.91	13015.36	0.135	0.131	10.537	12015.91	12134.11	0.12	0.121	0.9741
156	12258.41	12752.5	0.148	0.148	3.8745	13073.49	13172.99	0.125	0.121	0.7553
157	11474.66	11333.83	0.115	0.124	-1.243	11634.37	11796.71	0.124	0.124	1.3761
158	11170.25	12711.62	0.138	0.132	12.126	15670.61	15755.55	0.125	0.124	0.5391
159	12670.22	12674.36	0.14	0.141	0.0327	12188.24	12253.3	0.121	0.121	0.531
160	12459.59	13129.88	0.115	0.124	5.1051	12305.76	12612.07	0.13	0.13	2.4287
161	14797.84	15136.34	0.132	0.13	2.2363	13708.72	15331.25	0.134	0.139	10.583
162	13372.97	15036.57	0.116	0.114	11.064	12191.51	12291.01	0.124	0.119	0.8095
163	11954.01	12422.66	0.122	0.12	3.7725	13081.09	13788.8	0.12	0.12	5.1325
164	15170.37	15702.5	0.129	0.124	3.3888	13971.96	14138.91	0.12	0.117	1.1808
165	15395.32	16254.61	0.129	0.128	5.2864	10607.49	10748.83	0.129	0.13	1.3149
166	11459.39	13183.61	0.143	0.141	13.078	12790.57	12981.61	0.126	0.126	1.4716
167	12198.76	12788.81	0.127	0.132	4.6138	12662.46	12761.55	0.126	0.12	0.7764
168	12765.36	12867.37	0.115	0.127	0.7928	13958.55	13970.27	0.126	0.125	0.0839
169	10918.11	11308.27	0.146	0.143	3.4502	12798.64	13197.97	0.13	0.128	3.0257
170	12157.98	12965.14	0.11	0.119	6.2256	14088.82	15070.25	0.138	0.138	6.5123
171	12480.59	12538.58	0.141	0.143	0.4625	14121.51	14272.8	0.124	0.122	1.0601
172	12041.94	12272.36	0.117	0.127	1.8775	14181.6	14269.47	0.128	0.127	0.6158
173	11129.54	14699.77	0.129	0.142	24.288	11513.99	11577.83	0.126	0.123	0.5515
174	12194.82	11998.01	0.123	0.129	-1.64	11748.63	12435.91	0.135	0.134	5.5266
175	11440.19	11499.89	0.14	0.14	0.5192	14088.36	14151.91	0.121	0.127	0.4491
176	13503.74	13600.98	0.119	0.121	0.715	11681.23	11725.79	0.13	0.13	0.38
177	11588.95	11676.61	0.115	0.121	0.7507	12016.66	12116.15	0.125	0.121	0.8212
178	12040.7	13133.42	0.126	0.135	8.3202	12503.95	12790.51	0.127	0.128	2.2405
179	11533.45	12097.68	0.116	0.129	4.6639	10971.39	12085.59	0.139	0.14	9.2192
180	12160.46	12310.08	0.14	0.14	1.2154	11846.06	12502.3	0.125	0.12	5.2489
181	11048.13	10728.47	0.126	0.132	-2.98	11360.47	11447.42	0.129	0.126	0.7596
182	12078.95	12625.76	0.149	0.148	4.3309	11590.96	11854.09	0.125	0.127	2.2198
183	11991.42	12510.59	0.135	0.134	4.1498	11653.8	11820.96	0.126	0.124	1.4141
184	12421.72	14361.21	0.141	0.144	13.505	11536.59	11875.62	0.133	0.131	2.8548
185	11186.37	11430.75	0.146	0.145	2.138	11490.46	11657.62	0.126	0.123	1.4339
186	11212.97	11701.59	0.128	0.131	4.1756	13848.65	14196.05	0.125	0.12	2.4472
187	12931.19	13057.34	0.137	0.14	0.9661	12308.89	12649.3	0.126	0.128	2.6912
188	13768.25	14827.08	0.128	0.129	7.1412	12394.67	12644	0.12	0.123	1.9719

189	12652.31	12740.55	0.123	0.128	0.6927	11724.68	12109	0.12	0.12	3.1738
190	12165.91	12223.78	0.14	0.139	0.4734	11481.4	11468.98	0.123	0.123	-0.108
191	10944.71	11313.95	0.13	0.126	3.2636	11406.23	11443.51	0.131	0.13	0.3258
192	11344.51	12068.73	0.124	0.125	6.0007	11305.92	11080.4	0.12	0.119	-2.035
193	13511.42	13784.82	0.104	0.119	1.9833	12113.7	12145.33	0.125	0.124	0.2604
194	11731.44	13867.71	0.145	0.149	15.405	10518.2	10582.55	0.13	0.129	0.6081
195	11147.58	12258.36	0.136	0.133	9.0614	12420.29	12867.22	0.122	0.126	3.4734
196	12849.83	13124.27	0.115	0.122	2.0911	15023.2	14879.89	0.128	0.128	-0.963
197	11675.63	12150.4	0.133	0.129	3.9074	10973.24	11123.15	0.125	0.124	1.3478
198	14584.24	15047.22	0.125	0.132	3.0768	10847.62	10871.26	0.125	0.127	0.2175
199	11561.24	11838.06	0.142	0.14	2.3383	11625.34	11690.4	0.123	0.123	0.5565
200	12879.14	14129.39	0.122	0.111	8.8485	14600.59	14522.51	0.114	0.121	-0.538
201	11715.16	13782.22	0.129	0.14	14.998	12126.19	12100.12	0.124	0.122	-0.215
202	13532.74	13936.26	0.13	0.131	2.8955	14058.72	16087.11	0.134	0.138	12.609
203	12748.61	13894.46	0.128	0.142	8.2469	10753.3	10856.23	0.123	0.119	0.9481
204	15678.77	15988.77	0.129	0.127	1.9389	12022.22	13120.03	0.133	0.134	8.3674
205	11151.38	13384.43	0.142	0.146	16.684	15152.1	16759.23	0.136	0.138	9.5895
206	11270.04	11290.75	0.141	0.144	0.1834	10286.37	10564.27	0.128	0.129	2.6306
207	12703.28	13562.27	0.113	0.122	6.3337	11531.59	11565.02	0.127	0.128	0.2891
208	11100.09	11485.1	0.149	0.148	3.3523	12460.34	12719.51	0.132	0.13	2.0376
209	13334.83	12676.37	0.136	0.14	-5.194	12351.33	12486.06	0.122	0.122	1.0791
210	16167.93	16693.73	0.124	0.134	3.1497	13282.75	13035.76	0.118	0.117	-1.895
211	10937.16	11065.36	0.135	0.131	1.1586	11735.79	11853.99	0.12	0.121	0.9971
212	12094.07	12293.36	0.136	0.133	1.6211	13032.29	13678.32	0.127	0.13	4.723
213	11355.31	11809.11	0.145	0.145	3.8428	12639.18	12413.66	0.118	0.117	-1.817
214	12259.93	12179.72	0.115	0.124	-0.659	10869.92	13085.71	0.131	0.137	16.933
215	11322.95	11507.88	0.114	0.122	1.6071	12842.97	12944.8	0.126	0.123	0.7867
216	12064.61	11731.94	0.118	0.124	-2.836	15033.78	16244.34	0.129	0.129	7.4522
217	15358.13	15763.99	0.129	0.133	2.5746	10965.42	11441.73	0.128	0.13	4.1629
218	12770.75	12772.46	0.142	0.142	0.0134	10521.6	11500.03	0.137	0.138	8.508
219	12798.56	14781.9	0.139	0.132	13.417	11488.01	12107.33	0.132	0.13	5.1153
220	13390.1	13373.53	0.14	0.14	-0.124	10750.47	11919.28	0.138	0.137	9.806
221	12856.69	14311.3	0.129	0.138	10.164	12991.23	12765.7	0.117	0.116	-1.767
222	12010.44	11895.76	0.119	0.125	-0.964	13241.62	13586.13	0.129	0.127	2.5357

223	11787	12555.65	0.138	0.132	6.1219	13255.77	13530.96	0.128	0.128	2.0337
224	11819.66	11874.18	0.117	0.124	0.4592	11815.02	12241.74	0.124	0.128	3.4858
225	13617.72	13965	0.135	0.133	2.4868	14907.6	16198.24	0.124	0.126	7.9678
226	11630.46	15149.09	0.124	0.143	23.227	11505.69	11647.03	0.123	0.124	1.2135
227	12138.94	12758.23	0.139	0.137	4.854	14448.25	14939.58	0.135	0.129	3.2888
228	11754.81	12228.36	0.137	0.132	3.8726	11991.4	12302.74	0.134	0.136	2.5306
229	11885.26	13764	0.125	0.12	13.65	10053.67	11299.59	0.138	0.135	11.026
230	12702.22	14299.41	0.108	0.111	11.17	12211.27	12329.46	0.122	0.123	0.9587
231	12548.58	12628.46	0.118	0.123	0.6325	11922.03	12070.22	0.127	0.132	1.2278
232	12026.97	12448.84	0.128	0.125	3.3889	13742.39	12763.86	0.126	0.129	-7.666
233	13022.31	15410.07	0.123	0.114	15.495	12706.28	12680.21	0.123	0.121	-0.206
234	11749.87	12345.1	0.14	0.142	4.8216	14780.88	16154.78	0.131	0.132	8.5046
235	14157.46	13486.79	0.137	0.141	-4.973	12350.21	12449.71	0.123	0.119	0.7992
236	11593.3	11910.11	0.127	0.128	2.66	12452.18	12668.21	0.12	0.113	1.7053
237	15427.22	15974.62	0.13	0.133	3.4267	12874.19	12992.39	0.116	0.117	0.9097
238	14446.46	14400.51	0.129	0.131	-0.319	12468.85	12660.9	0.127	0.129	1.5168
239	12039.76	13851.18	0.145	0.148	13.078	11794.93	12026.47	0.128	0.128	1.9253
240	11756.82	12270.91	0.135	0.133	4.1895	11773.5	11547.97	0.122	0.121	-1.953
241	10634.86	14687.34	0.126	0.141	27.592	11284.96	11148.06	0.127	0.121	-1.228
242	11414.53	11601.43	0.144	0.144	1.611	11770.85	12042.31	0.123	0.126	2.2542
243	12160.43	14111.39	0.139	0.146	13.825	16318.79	17614.2	0.131	0.134	7.3543
244	12154.52	13144.06	0.138	0.133	7.5284	12694.35	12885.39	0.128	0.127	1.4826
245	12150.49	12468.78	0.138	0.135	2.5527	10913.39	10964.01	0.129	0.127	0.4617
246	11469.39	11879.05	0.131	0.129	3.4486	14624.83	14683.4	0.123	0.123	0.3989
247	12505.94	12466.73	0.144	0.143	-0.314	11714.82	11868.58	0.126	0.127	1.2955
248	12122.03	12491.47	0.137	0.139	2.9576	11149.6	11554.99	0.12	0.124	3.5084
249	13670.75	14336.4	0.133	0.137	4.6431	12229.34	12206.49	0.126	0.123	-0.187
250	12990.69	13131.24	0.115	0.114	1.0704	15090.41	15952.6	0.128	0.132	5.4047
251	11337.62	12393.3	0.148	0.146	8.5182	14257.3	14332.95	0.118	0.122	0.5278
252	11988.47	11953.62	0.143	0.144	-0.292	13141.58	13126.73	0.121	0.127	-0.113
253	11045.53	11435.69	0.15	0.148	3.4118	12296.56	12424.46	0.13	0.13	1.0295
254	14294.61	14728.25	0.132	0.131	2.9443	10933.45	10804.83	0.122	0.115	-1.19
255	16643.34	17275.47	0.124	0.123	3.6591	14011.81	13459.37	0.126	0.121	-4.105
256	14352.38	15560.12	0.113	0.114	7.7618	11877.71	12174.73	0.13	0.129	2.4396

257	11567.4	11766.72	0.147	0.146	1.694	13057.28	13196.15	0.12	0.12	1.0524
258	13155.21	13337.51	0.137	0.138	1.3669	12568.04	12842.22	0.119	0.124	2.135
259	12993.52	15280.25	0.115	0.112	14.965	12401.97	12749.51	0.126	0.124	2.7259
260	13228.82	14996.73	0.139	0.132	11.789	12584.44	12338.67	0.124	0.124	-1.992
261	12238.24	12878.69	0.122	0.123	4.973	12381.18	12582.27	0.124	0.121	1.5982
262	12919.36	14870.58	0.135	0.135	13.121	12297.59	12367.17	0.114	0.115	0.5626
263	11632.62	12306.59	0.147	0.147	5.4765	11816.3	11926.3	0.134	0.132	0.9223
264	11552.91	11965.87	0.131	0.124	3.4512	13111.44	12885.91	0.116	0.115	-1.75
265	15306.71	15791.06	0.132	0.133	3.0672	13101.45	13236.18	0.12	0.12	1.0179
266	11494.24	11939.05	0.146	0.147	3.7256	12765.07	12644.99	0.126	0.128	-0.95
267	11807.55	12699.55	0.131	0.122	7.0238	13749.95	12667.56	0.12	0.129	-8.545
268	11072.62	12668.51	0.141	0.147	12.597	13766.06	13801.8	0.128	0.125	0.2589
269	12029.97	12874.06	0.138	0.133	6.5565	14924.58	15767.98	0.134	0.137	5.3488
270	11081.99	11675.74	0.129	0.138	5.0853	14763.32	14821.9	0.123	0.123	0.3952
271	11707.42	11770.55	0.139	0.14	0.5364	11968.53	12379.07	0.132	0.13	3.3164
272	12836.99	14429.03	0.137	0.131	11.034	11212.77	11398.75	0.12	0.126	1.6316
273	11202.7	14834.89	0.131	0.145	24.484	11114.12	11255.46	0.128	0.13	1.2557
274	11856.71	11905.79	0.145	0.144	0.4122	12355.42	12454.92	0.126	0.122	0.7989
275	13606.88	13662.02	0.136	0.137	0.4037	12994.99	13364.41	0.122	0.12	2.7643
276	11955.4	12542.33	0.126	0.123	4.6796	10541.38	11131.67	0.132	0.111	5.3028
277	12526.33	12468.84	0.142	0.141	-0.461	11448.06	11161.28	0.125	0.128	-2.569
278	11037.17	13067.04	0.125	0.14	15.534	14417.59	14621.56	0.125	0.124	1.395
279	14195.59	14565.13	0.123	0.13	2.5372	11526.71	12093.02	0.134	0.127	4.6829
280	11954.87	12570.09	0.122	0.119	4.8943	11719.42	12220.08	0.133	0.133	4.097
281	12780.21	13845.1	0.122	0.115	7.6914	12293.75	12422.66	0.134	0.133	1.0377
282	13561.73	13610.13	0.136	0.137	0.3557	11003.03	11140.52	0.122	0.121	1.2341
283	12606.48	12597.7	0.143	0.143	-0.07	11112.91	11114.12	0.123	0.124	0.0109
284	10373.05	10754.92	0.149	0.147	3.5507	11090.28	11142.91	0.12	0.121	0.4724
285	12410.34	14088.05	0.136	0.139	11.909	12349.16	12336.73	0.12	0.12	-0.101
286	12594.99	12509.93	0.132	0.134	-0.68	12287.48	12295.05	0.122	0.123	0.0616
287	11391.83	11827.97	0.146	0.144	3.6873	13473.91	13447.84	0.122	0.121	-0.194
288	15275.04	15716.58	0.131	0.126	2.8094	11211.8	12126.73	0.12	0.12	7.5447
289	12697.04	12661.47	0.137	0.137	-0.281	11020.72	11008.29	0.126	0.126	-0.113
290	13903.58	13278.05	0.136	0.139	-4.711	11022.86	11196.62	0.125	0.125	1.5519

291	11608.06	12073.36	0.123	0.124	3.854	11658.1	11732.83	0.127	0.125	0.6369
292	12660.28	12627.94	0.128	0.13	-0.256	11187.94	11286.64	0.132	0.134	0.8745
293	11611.76	11909.99	0.146	0.145	2.5041	14731.45	15054.76	0.122	0.123	2.1476
294	12989.11	13314.67	0.131	0.133	2.4451	15252.87	15255	0.116	0.115	0.014
295	16449.08	16866.57	0.13	0.125	2.4752	12596.51	13475.59	0.135	0.134	6.5235
296	13541.84	15591.41	0.119	0.122	13.146	12285.61	12060.08	0.119	0.118	-1.87
297	11855.36	11895.36	0.143	0.144	0.3363	11952.38	12039.16	0.128	0.128	0.7208
298	12252.42	14126.77	0.145	0.148	13.268	14304.58	13264.13	0.125	0.126	-7.844
299	10547.43	10727.05	0.143	0.141	1.6745	11935.31	12000.37	0.118	0.119	0.5422
300	12117.81	12038.86	0.121	0.131	-0.656	15096.52	15566.57	0.129	0.128	3.0196
301	11709.39	13389.05	0.138	0.132	12.545	11939.54	11759.89	0.129	0.122	-1.528
302	11897.98	13266.68	0.126	0.133	10.317	11842.81	11934.52	0.115	0.118	0.7685
303	11098.11	11400.78	0.144	0.143	2.6548	13985.13	14859.83	0.12	0.126	5.8863
304	12788.27	13553.31	0.124	0.119	5.6447	12180.45	12102.17	0.124	0.123	-0.647
305	14482	15239	0.109	0.115	4.9675	11542.42	11582.12	0.126	0.123	0.3428
306	16606.21	16489.26	0.128	0.133	-0.709	14473.87	15838.98	0.124	0.126	8.6187
307	10755.36	11441.55	0.132	0.131	5.9973	15795.01	16007.81	0.127	0.129	1.3294
308	10701.06	11270.01	0.147	0.146	5.0483	12459.45	12746.02	0.121	0.122	2.2483
309	11830.31	11687.92	0.138	0.138	-1.218	11043.6	11200.29	0.128	0.123	1.399
310	15582.73	16244.28	0.131	0.125	4.0725	10797.7	10850.34	0.118	0.119	0.4851
311	12948.51	13125.62	0.14	0.139	1.3493	10822.44	10945.08	0.138	0.135	1.1205
312	12745.07	13199.11	0.126	0.127	3.4399	12705.06	12789.71	0.126	0.127	0.6618
313	11818.96	11826	0.121	0.128	0.0595	10923.02	10981.01	0.132	0.132	0.5281
314	14552.39	14265.07	0.121	0.127	-2.014	12358.58	12525.53	0.127	0.123	1.3329
315	11336.12	11612.94	0.147	0.145	2.3837	14242.56	14557.33	0.12	0.125	2.1623
316	14600.39	14836.96	0.128	0.125	1.5945	15579.74	16530.21	0.137	0.139	5.7499
317	15744.16	16165.79	0.129	0.124	2.6082	11481.32	11620.73	0.124	0.123	1.1997
318	12693.65	12648.59	0.132	0.134	-0.356	11377.53	11876.94	0.125	0.124	4.2049
319	14942.6	14979.96	0.135	0.135	0.2494	11939.26	11957.04	0.121	0.121	0.1487
320	14314.27	14134.8	0.13	0.14	-1.27	15698	15878.38	0.129	0.128	1.136
321	10965.12	11266.07	0.145	0.144	2.6713	9990.828	10645.16	0.141	0.138	6.1468
322	12001.14	12372.56	0.137	0.133	3.002	12672.12	13142.07	0.13	0.128	3.5759
323	12613.38	13028.46	0.127	0.132	3.1859	12578.75	12591.05	0.126	0.123	0.0977
324	11992.45	13160.98	0.124	0.113	8.8787	14460.23	14365.88	0.122	0.119	-0.657

325	11094.65	11488.95	0.149	0.147	3.432	11884.95	11876.16	0.129	0.129	-0.074
326	14913.64	14619.29	0.125	0.133	-2.013	11936.17	11988.8	0.119	0.119	0.439
327	10934.04	10934.04	0.145	0.145	0	12872.55	12846.48	0.127	0.125	-0.203
328	11917.33	13875.65	0.139	0.148	14.113	12013.79	12202.91	0.113	0.119	1.5498
329	12245.4	14985.75	0.125	0.145	18.286	14267.18	14447.09	0.129	0.131	1.2453
330	11530.19	15436.4	0.125	0.144	25.305	10900.81	11003.74	0.125	0.121	0.9354
331	12401.34	12485.77	0.144	0.144	0.6763	11209.18	11963.31	0.13	0.127	6.3037
332	12722.72	12819.93	0.116	0.126	0.7583	11196.55	11235.04	0.127	0.126	0.3426
333	13756.43	14908.95	0.118	0.122	7.7303	11741.56	11758.42	0.129	0.129	0.1434
334	12424.29	12568.1	0.117	0.127	1.1443	12088.19	12861.03	0.126	0.128	6.0092
335	13353.97	15097.52	0.139	0.133	11.549	12023.19	12623.47	0.132	0.13	4.7553
336	13909.74	14157.73	0.132	0.137	1.7516	11343.3	11897.65	0.122	0.121	4.6593
337	12087.15	11949.04	0.114	0.12	-1.156	13985.02	13939.46	0.117	0.12	-0.327
338	11876.41	11991.56	0.142	0.142	0.9602	12748.85	12955.04	0.128	0.13	1.5916
339	11078.8	11375.16	0.112	0.121	2.6053	12511.4	12660.27	0.119	0.118	1.1759
340	11627.33	12350.38	0.124	0.122	5.8545	11087.27	11285.88	0.131	0.131	1.7598
341	12582.25	12628.4	0.142	0.142	0.3655	14777.63	14974.08	0.13	0.129	1.3119
342	11917.62	13792.45	0.122	0.122	13.593	12876.91	13685.54	0.126	0.129	5.9086
343	12286.65	14294.92	0.128	0.134	14.049	11571.49	12503.85	0.135	0.136	7.4566
344	12079.35	14087.22	0.143	0.147	14.253	11113.83	11280.52	0.124	0.122	1.4777
345	12501.78	13188.61	0.118	0.119	5.2077	11671.41	12426.51	0.123	0.128	6.0765
346	10900.15	11288.6	0.149	0.147	3.441	11096.32	11426.06	0.123	0.127	2.8859
347	11698.08	11979.04	0.145	0.144	2.3454	12528.47	12526.55	0.116	0.116	-0.015
348	12352.75	14012.45	0.115	0.117	11.845	13679.84	13726.49	0.118	0.119	0.3399
349	12889.38	13151.8	0.138	0.135	1.9954	11316.57	11664.31	0.132	0.131	2.9812
350	11440.21	11604.69	0.145	0.146	1.4173	12771.57	12531.83	0.123	0.12	-1.913
351	13749.53	14629.2	0.118	0.115	6.0131	12625.43	12871.37	0.125	0.127	1.9108
352	13871.81	13753.96	0.115	0.113	-0.857	11334.72	11532.33	0.13	0.127	1.7135
353	11858.47	12271.56	0.142	0.143	3.3662	11789.54	12055.43	0.126	0.126	2.2056
354	16541.36	16855.92	0.12	0.127	1.8662	13460.26	13525.32	0.118	0.118	0.481
355	12209.31	12603.78	0.123	0.129	3.1298	11405.86	12639.37	0.14	0.139	9.7592
356	13369.51	14191.78	0.121	0.127	5.794	10492.08	10633.41	0.126	0.127	1.3292
357	12187.36	12729.82	0.134	0.134	4.2613	10882.76	10906.4	0.125	0.126	0.2167
358	11720.63	12160.37	0.129	0.128	3.6162	12939.3	13323.62	0.118	0.118	2.8845

359	12700.05	12995.08	0.113	0.121	2.2703	12266.04	12365.12	0.126	0.12	0.8013
360	11886.24	11897.66	0.14	0.141	0.096	11153.83	11295.16	0.125	0.126	1.2513
361	13349.83	13361.55	0.14	0.139	0.0877	15301.9	16278.81	0.117	0.121	6.0011
362	11313.47	11488.03	0.12	0.126	1.5195	11743.23	11859.59	0.117	0.117	0.9812
363	12555.7	13524.4	0.114	0.124	7.1626	12179.43	12502.1	0.121	0.125	2.5809
364	13186.53	13344.19	0.132	0.133	1.1815	11723.93	12035.09	0.125	0.128	2.5855
365	12965.53	12310.71	0.138	0.142	-5.319	15193.59	15633.85	0.129	0.128	2.8161
366	11070.36	12317.71	0.133	0.131	10.126	11638.74	11691.38	0.118	0.118	0.4502
367	15926.03	15722.13	0.123	0.132	-1.297	11599.28	11734.01	0.127	0.127	1.1482
368	16001.3	16423.43	0.131	0.125	2.5703	12425.85	12544.05	0.121	0.122	0.9423
369	12850.47	12386.57	0.137	0.14	-3.745	12199.58	12414.97	0.129	0.126	1.7349
370	12640.29	12868.61	0.139	0.139	1.7742	12568.62	12542.55	0.124	0.122	-0.208
371	12771.12	12934.17	0.134	0.134	1.2606	11481.27	11580.76	0.129	0.124	0.8592
372	12082.88	13858.78	0.142	0.147	12.814	11700.58	12182.04	0.131	0.13	3.9522
373	12734.98	16454.13	0.142	0.141	22.603	11038.47	11197.35	0.126	0.125	1.4188
374	10116.5	10464.95	0.148	0.145	3.3296	12051.85	11852.36	0.12	0.118	-1.683
375	11168.83	11405.94	0.145	0.144	2.0788	13976.37	14068.8	0.128	0.129	0.657
376	13510.65	13650.18	0.134	0.139	1.0222	12098.41	12085.99	0.122	0.122	-0.103
377	12404.27	12612.17	0.138	0.135	1.6484	12818.07	12980.41	0.119	0.119	1.2507
378	11799.22	11820.94	0.145	0.145	0.1837	12058.06	11832.53	0.121	0.12	-1.906
379	13733.98	14338.85	0.121	0.123	4.2184	14314.56	14717.03	0.122	0.122	2.7348
380	12083.92	15973.12	0.135	0.132	24.348	12864.41	12609.85	0.123	0.12	-2.019
381	12196	12920.97	0.147	0.147	5.6108	11907	12025.2	0.119	0.12	0.9829
382	13954.94	15600.72	0.135	0.137	10.549	10242.75	10743.53	0.135	0.129	4.6612
383	13961.4	15433.44	0.138	0.134	9.538	12434.38	12573.25	0.121	0.121	1.1045
384	13943.53	15611.56	0.12	0.11	10.685	11281.46	11721.41	0.132	0.13	3.7534
385	11037.37	11352.47	0.145	0.145	2.7756	13570.14	13967.47	0.125	0.123	2.8447
386	13282.76	13587.75	0.118	0.113	2.2446	14275.82	14181.97	0.122	0.12	-0.662
387	11320.67	11621.46	0.141	0.139	2.5883	11483.6	11525.31	0.127	0.127	0.3619
388	12432.69	13465.98	0.114	0.119	7.6734	12532.98	14198.05	0.134	0.138	11.727
389	11501.82	13092.22	0.125	0.122	12.148	10581.01	10838.62	0.131	0.131	2.3768
390	10557.41	13849.23	0.126	0.141	23.769	13118.22	13825.93	0.119	0.119	5.1187
391	14130.56	16426.97	0.13	0.137	13.98	11575.69	11766.23	0.127	0.128	1.6194
392	11567.86	12346.77	0.138	0.133	6.3086	10491.96	11096.26	0.133	0.133	5.446

393	15882.78	15886.92	0.129	0.129	0.0261	10131.6	10634.98	0.131	0.132	4.7333
394	12406.1	13125.53	0.127	0.13	5.4811	14551.65	14500.02	0.118	0.122	-0.356
395	14119.44	14862.45	0.107	0.115	4.9993	14525.25	14564.74	0.138	0.137	0.2712
396	13146.16	13692.19	0.139	0.137	3.9879	11847.38	11685.84	0.125	0.122	-1.382
397	13017.53	13183.72	0.142	0.142	1.2606	15821.37	16795.35	0.117	0.121	5.7991
398	13171.41	16292.62	0.136	0.134	19.157	13362.55	13344.77	0.12	0.118	-0.133
399	13367.61	13581.3	0.115	0.111	1.5734	10620.66	11729.22	0.128	0.128	9.4513
400	10488.25	10778.2	0.146	0.145	2.6901	10682.2	10901.73	0.132	0.132	2.0137
401	10872.85	11210.16	0.122	0.126	3.009	11650.41	12603.75	0.136	0.135	7.564
402	11899.12	12082.47	0.133	0.129	1.5174	13906.19	14045.06	0.118	0.118	0.9888
403	12767.08	12771.23	0.14	0.141	0.0324	11447.77	11306.73	0.123	0.116	-1.247
404	12135.08	13099.08	0.123	0.118	7.3593	12196.94	12476.18	0.131	0.128	2.2382
405	13321.08	14182.72	0.126	0.124	6.0753	13950.28	14048.19	0.122	0.128	0.6969
406	13569.9	16259.07	0.136	0.134	16.539	12016.47	12501.29	0.125	0.119	3.8781
407	11636.24	12254.89	0.143	0.14	5.0482	12115.16	12585.74	0.127	0.126	3.7389
408	12790.47	13781.77	0.129	0.135	7.1928	11083.71	11532.53	0.131	0.131	3.8918
409	12204.52	12194.37	0.12	0.129	-0.083	10867.14	10854.71	0.121	0.121	-0.114
410	10203.7	10523.14	0.149	0.147	3.0357	13005.09	13067.72	0.139	0.138	0.4793
411	11388.27	11585.16	0.141	0.141	1.6996	12683.07	13068.08	0.129	0.126	2.9462
412	11913.6	12618.81	0.131	0.127	5.5886	12521.88	12428.03	0.126	0.124	-0.755
413	14465.11	14615.91	0.132	0.136	1.0317	11392.51	11500.92	0.127	0.122	0.9426
414	13559.13	13861.56	0.132	0.139	2.1818	10557.97	10716.84	0.125	0.124	1.4825
415	16009.64	16621.65	0.124	0.121	3.682	14709.35	14733.37	0.122	0.119	0.163
416	13104.29	14517.97	0.123	0.115	9.7374	11688.36	11938.9	0.122	0.126	2.0985
417	12523.25	14119.47	0.123	0.118	11.305	10539	11009.33	0.129	0.129	4.2721
418	11736.19	12183.21	0.122	0.124	3.6692	11190.69	11255.75	0.127	0.127	0.578
419	12634.19	13389.64	0.107	0.116	5.642	11655.43	11732.42	0.123	0.12	0.6562
420	11849.72	12757.58	0.121	0.115	7.1162	11438.77	11213.24	0.122	0.121	-2.011
421	14124.49	14928.86	0.126	0.127	5.388	11135.63	11415.46	0.13	0.13	2.4513
422	11263.41	12047.88	0.145	0.147	6.5113	12953.67	13114.79	0.119	0.119	1.2286
423	12968.49	13112.93	0.139	0.142	1.1015	12736.34	12812.19	0.125	0.126	0.5921
424	13789.63	13805.49	0.14	0.14	0.1149	12431.2	12674.3	0.126	0.125	1.9181
425	11298.29	11765.61	0.131	0.13	3.9719	11822.71	11940.91	0.119	0.119	0.9899
426	10995.3	12313.94	0.136	0.129	10.708	15796.96	17256.84	0.137	0.134	8.4597

427	11588.56	11416.17	0.138	0.14	-1.51	12052.59	11933.03	0.128	0.122	-1.002
428	12249.42	16316.82	0.137	0.131	24.928	11294.84	11302.42	0.124	0.125	0.067
429	10673.2	10942.95	0.118	0.124	2.465	15308.56	15571.66	0.127	0.126	1.6896
430	12309.37	12763.87	0.117	0.114	3.5609	13677.24	13652.18	0.123	0.12	-0.184
431	12025.97	12121.24	0.135	0.139	0.786	11186.17	11258.8	0.128	0.129	0.6451
432	13013.52	16148.74	0.113	0.111	19.415	13504.83	13643.7	0.118	0.117	1.0179
433	11848.24	13391.99	0.125	0.139	11.527	11747.54	12073.14	0.122	0.125	2.6969
434	11825.97	11947.65	0.123	0.129	1.0184	10619.21	11646.4	0.134	0.134	8.8198
435	11446	11497.17	0.122	0.129	0.4451	12584.69	13021.52	0.124	0.124	3.3547
436	13747.28	13643.1	0.104	0.115	-0.764	11805.1	11981.08	0.125	0.131	1.4688
437	15957.27	15819.61	0.128	0.134	-0.87	12546.48	12767.91	0.128	0.127	1.7342
438	11966.92	13432.06	0.117	0.12	10.908	10992.97	11167.74	0.128	0.128	1.5649
439	12981.12	13724.13	0.108	0.118	5.4139	12786.65	12851.71	0.121	0.121	0.5062
440	17085.28	17212.31	0.127	0.134	0.738	13561.97	13907.54	0.127	0.129	2.4847
441	12878.31	13803.13	0.106	0.118	6.7001	11437.03	11685.55	0.128	0.127	2.1268
442	11838.99	12392.8	0.107	0.121	4.4688	12608.09	12599.3	0.129	0.129	-0.07
443	10814.89	11076.4	0.144	0.141	2.3609	11090.81	11212.74	0.127	0.124	1.0874
444	13069.89	13196.04	0.138	0.141	0.956	12618.08	12761.89	0.121	0.117	1.1269
445	12655.5	14478.43	0.115	0.117	12.591	11761.03	11836.39	0.125	0.125	0.6366
446	12690.78	13478.37	0.13	0.133	5.8433	13300.25	13584.72	0.119	0.123	2.0941
447	11973.27	12529.11	0.134	0.131	4.4364	12444.42	12533.3	0.122	0.125	0.7091
448	11624.01	12566.89	0.124	0.122	7.5029	11959.04	12524.76	0.133	0.134	4.5168
449	12490.05	12521.77	0.14	0.14	0.2533	11279.15	12043.61	0.136	0.136	6.3474
450	12203.21	12683.3	0.123	0.126	3.7852	12150.31	12436.88	0.123	0.125	2.3042
451	11698.83	12290.2	0.145	0.139	4.8117	11820.81	12574.94	0.127	0.126	5.9971
452	11519.51	12040.47	0.146	0.146	4.3267	11098.77	11163.83	0.123	0.123	0.5828
453	12827.1	14221.69	0.14	0.132	9.8061	10551.78	11023.45	0.133	0.131	4.2787
454	12624.4	12955.86	0.136	0.133	2.5584	12610.9	13891.78	0.138	0.137	9.2204
455	11028.29	11643.84	0.134	0.131	5.2865	12939.98	13227.88	0.119	0.123	2.1765
456	11616.84	12440.19	0.137	0.13	6.6184	11442.8	11725.35	0.133	0.132	2.4097
457	13505.33	13784.71	0.133	0.135	2.0267	14083.71	14272.92	0.121	0.122	1.3256
458	11200.16	13053.84	0.13	0.139	14.2	10957.44	11283.13	0.139	0.135	2.8865
459	12824.46	12808.4	0.14	0.14	-0.125	10888.65	11125.75	0.132	0.132	2.1312
460	14285.65	14690.97	0.122	0.128	2.759	13184.55	13302.75	0.116	0.117	0.8885

461	11430.13	12080.67	0.149	0.149	5.385	10940.28	10946.13	0.129	0.129	0.0535
462	11937.77	12752.04	0.126	0.138	6.3854	13119.41	13301.96	0.128	0.13	1.3723
463	12564.01	12876.02	0.127	0.131	2.4232	10962.73	11620.04	0.132	0.132	5.6567
464	10972.07	11324.65	0.148	0.145	3.1134	15579.04	15904.65	0.129	0.127	2.0473
465	13927.47	13854.51	0.123	0.131	-0.527	11553.46	11652.96	0.127	0.122	0.8538
466	13064.6	13392.33	0.141	0.14	2.4472	14730	14713.72	0.132	0.133	-0.111
467	11187.22	12134.75	0.132	0.127	7.8083	11831.99	11998.97	0.125	0.126	1.3917
468	10572.19	10958.2	0.15	0.148	3.5226	14857.79	15190.89	0.128	0.126	2.1928
469	12345.8	13411.86	0.136	0.136	7.9487	14815.89	15824.61	0.138	0.143	6.3743
470	11017.6	11403.91	0.145	0.149	3.3875	13421.01	12255.7	0.116	0.119	-9.508
471	12398.57	12199.37	0.113	0.12	-1.633	12023.51	12422.25	0.133	0.132	3.2099
472	13101.64	13223.36	0.136	0.14	0.9205	11065.86	11053.44	0.123	0.123	-0.112
473	11157.87	12523.42	0.126	0.126	10.904	13300.82	14955.18	0.134	0.138	11.062
474	11284.63	12514.45	0.142	0.148	9.8273	11419.97	11516.24	0.124	0.126	0.836
475	11385.42	11622.53	0.132	0.131	2.0401	14652.33	17213.12	0.124	0.124	14.877
476	12524.26	12851.5	0.111	0.122	2.5463	12204.97	12529.85	0.132	0.131	2.5929
477	15958.1	16321.95	0.13	0.124	2.2292	13340.4	13793.04	0.12	0.124	3.2816
478	13655.37	13773.44	0.13	0.134	0.8573	13096.42	13373.66	0.127	0.126	2.0731
479	12380.91	13188.07	0.11	0.119	6.1204	12180.92	12398.11	0.116	0.121	1.7518
480	12047.47	13620.76	0.129	0.126	11.551	11745.3	12084.83	0.13	0.124	2.8096
481	13252.85	14313.79	0.126	0.13	7.412	12798.13	13216.57	0.129	0.126	3.166
482	12413.41	12984.29	0.137	0.135	4.3967	15222.34	16605.73	0.131	0.132	8.3308
483	12343.21	13768.52	0.138	0.133	10.352	11091.65	11109.43	0.12	0.121	0.1601
484	16395.51	16871.92	0.123	0.129	2.8237	12992.01	12749.17	0.119	0.117	-1.905
485	13836.7	13840.84	0.133	0.134	0.0299	12991.7	12929.62	0.125	0.123	-0.48
486	11892.11	11896.25	0.143	0.144	0.0348	13222.02	13315.78	0.123	0.127	0.7041
487	12531.15	12385.68	0.119	0.125	-1.175	11586.09	11642.16	0.121	0.123	0.4816
488	12295.03	13966.36	0.112	0.109	11.967	13406.46	13498.89	0.124	0.126	0.6847
489	13060.06	12978.43	0.134	0.136	-0.629	12788.28	12853.34	0.117	0.117	0.5062
490	13505.77	14272.46	0.136	0.132	5.3718	10920.57	11138.89	0.132	0.129	1.96
491	13599.06	15583.65	0.138	0.13	12.735	13912.51	14135.73	0.126	0.124	1.5791
492	12354.27	12677.58	0.135	0.139	2.5502	16150.51	17229.56	0.129	0.131	6.2628
493	15135.56	15488.66	0.131	0.133	2.2797	12078.31	12181.24	0.124	0.12	0.845
494	12592.75	13393.84	0.109	0.119	5.981	14496.75	14508.46	0.122	0.121	0.0808

495	12662.96	14166.21	0.116	0.117	10.612	11735.64	11861.2	0.121	0.121	1.0586
496	13138.2	14804.18	0.141	0.145	11.253	12558.21	12756.12	0.124	0.128	1.5514
497	11123.06	11354.22	0.123	0.126	2.0359	11783.46	11882.96	0.122	0.117	0.8373
498	15852.89	15536.65	0.125	0.131	-2.035	12280.03	12464	0.119	0.122	1.476
499	12709.35	13205.21	0.134	0.139	3.755	13323.93	13388.99	0.122	0.122	0.4859
500	12172.71	12375.64	0.136	0.134	1.6397	10898.34	11883.21	0.14	0.139	8.2879
501	11090.42	11528.86	0.134	0.129	3.803	11421	11718.52	0.124	0.128	2.5389
502	14484.13	15997.56	0.127	0.131	9.4604	10688.94	11137.88	0.131	0.134	4.0308
503	11011.31	11430.75	0.148	0.148	3.6695	15130.41	16170.59	0.128	0.134	6.4325
504	13481.52	14113.82	0.117	0.123	4.48	14039.33	14078.82	0.133	0.132	0.2805
505	12124.48	12376.44	0.141	0.141	2.0358	12862.92	12927.98	0.121	0.122	0.5033
506	11167.56	15131.36	0.143	0.141	26.196	11026.03	11649.92	0.12	0.119	5.3553
507	16177.7	16633.4	0.124	0.129	2.7397	10793.42	10868.78	0.126	0.127	0.6933
508	10443.64	10724.59	0.145	0.143	2.6197	14918.93	14898.72	0.114	0.118	-0.136
509	11402.49	12082.32	0.149	0.149	5.6266	11237.76	11332.53	0.128	0.128	0.8362
510	13448.16	13453.19	0.107	0.117	0.0374	11904.64	12022.83	0.12	0.12	0.9831
511	17595.27	18197.81	0.127	0.122	3.3111	10396.72	11514.24	0.128	0.129	9.7056
512	16754.94	16762.25	0.12	0.131	0.0436	12534.5	12725.54	0.128	0.127	1.5012
513	10608.91	10677.49	0.115	0.122	0.6423	12131.53	12294.93	0.12	0.113	1.329
514	11599.64	11613.28	0.142	0.144	0.1174	15995.33	17092.81	0.132	0.13	6.4208
515	13404.17	13884.59	0.135	0.132	3.4601	11446.27	12222.66	0.135	0.132	6.3521
516	12404.56	12430.14	0.117	0.117	0.2058	12562.13	12598.91	0.122	0.119	0.2919
517	13863.87	14370.82	0.131	0.133	3.5276	13008.08	13779.71	0.139	0.138	5.5998
518	14536.59	15277.01	0.13	0.133	4.8466	12187.51	12201.24	0.123	0.117	0.1125
519	13333.95	14574.2	0.122	0.125	8.51	11867.62	12102.44	0.121	0.124	1.9402
520	13850.48	15050.95	0.113	0.117	7.976	12234.93	12353.13	0.118	0.119	0.9568
521	12657.72	13460.95	0.115	0.125	5.9671	11575.9	11717.23	0.129	0.13	1.2062
522	11511.56	11979.34	0.14	0.136	3.9049	12249.45	12189.87	0.127	0.129	-0.489
523	13074.93	13241.58	0.132	0.137	1.2586	11948.71	11723.18	0.121	0.12	-1.924
524	11959.22	12401.09	0.144	0.145	3.5632	11803.07	11922.98	0.126	0.125	1.0057
525	12673.66	13347.63	0.145	0.146	5.0494	13372.88	13415.6	0.121	0.122	0.3184
526	12285.45	13055.88	0.131	0.139	5.901	13622.4	13826.37	0.128	0.127	1.4752
527	12247.04	13463.02	0.141	0.148	9.032	12803.23	12902.72	0.123	0.119	0.7711
528	13915.14	15830.01	0.136	0.138	12.096	11458.45	11921.5	0.14	0.136	3.8842

529	16773.32	17549.59	0.122	0.131	4.4233	11509.75	11562.38	0.118	0.119	0.4552
530	11529.77	12266.38	0.148	0.148	6.0051	14363.64	14583.52	0.128	0.128	1.5077
531	12056.26	13080.38	0.122	0.121	7.8295	16234.84	16584.3	0.131	0.129	2.1072
532	12629.79	14706.36	0.139	0.144	14.12	13415.4	13405.11	0.116	0.122	-0.077
533	14180.59	14714.02	0.132	0.134	3.6253	12543.23	12411.34	0.124	0.121	-1.063
534	12655.4	16652.89	0.135	0.131	24.005	11083.54	11183.04	0.127	0.123	0.8897
535	12700.71	13116.24	0.126	0.126	3.168	11343.53	11432.53	0.127	0.127	0.7784
536	11687.7	14299.06	0.128	0.141	18.262	11250.73	11289.72	0.126	0.121	0.3454
537	13784.15	13764.66	0.136	0.136	-0.142	11931.85	11942.65	0.124	0.122	0.0904
538	11592.6	12832.6	0.139	0.137	9.6629	11231.9	11284.54	0.122	0.122	0.4664
539	13232.67	13195.24	0.114	0.112	-0.284	11726.63	11893.62	0.124	0.125	1.404
540	12499.66	12503.8	0.142	0.142	0.0331	12500.6	12930.72	0.124	0.125	3.3264
541	13321.23	13439.3	0.134	0.138	0.8786	12852	12925.01	0.122	0.124	0.5649
542	11107.85	11547	0.124	0.12	3.8032	12302.77	12545.03	0.121	0.125	1.9311
543	12792.07	12867.13	0.142	0.142	0.5834	12672.01	12911.21	0.134	0.133	1.8527
544	12534.95	12542.82	0.127	0.128	0.0627	11883.26	11912.26	0.125	0.125	0.2434
545	11834.64	12641.79	0.111	0.121	6.3848	15097.63	16126.47	0.119	0.124	6.3798
546	12618.43	13003.96	0.135	0.137	2.9647	12010.43	12172.77	0.121	0.12	1.3336
547	15060.65	15618.72	0.128	0.13	3.5731	12523.61	12765.03	0.13	0.129	1.8913
548	10967.94	14276.86	0.127	0.14	23.177	15028.26	15199.05	0.129	0.129	1.1237
549	16348.64	16784.29	0.125	0.123	2.5956	16356.28	16385.57	0.129	0.128	0.1788
550	12174.08	13134.46	0.116	0.125	7.3119	10953.88	11103.79	0.134	0.134	1.3501
551	11430.85	12833.99	0.115	0.117	10.933	11576.5	11665.91	0.126	0.116	0.7664
552	11772.7	12129.51	0.145	0.146	2.9417	10335.89	11046.38	0.141	0.139	6.4319
553	12534.72	12907.06	0.113	0.124	2.8848	12828.97	12871.69	0.123	0.123	0.3319
554	14778.46	14862.36	0.121	0.128	0.5645	15499.2	15404.97	0.125	0.128	-0.612
555	11805.41	11805.41	0.144	0.144	0	11911.74	12118.23	0.121	0.126	1.7039
556	11968.4	13141.66	0.123	0.12	8.9278	10368.11	10779.48	0.14	0.14	3.8162
557	13522.17	14126.73	0.132	0.138	4.2795	11995.6	12177.11	0.123	0.125	1.4906
558	10681.15	11004.03	0.147	0.145	2.9342	11082.29	12173.35	0.139	0.139	8.9627
559	11468.35	12429.97	0.135	0.123	7.7363	11287.91	11532.38	0.137	0.139	2.1199
560	14338.04	14433.48	0.133	0.136	0.6613	11552.92	11671.12	0.122	0.123	1.0127
561	11356.39	11633.2	0.142	0.14	2.3795	10920.86	11078.77	0.131	0.132	1.4253
562	15785.8	16055.27	0.125	0.132	1.6783	13261.56	13607.12	0.126	0.129	2.5396

563	11176.22	11482.74	0.146	0.144	2.6694	11557.5	11675.7	0.122	0.123	1.0123
564	11682.33	13495.8	0.115	0.112	13.437	9907.128	11284.81	0.138	0.138	12.208
565	11393.2	11955.29	0.123	0.129	4.7015	11969.2	12081.72	0.127	0.125	0.9313
566	15887.84	16149.05	0.133	0.134	1.6175	12107.38	12423.9	0.132	0.129	2.5477
567	12281.23	12602.36	0.136	0.131	2.5482	13663	13817.73	0.126	0.12	1.1198
568	12791.89	14425.65	0.142	0.145	11.325	11415.82	11741.42	0.123	0.127	2.7731
569	11824.54	12503.86	0.148	0.147	5.4329	12483.1	12610.09	0.139	0.137	1.007
570	15881.89	16621.68	0.129	0.129	4.4508	10804.12	11244.07	0.134	0.131	3.9127
571	11066.28	12275.4	0.142	0.149	9.8499	11878.15	12015.64	0.121	0.12	1.1442
572	12993.58	13007.22	0.137	0.139	0.1049	11188.18	11253.24	0.121	0.122	0.5782
573	17040.41	17719.32	0.124	0.122	3.8315	14207.94	14281.91	0.12	0.124	0.5179
574	12456.03	15349.92	0.114	0.111	18.853	12672.33	12912.45	0.121	0.124	1.8596
575	12328.72	12852.31	0.121	0.118	4.0739	14731.4	14837.17	0.139	0.137	0.7129
576	11613.62	12107.3	0.137	0.134	4.0775	11578.01	12069.88	0.12	0.127	4.0752
577	12527.63	13013.43	0.14	0.142	3.7331	11028.83	11891.24	0.127	0.124	7.2525
578	11270.73	12303.99	0.136	0.132	8.3978	14099.95	14140.87	0.12	0.118	0.2894
579	11743.14	15355.25	0.135	0.14	23.524	14219.48	14334.93	0.123	0.122	0.8053
580	12329.38	12888.49	0.134	0.131	4.3381	14205.37	14442.47	0.125	0.123	1.6417
581	13812.78	14435.97	0.124	0.131	4.3169	10872.22	11106.19	0.131	0.13	2.1067
582	11540.48	12919.55	0.132	0.131	10.674	9966.747	10308.91	0.127	0.129	3.3191
583	13419.41	14057.83	0.124	0.139	4.5414	11586.45	11725.32	0.125	0.124	1.1844
584	11749.96	11951.79	0.136	0.132	1.6888	12757.56	13121.33	0.126	0.126	2.7723
585	12765.78	15882.06	0.135	0.136	19.621	11666.24	11690.68	0.128	0.127	0.209
586	13943.04	14079.19	0.137	0.141	0.967	15160.55	15373.01	0.122	0.121	1.382
587	11820.24	13832.25	0.143	0.148	14.546	12470.39	12569.47	0.127	0.121	0.7883
588	11523.77	12393.04	0.133	0.124	7.0142	12082.7	12182.19	0.124	0.12	0.8167
589	17123.05	17672.75	0.124	0.122	3.1105	12203.72	12470.53	0.13	0.128	2.1395
590	12560.09	14663.05	0.108	0.111	14.342	10584.48	10743.35	0.127	0.126	1.4788
591	12994.18	13209.17	0.113	0.11	1.6276	12373.52	13081.23	0.122	0.123	5.4101
592	11942.19	12199.68	0.143	0.144	2.1106	11542.67	12575.74	0.141	0.14	8.2148
593	11957.69	11999.11	0.144	0.145	0.3452	15272.94	15748.85	0.132	0.129	3.0219
594	12943.41	13280.62	0.127	0.139	2.5391	11340.46	11554.64	0.131	0.13	1.8536
595	12075.3	12473.24	0.143	0.141	3.1903	12654.82	12757.75	0.123	0.119	0.8068
596	11302.69	11779.92	0.15	0.147	4.0512	10209.09	10431.13	0.137	0.141	2.1287

597	14320.07	14922.88	0.134	0.133	4.0395	11406.07	11381.22	0.123	0.123	-0.218
598	13920.26	14693.29	0.121	0.123	5.2611	11760.03	11528.57	0.124	0.12	-2.008
599	13174.79	13586.04	0.135	0.132	3.027	12757.41	13176.29	0.131	0.128	3.179
600	13202.07	14766.37	0.123	0.116	10.594	11652.3	11618.15	0.116	0.116	-0.294
601	10772.14	10784.56	0.143	0.143	0.1152	15957.5	16134.95	0.13	0.129	1.0998
602	16461.06	17148.55	0.124	0.12	4.009	12401.79	12640.87	0.126	0.128	1.8913
603	11751.55	12470.37	0.145	0.145	5.7642	12356.84	12396.75	0.127	0.127	0.322
604	12328.33	13079.78	0.141	0.142	5.7452	15041.95	16286.43	0.125	0.128	7.6412
605	12753.06	13075.49	0.132	0.133	2.4659	12413.48	12692.12	0.121	0.116	2.1954
606	13297.69	13451.33	0.113	0.123	1.1422	13256.19	13230.12	0.122	0.121	-0.197
607	10697.35	14241.63	0.128	0.141	24.887	14362.5	15744.47	0.127	0.129	8.7775
608	12369.06	12369.06	0.139	0.139	0	11871.99	12005	0.13	0.129	1.108
609	14536.84	14301.32	0.124	0.132	-1.647	11567.64	11542.79	0.124	0.124	-0.215
610	11351.9	11590.4	0.12	0.129	2.0577	11094.93	11217.23	0.123	0.123	1.0903
611	13374.72	14767.6	0.118	0.126	9.432	11534.01	12187.27	0.131	0.129	5.3602
612	10462.63	10852.79	0.15	0.148	3.595	11154.04	11234.24	0.129	0.129	0.714
613	13199.83	13268.08	0.123	0.125	0.5144	12046.05	12218.8	0.13	0.129	1.4139
614	13005.8	15058.89	0.12	0.116	13.634	13482.62	13737.27	0.126	0.129	1.8537
615	11390.37	13494.17	0.125	0.143	15.59	10458.85	10756.46	0.137	0.14	2.7668
616	13583.11	13583.11	0.14	0.14	0	12312.48	12549.72	0.122	0.121	1.8904
617	14803.26	14834.94	0.124	0.132	0.2136	14499.61	14501.82	0.121	0.127	0.0153
618	11490.02	13010.68	0.138	0.133	11.688	11974.07	12103.66	0.124	0.122	1.0706
619	12044.17	11898.48	0.121	0.13	-1.224	13983.11	13914.75	0.125	0.12	-0.491
620	12887.06	12781.71	0.113	0.119	-0.824	11329.37	11576.68	0.128	0.128	2.1363
621	11671.46	13531.38	0.136	0.146	13.745	15411.19	16664.93	0.128	0.137	7.5232
622	14594.56	15126.03	0.122	0.127	3.5136	10503.27	11438.1	0.129	0.124	8.173
623	13591.79	14907.52	0.134	0.135	8.826	12313.47	12087.95	0.118	0.117	-1.866
624	12669.15	12940.66	0.13	0.13	2.0981	13485.58	13652.56	0.126	0.127	1.2231
625	12534.61	14921.88	0.124	0.117	15.998	11745.99	12072.59	0.133	0.132	2.7053
626	11454.43	11461.5	0.144	0.144	0.0617	12712.18	13151.52	0.13	0.128	3.3406
627	11189.37	12549.91	0.131	0.14	10.841	10952.77	11237.45	0.124	0.123	2.5333
628	13171.39	13564.4	0.131	0.133	2.8974	11639.7	12049.14	0.121	0.124	3.3981
629	10897.42	11233.44	0.15	0.147	2.9912	14882.3	16039.93	0.117	0.121	7.2171
630	11240.75	11283.68	0.12	0.125	0.3805	10578.68	10923.15	0.132	0.131	3.1536

631	13848.73	13186.63	0.136	0.139	-5.021	12095.64	12198.69	0.118	0.12	0.8448
632	12646.8	13472.78	0.14	0.135	6.1307	12842.1	12701.06	0.122	0.115	-1.11
633	11643.19	11778.13	0.122	0.126	1.1457	11656.47	11773.04	0.117	0.119	0.9901
634	11066.16	15656.37	0.135	0.144	29.319	14060.11	14296.47	0.132	0.135	1.6533
635	12946.69	14700.3	0.115	0.117	11.929	12780.83	13265.23	0.128	0.124	3.6517
636	13905.45	13185.58	0.132	0.136	-5.46	12701.09	13005.57	0.117	0.116	2.3411
637	11201.88	11393.01	0.128	0.129	1.6776	12871.29	13151.33	0.118	0.119	2.1293
638	11000.89	11403.89	0.145	0.144	3.5339	12089.05	12178.96	0.128	0.125	0.7383
639	14606.74	14737.03	0.133	0.137	0.8841	12844.76	12962.96	0.12	0.12	0.9118
640	10844.12	12349.51	0.14	0.147	12.19	12883.77	13142.94	0.134	0.132	1.9719
641	11897.3	12507.21	0.137	0.133	4.8765	14340.08	15634.57	0.131	0.131	8.2796
642	11211.26	11539.75	0.119	0.127	2.8466	14117.19	14128.91	0.126	0.126	0.0829
643	13201.18	13364.23	0.137	0.137	1.2201	11285.31	11090.34	0.121	0.118	-1.758
644	12222.56	13660.38	0.136	0.141	10.525	9968.524	9986.808	0.132	0.134	0.1831
645	14321.62	14325.76	0.137	0.138	0.0289	14981.1	15068.97	0.12	0.118	0.5831
646	12563.62	12362.87	0.12	0.125	-1.624	11551.34	11538.91	0.121	0.121	-0.108
647	13089.77	13187.48	0.118	0.115	0.7409	14419.23	15744.42	0.131	0.131	8.4169
648	12192.3	12337.03	0.109	0.121	1.1731	12672.58	12877.76	0.129	0.128	1.5933
649	13259.85	14577.67	0.121	0.117	9.04	11846.88	12011.35	0.126	0.126	1.3693
650	11209.87	11611.88	0.111	0.121	3.4621	12397.55	12214.19	0.128	0.121	-1.501
651	11036.9	11498.78	0.143	0.143	4.0167	15076.53	15056.74	0.117	0.117	-0.131
652	10849.71	11003.14	0.119	0.127	1.3944	16189.47	17163.96	0.113	0.117	5.6775

653	12601.56	12437.38	0.117	0.124	-1.32	11175.11	11274.61	0.124	0.119	0.8825
654	14861.96	15013.89	0.13	0.129	1.0119	11922.26	12010.54	0.125	0.123	0.7351
655	12266.39	12694.2	0.136	0.133	3.3702	12687.16	13406.78	0.128	0.128	5.3676
656	10747.42	11236.37	0.141	0.144	4.3514	12701.14	13059.08	0.128	0.125	2.7409
657	12345.24	14010.88	0.111	0.114	11.888	12997.17	13097.97	0.122	0.12	0.7696
658	12342.04	13998.61	0.144	0.147	11.834	16898.89	17076.34	0.129	0.129	1.0392
659	12429.82	12442.25	0.143	0.143	0.0999	13707.97	13900.01	0.128	0.13	1.3816
660	11946.6	11959.02	0.141	0.14	0.1039	12587.76	12561.69	0.12	0.118	-0.208
661	11108.91	12546.09	0.136	0.132	11.455	13554.64	13867.03	0.126	0.124	2.2528
662	12110.13	12359.16	0.137	0.138	2.0149	11523.24	11588.3	0.123	0.123	0.5614
663	11566.84	11843.53	0.133	0.128	2.3362	11624.98	11399.45	0.122	0.121	-1.978
664	13709.68	14157.76	0.133	0.137	3.1649	11700.92	11969.45	0.132	0.133	2.2434
665	12267.38	12657.63	0.137	0.142	3.0831	11526.85	12564.43	0.132	0.13	8.258
666	12182.5	12331.59	0.113	0.116	1.2089	10958.91	11572.04	0.123	0.12	5.2983
667	13528.95	13425.15	0.112	0.114	-0.773	13255.02	13962.73	0.121	0.122	5.0686
668	12210.46	13794.97	0.137	0.131	11.486	13115.04	13250.98	0.125	0.125	1.0259
669	11266.61	14434.62	0.127	0.145	21.947	13115.63	13285.5	0.122	0.119	1.2787
670	12712.66	13956.63	0.122	0.115	8.9131	13161.3	13269.59	0.116	0.117	0.816
671	14312.61	13653.44	0.135	0.139	-4.828	12343.74	12249.89	0.128	0.126	-0.766
673	12744.5	12326.98	0.113	0.125	-3.387	12076.47	12485.92	0.12	0.124	3.2793
674	12874.76	13819.11	0.112	0.12	6.8337	15192.13	16028.96	0.134	0.137	5.2207
675	10899.21	11647.36	0.135	0.131	6.4233	12432.18	12706.36	0.119	0.124	2.1578
676	11218.43	11858.79	0.147	0.143	5.3999	10862.31	11019.71	0.134	0.134	1.4284
677	10536.66	11123.47	0.146	0.147	5.2754	13233.31	13346.33	0.117	0.114	0.8468
678	11316.55	11785.2	0.123	0.121	3.9766	14949.01	15005.82	0.125	0.123	0.3786
679	12879.72	12922.86	0.12	0.121	0.3338	11514.14	11496.36	0.123	0.12	-0.155
680	11996.46	12142.95	0.14	0.138	1.2063	10898.68	11272.18	0.12	0.126	3.3135
681	12476.66	13956.1	0.119	0.128	10.601	12682.91	12971.52	0.119	0.124	2.225
682	11687.97	13307.25	0.124	0.124	12.168	12890.53	13401.08	0.125	0.126	3.8098
683	13105.42	13654.71	0.131	0.132	4.0227	14120.77	14199.05	0.123	0.124	0.5513
684	11412.64	11832.09	0.146	0.146	3.545	11552.38	11639.96	0.119	0.121	0.7524
685	10874.33	14346.36	0.127	0.144	24.201	11288.79	11263.94	0.12	0.12	-0.221
686	12292.55	13385.24	0.121	0.129	8.1634	11762.92	11878.28	0.122	0.119	0.9711
687	11416.52	11768.99	0.137	0.133	2.9948	12847.69	12965.88	0.119	0.12	0.9116
688	11930.81	12395.11	0.137	0.132	3.7458	11495.73	11662.88	0.126	0.124	1.4332
689	12452.85	12624.18	0.138	0.136	1.3572	10361.72	10503.06	0.126	0.127	1.3457
690	12651.99	15216.88	0.136	0.136	16.856	12078.77	11575.04	0.123	0.125	-4.352
691	11439.12	12442.54	0.133	0.128	8.0644	11697.76	11941.52	0.126	0.124	2.0413
692	12207.93	11949.91	0.128	0.13	-2.159	11969.13	12002.56	0.128	0.128	0.2785
693	11697.51	11483.04	0.125	0.129	-1.868	12029.8	12431.02	0.127	0.128	3.2275
694	13480.51	13564.36	0.14	0.141	0.6181	11120.25	11237.95	0.131	0.129	1.0473
695	11945.48	12320.7	0.145	0.143	3.0454	12530.75	12703.59	0.126	0.127	1.3606
696	13438.63	13454.48	0.137	0.136	0.1179	12920.81	13019.89	0.126	0.12	0.761
697	12156.71	12920.38	0.142	0.142	5.9106	12597.14	13019.45	0.125	0.119	3.2436
698	14987.32	14625.93	0.127	0.137	-2.471	12569.29	12708.16	0.122	0.121	1.0928
699	12607.72	13967.05	0.119	0.115	9.7324	11582.63	11796.23	0.123	0.115	1.8108
700	13121.14	12727.97	0.127	0.13	-3.089	11268.71	11321.34	0.121	0.122	0.4649
701	12415.36	14526.66	0.144	0.148	14.534	12061.64	12213.41	0.118	0.114	1.2426
702	13372.11	13776.84	0.113	0.122	2.9378	11337.75	11471.09	0.12	0.118	1.1624
703	11437.53	11519.12	0.12	0.126	0.7083	14829.58	14905.14	0.129	0.132	0.507
704	13920.61	14761.42	0.123	0.123	5.696	11603.6	12173.63	0.126	0.124	4.6825

705	11501.76	11902.26	0.118	0.123	3.3649	11560.64	11984.99	0.122	0.122	3.5407
706	11053.38	11347.47	0.147	0.146	2.5917	13189.15	13344.51	0.12	0.124	1.1642
707	11357.33	11527.63	0.121	0.125	1.4773	13244.72	13629.03	0.119	0.119	2.8198
708	12704.92	12575.88	0.118	0.124	-1.026	12074.97	12415.42	0.116	0.121	2.7422
709	13927.51	15649.85	0.139	0.142	11.005	11249.19	11349.19	0.136	0.134	0.8811
710	12407.56	14219.92	0.134	0.136	12.745	14967.04	15116.63	0.127	0.127	0.9895
711	11286.72	12677.68	0.131	0.129	10.972	11067.45	11126.45	0.12	0.123	0.5302
712	12336	12730.94	0.117	0.126	3.1022	12423.61	12833.05	0.119	0.122	3.1906
713	15390.11	15704.25	0.129	0.127	2.0004	10743.95	10745.96	0.12	0.124	0.0187
714	10967.91	11382	0.133	0.128	3.6381	12958.33	13219.42	0.125	0.123	1.9751
715	12236.11	12845.35	0.146	0.145	4.7429	14301.17	13439.22	0.123	0.121	-6.414
716	13931.82	14181.49	0.121	0.129	1.7605	11069.95	11291.28	0.132	0.134	1.9602
717	11385.87	11319.39	0.114	0.121	-0.587	10739.31	10857.5	0.126	0.127	1.0886
718	12099.22	12199.93	0.109	0.118	0.8255	11661.05	12275.85	0.128	0.13	5.0082
719	11527.84	12149.7	0.128	0.131	5.1183	12547.97	12469.68	0.123	0.122	-0.628
720	10164.22	10317.99	0.146	0.147	1.4902	13973.17	14391.8	0.13	0.128	2.9088
721	12812.51	13983.05	0.136	0.143	8.3711	13107.18	13156.76	0.119	0.122	0.3769
722	11547.11	11941.41	0.145	0.143	3.302	12734.94	12861.93	0.139	0.137	0.9873
723	11991.55	12718.66	0.146	0.145	5.7169	10485.45	10460.59	0.119	0.119	-0.238
724	11821.68	12995.44	0.124	0.122	9.0321	11591.5	11641.2	0.125	0.12	0.427
725	14051.86	15032.29	0.131	0.132	6.5222	14603.76	15051.38	0.127	0.126	2.974
726	13125.77	14466.43	0.121	0.113	9.2674	11846.11	12135.94	0.126	0.128	2.3882
727	13241.33	13461.12	0.112	0.121	1.6328	11580.46	11816.44	0.125	0.128	1.997
728	11140.81	11166.97	0.144	0.143	0.2342	11554.93	11670.29	0.121	0.117	0.9885
729	10823.44	11226.02	0.147	0.147	3.5862	11648.63	11674.7	0.126	0.128	0.2233
730	12201.86	12777.1	0.115	0.125	4.5021	13348.86	13255.01	0.123	0.122	-0.708
731	11274.72	11564.93	0.137	0.136	2.5094	11368.27	11550.52	0.132	0.129	1.5779
732	11269.63	13924.08	0.126	0.141	19.064	13601.21	13824.31	0.115	0.117	1.6138
733	12909.33	13041.34	0.139	0.142	1.0122	11561.19	11667.68	0.129	0.128	0.9126
734	12335.97	15567.76	0.113	0.112	20.759	11301.22	13390.36	0.139	0.14	15.602
735	11243.63	14997.22	0.144	0.141	25.029	12147.33	12006.29	0.126	0.118	-1.175
736	13807.71	14410.26	0.133	0.134	4.1814	13272.95	13193.37	0.126	0.129	-0.603
737	14947.29	15365.4	0.131	0.127	2.7211	13389.29	13849.34	0.128	0.126	3.3218
738	13526.2	13657.59	0.126	0.13	0.962	11613.57	11923.74	0.12	0.116	2.6013
739	10929.55	11210.51	0.146	0.144	2.5062	14671.24	14571.15	0.127	0.129	-0.687
740	14084.4	14226.58	0.123	0.13	0.9994	11878.19	11981.12	0.12	0.116	0.8591
741	12171.12	14852.61	0.113	0.112	18.054	11118.27	11115.84	0.129	0.128	-0.022
742	12750.84	13225.28	0.133	0.132	3.5873	10218.19	11057.17	0.127	0.126	7.5877
743	12537.07	13923.47	0.133	0.135	9.9573	12778.14	12969.18	0.126	0.126	1.473
744	13766.81	14285.06	0.114	0.115	3.6279	11651.56	11818.72	0.122	0.12	1.4143
745	12445.37	12788.13	0.131	0.133	2.6803	11437.91	11568.03	0.123	0.122	1.1248
746	12928.7	12950.88	0.116	0.127	0.1713	12869.3	13201.94	0.127	0.128	2.5196
747	14618.93	14928.81	0.13	0.131	2.0757	11270.84	11412.17	0.127	0.128	1.2385
748	11412.11	11982.36	0.146	0.145	4.759	11552.64	11526.57	0.122	0.12	-0.226
749	11634.4	12338.34	0.122	0.125	5.7053	10904.43	10592.17	0.121	0.122	-2.948
750	14470.9	14193.65	0.132	0.14	-1.953	11507.49	11740.16	0.123	0.125	1.9818

751	9867.742	10144.55	0.148	0.146	2.7287	13353.01	13158.99	0.128	0.128	-1.474
752	12211.45	14026.72	0.113	0.112	12.942	11511.08	11947.31	0.123	0.128	3.6512
753	11570.61	12039.26	0.122	0.12	3.8927	12359.75	12347.32	0.121	0.121	-0.101
754	12777.58	12803.64	0.14	0.14	0.2036	12437.01	12563.46	0.118	0.118	1.0065
755	13414.1	14236.25	0.127	0.124	5.775	10515.8	10795.04	0.132	0.131	2.5867
756	11588.3	13769.38	0.129	0.14	15.84	11897.77	12067.98	0.135	0.132	1.4104
757	12759	14963.59	0.138	0.132	14.733	10986.35	11012.42	0.125	0.126	0.2367
758	11848.62	12377.06	0.142	0.136	4.2695	11563.43	11830.83	0.12	0.125	2.2602
759	12591.36	12639.32	0.118	0.123	0.3794	13561.27	13750.53	0.121	0.123	1.3763
760	11083.94	12221	0.125	0.125	9.3041	14737.79	14828.59	0.125	0.122	0.6123
761	11828.95	13857.01	0.123	0.124	14.636	13138.72	13126.29	0.121	0.12	-0.095
762	12376.33	12434.96	0.112	0.125	0.4715	13265.22	13263.8	0.12	0.126	-0.011
763	10357.1	10554	0.145	0.146	1.8656	12113.51	12328.9	0.131	0.13	1.747
764	12612.2	14231.93	0.125	0.122	11.381	15692.2	16026.31	0.129	0.127	2.0847
765	12763.09	13880.63	0.136	0.135	8.0511	11067.6	11643.29	0.125	0.118	4.9444
766	12611.51	13758.04	0.127	0.135	8.3335	11608.45	11745.14	0.129	0.126	1.1638
767	14942.83	15205.55	0.133	0.129	1.7278	13778.22	13782.95	0.125	0.123	0.0343
768	15454.68	15173.71	0.125	0.135	-1.852	12692.25	12806.34	0.12	0.124	0.8909
769	10833.97	11066.93	0.147	0.146	2.1051	10710.36	11650.3	0.127	0.135	8.0679
770	11656.31	11966.46	0.146	0.145	2.5919	11340.29	11848.9	0.12	0.125	4.2925
771	12326.74	12673.07	0.109	0.121	2.7328	11571.92	11525.94	0.124	0.117	-0.399
772	12736.99	13103.01	0.144	0.142	2.7934	14232.48	14651.11	0.13	0.128	2.8573
773	14487.92	14612.27	0.129	0.129	0.851	10626.32	10696.4	0.124	0.123	0.6552
774	16316.77	17074.05	0.125	0.123	4.4353	11110.34	11225.69	0.125	0.121	1.0276
775	11100.33	11429.27	0.147	0.145	2.8781	13089.79	13959.2	0.139	0.138	6.2282
776	11599.77	11771.11	0.14	0.139	1.4556	15334.51	15849.91	0.129	0.128	3.2518
777	12076.23	12472.75	0.131	0.128	3.1791	11838.63	12352.31	0.117	0.125	4.1585
778	13349.27	14689.93	0.12	0.112	9.1264	14456.45	14499.18	0.127	0.127	0.2946
779	15269.52	15399.81	0.136	0.139	0.8461	13157.45	13138.25	0.129	0.126	-0.146
780	11598.72	11685.7	0.14	0.142	0.7444	11350.45	13492.6	0.139	0.141	15.877
781	11090.72	11339.24	0.145	0.145	2.1918	11387.3	11882.48	0.123	0.126	4.1673
782	12045.64	12538.15	0.126	0.138	3.9281	11761.95	11897.9	0.13	0.128	1.1426
783	12923.85	12819.81	0.12	0.128	-0.812	10766.22	11472.82	0.133	0.134	6.1589
784	11986.52	12825.55	0.123	0.124	6.5419	11682.01	11781.51	0.127	0.123	0.8445
785	13118.46	13231.8	0.13	0.13	0.8566	13335	13332.99	0.138	0.137	-0.015
786	13867	13541.73	0.12	0.128	-2.402	13261.95	13653.92	0.123	0.124	2.8708
787	12298.15	13728.31	0.138	0.13	10.418	12443.69	12370.35	0.122	0.12	-0.593
788	14274.66	17067.03	0.139	0.132	16.361	13103.26	13307.23	0.125	0.124	1.5328
789	12148.76	12546.75	0.126	0.13	3.1721	13705.67	13832.83	0.122	0.121	0.9192
790	16084.24	17002.61	0.126	0.132	5.4014	14063.59	14103.09	0.138	0.137	0.2801
791	11542.55	12223.8	0.12	0.122	5.5731	12526.24	12794.56	0.122	0.127	2.0971
792	13068.05	12543.46	0.111	0.123	-4.182	14446	14893.63	0.131	0.129	3.0055
793	12961.08	13205.47	0.143	0.142	1.8506	11750.64	11915.2	0.135	0.135	1.3811
794	11502.27	11758.3	0.112	0.12	2.1774	10590.39	10931.05	0.131	0.133	3.1164
795	12439.78	12602.83	0.14	0.139	1.2938	13262.17	13429.15	0.126	0.127	1.2435
796	11593.27	14019.06	0.129	0.14	17.304	11189.21	11979.54	0.138	0.141	6.5973

797	12589.45	12870.66	0.126	0.131	2.1849	12815.25	12951.19	0.125	0.123	1.0497
798	13386.34	14068.23	0.113	0.122	4.847	12420.71	12394.65	0.124	0.122	-0.21
799	14141.74	14351.51	0.124	0.131	1.4617	11962.74	12254.4	0.126	0.127	2.3801
800	13240.06	14001.15	0.115	0.123	5.4359	11503.16	12141.66	0.127	0.128	5.2587
801	12729.02	13005.8	0.137	0.134	2.1281	10856.06	10994.93	0.13	0.13	1.2631
802	13429.6	14099.27	0.117	0.124	4.7497	13453.34	13792.09	0.128	0.126	2.4561
803	12663.61	15095.57	0.141	0.145	16.11	11202.45	11253.37	0.126	0.125	0.4525
804	13863.09	13690.21	0.118	0.121	-1.263	11620.96	12960.1	0.119	0.12	10.333
805	11515.68	11868.27	0.143	0.14	2.9708	10744.59	10987.76	0.127	0.127	2.2131
806	12284.23	12605.53	0.133	0.138	2.5489	14368.9	14516.68	0.13	0.132	1.018
807	13634.57	13165.16	0.12	0.128	-3.566	15062.56	15281.8	0.124	0.124	1.4346
808	13385.07	14199.34	0.119	0.128	5.7345	12188.17	11916.82	0.123	0.12	-2.277
809	11104.86	11463.6	0.144	0.145	3.1294	10058.49	10896.97	0.142	0.14	7.6946
810	14717.11	15284.8	0.131	0.125	3.7141	11697.98	11778.9	0.129	0.125	0.687
811	11442.11	11989.05	0.129	0.125	4.562	13629.68	13569.72	0.124	0.117	-0.442
812	13055.75	13681.19	0.12	0.124	4.5715	13843.68	14047.65	0.124	0.123	1.452
813	11803.35	12245.94	0.144	0.145	3.6141	15018.39	16420.07	0.126	0.127	8.5364
814	11132.54	11505.63	0.147	0.146	3.2426	11178.38	11153.52	0.124	0.124	-0.223
815	10913.2	11307.5	0.149	0.147	3.4871	16041.42	17448.25	0.122	0.124	8.0629
816	12986.69	13146.99	0.136	0.142	1.2192	10638.08	10613.23	0.12	0.12	-0.234
817	15497.9	15857.57	0.131	0.132	2.2681	10769.37	10904.1	0.128	0.127	1.2356
818	12279.09	12547.67	0.129	0.13	2.1405	11396.99	11595.69	0.129	0.132	1.7136
819	15767.87	16121.21	0.128	0.126	2.1918	13659.94	13856.26	0.127	0.129	1.4169
820	10426.3	10846.66	0.15	0.149	3.8755	12930.8	13030.3	0.122	0.119	0.7636
821	13979.6	14144.74	0.135	0.137	1.1676	13191.36	13488.6	0.129	0.125	2.2037
822	15492.24	15831.15	0.129	0.125	2.1408	13720.25	13893.56	0.12	0.116	1.2474
823	14287.54	14291.68	0.134	0.135	0.029	12399.52	12512.58	0.119	0.122	0.9035
824	11101.61	13344.52	0.126	0.14	16.808	11807.65	11933.21	0.118	0.119	1.0522
825	12819.38	12907.78	0.139	0.14	0.6849	11049.6	11309.34	0.131	0.131	2.2967
826	12755.15	12897.2	0.14	0.14	1.1014	10991.07	11204.83	0.138	0.141	1.9078
827	16395.94	16685.23	0.128	0.126	1.7338	10429.62	11365.54	0.123	0.125	8.2348
828	11679.19	11775.14	0.141	0.14	0.8148	12195.64	12336.47	0.129	0.126	1.1416
829	14505.17	14509.31	0.137	0.137	0.0285	11717.03	11846.23	0.123	0.124	1.0907
830	13703.37	14122.41	0.122	0.128	2.9672	12090.05	12213.81	0.12	0.121	1.0133
831	11472.46	11919.69	0.147	0.147	3.752	12386.39	12494.67	0.12	0.121	0.8666
832	13505.06	13647.78	0.138	0.141	1.0457	12336.95	12433.23	0.119	0.121	0.7743
833	13150.5	13693.23	0.131	0.132	3.9634	14134.35	14590.26	0.129	0.127	3.1247
834	12797.58	13091.35	0.104	0.12	2.244	11533.86	12004.11	0.126	0.127	3.9174
835	12130.15	12117.72	0.141	0.14	-0.103	13027.14	12929.15	0.125	0.123	-0.758
836	12013.63	12725.88	0.147	0.148	5.5969	10854.78	10970.14	0.122	0.119	1.0515
837	15117.45	15121.59	0.135	0.135	0.0274	11048.65	11764.49	0.128	0.127	6.0848
838	12949.18	13500.82	0.115	0.116	4.086	11667.31	12001.78	0.129	0.126	2.7869
839	10867.53	12401.79	0.139	0.146	12.371	14359.68	14660.35	0.126	0.124	2.0509
840	11285.63	11817.59	0.145	0.146	4.5014	15558.5	15643.44	0.121	0.12	0.543
841	11420.02	12782.6	0.129	0.142	10.66	14368.26	14175.37	0.124	0.119	-1.361
842	12486.15	13795.69	0.122	0.115	9.4923	12231.46	13126.92	0.121	0.116	6.8215

843	11619.26	11611.47	0.143	0.143	-0.067	12316.12	12434.32	0.125	0.126	0.9506
844	11008.27	11245.92	0.119	0.123	2.1133	11378.27	11516.17	0.129	0.128	1.1975
845	11824.91	13814.23	0.112	0.113	14.401	11502.71	11601.62	0.121	0.122	0.8525
846	11779.28	12057.82	0.111	0.119	2.3101	15705.13	15844.8	0.131	0.13	0.8815
847	12830.53	15034.95	0.123	0.114	14.662	11473.58	11573.08	0.121	0.117	0.8597
848	13018.2	13439.29	0.126	0.124	3.1333	12075.92	12175.42	0.125	0.121	0.8172
849	12456.46	12918.87	0.123	0.12	3.5793	15046.37	15246.75	0.125	0.126	1.3143
850	13125.48	14893.97	0.143	0.147	11.874	11877.71	11993.19	0.118	0.119	0.9629
851	12898.85	12446.89	0.111	0.124	-3.631	11957.86	11710.87	0.122	0.12	-2.109
852	12426.78	13238.87	0.115	0.125	6.1342	12378.66	12443.72	0.123	0.123	0.5228
853	10445.89	10810.69	0.143	0.142	3.3745	14660.88	14560.79	0.127	0.129	-0.687
854	11909.04	13298.86	0.144	0.148	10.451	13230.68	13337.87	0.119	0.12	0.8037
855	12582.78	12637.93	0.14	0.14	0.4364	11493.48	11891.51	0.123	0.128	3.3471
856	13165.69	13144.4	0.119	0.118	-0.162	11937.65	12152.12	0.123	0.128	1.7649
857	10482.05	12328.36	0.142	0.148	14.976	12054.36	13141.86	0.133	0.134	8.2751
858	10980.84	11753.54	0.136	0.133	6.5742	12222.3	12359.78	0.12	0.119	1.1124
859	11781.62	12002.38	0.11	0.121	1.8393	13318	14213.16	0.121	0.116	6.2981
860	12485.12	14413.91	0.143	0.147	13.381	12609.2	11994.39	0.124	0.129	-5.126
861	11803.46	13522.66	0.139	0.146	12.713	15512.03	15617.51	0.124	0.122	0.6754
862	12453.33	15273.68	0.126	0.144	18.465	11986	11849.1	0.125	0.119	-1.155
863	13587.98	13136.02	0.126	0.127	-3.441	10839.59	11807.51	0.135	0.137	8.1975
864	13161.6	13558.25	0.106	0.122	2.9256	12603.81	12914.77	0.126	0.128	2.4077
865	14608.5	15359.72	0.135	0.134	4.8908	12019.76	12467.8	0.119	0.116	3.5936
866	12183.6	13361.5	0.139	0.145	8.8157	13660.28	13567.56	0.115	0.119	-0.683
867	13091.78	13071.45	0.12	0.125	-0.156	14047.18	13928.31	0.126	0.128	-0.853
868	11796.19	11939.75	0.133	0.128	1.2023	13098.64	13563.54	0.131	0.126	3.4276
869	12825.66	13830.03	0.125	0.13	7.2622	12762.59	12827.65	0.121	0.121	0.5072
870	13258.75	13447.63	0.108	0.118	1.4045	12312.36	12430.55	0.122	0.123	0.9509
871	12280.04	13067.95	0.133	0.128	6.0293	11303.41	11077.88	0.122	0.121	-2.036
872	12028.45	12277.36	0.117	0.123	2.0274	12119.87	11563.8	0.118	0.115	-4.809
873	16127.08	16603.49	0.124	0.13	2.8693	10469.41	11170.02	0.14	0.139	6.2722
874	14911.43	15165.78	0.13	0.126	1.6771	13216.25	13190.18	0.119	0.117	-0.198
875	12719.91	13394.34	0.109	0.121	5.0352	10712.76	11379.96	0.125	0.13	5.8629
876	13552.89	17075.02	0.133	0.131	20.627	15176.41	15121.59	0.122	0.117	-0.363
877	15390.86	15639.64	0.134	0.135	1.5907	11134.38	11557.14	0.137	0.124	3.658
878	11820.76	13269.55	0.117	0.115	10.918	12004.23	12104.23	0.134	0.133	0.8262
879	12280.15	12335.68	0.119	0.127	0.4501	13036.34	13203.32	0.12	0.121	1.2647
880	13744.52	13992.06	0.124	0.131	1.7691	12857.97	13040.31	0.124	0.125	1.3983
881	11334.63	11716.79	0.14	0.141	3.2617	14633.46	14791.84	0.124	0.124	1.0707
882	11651.88	11615.1	0.142	0.142	-0.317	11574.64	11582.21	0.125	0.126	0.0654
883	12313.23	12775.41	0.115	0.125	3.6178	13268.15	13192.79	0.122	0.121	-0.571
884	14425.49	14508.25	0.13	0.136	0.5704	11593.36	11700.14	0.123	0.119	0.9126
885	12050.19	12452.56	0.126	0.122	3.2313	11617.11	11682.17	0.124	0.125	0.5569
886	12287.44	12167.32	0.118	0.125	-0.987	13358.78	13423.84	0.117	0.118	0.4847
887	15004.61	14629.37	0.128	0.134	-2.565	13901.32	13785.38	0.126	0.128	-0.841
888	12074.51	12527.06	0.116	0.127	3.6126	10076.1	10385.13	0.138	0.14	2.9757

889	11258.48	13009.52	0.136	0.143	13.46	11514.94	11965.77	0.13	0.124	3.7677
890	12849.77	12955.17	0.121	0.128	0.8136	11606.71	11751.52	0.122	0.119	1.2323
891	13104.11	13970.75	0.12	0.118	6.2032	11341	11347.56	0.126	0.122	0.0579
892	13683.85	14849.74	0.12	0.114	7.8513	11650.4	11715.46	0.121	0.121	0.5553
893	13326.76	13607.71	0.137	0.136	2.0647	12345.06	12549.03	0.127	0.125	1.6254
894	13862.91	13354.24	0.133	0.136	-3.809	12594.59	12694.08	0.123	0.119	0.7838
895	15055.58	14880.64	0.126	0.132	-1.176	14808.97	14844.2	0.124	0.121	0.2374
896	11744.54	12123.57	0.136	0.131	3.1264	12302	12840.65	0.127	0.127	4.1949
897	11320.86	11762.74	0.147	0.149	3.7566	14731.36	15610.11	0.136	0.138	5.6294
898	13105.6	13109.74	0.138	0.139	0.0316	11844.64	12014.81	0.122	0.119	1.4164
899	11535.35	13578.1	0.113	0.116	15.044	11168.14	11197.13	0.124	0.124	0.2589
900	12256.18	13388.52	0.124	0.12	8.4575	12373.79	12488.73	0.125	0.125	0.9203
901	13649.74	14510.33	0.117	0.119	5.9309	14492.68	15824.95	0.124	0.125	8.4188
902	13486.34	13733.91	0.132	0.13	1.8026	14014.74	15400.86	0.127	0.129	9.0003
903	13119.79	13015.49	0.101	0.118	-0.801	11329.63	11632.3	0.13	0.128	2.602
904	13673.95	13649.44	0.113	0.118	-0.18	11303.51	11421.71	0.124	0.125	1.0349
905	13003.54	13181.62	0.135	0.133	1.3509	11854.64	12128.81	0.119	0.125	2.2605
906	10925.71	11454.56	0.151	0.147	4.617	13644.17	13762.37	0.116	0.117	0.8588
907	11906.18	12252.91	0.144	0.141	2.8297	12905.46	12679.93	0.12	0.119	-1.779
908	11430.46	12252.75	0.137	0.132	6.7111	15655.86	16843.36	0.122	0.122	7.0503
909	16897.13	17187.46	0.121	0.132	1.6892	13682.57	14107.98	0.123	0.123	3.0154
910	12219.6	12378.51	0.135	0.134	1.2837	11227.41	11301.26	0.129	0.129	0.6534
911	11508.45	11991.88	0.111	0.123	4.0313	14066.33	14484.96	0.131	0.129	2.8901
912	13989.77	13974.92	0.135	0.135	-0.106	14053.91	14416.09	0.125	0.123	2.5123
913	11767.76	13068.29	0.135	0.133	9.9518	12196.83	12721.55	0.131	0.129	4.1246
914	12074.4	12728.54	0.14	0.136	5.1392	13373.4	13491.6	0.119	0.12	0.8761
915	9992.803	10185.56	0.147	0.147	1.8924	13353.87	14307.16	0.121	0.113	6.663
916	16094.34	16247.8	0.131	0.133	0.9445	10677.52	11274.54	0.135	0.138	5.2953
917	11846.44	11850.67	0.114	0.118	0.0357	11752.8	11817.86	0.123	0.123	0.5505
918	12092.17	13429.07	0.139	0.146	9.9553	12391.01	12546.24	0.127	0.124	1.2373
919	15402.69	15963.91	0.132	0.134	3.5155	12390.48	12992.52	0.129	0.122	4.6338
920	12504.82	13643.85	0.139	0.134	8.3483	12503.34	12789.44	0.129	0.126	2.237
921	11708.51	12234.7	0.136	0.133	4.3008	13642.67	13741.75	0.126	0.12	0.721
922	15347.88	15196.54	0.126	0.133	-0.996	12743.85	12874.27	0.126	0.129	1.013
923	13155.6	13989.79	0.126	0.132	5.9629	13328.39	13557.77	0.127	0.128	1.6918
924	14782.19	15275.17	0.124	0.13	3.2273	11943.36	12080.85	0.12	0.119	1.1381
925	13028.63	14284.52	0.141	0.145	8.792	11944.04	11931.61	0.119	0.119	-0.104
926	11862.5	13074.05	0.142	0.147	9.2668	12364.87	12808.59	0.133	0.129	3.4643
927	12348.28	12735.35	0.108	0.119	3.0393	11819.87	11995.85	0.13	0.129	1.467
928	13342.23	14291.19	0.119	0.123	6.6402	10351.22	10492.55	0.126	0.127	1.347
929	12034.19	13602.1	0.126	0.133	11.527	11144.42	11285.75	0.125	0.126	1.2523
930	13264.68	12879.57	0.136	0.139	-2.99	13481.89	13895.28	0.121	0.121	2.9751
931	11206.28	11615.22	0.124	0.126	3.5208	14856.39	15948.16	0.135	0.135	6.8457
932	13958.94	13516.84	0.135	0.138	-3.271	11943.85	12307.65	0.132	0.134	2.9559
933	11396.59	11414.37	0.142	0.144	0.1558	12312.09	12253.89	0.122	0.115	-0.475
934	12549.92	13212.01	0.117	0.125	5.0113	14140.76	15459.68	0.126	0.128	8.5314

935	12054.33	12343.62	0.129	0.131	2.3436	11949.46	12026.74	0.119	0.118	0.6426
936	12751.6	14865.15	0.141	0.145	14.218	10462.52	10437.67	0.119	0.119	-0.238
937	12118.52	12401.4	0.139	0.138	2.281	11477.17	11542.23	0.122	0.122	0.5637
938	11411.43	11965.52	0.145	0.143	4.6307	15184.35	15933.9	0.137	0.139	4.7041
939	12765.7	12865.7	0.107	0.115	0.7773	11579.79	11712.81	0.13	0.129	1.1356
940	15755.88	16191.15	0.125	0.128	2.6883	12644.99	12491.51	0.126	0.12	-1.229
941	14508.24	14415.22	0.126	0.129	-0.645	14273.01	14496.24	0.126	0.124	1.5399
942	11933.73	15457.82	0.14	0.139	22.798	15689.76	15939.56	0.132	0.132	1.5671
943	12770.7	16008.06	0.136	0.134	20.223	12453.67	13511.95	0.134	0.133	7.8322
944	12446.3	13744.41	0.124	0.117	9.4447	11548.33	11677.95	0.13	0.129	1.11
945	15568.5	15990.77	0.123	0.129	2.6407	12578.58	12728.7	0.128	0.129	1.1794
946	11393.07	11571.69	0.147	0.147	1.5435	13492.7	13797.38	0.131	0.129	2.2082
947	10963.02	12053.18	0.132	0.13	9.0446	10394.21	11290.99	0.132	0.133	7.9424
948	12340.05	13420.54	0.121	0.117	8.051	14345.32	15168.09	0.132	0.135	5.4244
949	11059.58	13231.41	0.139	0.147	16.414	11096.82	11124.6	0.124	0.125	0.2497
950	11559.71	11994.51	0.147	0.147	3.625	15620.72	15858.17	0.128	0.127	1.4973
951	11949.51	12011.65	0.143	0.144	0.5173	11504.88	11643.75	0.125	0.125	1.1927
952	11212.23	13019.88	0.13	0.141	13.884	13133.25	13035.26	0.125	0.124	-0.752
953	15452.19	15019.05	0.126	0.133	-2.884	15619.74	16561.21	0.132	0.132	5.6848
954	13440.38	14166.83	0.106	0.115	5.1278	14692.78	14837.51	0.122	0.121	0.9754
955	12653.08	12100.2	0.112	0.124	-4.569	11803.21	11906.14	0.12	0.116	0.8645
956	10130.98	10272.31	0.147	0.147	1.3759	15441.15	16839.36	0.124	0.124	8.3032
957	13022.13	14604.01	0.121	0.111	10.832	13450.42	13207.58	0.116	0.114	-1.839
958	10933.13	15265.92	0.143	0.141	28.382	11321.79	11282.88	0.125	0.119	-0.345
959	12010.07	12406.88	0.138	0.141	3.1983	13543.93	13896.91	0.132	0.128	2.54
960	13432.98	13663.61	0.113	0.123	1.6879	12754.82	12944.94	0.127	0.126	1.4687
961	12107.15	12338.07	0.11	0.122	1.8716	12660.4	13097.23	0.124	0.123	3.3353
962	11947.38	12403.9	0.146	0.148	3.6804	13853.48	13755.49	0.121	0.119	-0.712
963	12807.82	12806.61	0.141	0.141	-0.009	12034.7	12179.51	0.125	0.121	1.189
964	12185.55	12164.34	0.144	0.144	-0.174	11179.36	11610.22	0.133	0.133	3.7111
965	11023.11	11487.11	0.146	0.143	4.0394	15624.05	16274.56	0.129	0.13	3.9971
966	14304.72	14563.21	0.13	0.126	1.775	12481.59	12789.63	0.122	0.124	2.4085
967	12763.37	12719.11	0.104	0.114	-0.348	11981.26	11997.53	0.127	0.127	0.1356
968	12900.17	12996.74	0.138	0.139	0.743	11650.8	13018.02	0.14	0.14	10.502
969	10767.99	11196.93	0.151	0.147	3.8309	11845.28	11832.85	0.122	0.122	-0.105
970	11121.57	11382.23	0.13	0.132	2.2901	13548.48	14393.59	0.128	0.13	5.8714
971	11986.61	12162.09	0.136	0.133	1.4428	12172.45	12253.37	0.138	0.137	0.6604
972	11963.16	12082.25	0.141	0.14	0.9856	13099.88	13268.75	0.125	0.124	1.2727
973	12079.08	12076.38	0.12	0.122	-0.022	13316.79	13353.65	0.12	0.125	0.2761
974	11766.88	12378.04	0.135	0.133	4.9375	10846.33	12520.87	0.139	0.14	13.374
975	12064.33	12570.88	0.126	0.123	4.0296	11248.09	12674.52	0.131	0.129	11.254
976	13657.27	15502.79	0.134	0.136	11.904	11680.46	12128.69	0.127	0.128	3.6956
977	12190.52	12659.17	0.12	0.118	3.7021	12816.52	12912.79	0.121	0.123	0.7456
978	12105.75	15170.33	0.125	0.141	20.201	13525.02	13985.07	0.131	0.129	3.2896
979	12383.94	12745.03	0.135	0.136	2.8332	12855.05	13291.07	0.129	0.126	3.2805
980	12114.52	13302.13	0.125	0.118	8.928	11896.76	11995.46	0.13	0.132	0.8228

981	12510.43	13459.84	0.113	0.123	7.0537	10666.07	10731.13	0.129	0.129	0.6063
982	11440.79	15129.47	0.105	0.113	24.381	11242.35	11217.49	0.119	0.119	-0.222
983	13937.28	17544.52	0.136	0.132	20.561	15204.81	15660.79	0.124	0.123	2.9116
984	12510.48	12791.44	0.144	0.143	2.1964	14622.02	14664.74	0.126	0.126	0.2913
985	13151.56	13100.81	0.123	0.131	-0.387	10179.03	10611.61	0.138	0.139	4.0765
986	14344.75	14363.33	0.13	0.135	0.1293	10978.62	11153.98	0.124	0.123	1.5721
987	12437.96	12252.86	0.119	0.123	-1.511	11153.13	11228.48	0.126	0.127	0.6711
988	15547.88	16105	0.125	0.131	3.4593	12993.16	13406.98	0.118	0.119	3.0865
989	12827.17	13121.56	0.14	0.14	2.2435	14553.59	14596.31	0.127	0.127	0.2927
990	12018.48	14079.32	0.117	0.117	14.637	15029.35	16239.31	0.137	0.135	7.4508
991	12911.74	13754.2	0.12	0.119	6.1251	15278.06	15406	0.126	0.124	0.8305
992	15572.3	16821.89	0.127	0.129	7.4283	12537.46	12638.26	0.123	0.121	0.7976
993	12650.68	12797.04	0.137	0.139	1.1437	15282.37	15492.55	0.132	0.13	1.3566
994	13217.43	13762.28	0.13	0.132	3.959	11080.14	11170.14	0.134	0.133	0.8057
995	12221.13	12355.48	0.141	0.142	1.0874	12610.49	12839.87	0.126	0.128	1.7864
996	11210.34	12244.55	0.133	0.127	8.4463	12299.4	12619.44	0.12	0.123	2.5361
997	14895.05	15085.05	0.133	0.13	1.2595	11135.04	11597.33	0.132	0.131	3.9862
998	12035.2	13104.52	0.147	0.146	8.16	14893.72	16247.83	0.131	0.131	8.3341
999	12371.93	12505.77	0.139	0.14	1.0703	10738.88	11148.83	0.126	0.125	3.6771
1000	13187.54	12744.85	0.136	0.139	-3.473	12386.15	12606.99	0.121	0.125	1.7517
	Rama sample unite (1) E-W					Yeha sample unite (2) E-W				
	UM L	M L	UM C	M C	L Ch %	UM L	M L	UM C	M C	L Ch %
1	15085.54	16622.45	0.117	0.123	9.246	16035.97	15635.67	0.0938	0.0987	-2.56
2	14590.11	14667.77	0.116	0.103	0.5295	18190.44	18212.15	0.1017	0.1044	0.1192
3	17899.53	16012.93	0.1281	0.107	-11.782	15058.89	14812.23	0.0958	0.0955	-1.665
4	12320.97	12258.54	0.1099	0.093	-0.5092	16805.61	16810.26	0.0961	0.1016	0.0276
5	12223.86	12378.84	0.1197	0.119	1.2519	12079.05	12333.31	0.0997	0.0987	2.0616
6	14504.19	15180.31	0.1087	0.109	4.4539	12802.31	12903.02	0.1109	0.1135	0.7805
7	13563.92	14776.09	0.1169	0.118	8.2036	13256.86	14968.03	0.1074	0.0993	11.432
8	12778.53	12846.31	0.119	0.119	0.5276	12942.86	15678.91	0.0992	0.0968	17.451
9	13164.72	13207.44	0.1142	0.118	0.3235	14087.92	13975.49	0.1029	0.1023	-0.804
10	12188.36	12326.77	0.1243	0.124	1.1228	15018.92	14999.55	0.0978	0.0962	-0.129
11	12213.96	12808.73	0.1149	0.109	4.6434	14741.95	14709.81	0.0994	0.0994	-0.218
12	11771.59	11916.56	0.0989	0.103	1.2166	15010.44	15041.44	0.0985	0.0978	0.2061
13	12390.85	12645.11	0.1216	0.122	2.0108	14521.47	14518.33	0.1006	0.0984	-0.022
14	15463.46	17085.02	0.1148	0.121	9.4911	15902.92	15956.64	0.0994	0.103	0.3367
15	17015.35	15387.28	0.1327	0.108	-10.581	15099.83	15087.4	0.0925	0.0919	-0.082
16	11790.37	11928.78	0.1226	0.122	1.1603	12916.63	13141.28	0.1084	0.11	1.7095
17	12562.4	12690.77	0.1244	0.126	1.0115	16246.47	16553.21	0.1022	0.0993	1.8531
18	11957.01	12330.03	0.126	0.13	3.0253	16151.43	16301.72	0.0913	0.0872	0.922
19	10388.05	11167.95	0.1292	0.126	6.9834	13311.13	13586.1	0.1003	0.0981	2.0239
20	14373.14	14824.09	0.1206	0.124	3.042	13179.66	13328.95	0.1084	0.1076	1.12
21	14606.58	16182.01	0.1203	0.107	9.7357	15138.71	15767.5	0.0935	0.095	3.9879
22	11340.69	11325.34	0.1277	0.128	-0.1356	15628.71	15863.36	0.1008	0.1054	1.4792
23	12069.28	12328.69	0.1188	0.12	2.1041	13651.19	14765.33	0.0975	0.099	7.5457

24	12418.48	13031.03	0.1133	0.108	4.7007	16797.13	15444.75	0.1028	0.0809	-8.756
25	12181.41	12470.53	0.1256	0.126	2.3184	13558.15	13627.44	0.1096	0.1089	0.5085
26	16300.34	17866.33	0.1117	0.118	8.7651	15228.2	15890.83	0.0955	0.0968	4.1699
27	14984.05	15089.49	0.1247	0.123	0.6988	14085.72	14352.59	0.1032	0.1038	1.8593
28	12835.32	12973.73	0.1188	0.118	1.0668	13302.49	13641.99	0.0955	0.1055	2.4886
29	15150.82	15098.31	0.1183	0.102	-0.3478	12910.98	12918.26	0.1067	0.1044	0.0563
30	10982.47	13245.71	0.1225	0.113	17.087	13599.36	13673.47	0.1058	0.1071	0.542
31	12616.24	12766.95	0.1206	0.102	1.1805	14621.05	14664.87	0.1	0.1022	0.2988
32	15735.36	15973.53	0.1185	0.116	1.491	15090.82	15412.92	0.1077	0.1071	2.0898
33	13294.28	13579.65	0.107	0.099	2.1015	13353.57	13450.72	0.1026	0.1044	0.7223
34	12421.66	12504.5	0.1145	0.113	0.6625	16087.21	16294.69	0.1016	0.1011	1.2733
35	13496.34	13901.31	0.1276	0.132	2.9132	16194.52	14765.58	0.1063	0.0837	-9.678
36	11692.83	12255.59	0.1321	0.126	4.5918	16377.44	17222.21	0.0958	0.0969	4.9051
37	14611.62	14679.4	0.1146	0.115	0.4617	13588.71	14008.09	0.1071	0.1031	2.9938
38	13568.48	13621.41	0.1164	0.118	0.3886	13755.63	13930.18	0.1033	0.0992	1.2531
39	14301.92	13849.37	0.1165	0.114	-3.2676	13740.87	13827.44	0.1121	0.1119	0.6261
40	13596.49	13664.28	0.1147	0.115	0.4961	14879.07	16620.4	0.0984	0.0957	10.477
41	12500.85	13285.24	0.1229	0.124	5.9042	14315.22	14612	0.1154	0.1031	2.031
42	13422.65	14062.82	0.1187	0.12	4.5522	13233.03	13244.53	0.0987	0.0983	0.0869
43	17585.5	16370.89	0.1333	0.108	-7.4193	13414.56	14012.46	0.1037	0.0992	4.2669
44	12957.69	13096.09	0.1173	0.117	1.0569	13404.3	13958.53	0.1148	0.1107	3.9705
45	12999.01	13853.69	0.1194	0.121	6.1693	15092.02	15814.66	0.0918	0.0933	4.5694
46	13700.3	14463.89	0.1195	0.121	5.2793	14964.01	14959.87	0.0959	0.0947	-0.028
47	13831.44	13837.68	0.1236	0.116	0.0451	14945.99	15626.2	0.0983	0.0981	4.353
48	11412.97	11397.62	0.1223	0.123	-0.1347	12961.25	13124.47	0.1015	0.1034	1.2437
49	12707.64	12747.1	0.1112	0.099	0.3096	16822.3	15877.99	0.1038	0.0971	-5.947
50	12349.64	12494.61	0.095	0.099	1.1603	14473.86	15158.5	0.1017	0.0994	4.5166
51	13124.78	14242.09	0.1192	0.12	7.8452	13721.29	13808.95	0.0968	0.0989	0.6348
52	12013.45	12561.56	0.1196	0.118	4.3634	16522.33	17518.52	0.0983	0.1015	5.6865
53	11718.06	13609.79	0.121	0.112	13.9	16784.19	17240.43	0.0949	0.0922	2.6463
54	12278.31	12548.73	0.1293	0.132	2.1549	14188.44	14868.65	0.0997	0.0995	4.5748
55	11970.79	11993.21	0.1236	0.124	0.187	14849.4	13736.94	0.1068	0.084	-8.098
56	11326.61	11863.51	0.1275	0.125	4.5256	14618.97	14544.53	0.0978	0.098	-0.512
57	14161.62	12407.28	0.1205	0.105	-14.14	16552.77	16340.05	0.0994	0.1043	-1.302
58	12306.01	12599.65	0.1177	0.103	2.3305	13413.38	13417.82	0.1039	0.1052	0.0331
59	12398.79	12471.06	0.1237	0.123	0.5795	13036.48	13316.48	0.1085	0.1103	2.1027
60	13903.07	14161.24	0.1254	0.123	1.823	15098.92	15724.78	0.0974	0.0986	3.9801
61	12459.05	12787.16	0.1302	0.13	2.5659	14606.61	15400.25	0.0932	0.0946	5.1534
62	11785.52	12345.14	0.1318	0.127	4.5331	15865.73	14483.86	0.1065	0.0842	-9.541
63	17522.17	15782.75	0.1323	0.109	-11.021	13297.11	13502.26	0.1091	0.1107	1.5194
64	11447.59	11938.39	0.1195	0.117	4.1111	16834.25	17302.45	0.1039	0.1007	2.706
65	13891.97	13476.29	0.1236	0.105	-3.0846	13646.81	13923.17	0.1086	0.11	1.9849
66	12963.94	13916.52	0.1172	0.12	6.845	13436.73	13324.3	0.1036	0.1029	-0.844
67	12352.23	12357.59	0.1272	0.128	0.0433	15100.58	15729.36	0.0971	0.0984	3.9975
68	13744.45	14629.63	0.1201	0.109	6.0506	13828.33	13859.34	0.1006	0.0998	0.2237
69	12735.39	12731.25	0.1118	0.11	-0.0325	12034.19	12288.46	0.0999	0.0988	2.0691

70	12040.82	12665.09	0.1146	0.109	4.929	13829.35	13752.28	0.0946	0.0942	-0.56
71	13079.84	13185.28	0.1292	0.127	0.7997	15576.32	15590.84	0.1028	0.0986	0.0931
72	16359.21	18042.9	0.1146	0.119	9.3316	15755.13	16090.4	0.1061	0.0827	2.0837
73	13139.36	13469.36	0.114	0.119	2.45	13650.96	13386.02	0.1119	0.1033	-1.979
74	11750.7	11849.19	0.1275	0.127	0.8312	13776.1	13945.1	0.0931	0.1007	1.2119
75	14039.16	14123.6	0.1185	0.118	0.5978	14793	14915.93	0.1002	0.0986	0.8241
76	13691.98	13808.25	0.1216	0.124	0.8421	14101.15	14767.22	0.0979	0.0991	4.5104
77	12557.05	12529.11	0.127	0.124	-0.223	15131.05	15835.4	0.0966	0.0964	4.4479
78	12427.58	12510.42	0.1151	0.114	0.6622	12709.08	12637.87	0.1023	0.104	-0.563
79	12721.63	13172.79	0.1271	0.122	3.425	17173.65	17375.66	0.1041	0.1009	1.1626
80	13948.95	14410.37	0.112	0.116	3.202	13031.42	13733.76	0.1185	0.1092	5.114
81	12794.01	13648.69	0.1194	0.121	6.262	11964.91	13260.21	0.0975	0.0955	9.7684
82	11719.51	11741.94	0.1235	0.124	0.191	15041.24	15092.54	0.1002	0.1005	0.3399
83	12184.7	12650.17	0.1134	0.11	3.6796	13236.4	13709.78	0.0963	0.1027	3.4529
84	14349.59	14556.28	0.1185	0.121	1.4199	12718.43	12705.3	0.1049	0.107	-0.103
85	12875.1	13311.37	0.1054	0.102	3.2775	15384.42	16013.21	0.0927	0.0941	3.9267
86	12577.81	12431.45	0.1283	0.126	-1.1773	15237.44	15406.23	0.1054	0.1057	1.0956
87	13329.93	13705.83	0.1143	0.111	2.7427	15719.09	15895.74	0.0987	0.0953	1.1113
88	11228.98	11383.95	0.1238	0.123	1.3613	13653.49	13739.14	0.1051	0.1072	0.6234
89	13708.38	13748.38	0.1094	0.109	0.2909	15097.28	16438.02	0.0953	0.0889	8.1564
90	13827.95	13917.74	0.1121	0.112	0.6452	13970.84	14058.71	0.1085	0.1077	0.625
91	11202.32	11761.94	0.1288	0.124	4.7579	15022.35	15224.69	0.1048	0.1043	1.329
92	11513.39	11767.65	0.1207	0.121	2.1607	13960.64	14374.45	0.1085	0.1064	2.8788
93	17458.07	17758.28	0.1202	0.119	1.6905	14867.03	15010.97	0.1042	0.1035	0.9589
94	13460.32	13482.75	0.1247	0.125	0.1663	14260.61	14453.92	0.1093	0.1051	1.3374
95	13966.68	14072.12	0.1284	0.126	0.7493	12281.89	12263.4	0.1067	0.1085	-0.151
96	12134.17	11997.06	0.1222	0.101	-1.1428	13817.55	13688.05	0.1054	0.1059	-0.946
97	15260.44	15320.44	0.1137	0.113	0.3916	15576.44	15780.76	0.1071	0.1056	1.2947
98	12187.78	12333.05	0.114	0.112	1.1779	13593.68	13629.03	0.1068	0.1046	0.2594
99	15947.5	16396.82	0.1295	0.115	2.7403	17700.3	17855.95	0.1069	0.1052	0.8717
100	15831.01	15826.96	0.1166	0.12	-0.0256	16760.89	17282.99	0.1151	0.1116	3.0209
101	13758.06	13825.84	0.1149	0.115	0.4903	14543.68	15181.46	0.0937	0.0954	4.2011
102	16709.16	17063.72	0.12	0.119	2.0778	12652.93	12886.07	0.1172	0.1153	1.8092
103	13826.16	14795.82	0.1126	0.115	6.5536	15374.93	15864.3	0.0987	0.0952	3.0848
104	12079	12762.1	0.1315	0.134	5.3526	13474.98	13759.95	0.1104	0.108	2.071
105	11509.34	11779.76	0.1269	0.13	2.2956	15491.64	15686.62	0.1053	0.0973	1.2429
106	12334.93	12500.24	0.1194	0.11	1.3224	16002.92	16076.26	0.107	0.1106	0.4562
107	11480.7	11521	0.1195	0.101	0.3497	13596.28	13871.25	0.0996	0.0974	1.9823
108	13320.77	14865.49	0.1267	0.112	10.391	13511.63	14271.55	0.0997	0.0972	5.3247
109	15986.66	17341.95	0.1148	0.12	7.8151	14354.6	14983.38	0.0969	0.0983	4.1966
110	12384.12	13390.8	0.1242	0.123	7.5177	14615.64	14395.6	0.0996	0.0978	-1.528
111	17840.79	17166.19	0.1333	0.113	-3.9299	14731.12	14881.42	0.0948	0.0904	1.0099
112	11845.21	12221.12	0.1213	0.117	3.0759	15037.24	15163.39	0.0974	0.0999	0.832
113	13311.79	13994.89	0.131	0.133	4.8811	13958.58	16099.15	0.0943	0.0945	13.296
114	15573.79	17133.93	0.1126	0.119	9.1055	14656.91	14910.43	0.1038	0.0988	1.7003
115	13578.97	14531.56	0.1115	0.114	6.5553	17023.96	17008.81	0.1027	0.1044	-0.089

116	14012.33	13796.05	0.1212	0.109	-1.5677	17074.4	17002.89	0.0966	0.1	-0.421
117	16506.38	16285.05	0.1256	0.11	-1.3591	13903.7	13888.14	0.0987	0.1002	-0.112
118	13417.73	13537.82	0.1221	0.123	0.887	14511.4	14705.04	0.1017	0.101	1.3168
119	12898.75	13153.02	0.1235	0.124	1.9331	15987.79	16644.61	0.1032	0.1004	3.9461
120	12185.95	12128.79	0.1121	0.11	-0.4713	14940.49	13546.9	0.1057	0.0823	-10.29
121	17436.57	17691.21	0.1191	0.118	1.4394	14680.15	15342.78	0.0956	0.097	4.3189
122	13335.99	14251.94	0.1252	0.129	6.4268	16854.75	16858.19	0.0961	0.1018	0.0204
123	17998.1	17901.01	0.1364	0.112	-0.5423	14768.8	14531.02	0.103	0.1008	-1.636
124	14384.57	15423.31	0.1178	0.103	6.7348	14371.13	14159.92	0.0967	0.094	-1.492
125	11235.96	11374.37	0.1249	0.124	1.2168	16358.02	16560.03	0.1063	0.1029	1.2199
126	15968.73	17329.29	0.1126	0.121	7.8512	13828.23	14502.07	0.097	0.0979	4.6466
127	18243.69	19052.75	0.1324	0.127	4.2465	16431.04	16398.91	0.0955	0.0955	-0.196
128	12433.36	13093.69	0.1253	0.128	5.0431	13082.49	12890.06	0.1061	0.1063	-1.493
129	11583.35	12636.72	0.1212	0.124	8.3358	15973.89	16908.9	0.0954	0.1046	5.5297
130	13674.36	13742.14	0.1099	0.11	0.4932	18220.56	18114.7	0.0951	0.0992	-0.584
131	12692.02	12951.23	0.1249	0.124	2.0014	13702.84	13586.28	0.104	0.1043	-0.858
132	14035.76	14154.55	0.1151	0.117	0.8392	13832.83	13800.7	0.1023	0.1023	-0.233
133	13017.28	13580.07	0.1098	0.103	4.1443	13381.79	13678.03	0.1089	0.1053	2.1658
134	13580.34	13648.12	0.1161	0.117	0.4966	12064.11	12070.47	0.1057	0.1079	0.0527
135	17646.51	18246.92	0.1229	0.122	3.2905	15350.4	15823.21	0.1022	0.0999	2.9881
136	11539.51	11828.63	0.1242	0.124	2.4442	13934.35	13880.92	0.1048	0.1042	-0.385
137	12879.24	12930.12	0.1204	0.121	0.3935	14413.36	15311.56	0.0924	0.0937	5.8661
138	11779.32	12078.69	0.1273	0.122	2.4785	13318.95	14145.6	0.1056	0.1082	5.8439
139	13353.38	14314.01	0.12	0.109	6.7111	15751.59	14475.23	0.1059	0.092	-8.818
140	11654.58	11799.55	0.0988	0.103	1.2286	13597.66	16254.51	0.0981	0.0965	16.345
141	13693.19	13780.55	0.1161	0.115	0.634	13978.11	13841.37	0.1057	0.099	-0.988
142	12966.92	13120.97	0.1256	0.128	1.1741	12845.15	13480.92	0.1047	0.0998	4.7161
143	13268.46	13406.86	0.1257	0.125	1.0324	14186.64	14182.71	0.1039	0.1019	-0.028
144	13419.52	13708.64	0.115	0.115	2.109	17163.15	16767.39	0.1019	0.0903	-2.36
145	11726.17	12133.99	0.1274	0.128	3.361	13433.59	13638.74	0.11	0.1116	1.5042
146	14189.81	14274.25	0.1173	0.117	0.5915	16061.2	15921.2	0.1024	0.1057	-0.879
147	13280.8	13682.81	0.1155	0.116	2.9381	13723.35	13732.43	0.1036	0.1059	0.0661
148	12774.2	13710.01	0.1157	0.121	6.8257	17512.66	17222.94	0.1021	0.0868	-1.682
149	11234.78	11643.07	0.1246	0.119	3.5067	12619.51	12857.42	0.097	0.0959	1.8503
150	11821.85	11960.26	0.1253	0.124	1.1572	14669.4	14795.55	0.0976	0.1002	0.8526
151	12327.21	12768.96	0.124	0.126	3.4596	14215.08	14422.01	0.0941	0.0932	1.4348
152	12317.81	12375.8	0.0981	0.101	0.4686	17027.04	17280.47	0.1086	0.1063	1.4666
153	13730.78	14030.71	0.1097	0.097	2.1377	17682.24	18036.59	0.099	0.1016	1.9646
154	12619.77	13115.45	0.1236	0.109	3.7794	15831.74	15885.08	0.1145	0.1057	0.3358
155	12102.69	12646.48	0.1285	0.123	4.3	11081.38	11725.35	0.1079	0.1039	5.4921
156	12489.66	13383.37	0.1196	0.104	6.6778	15842.51	14636.79	0.097	0.0777	-8.238
157	14135.59	14153.66	0.1137	0.115	0.1277	14356.43	14682.17	0.1038	0.1005	2.2186
158	11744.29	12424.46	0.1279	0.131	5.4745	16415.57	16581.52	0.0972	0.0937	1.0008
159	13233.57	14349.46	0.118	0.122	7.7766	14869.8	15151.85	0.1094	0.106	1.8615
160	12656.9	12548.79	0.1193	0.121	-0.8615	15485.78	16797.62	0.0957	0.0942	7.8097
161	14844.16	15698.85	0.1134	0.115	5.4442	13653.8	14059.45	0.1052	0.1047	2.8852

162	12396.4	12486.19	0.1258	0.125	0.7191	12840.06	12981.28	0.1092	0.1111	1.0878
163	15038.19	15623.87	0.1153	0.101	3.7487	13163.29	13147.22	0.1053	0.1074	-0.122
164	12993.77	12466.98	0.1223	0.12	-4.2255	12614.59	12606.21	0.1068	0.1068	-0.066
165	12140.5	12186.07	0.1154	0.113	0.3739	17923.22	17586.86	0.097	0.1018	-1.913
166	12861.45	13558.64	0.1135	0.11	5.1421	15848.06	17106.89	0.0991	0.0964	7.3586
167	15222.46	17082.3	0.1156	0.12	10.888	14899.26	15055.21	0.1026	0.0993	1.0358
168	15155.17	15222.95	0.1134	0.114	0.4453	13373.49	13586.84	0.0886	0.0965	1.5702
169	12153.1	11753.28	0.1174	0.099	-3.4018	13039.56	13731.9	0.1166	0.1066	5.0418
170	11631.02	11687.09	0.1279	0.127	0.4797	17265.53	17270.17	0.0951	0.1005	0.0269
171	11804.16	11942.56	0.1218	0.121	1.1589	12885.5	13083.79	0.1065	0.1078	1.5155
172	12791.69	13474.79	0.1313	0.134	5.0695	14384.6	15016.23	0.0976	0.099	4.2063
173	11334.16	12177.04	0.1231	0.105	6.9219	14152.07	14795.21	0.0969	0.0978	4.3469
174	14307.45	14397.24	0.1195	0.119	0.6237	15495.05	15659.48	0.0996	0.0985	1.0501
175	11402.09	11406.23	0.1225	0.122	0.0363	14551.2	14623.42	0.1033	0.1038	0.4939
176	14600.73	14837.6	0.1165	0.117	1.5964	14941.44	15087.01	0.1092	0.1062	0.9648
177	12658.73	13254.71	0.1118	0.106	4.4964	16644.57	16389.38	0.1001	0.1003	-1.557
178	12876.65	12879.07	0.1236	0.124	0.0188	12138.02	12362.66	0.1098	0.1115	1.8171
179	15511.31	15606.75	0.1162	0.12	0.6115	14785.38	14860.11	0.1011	0.1032	0.5029
180	12124.64	12630.65	0.1125	0.106	4.0063	14231.05	14262.06	0.1007	0.0999	0.2174
181	14845.94	14918.66	0.1146	0.115	0.4874	12446.28	12651.42	0.1092	0.1109	1.6215
182	13675.55	14530.23	0.1159	0.117	5.8821	13379.89	13623.95	0.1046	0.1043	1.7914
183	13826	13931.44	0.1167	0.114	0.7569	12926.48	13137.49	0.1098	0.1117	1.6061
184	11960.49	12204.55	0.1284	0.13	1.9997	14633.89	15262.67	0.0945	0.096	4.1198
185	12766.85	12751.5	0.1231	0.123	-0.1204	16813.19	16679.25	0.0963	0.0995	-0.803
186	13839.96	13929.75	0.1198	0.119	0.6446	12855.78	12823.65	0.1043	0.1043	-0.251
187	14462.08	15550.02	0.1203	0.108	6.9964	13469.24	13527.82	0.1041	0.105	0.433
188	11922.6	12193.02	0.1298	0.133	2.2178	13654.89	13823.89	0.0943	0.1019	1.2225
189	11313.03	11716.74	0.1038	0.105	3.4456	13516.48	13647.4	0.107	0.1086	0.9593
190	14285.99	14245.78	0.1116	0.103	-0.2822	13266.08	13297.08	0.1032	0.1023	0.2332
191	11995.22	12518.28	0.1272	0.124	4.1783	14774.95	15403.74	0.0953	0.0966	4.082
192	13554.48	14409.16	0.1163	0.118	5.9315	13240.53	13167.6	0.0991	0.0991	-0.554
193	11382.41	11622.23	0.1248	0.127	2.0635	14212.37	15538.38	0.1008	0.0909	8.5338
194	12555.14	12539.78	0.1254	0.126	-0.1225	14498.04	14711.76	0.099	0.101	1.4528
195	12113.54	12809.73	0.1134	0.109	5.4348	12538.58	13021.01	0.096	0.1096	3.705
196	13331.9	13425.33	0.1097	0.109	0.6959	15347.17	15311.52	0.101	0.1046	-0.233
197	11365.25	12007.54	0.1222	0.12	5.3491	17218.16	17725.35	0.101	0.101	2.8614
198	11801.5	12055.76	0.1187	0.119	2.1091	16720.84	16898	0.099	0.0955	1.0484
199	12233.18	12868.1	0.1207	0.118	4.9341	17398.97	17589.47	0.1066	0.1054	1.083
200	11380.96	11365.61	0.1232	0.124	-0.1351	15307.28	15472.42	0.0925	0.0906	1.0674
201	11849.51	11921.65	0.1237	0.125	0.6051	14101.34	14068.2	0.1055	0.1061	-0.236
202	11995.52	12067.65	0.1228	0.124	0.5977	14108.44	14333.09	0.1092	0.1106	1.5673
203	11911.59	12024.31	0.1268	0.127	0.9374	16160.08	14720.5	0.1048	0.091	-9.779
204	15118.17	15738.83	0.1292	0.125	3.9435	11895.24	12154.44	0.0987	0.1091	2.1326
205	13138.35	13652.32	0.127	0.11	3.7647	15510.4	15843.96	0.1088	0.1066	2.1052
206	12445.05	12601.33	0.1192	0.102	1.2401	14705.5	14817.72	0.0942	0.0923	0.7573
207	11728.19	11998.61	0.1287	0.132	2.2537	16912.89	16936.24	0.0967	0.1007	0.1378

208	12690.33	12758.11	0.1177	0.118	0.5313	13649.56	13649.85	0.1047	0.1069	0.0022
209	13278.42	13368.21	0.1223	0.122	0.6717	14441.85	14848.33	0.095	0.0974	2.7376
210	11774.58	13568.11	0.1191	0.11	13.219	15643.33	16011.74	0.1045	0.0813	2.3009
211	14355.62	14593.78	0.1208	0.118	1.6319	17314.81	17115.73	0.0976	0.1023	-1.163
212	12290.49	12428.9	0.1217	0.121	1.1136	14470.36	15135.92	0.0971	0.0985	4.3972
213	11867.47	13580.8	0.1202	0.105	12.616	14792.66	14899.02	0.0918	0.09	0.7139
214	12270.25	11518.46	0.1273	0.107	-6.5268	16453.46	16655.47	0.104	0.1007	1.2129
215	14083.49	14319.47	0.1231	0.127	1.648	17007.58	16406.26	0.1022	0.0928	-3.665
216	12177.82	13039.65	0.1203	0.118	6.6093	14926.4	17264.04	0.0947	0.0947	13.541
217	12647	14000.2	0.1227	0.124	9.6655	13917.35	14231.67	0.1097	0.1093	2.2086
218	15381.65	15449.43	0.1122	0.113	0.4387	14699.28	15382.41	0.0987	0.0986	4.441
219	15369.49	15147.95	0.1172	0.109	-1.4625	13685.58	13801.23	0.1057	0.1042	0.838
220	14252.84	14491	0.123	0.12	1.6435	15735.37	15598.71	0.0968	0.0949	-0.876
221	12769.72	13886.82	0.1195	0.124	8.0444	14802.68	15191.43	0.1105	0.1093	2.559
222	12812.69	13218.84	0.121	0.12	3.0725	18172.66	17982.95	0.1015	0.1015	-1.055
223	11086.02	11489.73	0.1081	0.109	3.5137	12649.35	12882.49	0.1185	0.1165	1.8097
224	11626.73	11587.74	0.1233	0.123	-0.3365	13832.49	14091.69	0.0969	0.0972	1.8394
225	12747.15	14328.85	0.1226	0.109	11.039	12050.11	12433.16	0.0994	0.0985	3.0809
226	14274.24	12577.39	0.1138	0.097	-13.491	17303.94	17785.54	0.1116	0.1074	2.7078
227	11747.83	11785.62	0.1248	0.124	0.3206	14455.91	14507.21	0.1007	0.101	0.3536
228	14587.1	14367.66	0.1113	0.108	-1.5274	16439.93	17461.59	0.1055	0.1004	5.8509
229	13117.42	14474.75	0.1217	0.123	9.3773	12325.38	12545.8	0.0939	0.0951	1.7569
230	14235.31	15183.12	0.1216	0.111	6.2426	16745.26	16610.61	0.0967	0.1008	-0.811
231	12961.88	12309.08	0.1301	0.109	-5.3033	14426.42	15069.56	0.097	0.0979	4.2678
232	14335.05	14402.83	0.1144	0.115	0.4706	14666.26	15014.22	0.1072	0.1045	2.3175
233	12947.82	13704.44	0.1123	0.102	5.521	16843.53	17038.46	0.103	0.1087	1.1441
234	14648.66	14885.73	0.1171	0.117	1.5926	13756.01	13780.06	0.1019	0.1005	0.1746
235	14137.69	14375.86	0.1222	0.12	1.6567	13821.78	15174.66	0.1041	0.0984	8.9154
236	16399.42	16496.77	0.1358	0.111	0.5901	14074.83	14083.91	0.1028	0.105	0.0645
237	12080.46	12110.96	0.1193	0.12	0.2519	16994.76	17149.49	0.1088	0.1099	0.9022
238	13198.04	13303.48	0.1286	0.126	0.7926	13083.67	13010.74	0.1009	0.1009	-0.561
239	19500.84	16785.03	0.1309	0.108	-16.18	15952.5	15880.99	0.0975	0.1012	-0.45
240	12634.38	12693.87	0.1173	0.123	0.4687	14214.93	14612.79	0.1098	0.1049	2.7227
241	16830.91	16080.94	0.1347	0.113	-4.6637	12356.6	12306.8	0.1101	0.1083	-0.405
242	13787.74	14234.36	0.1176	0.12	3.1376	14505.08	14620.23	0.0967	0.0949	0.7876
243	12420.05	12697.83	0.126	0.123	2.1876	15963.98	16589.84	0.0919	0.0933	3.7725
244	18361.42	17347.94	0.1335	0.11	-5.8421	14759.01	15640.93	0.096	0.0972	5.6386
245	16638.06	15933.87	0.1261	0.115	-4.4195	13250.12	13436.9	0.0939	0.0954	1.39
246	12581.62	12714.67	0.1172	0.116	1.0464	15997.51	16217.98	0.1064	0.1056	1.3594
247	16749.88	17050.08	0.1202	0.119	1.7607	13704.39	13915.39	0.1096	0.1113	1.5163
248	13779.48	13360.66	0.1246	0.107	-3.1347	15799.37	16177.12	0.1057	0.1051	2.3351
249	15788.5	15955.99	0.1261	0.125	1.0497	15004.31	15152.68	0.0999	0.1019	0.9792
250	14332.37	14757.93	0.116	0.119	2.8836	12395.5	12618.14	0.1003	0.1088	1.7644
251	13063.89	13183.97	0.1212	0.122	0.9109	16932.15	15987.84	0.1039	0.0972	-5.906
252	12141.09	12499.92	0.1266	0.12	2.8706	13142.58	13072.78	0.1061	0.1054	-0.534
253	12208.64	13237.76	0.1256	0.114	7.7741	16356.56	16285.05	0.0972	0.1007	-0.439

254	13138.94	13417.64	0.127	0.129	2.0771	13525.04	13740.39	0.0981	0.1088	1.5673
255	11782.05	11903.89	0.1197	0.12	1.0235	15809.19	15763.75	0.1159	0.1073	-0.288
256	12535.6	12625.39	0.1244	0.124	0.7112	12581.24	13081.66	0.1136	0.1048	3.8253
257	12861.18	13115.44	0.119	0.119	1.9387	14410.66	16198.69	0.0997	0.0961	11.038
258	12742.04	12880.44	0.1211	0.12	1.0745	14165.81	14334.6	0.1091	0.1093	1.1775
259	15429.45	15674.01	0.1188	0.119	1.5603	14353.17	14521.96	0.1076	0.1078	1.1623
260	12433.38	12523.17	0.1253	0.125	0.717	15075.99	15704.78	0.0953	0.0967	4.0038
261	13039.64	13246.33	0.1236	0.127	1.5604	11248.35	11685.46	0.105	0.1035	3.7406
262	11449.96	11772.16	0.11	0.106	2.737	13088.32	13084.39	0.1051	0.1029	-0.03
263	13157.35	13247.14	0.1203	0.12	0.6778	15757.51	15788.52	0.0968	0.0961	0.1964
264	14330.91	14398.69	0.1162	0.117	0.4707	15695.51	15736.73	0.0941	0.0925	0.2619
265	11798.04	12068.46	0.1286	0.131	2.2407	14925.21	16231.31	0.0944	0.089	8.0468
266	12592.31	13151.25	0.1093	0.103	4.2501	15927.46	17166.78	0.094	0.0883	7.2193
267	11111.99	11450.52	0.126	0.127	2.9564	13402.78	13526.42	0.1033	0.1017	0.9141
268	11924.2	11815.71	0.1178	0.113	-0.9182	13375.1	13460.45	0.1116	0.1115	0.6341
269	12171.92	12254.13	0.1214	0.123	0.6709	16951.81	17209.68	0.1036	0.1083	1.4984
270	14189.34	13999.63	0.1197	0.108	-1.3551	13329.83	13540.83	0.1084	0.1102	1.5583
271	12500.11	12800.82	0.1264	0.123	2.3492	14218.48	14373.63	0.1054	0.1049	1.0794
272	13875.77	12323.4	0.1086	0.1	-12.597	15875.39	16070.62	0.1015	0.1079	1.2148
273	13109.01	14195.82	0.1176	0.118	7.6559	15221.92	16333.17	0.0926	0.0895	6.8036
274	11104.22	11382.92	0.1261	0.129	2.4484	13126.07	12922.72	0.1107	0.108	-1.574
275	12990.03	12932.04	0.1221	0.124	-0.4484	13416.94	13532.59	0.1086	0.1104	0.8546
276	17165.14	17465.35	0.1193	0.118	1.7189	15293.19	15976.32	0.0983	0.0981	4.2759
277	12931.31	12459.35	0.1272	0.108	-3.788	13526.48	15757.94	0.0883	0.0943	14.161
278	16009.85	15792.28	0.1082	0.107	-1.3777	12186.83	12207.04	0.1095	0.1107	0.1655
279	14148.12	14215.91	0.1152	0.116	0.4768	14602.71	14652.08	0.101	0.0997	0.337
280	17567.87	17068.61	0.1266	0.11	-2.925	15385.26	15399.4	0.1095	0.1025	0.0918
281	12776.68	12772.63	0.1236	0.123	-0.0318	13378.58	13401.3	0.1043	0.1063	0.1695
282	13590.6	13658.38	0.1182	0.119	0.4963	15139.79	15170.79	0.0984	0.0976	0.2044
283	15112.47	15849.04	0.1184	0.124	4.6474	16184.99	16062.77	0.0989	0.1031	-0.761
284	11464.81	12915.99	0.1207	0.123	11.236	13076.72	12960.15	0.1054	0.1058	-0.899
285	12777.71	13012.48	0.1221	0.125	1.8042	15928.21	16505.2	0.0941	0.0918	3.4958
286	12849.7	14219.46	0.1227	0.124	9.633	13642.91	14326.34	0.1033	0.1019	4.7705
287	13765.86	13871.3	0.1235	0.121	0.7601	13060.96	12948.53	0.1052	0.1046	-0.868
288	11390.4	11878.3	0.1259	0.126	4.1075	14293.57	14555.7	0.1032	0.1093	1.8009
289	14461.2	13678.65	0.1121	0.112	-5.7209	15474.9	14081.31	0.1043	0.0815	-9.897
290	13762.59	13860.37	0.1139	0.114	0.7055	14222.47	14382.06	0.0986	0.1026	1.1096
291	13365.2	13900.17	0.1233	0.125	3.8487	17493.52	17358.87	0.0981	0.102	-0.776
292	12105.64	12598.4	0.1259	0.123	3.9113	14759.98	14724.33	0.0926	0.0942	-0.242
293	15997.63	15788.13	0.1121	0.111	-1.3269	13256.84	13487.34	0.1088	0.1104	1.709
294	11711.55	12208.57	0.1272	0.122	4.0711	14642.29	14630.78	0.099	0.098	-0.079
295	12738.64	12839.06	0.1108	0.11	0.7821	14481.26	14690.76	0.1063	0.1053	1.426
296	12679.26	13023.73	0.121	0.103	2.645	14559.3	14549.89	0.1077	0.1092	-0.065
297	12967.94	13058.91	0.1257	0.124	0.6966	13397.58	13420.3	0.1064	0.1085	0.1693
298	17623.97	15665.73	0.1255	0.104	-12.5	14437.02	14785.43	0.1066	0.1069	2.3564
299	12968.19	13073.63	0.1284	0.126	0.8065	18945.1	18360.06	0.099	0.09	-3.187

300	14227.54	14347.62	0.1145	0.116	0.837	14196.96	14552.73	0.1044	0.1045	2.4447
301	14758.85	14864.29	0.1091	0.107	0.7094	13252.65	13359.8	0.1012	0.103	0.8021
302	11102.97	11639.87	0.1237	0.121	4.6126	13224.73	13246.36	0.1024	0.1024	0.1633
303	13070.84	13155.28	0.1194	0.119	0.6418	16230.44	14874.93	0.1029	0.081	-9.113
304	12803.79	12518.9	0.1227	0.125	-2.2757	14384.51	14776.1	0.1026	0.0996	2.6502
305	11675.87	13107.65	0.1199	0.122	10.923	15667.56	16033.3	0.0971	0.0933	2.2811
306	11649.2	12080.26	0.1272	0.125	3.5683	14365.04	14248.47	0.1049	0.1052	-0.818
307	14581.61	15345.78	0.1304	0.115	4.9797	14233.68	14059.03	0.1022	0.0991	-1.242
308	11819.88	12652.93	0.1279	0.115	6.5839	13875.72	13961.08	0.1101	0.1099	0.6114
309	12698.21	12720.64	0.1223	0.122	0.1763	11567.47	11869.01	0.103	0.1022	2.5406
310	12927.79	13123.96	0.1101	0.103	1.4947	15246.04	15365.83	0.0948	0.0929	0.7796
311	19377.2	16673.82	0.1328	0.109	-16.213	15709.19	15817.65	0.1009	0.0979	0.6857
312	16846.92	14990.7	0.1282	0.099	-12.383	14289.89	14184.33	0.1027	0.1023	-0.744
313	12448.72	13882.41	0.1201	0.124	10.327	13139.29	13349.5	0.1036	0.1015	1.5747
314	12499.27	12589.06	0.1242	0.124	0.7133	12574.52	12597.25	0.1062	0.1084	0.1804
315	11733.78	12836.86	0.1209	0.105	8.5931	16191.86	16376.76	0.1071	0.1007	1.1291
316	12143.84	12381.53	0.1285	0.129	1.9198	15330.7	15959.48	0.0957	0.0971	3.9399
317	14027.61	14299.74	0.1138	0.117	1.9031	12750.81	12941.1	0.1095	0.1108	1.4705
318	16065.38	16748.48	0.113	0.116	4.0786	15698.92	16407.21	0.097	0.0978	4.3169
319	12991.13	13687.54	0.1054	0.111	5.0879	14535.64	14531.7	0.1033	0.1014	-0.027
320	12149.12	12167.19	0.1154	0.117	0.1486	14576.28	14715.57	0.0914	0.0957	0.9465
321	13216.14	13303.42	0.1188	0.119	0.6561	14175.43	14493.59	0.1031	0.0992	2.1952
322	15301.77	15078.43	0.1197	0.109	-1.4812	15892.83	16575.97	0.0962	0.0962	4.1213
323	12587.33	12228.75	0.1242	0.118	-2.9323	15600.05	16283.19	0.0973	0.0972	4.1954
324	11520.85	12286.53	0.1152	0.109	6.2319	13485.1	13710.87	0.0951	0.1008	1.6467
325	11837.77	12071.33	0.1293	0.131	1.9348	17234.26	17424.76	0.1072	0.106	1.0933
326	12182.39	13108.41	0.1201	0.122	7.0643	12188.4	12371.24	0.1022	0.1038	1.478
327	12488.99	12743.25	0.1204	0.121	1.9953	15840.16	16016.81	0.0999	0.0964	1.1029
328	14564.67	14309.36	0.1234	0.121	-1.7842	16042.27	16314.57	0.0967	0.093	1.6691
329	13518.76	13974.07	0.1254	0.12	3.2582	14361.85	14373.36	0.0961	0.0958	0.0801
330	17080.89	15319.14	0.1318	0.107	-11.5	13733.92	14157.44	0.1066	0.1026	2.9915
331	12942.45	13080.86	0.1164	0.116	1.0581	13022.58	13151.57	0.104	0.1035	0.9808
332	16183.25	13916.86	0.1228	0.098	-16.285	13694.83	13942.02	0.1128	0.1116	1.773
333	12131.23	12203.36	0.1262	0.128	0.5911	14586.1	14402.97	0.1037	0.1019	-1.272
334	14462.99	14886.67	0.1183	0.12	2.846	16210.74	17881.4	0.0943	0.0869	9.343
335	12699.98	12767.76	0.1177	0.118	0.5309	14445.58	14517.79	0.1038	0.1043	0.4974
336	14877.54	15560.64	0.1176	0.12	4.3899	16719.24	16921.25	0.1057	0.1024	1.1938
337	11763.51	11726.23	0.1252	0.124	-0.3179	14841.54	14508.02	0.1005	0.0954	-2.299
338	11507.95	11646.35	0.125	0.124	1.1884	12027.18	12019.91	0.1069	0.1088	-0.061
339	12379.51	13523.69	0.12	0.122	8.4605	13264.44	13290.09	0.1066	0.1087	0.193
340	11565.87	11588.3	0.1247	0.125	0.1935	13235.18	13544.18	0.0957	0.1058	2.2814
341	13689.06	14007.71	0.1043	0.098	2.2748	15831.08	15846.64	0.1022	0.1055	0.0982
342	13396.02	13507.52	0.1187	0.119	0.8255	12568.96	12583.81	0.1109	0.1094	0.118
343	11684.72	11873.21	0.1259	0.123	1.5875	12865.12	12850.48	0.106	0.104	-0.114
344	12676.65	12673.72	0.1232	0.123	-0.0231	18217.7	17594.37	0.0997	0.0907	-3.543
345	13828.42	13948.5	0.1181	0.119	0.8609	12624.67	12676.09	0.1007	0.0989	0.4057

346	18954.65	16543.32	0.1337	0.106	-14.576	14121.41	14228.57	0.0999	0.1016	0.7531
347	15345.93	16069.69	0.1188	0.122	4.5039	14346.75	15376.67	0.0982	0.0965	6.6979
348	11824.43	11962.83	0.1214	0.121	1.157	14821.94	14837	0.103	0.0803	0.1015
349	12217.65	12754.55	0.1256	0.123	4.2095	14225.15	16386.94	0.0917	0.0931	13.192
350	13108.97	12193.25	0.1108	0.1	-7.5101	14770.53	14855.26	0.0995	0.1012	0.5704
351	12345.88	12202.21	0.1224	0.121	-1.1775	13488.2	14084.39	0.1037	0.0997	4.233
352	11985.58	12543.61	0.1207	0.103	4.4487	15564.81	14062.73	0.1073	0.0841	-10.68
353	14806.93	15751.17	0.1272	0.109	5.9948	14388.03	15013.89	0.0962	0.0976	4.1685
354	15441.19	16921.24	0.1182	0.123	8.7467	13824.28	13937.88	0.1081	0.1074	0.8151
355	13525.45	13521.31	0.1107	0.109	-0.0306	14727.12	15035.58	0.1063	0.1059	2.0515
356	12314.68	12997.78	0.1315	0.134	5.2555	13251.61	13426.96	0.1087	0.1072	1.306
357	13861.41	13929.19	0.1171	0.117	0.4866	13950.43	14295.87	0.1128	0.1081	2.4164
358	12152.98	12223.4	0.0981	0.1	0.5761	14313.24	14942.02	0.0965	0.0979	4.2082
359	11488.83	11485.9	0.1212	0.121	-0.0255	15013.85	15090.21	0.0925	0.0909	0.506
360	11635.82	12015.44	0.1215	0.107	3.1594	14158.03	14433	0.0995	0.0974	1.9052
361	17607.31	15612.01	0.1289	0.107	-12.781	14162.47	14522.85	0.108	0.105	2.4815
362	11406.4	11880.79	0.123	0.127	3.9929	13590.77	15883.15	0.0995	0.0986	14.433
363	13529.76	14039.38	0.1227	0.124	3.6299	15821.42	15975.53	0.1082	0.1049	0.9646
364	14543.66	15092.41	0.1153	0.119	3.6359	15500.34	16126.2	0.0946	0.0959	3.881
365	18940.42	16500.06	0.1329	0.107	-14.79	16665.05	17048.9	0.1095	0.1022	2.2515
366	11324.04	11966.33	0.1226	0.12	5.3675	13529.94	15282.02	0.1012	0.0976	11.465
367	12412	12424.43	0.1268	0.129	0.1	13903.36	14220.01	0.1126	0.1105	2.2268
368	16633.91	16108.6	0.1215	0.106	-3.261	15934.07	16400.05	0.1022	0.1007	2.8413
369	15240.39	15489.51	0.1112	0.113	1.6083	14129.42	14555.16	0.1077	0.1068	2.925
370	12344.6	12106.33	0.1235	0.122	-1.9681	14558.79	14341.21	0.0991	0.0988	-1.517
371	12582.46	11918.46	0.1272	0.108	-5.5712	18136.57	18040.92	0.0982	0.1017	-0.53
372	12302.25	12527.39	0.1223	0.103	1.7972	12902.97	13129.24	0.1043	0.1107	1.7234
373	12293.72	12325.64	0.1299	0.131	0.259	17141.44	16980.8	0.1025	0.0879	-0.946
374	11549.39	11736.17	0.1226	0.12	1.5915	13203.02	13550.71	0.0993	0.0972	2.5659
375	14087.21	13912.14	0.1187	0.109	-1.2583	13107.11	13325.69	0.1046	0.1049	1.6403
376	11674.99	12188.34	0.1218	0.108	4.2118	13492.38	13725.01	0.1042	0.1021	1.695
377	13401.08	13468.86	0.1167	0.117	0.5032	12537.96	12812.1	0.1123	0.1065	2.1397
378	18141.04	15679.88	0.1326	0.107	-15.696	12677.51	12824.29	0.1085	0.1063	1.1445
379	13268.86	13286.94	0.1138	0.115	0.136	14802.14	14818.5	0.1032	0.1024	0.1104
380	15331.53	15399.31	0.1138	0.114	0.4402	17453.6	16946.24	0.0957	0.1015	-2.994
381	12877.76	12967.55	0.1277	0.127	0.6924	14072.79	14221.29	0.1077	0.1068	1.0442
382	13907.8	14013.25	0.1258	0.124	0.7524	14150.31	14178.09	0.1042	0.1022	0.1959
383	12903.68	13586.78	0.1283	0.131	5.0277	15842.28	15893.58	0.0983	0.0986	0.3228
384	11940.63	12922.66	0.1244	0.126	7.5993	13299.5	13256.66	0.0995	0.1007	-0.323
385	12942.35	13032.14	0.1162	0.116	0.689	12731.3	12740.38	0.1063	0.1088	0.0713
386	13753.26	14203.92	0.1057	0.1	3.1728	12800.88	12862.81	0.1117	0.1115	0.4814
387	13018.89	13169.6	0.1138	0.114	1.1444	15303.75	14801.74	0.1097	0.0999	-3.392
388	13570.31	13714.57	0.1242	0.106	1.0519	17345.02	17249.37	0.0976	0.1012	-0.555
389	11854.67	11892.45	0.1244	0.124	0.3177	16179.45	16850.87	0.0956	0.0967	3.9845
390	12592.36	12737.33	0.0936	0.097	1.1382	13127.39	13829.52	0.1019	0.1027	5.0771
391	12785.98	12868.82	0.1174	0.116	0.6437	14533.12	15057.65	0.1054	0.1048	3.4834

392	13351.29	12445.65	0.1245	0.105	-7.2767	16130.23	14737.14	0.1051	0.0832	-9.453
393	13030.26	13052.69	0.1264	0.126	0.1718	15049.28	15678.06	0.0963	0.0977	4.0106
394	12097.63	12344.11	0.1291	0.13	1.9968	16334.46	16963.25	0.094	0.0953	3.7068
395	12341.3	13281.46	0.1172	0.119	7.0787	13275.51	13332.88	0.1019	0.1024	0.4303
396	13543.09	12423.23	0.1243	0.105	-9.0143	16210.61	16994.75	0.0951	0.0956	4.614
397	12144.82	11469.22	0.1156	0.104	-5.8905	14166.08	14308.5	0.1026	0.1005	0.9954
398	14033.33	14153.42	0.1181	0.119	0.8485	14206.4	14335.39	0.1013	0.1009	0.8998
399	12508.49	12419.38	0.1221	0.123	-0.7176	17001.53	16866.89	0.096	0.1	-0.798
400	11910.82	12278.61	0.1181	0.12	2.9953	15409.81	14066.02	0.1054	0.0839	-9.554
401	18836.01	16385.89	0.1334	0.106	-14.953	13742.38	13827.73	0.1114	0.1112	0.6173
402	15111.03	15053.66	0.1171	0.1	-0.3811	12177.54	12130.97	0.1047	0.1039	-0.384
403	13552.73	13691.02	0.1167	0.117	1.01	16335.73	14999.93	0.1048	0.0832	-8.905
404	13043.23	13651.63	0.1111	0.106	4.4567	13096.86	13139.2	0.1004	0.0993	0.3222
405	13492.09	13597.54	0.1281	0.126	0.7754	17227.74	17211.68	0.0954	0.1006	-0.093
406	12712.54	12850.95	0.1165	0.116	1.077	14602.29	14775.72	0.0997	0.0985	1.1738
407	12667.82	13084.6	0.1283	0.128	3.1852	13459.88	13386.95	0.1015	0.1015	-0.545
408	11913.16	13040.98	0.1212	0.119	8.6483	15086.91	15770.05	0.0967	0.0966	4.3319
409	14315.32	12898.17	0.1165	0.101	-10.987	14831.73	15460.51	0.0947	0.0961	4.067
410	12169.37	11724.31	0.1259	0.12	-3.7961	14114.95	14183.44	0.1078	0.102	0.4829
411	18715.68	17046.72	0.1336	0.109	-9.7905	15040.76	14601.68	0.109	0.1	-3.007
412	12511.42	12929.24	0.1277	0.11	3.2316	13662.92	13812.21	0.1099	0.1091	1.0809
413	13587.93	14196.34	0.1093	0.105	4.2857	12110.32	12163.75	0.1061	0.1067	0.4393
414	12981.15	13455.96	0.1285	0.112	3.5286	14707.21	14757	0.1032	0.1039	0.3374
415	13699.61	13789.4	0.1209	0.121	0.6512	17394.67	17323.16	0.0935	0.0968	-0.413
416	13485.99	14585.28	0.1253	0.129	7.537	13560.16	13861.55	0.1093	0.1087	2.1743
417	14797.21	13390.06	0.1125	0.099	-10.509	14480.49	14413.42	0.1035	0.1024	-0.465
418	11636.14	11890.41	0.1243	0.125	2.1384	14147.61	14810.04	0.0961	0.0972	4.4728
419	10877.53	11163.72	0.1252	0.127	2.5636	12253.61	12311.68	0.1024	0.1063	0.4717
420	12972.29	13254.73	0.1129	0.104	2.1309	13128.32	13235.18	0.1052	0.1054	0.8074
421	12382.99	12831.2	0.1154	0.104	3.4931	13439.56	13322.99	0.1059	0.1063	-0.875
422	16503.39	16621.17	0.1223	0.122	0.7086	16558.48	16558.48	0.101	0.1058	0
423	13087.23	13105.31	0.1158	0.117	0.1379	13816.11	13783.98	0.1018	0.1018	-0.233
424	12233.34	12712.78	0.1138	0.106	3.7714	13960.83	14589.62	0.0951	0.0965	4.3098
425	12995.27	14132.17	0.1161	0.116	8.0448	15808.42	15868.42	0.0942	0.0924	0.3781
426	11914.31	13486.6	0.114	0.106	11.658	13144.14	13364.77	0.0978	0.0972	1.6508
427	14753.31	14821.09	0.1147	0.115	0.4573	13236.09	13501.07	0.0957	0.0952	1.9626
428	16040.62	16195.89	0.1109	0.107	0.9587	13977.49	15440.37	0.1052	0.0963	9.4744
429	12443.75	13763.29	0.1155	0.106	9.5873	12391.18	13103.43	0.1093	0.1035	5.4356
430	13606.35	13903.35	0.1081	0.095	2.1362	15068.57	15039.57	0.0995	0.0993	-0.193
431	12678.1	12816.51	0.1202	0.119	1.0799	15205.7	15368.42	0.1027	0.1018	1.0588
432	12990.95	13269.65	0.1276	0.13	2.1003	16691.97	17368.07	0.1025	0.0999	3.8928
433	10718.73	11589.01	0.1328	0.123	7.5095	14917.08	15557.08	0.0971	0.0973	4.1139
434	13714.66	13670.72	0.1104	0.111	-0.3214	12989.02	12967.31	0.1049	0.1043	-0.167
435	12233.61	12876.15	0.1133	0.109	4.9902	13375.43	13406.43	0.1026	0.1018	0.2313
436	10775.63	10772.7	0.1308	0.13	-0.0272	14927.56	15610.7	0.0995	0.0993	4.3761
437	13782.02	12996.55	0.1105	0.111	-6.0437	14235.61	14323.27	0.099	0.1008	0.612

438	12009.07	11954.31	0.1198	0.115	-0.4581	12964.27	12890.83	0.1045	0.1017	-0.57
439	12017.27	12423.42	0.1215	0.121	3.2692	12881.55	12953.76	0.1045	0.105	0.5575
440	12082.44	12286.59	0.1261	0.128	1.6615	16504.68	15581.94	0.1022	0.0923	-5.922
441	11943.36	12015.49	0.1198	0.121	0.6003	12399.82	12664.79	0.098	0.0974	2.0922
442	12548.73	12491.33	0.1205	0.101	-0.4595	17679.73	17726.51	0.1001	0.1035	0.2639
443	16537.98	17817.39	0.1249	0.125	7.1807	15219.28	15848.06	0.0973	0.0986	3.9676
444	14792.26	15491.58	0.1143	0.116	4.5142	13795.48	13930.58	0.1052	0.0992	0.9698
445	12596.51	12660.82	0.1105	0.099	0.508	14534.74	15244.24	0.1045	0.0972	4.6542
446	12856.99	12924.77	0.1104	0.111	0.5244	14336.11	14303.98	0.1012	0.1012	-0.225
447	13173.61	13144.7	0.1249	0.122	-0.2199	14634.45	15472.73	0.0945	0.0962	5.4178
448	13695.36	13895.77	0.1213	0.124	1.4423	14105.92	14326.55	0.0956	0.0951	1.54
449	16152.74	15791.58	0.1283	0.113	-2.2871	15113.71	15742.5	0.0937	0.0951	3.9942
450	14158.28	14403.72	0.1212	0.118	1.704	15563.39	15903.77	0.1059	0.1028	2.1403
451	12017.79	12123.24	0.1311	0.128	0.8697	16617.22	15227.77	0.1035	0.0821	-9.124
452	14976.9	15215.06	0.1229	0.12	1.5653	15525.28	16339.42	0.0945	0.0951	4.9827
453	12593.57	12665.7	0.1209	0.122	0.5695	13594.89	14094.6	0.1137	0.1077	3.5454
454	16277.85	16812.24	0.1255	0.111	3.1786	14164.98	14111.55	0.104	0.1034	-0.379
455	12469.58	12492	0.1231	0.123	0.1795	16768.55	17427.88	0.1049	0.0953	3.7832
456	11653.09	11650.16	0.125	0.125	-0.0251	14577.27	14899.36	0.1101	0.1094	2.1618
457	14513.23	14719.92	0.1181	0.121	1.4042	15235.41	16112.81	0.0927	0.0905	5.4454
458	11901.27	12184.11	0.1294	0.132	2.3214	13390	14425.18	0.1106	0.0971	7.1762
459	12363.28	12310.64	0.1138	0.115	-0.4276	15153.12	15833.33	0.0979	0.0977	4.2961
460	11666.52	12089.49	0.1265	0.127	3.4986	16143.57	16754.31	0.1042	0.1013	3.6453
461	12224.82	12495.24	0.128	0.131	2.1642	16611.97	16552.89	0.0978	0.1012	-0.357
462	12751.81	12786.46	0.1143	0.115	0.2709	14952.39	14804.48	0.0991	0.099	-0.999
463	14207.28	14519.53	0.1141	0.116	2.1506	13728.09	13813.44	0.11	0.1099	0.6179
464	12216.56	12354.97	0.1189	0.118	1.1202	13324.47	13255.69	0.0995	0.0985	-0.519
465	16446.13	18233.34	0.1159	0.121	9.8019	13669.39	13871.61	0.1093	0.1109	1.4578
466	15439.74	17227.36	0.1136	0.119	10.377	15127.92	15756.7	0.0966	0.0979	3.9906
467	12784.03	12052.96	0.1259	0.107	-6.0655	12754.29	12934.5	0.1109	0.1097	1.3932
468	13149.23	12720.24	0.1235	0.121	-3.3725	15762.92	16388.77	0.0933	0.0946	3.8188
469	12080.65	12351.07	0.1298	0.133	2.1894	14329.16	14297.03	0.1008	0.1007	-0.225
470	14321.63	15038.74	0.1189	0.12	4.7684	12849.29	13018.29	0.0909	0.099	1.2981
471	16356.85	17913.34	0.1136	0.119	8.689	12519.41	12696.28	0.1056	0.1054	1.393
472	14706.65	14435.32	0.1146	0.106	-1.8797	15041.64	15670.93	0.0958	0.097	4.0156
473	16413.69	15418.37	0.1299	0.107	-6.4554	13268.73	13489.35	0.0964	0.0959	1.6355
474	13348.19	13432.62	0.1115	0.111	0.6286	14133.25	14096.97	0.1011	0.101	-0.257
475	14187.94	12741.8	0.1133	0.099	-11.35	12787.75	13914.68	0.1038	0.0977	8.0989
476	13682.94	14136.08	0.1145	0.118	3.2055	15453.77	16082.56	0.0938	0.0952	3.9097
477	13832.87	13938.31	0.1237	0.121	0.7565	14445.64	14437.35	0.1091	0.1017	-0.057
478	12821.3	13467.45	0.1196	0.115	4.7979	12885.09	12863.37	0.107	0.1063	-0.169
479	14717.85	13327.07	0.1122	0.098	-10.436	13653.75	13704.25	0.0954	0.0914	0.3685
480	12663.05	13628.57	0.1145	0.117	7.0845	15035.78	14739.84	0.1139	0.102	-2.008
481	11361.95	12478.14	0.1214	0.12	8.9451	15165.81	15365.31	0.096	0.0979	1.2984
482	12776.62	12882.06	0.1278	0.125	0.8185	17308.66	17338.58	0.1002	0.1004	0.1725
483	13520.28	13610.07	0.1243	0.124	0.6597	15290.64	15919.42	0.0933	0.0947	3.9498

484	10886.66	11923.46	0.128	0.128	8.6954	15283.19	15776.7	0.1022	0.0998	3.1281
485	13421.47	12677	0.1237	0.118	-5.8726	13972.24	14215.67	0.0951	0.0933	1.7124
486	12061	12199.4	0.1162	0.115	1.1345	14182.05	14253.68	0.101	0.0969	0.5025
487	11831.38	11874.51	0.1274	0.125	0.3633	16581.17	16541.56	0.0914	0.0908	-0.24
488	12825.36	13899.15	0.115	0.117	7.7256	15883.06	15848.87	0.0963	0.0999	-0.216
489	13003.87	13964.03	0.1189	0.121	6.8759	14944.96	13615.81	0.1083	0.0853	-9.762
490	12129.19	12096.06	0.1225	0.125	-0.2739	16370.84	16417.62	0.1025	0.1061	0.2849
491	12940.96	13030.75	0.1267	0.126	0.6891	14431.43	14649.42	0.1053	0.1096	1.488
492	14599.96	14104.87	0.1212	0.103	-3.5101	14798.63	14848	0.0996	0.1008	0.3325
493	13119.95	11995.95	0.1215	0.105	-9.3699	15064.25	15045.84	0.1055	0.1037	-0.122
494	12696.12	12834.52	0.1187	0.118	1.0784	13852.23	13883.44	0.1036	0.1046	0.2248
495	13617.52	13685.31	0.1159	0.116	0.4953	17904.86	18095.03	0.1124	0.1117	1.051
496	13282.76	12595.65	0.1153	0.092	-5.4551	17022.33	17131.03	0.1038	0.1076	0.6345
497	12961.14	13578.04	0.1255	0.128	4.5434	15089.73	15177.39	0.098	0.0996	0.5776
498	12212.06	12270.55	0.1216	0.126	0.4767	16111.92	14686.62	0.106	0.0841	-9.705
499	12254.26	12909.73	0.1158	0.111	5.0774	16231.39	17348.79	0.0931	0.0901	6.4408
500	13849.52	13745.34	0.123	0.118	-0.7579	12112.3	12406.27	0.102	0.1008	2.3695
501	14537.33	14605.11	0.115	0.115	0.4641	13333.64	14157.91	0.0998	0.0972	5.8219
502	11264.83	11249.48	0.1243	0.125	-0.1365	12878.73	12873.16	0.1064	0.108	-0.043
503	12002.5	12045.64	0.1295	0.127	0.3581	14598.6	14685.05	0.1	0.1014	0.5887
504	14677.5	13194.5	0.1115	0.096	-11.24	17058.98	17249.77	0.0963	0.0931	1.1061
505	11833.8	12486.98	0.1231	0.123	5.2308	15553.3	15578.86	0.1048	0.1078	0.1641
506	16975.86	14935.83	0.1252	0.098	-13.659	12968.56	13148.76	0.1123	0.1111	1.3705
507	11569.98	11637.97	0.1184	0.117	0.5842	13956.97	13924.84	0.1012	0.1012	-0.231
508	11998.34	11953.45	0.1201	0.118	-0.3755	16028.97	15106.23	0.1039	0.0938	-6.108
509	14324.61	14459.85	0.108	0.102	0.9353	14677.01	16155.03	0.0961	0.0888	9.149
510	12477.75	12097.83	0.114	0.098	-3.1403	15459.07	17054.67	0.1027	0.0983	9.3558
511	13058.48	13076.56	0.1148	0.116	0.1382	13862.88	13787.06	0.1002	0.1033	-0.55
512	13745.34	13850.78	0.1213	0.119	0.7613	13502.49	13385.92	0.1066	0.1069	-0.871
513	13263.66	13369.1	0.1276	0.125	0.7887	14126.81	14089.95	0.0998	0.0987	-0.262
514	15089.43	14708.39	0.1136	0.107	-2.5906	14375.49	14308.42	0.1041	0.1029	-0.469
515	12101.07	12096.93	0.115	0.113	-0.0342	15008.45	15161.17	0.099	0.1005	1.0073
516	13390.47	13929.59	0.1226	0.124	3.8703	15600.4	16229.19	0.0973	0.0985	3.8744
517	14802.45	13750.87	0.1219	0.103	-7.6474	14513.42	14627.77	0.112	0.1102	0.7817
518	11155.43	11326.47	0.0925	0.091	1.5101	13136.86	13810.42	0.1042	0.1013	4.8771
519	15751.27	15533.7	0.1083	0.107	-1.4007	11980.41	11831.12	0.1085	0.1046	-1.262
520	13501.86	13734.88	0.123	0.12	1.6965	13561.75	13620.75	0.1066	0.1063	0.4331
521	11942.27	12080.68	0.1215	0.121	1.1457	14017.82	14871.96	0.0949	0.097	5.7433
522	12983.82	12979.68	0.1121	0.11	-0.0319	16155.58	16417	0.1004	0.1017	1.5924
523	11994.76	12548.26	0.1304	0.124	4.411	11784.91	11772.48	0.1118	0.1111	-0.106
524	13268.86	14088.39	0.1183	0.12	5.8171	14748.53	17551.24	0.0992	0.0976	15.969
525	17713.85	16242.96	0.1327	0.107	-9.0555	13797.55	13680.98	0.1062	0.1064	-0.852
526	13998.16	14555.77	0.1191	0.122	3.8308	13069.57	13226.23	0.099	0.1034	1.1844
527	11849.01	11871.44	0.131	0.131	0.1889	14215.54	14433.24	0.0981	0.0973	1.5083
528	12749.56	13517.9	0.1066	0.11	5.6838	15281.91	15298.27	0.1017	0.1009	0.1069
529	12516.65	12501.29	0.1251	0.125	-0.1228	14595.6	14870.58	0.0982	0.0961	1.8491

530	12496.85	12481.5	0.1173	0.118	-0.123	16256.89	16885.67	0.0947	0.0961	3.7238
531	12271.27	12407.25	0.1159	0.115	1.096	13106.08	13193.74	0.1007	0.1026	0.6644
532	12620.9	12688.68	0.1168	0.117	0.5342	14911.56	15595.2	0.0987	0.0983	4.3837
533	14383.54	13042.26	0.1226	0.105	-10.284	17379.23	17684.46	0.0973	0.0926	1.726
534	15704.26	15365.94	0.1149	0.109	-2.2018	17974.51	18752.67	0.1081	0.1045	4.1496
535	17567.52	15448.16	0.1277	0.105	-13.719	13313.94	13464.56	0.1148	0.1128	1.1187
536	13212.52	12448.23	0.1209	0.105	-6.1398	14030.72	14030.6	0.1056	0.1041	-9.00E-04
537	13016.94	13101.37	0.1179	0.117	0.6445	12448.23	13011.78	0.0957	0.1009	4.3311
538	13270.93	13355.37	0.119	0.118	0.6322	13228.26	13416.96	0.1185	0.1178	1.4064
539	14614.61	15617.92	0.1263	0.13	6.4241	13252.99	13099.35	0.1065	0.1065	-1.173
540	11901.59	12543.87	0.1226	0.12	5.1203	14638.96	14593.9	0.0998	0.0999	-0.309
541	16043.25	15318.82	0.1249	0.109	-4.729	15598.45	15989.84	0.1084	0.1066	2.4477
542	17182.95	16623.91	0.1332	0.112	-3.3629	14948.59	15169.22	0.0961	0.0956	1.4544
543	18789.51	16218.85	0.1314	0.107	-15.85	18009.39	17137.74	0.0986	0.0903	-5.086
544	12947.81	13217.93	0.1277	0.13	2.0436	14638.29	15306.78	0.0958	0.097	4.3673
545	11822.5	11718.53	0.1255	0.125	-0.8872	15207.92	15823.77	0.0984	0.0995	3.892
546	13166.4	13533.17	0.1282	0.127	2.7102	17645.44	17556.65	0.1019	0.1038	-0.506
547	13181.4	13585.78	0.1219	0.115	2.9765	13951.75	14080.75	0.1051	0.1047	0.9161
548	11516.26	11538.68	0.1261	0.126	0.1944	13101.13	13109	0.1071	0.109	0.06
549	13262.18	13960.3	0.1221	0.125	5.0007	15851.14	15716.49	0.0974	0.1018	-0.857
550	13580.09	13850.12	0.1211	0.122	1.9497	14794.51	17640.86	0.098	0.0942	16.135
551	12636.55	12610.86	0.1191	0.12	-0.2037	13668.58	16136.73	0.0989	0.0967	15.295
552	13805.55	13903.33	0.115	0.115	0.7033	18386.99	18982.02	0.1113	0.1072	3.1347
553	11988.03	12029.45	0.1157	0.115	0.3443	14154.6	14277.52	0.1005	0.0988	0.861
554	13039.56	12884.92	0.1274	0.125	-1.2002	14597.06	15103.3	0.1045	0.1034	3.3518
555	12784.82	13207.37	0.1219	0.123	3.1993	14239.74	14868.53	0.0964	0.0977	4.229
556	12794.01	13469.03	0.1278	0.13	5.0117	13994.95	13938.09	0.0983	0.0978	-0.408
557	14359.1	14940.58	0.1209	0.119	3.8919	15708.42	14789.46	0.1077	0.1009	-6.214
558	16921.27	15431.06	0.1333	0.109	-9.6572	12783.87	12902.37	0.0984	0.1	0.9184
559	12583.86	12612.15	0.1239	0.126	0.2243	13590.45	13703.89	0.1042	0.1051	0.8277
560	16571.47	16027.78	0.1346	0.113	-3.3922	14938.98	14874.04	0.1089	0.0994	-0.437
561	12787.34	12949.89	0.1275	0.11	1.2552	13988.62	14292.97	0.0905	0.1013	2.1294
562	11794.01	12378.69	0.1303	0.131	4.7233	14669.22	14975.96	0.1066	0.1032	2.0482
563	13706.33	13863.31	0.1218	0.124	1.1324	17304.53	15888.72	0.1042	0.084	-8.911
564	13277.49	13508.11	0.1074	0.108	1.7073	12853.08	13014.29	0.104	0.1037	1.2387
565	12149.1	12886.66	0.1198	0.121	5.7234	12952.19	13131.9	0.113	0.1102	1.3685
566	10892.03	11451.65	0.1318	0.126	4.8868	14804.22	15159.4	0.109	0.1051	2.343
567	16877.87	16226.27	0.1314	0.11	-4.0157	13356.04	13558.26	0.1086	0.1103	1.4915
568	12044.61	12306.07	0.0922	0.095	2.1246	17253.89	17430.55	0.0966	0.0934	1.0135
569	12574.08	13693.24	0.1189	0.116	8.173	14398.12	14644.07	0.1049	0.1014	1.6795
570	11346.43	12207.54	0.1287	0.129	7.0539	16145.32	16656.53	0.1049	0.1024	3.0691
571	13770	14024.27	0.1131	0.114	1.813	13017.16	13105.44	0.1056	0.1076	0.6736
572	12449.98	12539.77	0.1239	0.123	0.7161	13868.7	13815.27	0.1047	0.1041	-0.387
573	12823.15	12912.94	0.1256	0.125	0.6954	13330.87	13826.4	0.1076	0.1063	3.5839
574	13464.03	14617.71	0.1201	0.117	7.8923	12576.03	12660.09	0.1156	0.1134	0.6639
575	13106.63	13144.41	0.1206	0.12	0.2874	15514.19	16198.54	0.0992	0.0969	4.2248

576	14152	13793.38	0.1248	0.108	-2.5999	14398.9	14483.63	0.1006	0.1024	0.585
577	17880.94	17131.9	0.1339	0.113	-4.3722	13292.97	13433.17	0.1097	0.1077	1.0437
578	11745.95	11794.94	0.1151	0.113	0.4154	17580	17748.87	0.0934	0.1009	0.9515
579	11926.18	12552.87	0.1189	0.105	4.9924	18291.65	18240.44	0.0933	0.0974	-0.281
580	12923.76	12991.55	0.1132	0.114	0.5217	15814.46	14420.87	0.1039	0.0816	-9.664
581	12671.41	13004.38	0.1279	0.13	2.5604	12869	12876.99	0.1082	0.1086	0.062
582	14346.53	14466.62	0.1143	0.115	0.8301	12627.51	12861.86	0.0988	0.0973	1.8221
583	18457.51	19625.95	0.1356	0.132	5.9536	16522.12	16626.97	0.1005	0.1007	0.6306
584	12622.49	13494.5	0.1294	0.132	6.462	15743.06	16368.92	0.0934	0.0947	3.8235
585	14643.58	16254.55	0.1145	0.12	9.9109	12047.86	12282.42	0.0936	0.1022	1.9097
586	12732.33	12504.97	0.1214	0.117	-1.8182	14316.47	14423.63	0.0994	0.1011	0.7429
587	11168.03	11202.38	0.1233	0.121	0.3066	13689.24	13355.48	0.1091	0.1075	-2.499
588	13798.43	14052.7	0.122	0.122	1.8094	12965.86	12721.01	0.1048	0.1023	-1.925
589	14837.67	14934.24	0.1273	0.117	0.6466	15105.46	15417.89	0.0957	0.0959	2.0264
590	17012.72	17312.93	0.1195	0.118	1.734	15586.76	16212.62	0.0954	0.0967	3.8603
591	12137.48	13156.21	0.1175	0.105	7.7434	13292.28	13530.06	0.103	0.1012	1.7574
592	13661.63	13964.77	0.1083	0.097	2.1707	16194.75	16405.26	0.0937	0.0924	1.2831
593	16699.31	16302.4	0.1349	0.113	-2.4347	12966.21	12920.57	0.1081	0.1065	-0.353
594	11797.44	11840.58	0.1312	0.129	0.3643	13122.61	13183.11	0.1085	0.1037	0.4589
595	13530.11	13635.55	0.1276	0.125	0.7733	13254.65	13212.72	0.1074	0.105	-0.317
596	14053.38	15351.84	0.1022	0.115	8.458	14170.27	14137.13	0.1039	0.1045	-0.234
597	16191.03	16196.05	0.1274	0.113	0.031	15643.12	16271.91	0.0952	0.0966	3.8642
598	12493.13	12565.26	0.117	0.119	0.5741	14913.93	14881.8	0.101	0.101	-0.216
599	11701.9	12428.67	0.1223	0.122	5.8475	14460.04	14653.68	0.101	0.1003	1.3214
600	14363.65	15482.6	0.1197	0.105	7.2271	15201.17	15263.9	0.0979	0.097	0.4109
601	12521.15	12799.85	0.1214	0.124	2.1774	16335.17	16093.37	0.0971	0.0993	-1.502
602	13140.95	12109.58	0.1192	0.111	-8.517	17638.72	17577.01	0.1039	0.1065	-0.351
603	11086.44	11365.14	0.1296	0.132	2.4522	13738.97	14367.76	0.0985	0.0999	4.3764
604	13806.29	13926.37	0.1183	0.119	0.8623	13317.17	13452.02	0.1047	0.102	1.0025
605	14262.51	14609	0.1201	0.121	2.3717	13516.34	14183.91	0.1038	0.1021	4.7066
606	12412.18	12849.59	0.1284	0.133	3.404	15958.02	16292.37	0.0929	0.091	2.0522
607	12153.52	12608.82	0.1277	0.123	3.611	14205.58	14264.15	0.102	0.1028	0.4107
608	16774.4	16941.89	0.1216	0.121	0.9886	14232.26	15676.64	0.0995	0.0965	9.2136
609	13872.06	14205.66	0.1192	0.119	2.3484	14463.9	14548.63	0.1012	0.1029	0.5824
610	12988.46	12615.62	0.1115	0.096	-2.9554	15759.58	14331.38	0.1076	0.0938	-9.966
611	17140.24	15179.08	0.1273	0.104	-12.92	14475.37	14463.86	0.0992	0.0982	-0.08
612	12787.9	12746.47	0.1199	0.122	-0.325	15281.75	15490.62	0.1035	0.1073	1.3484
613	13538.33	13622.77	0.1193	0.119	0.6198	14485.58	14634.07	0.1055	0.1046	1.0147
614	12620.7	12695.35	0.1193	0.12	0.588	16790.38	17425.02	0.0935	0.0946	3.6421
615	12542.39	13647.91	0.1292	0.116	8.1002	15933.39	16562.68	0.0942	0.0953	3.7994
616	12876.41	12948.54	0.1201	0.122	0.5571	14850.99	15077.44	0.1034	0.1009	1.5019
617	12649.78	12721.92	0.1248	0.126	0.567	13434.22	13552.59	0.1019	0.1036	0.8734
618	12991.19	13827.43	0.13	0.133	6.0477	15931.66	16108.32	0.0969	0.0936	1.0967
619	14001.53	13350.96	0.1223	0.104	-4.8729	16708.69	16782.19	0.104	0.0955	0.438
620	12293.78	14182.74	0.1175	0.124	13.319	15421.53	14054.3	0.104	0.0822	-9.728
621	11677.56	11771.92	0.126	0.125	0.8015	14743.03	16106.29	0.0964	0.0953	8.4641

622	12427.63	13211.01	0.1213	0.103	5.9298	13868.77	14055.72	0.1075	0.1042	1.3301
623	15630.06	15408.52	0.1167	0.109	-1.4378	12325.59	12957.93	0.0953	0.1012	4.8799
624	17697.57	16281.04	0.1348	0.109	-8.7005	13831.37	14154.55	0.0971	0.1037	2.2832
625	12412.77	12914.65	0.1121	0.105	3.8861	14178.83	14452.65	0.1096	0.1064	1.8945
626	13893.69	14421.89	0.1142	0.114	3.6625	15879.79	14492.09	0.1064	0.0941	-9.576
627	12320.54	12338.62	0.117	0.118	0.1465	15629.26	15831.27	0.1052	0.1018	1.276
628	12046.23	11526.82	0.1259	0.122	-4.5061	12510.18	14059.18	0.105	0.1089	11.018
629	12752.72	13319.59	0.1165	0.117	4.2559	17548.78	16615.68	0.1011	0.0947	-5.616
630	17036.12	15095.17	0.1302	0.108	-12.858	13121.86	14389.6	0.1056	0.0977	8.8101
631	11402.36	12178.75	0.1192	0.113	6.375	14408.27	14523.92	0.1047	0.1032	0.7963
632	13684.95	12919.68	0.1135	0.114	-5.9233	13476.53	14142.1	0.097	0.0985	4.7063
633	12788.26	13457.38	0.1169	0.115	4.9721	13402.52	13474.74	0.1041	0.1046	0.536
634	11158.39	11473.57	0.1255	0.126	2.747	13339.41	13965.27	0.0978	0.0992	4.4815
635	11911.28	13114.23	0.1278	0.123	9.1729	13486.9	13227.49	0.1076	0.109	-1.961
636	14023.48	15044.71	0.1084	0.106	6.788	17771.7	16986.74	0.1011	0.0922	-4.621
637	11851.67	11923.8	0.1239	0.125	0.6049	17034.71	17131.07	0.0889	0.0876	0.5625
638	16622.36	15534.88	0.1233	0.102	-7.0003	15482.13	15657.78	0.1009	0.0967	1.1218
639	14788.86	14523.76	0.1288	0.113	-1.8253	15630.4	14396.68	0.1022	0.0976	-8.57
640	13284.56	13573.09	0.1074	0.102	2.1257	13580.43	13990.51	0.1067	0.1036	2.9312
641	12271.52	12367.6	0.1266	0.125	0.7769	13768.85	16409.42	0.0945	0.0942	16.092
642	11534.78	11813.48	0.1269	0.13	2.3592	13037.07	13229.5	0.1059	0.1061	1.4545
643	14834.14	15289.12	0.1173	0.119	2.9758	18068.16	18055.94	0.0959	0.0997	-0.068
644	12942.54	13047.98	0.1272	0.125	0.8081	14310.6	14939.39	0.0943	0.0957	4.2089
645	12834.35	12976.07	0.1274	0.113	1.0921	15789.75	15778.25	0.0969	0.096	-0.073
646	12169.24	12219.45	0.1234	0.122	0.4109	14571.07	15294.62	0.0944	0.097	4.7308
647	16760.73	17277.01	0.1208	0.119	2.9882	16554.99	16495.91	0.0973	0.1007	-0.358
648	12809.57	13287.7	0.1269	0.125	3.5983	14966.24	15073.39	0.0992	0.1008	0.7109
649	18336.86	16684.97	0.1349	0.11	-9.9005	14621.23	14801.64	0.0995	0.0983	1.2189
650	12393.31	12476.15	0.1123	0.111	0.664	12637.6	12702.45	0.1124	0.1119	0.5106
651	14556.63	14814.79	0.1246	0.122	1.7426	13506.13	13389.56	0.1033	0.1037	-0.871
652	12667.88	12735.66	0.1159	0.116	0.5322	13245.39	13330.75	0.1126	0.1124	0.6403
653	12321.23	11737.68	0.1257	0.121	-4.9716	15972.72	14628.92	0.1052	0.0844	-9.186
654	11027.32	11316.44	0.1273	0.127	2.5548	13411.93	13722.34	0.1032	0.1004	2.2621
655	11462.53	11447.17	0.122	0.122	-0.1341	12750.38	12701.09	0.1076	0.1072	-0.388
656	12767.11	13828.44	0.1231	0.112	7.675	17053	16537	0.1042	0.093	-3.12
657	14176.34	14992.94	0.1217	0.125	5.4466	16070.88	16754.02	0.096	0.096	4.0775
658	11097.22	12141.6	0.1223	0.125	8.6016	15309.12	15296.69	0.0911	0.0904	-0.081
659	12592.42	14044.71	0.1182	0.108	10.34	12776.44	13033.84	0.0978	0.0972	1.9749
660	14058.16	14680.54	0.1315	0.127	4.2395	16327.06	16330.49	0.0984	0.1043	0.021
661	11348.68	11939.1	0.1201	0.124	4.9452	16798.33	16849.55	0.0961	0.1016	0.3039
662	12122.86	13719.41	0.1221	0.11	11.637	17146.55	17323.21	0.097	0.0938	1.0198
663	11980.1	12064.53	0.1225	0.122	0.6999	13858.11	13603.26	0.1033	0.101	-1.873
664	13039.83	13090.71	0.121	0.122	0.3887	15205.22	16075.01	0.0956	0.0972	5.4108
665	13387.21	13684.2	0.1077	0.095	2.1704	12597.31	13005	0.1121	0.1065	3.1349
666	13962.76	14599.95	0.1239	0.127	4.3644	12949.98	12960.18	0.1066	0.103	0.0788
667	12427.75	12807.37	0.1248	0.127	2.9641	14843.39	14984.9	0.0997	0.1011	0.9443

668	14093.77	14161.56	0.1151	0.116	0.4786	13132.4	13306.55	0.1063	0.1038	1.3087
669	12415.18	12916.4	0.1246	0.111	3.8804	15275.55	15553.45	0.1075	0.1056	1.7868
670	13406.91	13524.07	0.1198	0.121	0.8663	13169.27	13402.4	0.1146	0.1128	1.7395
671	13296.29	13175.58	0.1254	0.11	-0.9162	13730.77	14390.27	0.0963	0.0973	4.5829
672	12963.63	13387.39	0.1253	0.127	3.1654	12873.16	12996.21	0.1079	0.1056	0.9468
673	11635.4	12372.96	0.1211	0.122	5.9611	16888.25	16811.38	0.0997	0.1022	-0.457
674	11573.37	11868.1	0.1293	0.132	2.4834	13808.57	13932.17	0.1063	0.1059	0.8872
675	12555.77	12467.19	0.1307	0.111	-0.7105	17064.25	17037.89	0.0979	0.1014	-0.155
676	12791.2	14632.02	0.1168	0.108	12.581	13644.18	13792.67	0.1086	0.1076	1.0766
677	10685.39	11497.21	0.13	0.127	7.061	13740.81	14006.67	0.1096	0.1115	1.8981
678	12682.23	12802.32	0.1197	0.121	0.938	11865.32	12347.16	0.097	0.1038	3.9024
679	13069.49	13273.25	0.1234	0.127	1.5351	13278.21	15940.63	0.0965	0.0951	16.702
680	13094.99	13199.42	0.1157	0.115	0.7912	16923.25	16914.25	0.0969	0.1024	-0.053
681	14556.03	15365.61	0.1229	0.127	5.2688	13241.39	13940.59	0.1011	0.1019	5.0156
682	13930.21	14035.65	0.116	0.114	0.7512	14275.25	14550.22	0.0985	0.0964	1.8898
683	15434.07	16166.41	0.129	0.118	4.53	14989.55	15030.22	0.1024	0.1023	0.2706
684	13295.11	12859.76	0.1216	0.118	-3.3854	16210.49	16322.71	0.1006	0.1027	0.6875
685	13011.01	13605.77	0.113	0.107	4.3714	17326.86	17728.45	0.0986	0.0951	2.2652
686	10771.7	10910.1	0.1238	0.123	1.2686	15104.92	15776.34	0.0962	0.0974	4.2559
687	11851.29	11885.64	0.1233	0.121	0.289	15307.47	15987.68	0.0973	0.0972	4.2546
688	12160.72	12266.16	0.1305	0.128	0.8596	14785.31	15795.72	0.0983	0.097	6.3968
689	19030.72	16219.18	0.1311	0.105	-17.335	15952.08	16128.73	0.1008	0.0974	1.0953
690	13237.44	13255.51	0.1164	0.118	0.1364	14437.68	14645.64	0.1094	0.1051	1.4199
691	17506.1	14941.47	0.1255	0.103	-17.165	16520.97	16522.25	0.1059	0.0908	0.0078
692	13024.28	12255.92	0.124	0.104	-6.2693	16853.9	16930.38	0.0996	0.1014	0.4517
693	12320.08	12458.48	0.1209	0.12	1.1109	15233.6	15557.74	0.0959	0.0961	2.0835
694	13061.21	13063.23	0.1078	0.107	0.0154	16854.35	17537.48	0.0962	0.0962	3.8953
695	11743.9	11876	0.122	0.12	1.1123	18120.44	18138.01	0.1014	0.1039	0.0969
696	13961.14	14778.8	0.1231	0.127	5.5327	16596.62	16620.76	0.1006	0.1047	0.1453
697	12563.35	12862.72	0.1252	0.12	2.3275	12684.91	13361.68	0.0996	0.1006	5.0651
698	14090.57	14734.03	0.1183	0.119	4.3672	15594.69	15422.3	0.116	0.1056	-1.118
699	13291.12	12685.35	0.1208	0.115	-4.7754	16804.24	16321.49	0.1018	0.0915	-2.958
700	11822.65	12139.05	0.1259	0.128	2.6064	15167.71	15621.43	0.0986	0.0957	2.9045
701	16839.08	14502.49	0.1232	0.097	-16.112	14568.52	14536.38	0.1032	0.1032	-0.221
702	11029.71	11075.28	0.1236	0.123	0.4114	14060.92	14252.05	0.0989	0.0976	1.341
703	11950.04	12623.54	0.125	0.124	5.3353	14262.32	14403.24	0.1032	0.1032	0.9784
704	11527.15	11665.55	0.1228	0.122	1.1865	16382.56	16824.69	0.1027	0.1	2.6279
705	15555.44	15390.59	0.1083	0.108	-1.0711	14118.53	14690.07	0.0998	0.1045	3.8907
706	12259.14	12634.92	0.1169	0.103	2.9741	16263.98	16128.12	0.1028	0.1055	-0.842
707	11442.97	11427.62	0.1291	0.129	-0.1344	15711.24	14323.5	0.103	0.0806	-9.688
708	12094.89	13770.15	0.1218	0.11	12.166	15724.85	15692.72	0.0971	0.0971	-0.205
709	11734.87	11989.13	0.1185	0.119	2.1208	17414.73	17328.37	0.0983	0.1016	-0.498
710	11377.7	12012.63	0.1241	0.121	5.2855	16504.7	16556	0.0968	0.0971	0.3099
711	14529.67	13491.73	0.1169	0.1	-7.6932	16220.78	16235.13	0.0936	0.0909	0.0884
712	12721.7	12827.14	0.1305	0.128	0.822	13482.51	14449.62	0.1018	0.099	6.693
713	12760.81	13458.56	0.1285	0.131	5.1844	14531.56	15055.37	0.1064	0.1056	3.4792

714	14015.35	14207.66	0.1222	0.12	1.3535	16955.53	16896.44	0.098	0.1013	-0.35
715	13754.69	14037.13	0.1098	0.101	2.0121	17548.01	17469.73	0.1021	0.1044	-0.448
716	13913.16	14018.6	0.1258	0.124	0.7522	13836.2	13975.78	0.1023	0.1044	0.9988
717	11804.72	12126.93	0.1093	0.105	2.6569	15616.64	15326.17	0.0941	0.0957	-1.895
718	13564.48	13632.27	0.1172	0.118	0.4972	12720.71	13013.64	0.0981	0.1093	2.2509
719	13220.6	13977.55	0.1268	0.129	5.4155	13032.94	13152.82	0.1006	0.1043	0.9114
720	12136.21	12219.06	0.1161	0.114	0.678	15519.67	15570.97	0.0986	0.0989	0.3295
721	11942.03	13697.14	0.1213	0.127	12.814	16725.7	16691.26	0.1069	0.1097	-0.206
722	16106.66	16465.74	0.1172	0.112	2.1808	14995.58	15092.85	0.1035	0.0811	0.6445
723	13495.97	13601.41	0.1279	0.126	0.7752	17072.6	17049.46	0.1007	0.1055	-0.136
724	13451.16	13732.64	0.1284	0.126	2.0497	15655.91	15967.24	0.1075	0.1062	1.9498
725	18050.01	15519.73	0.1268	0.104	-16.304	17907.47	17259.75	0.1051	0.0938	-3.753
726	13303.61	13375.74	0.1218	0.123	0.5393	13514.09	13521.46	0.1012	0.1024	0.0545
727	12361.85	12467.29	0.1289	0.126	0.8457	14931.31	15560.1	0.0948	0.0961	4.041
728	12755.41	12988.25	0.1198	0.119	1.7927	14317.79	14243.24	0.1083	0.111	-0.523
729	13621.68	13727.12	0.1268	0.124	0.7681	18128.83	17455.97	0.1059	0.0963	-3.855
730	12757.31	11762.5	0.1087	0.098	-8.4574	16040.54	16965.42	0.1056	0.0928	5.4516
731	11628.15	11776.06	0.0969	0.101	1.256	13153.41	13238.76	0.1108	0.1107	0.6447
732	11863.72	12052.21	0.1232	0.12	1.564	15034.13	15029.48	0.11	0.0993	-0.031
733	13564.92	14323.95	0.1236	0.129	5.299	16352.83	16412.83	0.0944	0.0927	0.3656
734	11629.7	12766.68	0.1239	0.121	8.9059	15885.05	16370.53	0.1046	0.0817	2.9656
735	14892.19	15157.46	0.1307	0.115	1.7501	13830.16	13826.23	0.1037	0.1017	-0.028
736	16496.89	15982.66	0.1228	0.103	-3.2174	12764.17	12776.6	0.1102	0.1093	0.0973
737	17444.94	15822.55	0.1362	0.112	-10.254	16102.35	16030.84	0.0977	0.1013	-0.446
738	13452.66	13690.82	0.1234	0.121	1.7396	14784.34	14582.41	0.1115	0.1023	-1.385
739	13055.53	13051.47	0.1242	0.124	-0.0311	14393.53	14587.17	0.103	0.1023	1.3275
740	16576.02	17817.6	0.1245	0.113	6.9683	14714.72	15611.29	0.0966	0.0977	5.7431
741	16466.92	14279.19	0.134	0.107	-15.321	12594.85	12794.85	0.1076	0.1098	1.5631
742	12066.88	12272.65	0.1257	0.128	1.6767	15069.97	15225.92	0.1051	0.1018	1.0242
743	11484.64	11476.44	0.1252	0.125	-0.0714	17079.31	17086.89	0.102	0.1033	0.0443
744	11474.23	12588.73	0.1319	0.125	8.8531	13933.48	14018.21	0.1016	0.1033	0.6044
745	16128.69	16419.19	0.1258	0.115	1.7693	14105.18	14380.16	0.0976	0.0955	1.9122
746	13485.58	12556.93	0.1248	0.105	-7.3955	13463.91	13443.11	0.0985	0.0983	-0.155
747	15143.38	15842.71	0.1142	0.116	4.4142	14439.63	14761.73	0.1105	0.1098	2.182
748	11545.99	11587.41	0.1195	0.118	0.3575	13209.79	14027.78	0.109	0.103	5.8312
749	17045.18	14990.59	0.1351	0.108	-13.706	16950.66	17446.64	0.1045	0.0937	2.8428
750	12395.81	13134.56	0.1305	0.132	5.6245	13841.64	14197.38	0.1071	0.1059	2.5056
751	12682.42	12994.67	0.1214	0.123	2.4029	12905.3	13060.86	0.1071	0.1098	1.1911
752	12010.1	12068.09	0.1156	0.115	0.4805	14553.54	14660.7	0.101	0.1026	0.7309
753	12205.1	13158.85	0.1158	0.118	7.2479	13017.84	13284.62	0.1168	0.1157	2.0082
754	17251.82	16946.12	0.1257	0.108	-1.804	15285.53	15655.91	0.1043	0.1019	2.3658
755	13430.45	14382.26	0.129	0.131	6.6179	13648.05	13531.48	0.1058	0.1061	-0.861
756	14069.25	14265.58	0.1195	0.118	1.3762	13481.81	14076.16	0.1121	0.1092	4.2224
757	16583.15	18055.21	0.1149	0.12	8.1531	17577.15	17442.51	0.0959	0.0998	-0.772
758	16418.45	16718.66	0.1206	0.119	1.7956	15403.23	15594.03	0.0995	0.096	1.2235
759	16291.38	15613.52	0.1291	0.111	-4.3415	13547.26	13632.61	0.1106	0.1105	0.6261

760	12418.44	12395.53	0.1191	0.117	-0.1849	15446.43	16221.79	0.0975	0.0976	4.7797
761	13355	13861.02	0.1101	0.104	3.6506	14144.18	14770.04	0.0957	0.0971	4.2373
762	11884.13	12206.34	0.1088	0.105	2.6396	13735.98	13554.27	0.1029	0.0997	-1.341
763	14595.6	15534.3	0.1295	0.118	6.0428	13319.17	13965.74	0.0981	0.099	4.6297
764	17059.43	15682.07	0.1298	0.107	-8.7831	16187.47	17201.15	0.1033	0.1013	5.8931
765	11164.93	12424.46	0.1209	0.109	10.138	13618.64	13839.27	0.0947	0.0942	1.5942
766	14055.86	14344.98	0.113	0.113	2.0155	14891.94	15203.27	0.1087	0.1074	2.0478
767	15417.69	16509.42	0.1111	0.115	6.6128	13760.3	13687.37	0.098	0.098	-0.533
768	11918.6	12594.82	0.1221	0.105	5.3691	15170.78	15458.69	0.1055	0.1043	1.8624
769	13637.36	13870.38	0.1217	0.119	1.6799	18167.01	18071.36	0.0963	0.0997	-0.529
770	13523.83	13716.35	0.1164	0.116	1.4035	17179.98	17356.64	0.0971	0.0939	1.0178
771	12811.62	12944.67	0.1116	0.111	1.0278	16806.01	17354.97	0.1115	0.1073	3.1631
772	12467.04	12789.24	0.1079	0.104	2.5193	17095.36	16442.62	0.1022	0.0928	-3.97
773	12952.65	12970.72	0.1155	0.117	0.1394	12626.03	12657.25	0.111	0.1097	0.2466
774	11474.54	13422.13	0.1242	0.112	14.51	16828.81	16813.96	0.0958	0.1014	-0.088
775	12271.08	12573.08	0.1098	0.106	2.4019	13791.34	15480.58	0.1034	0.0988	10.912
776	11005.72	11881.39	0.1262	0.126	7.3701	12548.81	12636.3	0.1036	0.1026	0.6923
777	12284.84	12844.46	0.1239	0.12	4.3569	14480.37	15163.5	0.099	0.0988	4.5051
778	12773.65	12883.37	0.124	0.122	0.8516	14992.29	17187.18	0.1017	0.0999	12.77
779	16558.42	15800.38	0.126	0.115	-4.7976	14584.57	14669.93	0.1062	0.1061	0.5818
780	11833.36	12021.85	0.1243	0.121	1.5679	15188.53	15155.39	0.0985	0.0991	-0.219
781	14947.57	13794.07	0.1206	0.102	-8.3623	14257.64	16529.42	0.0985	0.0972	13.744
782	16487.12	17566.86	0.1243	0.114	6.1465	15122.3	15153.31	0.0976	0.0969	0.2046
783	15585.86	15653.64	0.1126	0.113	0.433	13989.87	14062.08	0.1055	0.106	0.5136
784	18368.28	17563.21	0.1308	0.11	-4.5839	14902.47	15168.71	0.1063	0.1044	1.7552
785	14739.1	14456.56	0.1088	0.106	-1.9545	13047.87	13028.87	0.1012	0.105	-0.146
786	13861.56	13929.34	0.1145	0.115	0.4866	12739.47	12848.76	0.1093	0.1092	0.8506
787	12436.94	12421.59	0.1191	0.119	-0.1236	14112.29	14116.73	0.1029	0.1041	0.0314
788	18339.2	16505.72	0.1337	0.109	-11.108	14818.57	15096.05	0.1042	0.1046	1.8381
789	11098.27	11120.69	0.1282	0.128	0.2017	13470.3	13535.15	0.1115	0.111	0.4791
790	13700.11	13791.03	0.1228	0.125	0.6593	13483.59	13726.43	0.1034	0.1099	1.7692
791	12625.51	12709.95	0.1221	0.121	0.6643	14390.51	14369.63	0.1095	0.1018	-0.145
792	13368.77	13708.41	0.1245	0.126	2.4776	14381.3	14496.44	0.0954	0.0936	0.7943
793	17608.39	18850.68	0.1355	0.131	6.5902	13181.25	13298.82	0.1075	0.1075	0.8841
794	13192.82	13875.92	0.1296	0.132	4.9229	14879.46	14942.18	0.0982	0.0974	0.4198
795	17033.37	18224.91	0.1328	0.128	6.538	14894.2	15013.99	0.0951	0.0931	0.7979
796	12993.71	13078.15	0.1221	0.121	0.6456	13649.42	13749.42	0.0989	0.1005	0.7273
797	11647.03	12216.47	0.1232	0.124	4.6613	12852.81	13361.93	0.1071	0.1014	3.8102
798	13675.91	13970.57	0.1067	0.1	2.1091	13205.83	13058.56	0.1076	0.1078	-1.128
799	11581.9	11703.74	0.1224	0.123	1.041	13518.89	13591.1	0.1047	0.1052	0.5314
800	13744.69	14599.37	0.1164	0.118	5.8542	17455.59	17440.73	0.0934	0.0988	-0.085
801	15136.93	16355.87	0.1283	0.119	7.4526	13798.53	14033.59	0.116	0.1138	1.675
802	12396.06	12285.73	0.1299	0.127	-0.898	15806.64	16101.49	0.0989	0.1056	1.8312
803	13838.6	14263.25	0.1111	0.114	2.9772	13489.13	15607.28	0.0949	0.0954	13.572
804	11164.6	12513.65	0.124	0.126	10.781	14916.32	14967.62	0.0999	0.1003	0.3427
805	13289.51	12791.48	0.1265	0.108	-3.8934	15478	15836.37	0.0956	0.0924	2.263

806	12318.95	12303.6	0.1237	0.124	-0.1248	14568.59	14330.81	0.1003	0.0981	-1.659
807	12628.52	12666.3	0.1221	0.121	0.2983	13350.71	13385.86	0.1075	0.1076	0.2626
808	16177.5	16468.28	0.1301	0.108	1.7657	12818.52	13241.78	0.1047	0.1015	3.1964
809	13898.03	14858.27	0.1218	0.111	6.4627	15383.25	15498.9	0.1005	0.0992	0.7462
810	12241.4	12331.19	0.1174	0.117	0.7282	15061.11	14976.35	0.0986	0.0979	-0.566
811	13874.19	14092.98	0.1174	0.117	1.5525	16057.08	16233.73	0.0978	0.0944	1.0882
812	15830.66	16080.24	0.1191	0.117	1.5521	13576.28	15219.15	0.102	0.0987	10.795
813	14197.41	14880.51	0.1306	0.133	4.5906	18157.64	18826.1	0.1094	0.1059	3.5507
814	13036.95	13363.3	0.1034	0.1	2.4421	14039.41	14936.9	0.099	0.0987	6.0085
815	11725.96	11706.46	0.1153	0.117	-0.1666	13042.51	14521.96	0.1075	0.0986	10.188
816	12853.67	12992.07	0.1166	0.116	1.0653	18293.72	18242.51	0.0939	0.098	-0.281
817	12337.28	13020.38	0.1219	0.125	5.2464	12600.24	12443.67	0.1058	0.1026	-1.258
818	12744.47	12812.26	0.1162	0.117	0.529	13368.65	13475.81	0.1017	0.1034	0.7952
819	10638.06	11249.51	0.125	0.122	5.4354	14728.35	14655.42	0.0951	0.0951	-0.498
820	13193.44	13617.72	0.1128	0.1	3.1156	15444.79	15311.74	0.1005	0.1025	-0.869
821	12283.16	13380.86	0.1236	0.113	8.2035	13768.5	14094.74	0.1118	0.1077	2.3146
822	12565.54	12633.32	0.1185	0.119	0.5365	12779.27	12864.62	0.1094	0.1093	0.6635
823	18005.87	15395.29	0.1231	0.104	-16.957	15170.97	13789.09	0.105	0.0821	-10.02
824	13321.05	13245.99	0.1154	0.114	-0.5667	14186.48	16295.13	0.0941	0.0945	12.94
825	17905.65	17172.88	0.1312	0.11	-4.267	13085.03	12903.81	0.1003	0.0974	-1.404
826	13173.86	13191.94	0.1153	0.117	0.137	15247.47	15258.69	0.1093	0.1023	0.0735
827	13451.12	13570.32	0.1234	0.125	0.8784	13380.28	13411.29	0.1016	0.1008	0.2312
828	13173.59	11963.61	0.1199	0.106	-10.114	16959.55	17305.32	0.1035	0.1059	1.9981
829	14363.91	14602.07	0.1212	0.118	1.631	13649.06	13813.7	0.1037	0.1041	1.1919
830	13368.38	13277.97	0.1189	0.118	-0.6809	14554.63	14982.21	0.1121	0.1109	2.8539
831	13129.03	13785.77	0.1293	0.131	4.7639	17535.94	17428.58	0.097	0.101	-0.616
832	13784.52	13375.03	0.1188	0.116	-3.0617	15740.28	16315.34	0.0964	0.1043	3.5247
833	17582.74	18759.47	0.1366	0.132	6.2727	12915.36	13000.92	0.1059	0.1044	0.6581
834	15989.13	16163.69	0.1248	0.124	1.0799	13660.93	13801.23	0.1012	0.103	1.0165
835	13277.11	13272.97	0.1119	0.11	-0.0312	15112.67	16052.21	0.0977	0.0911	5.853
836	11291.97	11446.94	0.1239	0.123	1.3539	12046.52	12284.43	0.0999	0.0988	1.9366
837	11978.27	13038.2	0.1334	0.129	8.1295	13007.19	13092.55	0.1097	0.1096	0.6519
838	13500.04	14335.95	0.1042	0.109	5.8309	14138.24	13975.22	0.1104	0.1011	-1.166
839	12084.26	12764.76	0.1221	0.118	5.3311	15326.91	14949.8	0.1006	0.0975	-2.522
840	12754.45	12069.73	0.1281	0.109	-5.673	14516.34	16478.42	0.0928	0.0934	11.907
841	15693.12	15941.7	0.1272	0.115	1.5593	14119.16	14238.45	0.0941	0.0921	0.8378
842	16133.42	16926.17	0.1265	0.114	4.6836	15356.32	13989.09	0.1058	0.0841	-9.774
843	14829.23	14919.02	0.1203	0.12	0.6019	14212.59	14157.44	0.1104	0.1036	-0.39
844	14863.39	15546.49	0.1181	0.121	4.3939	15210.7	15488.6	0.1061	0.1042	1.7942
845	15049.09	15335.07	0.1312	0.116	1.8649	15314.35	15429.49	0.0928	0.091	0.7463
846	11660.22	11798.63	0.1194	0.119	1.1731	13954.24	14229.22	0.0997	0.0976	1.9325
847	12417.56	12985.71	0.1176	0.115	4.3752	14893.27	14774.07	0.1032	0.1046	-0.807
848	16963.37	16619.69	0.1238	0.108	-2.0679	13042.84	13748.62	0.1157	0.106	5.1334
849	14044.61	14181.17	0.1155	0.116	0.963	12190.26	12476.53	0.1039	0.1059	2.2945
850	14171.11	14342.84	0.1051	0.096	1.1973	17409.41	16798.4	0.108	0.0988	-3.637
851	12898.07	13013.34	0.1241	0.126	0.8858	13000.63	13259.12	0.1176	0.1167	1.9495

852	13950.16	14719.53	0.127	0.131	5.2269	16746.53	17117.92	0.0992	0.0961	2.1696
853	16128.77	16296.26	0.1247	0.124	1.0278	14179.07	14592.88	0.1096	0.1075	2.8357
854	16254.96	15420.94	0.1329	0.11	-5.4084	13280.72	13672.11	0.1088	0.1066	2.8627
855	14680.29	14819.88	0.1146	0.116	0.9419	12871.4	12996.42	0.1123	0.11	0.962
856	11346.92	11010.52	0.119	0.101	-3.0552	13832.51	14479.08	0.0975	0.0983	4.4655
857	12163.8	12148.45	0.1246	0.125	-0.1264	15552.54	15862.92	0.1011	0.0969	1.9566
858	12824.79	12775.38	0.1084	0.108	-0.3868	16091.79	16090.78	0.1063	0.1083	-0.006
859	11830.52	11968.93	0.1173	0.117	1.1564	16951.62	16847.47	0.1088	0.1082	-0.618
860	12638.63	12777.04	0.1199	0.119	1.0832	14501.7	14389.28	0.1011	0.1004	-0.781
861	13083.84	13068.48	0.1174	0.118	-0.1175	18347.93	18253.49	0.0952	0.0987	-0.517
862	11766.05	11807.47	0.1203	0.119	0.3508	13766.4	13666.52	0.1186	0.1096	-0.731
863	12499.91	13112.45	0.1131	0.108	4.6715	13747.17	13819.39	0.1027	0.1032	0.5226
864	13415.11	13504.9	0.1161	0.116	0.6649	13503.09	13514.6	0.0979	0.0975	0.0851
865	12300.62	12194.22	0.1242	0.123	-0.8725	15168.37	15317.66	0.1051	0.1045	0.9746
866	12263.66	12286.08	0.1221	0.122	0.1825	13664.03	13930.81	0.1158	0.1148	1.915
867	13590.7	13378.86	0.1225	0.107	-1.5834	15267.59	15267.29	0.1025	0.1022	-0.002
868	12067.54	12393.61	0.1216	0.119	2.6309	13864.18	14050.96	0.0939	0.0953	1.3293
869	16904.18	15014.02	0.1272	0.105	-12.589	14451.14	14455.58	0.1026	0.1038	0.0307
870	11692.53	12056.08	0.1203	0.113	3.0155	15761.68	15475.94	0.1097	0.101	-1.846
871	12510.25	12578.03	0.1172	0.118	0.5389	13142.5	13173.5	0.1027	0.1018	0.2354
872	15569.9	13529.08	0.1257	0.101	-15.085	14610.75	16711.62	0.0948	0.0956	12.571
873	15781.6	15662.9	0.1174	0.121	-0.7578	18200.06	17892.48	0.0977	0.1024	-1.719
874	11544.39	11616.52	0.1224	0.124	0.6209	13569.77	14254.41	0.1041	0.1023	4.803
875	12467.01	11639.19	0.1153	0.1	-7.1123	14522.36	14641.65	0.0957	0.0938	0.8147
876	12536.2	12645.91	0.1205	0.123	0.8675	17891.46	17362.74	0.1025	0.0928	-3.045
877	12417.4	12485.18	0.1159	0.116	0.5429	12804.24	13003.03	0.1091	0.1107	1.5288
878	12473.04	12468.99	0.1275	0.127	-0.0325	14306.46	14285.66	0.0998	0.0997	-0.146
879	11692.1	11774.94	0.1146	0.113	0.7036	15210.84	15373.57	0.1027	0.1017	1.0584
880	12867.32	13298.49	0.1287	0.127	3.2423	12462.75	12623.37	0.1068	0.1058	1.2724
881	15479.59	14808.05	0.1157	0.113	-4.535	15482.74	15866.56	0.1053	0.1028	2.419
882	12604.58	12667.71	0.121	0.121	0.4984	14353.79	15052.99	0.0979	0.0988	4.6449
883	15013.16	15080.94	0.1156	0.116	0.4495	14335.51	14270.58	0.1098	0.1038	-0.455
884	14160.11	14244.55	0.1162	0.116	0.5928	13491.9	13766.96	0.1135	0.1086	1.998
885	16257.14	15921.12	0.113	0.115	-2.1105	14062.39	14150.05	0.099	0.1007	0.6195
886	12093.12	12385.37	0.1259	0.126	2.3597	16782.28	15438.48	0.1014	0.0814	-8.704
887	12629.39	12719.18	0.1233	0.123	0.706	13032.86	13309.05	0.0962	0.0957	2.0752
888	12921.52	12120.36	0.123	0.105	-6.6101	12383.04	12704.88	0.1076	0.1045	2.5332
889	13190.77	13205	0.1074	0.106	0.1077	13322.4	13275.04	0.1163	0.1062	-0.357
890	12963.27	13047.71	0.1204	0.12	0.6471	14337.27	14701.49	0.1148	0.1117	2.4775
891	14448.41	15429.03	0.1281	0.118	6.3557	14139.3	14363.95	0.1084	0.1099	1.5639
892	11656.73	11801.71	0.0955	0.099	1.2284	13338.73	13361.45	0.1043	0.1064	0.17
893	12850.51	13226.42	0.1171	0.113	2.8421	13454.98	13679.62	0.1083	0.1098	1.6422
894	12655.38	13219.11	0.1192	0.115	4.2645	14271.94	14538.71	0.1135	0.1125	1.8349
895	12381.5	14055.7	0.1215	0.127	11.911	12991.84	13202.84	0.1093	0.1112	1.5982
896	13102.75	13425.21	0.1239	0.125	2.4019	15232.44	15861.23	0.0929	0.0944	3.9643
897	15171.52	15450.22	0.1122	0.115	1.8039	14748.52	14842.03	0.0989	0.1008	0.6301

898	13468.83	13558.63	0.1193	0.119	0.6622	16146.47	16548.06	0.1003	0.0964	2.4268
899	13290.22	13973.32	0.1289	0.131	4.8886	14925.32	15335.4	0.1055	0.1027	2.6741
900	13580.53	13685.97	0.1277	0.125	0.7704	15213.05	15325.27	0.0942	0.0924	0.7322
901	11988.8	11935.67	0.1211	0.12	-0.4452	13649.22	13924.24	0.1078	0.1061	1.9752
902	13458.7	15204.89	0.1061	0.117	11.484	16037.39	16666.17	0.0959	0.0972	3.7728
903	14414.53	14827.79	0.1231	0.127	2.7871	14579.85	15242.49	0.0971	0.0984	4.3473
904	12859.19	12843.84	0.1197	0.12	-0.1196	16063.95	16514.87	0.1017	0.0994	2.7304
905	12099.07	12454.76	0.1279	0.13	2.8558	15113.7	15329.85	0.1093	0.1056	1.41
906	13242.23	14143.15	0.12	0.108	6.37	14779.84	15212.44	0.1096	0.1086	2.8437
907	12342.81	12901.75	0.11	0.103	4.3323	16653.16	17002.33	0.0973	0.0948	2.0536
908	12706.39	12960.65	0.1208	0.121	1.9618	13258.7	13125.77	0.1045	0.1047	-1.013
909	12334.22	12397.36	0.1205	0.121	0.5093	13735.48	13596.28	0.1024	0.1021	-1.024
910	12685.08	13288.67	0.1199	0.112	4.5421	14846.02	15471.88	0.0949	0.0963	4.0451
911	12307.38	12397.17	0.1165	0.116	0.7243	14340.43	14559.01	0.104	0.1043	1.5013
912	13200.88	13662.18	0.1246	0.122	3.3765	13763.77	14438.04	0.1077	0.0983	4.6701
913	13281.21	13973.26	0.1112	0.107	4.9526	15050.73	15056.97	0.1003	0.1018	0.0414
914	12137.06	12574.17	0.1318	0.133	3.4762	12523.96	12627.6	0.1026	0.1063	0.8207
915	12913.36	13003.15	0.1149	0.115	0.6905	18460.9	17879.75	0.1047	0.0941	-3.25
916	12171.4	12261.19	0.1234	0.123	0.7323	13477.32	13688.32	0.1066	0.1085	1.5415
917	11325.16	12987.14	0.1233	0.126	12.797	17744.29	17609.64	0.0959	0.0998	-0.765
918	12922.21	13027.65	0.13	0.128	0.8094	12653.31	12776.45	0.0997	0.1013	0.9638
919	14293.39	14417.62	0.1162	0.118	0.8616	13730.31	13815.66	0.1095	0.1094	0.6178
920	11812.8	11835.22	0.1225	0.123	0.1895	15837.05	15828.76	0.0954	0.095	-0.052
921	15353.59	16294.01	0.1255	0.116	5.7715	12749.52	12772.25	0.1059	0.1081	0.1779
922	13096.6	13418.8	0.1034	0.1	2.4011	13632.02	13768.26	0.1065	0.1046	0.9895
923	12196.73	12554.26	0.1211	0.121	2.8478	14520.93	15204.07	0.0995	0.0993	4.4931
924	12747.56	12853	0.1221	0.12	0.8204	14412.52	15096.46	0.1016	0.1005	4.5304
925	14936.03	14726.53	0.1126	0.111	-1.4226	15093.33	15776.47	0.0971	0.097	4.3301
926	12955.69	13075.77	0.121	0.122	0.9184	16722.43	16899.09	0.0964	0.0932	1.0454
927	11190.07	11824.99	0.1246	0.121	5.3693	14711.82	14763.12	0.0998	0.1002	0.3475
928	17297.48	15865.27	0.128	0.106	-9.0274	15328.36	15797.27	0.1017	0.1012	2.9683
929	12455.63	13531.01	0.1245	0.119	7.9475	15168.96	15133.39	0.1016	0.0989	-0.235
930	12413.63	13792.18	0.1136	0.117	9.9951	16736.36	17419.49	0.095	0.095	3.9217
931	11670.52	12230.14	0.1283	0.123	4.5757	14287.65	14685.01	0.1016	0.0993	2.7059
932	13871.9	13741.69	0.1169	0.117	-0.9475	16495.29	15101.7	0.1035	0.0822	-9.228
933	16159.8	17392.74	0.113	0.116	7.0888	15573.58	15541.44	0.0993	0.0992	-0.207
934	12786.48	13824.72	0.1269	0.113	7.51	15732.56	15914.78	0.0948	0.0927	1.145
935	12140.17	12595.48	0.1289	0.124	3.6148	16735.57	16824.86	0.0889	0.0875	0.5307
936	13085.2	13472.31	0.1201	0.12	2.8734	12314.79	12495	0.1119	0.1107	1.4422
937	14442.28	14831.1	0.1173	0.119	2.6217	17454.24	18164.11	0.1099	0.1063	3.9081
938	11928.13	13640.04	0.1174	0.109	12.551	13073.76	13159.12	0.1081	0.108	0.6486
939	16415.46	16685.88	0.1199	0.118	1.6206	14913.91	16016.96	0.097	0.0966	6.8868
940	11388.09	11410.52	0.1242	0.124	0.1965	13085.83	13234.33	0.1088	0.1078	1.122
941	15290.72	15458.21	0.1246	0.124	1.0835	14739.39	14572.94	0.1037	0.0958	-1.142
942	16770.08	16043.13	0.1324	0.11	-4.5312	15342.06	15971.35	0.0952	0.0964	3.9401
943	12129.16	13478.21	0.1252	0.127	10.009	14197.97	14463.82	0.1084	0.1103	1.8381

944	12702.16	12785	0.114	0.112	0.648	14093.3	14241.79	0.1069	0.1059	1.0427
945	13276.81	13105.27	0.1263	0.123	-1.309	13926.1	13901.96	0.0996	0.0983	-0.174
946	12883.78	12378.51	0.1225	0.118	-4.0818	13206.01	13168.73	0.1049	0.107	-0.283
947	12570.12	13690.45	0.1228	0.122	8.1833	16663.45	16989.19	0.0981	0.0944	1.9173
948	13623.19	13712.98	0.1222	0.122	0.6548	16611.47	16552.39	0.0987	0.102	-0.357
949	12260.81	12306.38	0.1201	0.119	0.3702	14826.3	14794.16	0.102	0.102	-0.217
950	17793.49	18093.7	0.1179	0.117	1.6592	15963.04	16174.34	0.1013	0.0998	1.3064
951	12248.46	12738.79	0.1188	0.105	3.8491	13587.46	13709.6	0.1049	0.1036	0.8909
952	12493.38	12580.75	0.1233	0.123	0.6944	12297.45	12709.29	0.0998	0.0995	3.2404
953	12730.81	12216.93	0.1269	0.108	-4.2063	13947.99	13780	0.1013	0.101	-1.219
954	13039	13014.23	0.1205	0.121	-0.1903	12512.93	12531.51	0.1033	0.1052	0.1483
955	12679.05	13678.41	0.1186	0.104	7.3061	16169.58	16041.51	0.11	0.102	-0.798
956	17875.39	15438.37	0.1336	0.107	-15.785	13982.76	14611.55	0.0959	0.0973	4.3034
957	13473.45	13578.9	0.1248	0.122	0.7765	16768.71	16934.15	0.0973	0.0965	0.977
958	12384.32	12663.02	0.1241	0.127	2.2009	17864.25	17409.46	0.1042	0.0941	-2.612
959	12307.13	12990.24	0.1315	0.134	5.2586	15284.13	15950.49	0.0961	0.0973	4.1777
960	13455.81	13575.9	0.1217	0.123	0.8846	16864.46	16888.6	0.0967	0.1019	0.1429
961	11834.04	12105.49	0.1183	0.124	2.2424	16807.13	17345.71	0.1167	0.1128	3.105
962	10990.25	11312.45	0.114	0.11	2.8482	13200.07	13424.22	0.1065	0.1082	1.6697
963	13151.66	13100.82	0.1196	0.118	-0.388	17226.62	17422.18	0.0993	0.0988	1.1225
964	14426.27	14664.43	0.1152	0.113	1.6241	14032.12	14139.28	0.1014	0.1031	0.7579
965	12657.83	13217.45	0.1275	0.123	4.2339	17048.81	17387.51	0.1021	0.1046	1.948
966	10718.47	10665.84	0.1197	0.121	-0.4935	12332.16	12886.96	0.1046	0.1104	4.3051
967	11510.16	13215.5	0.1195	0.109	12.904	13069.92	13280.92	0.1087	0.1107	1.5888
968	12872.49	12826.01	0.1062	0.105	-0.3624	15779.78	15643.92	0.1021	0.1058	-0.868
969	12037.9	12565.66	0.1144	0.119	4.2001	14420.23	14535.38	0.0952	0.0934	0.7922
970	15379.14	14998.39	0.1137	0.108	-2.5386	15100.18	14737.16	0.1004	0.0953	-2.463
971	13774.52	13879.96	0.1256	0.123	0.7597	13044.79	13231.57	0.0909	0.0925	1.4116
972	14179.52	14270.44	0.1222	0.124	0.6371	17529.31	17304.88	0.0973	0.1018	-1.297
973	12261.6	12820.54	0.1105	0.104	4.3598	15060.13	15501.43	0.1026	0.0995	2.8468
974	13006.01	13465.45	0.1288	0.124	3.412	18299.36	18925.6	0.1127	0.109	3.3089
975	11478.74	11463.39	0.1285	0.129	-0.134	12942.93	12826.36	0.1082	0.1085	-0.909
976	12863.38	12953.17	0.1261	0.126	0.6932	17908.03	17372.95	0.1063	0.0968	-3.08
977	12196.41	12736.95	0.1265	0.128	4.2439	16076.3	14685.64	0.1021	0.0806	-9.47
978	15700.6	16301.76	0.1314	0.127	3.6877	18511.71	18529.29	0.1014	0.1038	0.0948
979	13506.46	14597.33	0.1125	0.115	7.4731	12251.18	12282.39	0.1133	0.1119	0.2541
980	13113.5	14170.61	0.1225	0.124	7.4599	15539.52	14154.72	0.1069	0.0841	-9.783
981	11046.19	12971.24	0.1204	0.108	14.841	14194.5	14896.63	0.0983	0.0992	4.7134
982	11822.55	12576.8	0.1255	0.119	5.9971	13531.02	13742.94	0.1037	0.1013	1.5421
983	12254.28	12988.58	0.1174	0.11	5.6534	14479.95	14456.52	0.097	0.0956	-0.162
984	14666.24	14684.31	0.1139	0.115	0.1231	15830.34	16286.58	0.0985	0.0956	2.8013
985	11716.97	12426.74	0.1225	0.122	5.7117	14917.38	17084.02	0.096	0.095	12.682
986	12341.74	13306.13	0.1282	0.116	7.2477	15031.43	15660.22	0.0948	0.0962	4.0152
987	12709.08	12773.4	0.1092	0.098	0.5035	15330.93	15103.48	0.0928	0.0937	-1.506
988	13891.61	15223.2	0.1049	0.119	8.7471	13175.69	13380.83	0.109	0.1106	1.5331
989	12960.28	13050.07	0.125	0.125	0.6881	16301.71	14919.84	0.1063	0.0847	-9.262

990	12950.57	13531.81	0.1274	0.111	4.2954	16030.67	15772.01	0.1096	0.1012	-1.64
991	12322.95	12649.29	0.1074	0.104	2.58	13929.5	13955.15	0.097	0.0989	0.1838
992	10728.38	11231.97	0.1238	0.113	4.4835	16961.73	17303.81	0.0986	0.1029	1.9769
993	12085.02	12148.15	0.1222	0.122	0.5197	14467.17	15093.03	0.0956	0.097	4.1467
994	17668.28	17968.49	0.1184	0.117	1.6707	13208.75	13874.32	0.0993	0.1007	4.7971
995	12410.63	12478.41	0.1167	0.117	0.5432	14804.16	14772.03	0.102	0.1019	-0.218
996	12666.03	12608.04	0.1184	0.121	-0.4599	14313.15	14263.86	0.1003	0.0989	-0.346
997	13299.67	13405.11	0.1272	0.125	0.7866	14341.82	14448.98	0.1023	0.104	0.7416
998	11803.3	11764.31	0.1232	0.122	-0.3315	17168.6	16876.89	0.0981	0.1033	-1.728
999	13306.43	13963.17	0.1296	0.132	4.7034	14216.61	16078.27	0.1009	0.0973	11.579
1000	13098.62	14248.15	0.1158	0.113	8.0679	11644.26	11523.54	0.107	0.1075	-1.048
	Daraga sample unite (3) N-S					Wuqro sample unite (4) N-S				
	UM L	M L	UM C	M C	L Ch %	UM L	M L	UM C	M C	L Ch %
1	11734.12	12194.07	0.149	0.147	3.7719	11322.5	11363.21	0.125	0.122	0.3583
2	13153.53	13222.94	0.14	0.14	0.5249	10794.69	10924.27	0.124	0.123	1.1862
3	12463.04	12530.41	0.138	0.137	0.5376	11964.24	12089.01	0.124	0.124	1.0321
4	14012.87	16096.76	0.134	0.135	12.946	14898.07	15047.66	0.129	0.128	0.9941
5	14612.57	14876.68	0.121	0.127	1.7753	11916.77	12476.51	0.13	0.129	4.4864
6	15328.17	15617.67	0.131	0.126	1.8537	11798.4	11989.44	0.127	0.126	1.5934
7	11564.84	13000.79	0.118	0.12	11.045	12730.63	12981.96	0.128	0.129	1.936
8	11601.9	11934.42	0.121	0.124	2.7862	12146.52	12048.53	0.125	0.123	-0.813
9	12069.96	12819.19	0.146	0.147	5.8447	11258.86	11377.06	0.127	0.128	1.0389
10	12656.18	12633.75	0.14	0.142	-0.178	11206.33	11302.6	0.12	0.121	0.8518
11	12033.66	13761.04	0.12	0.139	12.553	11847.64	13522.22	0.14	0.139	12.384
12	11153.62	11992.95	0.144	0.145	6.9985	11587.87	12113.93	0.122	0.122	4.3425
13	11452.42	15615.42	0.143	0.14	26.66	12093.4	12238.21	0.122	0.118	1.1833
14	12514.28	12400.61	0.115	0.123	-0.917	12689.84	12782.69	0.13	0.129	0.7263
15	12254.87	13149.22	0.114	0.122	6.8015	11293.95	11499.72	0.139	0.136	1.7894
16	10859	11158.15	0.124	0.127	2.681	12327.48	12633.79	0.13	0.13	2.4245
17	11804.75	12199.05	0.148	0.146	3.2322	12635.29	12738.21	0.124	0.121	0.808
18	13873.2	13967.56	0.128	0.133	0.6756	13866.81	14005.69	0.118	0.118	0.9915
19	10665.21	14303.64	0.125	0.141	25.437	12002.03	12365.29	0.124	0.122	2.9377
20	11678.41	11757.11	0.131	0.129	0.6694	14220.53	14001.53	0.112	0.117	-1.564
21	15187.62	14843.11	0.108	0.111	-2.321	15619.65	15726.81	0.128	0.127	0.6814
22	12887.12	12422.86	0.107	0.118	-3.737	12122.02	12113.24	0.129	0.129	-0.073
23	11858.84	11902.77	0.142	0.142	0.3691	14123.41	14311.47	0.128	0.121	1.3141
24	11038.18	10971.7	0.117	0.124	-0.606	10577.26	10766.88	0.127	0.122	1.7611
25	12814.46	12838.31	0.14	0.141	0.1858	13541.37	13584.09	0.122	0.123	0.3145
26	14716.63	17048.1	0.127	0.134	13.676	16098.59	17608.64	0.134	0.137	8.5756
27	11934.14	13029.71	0.135	0.134	8.4082	12290.35	12567.45	0.118	0.122	2.205
28	11998.78	13283.25	0.143	0.148	9.6699	15335.51	15596.39	0.128	0.128	1.6727
29	13985.31	14002.88	0.139	0.139	0.1255	14025.11	13946.16	0.123	0.122	-0.566
30	11502.29	12430.64	0.127	0.128	7.4683	11023.21	11302.42	0.135	0.134	2.4703
31	12939.91	13606.3	0.146	0.147	4.8977	11095.51	11318.47	0.131	0.13	1.9699
32	11321.71	11903.93	0.139	0.136	4.891	12751.44	12776.59	0.125	0.126	0.1968

33	12513.81	12025.49	0.102	0.118	-4.061	10248.85	11453.76	0.137	0.134	10.52
34	15312.1	15491.77	0.124	0.13	1.1598	10942.26	11264.43	0.12	0.127	2.86
35	13486.02	14227.18	0.117	0.13	5.2095	12359.44	12434.79	0.124	0.124	0.606
36	14272.39	14805.94	0.132	0.135	3.6036	12295.05	12791.31	0.129	0.124	3.8797
37	12812.69	12879.64	0.112	0.121	0.5198	15486.9	16436.74	0.119	0.124	5.7788
38	14310.7	15269.66	0.128	0.127	6.2802	13279.26	13221.06	0.119	0.113	-0.44
39	11828.54	11886.53	0.141	0.143	0.4879	11505.59	11615.59	0.136	0.134	0.947
40	12214.82	12280.88	0.138	0.14	0.538	13971.77	14322.24	0.129	0.127	2.447
41	12906.3	13172.66	0.136	0.134	2.0221	12121.88	12372.12	0.131	0.128	2.0226
42	11945.16	13658.91	0.123	0.121	12.547	15999.42	16132.94	0.128	0.127	0.8276
43	14442.68	14572.98	0.137	0.14	0.8941	13161.79	13226.85	0.118	0.119	0.4919
44	13071.2	13414.01	0.131	0.138	2.5556	10692.41	10747.76	0.129	0.128	0.515
45	14511.96	14747.02	0.13	0.128	1.594	12324.09	12538.11	0.121	0.118	1.707
46	12802.65	13346.74	0.135	0.133	4.0766	11306.07	11297.79	0.125	0.125	-0.073
47	12944.35	12912.56	0.119	0.119	-0.246	12101.71	12217.06	0.12	0.117	0.9442
48	11428.91	12066.27	0.125	0.121	5.2821	13078.51	13143.57	0.121	0.121	0.495
49	11402.34	12109.56	0.146	0.143	5.8402	13038.16	13189.46	0.124	0.123	1.1471
50	11975.09	11979.23	0.143	0.143	0.0346	16754.33	16864.42	0.127	0.127	0.6528
51	13739.38	13432.18	0.106	0.113	-2.287	14630.74	14891.12	0.131	0.13	1.7486
52	10829.21	11179.45	0.137	0.132	3.1329	12484.97	12894.41	0.12	0.123	3.1754
53	11316.38	11761.85	0.136	0.14	3.7875	10565.53	11541.74	0.135	0.138	8.4581
54	12605.7	12683.86	0.112	0.12	0.6162	10275.28	11509.92	0.133	0.134	10.727
55	11712.63	12239.37	0.108	0.121	4.3037	12205.11	12304.61	0.125	0.12	0.8086
56	14425.88	14839.52	0.131	0.136	2.7874	13322.31	13409.97	0.116	0.113	0.6537
57	12260.31	12922.56	0.148	0.148	5.1248	12584.81	12597.12	0.126	0.123	0.0977
58	10787.73	12123.28	0.136	0.133	11.016	13527.68	13429.69	0.123	0.121	-0.73
59	11700.52	11927.17	0.117	0.12	1.9003	13007.51	13142.25	0.12	0.12	1.0252
60	11626.59	12544.32	0.134	0.132	7.3159	11970.33	12423.47	0.126	0.126	3.6474
61	12444.08	14674.29	0.14	0.145	15.198	13423.97	13527.11	0.116	0.119	0.7624
62	13872.46	14049.53	0.134	0.13	1.2603	14555.29	15808.06	0.131	0.131	7.9249
63	10895.28	11334.72	0.13	0.125	3.877	11980.71	11962.93	0.123	0.121	-0.149
64	13054.08	16030.9	0.112	0.109	18.569	11358.07	11492.8	0.129	0.129	1.1723
65	14982.35	14971.68	0.127	0.135	-0.071	14272.62	15678.74	0.126	0.129	8.9683
66	12807.93	12765.8	0.142	0.142	-0.33	12584.73	12775.77	0.123	0.122	1.4953
67	11358.24	11712.17	0.138	0.135	3.0219	11382.62	11447.68	0.123	0.124	0.5683
68	13220.34	13224.48	0.138	0.139	0.0313	12953.91	13092.78	0.121	0.12	1.0607
69	10745.77	10903.67	0.147	0.147	1.4482	15211.93	15453.53	0.124	0.123	1.5634
70	10300.14	10581.1	0.147	0.145	2.6552	12092.15	12210.35	0.124	0.124	0.968
71	11517.23	11556.23	0.144	0.144	0.3374	11461.27	11777.87	0.131	0.127	2.6881
72	10792.94	11099.96	0.149	0.146	2.766	13478.66	13253.13	0.114	0.113	-1.702
73	12279.33	13808.69	0.128	0.124	11.075	13022.12	13293.63	0.134	0.135	2.0424
74	11671.34	12192	0.145	0.146	4.2705	12152.27	12270.47	0.123	0.123	0.9633
75	13513.1	13596.78	0.133	0.14	0.6154	11399.12	12006.14	0.128	0.131	5.0559
76	10828.61	11201.7	0.146	0.145	3.3306	10846.61	11016.52	0.138	0.139	1.5424
77	10937.64	11037.05	0.141	0.144	0.9007	11205.57	12908.23	0.139	0.137	13.19
78	11056.22	11382.74	0.126	0.127	2.8685	13782.21	12889.92	0.115	0.117	-6.922

79	12968.25	13170.68	0.136	0.134	1.5369	13326.32	13401.76	0.119	0.121	0.5629
80	11956.29	11956.29	0.139	0.139	0	11564	11537.93	0.121	0.119	-0.226
81	11245.73	11534.97	0.146	0.144	2.5075	11801.95	12015.21	0.129	0.127	1.7749
82	13309.85	13371.9	0.131	0.137	0.464	13450.22	13546.49	0.123	0.125	0.7107
83	11795.14	13704.67	0.143	0.148	13.933	10924.04	11166.29	0.122	0.126	2.1695
84	13872.82	13889.39	0.134	0.133	0.1193	13749.74	13824.6	0.12	0.116	0.5414
85	12008.75	13628.25	0.143	0.146	11.883	12936.09	12975.59	0.128	0.127	0.3044
86	11705.37	13989.79	0.124	0.142	16.329	12731.37	12890.96	0.118	0.119	1.238
87	12847.66	14048.2	0.121	0.114	8.5459	11816.14	11569.16	0.123	0.122	-2.135
88	12918.85	14529.01	0.122	0.111	11.082	12877.32	12794.89	0.123	0.121	-0.644
89	14560.31	14917.5	0.13	0.126	2.3945	13386.86	13582.64	0.138	0.137	1.4413
90	12204.77	13127.75	0.125	0.128	7.0308	11269.4	11408.28	0.128	0.127	1.2173
91	12357.1	13264.13	0.129	0.139	6.8383	11821.24	11931.24	0.135	0.133	0.9219
92	11447.55	11658.51	0.132	0.13	1.8094	13043.91	13208.43	0.122	0.119	1.2456
93	12178.29	12386.66	0.137	0.141	1.6822	12440.2	12770.24	0.131	0.129	2.5844
94	12051.88	14247.34	0.125	0.137	15.41	12030.05	12474.07	0.135	0.12	3.5595
95	14635.13	14756.85	0.134	0.137	0.8248	11957.74	12060.67	0.127	0.123	0.8534
96	14901.31	14625.99	0.132	0.14	-1.882	12875.65	13305.39	0.126	0.125	3.2298
97	11666.9	14726.04	0.131	0.144	20.774	12089.66	12077.23	0.12	0.12	-0.103
98	17259.56	17797.04	0.125	0.12	3.0201	11011.31	11123.65	0.133	0.133	1.0099
99	11173.68	11857.65	0.146	0.146	5.7682	12346.06	12390.58	0.12	0.12	0.3593
100	12429.84	12455.91	0.142	0.143	0.2093	13614.51	13769.24	0.125	0.119	1.1237
101	12962.21	15056.64	0.133	0.136	13.91	12985.62	13217.58	0.115	0.122	1.7549
102	13340.47	13231.77	0.137	0.136	-0.822	14777.25	15131.69	0.122	0.123	2.3423
103	13691.25	13213.21	0.136	0.139	-3.618	11575.58	12316.88	0.129	0.129	6.0186
104	11845.79	12422.23	0.112	0.121	4.6404	14987.72	15324.49	0.134	0.129	2.1976
105	12430.94	12639.01	0.112	0.123	1.6463	12576.4	12675.48	0.127	0.12	0.7817
106	12465.73	13036.6	0.136	0.137	4.379	10585.68	11868.37	0.135	0.134	10.808
107	11682.33	12359.23	0.135	0.134	5.4769	16249.54	16741.01	0.132	0.129	2.9357
108	11554.3	11868.6	0.146	0.145	2.6482	11082.94	11058.08	0.12	0.12	-0.225
109	13021.55	13389.97	0.127	0.138	2.7515	13252.76	13443.8	0.124	0.123	1.421
110	11740.26	13319.46	0.115	0.115	11.856	12058.02	12157.51	0.125	0.12	0.8184
111	11805.25	12481.89	0.123	0.118	5.421	11393	11624.33	0.138	0.141	1.9901
112	14724.97	15115.73	0.122	0.128	2.5851	12960.87	13115.6	0.125	0.119	1.1797
113	11947.72	11951.86	0.141	0.141	0.0347	11615.96	11668.6	0.119	0.119	0.4511
114	15176.61	15743.8	0.132	0.126	3.6026	12366.28	12781.96	0.128	0.121	3.2521
115	12166.4	13623.64	0.122	0.125	10.696	10951.39	12070.08	0.123	0.122	9.2683
116	12874.82	14404.94	0.127	0.134	10.622	13125.77	13329.74	0.129	0.128	1.5302
117	11949.47	12234.06	0.141	0.14	2.3262	11206.17	11244.66	0.132	0.131	0.3423
118	12372.65	12817.45	0.145	0.147	3.4703	11356.17	11766.53	0.123	0.127	3.4876
119	13320.33	13188.08	0.114	0.121	-1.003	12551.12	13165.11	0.127	0.127	4.6637
120	11621.02	11623.95	0.146	0.146	0.0252	12426.96	13234.92	0.125	0.125	6.1047
121	13131.14	13129.42	0.142	0.142	-0.013	11707.98	11810.91	0.121	0.117	0.8715
122	13425.1	14829.12	0.118	0.123	9.468	11905.17	12013.46	0.121	0.123	0.9014
123	12478.99	12613.42	0.111	0.117	1.0658	15129.35	16402.41	0.127	0.128	7.7615
124	13789.24	14216.81	0.136	0.133	3.0075	12155.81	12489.58	0.135	0.137	2.6723

125	11920.04	12623.25	0.131	0.122	5.5707	10638.71	10791.97	0.13	0.129	1.4201
126	11325.1	12078.9	0.123	0.123	6.2406	11660.81	12466.59	0.133	0.133	6.4635
127	12846.17	17625.08	0.138	0.132	27.114	12584.99	12864.61	0.132	0.136	2.1736
128	13596.67	15330.81	0.138	0.132	11.311	12996.07	13200.04	0.129	0.127	1.5452
129	15805.8	15996.69	0.123	0.129	1.1933	10741.55	11783.49	0.125	0.121	8.8424
130	11991.56	11964.28	0.143	0.142	-0.228	12421.53	12648.52	0.133	0.132	1.7946
131	14084.31	14480.43	0.119	0.125	2.7355	11099.77	11164.83	0.124	0.124	0.5827
132	11391.96	11836.26	0.148	0.149	3.7537	14012.06	14073.77	0.12	0.124	0.4385
133	11809.92	12676.11	0.145	0.146	6.8332	11943.83	11996.46	0.121	0.121	0.4388
134	15333.39	15694.4	0.129	0.127	2.3002	12531.41	12371.59	0.122	0.117	-1.292
135	12278.31	12290.74	0.145	0.145	0.1011	11223.12	11380.52	0.13	0.131	1.3831
136	12093.58	12250.99	0.146	0.146	1.2848	12142.13	12116.07	0.124	0.122	-0.215
137	11394.18	13072	0.144	0.149	12.835	11734.85	11708.79	0.126	0.124	-0.223
138	11879.15	16237.85	0.133	0.136	26.843	11666	11865.82	0.128	0.128	1.6841
139	14926.35	14425.77	0.107	0.111	-3.47	11452.91	11867.59	0.132	0.13	3.4942
140	11915.51	12344.66	0.142	0.14	3.4764	11035.73	11051.59	0.124	0.125	0.1435
141	12556.27	12810.03	0.133	0.135	1.981	13462.76	13562.26	0.121	0.117	0.7336
142	14116.02	13683.05	0.117	0.121	-3.164	15222.88	16329.29	0.137	0.143	6.7756
143	10843.85	11633.51	0.124	0.126	6.7878	13719.96	13621.97	0.123	0.122	-0.719
144	13330.65	15596.29	0.121	0.114	14.527	14156.1	14356.48	0.128	0.125	1.3958
145	11711.38	13684.76	0.143	0.148	14.42	10874.44	11492.8	0.131	0.13	5.3804
146	13546.04	16251.35	0.119	0.124	16.647	15547.64	15647.23	0.129	0.126	0.6364
147	13157.64	13343.29	0.116	0.127	1.3913	12880.77	13071.81	0.127	0.126	1.4615
148	11317.83	13765.95	0.143	0.147	17.784	13923.57	14039.01	0.122	0.121	0.8223
149	11428.47	11928.34	0.128	0.124	4.1906	10666.02	10553.98	0.122	0.116	-1.062
150	12267.67	12283.53	0.142	0.141	0.1291	15143.02	16084.37	0.125	0.128	5.8526
151	11900.19	12664.19	0.137	0.131	6.0328	11437.05	11502.11	0.122	0.123	0.5656
152	11515.78	11739.96	0.145	0.144	1.9095	12592.65	12963.79	0.124	0.122	2.8629
153	11674.27	12014.43	0.147	0.145	2.8312	15351.48	15273.28	0.116	0.119	-0.512
154	15384.08	15388.22	0.129	0.13	0.0269	11037.46	11676.52	0.139	0.138	5.4731
155	11643.91	13015.36	0.135	0.131	10.537	12015.91	12134.11	0.12	0.121	0.9741
156	12258.41	12752.5	0.148	0.148	3.8745	13073.49	13172.99	0.125	0.121	0.7553
157	11474.66	11333.83	0.115	0.124	-1.243	11634.37	11796.71	0.124	0.124	1.3761
158	11170.25	12711.62	0.138	0.132	12.126	15670.61	15755.55	0.125	0.124	0.5391
159	12670.22	12674.36	0.14	0.141	0.0327	12188.24	12253.3	0.121	0.121	0.531
160	12459.59	13129.88	0.115	0.124	5.1051	12305.76	12612.07	0.13	0.13	2.4287
161	14797.84	15136.34	0.132	0.13	2.2363	13708.72	15331.25	0.134	0.139	10.583
162	13372.97	15036.57	0.116	0.114	11.064	12191.51	12291.01	0.124	0.119	0.8095
163	11954.01	12422.66	0.122	0.12	3.7725	13081.09	13788.8	0.12	0.12	5.1325
164	15170.37	15702.5	0.129	0.124	3.3888	13971.96	14138.91	0.12	0.117	1.1808
165	15395.32	16254.61	0.129	0.128	5.2864	10607.49	10748.83	0.129	0.13	1.3149
166	11459.39	13183.61	0.143	0.141	13.078	12790.57	12981.61	0.126	0.126	1.4716
167	12198.76	12788.81	0.127	0.132	4.6138	12662.46	12761.55	0.126	0.12	0.7764
168	12765.36	12867.37	0.115	0.127	0.7928	13958.55	13970.27	0.126	0.125	0.0839
169	10918.11	11308.27	0.146	0.143	3.4502	12798.64	13197.97	0.13	0.128	3.0257
170	12157.98	12965.14	0.11	0.119	6.2256	14088.82	15070.25	0.138	0.138	6.5123

171	12480.59	12538.58	0.141	0.143	0.4625	14121.51	14272.8	0.124	0.122	1.0601
172	12041.94	12272.36	0.117	0.127	1.8775	14181.6	14269.47	0.128	0.127	0.6158
173	11129.54	14699.77	0.129	0.142	24.288	11513.99	11577.83	0.126	0.123	0.5515
174	12194.82	11998.01	0.123	0.129	-1.64	11748.63	12435.91	0.135	0.134	5.5266
175	11440.19	11499.89	0.14	0.14	0.5192	14088.36	14151.91	0.121	0.127	0.4491
176	13503.74	13600.98	0.119	0.121	0.715	11681.23	11725.79	0.13	0.13	0.38
177	11588.95	11676.61	0.115	0.121	0.7507	12016.66	12116.15	0.125	0.121	0.8212
178	12040.7	13133.42	0.126	0.135	8.3202	12503.95	12790.51	0.127	0.128	2.2405
179	11533.45	12097.68	0.116	0.129	4.6639	10971.39	12085.59	0.139	0.14	9.2192
180	12160.46	12310.08	0.14	0.14	1.2154	11846.06	12502.3	0.125	0.12	5.2489
181	11048.13	10728.47	0.126	0.132	-2.98	11360.47	11447.42	0.129	0.126	0.7596
182	12078.95	12625.76	0.149	0.148	4.3309	11590.96	11854.09	0.125	0.127	2.2198
183	11991.42	12510.59	0.135	0.134	4.1498	11653.8	11820.96	0.126	0.124	1.4141
184	12421.72	14361.21	0.141	0.144	13.505	11536.59	11875.62	0.133	0.131	2.8548
185	11186.37	11430.75	0.146	0.145	2.138	11490.46	11657.62	0.126	0.123	1.4339
186	11212.97	11701.59	0.128	0.131	4.1756	13848.65	14196.05	0.125	0.12	2.4472
187	12931.19	13057.34	0.137	0.14	0.9661	12308.89	12649.3	0.126	0.128	2.6912
188	13768.25	14827.08	0.128	0.129	7.1412	12394.67	12644	0.12	0.123	1.9719
189	12652.31	12740.55	0.123	0.128	0.6927	11724.68	12109	0.12	0.12	3.1738
190	12165.91	12223.78	0.14	0.139	0.4734	11481.4	11468.98	0.123	0.123	-0.108
191	10944.71	11313.95	0.13	0.126	3.2636	11406.23	11443.51	0.131	0.13	0.3258
192	11344.51	12068.73	0.124	0.125	6.0007	11305.92	11080.4	0.12	0.119	-2.035
193	13511.42	13784.82	0.104	0.119	1.9833	12113.7	12145.33	0.125	0.124	0.2604
194	11731.44	13867.71	0.145	0.149	15.405	10518.2	10582.55	0.13	0.129	0.6081
195	11147.58	12258.36	0.136	0.133	9.0614	12420.29	12867.22	0.122	0.126	3.4734
196	12849.83	13124.27	0.115	0.122	2.0911	15023.2	14879.89	0.128	0.128	-0.963
197	11675.63	12150.4	0.133	0.129	3.9074	10973.24	11123.15	0.125	0.124	1.3478
198	14584.24	15047.22	0.125	0.132	3.0768	10847.62	10871.26	0.125	0.127	0.2175
199	11561.24	11838.06	0.142	0.14	2.3383	11625.34	11690.4	0.123	0.123	0.5565
200	12879.14	14129.39	0.122	0.111	8.8485	14600.59	14522.51	0.114	0.121	-0.538
201	11715.16	13782.22	0.129	0.14	14.998	12126.19	12100.12	0.124	0.122	-0.215
202	13532.74	13936.26	0.13	0.131	2.8955	14058.72	16087.11	0.134	0.138	12.609
203	12748.61	13894.46	0.128	0.142	8.2469	10753.3	10856.23	0.123	0.119	0.9481
204	15678.77	15988.77	0.129	0.127	1.9389	12022.22	13120.03	0.133	0.134	8.3674
205	11151.38	13384.43	0.142	0.146	16.684	15152.1	16759.23	0.136	0.138	9.5895
206	11270.04	11290.75	0.141	0.144	0.1834	10286.37	10564.27	0.128	0.129	2.6306
207	12703.28	13562.27	0.113	0.122	6.3337	11531.59	11565.02	0.127	0.128	0.2891
208	11100.09	11485.1	0.149	0.148	3.3523	12460.34	12719.51	0.132	0.13	2.0376
209	13334.83	12676.37	0.136	0.14	-5.194	12351.33	12486.06	0.122	0.122	1.0791
210	16167.93	16693.73	0.124	0.134	3.1497	13282.75	13035.76	0.118	0.117	-1.895
211	10937.16	11065.36	0.135	0.131	1.1586	11735.79	11853.99	0.12	0.121	0.9971
212	12094.07	12293.36	0.136	0.133	1.6211	13032.29	13678.32	0.127	0.13	4.723
213	11355.31	11809.11	0.145	0.145	3.8428	12639.18	12413.66	0.118	0.117	-1.817
214	12259.93	12179.72	0.115	0.124	-0.659	10869.92	13085.71	0.131	0.137	16.933
215	11322.95	11507.88	0.114	0.122	1.6071	12842.97	12944.8	0.126	0.123	0.7867
216	12064.61	11731.94	0.118	0.124	-2.836	15033.78	16244.34	0.129	0.129	7.4522

217	15358.13	15763.99	0.129	0.133	2.5746	10965.42	11441.73	0.128	0.13	4.1629
218	12770.75	12772.46	0.142	0.142	0.0134	10521.6	11500.03	0.137	0.138	8.508
219	12798.56	14781.9	0.139	0.132	13.417	11488.01	12107.33	0.132	0.13	5.1153
220	13390.1	13373.53	0.14	0.14	-0.124	10750.47	11919.28	0.138	0.137	9.806
221	12856.69	14311.3	0.129	0.138	10.164	12991.23	12765.7	0.117	0.116	-1.767
222	12010.44	11895.76	0.119	0.125	-0.964	13241.62	13586.13	0.129	0.127	2.5357
223	11787	12555.65	0.138	0.132	6.1219	13255.77	13530.96	0.128	0.128	2.0337
224	11819.66	11874.18	0.117	0.124	0.4592	11815.02	12241.74	0.124	0.128	3.4858
225	13617.72	13965	0.135	0.133	2.4868	14907.6	16198.24	0.124	0.126	7.9678
226	11630.46	15149.09	0.124	0.143	23.227	11505.69	11647.03	0.123	0.124	1.2135
227	12138.94	12758.23	0.139	0.137	4.854	14448.25	14939.58	0.135	0.129	3.2888
228	11754.81	12228.36	0.137	0.132	3.8726	11991.4	12302.74	0.134	0.136	2.5306
229	11885.26	13764	0.125	0.12	13.65	10053.67	11299.59	0.138	0.135	11.026
230	12702.22	14299.41	0.108	0.111	11.17	12211.27	12329.46	0.122	0.123	0.9587
231	12548.58	12628.46	0.118	0.123	0.6325	11922.03	12070.22	0.127	0.132	1.2278
232	12026.97	12448.84	0.128	0.125	3.3889	13742.39	12763.86	0.126	0.129	-7.666
233	13022.31	15410.07	0.123	0.114	15.495	12706.28	12680.21	0.123	0.121	-0.206
234	11749.87	12345.1	0.14	0.142	4.8216	14780.88	16154.78	0.131	0.132	8.5046
235	14157.46	13486.79	0.137	0.141	-4.973	12350.21	12449.71	0.123	0.119	0.7992
236	11593.3	11910.11	0.127	0.128	2.66	12452.18	12668.21	0.12	0.113	1.7053
237	15427.22	15974.62	0.13	0.133	3.4267	12874.19	12992.39	0.116	0.117	0.9097
238	14446.46	14400.51	0.129	0.131	-0.319	12468.85	12660.9	0.127	0.129	1.5168
239	12039.76	13851.18	0.145	0.148	13.078	11794.93	12026.47	0.128	0.128	1.9253
240	11756.82	12270.91	0.135	0.133	4.1895	11773.5	11547.97	0.122	0.121	-1.953
241	10634.86	14687.34	0.126	0.141	27.592	11284.96	11148.06	0.127	0.121	-1.228
242	11414.53	11601.43	0.144	0.144	1.611	11770.85	12042.31	0.123	0.126	2.2542
243	12160.43	14111.39	0.139	0.146	13.825	16318.79	17614.2	0.131	0.134	7.3543
244	12154.52	13144.06	0.138	0.133	7.5284	12694.35	12885.39	0.128	0.127	1.4826
245	12150.49	12468.78	0.138	0.135	2.5527	10913.39	10964.01	0.129	0.127	0.4617
246	11469.39	11879.05	0.131	0.129	3.4486	14624.83	14683.4	0.123	0.123	0.3989
247	12505.94	12466.73	0.144	0.143	-0.314	11714.82	11868.58	0.126	0.127	1.2955
248	12122.03	12491.47	0.137	0.139	2.9576	11149.6	11554.99	0.12	0.124	3.5084
249	13670.75	14336.4	0.133	0.137	4.6431	12229.34	12206.49	0.126	0.123	-0.187
250	12990.69	13131.24	0.115	0.114	1.0704	15090.41	15952.6	0.128	0.132	5.4047
251	11337.62	12393.3	0.148	0.146	8.5182	14257.3	14332.95	0.118	0.122	0.5278
252	11988.47	11953.62	0.143	0.144	-0.292	13141.58	13126.73	0.121	0.127	-0.113
253	11045.53	11435.69	0.15	0.148	3.4118	12296.56	12424.46	0.13	0.13	1.0295
254	14294.61	14728.25	0.132	0.131	2.9443	10933.45	10804.83	0.122	0.115	-1.19
255	16643.34	17275.47	0.124	0.123	3.6591	14011.81	13459.37	0.126	0.121	-4.105
256	14352.38	15560.12	0.113	0.114	7.7618	11877.71	12174.73	0.13	0.129	2.4396
257	11567.4	11766.72	0.147	0.146	1.694	13057.28	13196.15	0.12	0.12	1.0524
258	13155.21	13337.51	0.137	0.138	1.3669	12568.04	12842.22	0.119	0.124	2.135
259	12993.52	15280.25	0.115	0.112	14.965	12401.97	12749.51	0.126	0.124	2.7259
260	13228.82	14996.73	0.139	0.132	11.789	12584.44	12338.67	0.124	0.124	-1.992
261	12238.24	12878.69	0.122	0.123	4.973	12381.18	12582.27	0.124	0.121	1.5982
262	12919.36	14870.58	0.135	0.135	13.121	12297.59	12367.17	0.114	0.115	0.5626

263	11632.62	12306.59	0.147	0.147	5.4765	11816.3	11926.3	0.134	0.132	0.9223
264	11552.91	11965.87	0.131	0.124	3.4512	13111.44	12885.91	0.116	0.115	-1.75
265	15306.71	15791.06	0.132	0.133	3.0672	13101.45	13236.18	0.12	0.12	1.0179
266	11494.24	11939.05	0.146	0.147	3.7256	12765.07	12644.99	0.126	0.128	-0.95
267	11807.55	12699.55	0.131	0.122	7.0238	13749.95	12667.56	0.12	0.129	-8.545
268	11072.62	12668.51	0.141	0.147	12.597	13766.06	13801.8	0.128	0.125	0.2589
269	12029.97	12874.06	0.138	0.133	6.5565	14924.58	15767.98	0.134	0.137	5.3488
270	11081.99	11675.74	0.129	0.138	5.0853	14763.32	14821.9	0.123	0.123	0.3952
271	11707.42	11770.55	0.139	0.14	0.5364	11968.53	12379.07	0.132	0.13	3.3164
272	12836.99	14429.03	0.137	0.131	11.034	11212.77	11398.75	0.12	0.126	1.6316
273	11202.7	14834.89	0.131	0.145	24.484	11114.12	11255.46	0.128	0.13	1.2557
274	11856.71	11905.79	0.145	0.144	0.4122	12355.42	12454.92	0.126	0.122	0.7989
275	13606.88	13662.02	0.136	0.137	0.4037	12994.99	13364.41	0.122	0.12	2.7643
276	11955.4	12542.33	0.126	0.123	4.6796	10541.38	11131.67	0.132	0.111	5.3028
277	12526.33	12468.84	0.142	0.141	-0.461	11448.06	11161.28	0.125	0.128	-2.569
278	11037.17	13067.04	0.125	0.14	15.534	14417.59	14621.56	0.125	0.124	1.395
279	14195.59	14565.13	0.123	0.13	2.5372	11526.71	12093.02	0.134	0.127	4.6829
280	11954.87	12570.09	0.122	0.119	4.8943	11719.42	12220.08	0.133	0.133	4.097
281	12780.21	13845.1	0.122	0.115	7.6914	12293.75	12422.66	0.134	0.133	1.0377
282	13561.73	13610.13	0.136	0.137	0.3557	11003.03	11140.52	0.122	0.121	1.2341
283	12606.48	12597.7	0.143	0.143	-0.07	11112.91	11114.12	0.123	0.124	0.0109
284	10373.05	10754.92	0.149	0.147	3.5507	11090.28	11142.91	0.12	0.121	0.4724
285	12410.34	14088.05	0.136	0.139	11.909	12349.16	12336.73	0.12	0.12	-0.101
286	12594.99	12509.93	0.132	0.134	-0.68	12287.48	12295.05	0.122	0.123	0.0616
287	11391.83	11827.97	0.146	0.144	3.6873	13473.91	13447.84	0.122	0.121	-0.194
288	15275.04	15716.58	0.131	0.126	2.8094	11211.8	12126.73	0.12	0.12	7.5447
289	12697.04	12661.47	0.137	0.137	-0.281	11020.72	11008.29	0.126	0.126	-0.113
290	13903.58	13278.05	0.136	0.139	-4.711	11022.86	11196.62	0.125	0.125	1.5519
291	11608.06	12073.36	0.123	0.124	3.854	11658.1	11732.83	0.127	0.125	0.6369
292	12660.28	12627.94	0.128	0.13	-0.256	11187.94	11286.64	0.132	0.134	0.8745
293	11611.76	11909.99	0.146	0.145	2.5041	14731.45	15054.76	0.122	0.123	2.1476
294	12989.11	13314.67	0.131	0.133	2.4451	15252.87	15255	0.116	0.115	0.014
295	16449.08	16866.57	0.13	0.125	2.4752	12596.51	13475.59	0.135	0.134	6.5235
296	13541.84	15591.41	0.119	0.122	13.146	12285.61	12060.08	0.119	0.118	-1.87
297	11855.36	11895.36	0.143	0.144	0.3363	11952.38	12039.16	0.128	0.128	0.7208
298	12252.42	14126.77	0.145	0.148	13.268	14304.58	13264.13	0.125	0.126	-7.844
299	10547.43	10727.05	0.143	0.141	1.6745	11935.31	12000.37	0.118	0.119	0.5422
300	12117.81	12038.86	0.121	0.131	-0.656	15096.52	15566.57	0.129	0.128	3.0196
301	11709.39	13389.05	0.138	0.132	12.545	11939.54	11759.89	0.129	0.122	-1.528
302	11897.98	13266.68	0.126	0.133	10.317	11842.81	11934.52	0.115	0.118	0.7685
303	11098.11	11400.78	0.144	0.143	2.6548	13985.13	14859.83	0.12	0.126	5.8863
304	12788.27	13553.31	0.124	0.119	5.6447	12180.45	12102.17	0.124	0.123	-0.647
305	14482	15239	0.109	0.115	4.9675	11542.42	11582.12	0.126	0.123	0.3428
306	16606.21	16489.26	0.128	0.133	-0.709	14473.87	15838.98	0.124	0.126	8.6187
307	10755.36	11441.55	0.132	0.131	5.9973	15795.01	16007.81	0.127	0.129	1.3294
308	10701.06	11270.01	0.147	0.146	5.0483	12459.45	12746.02	0.121	0.122	2.2483

309	11830.31	11687.92	0.138	0.138	-1.218	11043.6	11200.29	0.128	0.123	1.399
310	15582.73	16244.28	0.131	0.125	4.0725	10797.7	10850.34	0.118	0.119	0.4851
311	12948.51	13125.62	0.14	0.139	1.3493	10822.44	10945.08	0.138	0.135	1.1205
312	12745.07	13199.11	0.126	0.127	3.4399	12705.06	12789.71	0.126	0.127	0.6618
313	11818.96	11826	0.121	0.128	0.0595	10923.02	10981.01	0.132	0.132	0.5281
314	14552.39	14265.07	0.121	0.127	-2.014	12358.58	12525.53	0.127	0.123	1.3329
315	11336.12	11612.94	0.147	0.145	2.3837	14242.56	14557.33	0.12	0.125	2.1623
316	14600.39	14836.96	0.128	0.125	1.5945	15579.74	16530.21	0.137	0.139	5.7499
317	15744.16	16165.79	0.129	0.124	2.6082	11481.32	11620.73	0.124	0.123	1.1997
318	12693.65	12648.59	0.132	0.134	-0.356	11377.53	11876.94	0.125	0.124	4.2049
319	14942.6	14979.96	0.135	0.135	0.2494	11939.26	11957.04	0.121	0.121	0.1487
320	14314.27	14134.8	0.13	0.14	-1.27	15698	15878.38	0.129	0.128	1.136
321	10965.12	11266.07	0.145	0.144	2.6713	9990.828	10645.16	0.141	0.138	6.1468
322	12001.14	12372.56	0.137	0.133	3.002	12672.12	13142.07	0.13	0.128	3.5759
323	12613.38	13028.46	0.127	0.132	3.1859	12578.75	12591.05	0.126	0.123	0.0977
324	11992.45	13160.98	0.124	0.113	8.8787	14460.23	14365.88	0.122	0.119	-0.657
325	11094.65	11488.95	0.149	0.147	3.432	11884.95	11876.16	0.129	0.129	-0.074
326	14913.64	14619.29	0.125	0.133	-2.013	11936.17	11988.8	0.119	0.119	0.439
327	10934.04	10934.04	0.145	0.145	0	12872.55	12846.48	0.127	0.125	-0.203
328	11917.33	13875.65	0.139	0.148	14.113	12013.79	12202.91	0.113	0.119	1.5498
329	12245.4	14985.75	0.125	0.145	18.286	14267.18	14447.09	0.129	0.131	1.2453
330	11530.19	15436.4	0.125	0.144	25.305	10900.81	11003.74	0.125	0.121	0.9354
331	12401.34	12485.77	0.144	0.144	0.6763	11209.18	11963.31	0.13	0.127	6.3037
332	12722.72	12819.93	0.116	0.126	0.7583	11196.55	11235.04	0.127	0.126	0.3426
333	13756.43	14908.95	0.118	0.122	7.7303	11741.56	11758.42	0.129	0.129	0.1434
334	12424.29	12568.1	0.117	0.127	1.1443	12088.19	12861.03	0.126	0.128	6.0092
335	13353.97	15097.52	0.139	0.133	11.549	12023.19	12623.47	0.132	0.13	4.7553
336	13909.74	14157.73	0.132	0.137	1.7516	11343.3	11897.65	0.122	0.121	4.6593
337	12087.15	11949.04	0.114	0.12	-1.156	13985.02	13939.46	0.117	0.12	-0.327
338	11876.41	11991.56	0.142	0.142	0.9602	12748.85	12955.04	0.128	0.13	1.5916
339	11078.8	11375.16	0.112	0.121	2.6053	12511.4	12660.27	0.119	0.118	1.1759
340	11627.33	12350.38	0.124	0.122	5.8545	11087.27	11285.88	0.131	0.131	1.7598
341	12582.25	12628.4	0.142	0.142	0.3655	14777.63	14974.08	0.13	0.129	1.3119
342	11917.62	13792.45	0.122	0.122	13.593	12876.91	13685.54	0.126	0.129	5.9086
343	12286.65	14294.92	0.128	0.134	14.049	11571.49	12503.85	0.135	0.136	7.4566
344	12079.35	14087.22	0.143	0.147	14.253	11113.83	11280.52	0.124	0.122	1.4777
345	12501.78	13188.61	0.118	0.119	5.2077	11671.41	12426.51	0.123	0.128	6.0765
346	10900.15	11288.6	0.149	0.147	3.441	11096.32	11426.06	0.123	0.127	2.8859
347	11698.08	11979.04	0.145	0.144	2.3454	12528.47	12526.55	0.116	0.116	-0.015
348	12352.75	14012.45	0.115	0.117	11.845	13679.84	13726.49	0.118	0.119	0.3399
349	12889.38	13151.8	0.138	0.135	1.9954	11316.57	11664.31	0.132	0.131	2.9812
350	11440.21	11604.69	0.145	0.146	1.4173	12771.57	12531.83	0.123	0.12	-1.913
351	13749.53	14629.2	0.118	0.115	6.0131	12625.43	12871.37	0.125	0.127	1.9108
352	13871.81	13753.96	0.115	0.113	-0.857	11334.72	11532.33	0.13	0.127	1.7135
353	11858.47	12271.56	0.142	0.143	3.3662	11789.54	12055.43	0.126	0.126	2.2056
354	16541.36	16855.92	0.12	0.127	1.8662	13460.26	13525.32	0.118	0.118	0.481

355	12209.31	12603.78	0.123	0.129	3.1298	11405.86	12639.37	0.14	0.139	9.7592
356	13369.51	14191.78	0.121	0.127	5.794	10492.08	10633.41	0.126	0.127	1.3292
357	12187.36	12729.82	0.134	0.134	4.2613	10882.76	10906.4	0.125	0.126	0.2167
358	11720.63	12160.37	0.129	0.128	3.6162	12939.3	13323.62	0.118	0.118	2.8845
359	12700.05	12995.08	0.113	0.121	2.2703	12266.04	12365.12	0.126	0.12	0.8013
360	11886.24	11897.66	0.14	0.141	0.096	11153.83	11295.16	0.125	0.126	1.2513
361	13349.83	13361.55	0.14	0.139	0.0877	15301.9	16278.81	0.117	0.121	6.0011
362	11313.47	11488.03	0.12	0.126	1.5195	11743.23	11859.59	0.117	0.117	0.9812
363	12555.7	13524.4	0.114	0.124	7.1626	12179.43	12502.1	0.121	0.125	2.5809
364	13186.53	13344.19	0.132	0.133	1.1815	11723.93	12035.09	0.125	0.128	2.5855
365	12965.53	12310.71	0.138	0.142	-5.319	15193.59	15633.85	0.129	0.128	2.8161
366	11070.36	12317.71	0.133	0.131	10.126	11638.74	11691.38	0.118	0.118	0.4502
367	15926.03	15722.13	0.123	0.132	-1.297	11599.28	11734.01	0.127	0.127	1.1482
368	16001.3	16423.43	0.131	0.125	2.5703	12425.85	12544.05	0.121	0.122	0.9423
369	12850.47	12386.57	0.137	0.14	-3.745	12199.58	12414.97	0.129	0.126	1.7349
370	12640.29	12868.61	0.139	0.139	1.7742	12568.62	12542.55	0.124	0.122	-0.208
371	12771.12	12934.17	0.134	0.134	1.2606	11481.27	11580.76	0.129	0.124	0.8592
372	12082.88	13858.78	0.142	0.147	12.814	11700.58	12182.04	0.131	0.13	3.9522
373	12734.98	16454.13	0.142	0.141	22.603	11038.47	11197.35	0.126	0.125	1.4188
374	10116.5	10464.95	0.148	0.145	3.3296	12051.85	11852.36	0.12	0.118	-1.683
375	11168.83	11405.94	0.145	0.144	2.0788	13976.37	14068.8	0.128	0.129	0.657
376	13510.65	13650.18	0.134	0.139	1.0222	12098.41	12085.99	0.122	0.122	-0.103
377	12404.27	12612.17	0.138	0.135	1.6484	12818.07	12980.41	0.119	0.119	1.2507
378	11799.22	11820.94	0.145	0.145	0.1837	12058.06	11832.53	0.121	0.12	-1.906
379	13733.98	14338.85	0.121	0.123	4.2184	14314.56	14717.03	0.122	0.122	2.7348
380	12083.92	15973.12	0.135	0.132	24.348	12864.41	12609.85	0.123	0.12	-2.019
381	12196	12920.97	0.147	0.147	5.6108	11907	12025.2	0.119	0.12	0.9829
382	13954.94	15600.72	0.135	0.137	10.549	10242.75	10743.53	0.135	0.129	4.6612
383	13961.4	15433.44	0.138	0.134	9.538	12434.38	12573.25	0.121	0.121	1.1045
384	13943.53	15611.56	0.12	0.11	10.685	11281.46	11721.41	0.132	0.13	3.7534
385	11037.37	11352.47	0.145	0.145	2.7756	13570.14	13967.47	0.125	0.123	2.8447
386	13282.76	13587.75	0.118	0.113	2.2446	14275.82	14181.97	0.122	0.12	-0.662
387	11320.67	11621.46	0.141	0.139	2.5883	11483.6	11525.31	0.127	0.127	0.3619
388	12432.69	13465.98	0.114	0.119	7.6734	12532.98	14198.05	0.134	0.138	11.727
389	11501.82	13092.22	0.125	0.122	12.148	10581.01	10838.62	0.131	0.131	2.3768
390	10557.41	13849.23	0.126	0.141	23.769	13118.22	13825.93	0.119	0.119	5.1187
391	14130.56	16426.97	0.13	0.137	13.98	11575.69	11766.23	0.127	0.128	1.6194
392	11567.86	12346.77	0.138	0.133	6.3086	10491.96	11096.26	0.133	0.133	5.446
393	15882.78	15886.92	0.129	0.129	0.0261	10131.6	10634.98	0.131	0.132	4.7333
394	12406.1	13125.53	0.127	0.13	5.4811	14551.65	14500.02	0.118	0.122	-0.356
395	14119.44	14862.45	0.107	0.115	4.9993	14525.25	14564.74	0.138	0.137	0.2712
396	13146.16	13692.19	0.139	0.137	3.9879	11847.38	11685.84	0.125	0.122	-1.382
397	13017.53	13183.72	0.142	0.142	1.2606	15821.37	16795.35	0.117	0.121	5.7991
398	13171.41	16292.62	0.136	0.134	19.157	13362.55	13344.77	0.12	0.118	-0.133
399	13367.61	13581.3	0.115	0.111	1.5734	10620.66	11729.22	0.128	0.128	9.4513
400	10488.25	10778.2	0.146	0.145	2.6901	10682.2	10901.73	0.132	0.132	2.0137

401	10872.85	11210.16	0.122	0.126	3.009	11650.41	12603.75	0.136	0.135	7.564
402	11899.12	12082.47	0.133	0.129	1.5174	13906.19	14045.06	0.118	0.118	0.9888
403	12767.08	12771.23	0.14	0.141	0.0324	11447.77	11306.73	0.123	0.116	-1.247
404	12135.08	13099.08	0.123	0.118	7.3593	12196.94	12476.18	0.131	0.128	2.2382
405	13321.08	14182.72	0.126	0.124	6.0753	13950.28	14048.19	0.122	0.128	0.6969
406	13569.9	16259.07	0.136	0.134	16.539	12016.47	12501.29	0.125	0.119	3.8781
407	11636.24	12254.89	0.143	0.14	5.0482	12115.16	12585.74	0.127	0.126	3.7389
408	12790.47	13781.77	0.129	0.135	7.1928	11083.71	11532.53	0.131	0.131	3.8918
409	12204.52	12194.37	0.12	0.129	-0.083	10867.14	10854.71	0.121	0.121	-0.114
410	10203.7	10523.14	0.149	0.147	3.0357	13005.09	13067.72	0.139	0.138	0.4793
411	11388.27	11585.16	0.141	0.141	1.6996	12683.07	13068.08	0.129	0.126	2.9462
412	11913.6	12618.81	0.131	0.127	5.5886	12521.88	12428.03	0.126	0.124	-0.755
413	14465.11	14615.91	0.132	0.136	1.0317	11392.51	11500.92	0.127	0.122	0.9426
414	13559.13	13861.56	0.132	0.139	2.1818	10557.97	10716.84	0.125	0.124	1.4825
415	16009.64	16621.65	0.124	0.121	3.682	14709.35	14733.37	0.122	0.119	0.163
416	13104.29	14517.97	0.123	0.115	9.7374	11688.36	11938.9	0.122	0.126	2.0985
417	12523.25	14119.47	0.123	0.118	11.305	10539	11009.33	0.129	0.129	4.2721
418	11736.19	12183.21	0.122	0.124	3.6692	11190.69	11255.75	0.127	0.127	0.578
419	12634.19	13389.64	0.107	0.116	5.642	11655.43	11732.42	0.123	0.12	0.6562
420	11849.72	12757.58	0.121	0.115	7.1162	11438.77	11213.24	0.122	0.121	-2.011
421	14124.49	14928.86	0.126	0.127	5.388	11135.63	11415.46	0.13	0.13	2.4513
422	11263.41	12047.88	0.145	0.147	6.5113	12953.67	13114.79	0.119	0.119	1.2286
423	12968.49	13112.93	0.139	0.142	1.1015	12736.34	12812.19	0.125	0.126	0.5921
424	13789.63	13805.49	0.14	0.14	0.1149	12431.2	12674.3	0.126	0.125	1.9181
425	11298.29	11765.61	0.131	0.13	3.9719	11822.71	11940.91	0.119	0.119	0.9899
426	10995.3	12313.94	0.136	0.129	10.708	15796.96	17256.84	0.137	0.134	8.4597
427	11588.56	11416.17	0.138	0.14	-1.51	12052.59	11933.03	0.128	0.122	-1.002
428	12249.42	16316.82	0.137	0.131	24.928	11294.84	11302.42	0.124	0.125	0.067
429	10673.2	10942.95	0.118	0.124	2.465	15308.56	15571.66	0.127	0.126	1.6896
430	12309.37	12763.87	0.117	0.114	3.5609	13677.24	13652.18	0.123	0.12	-0.184
431	12025.97	12121.24	0.135	0.139	0.786	11186.17	11258.8	0.128	0.129	0.6451
432	13013.52	16148.74	0.113	0.111	19.415	13504.83	13643.7	0.118	0.117	1.0179
433	11848.24	13391.99	0.125	0.139	11.527	11747.54	12073.14	0.122	0.125	2.6969
434	11825.97	11947.65	0.123	0.129	1.0184	10619.21	11646.4	0.134	0.134	8.8198
435	11446	11497.17	0.122	0.129	0.4451	12584.69	13021.52	0.124	0.124	3.3547
436	13747.28	13643.1	0.104	0.115	-0.764	11805.1	11981.08	0.125	0.131	1.4688
437	15957.27	15819.61	0.128	0.134	-0.87	12546.48	12767.91	0.128	0.127	1.7342
438	11966.92	13432.06	0.117	0.12	10.908	10992.97	11167.74	0.128	0.128	1.5649
439	12981.12	13724.13	0.108	0.118	5.4139	12786.65	12851.71	0.121	0.121	0.5062
440	17085.28	17212.31	0.127	0.134	0.738	13561.97	13907.54	0.127	0.129	2.4847
441	12878.31	13803.13	0.106	0.118	6.7001	11437.03	11685.55	0.128	0.127	2.1268
442	11838.99	12392.8	0.107	0.121	4.4688	12608.09	12599.3	0.129	0.129	-0.07
443	10814.89	11076.4	0.144	0.141	2.3609	11090.81	11212.74	0.127	0.124	1.0874
444	13069.89	13196.04	0.138	0.141	0.956	12618.08	12761.89	0.121	0.117	1.1269
445	12655.5	14478.43	0.115	0.117	12.591	11761.03	11836.39	0.125	0.125	0.6366
446	12690.78	13478.37	0.13	0.133	5.8433	13300.25	13584.72	0.119	0.123	2.0941

447	11973.27	12529.11	0.134	0.131	4.4364	12444.42	12533.3	0.122	0.125	0.7091
448	11624.01	12566.89	0.124	0.122	7.5029	11959.04	12524.76	0.133	0.134	4.5168
449	12490.05	12521.77	0.14	0.14	0.2533	11279.15	12043.61	0.136	0.136	6.3474
450	12203.21	12683.3	0.123	0.126	3.7852	12150.31	12436.88	0.123	0.125	2.3042
451	11698.83	12290.2	0.145	0.139	4.8117	11820.81	12574.94	0.127	0.126	5.9971
452	11519.51	12040.47	0.146	0.146	4.3267	11098.77	11163.83	0.123	0.123	0.5828
453	12827.1	14221.69	0.14	0.132	9.8061	10551.78	11023.45	0.133	0.131	4.2787
454	12624.4	12955.86	0.136	0.133	2.5584	12610.9	13891.78	0.138	0.137	9.2204
455	11028.29	11643.84	0.134	0.131	5.2865	12939.98	13227.88	0.119	0.123	2.1765
456	11616.84	12440.19	0.137	0.13	6.6184	11442.8	11725.35	0.133	0.132	2.4097
457	13505.33	13784.71	0.133	0.135	2.0267	14083.71	14272.92	0.121	0.122	1.3256
458	11200.16	13053.84	0.13	0.139	14.2	10957.44	11283.13	0.139	0.135	2.8865
459	12824.46	12808.4	0.14	0.14	-0.125	10888.65	11125.75	0.132	0.132	2.1312
460	14285.65	14690.97	0.122	0.128	2.759	13184.55	13302.75	0.116	0.117	0.8885
461	11430.13	12080.67	0.149	0.149	5.385	10940.28	10946.13	0.129	0.129	0.0535
462	11937.77	12752.04	0.126	0.138	6.3854	13119.41	13301.96	0.128	0.13	1.3723
463	12564.01	12876.02	0.127	0.131	2.4232	10962.73	11620.04	0.132	0.132	5.6567
464	10972.07	11324.65	0.148	0.145	3.1134	15579.04	15904.65	0.129	0.127	2.0473
465	13927.47	13854.51	0.123	0.131	-0.527	11553.46	11652.96	0.127	0.122	0.8538
466	13064.6	13392.33	0.141	0.14	2.4472	14730	14713.72	0.132	0.133	-0.111
467	11187.22	12134.75	0.132	0.127	7.8083	11831.99	11998.97	0.125	0.126	1.3917
468	10572.19	10958.2	0.15	0.148	3.5226	14857.79	15190.89	0.128	0.126	2.1928
469	12345.8	13411.86	0.136	0.136	7.9487	14815.89	15824.61	0.138	0.143	6.3743
470	11017.6	11403.91	0.145	0.149	3.3875	13421.01	12255.7	0.116	0.119	-9.508
471	12398.57	12199.37	0.113	0.12	-1.633	12023.51	12422.25	0.133	0.132	3.2099
472	13101.64	13223.36	0.136	0.14	0.9205	11065.86	11053.44	0.123	0.123	-0.112
473	11157.87	12523.42	0.126	0.126	10.904	13300.82	14955.18	0.134	0.138	11.062
474	11284.63	12514.45	0.142	0.148	9.8273	11419.97	11516.24	0.124	0.126	0.836
475	11385.42	11622.53	0.132	0.131	2.0401	14652.33	17213.12	0.124	0.124	14.877
476	12524.26	12851.5	0.111	0.122	2.5463	12204.97	12529.85	0.132	0.131	2.5929
477	15958.1	16321.95	0.13	0.124	2.2292	13340.4	13793.04	0.12	0.124	3.2816
478	13655.37	13773.44	0.13	0.134	0.8573	13096.42	13373.66	0.127	0.126	2.0731
479	12380.91	13188.07	0.11	0.119	6.1204	12180.92	12398.11	0.116	0.121	1.7518
480	12047.47	13620.76	0.129	0.126	11.551	11745.3	12084.83	0.13	0.124	2.8096
481	13252.85	14313.79	0.126	0.13	7.412	12798.13	13216.57	0.129	0.126	3.166
482	12413.41	12984.29	0.137	0.135	4.3967	15222.34	16605.73	0.131	0.132	8.3308
483	12343.21	13768.52	0.138	0.133	10.352	11091.65	11109.43	0.12	0.121	0.1601
484	16395.51	16871.92	0.123	0.129	2.8237	12992.01	12749.17	0.119	0.117	-1.905
485	13836.7	13840.84	0.133	0.134	0.0299	12991.7	12929.62	0.125	0.123	-0.48
486	11892.11	11896.25	0.143	0.144	0.0348	13222.02	13315.78	0.123	0.127	0.7041
487	12531.15	12385.68	0.119	0.125	-1.175	11586.09	11642.16	0.121	0.123	0.4816
488	12295.03	13966.36	0.112	0.109	11.967	13406.46	13498.89	0.124	0.126	0.6847
489	13060.06	12978.43	0.134	0.136	-0.629	12788.28	12853.34	0.117	0.117	0.5062
490	13505.77	14272.46	0.136	0.132	5.3718	10920.57	11138.89	0.132	0.129	1.96
491	13599.06	15583.65	0.138	0.13	12.735	13912.51	14135.73	0.126	0.124	1.5791
492	12354.27	12677.58	0.135	0.139	2.5502	16150.51	17229.56	0.129	0.131	6.2628

493	15135.56	15488.66	0.131	0.133	2.2797	12078.31	12181.24	0.124	0.12	0.845
494	12592.75	13393.84	0.109	0.119	5.981	14496.75	14508.46	0.122	0.121	0.0808
495	12662.96	14166.21	0.116	0.117	10.612	11735.64	11861.2	0.121	0.121	1.0586
496	13138.2	14804.18	0.141	0.145	11.253	12558.21	12756.12	0.124	0.128	1.5514
497	11123.06	11354.22	0.123	0.126	2.0359	11783.46	11882.96	0.122	0.117	0.8373
498	15852.89	15536.65	0.125	0.131	-2.035	12280.03	12464	0.119	0.122	1.476
499	12709.35	13205.21	0.134	0.139	3.755	13323.93	13388.99	0.122	0.122	0.4859
500	12172.71	12375.64	0.136	0.134	1.6397	10898.34	11883.21	0.14	0.139	8.2879
501	11090.42	11528.86	0.134	0.129	3.803	11421	11718.52	0.124	0.128	2.5389
502	14484.13	15997.56	0.127	0.131	9.4604	10688.94	11137.88	0.131	0.134	4.0308
503	11011.31	11430.75	0.148	0.148	3.6695	15130.41	16170.59	0.128	0.134	6.4325
504	13481.52	14113.82	0.117	0.123	4.48	14039.33	14078.82	0.133	0.132	0.2805
505	12124.48	12376.44	0.141	0.141	2.0358	12862.92	12927.98	0.121	0.122	0.5033
506	11167.56	15131.36	0.143	0.141	26.196	11026.03	11649.92	0.12	0.119	5.3553
507	16177.7	16633.4	0.124	0.129	2.7397	10793.42	10868.78	0.126	0.127	0.6933
508	10443.64	10724.59	0.145	0.143	2.6197	14918.93	14898.72	0.114	0.118	-0.136
509	11402.49	12082.32	0.149	0.149	5.6266	11237.76	11332.53	0.128	0.128	0.8362
510	13448.16	13453.19	0.107	0.117	0.0374	11904.64	12022.83	0.12	0.12	0.9831
511	17595.27	18197.81	0.127	0.122	3.3111	10396.72	11514.24	0.128	0.129	9.7056
512	16754.94	16762.25	0.12	0.131	0.0436	12534.5	12725.54	0.128	0.127	1.5012
513	10608.91	10677.49	0.115	0.122	0.6423	12131.53	12294.93	0.12	0.113	1.329
514	11599.64	11613.28	0.142	0.144	0.1174	15995.33	17092.81	0.132	0.13	6.4208
515	13404.17	13884.59	0.135	0.132	3.4601	11446.27	12222.66	0.135	0.132	6.3521
516	12404.56	12430.14	0.117	0.117	0.2058	12562.13	12598.91	0.122	0.119	0.2919
517	13863.87	14370.82	0.131	0.133	3.5276	13008.08	13779.71	0.139	0.138	5.5998
518	14536.59	15277.01	0.13	0.133	4.8466	12187.51	12201.24	0.123	0.117	0.1125
519	13333.95	14574.2	0.122	0.125	8.51	11867.62	12102.44	0.121	0.124	1.9402
520	13850.48	15050.95	0.113	0.117	7.976	12234.93	12353.13	0.118	0.119	0.9568
521	12657.72	13460.95	0.115	0.125	5.9671	11575.9	11717.23	0.129	0.13	1.2062
522	11511.56	11979.34	0.14	0.136	3.9049	12249.45	12189.87	0.127	0.129	-0.489
523	13074.93	13241.58	0.132	0.137	1.2586	11948.71	11723.18	0.121	0.12	-1.924
524	11959.22	12401.09	0.144	0.145	3.5632	11803.07	11922.98	0.126	0.125	1.0057
525	12673.66	13347.63	0.145	0.146	5.0494	13372.88	13415.6	0.121	0.122	0.3184
526	12285.45	13055.88	0.131	0.139	5.901	13622.4	13826.37	0.128	0.127	1.4752
527	12247.04	13463.02	0.141	0.148	9.032	12803.23	12902.72	0.123	0.119	0.7711
528	13915.14	15830.01	0.136	0.138	12.096	11458.45	11921.5	0.14	0.136	3.8842
529	16773.32	17549.59	0.122	0.131	4.4233	11509.75	11562.38	0.118	0.119	0.4552
530	11529.77	12266.38	0.148	0.148	6.0051	14363.64	14583.52	0.128	0.128	1.5077
531	12056.26	13080.38	0.122	0.121	7.8295	16234.84	16584.3	0.131	0.129	2.1072
532	12629.79	14706.36	0.139	0.144	14.12	13415.4	13405.11	0.116	0.122	-0.077
533	14180.59	14714.02	0.132	0.134	3.6253	12543.23	12411.34	0.124	0.121	-1.063
534	12655.4	16652.89	0.135	0.131	24.005	11083.54	11183.04	0.127	0.123	0.8897
535	12700.71	13116.24	0.126	0.126	3.168	11343.53	11432.53	0.127	0.127	0.7784
536	11687.7	14299.06	0.128	0.141	18.262	11250.73	11289.72	0.126	0.121	0.3454
537	13784.15	13764.66	0.136	0.136	-0.142	11931.85	11942.65	0.124	0.122	0.0904
538	11592.6	12832.6	0.139	0.137	9.6629	11231.9	11284.54	0.122	0.122	0.4664

539	13232.67	13195.24	0.114	0.112	-0.284	11726.63	11893.62	0.124	0.125	1.404
540	12499.66	12503.8	0.142	0.142	0.0331	12500.6	12930.72	0.124	0.125	3.3264
541	13321.23	13439.3	0.134	0.138	0.8786	12852	12925.01	0.122	0.124	0.5649
542	11107.85	11547	0.124	0.12	3.8032	12302.77	12545.03	0.121	0.125	1.9311
543	12792.07	12867.13	0.142	0.142	0.5834	12672.01	12911.21	0.134	0.133	1.8527
544	12534.95	12542.82	0.127	0.128	0.0627	11883.26	11912.26	0.125	0.125	0.2434
545	11834.64	12641.79	0.111	0.121	6.3848	15097.63	16126.47	0.119	0.124	6.3798
546	12618.43	13003.96	0.135	0.137	2.9647	12010.43	12172.77	0.121	0.12	1.3336
547	15060.65	15618.72	0.128	0.13	3.5731	12523.61	12765.03	0.13	0.129	1.8913
548	10967.94	14276.86	0.127	0.14	23.177	15028.26	15199.05	0.129	0.129	1.1237
549	16348.64	16784.29	0.125	0.123	2.5956	16356.28	16385.57	0.129	0.128	0.1788
550	12174.08	13134.46	0.116	0.125	7.3119	10953.88	11103.79	0.134	0.134	1.3501
551	11430.85	12833.99	0.115	0.117	10.933	11576.5	11665.91	0.126	0.116	0.7664
552	11772.7	12129.51	0.145	0.146	2.9417	10335.89	11046.38	0.141	0.139	6.4319
553	12534.72	12907.06	0.113	0.124	2.8848	12828.97	12871.69	0.123	0.123	0.3319
554	14778.46	14862.36	0.121	0.128	0.5645	15499.2	15404.97	0.125	0.128	-0.612
555	11805.41	11805.41	0.144	0.144	0	11911.74	12118.23	0.121	0.126	1.7039
556	11968.4	13141.66	0.123	0.12	8.9278	10368.11	10779.48	0.14	0.14	3.8162
557	13522.17	14126.73	0.132	0.138	4.2795	11995.6	12177.11	0.123	0.125	1.4906
558	10681.15	11004.03	0.147	0.145	2.9342	11082.29	12173.35	0.139	0.139	8.9627
559	11468.35	12429.97	0.135	0.123	7.7363	11287.91	11532.38	0.137	0.139	2.1199
560	14338.04	14433.48	0.133	0.136	0.6613	11552.92	11671.12	0.122	0.123	1.0127
561	11356.39	11633.2	0.142	0.14	2.3795	10920.86	11078.77	0.131	0.132	1.4253
562	15785.8	16055.27	0.125	0.132	1.6783	13261.56	13607.12	0.126	0.129	2.5396
563	11176.22	11482.74	0.146	0.144	2.6694	11557.5	11675.7	0.122	0.123	1.0123
564	11682.33	13495.8	0.115	0.112	13.437	9907.128	11284.81	0.138	0.138	12.208
565	11393.2	11955.29	0.123	0.129	4.7015	11969.2	12081.72	0.127	0.125	0.9313
566	15887.84	16149.05	0.133	0.134	1.6175	12107.38	12423.9	0.132	0.129	2.5477
567	12281.23	12602.36	0.136	0.131	2.5482	13663	13817.73	0.126	0.12	1.1198
568	12791.89	14425.65	0.142	0.145	11.325	11415.82	11741.42	0.123	0.127	2.7731
569	11824.54	12503.86	0.148	0.147	5.4329	12483.1	12610.09	0.139	0.137	1.007
570	15881.89	16621.68	0.129	0.129	4.4508	10804.12	11244.07	0.134	0.131	3.9127
571	11066.28	12275.4	0.142	0.149	9.8499	11878.15	12015.64	0.121	0.12	1.1442
572	12993.58	13007.22	0.137	0.139	0.1049	11188.18	11253.24	0.121	0.122	0.5782
573	17040.41	17719.32	0.124	0.122	3.8315	14207.94	14281.91	0.12	0.124	0.5179
574	12456.03	15349.92	0.114	0.111	18.853	12672.33	12912.45	0.121	0.124	1.8596
575	12328.72	12852.31	0.121	0.118	4.0739	14731.4	14837.17	0.139	0.137	0.7129
576	11613.62	12107.3	0.137	0.134	4.0775	11578.01	12069.88	0.12	0.127	4.0752
577	12527.63	13013.43	0.14	0.142	3.7331	11028.83	11891.24	0.127	0.124	7.2525
578	11270.73	12303.99	0.136	0.132	8.3978	14099.95	14140.87	0.12	0.118	0.2894
579	11743.14	15355.25	0.135	0.14	23.524	14219.48	14334.93	0.123	0.122	0.8053
580	12329.38	12888.49	0.134	0.131	4.3381	14205.37	14442.47	0.125	0.123	1.6417
581	13812.78	14435.97	0.124	0.131	4.3169	10872.22	11106.19	0.131	0.13	2.1067
582	11540.48	12919.55	0.132	0.131	10.674	9966.747	10308.91	0.127	0.129	3.3191
583	13419.41	14057.83	0.124	0.139	4.5414	11586.45	11725.32	0.125	0.124	1.1844
584	11749.96	11951.79	0.136	0.132	1.6888	12757.56	13121.33	0.126	0.126	2.7723

585	12765.78	15882.06	0.135	0.136	19.621	11666.24	11690.68	0.128	0.127	0.209
586	13943.04	14079.19	0.137	0.141	0.967	15160.55	15373.01	0.122	0.121	1.382
587	11820.24	13832.25	0.143	0.148	14.546	12470.39	12569.47	0.127	0.121	0.7883
588	11523.77	12393.04	0.133	0.124	7.0142	12082.7	12182.19	0.124	0.12	0.8167
589	17123.05	17672.75	0.124	0.122	3.1105	12203.72	12470.53	0.13	0.128	2.1395
590	12560.09	14663.05	0.108	0.111	14.342	10584.48	10743.35	0.127	0.126	1.4788
591	12994.18	13209.17	0.113	0.11	1.6276	12373.52	13081.23	0.122	0.123	5.4101
592	11942.19	12199.68	0.143	0.144	2.1106	11542.67	12575.74	0.141	0.14	8.2148
593	11957.69	11999.11	0.144	0.145	0.3452	15272.94	15748.85	0.132	0.129	3.0219
594	12943.41	13280.62	0.127	0.139	2.5391	11340.46	11554.64	0.131	0.13	1.8536
595	12075.3	12473.24	0.143	0.141	3.1903	12654.82	12757.75	0.123	0.119	0.8068
596	11302.69	11779.92	0.15	0.147	4.0512	10209.09	10431.13	0.137	0.141	2.1287
597	14320.07	14922.88	0.134	0.133	4.0395	11406.07	11381.22	0.123	0.123	-0.218
598	13920.26	14693.29	0.121	0.123	5.2611	11760.03	11528.57	0.124	0.12	-2.008
599	13174.79	13586.04	0.135	0.132	3.027	12757.41	13176.29	0.131	0.128	3.179
600	13202.07	14766.37	0.123	0.116	10.594	11652.3	11618.15	0.116	0.116	-0.294
601	10772.14	10784.56	0.143	0.143	0.1152	15957.5	16134.95	0.13	0.129	1.0998
602	16461.06	17148.55	0.124	0.12	4.009	12401.79	12640.87	0.126	0.128	1.8913
603	11751.55	12470.37	0.145	0.145	5.7642	12356.84	12396.75	0.127	0.127	0.322
604	12328.33	13079.78	0.141	0.142	5.7452	15041.95	16286.43	0.125	0.128	7.6412
605	12753.06	13075.49	0.132	0.133	2.4659	12413.48	12692.12	0.121	0.116	2.1954
606	13297.69	13451.33	0.113	0.123	1.1422	13256.19	13230.12	0.122	0.121	-0.197
607	10697.35	14241.63	0.128	0.141	24.887	14362.5	15744.47	0.127	0.129	8.7775
608	12369.06	12369.06	0.139	0.139	0	11871.99	12005	0.13	0.129	1.108
609	14536.84	14301.32	0.124	0.132	-1.647	11567.64	11542.79	0.124	0.124	-0.215
610	11351.9	11590.4	0.12	0.129	2.0577	11094.93	11217.23	0.123	0.123	1.0903
611	13374.72	14767.6	0.118	0.126	9.432	11534.01	12187.27	0.131	0.129	5.3602
612	10462.63	10852.79	0.15	0.148	3.595	11154.04	11234.24	0.129	0.129	0.714
613	13199.83	13268.08	0.123	0.125	0.5144	12046.05	12218.8	0.13	0.129	1.4139
614	13005.8	15058.89	0.12	0.116	13.634	13482.62	13737.27	0.126	0.129	1.8537
615	11390.37	13494.17	0.125	0.143	15.59	10458.85	10756.46	0.137	0.14	2.7668
616	13583.11	13583.11	0.14	0.14	0	12312.48	12549.72	0.122	0.121	1.8904
617	14803.26	14834.94	0.124	0.132	0.2136	14499.61	14501.82	0.121	0.127	0.0153
618	11490.02	13010.68	0.138	0.133	11.688	11974.07	12103.66	0.124	0.122	1.0706
619	12044.17	11898.48	0.121	0.13	-1.224	13983.11	13914.75	0.125	0.12	-0.491
620	12887.06	12781.71	0.113	0.119	-0.824	11329.37	11576.68	0.128	0.128	2.1363
621	11671.46	13531.38	0.136	0.146	13.745	15411.19	16664.93	0.128	0.137	7.5232
622	14594.56	15126.03	0.122	0.127	3.5136	10503.27	11438.1	0.129	0.124	8.173
623	13591.79	14907.52	0.134	0.135	8.826	12313.47	12087.95	0.118	0.117	-1.866
624	12669.15	12940.66	0.13	0.13	2.0981	13485.58	13652.56	0.126	0.127	1.2231
625	12534.61	14921.88	0.124	0.117	15.998	11745.99	12072.59	0.133	0.132	2.7053
626	11454.43	11461.5	0.144	0.144	0.0617	12712.18	13151.52	0.13	0.128	3.3406
627	11189.37	12549.91	0.131	0.14	10.841	10952.77	11237.45	0.124	0.123	2.5333
628	13171.39	13564.4	0.131	0.133	2.8974	11639.7	12049.14	0.121	0.124	3.3981
629	10897.42	11233.44	0.15	0.147	2.9912	14882.3	16039.93	0.117	0.121	7.2171
630	11240.75	11283.68	0.12	0.125	0.3805	10578.68	10923.15	0.132	0.131	3.1536

631	13848.73	13186.63	0.136	0.139	-5.021	12095.64	12198.69	0.118	0.12	0.8448
632	12646.8	13472.78	0.14	0.135	6.1307	12842.1	12701.06	0.122	0.115	-1.11
633	11643.19	11778.13	0.122	0.126	1.1457	11656.47	11773.04	0.117	0.119	0.9901
634	11066.16	15656.37	0.135	0.144	29.319	14060.11	14296.47	0.132	0.135	1.6533
635	12946.69	14700.3	0.115	0.117	11.929	12780.83	13265.23	0.128	0.124	3.6517
636	13905.45	13185.58	0.132	0.136	-5.46	12701.09	13005.57	0.117	0.116	2.3411
637	11201.88	11393.01	0.128	0.129	1.6776	12871.29	13151.33	0.118	0.119	2.1293
638	11000.89	11403.89	0.145	0.144	3.5339	12089.05	12178.96	0.128	0.125	0.7383
639	14606.74	14737.03	0.133	0.137	0.8841	12844.76	12962.96	0.12	0.12	0.9118
640	10844.12	12349.51	0.14	0.147	12.19	12883.77	13142.94	0.134	0.132	1.9719
641	11897.3	12507.21	0.137	0.133	4.8765	14340.08	15634.57	0.131	0.131	8.2796
642	11211.26	11539.75	0.119	0.127	2.8466	14117.19	14128.91	0.126	0.126	0.0829
643	13201.18	13364.23	0.137	0.137	1.2201	11285.31	11090.34	0.121	0.118	-1.758
644	12222.56	13660.38	0.136	0.141	10.525	9968.524	9986.808	0.132	0.134	0.1831
645	14321.62	14325.76	0.137	0.138	0.0289	14981.1	15068.97	0.12	0.118	0.5831
646	12563.62	12362.87	0.12	0.125	-1.624	11551.34	11538.91	0.121	0.121	-0.108
647	13089.77	13187.48	0.118	0.115	0.7409	14419.23	15744.42	0.131	0.131	8.4169
648	12192.3	12337.03	0.109	0.121	1.1731	12672.58	12877.76	0.129	0.128	1.5933
649	13259.85	14577.67	0.121	0.117	9.04	11846.88	12011.35	0.126	0.126	1.3693
650	11209.87	11611.88	0.111	0.121	3.4621	12397.55	12214.19	0.128	0.121	-1.501
651	11036.9	11498.78	0.143	0.143	4.0167	15076.53	15056.74	0.117	0.117	-0.131
652	10849.71	11003.14	0.119	0.127	1.3944	16189.47	17163.96	0.113	0.117	5.6775
653	12601.56	12437.38	0.117	0.124	-1.32	11175.11	11274.61	0.124	0.119	0.8825
654	14861.96	15013.89	0.13	0.129	1.0119	11922.26	12010.54	0.125	0.123	0.7351
655	12266.39	12694.2	0.136	0.133	3.3702	12687.16	13406.78	0.128	0.128	5.3676
656	10747.42	11236.37	0.141	0.144	4.3514	12701.14	13059.08	0.128	0.125	2.7409
657	12345.24	14010.88	0.111	0.114	11.888	12997.17	13097.97	0.122	0.12	0.7696
658	12342.04	13998.61	0.144	0.147	11.834	16898.89	17076.34	0.129	0.129	1.0392
659	12429.82	12442.25	0.143	0.143	0.0999	13707.97	13900.01	0.128	0.13	1.3816
660	11946.6	11959.02	0.141	0.14	0.1039	12587.76	12561.69	0.12	0.118	-0.208
661	11108.91	12546.09	0.136	0.132	11.455	13554.64	13867.03	0.126	0.124	2.2528
662	12110.13	12359.16	0.137	0.138	2.0149	11523.24	11588.3	0.123	0.123	0.5614
663	11566.84	11843.53	0.133	0.128	2.3362	11624.98	11399.45	0.122	0.121	-1.978
664	13709.68	14157.76	0.133	0.137	3.1649	11700.92	11969.45	0.132	0.133	2.2434
665	12267.38	12657.63	0.137	0.142	3.0831	11526.85	12564.43	0.132	0.13	8.258
666	12182.5	12331.59	0.113	0.116	1.2089	10958.91	11572.04	0.123	0.12	5.2983
667	13528.95	13425.15	0.112	0.114	-0.773	13255.02	13962.73	0.121	0.122	5.0686
668	12210.46	13794.97	0.137	0.131	11.486	13115.04	13250.98	0.125	0.125	1.0259
669	11266.61	14434.62	0.127	0.145	21.947	13115.63	13285.5	0.122	0.119	1.2787
670	12712.66	13956.63	0.122	0.115	8.9131	13161.3	13269.59	0.116	0.117	0.816
671	14312.61	13653.44	0.135	0.139	-4.828	12343.74	12249.89	0.128	0.126	-0.766
672	12955.83	13604	0.14	0.138	4.7645	11010.58	11018.15	0.124	0.125	0.0687
673	12744.5	12326.98	0.113	0.125	-3.387	12076.47	12485.92	0.12	0.124	3.2793
674	12874.76	13819.11	0.112	0.12	6.8337	15192.13	16028.96	0.134	0.137	5.2207
675	10899.21	11647.36	0.135	0.131	6.4233	12432.18	12706.36	0.119	0.124	2.1578
676	11218.43	11858.79	0.147	0.143	5.3999	10862.31	11019.71	0.134	0.134	1.4284

677	10536.66	11123.47	0.146	0.147	5.2754	13233.31	13346.33	0.117	0.114	0.8468
678	11316.55	11785.2	0.123	0.121	3.9766	14949.01	15005.82	0.125	0.123	0.3786
679	12879.72	12922.86	0.12	0.121	0.3338	11514.14	11496.36	0.123	0.12	-0.155
680	11996.46	12142.95	0.14	0.138	1.2063	10898.68	11272.18	0.12	0.126	3.3135
681	12476.66	13956.1	0.119	0.128	10.601	12682.91	12971.52	0.119	0.124	2.225
682	11687.97	13307.25	0.124	0.124	12.168	12890.53	13401.08	0.125	0.126	3.8098
683	13105.42	13654.71	0.131	0.132	4.0227	14120.77	14199.05	0.123	0.124	0.5513
684	11412.64	11832.09	0.146	0.146	3.545	11552.38	11639.96	0.119	0.121	0.7524
685	10874.33	14346.36	0.127	0.144	24.201	11288.79	11263.94	0.12	0.12	-0.221
686	12292.55	13385.24	0.121	0.129	8.1634	11762.92	11878.28	0.122	0.119	0.9711
687	11416.52	11768.99	0.137	0.133	2.9948	12847.69	12965.88	0.119	0.12	0.9116
688	11930.81	12395.11	0.137	0.132	3.7458	11495.73	11662.88	0.126	0.124	1.4332
689	12452.85	12624.18	0.138	0.136	1.3572	10361.72	10503.06	0.126	0.127	1.3457
690	12651.99	15216.88	0.136	0.136	16.856	12078.77	11575.04	0.123	0.125	-4.352
691	11439.12	12442.54	0.133	0.128	8.0644	11697.76	11941.52	0.126	0.124	2.0413
692	12207.93	11949.91	0.128	0.13	-2.159	11969.13	12002.56	0.128	0.128	0.2785
693	11697.51	11483.04	0.125	0.129	-1.868	12029.8	12431.02	0.127	0.128	3.2275
694	13480.51	13564.36	0.14	0.141	0.6181	11120.25	11237.95	0.131	0.129	1.0473
695	11945.48	12320.7	0.145	0.143	3.0454	12530.75	12703.59	0.126	0.127	1.3606
696	13438.63	13454.48	0.137	0.136	0.1179	12920.81	13019.89	0.126	0.12	0.761
697	12156.71	12920.38	0.142	0.142	5.9106	12597.14	13019.45	0.125	0.119	3.2436
698	14987.32	14625.93	0.127	0.137	-2.471	12569.29	12708.16	0.122	0.121	1.0928
699	12607.72	13967.05	0.119	0.115	9.7324	11582.63	11796.23	0.123	0.115	1.8108
700	13121.14	12727.97	0.127	0.13	-3.089	11268.71	11321.34	0.121	0.122	0.4649
701	12415.36	14526.66	0.144	0.148	14.534	12061.64	12213.41	0.118	0.114	1.2426
702	13372.11	13776.84	0.113	0.122	2.9378	11337.75	11471.09	0.12	0.118	1.1624
703	11437.53	11519.12	0.12	0.126	0.7083	14829.58	14905.14	0.129	0.132	0.507
704	13920.61	14761.42	0.123	0.123	5.696	11603.6	12173.63	0.126	0.124	4.6825
705	11501.76	11902.26	0.118	0.123	3.3649	11560.64	11984.99	0.122	0.122	3.5407
706	11053.38	11347.47	0.147	0.146	2.5917	13189.15	13344.51	0.12	0.124	1.1642
707	11357.33	11527.63	0.121	0.125	1.4773	13244.72	13629.03	0.119	0.119	2.8198
708	12704.92	12575.88	0.118	0.124	-1.026	12074.97	12415.42	0.116	0.121	2.7422
709	13927.51	15649.85	0.139	0.142	11.005	11249.19	11349.19	0.136	0.134	0.8811
710	12407.56	14219.92	0.134	0.136	12.745	14967.04	15116.63	0.127	0.127	0.9895
711	11286.72	12677.68	0.131	0.129	10.972	11067.45	11126.45	0.12	0.123	0.5302
712	12336	12730.94	0.117	0.126	3.1022	12423.61	12833.05	0.119	0.122	3.1906
713	15390.11	15704.25	0.129	0.127	2.0004	10743.95	10745.96	0.12	0.124	0.0187
714	10967.91	11382	0.133	0.128	3.6381	12958.33	13219.42	0.125	0.123	1.9751
715	12236.11	12845.35	0.146	0.145	4.7429	14301.17	13439.22	0.123	0.121	-6.414
716	13931.82	14181.49	0.121	0.129	1.7605	11069.95	11291.28	0.132	0.134	1.9602
717	11385.87	11319.39	0.114	0.121	-0.587	10739.31	10857.5	0.126	0.127	1.0886
718	12099.22	12199.93	0.109	0.118	0.8255	11661.05	12275.85	0.128	0.13	5.0082
719	11527.84	12149.7	0.128	0.131	5.1183	12547.97	12469.68	0.123	0.122	-0.628
720	10164.22	10317.99	0.146	0.147	1.4902	13973.17	14391.8	0.13	0.128	2.9088
721	12812.51	13983.05	0.136	0.143	8.3711	13107.18	13156.76	0.119	0.122	0.3769
722	11547.11	11941.41	0.145	0.143	3.302	12734.94	12861.93	0.139	0.137	0.9873

723	11991.55	12718.66	0.146	0.145	5.7169	10485.45	10460.59	0.119	0.119	-0.238
724	11821.68	12995.44	0.124	0.122	9.0321	11591.5	11641.2	0.125	0.12	0.427
725	14051.86	15032.29	0.131	0.132	6.5222	14603.76	15051.38	0.127	0.126	2.974
726	13125.77	14466.43	0.121	0.113	9.2674	11846.11	12135.94	0.126	0.128	2.3882
727	13241.33	13461.12	0.112	0.121	1.6328	11580.46	11816.44	0.125	0.128	1.997
728	11140.81	11166.97	0.144	0.143	0.2342	11554.93	11670.29	0.121	0.117	0.9885
729	10823.44	11226.02	0.147	0.147	3.5862	11648.63	11674.7	0.126	0.128	0.2233
730	12201.86	12777.1	0.115	0.125	4.5021	13348.86	13255.01	0.123	0.122	-0.708
731	11274.72	11564.93	0.137	0.136	2.5094	11368.27	11550.52	0.132	0.129	1.5779
732	11269.63	13924.08	0.126	0.141	19.064	13601.21	13824.31	0.115	0.117	1.6138
733	12909.33	13041.34	0.139	0.142	1.0122	11561.19	11667.68	0.129	0.128	0.9126
734	12335.97	15567.76	0.113	0.112	20.759	11301.22	13390.36	0.139	0.14	15.602
735	11243.63	14997.22	0.144	0.141	25.029	12147.33	12006.29	0.126	0.118	-1.175
736	13807.71	14410.26	0.133	0.134	4.1814	13272.95	13193.37	0.126	0.129	-0.603
737	14947.29	15365.4	0.131	0.127	2.7211	13389.29	13849.34	0.128	0.126	3.3218
738	13526.2	13657.59	0.126	0.13	0.962	11613.57	11923.74	0.12	0.116	2.6013
739	10929.55	11210.51	0.146	0.144	2.5062	14671.24	14571.15	0.127	0.129	-0.687
740	14084.4	14226.58	0.123	0.13	0.9994	11878.19	11981.12	0.12	0.116	0.8591
741	12171.12	14852.61	0.113	0.112	18.054	11118.27	11115.84	0.129	0.128	-0.022
742	12750.84	13225.28	0.133	0.132	3.5873	10218.19	11057.17	0.127	0.126	7.5877
743	12537.07	13923.47	0.133	0.135	9.9573	12778.14	12969.18	0.126	0.126	1.473
744	13766.81	14285.06	0.114	0.115	3.6279	11651.56	11818.72	0.122	0.12	1.4143
745	12445.37	12788.13	0.131	0.133	2.6803	11437.91	11568.03	0.123	0.122	1.1248
746	12928.7	12950.88	0.116	0.127	0.1713	12869.3	13201.94	0.127	0.128	2.5196
747	14618.93	14928.81	0.13	0.131	2.0757	11270.84	11412.17	0.127	0.128	1.2385
748	11412.11	11982.36	0.146	0.145	4.759	11552.64	11526.57	0.122	0.12	-0.226
749	11634.4	12338.34	0.122	0.125	5.7053	10904.43	10592.17	0.121	0.122	-2.948
750	14470.9	14193.65	0.132	0.14	-1.953	11507.49	11740.16	0.123	0.125	1.9818
751	9867.742	10144.55	0.148	0.146	2.7287	13353.01	13158.99	0.128	0.128	-1.474
752	12211.45	14026.72	0.113	0.112	12.942	11511.08	11947.31	0.123	0.128	3.6512
753	11570.61	12039.26	0.122	0.12	3.8927	12359.75	12347.32	0.121	0.121	-0.101
754	12777.58	12803.64	0.14	0.14	0.2036	12437.01	12563.46	0.118	0.118	1.0065
755	13414.1	14236.25	0.127	0.124	5.775	10515.8	10795.04	0.132	0.131	2.5867
756	11588.3	13769.38	0.129	0.14	15.84	11897.77	12067.98	0.135	0.132	1.4104
757	12759	14963.59	0.138	0.132	14.733	10986.35	11012.42	0.125	0.126	0.2367
758	11848.62	12377.06	0.142	0.136	4.2695	11563.43	11830.83	0.12	0.125	2.2602
759	12591.36	12639.32	0.118	0.123	0.3794	13561.27	13750.53	0.121	0.123	1.3763
760	11083.94	12221	0.125	0.125	9.3041	14737.79	14828.59	0.125	0.122	0.6123
761	11828.95	13857.01	0.123	0.124	14.636	13138.72	13126.29	0.121	0.12	-0.095
762	12376.33	12434.96	0.112	0.125	0.4715	13265.22	13263.8	0.12	0.126	-0.011
763	10357.1	10554	0.145	0.146	1.8656	12113.51	12328.9	0.131	0.13	1.747
764	12612.2	14231.93	0.125	0.122	11.381	15692.2	16026.31	0.129	0.127	2.0847
765	12763.09	13880.63	0.136	0.135	8.0511	11067.6	11643.29	0.125	0.118	4.9444
766	12611.51	13758.04	0.127	0.135	8.3335	11608.45	11745.14	0.129	0.126	1.1638
767	14942.83	15205.55	0.133	0.129	1.7278	13778.22	13782.95	0.125	0.123	0.0343
768	15454.68	15173.71	0.125	0.135	-1.852	12692.25	12806.34	0.12	0.124	0.8909

769	10833.97	11066.93	0.147	0.146	2.1051	10710.36	11650.3	0.127	0.135	8.0679
770	11656.31	11966.46	0.146	0.145	2.5919	11340.29	11848.9	0.12	0.125	4.2925
771	12326.74	12673.07	0.109	0.121	2.7328	11571.92	11525.94	0.124	0.117	-0.399
772	12736.99	13103.01	0.144	0.142	2.7934	14232.48	14651.11	0.13	0.128	2.8573
773	14487.92	14612.27	0.129	0.129	0.851	10626.32	10696.4	0.124	0.123	0.6552
774	16316.77	17074.05	0.125	0.123	4.4353	11110.34	11225.69	0.125	0.121	1.0276
775	11100.33	11429.27	0.147	0.145	2.8781	13089.79	13959.2	0.139	0.138	6.2282
776	11599.77	11771.11	0.14	0.139	1.4556	15334.51	15849.91	0.129	0.128	3.2518
777	12076.23	12472.75	0.131	0.128	3.1791	11838.63	12352.31	0.117	0.125	4.1585
778	13349.27	14689.93	0.12	0.112	9.1264	14456.45	14499.18	0.127	0.127	0.2946
779	15269.52	15399.81	0.136	0.139	0.8461	13157.45	13138.25	0.129	0.126	-0.146
780	11598.72	11685.7	0.14	0.142	0.7444	11350.45	13492.6	0.139	0.141	15.877
781	11090.72	11339.24	0.145	0.145	2.1918	11387.3	11882.48	0.123	0.126	4.1673
782	12045.64	12538.15	0.126	0.138	3.9281	11761.95	11897.9	0.13	0.128	1.1426
783	12923.85	12819.81	0.12	0.128	-0.812	10766.22	11472.82	0.133	0.134	6.1589
784	11986.52	12825.55	0.123	0.124	6.5419	11682.01	11781.51	0.127	0.123	0.8445
785	13118.46	13231.8	0.13	0.13	0.8566	13335	13332.99	0.138	0.137	-0.015
786	13867	13541.73	0.12	0.128	-2.402	13261.95	13653.92	0.123	0.124	2.8708
787	12298.15	13728.31	0.138	0.13	10.418	12443.69	12370.35	0.122	0.12	-0.593
788	14274.66	17067.03	0.139	0.132	16.361	13103.26	13307.23	0.125	0.124	1.5328
789	12148.76	12546.75	0.126	0.13	3.1721	13705.67	13832.83	0.122	0.121	0.9192
790	16084.24	17002.61	0.126	0.132	5.4014	14063.59	14103.09	0.138	0.137	0.2801
791	11542.55	12223.8	0.12	0.122	5.5731	12526.24	12794.56	0.122	0.127	2.0971
792	13068.05	12543.46	0.111	0.123	-4.182	14446	14893.63	0.131	0.129	3.0055
793	12961.08	13205.47	0.143	0.142	1.8506	11750.64	11915.2	0.135	0.135	1.3811
794	11502.27	11758.3	0.112	0.12	2.1774	10590.39	10931.05	0.131	0.133	3.1164
795	12439.78	12602.83	0.14	0.139	1.2938	13262.17	13429.15	0.126	0.127	1.2435
796	11593.27	14019.06	0.129	0.14	17.304	11189.21	11979.54	0.138	0.141	6.5973
797	12589.45	12870.66	0.126	0.131	2.1849	12815.25	12951.19	0.125	0.123	1.0497
798	13386.34	14068.23	0.113	0.122	4.847	12420.71	12394.65	0.124	0.122	-0.21
799	14141.74	14351.51	0.124	0.131	1.4617	11962.74	12254.4	0.126	0.127	2.3801
800	13240.06	14001.15	0.115	0.123	5.4359	11503.16	12141.66	0.127	0.128	5.2587
801	12729.02	13005.8	0.137	0.134	2.1281	10856.06	10994.93	0.13	0.13	1.2631
802	13429.6	14099.27	0.117	0.124	4.7497	13453.34	13792.09	0.128	0.126	2.4561
803	12663.61	15095.57	0.141	0.145	16.11	11202.45	11253.37	0.126	0.125	0.4525
804	13863.09	13690.21	0.118	0.121	-1.263	11620.96	12960.1	0.119	0.12	10.333
805	11515.68	11868.27	0.143	0.14	2.9708	10744.59	10987.76	0.127	0.127	2.2131
806	12284.23	12605.53	0.133	0.138	2.5489	14368.9	14516.68	0.13	0.132	1.018
807	13634.57	13165.16	0.12	0.128	-3.566	15062.56	15281.8	0.124	0.124	1.4346
808	13385.07	14199.34	0.119	0.128	5.7345	12188.17	11916.82	0.123	0.12	-2.277
809	11104.86	11463.6	0.144	0.145	3.1294	10058.49	10896.97	0.142	0.14	7.6946
810	14717.11	15284.8	0.131	0.125	3.7141	11697.98	11778.9	0.129	0.125	0.687
811	11442.11	11989.05	0.129	0.125	4.562	13629.68	13569.72	0.124	0.117	-0.442
812	13055.75	13681.19	0.12	0.124	4.5715	13843.68	14047.65	0.124	0.123	1.452
813	11803.35	12245.94	0.144	0.145	3.6141	15018.39	16420.07	0.126	0.127	8.5364
814	11132.54	11505.63	0.147	0.146	3.2426	11178.38	11153.52	0.124	0.124	-0.223

815	10913.2	11307.5	0.149	0.147	3.4871	16041.42	17448.25	0.122	0.124	8.0629
816	12986.69	13146.99	0.136	0.142	1.2192	10638.08	10613.23	0.12	0.12	-0.234
817	15497.9	15857.57	0.131	0.132	2.2681	10769.37	10904.1	0.128	0.127	1.2356
818	12279.09	12547.67	0.129	0.13	2.1405	11396.99	11595.69	0.129	0.132	1.7136
819	15767.87	16121.21	0.128	0.126	2.1918	13659.94	13856.26	0.127	0.129	1.4169
820	10426.3	10846.66	0.15	0.149	3.8755	12930.8	13030.3	0.122	0.119	0.7636
821	13979.6	14144.74	0.135	0.137	1.1676	13191.36	13488.6	0.129	0.125	2.2037
822	15492.24	15831.15	0.129	0.125	2.1408	13720.25	13893.56	0.12	0.116	1.2474
823	14287.54	14291.68	0.134	0.135	0.029	12399.52	12512.58	0.119	0.122	0.9035
824	11101.61	13344.52	0.126	0.14	16.808	11807.65	11933.21	0.118	0.119	1.0522
825	12819.38	12907.78	0.139	0.14	0.6849	11049.6	11309.34	0.131	0.131	2.2967
826	12755.15	12897.2	0.14	0.14	1.1014	10991.07	11204.83	0.138	0.141	1.9078
827	16395.94	16685.23	0.128	0.126	1.7338	10429.62	11365.54	0.123	0.125	8.2348
828	11679.19	11775.14	0.141	0.14	0.8148	12195.64	12336.47	0.129	0.126	1.1416
829	14505.17	14509.31	0.137	0.137	0.0285	11717.03	11846.23	0.123	0.124	1.0907
830	13703.37	14122.41	0.122	0.128	2.9672	12090.05	12213.81	0.12	0.121	1.0133
831	11472.46	11919.69	0.147	0.147	3.752	12386.39	12494.67	0.12	0.121	0.8666
832	13505.06	13647.78	0.138	0.141	1.0457	12336.95	12433.23	0.119	0.121	0.7743
833	13150.5	13693.23	0.131	0.132	3.9634	14134.35	14590.26	0.129	0.127	3.1247
834	12797.58	13091.35	0.104	0.12	2.244	11533.86	12004.11	0.126	0.127	3.9174
835	12130.15	12117.72	0.141	0.14	-0.103	13027.14	12929.15	0.125	0.123	-0.758
836	12013.63	12725.88	0.147	0.148	5.5969	10854.78	10970.14	0.122	0.119	1.0515
837	15117.45	15121.59	0.135	0.135	0.0274	11048.65	11764.49	0.128	0.127	6.0848
838	12949.18	13500.82	0.115	0.116	4.086	11667.31	12001.78	0.129	0.126	2.7869
839	10867.53	12401.79	0.139	0.146	12.371	14359.68	14660.35	0.126	0.124	2.0509
840	11285.63	11817.59	0.145	0.146	4.5014	15558.5	15643.44	0.121	0.12	0.543
841	11420.02	12782.6	0.129	0.142	10.66	14368.26	14175.37	0.124	0.119	-1.361
842	12486.15	13795.69	0.122	0.115	9.4923	12231.46	13126.92	0.121	0.116	6.8215
843	11619.26	11611.47	0.143	0.143	-0.067	12316.12	12434.32	0.125	0.126	0.9506
844	11008.27	11245.92	0.119	0.123	2.1133	11378.27	11516.17	0.129	0.128	1.1975
845	11824.91	13814.23	0.112	0.113	14.401	11502.71	11601.62	0.121	0.122	0.8525
846	11779.28	12057.82	0.111	0.119	2.3101	15705.13	15844.8	0.131	0.13	0.8815
847	12830.53	15034.95	0.123	0.114	14.662	11473.58	11573.08	0.121	0.117	0.8597
848	13018.2	13439.29	0.126	0.124	3.1333	12075.92	12175.42	0.125	0.121	0.8172
849	12456.46	12918.87	0.123	0.12	3.5793	15046.37	15246.75	0.125	0.126	1.3143
850	13125.48	14893.97	0.143	0.147	11.874	11877.71	11993.19	0.118	0.119	0.9629
851	12898.85	12446.89	0.111	0.124	-3.631	11957.86	11710.87	0.122	0.12	-2.109
852	12426.78	13238.87	0.115	0.125	6.1342	12378.66	12443.72	0.123	0.123	0.5228
853	10445.89	10810.69	0.143	0.142	3.3745	14660.88	14560.79	0.127	0.129	-0.687
854	11909.04	13298.86	0.144	0.148	10.451	13230.68	13337.87	0.119	0.12	0.8037
855	12582.78	12637.93	0.14	0.14	0.4364	11493.48	11891.51	0.123	0.128	3.3471
856	13165.69	13144.4	0.119	0.118	-0.162	11937.65	12152.12	0.123	0.128	1.7649
857	10482.05	12328.36	0.142	0.148	14.976	12054.36	13141.86	0.133	0.134	8.2751
858	10980.84	11753.54	0.136	0.133	6.5742	12222.3	12359.78	0.12	0.119	1.1124
859	11781.62	12002.38	0.11	0.121	1.8393	13318	14213.16	0.121	0.116	6.2981
860	12485.12	14413.91	0.143	0.147	13.381	12609.2	11994.39	0.124	0.129	-5.126

861	11803.46	13522.66	0.139	0.146	12.713	15512.03	15617.51	0.124	0.122	0.6754
862	12453.33	15273.68	0.126	0.144	18.465	11986	11849.1	0.125	0.119	-1.155
863	13587.98	13136.02	0.126	0.127	-3.441	10839.59	11807.51	0.135	0.137	8.1975
864	13161.6	13558.25	0.106	0.122	2.9256	12603.81	12914.77	0.126	0.128	2.4077
865	14608.5	15359.72	0.135	0.134	4.8908	12019.76	12467.8	0.119	0.116	3.5936
866	12183.6	13361.5	0.139	0.145	8.8157	13660.28	13567.56	0.115	0.119	-0.683
867	13091.78	13071.45	0.12	0.125	-0.156	14047.18	13928.31	0.126	0.128	-0.853
868	11796.19	11939.75	0.133	0.128	1.2023	13098.64	13563.54	0.131	0.126	3.4276
869	12825.66	13830.03	0.125	0.13	7.2622	12762.59	12827.65	0.121	0.121	0.5072
870	13258.75	13447.63	0.108	0.118	1.4045	12312.36	12430.55	0.122	0.123	0.9509
871	12280.04	13067.95	0.133	0.128	6.0293	11303.41	11077.88	0.122	0.121	-2.036
872	12028.45	12277.36	0.117	0.123	2.0274	12119.87	11563.8	0.118	0.115	-4.809
873	16127.08	16603.49	0.124	0.13	2.8693	10469.41	11170.02	0.14	0.139	6.2722
874	14911.43	15165.78	0.13	0.126	1.6771	13216.25	13190.18	0.119	0.117	-0.198
875	12719.91	13394.34	0.109	0.121	5.0352	10712.76	11379.96	0.125	0.13	5.8629
876	13552.89	17075.02	0.133	0.131	20.627	15176.41	15121.59	0.122	0.117	-0.363
877	15390.86	15639.64	0.134	0.135	1.5907	11134.38	11557.14	0.137	0.124	3.658
878	11820.76	13269.55	0.117	0.115	10.918	12004.23	12104.23	0.134	0.133	0.8262
879	12280.15	12335.68	0.119	0.127	0.4501	13036.34	13203.32	0.12	0.121	1.2647
880	13744.52	13992.06	0.124	0.131	1.7691	12857.97	13040.31	0.124	0.125	1.3983
881	11334.63	11716.79	0.14	0.141	3.2617	14633.46	14791.84	0.124	0.124	1.0707
882	11651.88	11615.1	0.142	0.142	-0.317	11574.64	11582.21	0.125	0.126	0.0654
883	12313.23	12775.41	0.115	0.125	3.6178	13268.15	13192.79	0.122	0.121	-0.571
884	14425.49	14508.25	0.13	0.136	0.5704	11593.36	11700.14	0.123	0.119	0.9126
885	12050.19	12452.56	0.126	0.122	3.2313	11617.11	11682.17	0.124	0.125	0.5569
886	12287.44	12167.32	0.118	0.125	-0.987	13358.78	13423.84	0.117	0.118	0.4847
887	15004.61	14629.37	0.128	0.134	-2.565	13901.32	13785.38	0.126	0.128	-0.841
888	12074.51	12527.06	0.116	0.127	3.6126	10076.1	10385.13	0.138	0.14	2.9757
889	11258.48	13009.52	0.136	0.143	13.46	11514.94	11965.77	0.13	0.124	3.7677
890	12849.77	12955.17	0.121	0.128	0.8136	11606.71	11751.52	0.122	0.119	1.2323
891	13104.11	13970.75	0.12	0.118	6.2032	11341	11347.56	0.126	0.122	0.0579
892	13683.85	14849.74	0.12	0.114	7.8513	11650.4	11715.46	0.121	0.121	0.5553
893	13326.76	13607.71	0.137	0.136	2.0647	12345.06	12549.03	0.127	0.125	1.6254
894	13862.91	13354.24	0.133	0.136	-3.809	12594.59	12694.08	0.123	0.119	0.7838
895	15055.58	14880.64	0.126	0.132	-1.176	14808.97	14844.2	0.124	0.121	0.2374
896	11744.54	12123.57	0.136	0.131	3.1264	12302	12840.65	0.127	0.127	4.1949
897	11320.86	11762.74	0.147	0.149	3.7566	14731.36	15610.11	0.136	0.138	5.6294
898	13105.6	13109.74	0.138	0.139	0.0316	11844.64	12014.81	0.122	0.119	1.4164
899	11535.35	13578.1	0.113	0.116	15.044	11168.14	11197.13	0.124	0.124	0.2589
900	12256.18	13388.52	0.124	0.12	8.4575	12373.79	12488.73	0.125	0.125	0.9203
901	13649.74	14510.33	0.117	0.119	5.9309	14492.68	15824.95	0.124	0.125	8.4188
902	13486.34	13733.91	0.132	0.13	1.8026	14014.74	15400.86	0.127	0.129	9.0003
903	13119.79	13015.49	0.101	0.118	-0.801	11329.63	11632.3	0.13	0.128	2.602
904	13673.95	13649.44	0.113	0.118	-0.18	11303.51	11421.71	0.124	0.125	1.0349
905	13003.54	13181.62	0.135	0.133	1.3509	11854.64	12128.81	0.119	0.125	2.2605
906	10925.71	11454.56	0.151	0.147	4.617	13644.17	13762.37	0.116	0.117	0.8588

907	11906.18	12252.91	0.144	0.141	2.8297	12905.46	12679.93	0.12	0.119	-1.779
908	11430.46	12252.75	0.137	0.132	6.7111	15655.86	16843.36	0.122	0.122	7.0503
909	16897.13	17187.46	0.121	0.132	1.6892	13682.57	14107.98	0.123	0.123	3.0154
910	12219.6	12378.51	0.135	0.134	1.2837	11227.41	11301.26	0.129	0.129	0.6534
911	11508.45	11991.88	0.111	0.123	4.0313	14066.33	14484.96	0.131	0.129	2.8901
912	13989.77	13974.92	0.135	0.135	-0.106	14053.91	14416.09	0.125	0.123	2.5123
913	11767.76	13068.29	0.135	0.133	9.9518	12196.83	12721.55	0.131	0.129	4.1246
914	12074.4	12728.54	0.14	0.136	5.1392	13373.4	13491.6	0.119	0.12	0.8761
915	9992.803	10185.56	0.147	0.147	1.8924	13353.87	14307.16	0.121	0.113	6.663
916	16094.34	16247.8	0.131	0.133	0.9445	10677.52	11274.54	0.135	0.138	5.2953
917	11846.44	11850.67	0.114	0.118	0.0357	11752.8	11817.86	0.123	0.123	0.5505
918	12092.17	13429.07	0.139	0.146	9.9553	12391.01	12546.24	0.127	0.124	1.2373
919	15402.69	15963.91	0.132	0.134	3.5155	12390.48	12992.52	0.129	0.122	4.6338
920	12504.82	13643.85	0.139	0.134	8.3483	12503.34	12789.44	0.129	0.126	2.237
921	11708.51	12234.7	0.136	0.133	4.3008	13642.67	13741.75	0.126	0.12	0.721
922	15347.88	15196.54	0.126	0.133	-0.996	12743.85	12874.27	0.126	0.129	1.013
923	13155.6	13989.79	0.126	0.132	5.9629	13328.39	13557.77	0.127	0.128	1.6918
924	14782.19	15275.17	0.124	0.13	3.2273	11943.36	12080.85	0.12	0.119	1.1381
925	13028.63	14284.52	0.141	0.145	8.792	11944.04	11931.61	0.119	0.119	-0.104
926	11862.5	13074.05	0.142	0.147	9.2668	12364.87	12808.59	0.133	0.129	3.4643
927	12348.28	12735.35	0.108	0.119	3.0393	11819.87	11995.85	0.13	0.129	1.467
928	13342.23	14291.19	0.119	0.123	6.6402	10351.22	10492.55	0.126	0.127	1.347
929	12034.19	13602.1	0.126	0.133	11.527	11144.42	11285.75	0.125	0.126	1.2523
930	13264.68	12879.57	0.136	0.139	-2.99	13481.89	13895.28	0.121	0.121	2.9751
931	11206.28	11615.22	0.124	0.126	3.5208	14856.39	15948.16	0.135	0.135	6.8457
932	13958.94	13516.84	0.135	0.138	-3.271	11943.85	12307.65	0.132	0.134	2.9559
933	11396.59	11414.37	0.142	0.144	0.1558	12312.09	12253.89	0.122	0.115	-0.475
934	12549.92	13212.01	0.117	0.125	5.0113	14140.76	15459.68	0.126	0.128	8.5314
935	12054.33	12343.62	0.129	0.131	2.3436	11949.46	12026.74	0.119	0.118	0.6426
936	12751.6	14865.15	0.141	0.145	14.218	10462.52	10437.67	0.119	0.119	-0.238
937	12118.52	12401.4	0.139	0.138	2.281	11477.17	11542.23	0.122	0.122	0.5637
938	11411.43	11965.52	0.145	0.143	4.6307	15184.35	15933.9	0.137	0.139	4.7041
939	12765.7	12865.7	0.107	0.115	0.7773	11579.79	11712.81	0.13	0.129	1.1356
940	15755.88	16191.15	0.125	0.128	2.6883	12644.99	12491.51	0.126	0.12	-1.229
941	14508.24	14415.22	0.126	0.129	-0.645	14273.01	14496.24	0.126	0.124	1.5399
942	11933.73	15457.82	0.14	0.139	22.798	15689.76	15939.56	0.132	0.132	1.5671
943	12770.7	16008.06	0.136	0.134	20.223	12453.67	13511.95	0.134	0.133	7.8322
944	12446.3	13744.41	0.124	0.117	9.4447	11548.33	11677.95	0.13	0.129	1.11
945	15568.5	15990.77	0.123	0.129	2.6407	12578.58	12728.7	0.128	0.129	1.1794
946	11393.07	11571.69	0.147	0.147	1.5435	13492.7	13797.38	0.131	0.129	2.2082
947	10963.02	12053.18	0.132	0.13	9.0446	10394.21	11290.99	0.132	0.133	7.9424
948	12340.05	13420.54	0.121	0.117	8.051	14345.32	15168.09	0.132	0.135	5.4244
949	11059.58	13231.41	0.139	0.147	16.414	11096.82	11124.6	0.124	0.125	0.2497
950	11559.71	11994.51	0.147	0.147	3.625	15620.72	15858.17	0.128	0.127	1.4973
951	11949.51	12011.65	0.143	0.144	0.5173	11504.88	11643.75	0.125	0.125	1.1927
952	11212.23	13019.88	0.13	0.141	13.884	13133.25	13035.26	0.125	0.124	-0.752

953	15452.19	15019.05	0.126	0.133	-2.884	15619.74	16561.21	0.132	0.132	5.6848
954	13440.38	14166.83	0.106	0.115	5.1278	14692.78	14837.51	0.122	0.121	0.9754
955	12653.08	12100.2	0.112	0.124	-4.569	11803.21	11906.14	0.12	0.116	0.8645
956	10130.98	10272.31	0.147	0.147	1.3759	15441.15	16839.36	0.124	0.124	8.3032
957	13022.13	14604.01	0.121	0.111	10.832	13450.42	13207.58	0.116	0.114	-1.839
958	10933.13	15265.92	0.143	0.141	28.382	11321.79	11282.88	0.125	0.119	-0.345
959	12010.07	12406.88	0.138	0.141	3.1983	13543.93	13896.91	0.132	0.128	2.54
960	13432.98	13663.61	0.113	0.123	1.6879	12754.82	12944.94	0.127	0.126	1.4687
961	12107.15	12338.07	0.11	0.122	1.8716	12660.4	13097.23	0.124	0.123	3.3353
962	11947.38	12403.9	0.146	0.148	3.6804	13853.48	13755.49	0.121	0.119	-0.712
963	12807.82	12806.61	0.141	0.141	-0.009	12034.7	12179.51	0.125	0.121	1.189
964	12185.55	12164.34	0.144	0.144	-0.174	11179.36	11610.22	0.133	0.133	3.7111
965	11023.11	11487.11	0.146	0.143	4.0394	15624.05	16274.56	0.129	0.13	3.9971
966	14304.72	14563.21	0.13	0.126	1.775	12481.59	12789.63	0.122	0.124	2.4085
967	12763.37	12719.11	0.104	0.114	-0.348	11981.26	11997.53	0.127	0.127	0.1356
968	12900.17	12996.74	0.138	0.139	0.743	11650.8	13018.02	0.14	0.14	10.502
969	10767.99	11196.93	0.151	0.147	3.8309	11845.28	11832.85	0.122	0.122	-0.105
970	11121.57	11382.23	0.13	0.132	2.2901	13548.48	14393.59	0.128	0.13	5.8714
971	11986.61	12162.09	0.136	0.133	1.4428	12172.45	12253.37	0.138	0.137	0.6604
972	11963.16	12082.25	0.141	0.14	0.9856	13099.88	13268.75	0.125	0.124	1.2727
973	12079.08	12076.38	0.12	0.122	-0.022	13316.79	13353.65	0.12	0.125	0.2761
974	11766.88	12378.04	0.135	0.133	4.9375	10846.33	12520.87	0.139	0.14	13.374
975	12064.33	12570.88	0.126	0.123	4.0296	11248.09	12674.52	0.131	0.129	11.254
976	13657.27	15502.79	0.134	0.136	11.904	11680.46	12128.69	0.127	0.128	3.6956
977	12190.52	12659.17	0.12	0.118	3.7021	12816.52	12912.79	0.121	0.123	0.7456
978	12105.75	15170.33	0.125	0.141	20.201	13525.02	13985.07	0.131	0.129	3.2896
979	12383.94	12745.03	0.135	0.136	2.8332	12855.05	13291.07	0.129	0.126	3.2805
980	12114.52	13302.13	0.125	0.118	8.928	11896.76	11995.46	0.13	0.132	0.8228
981	12510.43	13459.84	0.113	0.123	7.0537	10666.07	10731.13	0.129	0.129	0.6063
982	11440.79	15129.47	0.105	0.113	24.381	11242.35	11217.49	0.119	0.119	-0.222
983	13937.28	17544.52	0.136	0.132	20.561	15204.81	15660.79	0.124	0.123	2.9116
984	12510.48	12791.44	0.144	0.143	2.1964	14622.02	14664.74	0.126	0.126	0.2913
985	13151.56	13100.81	0.123	0.131	-0.387	10179.03	10611.61	0.138	0.139	4.0765
986	14344.75	14363.33	0.13	0.135	0.1293	10978.62	11153.98	0.124	0.123	1.5721
987	12437.96	12252.86	0.119	0.123	-1.511	11153.13	11228.48	0.126	0.127	0.6711
988	15547.88	16105	0.125	0.131	3.4593	12993.16	13406.98	0.118	0.119	3.0865
989	12827.17	13121.56	0.14	0.14	2.2435	14553.59	14596.31	0.127	0.127	0.2927
990	12018.48	14079.32	0.117	0.117	14.637	15029.35	16239.31	0.137	0.135	7.4508
991	12911.74	13754.2	0.12	0.119	6.1251	15278.06	15406	0.126	0.124	0.8305
992	15572.3	16821.89	0.127	0.129	7.4283	12537.46	12638.26	0.123	0.121	0.7976
993	12650.68	12797.04	0.137	0.139	1.1437	15282.37	15492.55	0.132	0.13	1.3566
994	13217.43	13762.28	0.13	0.132	3.959	11080.14	11170.14	0.134	0.133	0.8057
995	12221.13	12355.48	0.141	0.142	1.0874	12610.49	12839.87	0.126	0.128	1.7864
996	11210.34	12244.55	0.133	0.127	8.4463	12299.4	12619.44	0.12	0.123	2.5361
997	14895.05	15085.05	0.133	0.13	1.2595	11135.04	11597.33	0.132	0.131	3.9862
998	12035.2	13104.52	0.147	0.146	8.16	14893.72	16247.83	0.131	0.131	8.3341

999	12371.93	12505.77	0.139	0.14	1.0703	10738.88	11148.83	0.126	0.125	3.6771
1000	13187.54	12744.85	0.136	0.139	-3.473	12386.15	12606.99	0.121	0.125	1.7517
49	11402.34	12109.56	0.146	0.143	5.8402	13038.16	13189.46	0.124	0.123	1.1471
50	11975.09	11979.23	0.143	0.143	0.0346	16754.33	16864.42	0.127	0.127	0.6528
51	13739.38	13432.18	0.106	0.113	-2.287	14630.74	14891.12	0.131	0.13	1.7486
52	10829.21	11179.45	0.137	0.132	3.1329	12484.97	12894.41	0.12	0.123	3.1754
53	11316.38	11761.85	0.136	0.14	3.7875	10565.53	11541.74	0.135	0.138	8.4581
54	12605.7	12683.86	0.112	0.12	0.6162	10275.28	11509.92	0.133	0.134	10.727
55	11712.63	12239.37	0.108	0.121	4.3037	12205.11	12304.61	0.125	0.12	0.8086
56	14425.88	14839.52	0.131	0.136	2.7874	13322.31	13409.97	0.116	0.113	0.6537
57	12260.31	12922.56	0.148	0.148	5.1248	12584.81	12597.12	0.126	0.123	0.0977
58	10787.73	12123.28	0.136	0.133	11.016	13527.68	13429.69	0.123	0.121	-0.73
59	11700.52	11927.17	0.117	0.12	1.9003	13007.51	13142.25	0.12	0.12	1.0252
60	11626.59	12544.32	0.134	0.132	7.3159	11970.33	12423.47	0.126	0.126	3.6474
61	12444.08	14674.29	0.14	0.145	15.198	13423.97	13527.11	0.116	0.119	0.7624
62	13872.46	14049.53	0.134	0.13	1.2603	14555.29	15808.06	0.131	0.131	7.9249
63	10895.28	11334.72	0.13	0.125	3.877	11980.71	11962.93	0.123	0.121	-0.149
64	13054.08	16030.9	0.112	0.109	18.569	11358.07	11492.8	0.129	0.129	1.1723
65	14982.35	14971.68	0.127	0.135	-0.071	14272.62	15678.74	0.126	0.129	8.9683
66	12807.93	12765.8	0.142	0.142	-0.33	12584.73	12775.77	0.123	0.122	1.4953
67	11358.24	11712.17	0.138	0.135	3.0219	11382.62	11447.68	0.123	0.124	0.5683
68	13220.34	13224.48	0.138	0.139	0.0313	12953.91	13092.78	0.121	0.12	1.0607
69	10745.77	10903.67	0.147	0.147	1.4482	15211.93	15453.53	0.124	0.123	1.5634
70	10300.14	10581.1	0.147	0.145	2.6552	12092.15	12210.35	0.124	0.124	0.968
71	11517.23	11556.23	0.144	0.144	0.3374	11461.27	11777.87	0.131	0.127	2.6881
72	10792.94	11099.96	0.149	0.146	2.766	13478.66	13253.13	0.114	0.113	-1.702
73	12279.33	13808.69	0.128	0.124	11.075	13022.12	13293.63	0.134	0.135	2.0424
74	11671.34	12192	0.145	0.146	4.2705	12152.27	12270.47	0.123	0.123	0.9633
75	13513.1	13596.78	0.133	0.14	0.6154	11399.12	12006.14	0.128	0.131	5.0559
76	10828.61	11201.7	0.146	0.145	3.3306	10846.61	11016.52	0.138	0.139	1.5424
77	10937.64	11037.05	0.141	0.144	0.9007	11205.57	12908.23	0.139	0.137	13.19
78	11056.22	11382.74	0.126	0.127	2.8685	13782.21	12889.92	0.115	0.117	-6.922
79	12968.25	13170.68	0.136	0.134	1.5369	13326.32	13401.76	0.119	0.121	0.5629
80	11956.29	11956.29	0.139	0.139	0	11564	11537.93	0.121	0.119	-0.226
81	11245.73	11534.97	0.146	0.144	2.5075	11801.95	12015.21	0.129	0.127	1.7749
82	13309.85	13371.9	0.131	0.137	0.464	13450.22	13546.49	0.123	0.125	0.7107
83	11795.14	13704.67	0.143	0.148	13.933	10924.04	11166.29	0.122	0.126	2.1695
84	13872.82	13889.39	0.134	0.133	0.1193	13749.74	13824.6	0.12	0.116	0.5414
85	12008.75	13628.25	0.143	0.146	11.883	12936.09	12975.59	0.128	0.127	0.3044
86	11705.37	13989.79	0.124	0.142	16.329	12731.37	12890.96	0.118	0.119	1.238
87	12847.66	14048.2	0.121	0.114	8.5459	11816.14	11569.16	0.123	0.122	-2.135
88	12918.85	14529.01	0.122	0.111	11.082	12877.32	12794.89	0.123	0.121	-0.644
89	14560.31	14917.5	0.13	0.126	2.3945	13386.86	13582.64	0.138	0.137	1.4413
90	12204.77	13127.75	0.125	0.128	7.0308	11269.4	11408.28	0.128	0.127	1.2173
91	12357.1	13264.13	0.129	0.139	6.8383	11821.24	11931.24	0.135	0.133	0.9219
92	11447.55	11658.51	0.132	0.13	1.8094	13043.91	13208.43	0.122	0.119	1.2456

93	12178.29	12386.66	0.137	0.141	1.6822	12440.2	12770.24	0.131	0.129	2.5844
94	12051.88	14247.34	0.125	0.137	15.41	12030.05	12474.07	0.135	0.12	3.5595
95	14635.13	14756.85	0.134	0.137	0.8248	11957.74	12060.67	0.127	0.123	0.8534
96	14901.31	14625.99	0.132	0.14	-1.882	12875.65	13305.39	0.126	0.125	3.2298
97	11666.9	14726.04	0.131	0.144	20.774	12089.66	12077.23	0.12	0.12	-0.103
98	17259.56	17797.04	0.125	0.12	3.0201	11011.31	11123.65	0.133	0.133	1.0099
99	11173.68	11857.65	0.146	0.146	5.7682	12346.06	12390.58	0.12	0.12	0.3593
100	12429.84	12455.91	0.142	0.143	0.2093	13614.51	13769.24	0.125	0.119	1.1237
101	12962.21	15056.64	0.133	0.136	13.91	12985.62	13217.58	0.115	0.122	1.7549
102	13340.47	13231.77	0.137	0.136	-0.822	14777.25	15131.69	0.122	0.123	2.3423
103	13691.25	13213.21	0.136	0.139	-3.618	11575.58	12316.88	0.129	0.129	6.0186
104	11845.79	12422.23	0.112	0.121	4.6404	14987.72	15324.49	0.134	0.129	2.1976
105	12430.94	12639.01	0.112	0.123	1.6463	12576.4	12675.48	0.127	0.12	0.7817
106	12465.73	13036.6	0.136	0.137	4.379	10585.68	11868.37	0.135	0.134	10.808
107	11682.33	12359.23	0.135	0.134	5.4769	16249.54	16741.01	0.132	0.129	2.9357
108	11554.3	11868.6	0.146	0.145	2.6482	11082.94	11058.08	0.12	0.12	-0.225
109	13021.55	13389.97	0.127	0.138	2.7515	13252.76	13443.8	0.124	0.123	1.421
110	11740.26	13319.46	0.115	0.115	11.856	12058.02	12157.51	0.125	0.12	0.8184
111	11805.25	12481.89	0.123	0.118	5.421	11393	11624.33	0.138	0.141	1.9901
112	14724.97	15115.73	0.122	0.128	2.5851	12960.87	13115.6	0.125	0.119	1.1797
113	11947.72	11951.86	0.141	0.141	0.0347	11615.96	11668.6	0.119	0.119	0.4511
114	15176.61	15743.8	0.132	0.126	3.6026	12366.28	12781.96	0.128	0.121	3.2521
115	12166.4	13623.64	0.122	0.125	10.696	10951.39	12070.08	0.123	0.122	9.2683
116	12874.82	14404.94	0.127	0.134	10.622	13125.77	13329.74	0.129	0.128	1.5302
117	11949.47	12234.06	0.141	0.14	2.3262	11206.17	11244.66	0.132	0.131	0.3423
118	12372.65	12817.45	0.145	0.147	3.4703	11356.17	11766.53	0.123	0.127	3.4876
119	13320.33	13188.08	0.114	0.121	-1.003	12551.12	13165.11	0.127	0.127	4.6637
120	11621.02	11623.95	0.146	0.146	0.0252	12426.96	13234.92	0.125	0.125	6.1047
121	13131.14	13129.42	0.142	0.142	-0.013	11707.98	11810.91	0.121	0.117	0.8715
122	13425.1	14829.12	0.118	0.123	9.468	11905.17	12013.46	0.121	0.123	0.9014
123	12478.99	12613.42	0.111	0.117	1.0658	15129.35	16402.41	0.127	0.128	7.7615
124	13789.24	14216.81	0.136	0.133	3.0075	12155.81	12489.58	0.135	0.137	2.6723
125	11920.04	12623.25	0.131	0.122	5.5707	10638.71	10791.97	0.13	0.129	1.4201
126	11325.1	12078.9	0.123	0.123	6.2406	11660.81	12466.59	0.133	0.133	6.4635
127	12846.17	17625.08	0.138	0.132	27.114	12584.99	12864.61	0.132	0.136	2.1736
128	13596.67	15330.81	0.138	0.132	11.311	12996.07	13200.04	0.129	0.127	1.5452
129	15805.8	15996.69	0.123	0.129	1.1933	10741.55	11783.49	0.125	0.121	8.8424
130	11991.56	11964.28	0.143	0.142	-0.228	12421.53	12648.52	0.133	0.132	1.7946
131	14084.31	14480.43	0.119	0.125	2.7355	11099.77	11164.83	0.124	0.124	0.5827
132	11391.96	11836.26	0.148	0.149	3.7537	14012.06	14073.77	0.12	0.124	0.4385
133	11809.92	12676.11	0.145	0.146	6.8332	11943.83	11996.46	0.121	0.121	0.4388
134	15333.39	15694.4	0.129	0.127	2.3002	12531.41	12371.59	0.122	0.117	-1.292
135	12278.31	12290.74	0.145	0.145	0.1011	11223.12	11380.52	0.13	0.131	1.3831
136	12093.58	12250.99	0.146	0.146	1.2848	12142.13	12116.07	0.124	0.122	-0.215
137	11394.18	13072	0.144	0.149	12.835	11734.85	11708.79	0.126	0.124	-0.223
138	11879.15	16237.85	0.133	0.136	26.843	11666	11865.82	0.128	0.128	1.6841

139	14926.35	14425.77	0.107	0.111	-3.47	11452.91	11867.59	0.132	0.13	3.4942
140	11915.51	12344.66	0.142	0.14	3.4764	11035.73	11051.59	0.124	0.125	0.1435
141	12556.27	12810.03	0.133	0.135	1.981	13462.76	13562.26	0.121	0.117	0.7336
142	14116.02	13683.05	0.117	0.121	-3.164	15222.88	16329.29	0.137	0.143	6.7756
143	10843.85	11633.51	0.124	0.126	6.7878	13719.96	13621.97	0.123	0.122	-0.719
144	13330.65	15596.29	0.121	0.114	14.527	14156.1	14356.48	0.128	0.125	1.3958
145	11711.38	13684.76	0.143	0.148	14.42	10874.44	11492.8	0.131	0.13	5.3804
146	13546.04	16251.35	0.119	0.124	16.647	15547.64	15647.23	0.129	0.126	0.6364
147	13157.64	13343.29	0.116	0.127	1.3913	12880.77	13071.81	0.127	0.126	1.4615
148	11317.83	13765.95	0.143	0.147	17.784	13923.57	14039.01	0.122	0.121	0.8223
149	11428.47	11928.34	0.128	0.124	4.1906	10666.02	10553.98	0.122	0.116	-1.062
150	12267.67	12283.53	0.142	0.141	0.1291	15143.02	16084.37	0.125	0.128	5.8526
151	11900.19	12664.19	0.137	0.131	6.0328	11437.05	11502.11	0.122	0.123	0.5656
152	11515.78	11739.96	0.145	0.144	1.9095	12592.65	12963.79	0.124	0.122	2.8629
153	11674.27	12014.43	0.147	0.145	2.8312	15351.48	15273.28	0.116	0.119	-0.512
154	15384.08	15388.22	0.129	0.13	0.0269	11037.46	11676.52	0.139	0.138	5.4731
155	11643.91	13015.36	0.135	0.131	10.537	12015.91	12134.11	0.12	0.121	0.9741
156	12258.41	12752.5	0.148	0.148	3.8745	13073.49	13172.99	0.125	0.121	0.7553
157	11474.66	11333.83	0.115	0.124	-1.243	11634.37	11796.71	0.124	0.124	1.3761
158	11170.25	12711.62	0.138	0.132	12.126	15670.61	15755.55	0.125	0.124	0.5391
159	12670.22	12674.36	0.14	0.141	0.0327	12188.24	12253.3	0.121	0.121	0.531
160	12459.59	13129.88	0.115	0.124	5.1051	12305.76	12612.07	0.13	0.13	2.4287
161	14797.84	15136.34	0.132	0.13	2.2363	13708.72	15331.25	0.134	0.139	10.583
162	13372.97	15036.57	0.116	0.114	11.064	12191.51	12291.01	0.124	0.119	0.8095
163	11954.01	12422.66	0.122	0.12	3.7725	13081.09	13788.8	0.12	0.12	5.1325
164	15170.37	15702.5	0.129	0.124	3.3888	13971.96	14138.91	0.12	0.117	1.1808
165	15395.32	16254.61	0.129	0.128	5.2864	10607.49	10748.83	0.129	0.13	1.3149
166	11459.39	13183.61	0.143	0.141	13.078	12790.57	12981.61	0.126	0.126	1.4716
167	12198.76	12788.81	0.127	0.132	4.6138	12662.46	12761.55	0.126	0.12	0.7764
168	12765.36	12867.37	0.115	0.127	0.7928	13958.55	13970.27	0.126	0.125	0.0839
169	10918.11	11308.27	0.146	0.143	3.4502	12798.64	13197.97	0.13	0.128	3.0257
170	12157.98	12965.14	0.11	0.119	6.2256	14088.82	15070.25	0.138	0.138	6.5123
171	12480.59	12538.58	0.141	0.143	0.4625	14121.51	14272.8	0.124	0.122	1.0601
172	12041.94	12272.36	0.117	0.127	1.8775	14181.6	14269.47	0.128	0.127	0.6158
173	11129.54	14699.77	0.129	0.142	24.288	11513.99	11577.83	0.126	0.123	0.5515
174	12194.82	11998.01	0.123	0.129	-1.64	11748.63	12435.91	0.135	0.134	5.5266
175	11440.19	11499.89	0.14	0.14	0.5192	14088.36	14151.91	0.121	0.127	0.4491
176	13503.74	13600.98	0.119	0.121	0.715	11681.23	11725.79	0.13	0.13	0.38
177	11588.95	11676.61	0.115	0.121	0.7507	12016.66	12116.15	0.125	0.121	0.8212
178	12040.7	13133.42	0.126	0.135	8.3202	12503.95	12790.51	0.127	0.128	2.2405
179	11533.45	12097.68	0.116	0.129	4.6639	10971.39	12085.59	0.139	0.14	9.2192
180	12160.46	12310.08	0.14	0.14	1.2154	11846.06	12502.3	0.125	0.12	5.2489
181	11048.13	10728.47	0.126	0.132	-2.98	11360.47	11447.42	0.129	0.126	0.7596
182	12078.95	12625.76	0.149	0.148	4.3309	11590.96	11854.09	0.125	0.127	2.2198
183	11991.42	12510.59	0.135	0.134	4.1498	11653.8	11820.96	0.126	0.124	1.4141
184	12421.72	14361.21	0.141	0.144	13.505	11536.59	11875.62	0.133	0.131	2.8548

185	11186.37	11430.75	0.146	0.145	2.138	11490.46	11657.62	0.126	0.123	1.4339
186	11212.97	11701.59	0.128	0.131	4.1756	13848.65	14196.05	0.125	0.12	2.4472
187	12931.19	13057.34	0.137	0.14	0.9661	12308.89	12649.3	0.126	0.128	2.6912
188	13768.25	14827.08	0.128	0.129	7.1412	12394.67	12644	0.12	0.123	1.9719
189	12652.31	12740.55	0.123	0.128	0.6927	11724.68	12109	0.12	0.12	3.1738
190	12165.91	12223.78	0.14	0.139	0.4734	11481.4	11468.98	0.123	0.123	-0.108
191	10944.71	11313.95	0.13	0.126	3.2636	11406.23	11443.51	0.131	0.13	0.3258
192	11344.51	12068.73	0.124	0.125	6.0007	11305.92	11080.4	0.12	0.119	-2.035
193	13511.42	13784.82	0.104	0.119	1.9833	12113.7	12145.33	0.125	0.124	0.2604
194	11731.44	13867.71	0.145	0.149	15.405	10518.2	10582.55	0.13	0.129	0.6081
195	11147.58	12258.36	0.136	0.133	9.0614	12420.29	12867.22	0.122	0.126	3.4734
196	12849.83	13124.27	0.115	0.122	2.0911	15023.2	14879.89	0.128	0.128	-0.963
197	11675.63	12150.4	0.133	0.129	3.9074	10973.24	11123.15	0.125	0.124	1.3478
198	14584.24	15047.22	0.125	0.132	3.0768	10847.62	10871.26	0.125	0.127	0.2175
199	11561.24	11838.06	0.142	0.14	2.3383	11625.34	11690.4	0.123	0.123	0.5565
200	12879.14	14129.39	0.122	0.111	8.8485	14600.59	14522.51	0.114	0.121	-0.538
201	11715.16	13782.22	0.129	0.14	14.998	12126.19	12100.12	0.124	0.122	-0.215
202	13532.74	13936.26	0.13	0.131	2.8955	14058.72	16087.11	0.134	0.138	12.609
203	12748.61	13894.46	0.128	0.142	8.2469	10753.3	10856.23	0.123	0.119	0.9481
204	15678.77	15988.77	0.129	0.127	1.9389	12022.22	13120.03	0.133	0.134	8.3674
205	11151.38	13384.43	0.142	0.146	16.684	15152.1	16759.23	0.136	0.138	9.5895
206	11270.04	11290.75	0.141	0.144	0.1834	10286.37	10564.27	0.128	0.129	2.6306
207	12703.28	13562.27	0.113	0.122	6.3337	11531.59	11565.02	0.127	0.128	0.2891
208	11100.09	11485.1	0.149	0.148	3.3523	12460.34	12719.51	0.132	0.13	2.0376
209	13334.83	12676.37	0.136	0.14	-5.194	12351.33	12486.06	0.122	0.122	1.0791
210	16167.93	16693.73	0.124	0.134	3.1497	13282.75	13035.76	0.118	0.117	-1.895
211	10937.16	11065.36	0.135	0.131	1.1586	11735.79	11853.99	0.12	0.121	0.9971
212	12094.07	12293.36	0.136	0.133	1.6211	13032.29	13678.32	0.127	0.13	4.723
213	11355.31	11809.11	0.145	0.145	3.8428	12639.18	12413.66	0.118	0.117	-1.817
214	12259.93	12179.72	0.115	0.124	-0.659	10869.92	13085.71	0.131	0.137	16.933
215	11322.95	11507.88	0.114	0.122	1.6071	12842.97	12944.8	0.126	0.123	0.7867
216	12064.61	11731.94	0.118	0.124	-2.836	15033.78	16244.34	0.129	0.129	7.4522
217	15358.13	15763.99	0.129	0.133	2.5746	10965.42	11441.73	0.128	0.13	4.1629
218	12770.75	12772.46	0.142	0.142	0.0134	10521.6	11500.03	0.137	0.138	8.508
219	12798.56	14781.9	0.139	0.132	13.417	11488.01	12107.33	0.132	0.13	5.1153
220	13390.1	13373.53	0.14	0.14	-0.124	10750.47	11919.28	0.138	0.137	9.806
221	12856.69	14311.3	0.129	0.138	10.164	12991.23	12765.7	0.117	0.116	-1.767
222	12010.44	11895.76	0.119	0.125	-0.964	13241.62	13586.13	0.129	0.127	2.5357
223	11787	12555.65	0.138	0.132	6.1219	13255.77	13530.96	0.128	0.128	2.0337
224	11819.66	11874.18	0.117	0.124	0.4592	11815.02	12241.74	0.124	0.128	3.4858
225	13617.72	13965	0.135	0.133	2.4868	14907.6	16198.24	0.124	0.126	7.9678
226	11630.46	15149.09	0.124	0.143	23.227	11505.69	11647.03	0.123	0.124	1.2135
227	12138.94	12758.23	0.139	0.137	4.854	14448.25	14939.58	0.135	0.129	3.2888
228	11754.81	12228.36	0.137	0.132	3.8726	11991.4	12302.74	0.134	0.136	2.5306
229	11885.26	13764	0.125	0.12	13.65	10053.67	11299.59	0.138	0.135	11.026
230	12702.22	14299.41	0.108	0.111	11.17	12211.27	12329.46	0.122	0.123	0.9587

231	12548.58	12628.46	0.118	0.123	0.6325	11922.03	12070.22	0.127	0.132	1.2278
232	12026.97	12448.84	0.128	0.125	3.3889	13742.39	12763.86	0.126	0.129	-7.666
233	13022.31	15410.07	0.123	0.114	15.495	12706.28	12680.21	0.123	0.121	-0.206
234	11749.87	12345.1	0.14	0.142	4.8216	14780.88	16154.78	0.131	0.132	8.5046
235	14157.46	13486.79	0.137	0.141	-4.973	12350.21	12449.71	0.123	0.119	0.7992
236	11593.3	11910.11	0.127	0.128	2.66	12452.18	12668.21	0.12	0.113	1.7053
237	15427.22	15974.62	0.13	0.133	3.4267	12874.19	12992.39	0.116	0.117	0.9097
238	14446.46	14400.51	0.129	0.131	-0.319	12468.85	12660.9	0.127	0.129	1.5168
239	12039.76	13851.18	0.145	0.148	13.078	11794.93	12026.47	0.128	0.128	1.9253
240	11756.82	12270.91	0.135	0.133	4.1895	11773.5	11547.97	0.122	0.121	-1.953
241	10634.86	14687.34	0.126	0.141	27.592	11284.96	11148.06	0.127	0.121	-1.228
242	11414.53	11601.43	0.144	0.144	1.611	11770.85	12042.31	0.123	0.126	2.2542
243	12160.43	14111.39	0.139	0.146	13.825	16318.79	17614.2	0.131	0.134	7.3543
244	12154.52	13144.06	0.138	0.133	7.5284	12694.35	12885.39	0.128	0.127	1.4826
245	12150.49	12468.78	0.138	0.135	2.5527	10913.39	10964.01	0.129	0.127	0.4617
246	11469.39	11879.05	0.131	0.129	3.4486	14624.83	14683.4	0.123	0.123	0.3989
247	12505.94	12466.73	0.144	0.143	-0.314	11714.82	11868.58	0.126	0.127	1.2955
248	12122.03	12491.47	0.137	0.139	2.9576	11149.6	11554.99	0.12	0.124	3.5084
249	13670.75	14336.4	0.133	0.137	4.6431	12229.34	12206.49	0.126	0.123	-0.187
250	12990.69	13131.24	0.115	0.114	1.0704	15090.41	15952.6	0.128	0.132	5.4047
251	11337.62	12393.3	0.148	0.146	8.5182	14257.3	14332.95	0.118	0.122	0.5278
252	11988.47	11953.62	0.143	0.144	-0.292	13141.58	13126.73	0.121	0.127	-0.113
253	11045.53	11435.69	0.15	0.148	3.4118	12296.56	12424.46	0.13	0.13	1.0295
254	14294.61	14728.25	0.132	0.131	2.9443	10933.45	10804.83	0.122	0.115	-1.19
255	16643.34	17275.47	0.124	0.123	3.6591	14011.81	13459.37	0.126	0.121	-4.105
256	14352.38	15560.12	0.113	0.114	7.7618	11877.71	12174.73	0.13	0.129	2.4396
257	11567.4	11766.72	0.147	0.146	1.694	13057.28	13196.15	0.12	0.12	1.0524
258	13155.21	13337.51	0.137	0.138	1.3669	12568.04	12842.22	0.119	0.124	2.135
259	12993.52	15280.25	0.115	0.112	14.965	12401.97	12749.51	0.126	0.124	2.7259
260	13228.82	14996.73	0.139	0.132	11.789	12584.44	12338.67	0.124	0.124	-1.992
261	12238.24	12878.69	0.122	0.123	4.973	12381.18	12582.27	0.124	0.121	1.5982
262	12919.36	14870.58	0.135	0.135	13.121	12297.59	12367.17	0.114	0.115	0.5626
263	11632.62	12306.59	0.147	0.147	5.4765	11816.3	11926.3	0.134	0.132	0.9223
264	11552.91	11965.87	0.131	0.124	3.4512	13111.44	12885.91	0.116	0.115	-1.75
265	15306.71	15791.06	0.132	0.133	3.0672	13101.45	13236.18	0.12	0.12	1.0179
266	11494.24	11939.05	0.146	0.147	3.7256	12765.07	12644.99	0.126	0.128	-0.95
267	11807.55	12699.55	0.131	0.122	7.0238	13749.95	12667.56	0.12	0.129	-8.545
268	11072.62	12668.51	0.141	0.147	12.597	13766.06	13801.8	0.128	0.125	0.2589
269	12029.97	12874.06	0.138	0.133	6.5565	14924.58	15767.98	0.134	0.137	5.3488
270	11081.99	11675.74	0.129	0.138	5.0853	14763.32	14821.9	0.123	0.123	0.3952
271	11707.42	11770.55	0.139	0.14	0.5364	11968.53	12379.07	0.132	0.13	3.3164
272	12836.99	14429.03	0.137	0.131	11.034	11212.77	11398.75	0.12	0.126	1.6316
273	11202.7	14834.89	0.131	0.145	24.484	11114.12	11255.46	0.128	0.13	1.2557
274	11856.71	11905.79	0.145	0.144	0.4122	12355.42	12454.92	0.126	0.122	0.7989
275	13606.88	13662.02	0.136	0.137	0.4037	12994.99	13364.41	0.122	0.12	2.7643
276	11955.4	12542.33	0.126	0.123	4.6796	10541.38	11131.67	0.132	0.111	5.3028

277	12526.33	12468.84	0.142	0.141	-0.461	11448.06	11161.28	0.125	0.128	-2.569
278	11037.17	13067.04	0.125	0.14	15.534	14417.59	14621.56	0.125	0.124	1.395
279	14195.59	14565.13	0.123	0.13	2.5372	11526.71	12093.02	0.134	0.127	4.6829
280	11954.87	12570.09	0.122	0.119	4.8943	11719.42	12220.08	0.133	0.133	4.097
281	12780.21	13845.1	0.122	0.115	7.6914	12293.75	12422.66	0.134	0.133	1.0377
282	13561.73	13610.13	0.136	0.137	0.3557	11003.03	11140.52	0.122	0.121	1.2341
283	12606.48	12597.7	0.143	0.143	-0.07	11112.91	11114.12	0.123	0.124	0.0109
284	10373.05	10754.92	0.149	0.147	3.5507	11090.28	11142.91	0.12	0.121	0.4724
285	12410.34	14088.05	0.136	0.139	11.909	12349.16	12336.73	0.12	0.12	-0.101
286	12594.99	12509.93	0.132	0.134	-0.68	12287.48	12295.05	0.122	0.123	0.0616
287	11391.83	11827.97	0.146	0.144	3.6873	13473.91	13447.84	0.122	0.121	-0.194
288	15275.04	15716.58	0.131	0.126	2.8094	11211.8	12126.73	0.12	0.12	7.5447
289	12697.04	12661.47	0.137	0.137	-0.281	11020.72	11008.29	0.126	0.126	-0.113
290	13903.58	13278.05	0.136	0.139	-4.711	11022.86	11196.62	0.125	0.125	1.5519
291	11608.06	12073.36	0.123	0.124	3.854	11658.1	11732.83	0.127	0.125	0.6369
292	12660.28	12627.94	0.128	0.13	-0.256	11187.94	11286.64	0.132	0.134	0.8745
293	11611.76	11909.99	0.146	0.145	2.5041	14731.45	15054.76	0.122	0.123	2.1476
294	12989.11	13314.67	0.131	0.133	2.4451	15252.87	15255	0.116	0.115	0.014
295	16449.08	16866.57	0.13	0.125	2.4752	12596.51	13475.59	0.135	0.134	6.5235
296	13541.84	15591.41	0.119	0.122	13.146	12285.61	12060.08	0.119	0.118	-1.87
297	11855.36	11895.36	0.143	0.144	0.3363	11952.38	12039.16	0.128	0.128	0.7208
298	12252.42	14126.77	0.145	0.148	13.268	14304.58	13264.13	0.125	0.126	-7.844
299	10547.43	10727.05	0.143	0.141	1.6745	11935.31	12000.37	0.118	0.119	0.5422
300	12117.81	12038.86	0.121	0.131	-0.656	15096.52	15566.57	0.129	0.128	3.0196
301	11709.39	13389.05	0.138	0.132	12.545	11939.54	11759.89	0.129	0.122	-1.528
302	11897.98	13266.68	0.126	0.133	10.317	11842.81	11934.52	0.115	0.118	0.7685
303	11098.11	11400.78	0.144	0.143	2.6548	13985.13	14859.83	0.12	0.126	5.8863
304	12788.27	13553.31	0.124	0.119	5.6447	12180.45	12102.17	0.124	0.123	-0.647
305	14482	15239	0.109	0.115	4.9675	11542.42	11582.12	0.126	0.123	0.3428
306	16606.21	16489.26	0.128	0.133	-0.709	14473.87	15838.98	0.124	0.126	8.6187
307	10755.36	11441.55	0.132	0.131	5.9973	15795.01	16007.81	0.127	0.129	1.3294
308	10701.06	11270.01	0.147	0.146	5.0483	12459.45	12746.02	0.121	0.122	2.2483
309	11830.31	11687.92	0.138	0.138	-1.218	11043.6	11200.29	0.128	0.123	1.399
310	15582.73	16244.28	0.131	0.125	4.0725	10797.7	10850.34	0.118	0.119	0.4851
311	12948.51	13125.62	0.14	0.139	1.3493	10822.44	10945.08	0.138	0.135	1.1205
312	12745.07	13199.11	0.126	0.127	3.4399	12705.06	12789.71	0.126	0.127	0.6618
313	11818.96	11826	0.121	0.128	0.0595	10923.02	10981.01	0.132	0.132	0.5281
314	14552.39	14265.07	0.121	0.127	-2.014	12358.58	12525.53	0.127	0.123	1.3329
315	11336.12	11612.94	0.147	0.145	2.3837	14242.56	14557.33	0.12	0.125	2.1623
316	14600.39	14836.96	0.128	0.125	1.5945	15579.74	16530.21	0.137	0.139	5.7499
317	15744.16	16165.79	0.129	0.124	2.6082	11481.32	11620.73	0.124	0.123	1.1997
318	12693.65	12648.59	0.132	0.134	-0.356	11377.53	11876.94	0.125	0.124	4.2049
319	14942.6	14979.96	0.135	0.135	0.2494	11939.26	11957.04	0.121	0.121	0.1487
320	14314.27	14134.8	0.13	0.14	-1.27	15698	15878.38	0.129	0.128	1.136
321	10965.12	11266.07	0.145	0.144	2.6713	9990.828	10645.16	0.141	0.138	6.1468
322	12001.14	12372.56	0.137	0.133	3.002	12672.12	13142.07	0.13	0.128	3.5759

323	12613.38	13028.46	0.127	0.132	3.1859	12578.75	12591.05	0.126	0.123	0.0977
324	11992.45	13160.98	0.124	0.113	8.8787	14460.23	14365.88	0.122	0.119	-0.657
325	11094.65	11488.95	0.149	0.147	3.432	11884.95	11876.16	0.129	0.129	-0.074
326	14913.64	14619.29	0.125	0.133	-2.013	11936.17	11988.8	0.119	0.119	0.439
327	10934.04	10934.04	0.145	0.145	0	12872.55	12846.48	0.127	0.125	-0.203
328	11917.33	13875.65	0.139	0.148	14.113	12013.79	12202.91	0.113	0.119	1.5498
329	12245.4	14985.75	0.125	0.145	18.286	14267.18	14447.09	0.129	0.131	1.2453
330	11530.19	15436.4	0.125	0.144	25.305	10900.81	11003.74	0.125	0.121	0.9354
331	12401.34	12485.77	0.144	0.144	0.6763	11209.18	11963.31	0.13	0.127	6.3037
332	12722.72	12819.93	0.116	0.126	0.7583	11196.55	11235.04	0.127	0.126	0.3426
333	13756.43	14908.95	0.118	0.122	7.7303	11741.56	11758.42	0.129	0.129	0.1434
334	12424.29	12568.1	0.117	0.127	1.1443	12088.19	12861.03	0.126	0.128	6.0092
335	13353.97	15097.52	0.139	0.133	11.549	12023.19	12623.47	0.132	0.13	4.7553
336	13909.74	14157.73	0.132	0.137	1.7516	11343.3	11897.65	0.122	0.121	4.6593
337	12087.15	11949.04	0.114	0.12	-1.156	13985.02	13939.46	0.117	0.12	-0.327
338	11876.41	11991.56	0.142	0.142	0.9602	12748.85	12955.04	0.128	0.13	1.5916
339	11078.8	11375.16	0.112	0.121	2.6053	12511.4	12660.27	0.119	0.118	1.1759
340	11627.33	12350.38	0.124	0.122	5.8545	11087.27	11285.88	0.131	0.131	1.7598
341	12582.25	12628.4	0.142	0.142	0.3655	14777.63	14974.08	0.13	0.129	1.3119
342	11917.62	13792.45	0.122	0.122	13.593	12876.91	13685.54	0.126	0.129	5.9086
343	12286.65	14294.92	0.128	0.134	14.049	11571.49	12503.85	0.135	0.136	7.4566
344	12079.35	14087.22	0.143	0.147	14.253	11113.83	11280.52	0.124	0.122	1.4777
345	12501.78	13188.61	0.118	0.119	5.2077	11671.41	12426.51	0.123	0.128	6.0765
346	10900.15	11288.6	0.149	0.147	3.441	11096.32	11426.06	0.123	0.127	2.8859
347	11698.08	11979.04	0.145	0.144	2.3454	12528.47	12526.55	0.116	0.116	-0.015
348	12352.75	14012.45	0.115	0.117	11.845	13679.84	13726.49	0.118	0.119	0.3399
349	12889.38	13151.8	0.138	0.135	1.9954	11316.57	11664.31	0.132	0.131	2.9812
350	11440.21	11604.69	0.145	0.146	1.4173	12771.57	12531.83	0.123	0.12	-1.913
351	13749.53	14629.2	0.118	0.115	6.0131	12625.43	12871.37	0.125	0.127	1.9108
352	13871.81	13753.96	0.115	0.113	-0.857	11334.72	11532.33	0.13	0.127	1.7135
353	11858.47	12271.56	0.142	0.143	3.3662	11789.54	12055.43	0.126	0.126	2.2056
354	16541.36	16855.92	0.12	0.127	1.8662	13460.26	13525.32	0.118	0.118	0.481
355	12209.31	12603.78	0.123	0.129	3.1298	11405.86	12639.37	0.14	0.139	9.7592
356	13369.51	14191.78	0.121	0.127	5.794	10492.08	10633.41	0.126	0.127	1.3292
357	12187.36	12729.82	0.134	0.134	4.2613	10882.76	10906.4	0.125	0.126	0.2167
358	11720.63	12160.37	0.129	0.128	3.6162	12939.3	13323.62	0.118	0.118	2.8845
359	12700.05	12995.08	0.113	0.121	2.2703	12266.04	12365.12	0.126	0.12	0.8013
360	11886.24	11897.66	0.14	0.141	0.096	11153.83	11295.16	0.125	0.126	1.2513
361	13349.83	13361.55	0.14	0.139	0.0877	15301.9	16278.81	0.117	0.121	6.0011
362	11313.47	11488.03	0.12	0.126	1.5195	11743.23	11859.59	0.117	0.117	0.9812
363	12555.7	13524.4	0.114	0.124	7.1626	12179.43	12502.1	0.121	0.125	2.5809
364	13186.53	13344.19	0.132	0.133	1.1815	11723.93	12035.09	0.125	0.128	2.5855
365	12965.53	12310.71	0.138	0.142	-5.319	15193.59	15633.85	0.129	0.128	2.8161
366	11070.36	12317.71	0.133	0.131	10.126	11638.74	11691.38	0.118	0.118	0.4502
367	15926.03	15722.13	0.123	0.132	-1.297	11599.28	11734.01	0.127	0.127	1.1482
368	16001.3	16423.43	0.131	0.125	2.5703	12425.85	12544.05	0.121	0.122	0.9423

369	12850.47	12386.57	0.137	0.14	-3.745	12199.58	12414.97	0.129	0.126	1.7349
370	12640.29	12868.61	0.139	0.139	1.7742	12568.62	12542.55	0.124	0.122	-0.208
371	12771.12	12934.17	0.134	0.134	1.2606	11481.27	11580.76	0.129	0.124	0.8592
372	12082.88	13858.78	0.142	0.147	12.814	11700.58	12182.04	0.131	0.13	3.9522
373	12734.98	16454.13	0.142	0.141	22.603	11038.47	11197.35	0.126	0.125	1.4188
374	10116.5	10464.95	0.148	0.145	3.3296	12051.85	11852.36	0.12	0.118	-1.683
375	11168.83	11405.94	0.145	0.144	2.0788	13976.37	14068.8	0.128	0.129	0.657
376	13510.65	13650.18	0.134	0.139	1.0222	12098.41	12085.99	0.122	0.122	-0.103
377	12404.27	12612.17	0.138	0.135	1.6484	12818.07	12980.41	0.119	0.119	1.2507
378	11799.22	11820.94	0.145	0.145	0.1837	12058.06	11832.53	0.121	0.12	-1.906
379	13733.98	14338.85	0.121	0.123	4.2184	14314.56	14717.03	0.122	0.122	2.7348
380	12083.92	15973.12	0.135	0.132	24.348	12864.41	12609.85	0.123	0.12	-2.019
381	12196	12920.97	0.147	0.147	5.6108	11907	12025.2	0.119	0.12	0.9829
382	13954.94	15600.72	0.135	0.137	10.549	10242.75	10743.53	0.135	0.129	4.6612
383	13961.4	15433.44	0.138	0.134	9.538	12434.38	12573.25	0.121	0.121	1.1045
384	13943.53	15611.56	0.12	0.11	10.685	11281.46	11721.41	0.132	0.13	3.7534
385	11037.37	11352.47	0.145	0.145	2.7756	13570.14	13967.47	0.125	0.123	2.8447
386	13282.76	13587.75	0.118	0.113	2.2446	14275.82	14181.97	0.122	0.12	-0.662
387	11320.67	11621.46	0.141	0.139	2.5883	11483.6	11525.31	0.127	0.127	0.3619
388	12432.69	13465.98	0.114	0.119	7.6734	12532.98	14198.05	0.134	0.138	11.727
389	11501.82	13092.22	0.125	0.122	12.148	10581.01	10838.62	0.131	0.131	2.3768
390	10557.41	13849.23	0.126	0.141	23.769	13118.22	13825.93	0.119	0.119	5.1187
391	14130.56	16426.97	0.13	0.137	13.98	11575.69	11766.23	0.127	0.128	1.6194
392	11567.86	12346.77	0.138	0.133	6.3086	10491.96	11096.26	0.133	0.133	5.446
393	15882.78	15886.92	0.129	0.129	0.0261	10131.6	10634.98	0.131	0.132	4.7333
394	12406.1	13125.53	0.127	0.13	5.4811	14551.65	14500.02	0.118	0.122	-0.356
395	14119.44	14862.45	0.107	0.115	4.9993	14525.25	14564.74	0.138	0.137	0.2712
396	13146.16	13692.19	0.139	0.137	3.9879	11847.38	11685.84	0.125	0.122	-1.382
397	13017.53	13183.72	0.142	0.142	1.2606	15821.37	16795.35	0.117	0.121	5.7991
398	13171.41	16292.62	0.136	0.134	19.157	13362.55	13344.77	0.12	0.118	-0.133
399	13367.61	13581.3	0.115	0.111	1.5734	10620.66	11729.22	0.128	0.128	9.4513
400	10488.25	10778.2	0.146	0.145	2.6901	10682.2	10901.73	0.132	0.132	2.0137
401	10872.85	11210.16	0.122	0.126	3.009	11650.41	12603.75	0.136	0.135	7.564
402	11899.12	12082.47	0.133	0.129	1.5174	13906.19	14045.06	0.118	0.118	0.9888
403	12767.08	12771.23	0.14	0.141	0.0324	11447.77	11306.73	0.123	0.116	-1.247
404	12135.08	13099.08	0.123	0.118	7.3593	12196.94	12476.18	0.131	0.128	2.2382
405	13321.08	14182.72	0.126	0.124	6.0753	13950.28	14048.19	0.122	0.128	0.6969
406	13569.9	16259.07	0.136	0.134	16.539	12016.47	12501.29	0.125	0.119	3.8781
407	11636.24	12254.89	0.143	0.14	5.0482	12115.16	12585.74	0.127	0.126	3.7389
408	12790.47	13781.77	0.129	0.135	7.1928	11083.71	11532.53	0.131	0.131	3.8918
409	12204.52	12194.37	0.12	0.129	-0.083	10867.14	10854.71	0.121	0.121	-0.114
410	10203.7	10523.14	0.149	0.147	3.0357	13005.09	13067.72	0.139	0.138	0.4793
411	11388.27	11585.16	0.141	0.141	1.6996	12683.07	13068.08	0.129	0.126	2.9462
412	11913.6	12618.81	0.131	0.127	5.5886	12521.88	12428.03	0.126	0.124	-0.755
413	14465.11	14615.91	0.132	0.136	1.0317	11392.51	11500.92	0.127	0.122	0.9426
414	13559.13	13861.56	0.132	0.139	2.1818	10557.97	10716.84	0.125	0.124	1.4825

415	16009.64	16621.65	0.124	0.121	3.682	14709.35	14733.37	0.122	0.119	0.163
416	13104.29	14517.97	0.123	0.115	9.7374	11688.36	11938.9	0.122	0.126	2.0985
417	12523.25	14119.47	0.123	0.118	11.305	10539	11009.33	0.129	0.129	4.2721
418	11736.19	12183.21	0.122	0.124	3.6692	11190.69	11255.75	0.127	0.127	0.578
419	12634.19	13389.64	0.107	0.116	5.642	11655.43	11732.42	0.123	0.12	0.6562
420	11849.72	12757.58	0.121	0.115	7.1162	11438.77	11213.24	0.122	0.121	-2.011
421	14124.49	14928.86	0.126	0.127	5.388	11135.63	11415.46	0.13	0.13	2.4513
422	11263.41	12047.88	0.145	0.147	6.5113	12953.67	13114.79	0.119	0.119	1.2286
423	12968.49	13112.93	0.139	0.142	1.1015	12736.34	12812.19	0.125	0.126	0.5921
424	13789.63	13805.49	0.14	0.14	0.1149	12431.2	12674.3	0.126	0.125	1.9181
425	11298.29	11765.61	0.131	0.13	3.9719	11822.71	11940.91	0.119	0.119	0.9899
426	10995.3	12313.94	0.136	0.129	10.708	15796.96	17256.84	0.137	0.134	8.4597
427	11588.56	11416.17	0.138	0.14	-1.51	12052.59	11933.03	0.128	0.122	-1.002
428	12249.42	16316.82	0.137	0.131	24.928	11294.84	11302.42	0.124	0.125	0.067
429	10673.2	10942.95	0.118	0.124	2.465	15308.56	15571.66	0.127	0.126	1.6896
430	12309.37	12763.87	0.117	0.114	3.5609	13677.24	13652.18	0.123	0.12	-0.184
431	12025.97	12121.24	0.135	0.139	0.786	11186.17	11258.8	0.128	0.129	0.6451
432	13013.52	16148.74	0.113	0.111	19.415	13504.83	13643.7	0.118	0.117	1.0179
433	11848.24	13391.99	0.125	0.139	11.527	11747.54	12073.14	0.122	0.125	2.6969
434	11825.97	11947.65	0.123	0.129	1.0184	10619.21	11646.4	0.134	0.134	8.8198
435	11446	11497.17	0.122	0.129	0.4451	12584.69	13021.52	0.124	0.124	3.3547
436	13747.28	13643.1	0.104	0.115	-0.764	11805.1	11981.08	0.125	0.131	1.4688
437	15957.27	15819.61	0.128	0.134	-0.87	12546.48	12767.91	0.128	0.127	1.7342
438	11966.92	13432.06	0.117	0.12	10.908	10992.97	11167.74	0.128	0.128	1.5649
439	12981.12	13724.13	0.108	0.118	5.4139	12786.65	12851.71	0.121	0.121	0.5062
440	17085.28	17212.31	0.127	0.134	0.738	13561.97	13907.54	0.127	0.129	2.4847
441	12878.31	13803.13	0.106	0.118	6.7001	11437.03	11685.55	0.128	0.127	2.1268
442	11838.99	12392.8	0.107	0.121	4.4688	12608.09	12599.3	0.129	0.129	-0.07
443	10814.89	11076.4	0.144	0.141	2.3609	11090.81	11212.74	0.127	0.124	1.0874
444	13069.89	13196.04	0.138	0.141	0.956	12618.08	12761.89	0.121	0.117	1.1269
445	12655.5	14478.43	0.115	0.117	12.591	11761.03	11836.39	0.125	0.125	0.6366
446	12690.78	13478.37	0.13	0.133	5.8433	13300.25	13584.72	0.119	0.123	2.0941
447	11973.27	12529.11	0.134	0.131	4.4364	12444.42	12533.3	0.122	0.125	0.7091
448	11624.01	12566.89	0.124	0.122	7.5029	11959.04	12524.76	0.133	0.134	4.5168
449	12490.05	12521.77	0.14	0.14	0.2533	11279.15	12043.61	0.136	0.136	6.3474
450	12203.21	12683.3	0.123	0.126	3.7852	12150.31	12436.88	0.123	0.125	2.3042
451	11698.83	12290.2	0.145	0.139	4.8117	11820.81	12574.94	0.127	0.126	5.9971
452	11519.51	12040.47	0.146	0.146	4.3267	11098.77	11163.83	0.123	0.123	0.5828
453	12827.1	14221.69	0.14	0.132	9.8061	10551.78	11023.45	0.133	0.131	4.2787
454	12624.4	12955.86	0.136	0.133	2.5584	12610.9	13891.78	0.138	0.137	9.2204
455	11028.29	11643.84	0.134	0.131	5.2865	12939.98	13227.88	0.119	0.123	2.1765
456	11616.84	12440.19	0.137	0.13	6.6184	11442.8	11725.35	0.133	0.132	2.4097
457	13505.33	13784.71	0.133	0.135	2.0267	14083.71	14272.92	0.121	0.122	1.3256
458	11200.16	13053.84	0.13	0.139	14.2	10957.44	11283.13	0.139	0.135	2.8865
459	12824.46	12808.4	0.14	0.14	-0.125	10888.65	11125.75	0.132	0.132	2.1312
460	14285.65	14690.97	0.122	0.128	2.759	13184.55	13302.75	0.116	0.117	0.8885

461	11430.13	12080.67	0.149	0.149	5.385	10940.28	10946.13	0.129	0.129	0.0535
462	11937.77	12752.04	0.126	0.138	6.3854	13119.41	13301.96	0.128	0.13	1.3723
463	12564.01	12876.02	0.127	0.131	2.4232	10962.73	11620.04	0.132	0.132	5.6567
464	10972.07	11324.65	0.148	0.145	3.1134	15579.04	15904.65	0.129	0.127	2.0473
465	13927.47	13854.51	0.123	0.131	-0.527	11553.46	11652.96	0.127	0.122	0.8538
466	13064.6	13392.33	0.141	0.14	2.4472	14730	14713.72	0.132	0.133	-0.111
467	11187.22	12134.75	0.132	0.127	7.8083	11831.99	11998.97	0.125	0.126	1.3917
468	10572.19	10958.2	0.15	0.148	3.5226	14857.79	15190.89	0.128	0.126	2.1928
469	12345.8	13411.86	0.136	0.136	7.9487	14815.89	15824.61	0.138	0.143	6.3743
470	11017.6	11403.91	0.145	0.149	3.3875	13421.01	12255.7	0.116	0.119	-9.508
471	12398.57	12199.37	0.113	0.12	-1.633	12023.51	12422.25	0.133	0.132	3.2099
472	13101.64	13223.36	0.136	0.14	0.9205	11065.86	11053.44	0.123	0.123	-0.112
473	11157.87	12523.42	0.126	0.126	10.904	13300.82	14955.18	0.134	0.138	11.062
474	11284.63	12514.45	0.142	0.148	9.8273	11419.97	11516.24	0.124	0.126	0.836
475	11385.42	11622.53	0.132	0.131	2.0401	14652.33	17213.12	0.124	0.124	14.877
476	12524.26	12851.5	0.111	0.122	2.5463	12204.97	12529.85	0.132	0.131	2.5929
477	15958.1	16321.95	0.13	0.124	2.2292	13340.4	13793.04	0.12	0.124	3.2816
478	13655.37	13773.44	0.13	0.134	0.8573	13096.42	13373.66	0.127	0.126	2.0731
479	12380.91	13188.07	0.11	0.119	6.1204	12180.92	12398.11	0.116	0.121	1.7518
480	12047.47	13620.76	0.129	0.126	11.551	11745.3	12084.83	0.13	0.124	2.8096
481	13252.85	14313.79	0.126	0.13	7.412	12798.13	13216.57	0.129	0.126	3.166
482	12413.41	12984.29	0.137	0.135	4.3967	15222.34	16605.73	0.131	0.132	8.3308
483	12343.21	13768.52	0.138	0.133	10.352	11091.65	11109.43	0.12	0.121	0.1601
484	16395.51	16871.92	0.123	0.129	2.8237	12992.01	12749.17	0.119	0.117	-1.905
485	13836.7	13840.84	0.133	0.134	0.0299	12991.7	12929.62	0.125	0.123	-0.48
486	11892.11	11896.25	0.143	0.144	0.0348	13222.02	13315.78	0.123	0.127	0.7041
487	12531.15	12385.68	0.119	0.125	-1.175	11586.09	11642.16	0.121	0.123	0.4816
488	12295.03	13966.36	0.112	0.109	11.967	13406.46	13498.89	0.124	0.126	0.6847
489	13060.06	12978.43	0.134	0.136	-0.629	12788.28	12853.34	0.117	0.117	0.5062
490	13505.77	14272.46	0.136	0.132	5.3718	10920.57	11138.89	0.132	0.129	1.96
491	13599.06	15583.65	0.138	0.13	12.735	13912.51	14135.73	0.126	0.124	1.5791
492	12354.27	12677.58	0.135	0.139	2.5502	16150.51	17229.56	0.129	0.131	6.2628
493	15135.56	15488.66	0.131	0.133	2.2797	12078.31	12181.24	0.124	0.12	0.845
494	12592.75	13393.84	0.109	0.119	5.981	14496.75	14508.46	0.122	0.121	0.0808
495	12662.96	14166.21	0.116	0.117	10.612	11735.64	11861.2	0.121	0.121	1.0586
496	13138.2	14804.18	0.141	0.145	11.253	12558.21	12756.12	0.124	0.128	1.5514
497	11123.06	11354.22	0.123	0.126	2.0359	11783.46	11882.96	0.122	0.117	0.8373
498	15852.89	15536.65	0.125	0.131	-2.035	12280.03	12464	0.119	0.122	1.476
499	12709.35	13205.21	0.134	0.139	3.755	13323.93	13388.99	0.122	0.122	0.4859
500	12172.71	12375.64	0.136	0.134	1.6397	10898.34	11883.21	0.14	0.139	8.2879
501	11090.42	11528.86	0.134	0.129	3.803	11421	11718.52	0.124	0.128	2.5389
502	14484.13	15997.56	0.127	0.131	9.4604	10688.94	11137.88	0.131	0.134	4.0308
503	11011.31	11430.75	0.148	0.148	3.6695	15130.41	16170.59	0.128	0.134	6.4325
504	13481.52	14113.82	0.117	0.123	4.48	14039.33	14078.82	0.133	0.132	0.2805
505	12124.48	12376.44	0.141	0.141	2.0358	12862.92	12927.98	0.121	0.122	0.5033
506	11167.56	15131.36	0.143	0.141	26.196	11026.03	11649.92	0.12	0.119	5.3553

507	16177.7	16633.4	0.124	0.129	2.7397	10793.42	10868.78	0.126	0.127	0.6933
508	10443.64	10724.59	0.145	0.143	2.6197	14918.93	14898.72	0.114	0.118	-0.136
509	11402.49	12082.32	0.149	0.149	5.6266	11237.76	11332.53	0.128	0.128	0.8362
510	13448.16	13453.19	0.107	0.117	0.0374	11904.64	12022.83	0.12	0.12	0.9831
511	17595.27	18197.81	0.127	0.122	3.3111	10396.72	11514.24	0.128	0.129	9.7056
512	16754.94	16762.25	0.12	0.131	0.0436	12534.5	12725.54	0.128	0.127	1.5012
513	10608.91	10677.49	0.115	0.122	0.6423	12131.53	12294.93	0.12	0.113	1.329
514	11599.64	11613.28	0.142	0.144	0.1174	15995.33	17092.81	0.132	0.13	6.4208
515	13404.17	13884.59	0.135	0.132	3.4601	11446.27	12222.66	0.135	0.132	6.3521
516	12404.56	12430.14	0.117	0.117	0.2058	12562.13	12598.91	0.122	0.119	0.2919
517	13863.87	14370.82	0.131	0.133	3.5276	13008.08	13779.71	0.139	0.138	5.5998
518	14536.59	15277.01	0.13	0.133	4.8466	12187.51	12201.24	0.123	0.117	0.1125
519	13333.95	14574.2	0.122	0.125	8.51	11867.62	12102.44	0.121	0.124	1.9402
520	13850.48	15050.95	0.113	0.117	7.976	12234.93	12353.13	0.118	0.119	0.9568
521	12657.72	13460.95	0.115	0.125	5.9671	11575.9	11717.23	0.129	0.13	1.2062
522	11511.56	11979.34	0.14	0.136	3.9049	12249.45	12189.87	0.127	0.129	-0.489
523	13074.93	13241.58	0.132	0.137	1.2586	11948.71	11723.18	0.121	0.12	-1.924
524	11959.22	12401.09	0.144	0.145	3.5632	11803.07	11922.98	0.126	0.125	1.0057
525	12673.66	13347.63	0.145	0.146	5.0494	13372.88	13415.6	0.121	0.122	0.3184
526	12285.45	13055.88	0.131	0.139	5.901	13622.4	13826.37	0.128	0.127	1.4752
527	12247.04	13463.02	0.141	0.148	9.032	12803.23	12902.72	0.123	0.119	0.7711
528	13915.14	15830.01	0.136	0.138	12.096	11458.45	11921.5	0.14	0.136	3.8842
529	16773.32	17549.59	0.122	0.131	4.4233	11509.75	11562.38	0.118	0.119	0.4552
530	11529.77	12266.38	0.148	0.148	6.0051	14363.64	14583.52	0.128	0.128	1.5077
531	12056.26	13080.38	0.122	0.121	7.8295	16234.84	16584.3	0.131	0.129	2.1072
532	12629.79	14706.36	0.139	0.144	14.12	13415.4	13405.11	0.116	0.122	-0.077
533	14180.59	14714.02	0.132	0.134	3.6253	12543.23	12411.34	0.124	0.121	-1.063
534	12655.4	16652.89	0.135	0.131	24.005	11083.54	11183.04	0.127	0.123	0.8897
535	12700.71	13116.24	0.126	0.126	3.168	11343.53	11432.53	0.127	0.127	0.7784
536	11687.7	14299.06	0.128	0.141	18.262	11250.73	11289.72	0.126	0.121	0.3454
537	13784.15	13764.66	0.136	0.136	-0.142	11931.85	11942.65	0.124	0.122	0.0904
538	11592.6	12832.6	0.139	0.137	9.6629	11231.9	11284.54	0.122	0.122	0.4664
539	13232.67	13195.24	0.114	0.112	-0.284	11726.63	11893.62	0.124	0.125	1.404
540	12499.66	12503.8	0.142	0.142	0.0331	12500.6	12930.72	0.124	0.125	3.3264
541	13321.23	13439.3	0.134	0.138	0.8786	12852	12925.01	0.122	0.124	0.5649
542	11107.85	11547	0.124	0.12	3.8032	12302.77	12545.03	0.121	0.125	1.9311
543	12792.07	12867.13	0.142	0.142	0.5834	12672.01	12911.21	0.134	0.133	1.8527
544	12534.95	12542.82	0.127	0.128	0.0627	11883.26	11912.26	0.125	0.125	0.2434
545	11834.64	12641.79	0.111	0.121	6.3848	15097.63	16126.47	0.119	0.124	6.3798
546	12618.43	13003.96	0.135	0.137	2.9647	12010.43	12172.77	0.121	0.12	1.3336
547	15060.65	15618.72	0.128	0.13	3.5731	12523.61	12765.03	0.13	0.129	1.8913
548	10967.94	14276.86	0.127	0.14	23.177	15028.26	15199.05	0.129	0.129	1.1237
549	16348.64	16784.29	0.125	0.123	2.5956	16356.28	16385.57	0.129	0.128	0.1788
550	12174.08	13134.46	0.116	0.125	7.3119	10953.88	11103.79	0.134	0.134	1.3501
551	11430.85	12833.99	0.115	0.117	10.933	11576.5	11665.91	0.126	0.116	0.7664
552	11772.7	12129.51	0.145	0.146	2.9417	10335.89	11046.38	0.141	0.139	6.4319

553	12534.72	12907.06	0.113	0.124	2.8848	12828.97	12871.69	0.123	0.123	0.3319
554	14778.46	14862.36	0.121	0.128	0.5645	15499.2	15404.97	0.125	0.128	-0.612
555	11805.41	11805.41	0.144	0.144	0	11911.74	12118.23	0.121	0.126	1.7039
556	11968.4	13141.66	0.123	0.12	8.9278	10368.11	10779.48	0.14	0.14	3.8162
557	13522.17	14126.73	0.132	0.138	4.2795	11995.6	12177.11	0.123	0.125	1.4906
558	10681.15	11004.03	0.147	0.145	2.9342	11082.29	12173.35	0.139	0.139	8.9627
559	11468.35	12429.97	0.135	0.123	7.7363	11287.91	11532.38	0.137	0.139	2.1199
560	14338.04	14433.48	0.133	0.136	0.6613	11552.92	11671.12	0.122	0.123	1.0127
561	11356.39	11633.2	0.142	0.14	2.3795	10920.86	11078.77	0.131	0.132	1.4253
562	15785.8	16055.27	0.125	0.132	1.6783	13261.56	13607.12	0.126	0.129	2.5396
563	11176.22	11482.74	0.146	0.144	2.6694	11557.5	11675.7	0.122	0.123	1.0123
564	11682.33	13495.8	0.115	0.112	13.437	9907.128	11284.81	0.138	0.138	12.208
565	11393.2	11955.29	0.123	0.129	4.7015	11969.2	12081.72	0.127	0.125	0.9313
566	15887.84	16149.05	0.133	0.134	1.6175	12107.38	12423.9	0.132	0.129	2.5477
567	12281.23	12602.36	0.136	0.131	2.5482	13663	13817.73	0.126	0.12	1.1198
568	12791.89	14425.65	0.142	0.145	11.325	11415.82	11741.42	0.123	0.127	2.7731
569	11824.54	12503.86	0.148	0.147	5.4329	12483.1	12610.09	0.139	0.137	1.007
570	15881.89	16621.68	0.129	0.129	4.4508	10804.12	11244.07	0.134	0.131	3.9127
571	11066.28	12275.4	0.142	0.149	9.8499	11878.15	12015.64	0.121	0.12	1.1442
572	12993.58	13007.22	0.137	0.139	0.1049	11188.18	11253.24	0.121	0.122	0.5782
573	17040.41	17719.32	0.124	0.122	3.8315	14207.94	14281.91	0.12	0.124	0.5179
574	12456.03	15349.92	0.114	0.111	18.853	12672.33	12912.45	0.121	0.124	1.8596
575	12328.72	12852.31	0.121	0.118	4.0739	14731.4	14837.17	0.139	0.137	0.7129
576	11613.62	12107.3	0.137	0.134	4.0775	11578.01	12069.88	0.12	0.127	4.0752
577	12527.63	13013.43	0.14	0.142	3.7331	11028.83	11891.24	0.127	0.124	7.2525
578	11270.73	12303.99	0.136	0.132	8.3978	14099.95	14140.87	0.12	0.118	0.2894
579	11743.14	15355.25	0.135	0.14	23.524	14219.48	14334.93	0.123	0.122	0.8053
580	12329.38	12888.49	0.134	0.131	4.3381	14205.37	14442.47	0.125	0.123	1.6417
581	13812.78	14435.97	0.124	0.131	4.3169	10872.22	11106.19	0.131	0.13	2.1067
582	11540.48	12919.55	0.132	0.131	10.674	9966.747	10308.91	0.127	0.129	3.3191
583	13419.41	14057.83	0.124	0.139	4.5414	11586.45	11725.32	0.125	0.124	1.1844
584	11749.96	11951.79	0.136	0.132	1.6888	12757.56	13121.33	0.126	0.126	2.7723
585	12765.78	15882.06	0.135	0.136	19.621	11666.24	11690.68	0.128	0.127	0.209
586	13943.04	14079.19	0.137	0.141	0.967	15160.55	15373.01	0.122	0.121	1.382
587	11820.24	13832.25	0.143	0.148	14.546	12470.39	12569.47	0.127	0.121	0.7883
588	11523.77	12393.04	0.133	0.124	7.0142	12082.7	12182.19	0.124	0.12	0.8167
589	17123.05	17672.75	0.124	0.122	3.1105	12203.72	12470.53	0.13	0.128	2.1395
590	12560.09	14663.05	0.108	0.111	14.342	10584.48	10743.35	0.127	0.126	1.4788
591	12994.18	13209.17	0.113	0.11	1.6276	12373.52	13081.23	0.122	0.123	5.4101
592	11942.19	12199.68	0.143	0.144	2.1106	11542.67	12575.74	0.141	0.14	8.2148
593	11957.69	11999.11	0.144	0.145	0.3452	15272.94	15748.85	0.132	0.129	3.0219
594	12943.41	13280.62	0.127	0.139	2.5391	11340.46	11554.64	0.131	0.13	1.8536
595	12075.3	12473.24	0.143	0.141	3.1903	12654.82	12757.75	0.123	0.119	0.8068
596	11302.69	11779.92	0.15	0.147	4.0512	10209.09	10431.13	0.137	0.141	2.1287
597	14320.07	14922.88	0.134	0.133	4.0395	11406.07	11381.22	0.123	0.123	-0.218
598	13920.26	14693.29	0.121	0.123	5.2611	11760.03	11528.57	0.124	0.12	-2.008

599	13174.79	13586.04	0.135	0.132	3.027	12757.41	13176.29	0.131	0.128	3.179
600	13202.07	14766.37	0.123	0.116	10.594	11652.3	11618.15	0.116	0.116	-0.294
601	10772.14	10784.56	0.143	0.143	0.1152	15957.5	16134.95	0.13	0.129	1.0998
602	16461.06	17148.55	0.124	0.12	4.009	12401.79	12640.87	0.126	0.128	1.8913
603	11751.55	12470.37	0.145	0.145	5.7642	12356.84	12396.75	0.127	0.127	0.322
604	12328.33	13079.78	0.141	0.142	5.7452	15041.95	16286.43	0.125	0.128	7.6412
605	12753.06	13075.49	0.132	0.133	2.4659	12413.48	12692.12	0.121	0.116	2.1954
606	13297.69	13451.33	0.113	0.123	1.1422	13256.19	13230.12	0.122	0.121	-0.197
607	10697.35	14241.63	0.128	0.141	24.887	14362.5	15744.47	0.127	0.129	8.7775
608	12369.06	12369.06	0.139	0.139	0	11871.99	12005	0.13	0.129	1.108
609	14536.84	14301.32	0.124	0.132	-1.647	11567.64	11542.79	0.124	0.124	-0.215
610	11351.9	11590.4	0.12	0.129	2.0577	11094.93	11217.23	0.123	0.123	1.0903
611	13374.72	14767.6	0.118	0.126	9.432	11534.01	12187.27	0.131	0.129	5.3602
612	10462.63	10852.79	0.15	0.148	3.595	11154.04	11234.24	0.129	0.129	0.714
613	13199.83	13268.08	0.123	0.125	0.5144	12046.05	12218.8	0.13	0.129	1.4139
614	13005.8	15058.89	0.12	0.116	13.634	13482.62	13737.27	0.126	0.129	1.8537
615	11390.37	13494.17	0.125	0.143	15.59	10458.85	10756.46	0.137	0.14	2.7668
616	13583.11	13583.11	0.14	0.14	0	12312.48	12549.72	0.122	0.121	1.8904
617	14803.26	14834.94	0.124	0.132	0.2136	14499.61	14501.82	0.121	0.127	0.0153
618	11490.02	13010.68	0.138	0.133	11.688	11974.07	12103.66	0.124	0.122	1.0706
619	12044.17	11898.48	0.121	0.13	-1.224	13983.11	13914.75	0.125	0.12	-0.491
620	12887.06	12781.71	0.113	0.119	-0.824	11329.37	11576.68	0.128	0.128	2.1363
621	11671.46	13531.38	0.136	0.146	13.745	15411.19	16664.93	0.128	0.137	7.5232
622	14594.56	15126.03	0.122	0.127	3.5136	10503.27	11438.1	0.129	0.124	8.173
623	13591.79	14907.52	0.134	0.135	8.826	12313.47	12087.95	0.118	0.117	-1.866
624	12669.15	12940.66	0.13	0.13	2.0981	13485.58	13652.56	0.126	0.127	1.2231
625	12534.61	14921.88	0.124	0.117	15.998	11745.99	12072.59	0.133	0.132	2.7053
626	11454.43	11461.5	0.144	0.144	0.0617	12712.18	13151.52	0.13	0.128	3.3406
627	11189.37	12549.91	0.131	0.14	10.841	10952.77	11237.45	0.124	0.123	2.5333
628	13171.39	13564.4	0.131	0.133	2.8974	11639.7	12049.14	0.121	0.124	3.3981
629	10897.42	11233.44	0.15	0.147	2.9912	14882.3	16039.93	0.117	0.121	7.2171
630	11240.75	11283.68	0.12	0.125	0.3805	10578.68	10923.15	0.132	0.131	3.1536
631	13848.73	13186.63	0.136	0.139	-5.021	12095.64	12198.69	0.118	0.12	0.8448
632	12646.8	13472.78	0.14	0.135	6.1307	12842.1	12701.06	0.122	0.115	-1.11
633	11643.19	11778.13	0.122	0.126	1.1457	11656.47	11773.04	0.117	0.119	0.9901
634	11066.16	15656.37	0.135	0.144	29.319	14060.11	14296.47	0.132	0.135	1.6533
635	12946.69	14700.3	0.115	0.117	11.929	12780.83	13265.23	0.128	0.124	3.6517
636	13905.45	13185.58	0.132	0.136	-5.46	12701.09	13005.57	0.117	0.116	2.3411
637	11201.88	11393.01	0.128	0.129	1.6776	12871.29	13151.33	0.118	0.119	2.1293
638	11000.89	11403.89	0.145	0.144	3.5339	12089.05	12178.96	0.128	0.125	0.7383
639	14606.74	14737.03	0.133	0.137	0.8841	12844.76	12962.96	0.12	0.12	0.9118
640	10844.12	12349.51	0.14	0.147	12.19	12883.77	13142.94	0.134	0.132	1.9719
641	11897.3	12507.21	0.137	0.133	4.8765	14340.08	15634.57	0.131	0.131	8.2796
642	11211.26	11539.75	0.119	0.127	2.8466	14117.19	14128.91	0.126	0.126	0.0829
643	13201.18	13364.23	0.137	0.137	1.2201	11285.31	11090.34	0.121	0.118	-1.758
644	12222.56	13660.38	0.136	0.141	10.525	9968.524	9986.808	0.132	0.134	0.1831

645	14321.62	14325.76	0.137	0.138	0.0289	14981.1	15068.97	0.12	0.118	0.5831
646	12563.62	12362.87	0.12	0.125	-1.624	11551.34	11538.91	0.121	0.121	-0.108
647	13089.77	13187.48	0.118	0.115	0.7409	14419.23	15744.42	0.131	0.131	8.4169
648	12192.3	12337.03	0.109	0.121	1.1731	12672.58	12877.76	0.129	0.128	1.5933
649	13259.85	14577.67	0.121	0.117	9.04	11846.88	12011.35	0.126	0.126	1.3693
650	11209.87	11611.88	0.111	0.121	3.4621	12397.55	12214.19	0.128	0.121	-1.501
651	11036.9	11498.78	0.143	0.143	4.0167	15076.53	15056.74	0.117	0.117	-0.131
652	10849.71	11003.14	0.119	0.127	1.3944	16189.47	17163.96	0.113	0.117	5.6775
653	12601.56	12437.38	0.117	0.124	-1.32	11175.11	11274.61	0.124	0.119	0.8825
654	14861.96	15013.89	0.13	0.129	1.0119	11922.26	12010.54	0.125	0.123	0.7351
655	12266.39	12694.2	0.136	0.133	3.3702	12687.16	13406.78	0.128	0.128	5.3676
656	10747.42	11236.37	0.141	0.144	4.3514	12701.14	13059.08	0.128	0.125	2.7409
657	12345.24	14010.88	0.111	0.114	11.888	12997.17	13097.97	0.122	0.12	0.7696
658	12342.04	13998.61	0.144	0.147	11.834	16898.89	17076.34	0.129	0.129	1.0392
659	12429.82	12442.25	0.143	0.143	0.0999	13707.97	13900.01	0.128	0.13	1.3816
660	11946.6	11959.02	0.141	0.14	0.1039	12587.76	12561.69	0.12	0.118	-0.208
661	11108.91	12546.09	0.136	0.132	11.455	13554.64	13867.03	0.126	0.124	2.2528
662	12110.13	12359.16	0.137	0.138	2.0149	11523.24	11588.3	0.123	0.123	0.5614
663	11566.84	11843.53	0.133	0.128	2.3362	11624.98	11399.45	0.122	0.121	-1.978
664	13709.68	14157.76	0.133	0.137	3.1649	11700.92	11969.45	0.132	0.133	2.2434
665	12267.38	12657.63	0.137	0.142	3.0831	11526.85	12564.43	0.132	0.13	8.258
666	12182.5	12331.59	0.113	0.116	1.2089	10958.91	11572.04	0.123	0.12	5.2983
667	13528.95	13425.15	0.112	0.114	-0.773	13255.02	13962.73	0.121	0.122	5.0686
668	12210.46	13794.97	0.137	0.131	11.486	13115.04	13250.98	0.125	0.125	1.0259
669	11266.61	14434.62	0.127	0.145	21.947	13115.63	13285.5	0.122	0.119	1.2787
670	12712.66	13956.63	0.122	0.115	8.9131	13161.3	13269.59	0.116	0.117	0.816
671	14312.61	13653.44	0.135	0.139	-4.828	12343.74	12249.89	0.128	0.126	-0.766
672	12955.83	13604	0.14	0.138	4.7645	11010.58	11018.15	0.124	0.125	0.0687
673	12744.5	12326.98	0.113	0.125	-3.387	12076.47	12485.92	0.12	0.124	3.2793
674	12874.76	13819.11	0.112	0.12	6.8337	15192.13	16028.96	0.134	0.137	5.2207
675	10899.21	11647.36	0.135	0.131	6.4233	12432.18	12706.36	0.119	0.124	2.1578
676	11218.43	11858.79	0.147	0.143	5.3999	10862.31	11019.71	0.134	0.134	1.4284
677	10536.66	11123.47	0.146	0.147	5.2754	13233.31	13346.33	0.117	0.114	0.8468
678	11316.55	11785.2	0.123	0.121	3.9766	14949.01	15005.82	0.125	0.123	0.3786
679	12879.72	12922.86	0.12	0.121	0.3338	11514.14	11496.36	0.123	0.12	-0.155
680	11996.46	12142.95	0.14	0.138	1.2063	10898.68	11272.18	0.12	0.126	3.3135
681	12476.66	13956.1	0.119	0.128	10.601	12682.91	12971.52	0.119	0.124	2.225
682	11687.97	13307.25	0.124	0.124	12.168	12890.53	13401.08	0.125	0.126	3.8098
683	13105.42	13654.71	0.131	0.132	4.0227	14120.77	14199.05	0.123	0.124	0.5513
684	11412.64	11832.09	0.146	0.146	3.545	11552.38	11639.96	0.119	0.121	0.7524
685	10874.33	14346.36	0.127	0.144	24.201	11288.79	11263.94	0.12	0.12	-0.221
686	12292.55	13385.24	0.121	0.129	8.1634	11762.92	11878.28	0.122	0.119	0.9711
687	11416.52	11768.99	0.137	0.133	2.9948	12847.69	12965.88	0.119	0.12	0.9116
688	11930.81	12395.11	0.137	0.132	3.7458	11495.73	11662.88	0.126	0.124	1.4332
689	12452.85	12624.18	0.138	0.136	1.3572	10361.72	10503.06	0.126	0.127	1.3457
690	12651.99	15216.88	0.136	0.136	16.856	12078.77	11575.04	0.123	0.125	-4.352

691	11439.12	12442.54	0.133	0.128	8.0644	11697.76	11941.52	0.126	0.124	2.0413
692	12207.93	11949.91	0.128	0.13	-2.159	11969.13	12002.56	0.128	0.128	0.2785
693	11697.51	11483.04	0.125	0.129	-1.868	12029.8	12431.02	0.127	0.128	3.2275
694	13480.51	13564.36	0.14	0.141	0.6181	11120.25	11237.95	0.131	0.129	1.0473
695	11945.48	12320.7	0.145	0.143	3.0454	12530.75	12703.59	0.126	0.127	1.3606
696	13438.63	13454.48	0.137	0.136	0.1179	12920.81	13019.89	0.126	0.12	0.761
697	12156.71	12920.38	0.142	0.142	5.9106	12597.14	13019.45	0.125	0.119	3.2436
698	14987.32	14625.93	0.127	0.137	-2.471	12569.29	12708.16	0.122	0.121	1.0928
699	12607.72	13967.05	0.119	0.115	9.7324	11582.63	11796.23	0.123	0.115	1.8108
700	13121.14	12727.97	0.127	0.13	-3.089	11268.71	11321.34	0.121	0.122	0.4649
701	12415.36	14526.66	0.144	0.148	14.534	12061.64	12213.41	0.118	0.114	1.2426
702	13372.11	13776.84	0.113	0.122	2.9378	11337.75	11471.09	0.12	0.118	1.1624
703	11437.53	11519.12	0.12	0.126	0.7083	14829.58	14905.14	0.129	0.132	0.507
704	13920.61	14761.42	0.123	0.123	5.696	11603.6	12173.63	0.126	0.124	4.6825
705	11501.76	11902.26	0.118	0.123	3.3649	11560.64	11984.99	0.122	0.122	3.5407
706	11053.38	11347.47	0.147	0.146	2.5917	13189.15	13344.51	0.12	0.124	1.1642
707	11357.33	11527.63	0.121	0.125	1.4773	13244.72	13629.03	0.119	0.119	2.8198
708	12704.92	12575.88	0.118	0.124	-1.026	12074.97	12415.42	0.116	0.121	2.7422
709	13927.51	15649.85	0.139	0.142	11.005	11249.19	11349.19	0.136	0.134	0.8811
710	12407.56	14219.92	0.134	0.136	12.745	14967.04	15116.63	0.127	0.127	0.9895
711	11286.72	12677.68	0.131	0.129	10.972	11067.45	11126.45	0.12	0.123	0.5302
712	12336	12730.94	0.117	0.126	3.1022	12423.61	12833.05	0.119	0.122	3.1906
713	15390.11	15704.25	0.129	0.127	2.0004	10743.95	10745.96	0.12	0.124	0.0187
714	10967.91	11382	0.133	0.128	3.6381	12958.33	13219.42	0.125	0.123	1.9751
715	12236.11	12845.35	0.146	0.145	4.7429	14301.17	13439.22	0.123	0.121	-6.414
716	13931.82	14181.49	0.121	0.129	1.7605	11069.95	11291.28	0.132	0.134	1.9602
717	11385.87	11319.39	0.114	0.121	-0.587	10739.31	10857.5	0.126	0.127	1.0886
718	12099.22	12199.93	0.109	0.118	0.8255	11661.05	12275.85	0.128	0.13	5.0082
719	11527.84	12149.7	0.128	0.131	5.1183	12547.97	12469.68	0.123	0.122	-0.628
720	10164.22	10317.99	0.146	0.147	1.4902	13973.17	14391.8	0.13	0.128	2.9088
721	12812.51	13983.05	0.136	0.143	8.3711	13107.18	13156.76	0.119	0.122	0.3769
722	11547.11	11941.41	0.145	0.143	3.302	12734.94	12861.93	0.139	0.137	0.9873
723	11991.55	12718.66	0.146	0.145	5.7169	10485.45	10460.59	0.119	0.119	-0.238
724	11821.68	12995.44	0.124	0.122	9.0321	11591.5	11641.2	0.125	0.12	0.427
725	14051.86	15032.29	0.131	0.132	6.5222	14603.76	15051.38	0.127	0.126	2.974
726	13125.77	14466.43	0.121	0.113	9.2674	11846.11	12135.94	0.126	0.128	2.3882
727	13241.33	13461.12	0.112	0.121	1.6328	11580.46	11816.44	0.125	0.128	1.997
728	11140.81	11166.97	0.144	0.143	0.2342	11554.93	11670.29	0.121	0.117	0.9885
729	10823.44	11226.02	0.147	0.147	3.5862	11648.63	11674.7	0.126	0.128	0.2233
730	12201.86	12777.1	0.115	0.125	4.5021	13348.86	13255.01	0.123	0.122	-0.708
731	11274.72	11564.93	0.137	0.136	2.5094	11368.27	11550.52	0.132	0.129	1.5779
732	11269.63	13924.08	0.126	0.141	19.064	13601.21	13824.31	0.115	0.117	1.6138
733	12909.33	13041.34	0.139	0.142	1.0122	11561.19	11667.68	0.129	0.128	0.9126
734	12335.97	15567.76	0.113	0.112	20.759	11301.22	13390.36	0.139	0.14	15.602
735	11243.63	14997.22	0.144	0.141	25.029	12147.33	12006.29	0.126	0.118	-1.175
736	13807.71	14410.26	0.133	0.134	4.1814	13272.95	13193.37	0.126	0.129	-0.603

737	14947.29	15365.4	0.131	0.127	2.7211	13389.29	13849.34	0.128	0.126	3.3218
738	13526.2	13657.59	0.126	0.13	0.962	11613.57	11923.74	0.12	0.116	2.6013
739	10929.55	11210.51	0.146	0.144	2.5062	14671.24	14571.15	0.127	0.129	-0.687
740	14084.4	14226.58	0.123	0.13	0.9994	11878.19	11981.12	0.12	0.116	0.8591
741	12171.12	14852.61	0.113	0.112	18.054	11118.27	11115.84	0.129	0.128	-0.022
742	12750.84	13225.28	0.133	0.132	3.5873	10218.19	11057.17	0.127	0.126	7.5877
743	12537.07	13923.47	0.133	0.135	9.9573	12778.14	12969.18	0.126	0.126	1.473
744	13766.81	14285.06	0.114	0.115	3.6279	11651.56	11818.72	0.122	0.12	1.4143
745	12445.37	12788.13	0.131	0.133	2.6803	11437.91	11568.03	0.123	0.122	1.1248
746	12928.7	12950.88	0.116	0.127	0.1713	12869.3	13201.94	0.127	0.128	2.5196
747	14618.93	14928.81	0.13	0.131	2.0757	11270.84	11412.17	0.127	0.128	1.2385
748	11412.11	11982.36	0.146	0.145	4.759	11552.64	11526.57	0.122	0.12	-0.226
749	11634.4	12338.34	0.122	0.125	5.7053	10904.43	10592.17	0.121	0.122	-2.948
750	14470.9	14193.65	0.132	0.14	-1.953	11507.49	11740.16	0.123	0.125	1.9818
751	9867.742	10144.55	0.148	0.146	2.7287	13353.01	13158.99	0.128	0.128	-1.474
752	12211.45	14026.72	0.113	0.112	12.942	11511.08	11947.31	0.123	0.128	3.6512
753	11570.61	12039.26	0.122	0.12	3.8927	12359.75	12347.32	0.121	0.121	-0.101
754	12777.58	12803.64	0.14	0.14	0.2036	12437.01	12563.46	0.118	0.118	1.0065
755	13414.1	14236.25	0.127	0.124	5.775	10515.8	10795.04	0.132	0.131	2.5867
756	11588.3	13769.38	0.129	0.14	15.84	11897.77	12067.98	0.135	0.132	1.4104
757	12759	14963.59	0.138	0.132	14.733	10986.35	11012.42	0.125	0.126	0.2367
758	11848.62	12377.06	0.142	0.136	4.2695	11563.43	11830.83	0.12	0.125	2.2602
759	12591.36	12639.32	0.118	0.123	0.3794	13561.27	13750.53	0.121	0.123	1.3763
760	11083.94	12221	0.125	0.125	9.3041	14737.79	14828.59	0.125	0.122	0.6123
761	11828.95	13857.01	0.123	0.124	14.636	13138.72	13126.29	0.121	0.12	-0.095
762	12376.33	12434.96	0.112	0.125	0.4715	13265.22	13263.8	0.12	0.126	-0.011
763	10357.1	10554	0.145	0.146	1.8656	12113.51	12328.9	0.131	0.13	1.747
764	12612.2	14231.93	0.125	0.122	11.381	15692.2	16026.31	0.129	0.127	2.0847
765	12763.09	13880.63	0.136	0.135	8.0511	11067.6	11643.29	0.125	0.118	4.9444
766	12611.51	13758.04	0.127	0.135	8.3335	11608.45	11745.14	0.129	0.126	1.1638
767	14942.83	15205.55	0.133	0.129	1.7278	13778.22	13782.95	0.125	0.123	0.0343
768	15454.68	15173.71	0.125	0.135	-1.852	12692.25	12806.34	0.12	0.124	0.8909
769	10833.97	11066.93	0.147	0.146	2.1051	10710.36	11650.3	0.127	0.135	8.0679
770	11656.31	11966.46	0.146	0.145	2.5919	11340.29	11848.9	0.12	0.125	4.2925
771	12326.74	12673.07	0.109	0.121	2.7328	11571.92	11525.94	0.124	0.117	-0.399
772	12736.99	13103.01	0.144	0.142	2.7934	14232.48	14651.11	0.13	0.128	2.8573
773	14487.92	14612.27	0.129	0.129	0.851	10626.32	10696.4	0.124	0.123	0.6552
774	16316.77	17074.05	0.125	0.123	4.4353	11110.34	11225.69	0.125	0.121	1.0276
775	11100.33	11429.27	0.147	0.145	2.8781	13089.79	13959.2	0.139	0.138	6.2282
776	11599.77	11771.11	0.14	0.139	1.4556	15334.51	15849.91	0.129	0.128	3.2518
777	12076.23	12472.75	0.131	0.128	3.1791	11838.63	12352.31	0.117	0.125	4.1585
778	13349.27	14689.93	0.12	0.112	9.1264	14456.45	14499.18	0.127	0.127	0.2946
779	15269.52	15399.81	0.136	0.139	0.8461	13157.45	13138.25	0.129	0.126	-0.146
780	11598.72	11685.7	0.14	0.142	0.7444	11350.45	13492.6	0.139	0.141	15.877
781	11090.72	11339.24	0.145	0.145	2.1918	11387.3	11882.48	0.123	0.126	4.1673
782	12045.64	12538.15	0.126	0.138	3.9281	11761.95	11897.9	0.13	0.128	1.1426

783	12923.85	12819.81	0.12	0.128	-0.812	10766.22	11472.82	0.133	0.134	6.1589
784	11986.52	12825.55	0.123	0.124	6.5419	11682.01	11781.51	0.127	0.123	0.8445
785	13118.46	13231.8	0.13	0.13	0.8566	13335	13332.99	0.138	0.137	-0.015
786	13867	13541.73	0.12	0.128	-2.402	13261.95	13653.92	0.123	0.124	2.8708
787	12298.15	13728.31	0.138	0.13	10.418	12443.69	12370.35	0.122	0.12	-0.593
788	14274.66	17067.03	0.139	0.132	16.361	13103.26	13307.23	0.125	0.124	1.5328
789	12148.76	12546.75	0.126	0.13	3.1721	13705.67	13832.83	0.122	0.121	0.9192
790	16084.24	17002.61	0.126	0.132	5.4014	14063.59	14103.09	0.138	0.137	0.2801
791	11542.55	12223.8	0.12	0.122	5.5731	12526.24	12794.56	0.122	0.127	2.0971
792	13068.05	12543.46	0.111	0.123	-4.182	14446	14893.63	0.131	0.129	3.0055
793	12961.08	13205.47	0.143	0.142	1.8506	11750.64	11915.2	0.135	0.135	1.3811
794	11502.27	11758.3	0.112	0.12	2.1774	10590.39	10931.05	0.131	0.133	3.1164
795	12439.78	12602.83	0.14	0.139	1.2938	13262.17	13429.15	0.126	0.127	1.2435
796	11593.27	14019.06	0.129	0.14	17.304	11189.21	11979.54	0.138	0.141	6.5973
797	12589.45	12870.66	0.126	0.131	2.1849	12815.25	12951.19	0.125	0.123	1.0497
798	13386.34	14068.23	0.113	0.122	4.847	12420.71	12394.65	0.124	0.122	-0.21
799	14141.74	14351.51	0.124	0.131	1.4617	11962.74	12254.4	0.126	0.127	2.3801
800	13240.06	14001.15	0.115	0.123	5.4359	11503.16	12141.66	0.127	0.128	5.2587
801	12729.02	13005.8	0.137	0.134	2.1281	10856.06	10994.93	0.13	0.13	1.2631
802	13429.6	14099.27	0.117	0.124	4.7497	13453.34	13792.09	0.128	0.126	2.4561
803	12663.61	15095.57	0.141	0.145	16.11	11202.45	11253.37	0.126	0.125	0.4525
804	13863.09	13690.21	0.118	0.121	-1.263	11620.96	12960.1	0.119	0.12	10.333
805	11515.68	11868.27	0.143	0.14	2.9708	10744.59	10987.76	0.127	0.127	2.2131
806	12284.23	12605.53	0.133	0.138	2.5489	14368.9	14516.68	0.13	0.132	1.018
807	13634.57	13165.16	0.12	0.128	-3.566	15062.56	15281.8	0.124	0.124	1.4346
808	13385.07	14199.34	0.119	0.128	5.7345	12188.17	11916.82	0.123	0.12	-2.277
809	11104.86	11463.6	0.144	0.145	3.1294	10058.49	10896.97	0.142	0.14	7.6946
810	14717.11	15284.8	0.131	0.125	3.7141	11697.98	11778.9	0.129	0.125	0.687
811	11442.11	11989.05	0.129	0.125	4.562	13629.68	13569.72	0.124	0.117	-0.442
812	13055.75	13681.19	0.12	0.124	4.5715	13843.68	14047.65	0.124	0.123	1.452
813	11803.35	12245.94	0.144	0.145	3.6141	15018.39	16420.07	0.126	0.127	8.5364
814	11132.54	11505.63	0.147	0.146	3.2426	11178.38	11153.52	0.124	0.124	-0.223
815	10913.2	11307.5	0.149	0.147	3.4871	16041.42	17448.25	0.122	0.124	8.0629
816	12986.69	13146.99	0.136	0.142	1.2192	10638.08	10613.23	0.12	0.12	-0.234
817	15497.9	15857.57	0.131	0.132	2.2681	10769.37	10904.1	0.128	0.127	1.2356
818	12279.09	12547.67	0.129	0.13	2.1405	11396.99	11595.69	0.129	0.132	1.7136
819	15767.87	16121.21	0.128	0.126	2.1918	13659.94	13856.26	0.127	0.129	1.4169
820	10426.3	10846.66	0.15	0.149	3.8755	12930.8	13030.3	0.122	0.119	0.7636
821	13979.6	14144.74	0.135	0.137	1.1676	13191.36	13488.6	0.129	0.125	2.2037
822	15492.24	15831.15	0.129	0.125	2.1408	13720.25	13893.56	0.12	0.116	1.2474
823	14287.54	14291.68	0.134	0.135	0.029	12399.52	12512.58	0.119	0.122	0.9035
824	11101.61	13344.52	0.126	0.14	16.808	11807.65	11933.21	0.118	0.119	1.0522
825	12819.38	12907.78	0.139	0.14	0.6849	11049.6	11309.34	0.131	0.131	2.2967
826	12755.15	12897.2	0.14	0.14	1.1014	10991.07	11204.83	0.138	0.141	1.9078
827	16395.94	16685.23	0.128	0.126	1.7338	10429.62	11365.54	0.123	0.125	8.2348
828	11679.19	11775.14	0.141	0.14	0.8148	12195.64	12336.47	0.129	0.126	1.1416

829	14505.17	14509.31	0.137	0.137	0.0285	11717.03	11846.23	0.123	0.124	1.0907
830	13703.37	14122.41	0.122	0.128	2.9672	12090.05	12213.81	0.12	0.121	1.0133
831	11472.46	11919.69	0.147	0.147	3.752	12386.39	12494.67	0.12	0.121	0.8666
832	13505.06	13647.78	0.138	0.141	1.0457	12336.95	12433.23	0.119	0.121	0.7743
833	13150.5	13693.23	0.131	0.132	3.9634	14134.35	14590.26	0.129	0.127	3.1247
834	12797.58	13091.35	0.104	0.12	2.244	11533.86	12004.11	0.126	0.127	3.9174
835	12130.15	12117.72	0.141	0.14	-0.103	13027.14	12929.15	0.125	0.123	-0.758
836	12013.63	12725.88	0.147	0.148	5.5969	10854.78	10970.14	0.122	0.119	1.0515
837	15117.45	15121.59	0.135	0.135	0.0274	11048.65	11764.49	0.128	0.127	6.0848
838	12949.18	13500.82	0.115	0.116	4.086	11667.31	12001.78	0.129	0.126	2.7869
839	10867.53	12401.79	0.139	0.146	12.371	14359.68	14660.35	0.126	0.124	2.0509
840	11285.63	11817.59	0.145	0.146	4.5014	15558.5	15643.44	0.121	0.12	0.543
841	11420.02	12782.6	0.129	0.142	10.66	14368.26	14175.37	0.124	0.119	-1.361
842	12486.15	13795.69	0.122	0.115	9.4923	12231.46	13126.92	0.121	0.116	6.8215
843	11619.26	11611.47	0.143	0.143	-0.067	12316.12	12434.32	0.125	0.126	0.9506
844	11008.27	11245.92	0.119	0.123	2.1133	11378.27	11516.17	0.129	0.128	1.1975
845	11824.91	13814.23	0.112	0.113	14.401	11502.71	11601.62	0.121	0.122	0.8525
846	11779.28	12057.82	0.111	0.119	2.3101	15705.13	15844.8	0.131	0.13	0.8815
847	12830.53	15034.95	0.123	0.114	14.662	11473.58	11573.08	0.121	0.117	0.8597
848	13018.2	13439.29	0.126	0.124	3.1333	12075.92	12175.42	0.125	0.121	0.8172
849	12456.46	12918.87	0.123	0.12	3.5793	15046.37	15246.75	0.125	0.126	1.3143
850	13125.48	14893.97	0.143	0.147	11.874	11877.71	11993.19	0.118	0.119	0.9629
851	12898.85	12446.89	0.111	0.124	-3.631	11957.86	11710.87	0.122	0.12	-2.109
852	12426.78	13238.87	0.115	0.125	6.1342	12378.66	12443.72	0.123	0.123	0.5228
853	10445.89	10810.69	0.143	0.142	3.3745	14660.88	14560.79	0.127	0.129	-0.687
854	11909.04	13298.86	0.144	0.148	10.451	13230.68	13337.87	0.119	0.12	0.8037
855	12582.78	12637.93	0.14	0.14	0.4364	11493.48	11891.51	0.123	0.128	3.3471
856	13165.69	13144.4	0.119	0.118	-0.162	11937.65	12152.12	0.123	0.128	1.7649
857	10482.05	12328.36	0.142	0.148	14.976	12054.36	13141.86	0.133	0.134	8.2751
858	10980.84	11753.54	0.136	0.133	6.5742	12222.3	12359.78	0.12	0.119	1.1124
859	11781.62	12002.38	0.11	0.121	1.8393	13318	14213.16	0.121	0.116	6.2981
860	12485.12	14413.91	0.143	0.147	13.381	12609.2	11994.39	0.124	0.129	-5.126
861	11803.46	13522.66	0.139	0.146	12.713	15512.03	15617.51	0.124	0.122	0.6754
862	12453.33	15273.68	0.126	0.144	18.465	11986	11849.1	0.125	0.119	-1.155
863	13587.98	13136.02	0.126	0.127	-3.441	10839.59	11807.51	0.135	0.137	8.1975
864	13161.6	13558.25	0.106	0.122	2.9256	12603.81	12914.77	0.126	0.128	2.4077
865	14608.5	15359.72	0.135	0.134	4.8908	12019.76	12467.8	0.119	0.116	3.5936
866	12183.6	13361.5	0.139	0.145	8.8157	13660.28	13567.56	0.115	0.119	-0.683
867	13091.78	13071.45	0.12	0.125	-0.156	14047.18	13928.31	0.126	0.128	-0.853
868	11796.19	11939.75	0.133	0.128	1.2023	13098.64	13563.54	0.131	0.126	3.4276
869	12825.66	13830.03	0.125	0.13	7.2622	12762.59	12827.65	0.121	0.121	0.5072
870	13258.75	13447.63	0.108	0.118	1.4045	12312.36	12430.55	0.122	0.123	0.9509
871	12280.04	13067.95	0.133	0.128	6.0293	11303.41	11077.88	0.122	0.121	-2.036
872	12028.45	12277.36	0.117	0.123	2.0274	12119.87	11563.8	0.118	0.115	-4.809
873	16127.08	16603.49	0.124	0.13	2.8693	10469.41	11170.02	0.14	0.139	6.2722
874	14911.43	15165.78	0.13	0.126	1.6771	13216.25	13190.18	0.119	0.117	-0.198

875	12719.91	13394.34	0.109	0.121	5.0352	10712.76	11379.96	0.125	0.13	5.8629
876	13552.89	17075.02	0.133	0.131	20.627	15176.41	15121.59	0.122	0.117	-0.363
877	15390.86	15639.64	0.134	0.135	1.5907	11134.38	11557.14	0.137	0.124	3.658
878	11820.76	13269.55	0.117	0.115	10.918	12004.23	12104.23	0.134	0.133	0.8262
879	12280.15	12335.68	0.119	0.127	0.4501	13036.34	13203.32	0.12	0.121	1.2647
880	13744.52	13992.06	0.124	0.131	1.7691	12857.97	13040.31	0.124	0.125	1.3983
881	11334.63	11716.79	0.14	0.141	3.2617	14633.46	14791.84	0.124	0.124	1.0707
882	11651.88	11615.1	0.142	0.142	-0.317	11574.64	11582.21	0.125	0.126	0.0654
883	12313.23	12775.41	0.115	0.125	3.6178	13268.15	13192.79	0.122	0.121	-0.571
884	14425.49	14508.25	0.13	0.136	0.5704	11593.36	11700.14	0.123	0.119	0.9126
885	12050.19	12452.56	0.126	0.122	3.2313	11617.11	11682.17	0.124	0.125	0.5569
886	12287.44	12167.32	0.118	0.125	-0.987	13358.78	13423.84	0.117	0.118	0.4847
887	15004.61	14629.37	0.128	0.134	-2.565	13901.32	13785.38	0.126	0.128	-0.841
888	12074.51	12527.06	0.116	0.127	3.6126	10076.1	10385.13	0.138	0.14	2.9757
889	11258.48	13009.52	0.136	0.143	13.46	11514.94	11965.77	0.13	0.124	3.7677
890	12849.77	12955.17	0.121	0.128	0.8136	11606.71	11751.52	0.122	0.119	1.2323
891	13104.11	13970.75	0.12	0.118	6.2032	11341	11347.56	0.126	0.122	0.0579
892	13683.85	14849.74	0.12	0.114	7.8513	11650.4	11715.46	0.121	0.121	0.5553
893	13326.76	13607.71	0.137	0.136	2.0647	12345.06	12549.03	0.127	0.125	1.6254
894	13862.91	13354.24	0.133	0.136	-3.809	12594.59	12694.08	0.123	0.119	0.7838
895	15055.58	14880.64	0.126	0.132	-1.176	14808.97	14844.2	0.124	0.121	0.2374
896	11744.54	12123.57	0.136	0.131	3.1264	12302	12840.65	0.127	0.127	4.1949
897	11320.86	11762.74	0.147	0.149	3.7566	14731.36	15610.11	0.136	0.138	5.6294
898	13105.6	13109.74	0.138	0.139	0.0316	11844.64	12014.81	0.122	0.119	1.4164
899	11535.35	13578.1	0.113	0.116	15.044	11168.14	11197.13	0.124	0.124	0.2589
900	12256.18	13388.52	0.124	0.12	8.4575	12373.79	12488.73	0.125	0.125	0.9203
901	13649.74	14510.33	0.117	0.119	5.9309	14492.68	15824.95	0.124	0.125	8.4188
902	13486.34	13733.91	0.132	0.13	1.8026	14014.74	15400.86	0.127	0.129	9.0003
903	13119.79	13015.49	0.101	0.118	-0.801	11329.63	11632.3	0.13	0.128	2.602
904	13673.95	13649.44	0.113	0.118	-0.18	11303.51	11421.71	0.124	0.125	1.0349
905	13003.54	13181.62	0.135	0.133	1.3509	11854.64	12128.81	0.119	0.125	2.2605
906	10925.71	11454.56	0.151	0.147	4.617	13644.17	13762.37	0.116	0.117	0.8588
907	11906.18	12252.91	0.144	0.141	2.8297	12905.46	12679.93	0.12	0.119	-1.779
908	11430.46	12252.75	0.137	0.132	6.7111	15655.86	16843.36	0.122	0.122	7.0503
909	16897.13	17187.46	0.121	0.132	1.6892	13682.57	14107.98	0.123	0.123	3.0154
910	12219.6	12378.51	0.135	0.134	1.2837	11227.41	11301.26	0.129	0.129	0.6534
911	11508.45	11991.88	0.111	0.123	4.0313	14066.33	14484.96	0.131	0.129	2.8901
912	13989.77	13974.92	0.135	0.135	-0.106	14053.91	14416.09	0.125	0.123	2.5123
913	11767.76	13068.29	0.135	0.133	9.9518	12196.83	12721.55	0.131	0.129	4.1246
914	12074.4	12728.54	0.14	0.136	5.1392	13373.4	13491.6	0.119	0.12	0.8761
915	9992.803	10185.56	0.147	0.147	1.8924	13353.87	14307.16	0.121	0.113	6.663
916	16094.34	16247.8	0.131	0.133	0.9445	10677.52	11274.54	0.135	0.138	5.2953
917	11846.44	11850.67	0.114	0.118	0.0357	11752.8	11817.86	0.123	0.123	0.5505
918	12092.17	13429.07	0.139	0.146	9.9553	12391.01	12546.24	0.127	0.124	1.2373
919	15402.69	15963.91	0.132	0.134	3.5155	12390.48	12992.52	0.129	0.122	4.6338
920	12504.82	13643.85	0.139	0.134	8.3483	12503.34	12789.44	0.129	0.126	2.237

921	11708.51	12234.7	0.136	0.133	4.3008	13642.67	13741.75	0.126	0.12	0.721
922	15347.88	15196.54	0.126	0.133	-0.996	12743.85	12874.27	0.126	0.129	1.013
923	13155.6	13989.79	0.126	0.132	5.9629	13328.39	13557.77	0.127	0.128	1.6918
924	14782.19	15275.17	0.124	0.13	3.2273	11943.36	12080.85	0.12	0.119	1.1381
925	13028.63	14284.52	0.141	0.145	8.792	11944.04	11931.61	0.119	0.119	-0.104
926	11862.5	13074.05	0.142	0.147	9.2668	12364.87	12808.59	0.133	0.129	3.4643
927	12348.28	12735.35	0.108	0.119	3.0393	11819.87	11995.85	0.13	0.129	1.467
928	13342.23	14291.19	0.119	0.123	6.6402	10351.22	10492.55	0.126	0.127	1.347
929	12034.19	13602.1	0.126	0.133	11.527	11144.42	11285.75	0.125	0.126	1.2523
930	13264.68	12879.57	0.136	0.139	-2.99	13481.89	13895.28	0.121	0.121	2.9751
931	11206.28	11615.22	0.124	0.126	3.5208	14856.39	15948.16	0.135	0.135	6.8457
932	13958.94	13516.84	0.135	0.138	-3.271	11943.85	12307.65	0.132	0.134	2.9559
933	11396.59	11414.37	0.142	0.144	0.1558	12312.09	12253.89	0.122	0.115	-0.475
934	12549.92	13212.01	0.117	0.125	5.0113	14140.76	15459.68	0.126	0.128	8.5314
935	12054.33	12343.62	0.129	0.131	2.3436	11949.46	12026.74	0.119	0.118	0.6426
936	12751.6	14865.15	0.141	0.145	14.218	10462.52	10437.67	0.119	0.119	-0.238
937	12118.52	12401.4	0.139	0.138	2.281	11477.17	11542.23	0.122	0.122	0.5637
938	11411.43	11965.52	0.145	0.143	4.6307	15184.35	15933.9	0.137	0.139	4.7041
939	12765.7	12865.7	0.107	0.115	0.7773	11579.79	11712.81	0.13	0.129	1.1356
940	15755.88	16191.15	0.125	0.128	2.6883	12644.99	12491.51	0.126	0.12	-1.229
941	14508.24	14415.22	0.126	0.129	-0.645	14273.01	14496.24	0.126	0.124	1.5399
942	11933.73	15457.82	0.14	0.139	22.798	15689.76	15939.56	0.132	0.132	1.5671
943	12770.7	16008.06	0.136	0.134	20.223	12453.67	13511.95	0.134	0.133	7.8322
944	12446.3	13744.41	0.124	0.117	9.4447	11548.33	11677.95	0.13	0.129	1.11
945	15568.5	15990.77	0.123	0.129	2.6407	12578.58	12728.7	0.128	0.129	1.1794
946	11393.07	11571.69	0.147	0.147	1.5435	13492.7	13797.38	0.131	0.129	2.2082
947	10963.02	12053.18	0.132	0.13	9.0446	10394.21	11290.99	0.132	0.133	7.9424
948	12340.05	13420.54	0.121	0.117	8.051	14345.32	15168.09	0.132	0.135	5.4244
949	11059.58	13231.41	0.139	0.147	16.414	11096.82	11124.6	0.124	0.125	0.2497
950	11559.71	11994.51	0.147	0.147	3.625	15620.72	15858.17	0.128	0.127	1.4973
951	11949.51	12011.65	0.143	0.144	0.5173	11504.88	11643.75	0.125	0.125	1.1927
952	11212.23	13019.88	0.13	0.141	13.884	13133.25	13035.26	0.125	0.124	-0.752
953	15452.19	15019.05	0.126	0.133	-2.884	15619.74	16561.21	0.132	0.132	5.6848
954	13440.38	14166.83	0.106	0.115	5.1278	14692.78	14837.51	0.122	0.121	0.9754
955	12653.08	12100.2	0.112	0.124	-4.569	11803.21	11906.14	0.12	0.116	0.8645
956	10130.98	10272.31	0.147	0.147	1.3759	15441.15	16839.36	0.124	0.124	8.3032
957	13022.13	14604.01	0.121	0.111	10.832	13450.42	13207.58	0.116	0.114	-1.839
958	10933.13	15265.92	0.143	0.141	28.382	11321.79	11282.88	0.125	0.119	-0.345
959	12010.07	12406.88	0.138	0.141	3.1983	13543.93	13896.91	0.132	0.128	2.54
960	13432.98	13663.61	0.113	0.123	1.6879	12754.82	12944.94	0.127	0.126	1.4687
961	12107.15	12338.07	0.11	0.122	1.8716	12660.4	13097.23	0.124	0.123	3.3353
962	11947.38	12403.9	0.146	0.148	3.6804	13853.48	13755.49	0.121	0.119	-0.712
963	12807.82	12806.61	0.141	0.141	-0.009	12034.7	12179.51	0.125	0.121	1.189
964	12185.55	12164.34	0.144	0.144	-0.174	11179.36	11610.22	0.133	0.133	3.7111
965	11023.11	11487.11	0.146	0.143	4.0394	15624.05	16274.56	0.129	0.13	3.9971
966	14304.72	14563.21	0.13	0.126	1.775	12481.59	12789.63	0.122	0.124	2.4085

967	12763.37	12719.11	0.104	0.114	-0.348	11981.26	11997.53	0.127	0.127	0.1356
968	12900.17	12996.74	0.138	0.139	0.743	11650.8	13018.02	0.14	0.14	10.502
969	10767.99	11196.93	0.151	0.147	3.8309	11845.28	11832.85	0.122	0.122	-0.105
970	11121.57	11382.23	0.13	0.132	2.2901	13548.48	14393.59	0.128	0.13	5.8714
971	11986.61	12162.09	0.136	0.133	1.4428	12172.45	12253.37	0.138	0.137	0.6604
972	11963.16	12082.25	0.141	0.14	0.9856	13099.88	13268.75	0.125	0.124	1.2727
973	12079.08	12076.38	0.12	0.122	-0.022	13316.79	13353.65	0.12	0.125	0.2761
974	11766.88	12378.04	0.135	0.133	4.9375	10846.33	12520.87	0.139	0.14	13.374
975	12064.33	12570.88	0.126	0.123	4.0296	11248.09	12674.52	0.131	0.129	11.254
976	13657.27	15502.79	0.134	0.136	11.904	11680.46	12128.69	0.127	0.128	3.6956
977	12190.52	12659.17	0.12	0.118	3.7021	12816.52	12912.79	0.121	0.123	0.7456
978	12105.75	15170.33	0.125	0.141	20.201	13525.02	13985.07	0.131	0.129	3.2896
979	12383.94	12745.03	0.135	0.136	2.8332	12855.05	13291.07	0.129	0.126	3.2805
980	12114.52	13302.13	0.125	0.118	8.928	11896.76	11995.46	0.13	0.132	0.8228
981	12510.43	13459.84	0.113	0.123	7.0537	10666.07	10731.13	0.129	0.129	0.6063
982	11440.79	15129.47	0.105	0.113	24.381	11242.35	11217.49	0.119	0.119	-0.222
983	13937.28	17544.52	0.136	0.132	20.561	15204.81	15660.79	0.124	0.123	2.9116
984	12510.48	12791.44	0.144	0.143	2.1964	14622.02	14664.74	0.126	0.126	0.2913
985	13151.56	13100.81	0.123	0.131	-0.387	10179.03	10611.61	0.138	0.139	4.0765
986	14344.75	14363.33	0.13	0.135	0.1293	10978.62	11153.98	0.124	0.123	1.5721
987	12437.96	12252.86	0.119	0.123	-1.511	11153.13	11228.48	0.126	0.127	0.6711
988	15547.88	16105	0.125	0.131	3.4593	12993.16	13406.98	0.118	0.119	3.0865
989	12827.17	13121.56	0.14	0.14	2.2435	14553.59	14596.31	0.127	0.127	0.2927
990	12018.48	14079.32	0.117	0.117	14.637	15029.35	16239.31	0.137	0.135	7.4508
991	12911.74	13754.2	0.12	0.119	6.1251	15278.06	15406	0.126	0.124	0.8305
992	15572.3	16821.89	0.127	0.129	7.4283	12537.46	12638.26	0.123	0.121	0.7976
993	12650.68	12797.04	0.137	0.139	1.1437	15282.37	15492.55	0.132	0.13	1.3566
994	13217.43	13762.28	0.13	0.132	3.959	11080.14	11170.14	0.134	0.133	0.8057
995	12221.13	12355.48	0.141	0.142	1.0874	12610.49	12839.87	0.126	0.128	1.7864
996	11210.34	12244.55	0.133	0.127	8.4463	12299.4	12619.44	0.12	0.123	2.5361
997	14895.05	15085.05	0.133	0.13	1.2595	11135.04	11597.33	0.132	0.131	3.9862
998	12035.2	13104.52	0.147	0.146	8.16	14893.72	16247.83	0.131	0.131	8.3341
999	12371.93	12505.77	0.139	0.14	1.0703	10738.88	11148.83	0.126	0.125	3.6771
1000	13187.54	12744.85	0.136	0.139	-3.473	12386.15	12606.99	0.121	0.125	1.7517
	Daraga sample unite (3) E-W					Wuqro sample unite (4) E-W				
	UM L	M L	UM C	M C	L Ch %	UM L	M L	UM C	M C	L Ch %
1	12565	21970.4	0.1265	0.1309	42.809	15315.4	16178.7	0.1255	0.1244	5.3361
2	13016	22460.6	0.1297	0.1319	42.05	12448	12503.9	0.115	0.1162	0.4467
3	12325.9	22561.8	0.1175	0.1344	45.368	13196.3	13216.8	0.131	0.1305	0.1551
4	11741.2	15556.5	0.1337	0.1235	24.525	14079.6	13992.4	0.1271	0.1304	-0.623
5	11522.7	11526.6	0.1155	0.1142	0.0334	12090.6	12487.4	0.1371	0.1346	3.1777
6	11911.2	11660	0.1327	0.1278	-2.154	12709	12442	0.1387	0.136	-2.146
7	13660.2	24111.1	0.1211	0.1323	43.345	11531.3	11674.4	0.1426	0.1428	1.2253
8	11342.3	19035.5	0.1355	0.1346	40.415	15295.1	15319.7	0.1228	0.1252	0.1603
9	13945.6	13962.5	0.1277	0.1267	0.1208	11968.2	12216.2	0.1308	0.1324	2.0303

10	14488.1	26213.1	0.1218	0.126	44.729	11287.4	11398.5	0.1417	0.1409	0.9749
11	11921.5	12220.7	0.1321	0.1343	2.4486	11102	12500.8	0.1432	0.1379	11.189
12	13278.9	25179	0.1117	0.1253	47.262	13631.9	14061.7	0.1237	0.1253	3.0564
13	11418.5	11577.9	0.1165	0.1226	1.3769	12707.3	12849.4	0.1285	0.1329	1.1055
14	11916.1	19011.7	0.1217	0.1323	37.323	12169.4	12190.9	0.1376	0.1364	0.1764
15	14058.1	14299.2	0.1218	0.1243	1.686	10817.7	12103.7	0.1376	0.1335	10.625
16	15898.5	16721.4	0.1274	0.1259	4.9214	12769.5	12925.5	0.1448	0.1454	1.2068
17	13919.9	15825.8	0.1263	0.1339	12.043	13197.2	13172.8	0.1314	0.1307	-0.186
18	12581.6	19612.5	0.12	0.1296	35.849	13268.7	13308.9	0.1287	0.1293	0.3021
19	12315.9	12346.6	0.1121	0.1181	0.2487	10163.2	10454.8	0.1388	0.1391	2.7898
20	11443.8	18388.2	0.1348	0.1309	37.766	13368.2	14043.4	0.1156	0.1154	4.8082
21	10977.8	14435.9	0.1362	0.1354	23.955	11474.4	11816.8	0.1341	0.1339	2.8978
22	13287.1	26440.4	0.1266	0.133	49.747	15182.1	15165.8	0.1285	0.1288	-0.108
23	11054.6	15727.7	0.1346	0.1322	29.713	12185.3	12311.4	0.1279	0.1321	1.025
24	14466.8	19671.3	0.1324	0.1306	26.457	13158.3	13267.3	0.1141	0.1153	0.8222
25	12251.2	15505.3	0.1435	0.1398	20.987	13898.7	13889.9	0.131	0.1307	-0.063
26	13358.3	14495	0.12	0.1155	7.842	14355	14412	0.125	0.1262	0.3954
27	13211.9	18771.9	0.1256	0.1325	29.619	11209.6	11434.5	0.1333	0.1339	1.9668
28	12246	12729.9	0.1318	0.1306	3.8016	12112.3	12165.7	0.1385	0.14	0.4385
29	11506.6	16208.3	0.1297	0.1343	29.008	11401.5	11450.4	0.1351	0.1351	0.4271
30	11803.9	16738.7	0.1455	0.1414	29.481	15235.4	19327.5	0.1267	0.1232	21.172
31	11368.5	11255.4	0.1294	0.1301	-1.004	12685.7	12900.6	0.1265	0.1287	1.6657
32	13420.4	14351.2	0.1252	0.1228	6.4855	11183.9	11481.7	0.1336	0.1364	2.5938
33	15576.3	16825.7	0.1168	0.1233	7.4259	10794.7	10972.4	0.1424	0.1407	1.6195
34	12452.5	20762.2	0.123	0.1242	40.023	16170.5	16201.6	0.1262	0.1285	0.1921
35	13614.7	21819.6	0.1263	0.1321	37.603	11755.9	11979.6	0.1334	0.1328	1.8671
36	10583	16972.9	0.141	0.1399	37.648	11848.9	11739.5	0.1382	0.1388	-0.932
37	13362.7	20108	0.1297	0.1296	33.546	12826.1	12976.4	0.1276	0.132	1.1585
38	14091.6	14104.3	0.1281	0.1273	0.0902	11602.5	11539	0.1351	0.1356	-0.551
39	12421	19012.1	0.1259	0.1365	34.668	14299.7	14283.4	0.1315	0.1316	-0.115
40	13507.4	24288.3	0.1118	0.1309	44.387	13150.5	13438.5	0.1388	0.1355	2.1428
41	15414.4	16715.5	0.1235	0.1298	7.7835	12355.2	13523.1	0.1268	0.1258	8.6358
42	11548	15491.9	0.1337	0.1344	25.458	12298.2	12520.6	0.1439	0.1446	1.7758
43	12362.2	25372.8	0.1159	0.1267	51.278	12956.1	13218.9	0.1151	0.1165	1.9884
44	12222.4	19999	0.1349	0.14	38.885	11892.8	12490.6	0.1411	0.1366	4.7858
45	11585.5	17308.8	0.1438	0.1417	33.065	12128.4	12076.6	0.1437	0.135	-0.429
46	15679.7	16809.8	0.1317	0.1341	6.7228	12466.4	12552.3	0.1287	0.1266	0.685
47	11390.3	16576.2	0.1396	0.1295	31.285	10974.1	11160.5	0.1327	0.1319	1.6701
48	13440.1	24443.9	0.1298	0.132	45.016	11946.7	11951.4	0.1378	0.1365	0.0389
49	14098.3	14440.9	0.1259	0.1221	2.3721	11361.9	11485.1	0.13	0.1341	1.0732
50	11984.3	11734.7	0.1102	0.1168	-2.127	13357.2	14910.8	0.1284	0.1272	10.419
51	11835.3	11536.2	0.1103	0.1134	-2.593	13465.7	13456.9	0.1326	0.1323	-0.065
52	11243.7	18624	0.1369	0.1396	39.628	13055.1	13154.7	0.1316	0.1293	0.757
53	13000.9	13361	0.1287	0.1282	2.6957	13599.8	13604	0.1179	0.118	0.0304
54	11981.8	14251.8	0.1421	0.1271	15.928	12965.5	12986	0.1315	0.131	0.1579
55	12334.3	22239.9	0.1346	0.1333	44.54	12848.3	16524	0.1309	0.1257	22.244

56	12465.7	14295	0.1257	0.1294	12.797	14271.6	14469.9	0.1266	0.128	1.3706
57	12333.6	23992.5	0.131	0.1309	48.594	10804.6	10927.7	0.1316	0.1308	1.126
58	11928.4	13470.4	0.1201	0.1301	11.447	11035.9	11311.1	0.1432	0.1423	2.4329
59	12275.2	19144.7	0.1342	0.1405	35.882	13985.1	14023.2	0.124	0.1233	0.2715
60	14166.5	14465.4	0.1273	0.12	2.0664	11647.8	11888	0.1341	0.1302	2.0209
61	11652.1	11745.2	0.1128	0.1125	0.793	10969.8	11315.9	0.1394	0.1381	3.0578
62	17001	17075.5	0.1286	0.1337	0.4364	11016.1	11041.5	0.1391	0.1367	0.2296
63	13100.6	13982.4	0.1208	0.1122	6.3065	11797.8	11969.5	0.1399	0.1367	1.4346
64	14438.6	14493.9	0.1298	0.1199	0.3813	12244.9	12249.1	0.1163	0.1162	0.0338
65	14825.2	16155.3	0.1231	0.1318	8.2327	12987.3	13869.1	0.1327	0.133	6.3578
66	12703.2	16623.7	0.1365	0.1386	23.584	11233.9	11386.3	0.1333	0.1308	1.3379
67	14132.7	19696.6	0.1313	0.1309	28.248	11672.5	11701.5	0.1122	0.1118	0.2478
68	12088.3	13650	0.1168	0.1116	11.441	12747.4	12751.5	0.1146	0.1144	0.0325
69	14502.8	15056.8	0.1244	0.1148	3.6792	11789.7	11796	0.1305	0.1307	0.0539
70	12473.3	15371.6	0.1437	0.1401	18.854	12280.6	12419	0.1347	0.1349	1.1142
71	13676.3	14292.7	0.1265	0.1251	4.3124	11026.5	11263.4	0.1392	0.1374	2.1033
72	11261	15041.1	0.144	0.1393	25.132	10285.4	10573.4	0.1411	0.1393	2.7241
73	12175.5	19437.7	0.1257	0.1329	37.361	11540	11494	0.1377	0.1358	-0.401
74	12090.5	13716.8	0.1421	0.1285	11.856	11101.5	11164.7	0.1408	0.14	0.5655
75	12083.6	19683.8	0.135	0.14	38.611	10845.8	11132.8	0.1375	0.1367	2.5781
76	13210	13291.2	0.115	0.1147	0.611	13159.6	14259	0.1447	0.1388	7.7098
77	11568.4	13446.9	0.1398	0.1258	13.97	11329.8	11713.4	0.1336	0.1326	3.2748
78	11116.8	17377.1	0.1351	0.1314	36.026	12300.6	12411.7	0.1363	0.1356	0.8953
79	13884.1	14693	0.1261	0.1307	5.5054	14398.8	15563.7	0.1373	0.1348	7.4848
80	12527.2	12400.2	0.1179	0.1146	-1.024	10864.5	11139.9	0.1316	0.1298	2.4721
81	11153.1	17949.2	0.1426	0.1416	37.863	14090.1	14128.2	0.122	0.1214	0.2695
82	12625.8	16570.6	0.1264	0.127	23.805	12791.9	12704.7	0.1296	0.1336	-0.686
83	13091.6	13327.6	0.1323	0.1261	1.7709	10656.5	11245.5	0.1438	0.1428	5.2375
84	12021.2	12155.7	0.1246	0.1169	1.107	10771.6	11349.4	0.1369	0.1338	5.0912
85	13077.4	22367.1	0.138	0.1259	41.533	12826.7	12961.9	0.1246	0.1247	1.0429
86	14883	21787.4	0.1197	0.1309	31.69	10775.3	13938.8	0.1365	0.129	22.696
87	11047.7	17010.7	0.1317	0.1376	35.055	14514.9	14640.3	0.1241	0.1231	0.8562
88	12004.2	15995.6	0.1307	0.129	24.953	11228.1	11291.2	0.1416	0.1409	0.5592
89	11334.4	18324.6	0.1415	0.1427	38.147	11239.1	11596.1	0.1367	0.1382	3.0781
90	12460.9	19270	0.1237	0.1258	35.335	11380.3	11651.8	0.1396	0.1374	2.3297
91	13111.6	13721.6	0.1216	0.1144	4.4449	12721.9	13196	0.1398	0.1399	3.5931
92	12215	16822.3	0.1237	0.1226	27.388	13279.4	17063.7	0.128	0.1236	22.178
93	11211.8	14564	0.1433	0.129	23.017	12267.6	12130.3	0.1307	0.1412	-1.132
94	13453.9	23845.1	0.1245	0.1304	43.578	14954.4	15974.2	0.1308	0.1299	6.384
95	14349	14040.9	0.1212	0.1163	-2.194	10466.3	10508.4	0.1421	0.1396	0.4009
96	12802.7	18666.5	0.1216	0.1207	31.413	13259.1	13242.7	0.1344	0.1346	-0.124
97	14107.2	19831.4	0.1323	0.1295	28.864	13230.2	13527.7	0.1364	0.1376	2.1988
98	13760.5	13422.7	0.1069	0.1104	-2.516	13272.4	13509.4	0.1346	0.1359	1.7542
99	15470.3	20401.4	0.1263	0.131	24.171	11241.4	11338.6	0.141	0.1342	0.8572
100	13212.9	23846.7	0.1276	0.1311	44.592	11633.4	11797.1	0.1355	0.1347	1.3881
101	12203.3	19859.8	0.1323	0.1315	38.552	12107.6	12270.8	0.1426	0.1437	1.3305

102	12079.5	11966.4	0.1093	0.1154	-0.945	13007.6	13219.3	0.1396	0.1393	1.6009
103	12041.3	12169.3	0.1347	0.139	1.0524	11549.1	11738.4	0.1336	0.1361	1.6129
104	11214.9	17034.5	0.1253	0.1344	34.164	12585.7	12871.7	0.1278	0.1293	2.2215
105	13088.1	12959.6	0.1358	0.1316	-0.991	11645.2	11645.2	0.1151	0.1151	0
106	13719.6	23098.2	0.1202	0.133	40.603	12618	12982.1	0.1336	0.1393	2.8043
107	14933.5	16668	0.1245	0.1244	10.407	13145.9	13347.3	0.1139	0.1149	1.5091
108	12689.1	12693.6	0.1339	0.1283	0.035	12403.5	12407.7	0.1127	0.1125	0.0334
109	12645.9	15199.3	0.123	0.1299	16.8	10918.6	11163	0.1327	0.1326	2.1892
110	12917.6	13321	0.1458	0.1448	3.0288	13838.4	13751.2	0.1284	0.1317	-0.634
111	12507.2	13108.3	0.1463	0.1455	4.5855	10878.4	11125	0.1418	0.141	2.2167
112	12991.8	14045	0.1213	0.1126	7.4989	12066.8	11979.6	0.1315	0.1352	-0.728
113	12989.6	25345.1	0.1144	0.1267	48.749	14602.2	14640.3	0.121	0.1204	0.2601
114	13248.5	18243.2	0.1146	0.1231	27.378	14186.6	15104.2	0.1353	0.1363	6.0753
115	12509.7	18399.9	0.1218	0.1298	32.012	15526.3	15842.1	0.1278	0.1267	1.9936
116	11166.8	18301.9	0.1328	0.1349	38.986	12954.5	13221	0.1309	0.1334	2.0153
117	13194.7	22334.7	0.128	0.1309	40.923	12830.3	13484.1	0.1361	0.1351	4.8488
118	13674.4	14079.6	0.1309	0.1307	2.8782	12153.5	12331.6	0.1271	0.1266	1.4444
119	15770.1	19886.9	0.1267	0.1323	20.701	13564.7	13540.8	0.124	0.125	-0.177
120	10717.1	14829.9	0.1375	0.1349	27.733	11299.9	11344.2	0.1279	0.1282	0.3909
121	12440.8	22699.8	0.137	0.1314	45.194	12641.6	12920	0.1455	0.1454	2.1548
122	13560.1	13347.1	0.1224	0.126	-1.596	11602.6	12063.1	0.1354	0.1342	3.818
123	13757.3	20949.2	0.1273	0.1335	34.33	11300.2	11714.5	0.1387	0.1371	3.5366
124	13421.5	15143.2	0.1288	0.1315	11.369	13925	13796.2	0.1269	0.1321	-0.934
125	13358.7	15482.2	0.1205	0.1299	13.716	14341.1	15050.9	0.1274	0.1261	4.7162
126	12909.3	13096.5	0.1285	0.1306	1.4293	11313	11603.7	0.1253	0.1247	2.5049
127	11736.3	15934.2	0.1189	0.1231	26.345	10178.1	10749.8	0.1367	0.1332	5.3182
128	11780.1	12270.1	0.1347	0.1392	3.9935	11673.1	12050.4	0.1345	0.1372	3.1304
129	12475.7	14435.1	0.1219	0.1071	13.573	11705.2	11956.4	0.1321	0.1339	2.1014
130	12930.2	22781.1	0.1187	0.1332	43.242	13787.8	14035.8	0.1239	0.1256	1.7671
131	10917.2	12716.5	0.1199	0.1109	14.149	11857.1	12733.3	0.1405	0.1372	6.8813
132	12992.2	23676.8	0.1136	0.1307	45.127	11765	11897.9	0.1387	0.1384	1.1172
133	12851.1	26053.2	0.1273	0.1333	50.674	10979.2	11222.6	0.1338	0.1331	2.1694
134	12365.4	20046.1	0.1328	0.1405	38.315	14387.5	14300.3	0.1271	0.1303	-0.609
135	11379.8	12073.9	0.1444	0.1469	5.749	11609.5	11699.6	0.1288	0.127	0.7703
136	15386.4	15947.8	0.129	0.1337	3.5201	13504.9	13488.5	0.1322	0.1322	-0.121
137	10530.9	15812.8	0.1352	0.1367	33.403	13069.2	13723	0.1348	0.1341	4.7644
138	11073.4	11085.2	0.1366	0.1395	0.1065	11668.5	11754.4	0.127	0.1296	0.7307
139	13417.5	14352.1	0.1301	0.1297	6.5119	11132	11360.6	0.1349	0.1424	2.0127
140	12475.1	12219.4	0.1135	0.1168	-2.092	14535.8	14592.8	0.1206	0.1218	0.3905
141	14151.6	18897.5	0.1379	0.1309	25.114	11651.9	11684.3	0.1394	0.1374	0.2768
142	14022	15789.9	0.1282	0.1313	11.196	11467.2	11757	0.1383	0.1455	2.4641
143	15933.2	19269.4	0.1242	0.1296	17.313	10745.6	11030.2	0.1335	0.1331	2.5801
144	12186.2	13778.8	0.1122	0.1115	11.558	10798.7	10813.9	0.1393	0.1366	0.1401
145	12682.8	13341.7	0.1174	0.1139	4.9387	12042.5	12029.6	0.1413	0.1395	-0.107
146	12307.9	12301.2	0.1147	0.1107	-0.054	11419	11651.9	0.1415	0.1368	1.9994
147	13651.3	21244.7	0.1228	0.1245	35.742	12932.6	13058.8	0.131	0.1348	0.9663

148	12512.1	14296.2	0.114	0.1091	12.479	12419.3	12573.6	0.1473	0.1466	1.2276
149	11311.7	17632.2	0.1261	0.135	35.846	12004.1	11741.1	0.1414	0.1429	-2.239
150	11751.2	17792.6	0.1278	0.1364	33.955	11642.4	11773.8	0.1422	0.1443	1.1155
151	11938.4	14421.5	0.1294	0.1305	17.218	11658.6	12117.3	0.1308	0.1297	3.7855
152	10988.1	17462.6	0.1431	0.1423	37.077	14954.2	14907.1	0.1279	0.1303	-0.316
153	12324.4	17696.2	0.1207	0.1287	30.356	11777.6	11834.6	0.1263	0.1279	0.4815
154	16242.6	19974.3	0.1244	0.1303	18.683	12232.9	12393.7	0.1238	0.1286	1.297
155	15515.9	19103.5	0.1294	0.1313	18.78	13110.7	17406.2	0.1271	0.1236	24.678
156	11138.3	19087.6	0.1363	0.1295	41.647	11507.8	12975.5	0.1423	0.1393	11.312
157	15336.7	21776.2	0.1193	0.1304	29.572	11106.5	11078.7	0.139	0.1401	-0.251
158	11436.5	20041.1	0.1311	0.1401	42.935	11314.5	11454.2	0.1446	0.1438	1.2197
159	12016.8	11994.3	0.1321	0.1292	-0.188	11140.1	11385.5	0.1292	0.131	2.1553
160	14052.3	26195.7	0.1129	0.1246	46.357	10947.2	10951.4	0.1368	0.1351	0.0386
161	12915.7	13338.5	0.1198	0.1161	3.1701	13242.5	13513.5	0.1412	0.1418	2.0048
162	12755.5	14803	0.1412	0.1376	13.831	10805.3	11024.9	0.1342	0.1376	1.9913
163	11302.3	15432.9	0.1294	0.1325	26.765	11394.9	11703.5	0.1335	0.1319	2.6362
164	11485.9	11659.5	0.133	0.1369	1.4885	11273.3	11449.7	0.1321	0.1386	1.5406
165	12168.8	15891.8	0.1269	0.1258	23.427	15077.4	16008.8	0.1352	0.128	5.8177
166	12808.5	12690.5	0.1355	0.1307	-0.93	12354.5	12749.2	0.1318	0.1302	3.0961
167	13355.9	24173.9	0.1122	0.1308	44.751	10893	10935.4	0.1387	0.137	0.388
168	13693.7	13706.6	0.1358	0.1307	0.0943	14255.4	14931.2	0.1248	0.1243	4.5265
169	12236.1	13775.1	0.1204	0.1112	11.173	11041	11145.5	0.1435	0.1408	0.9381
170	11001.1	15737.8	0.1476	0.1429	30.098	11838.8	12558.2	0.1291	0.1286	5.7279
171	12094.8	12459.7	0.1248	0.1183	2.9292	13321	13877	0.1267	0.1257	4.0067
172	12981.7	14818	0.1364	0.1241	12.392	15979.4	16987.2	0.1237	0.1238	5.9331
173	11660.3	13311.4	0.1224	0.1308	12.404	14601.7	15255.6	0.1306	0.1302	4.2857
174	12553.6	21591.8	0.123	0.1337	41.859	10409.9	10648.2	0.1394	0.1376	2.2381
175	11934.3	19688.5	0.1325	0.1255	39.384	11092.6	11402.3	0.1378	0.1362	2.7165
176	12490.7	22680.8	0.1366	0.1312	44.928	11602.5	11768.2	0.1409	0.1413	1.4086
177	14427.9	22112.6	0.1255	0.133	34.753	14500.9	14922.9	0.1252	0.1253	2.8278
178	12377.5	13466.6	0.1153	0.1119	8.0873	13748.3	13874.5	0.1287	0.1323	0.9095
179	13400.9	14596.4	0.1206	0.1322	8.1907	12934.2	13170.1	0.1279	0.1287	1.7915
180	13231.5	20745	0.1284	0.1305	36.218	12319	12558.7	0.1324	0.1292	1.909
181	12820.4	13391.5	0.144	0.1439	4.2642	12400.8	12449.5	0.1373	0.1364	0.3912
182	12252.5	20849.2	0.1371	0.1404	41.233	11897.5	15702.4	0.1353	0.1286	24.231
183	14933.5	14878.2	0.1216	0.1138	-0.372	11518.6	11644.8	0.1288	0.1332	1.0836
184	11829	19096	0.1269	0.1342	38.055	12606.5	12663.5	0.1245	0.126	0.45
185	13346.6	19108	0.1296	0.1323	30.152	11780.4	12237.6	0.1315	0.1332	3.7356
186	14079.9	15726.6	0.1257	0.1317	10.471	11525.9	11524.2	0.1355	0.1335	-0.014
187	12683.1	12651.8	0.1269	0.1269	-0.247	15104.6	16147.5	0.1244	0.1258	6.4587
188	12115.5	12396.9	0.1166	0.1154	2.2701	11834	12062.6	0.1305	0.1295	1.8945
189	12446.4	13277.7	0.1115	0.113	6.2608	15100.6	15157.5	0.1182	0.1194	0.376
190	11752.1	19766.5	0.1363	0.1396	40.545	12912	12923.7	0.1347	0.1354	0.0907
191	11180.7	16127	0.1408	0.1301	30.671	10336.3	10463.5	0.1445	0.1455	1.2156
192	12042.5	26739.1	0.1303	0.1321	54.963	12125.7	12125.7	0.1189	0.1189	0
193	13017.7	12858	0.1343	0.1321	-1.242	11220.4	11405.6	0.1398	0.1408	1.6236

194	12504.9	17810.9	0.124	0.133	29.791	12513.8	12456.1	0.1446	0.1369	-0.463
195	12407.5	18115.5	0.1248	0.1239	31.509	15165.9	15301.1	0.1247	0.1247	0.8835
196	11891.4	18916.9	0.1415	0.1406	37.138	11819.3	11898.2	0.1362	0.136	0.6629
197	13926.1	21646.6	0.1233	0.1332	35.666	11703.7	11928.6	0.1355	0.1362	1.8853
198	15594.2	18955	0.1253	0.1311	17.73	11232.2	11371.9	0.1458	0.145	1.2285
199	14429.2	18145.4	0.1338	0.1332	20.48	11590.2	11691.7	0.1287	0.1336	0.8685
200	13147.7	22803.8	0.1384	0.1262	42.344	12372	16447.9	0.1276	0.1237	24.781
201	11062.9	17741.7	0.1445	0.1429	37.645	12261.4	12753.9	0.1454	0.1452	3.861
202	11647.4	11594.5	0.1178	0.1204	-0.457	11278	11334.1	0.1462	0.1449	0.4947
203	12809.1	13705	0.1128	0.1144	6.5367	11141.1	11790.7	0.1345	0.1336	5.5099
204	13128.7	22472	0.1211	0.1332	41.578	13208	13462.7	0.1355	0.1309	1.8919
205	12846.3	23922.7	0.1257	0.1325	46.301	12368.6	12404.3	0.1373	0.137	0.2874
206	11596.6	16028.1	0.1398	0.136	27.648	16294.7	16420.1	0.1229	0.1221	0.7634
207	13284.5	13850.7	0.128	0.1321	4.0875	12362.5	12444.3	0.131	0.1309	0.6576
208	10991.5	17534.5	0.1367	0.1302	37.315	11936.8	12106.9	0.1312	0.1369	1.4052
209	12436.8	22608.1	0.114	0.133	44.989	13138.1	13279.1	0.1343	0.1317	1.0619
210	12845.2	14570.3	0.1286	0.133	11.839	13332.6	13391.8	0.1128	0.1138	0.4427
211	12662.4	19645.6	0.1199	0.1242	35.546	10711.7	11076	0.1353	0.1357	3.2891
212	12135.9	15804.4	0.1296	0.1345	23.212	13395.6	13812.3	0.138	0.1353	3.0169
213	12424.5	12103.1	0.1303	0.134	-2.655	10243.1	10612.9	0.1379	0.135	3.485
214	11411.1	17811.8	0.1346	0.1364	35.935	11718.8	11722.2	0.1315	0.132	0.0293
215	10807.1	11597.1	0.1362	0.1263	6.8122	14877.2	15278.3	0.1315	0.1301	2.6252
216	13927.7	14568.8	0.1284	0.1315	4.4004	10823.3	11165.9	0.1354	0.1367	3.0689
217	11636.8	15407.2	0.1439	0.1275	24.472	14059.1	14042.7	0.1327	0.133	-0.117
218	14580.9	16271.3	0.1232	0.126	10.389	13401.2	13384.8	0.1346	0.1348	-0.122
219	13617.9	26647.1	0.1235	0.1245	48.895	11724.4	12025.5	0.1341	0.1341	2.5044
220	11947.5	11836.3	0.1362	0.1313	-0.94	11497.9	15662.1	0.1373	0.1298	26.588
221	11386.6	13835.9	0.1371	0.1359	17.702	11089	11431.1	0.1328	0.1295	2.9933
222	11774.7	15862.1	0.1349	0.1332	25.769	11919.5	11976.2	0.1329	0.1315	0.4741
223	15816.6	16765.4	0.1259	0.1229	5.6592	13655.7	13884.2	0.1247	0.1239	1.646
224	11895.8	16029	0.1328	0.1302	25.786	14351.4	15497	0.1382	0.1348	7.3925
225	12254.1	19679.9	0.1246	0.1346	37.733	14688.2	15684.7	0.1365	0.1421	6.3533
226	12535.1	17098.3	0.1225	0.128	26.688	11655.2	15594.1	0.1382	0.1304	25.259
227	12530.9	23607.9	0.1342	0.1317	46.921	11219.8	11608.8	0.1362	0.1348	3.3512
228	13341.9	13925.2	0.1339	0.1321	4.1891	13001.3	13005.4	0.1148	0.1147	0.0318
229	15436.7	16169.8	0.1271	0.1247	4.5332	12759.9	12776.3	0.1331	0.1308	0.1281
230	12762.8	13311	0.1415	0.1403	4.1184	14449.6	15858.3	0.1221	0.1217	8.8833
231	13762.5	13636.9	0.1199	0.1223	-0.921	16946	17048.6	0.13	0.1286	0.6013
232	13555.7	15938.1	0.1332	0.1293	14.948	15297.5	16393.9	0.1435	0.1387	6.6879
233	12262.8	14992.6	0.1366	0.1325	18.207	11622.9	11885.4	0.1459	0.146	2.209
234	11751	16624.5	0.1334	0.1252	29.315	12525	12525	0.1119	0.1119	0
235	14159	21991.3	0.1249	0.1331	35.616	12477.8	12477.8	0.1165	0.1166	0
236	11896.2	13534	0.1185	0.1282	12.102	12623.4	12820.6	0.1431	0.1444	1.5381
237	12517.4	17608.3	0.1304	0.1362	28.912	11690	11690	0.1153	0.1153	0
238	11547.6	11890.2	0.1349	0.1323	2.8819	12306	12526.1	0.1371	0.137	1.757
239	12288.4	19561.8	0.1277	0.133	37.181	11395.6	11468.2	0.1392	0.1378	0.6334

240	11415.5	11669.6	0.1406	0.1399	2.1771	13661.3	13645	0.1325	0.1327	-0.12
241	13431.7	13501.3	0.1308	0.1277	0.5156	11242.3	11563.4	0.1471	0.1452	2.7771
242	12295.9	17960.5	0.1309	0.1289	31.539	12074.7	12078.9	0.1355	0.1341	0.035
243	12759.3	22257	0.1219	0.1361	42.673	12882.5	13767.2	0.1347	0.1349	6.4261
244	11454.9	18765.2	0.1376	0.1397	38.957	12216	12340.1	0.1372	0.1339	1.0053
245	16463.4	16785.9	0.127	0.1267	1.9208	10656.4	10859.3	0.1365	0.1364	1.869
246	12602	13173	0.1334	0.1314	4.334	11046.2	11079.4	0.1417	0.1416	0.2991
247	10081.1	16370.7	0.1457	0.1423	38.42	12298.7	12315.9	0.1397	0.1417	0.1396
248	10754.7	16353.8	0.1332	0.127	34.237	12776.1	12776.1	0.117	0.117	0
249	11269.8	11323.8	0.1117	0.1187	0.4766	11957.7	12050.6	0.1462	0.1427	0.7704
250	13674.9	20567.8	0.1235	0.1338	33.513	13810.1	13867.1	0.125	0.1263	0.4109
251	11587	20460.1	0.1309	0.1371	43.368	10633.6	12593.3	0.1447	0.1406	15.561
252	12175.3	12116.9	0.1186	0.1136	-0.483	12325.5	12392.6	0.1255	0.1253	0.5412
253	11999.7	12054.5	0.1153	0.1149	0.455	15020.5	15674.3	0.1296	0.1294	4.1712
254	14095.5	21526.3	0.1272	0.1327	34.519	11661.1	11717.9	0.1275	0.1261	0.4845
255	17088.6	20262	0.1243	0.128	15.662	13464.3	13447.9	0.1308	0.1311	-0.122
256	14408.8	16660	0.1243	0.1339	13.512	10689.2	10886.3	0.1349	0.1345	1.8106
257	14746.3	16047	0.1308	0.1308	8.1059	11928.3	12345.2	0.1318	0.1344	3.3773
258	15229.4	15161.9	0.1275	0.1268	-0.445	11900.7	12139.9	0.1383	0.136	1.9704
259	12575.4	18081.2	0.1238	0.1226	30.451	10936.6	11115.5	0.1354	0.1364	1.6088
260	15379.2	17248	0.1248	0.1315	10.834	14825.1	15478.9	0.1308	0.1305	4.2239
261	13032	25431.3	0.1143	0.1261	48.756	11527.4	11775.2	0.1341	0.1295	2.1046
262	13571.1	14192.2	0.1353	0.1353	4.3763	12064	12307.9	0.1389	0.1386	1.9822
263	12145.4	20062.7	0.1312	0.1285	39.463	15316.5	15311.8	0.1248	0.1257	-0.03
264	13201.2	13314.6	0.1149	0.1146	0.8513	11978.7	12048.6	0.1357	0.137	0.5803
265	16648	17545.2	0.1266	0.122	5.1136	12658.6	16556.2	0.1274	0.1231	23.541
266	14664.6	15019.5	0.1247	0.1174	2.3629	12464.7	12754.7	0.1314	0.1284	2.274
267	11248.6	11247.5	0.113	0.1134	-0.01	13343.7	13443.3	0.1331	0.1307	0.7408
268	14153.6	16200	0.1282	0.131	12.633	12980	12892.9	0.1301	0.1338	-0.676
269	14546.3	18209.2	0.1342	0.1333	20.116	14380.7	14418.8	0.1218	0.1211	0.2641
270	13573.6	21804.1	0.1257	0.1313	37.748	13170.8	13619.4	0.132	0.131	3.2934
271	11332.1	16907.4	0.126	0.1332	32.976	11927.4	11876.5	0.1289	0.1304	-0.429
272	13682.3	22090.3	0.1344	0.1312	38.062	11055.3	11241	0.1355	0.1342	1.6519
273	11802	18324.1	0.1325	0.1399	35.593	15267.9	15474.1	0.1282	0.1291	1.3328
274	13123.7	21450.8	0.1297	0.1214	38.819	11376.4	11376.4	0.1117	0.1117	0
275	11480.1	15005.2	0.1433	0.1399	23.492	13079.9	13216.9	0.1329	0.1314	1.0371
276	13733.8	13442.2	0.1062	0.1124	-2.169	14287.5	14465	0.1284	0.1292	1.2268
277	11326.7	11330.6	0.1134	0.1136	0.0347	11652.8	12646.3	0.1456	0.1399	7.8561
278	16255.1	19314.3	0.1247	0.1295	15.839	11780.3	12434.1	0.1353	0.1348	5.2582
279	11786.2	18632.8	0.1254	0.1327	36.745	10513.5	10734.3	0.1356	0.1377	2.0565
280	11812.6	18614.8	0.1236	0.1333	36.542	13760.6	14896.6	0.1377	0.1433	7.6253
281	12652.1	15413.2	0.1427	0.1404	17.914	12386.2	12386.2	0.1131	0.1131	0
282	13942.8	21667.8	0.1289	0.1295	35.652	11057.9	11115.1	0.1359	0.1355	0.5146
283	11911.5	15513.1	0.1423	0.1267	23.217	13723.3	13849.5	0.1298	0.1335	0.9111
284	11727.2	11812.8	0.1166	0.1198	0.7243	11230.3	11752.5	0.1379	0.1338	4.4433
285	11741.7	12092	0.1283	0.1267	2.8972	12448.2	12452.3	0.1161	0.116	0.0333

286	14210.8	21578.4	0.1195	0.1319	34.143	12532.7	12586.1	0.1353	0.1368	0.4238
287	11718.5	11741.3	0.1328	0.1382	0.1942	13139.1	13237.7	0.1298	0.1291	0.745
288	11866.1	18140.1	0.1385	0.1371	34.586	13128.2	13407.2	0.1428	0.1427	2.0809
289	13360.6	20516.2	0.1232	0.1213	34.878	14915.3	15569.1	0.1315	0.1312	4.1994
290	16972.3	17261.6	0.1227	0.1208	1.6759	10635.6	10807.8	0.1411	0.1383	1.5935
291	15837.4	16758.1	0.1263	0.1217	5.4936	11638.9	11761.1	0.1384	0.1397	1.0392
292	11144.5	11425.6	0.1332	0.1389	2.4608	11738.5	11830.2	0.1378	0.1372	0.7745
293	13767.1	21639.8	0.1322	0.129	36.381	11315.8	11331.3	0.1392	0.1459	0.1366
294	13593.3	20465	0.1383	0.1277	33.578	12222.5	12222.5	0.1171	0.1171	0
295	11517.7	16339.7	0.1413	0.1302	29.511	12619.8	12603.4	0.134	0.1342	-0.13
296	11403.1	14175.2	0.1143	0.1107	19.556	10659.9	11163	0.1298	0.1306	4.507
297	13064.3	23891.1	0.1249	0.1299	45.317	13451.3	13641.5	0.1278	0.1291	1.3943
298	13283.7	23649.4	0.113	0.1298	43.831	10294.6	10594.8	0.1311	0.1295	2.8339
299	14138	16454.1	0.1226	0.1215	14.076	12970.1	13252.7	0.1272	0.1274	2.1327
300	11512	14221.6	0.1167	0.1082	19.052	12311	12406.7	0.1348	0.1321	0.771
301	15430.9	16412.8	0.1285	0.1271	5.9827	14274.5	15253.3	0.1261	0.1273	6.4171
302	14552.4	21947.6	0.1254	0.1303	33.695	11848.4	12227.6	0.137	0.1344	3.1015
303	13029.6	25197.2	0.1299	0.1327	48.29	11132.3	11482.5	0.1448	0.1421	3.0495
304	13303.7	20568.6	0.1352	0.1286	35.32	10983.4	11663.5	0.1403	0.1371	5.8311
305	15407.5	15844.7	0.1272	0.1265	2.759	11990.2	11994.3	0.1134	0.1133	0.0345
306	11847.7	11759.2	0.1182	0.1145	-0.753	10878.3	16509.1	0.1375	0.1294	34.107
307	12683.4	23231.2	0.1167	0.1334	45.404	15618.4	15531.2	0.1283	0.1313	-0.561
308	11469.3	15471.3	0.1461	0.1401	25.867	13650.4	13751.5	0.1303	0.1297	0.7348
309	12972.4	13580.5	0.1297	0.1286	4.4776	11434.1	11716.1	0.1408	0.1405	2.4066
310	13650.4	13539.9	0.1365	0.1319	-0.816	12422.2	12568.8	0.1282	0.1266	1.1664
311	14525.9	14487	0.1263	0.1194	-0.269	15415.1	16995.8	0.1264	0.1251	9.3008
312	12625.8	16999.5	0.1447	0.1402	25.729	13505.4	13613.5	0.1237	0.1273	0.7942
313	15459.1	19858	0.1291	0.1298	22.152	15124.5	16022.4	0.1278	0.1264	5.604
314	11167	11411.1	0.1404	0.141	2.1388	13520.2	13975.1	0.1339	0.1312	3.2551
315	10985.8	19175.1	0.1402	0.1408	42.708	11981.5	11994.4	0.1301	0.1326	0.1078
316	11529.3	11733.4	0.1143	0.1164	1.7398	11927.1	11970.3	0.1452	0.1453	0.3604
317	12080.3	18869.8	0.1241	0.1322	35.981	11771.4	12240.4	0.142	0.1423	3.8318
318	13501.2	13381	0.1329	0.1273	-0.898	13073.1	13111.2	0.1242	0.1234	0.2904
319	11319	16347	0.137	0.1386	30.758	11392.9	11726	0.1334	0.1355	2.8406
320	12603.9	21196.1	0.134	0.1336	40.537	15089.5	15971.3	0.1315	0.1324	5.521
321	11703.7	15168.5	0.1322	0.1342	22.842	10563.1	10601.4	0.1414	0.1395	0.3611
322	12490.1	17737.4	0.1381	0.1394	29.583	14709.1	15727.2	0.1354	0.1404	6.4737
323	16127.9	16844.4	0.1258	0.1211	4.2533	12493.5	12597.5	0.1251	0.1283	0.8253
324	13548.8	24344.6	0.1142	0.1294	44.346	11152.1	11214.4	0.1335	0.1407	0.5559
325	12272.7	12091.7	0.1321	0.1331	-1.496	14468.9	15350.7	0.1332	0.1335	5.7441
326	12713.2	13258.3	0.1138	0.114	4.1108	11931	12039.9	0.1287	0.131	0.9046
327	11934.2	16334.9	0.1315	0.1267	26.94	11129.2	11203.2	0.137	0.1376	0.661
328	13014.9	18191.9	0.1342	0.1305	28.458	13706	14393.2	0.1343	0.1339	4.7748
329	11900.3	12009.3	0.1126	0.1138	0.9076	14181.2	14852.1	0.1338	0.1347	4.5171
330	12593	19095.7	0.1361	0.1407	34.053	15805.3	13617.2	0.122	0.113	-16.07
331	12562	12856.7	0.1178	0.1123	2.2924	11864.6	11976.9	0.1279	0.1262	0.9373

332	12635	20660.6	0.1349	0.139	38.845	12421.4	12708	0.1311	0.1308	2.255
333	12746.4	19209.1	0.1368	0.1413	33.644	11106.5	11097	0.1334	0.1351	-0.086
334	12172.8	14579.3	0.1437	0.1294	16.507	14331.7	14560.2	0.1255	0.1248	1.5695
335	11554	16055	0.1283	0.1324	28.035	15098.8	15939.8	0.1398	0.1412	5.2759
336	14410.9	17080.9	0.1292	0.1303	15.631	11646.5	11935.1	0.1323	0.1336	2.4175
337	11545.4	18277.9	0.1322	0.1395	36.834	12007.7	16090	0.1345	0.1291	25.372
338	13715.3	13627.5	0.1257	0.1252	-0.644	11976.5	11976.5	0.1122	0.1123	0
339	12392.4	12657.9	0.1133	0.1157	2.0977	13443.7	13901.5	0.1316	0.129	3.2934
340	13196.4	13798.9	0.1289	0.1308	4.3664	12761	12818	0.1238	0.1252	0.4446
341	11721.3	14906.4	0.1289	0.1309	21.367	13142	13199	0.1249	0.1263	0.4317
342	13124.6	13820.9	0.1279	0.1255	5.0384	13720.8	14401	0.1343	0.134	4.7231
343	12055.8	18127	0.1252	0.1335	33.492	14047.3	14084.5	0.1154	0.1151	0.2647
344	11833.5	14839.3	0.1452	0.1422	20.256	12037.1	12099.3	0.1294	0.1308	0.5135
345	11723.9	18980.5	0.1395	0.1424	38.232	11229.8	11356	0.129	0.1335	1.1112
346	14594	19977.3	0.1286	0.1318	26.947	13408.8	13495.3	0.1282	0.1286	0.6415
347	12349.1	12169.4	0.1092	0.1155	-1.476	12267.2	12326.7	0.134	0.13	0.4827
348	12158.7	18599.1	0.124	0.1362	34.627	15060.7	16543.3	0.1267	0.1258	8.9623
349	12191.7	12724.1	0.11	0.1112	4.184	11084.8	11109.2	0.1286	0.1291	0.2192
350	13461.4	22682.5	0.1235	0.1327	40.653	10838.6	10862.3	0.136	0.1373	0.2176
351	15787.2	22157.8	0.1182	0.1296	28.751	11579.4	11875.2	0.1346	0.1371	2.491
352	14420.1	20165.3	0.1291	0.1314	28.49	13648.1	13844.4	0.1283	0.1286	1.4177
353	11328.2	12058.7	0.1332	0.1358	6.0578	12885.5	13058.7	0.1275	0.1299	1.3268
354	12397.9	19475.3	0.1366	0.1407	36.341	10450.1	10635.2	0.1449	0.1456	1.7412
355	13422.9	23407.6	0.1142	0.1331	42.656	11992.8	12061.6	0.1308	0.1338	0.5706
356	12750.9	14883.2	0.1216	0.132	14.327	13869.4	14287.2	0.1294	0.1305	2.9242
357	11360	19307.9	0.1358	0.1301	41.164	12103.5	12154.1	0.1307	0.1307	0.4165
358	14080.1	23150.9	0.1207	0.1331	39.181	11209.9	11375.6	0.1335	0.1371	1.4565
359	14192.3	16100.9	0.125	0.1307	11.854	14149	14377.3	0.1214	0.124	1.5878
360	12460.8	12459.9	0.1272	0.119	-0.007	11973.7	11977.9	0.1156	0.1155	0.0346
361	11637.6	18561.2	0.1243	0.1337	37.301	13200.9	13257.9	0.1232	0.1245	0.4298
362	14681	20137.8	0.1267	0.1319	27.097	11456.4	11538.1	0.1309	0.1309	0.7075
363	12611.5	13253.6	0.1455	0.1468	4.8446	11151.9	11378.3	0.1332	0.1343	1.9897
364	13208.9	23142.5	0.1148	0.134	42.924	13244.9	13304.1	0.1293	0.1313	0.445
365	11953.8	13831.4	0.1155	0.1058	13.575	12434.2	12484.9	0.131	0.1312	0.4055
366	14430	14434.5	0.1299	0.1289	0.0307	11796.7	11847.3	0.1319	0.132	0.4273
367	13418.9	19207.7	0.1287	0.129	30.138	15247.6	15453.9	0.1275	0.1283	1.3345
368	14187.9	21148.9	0.1195	0.1329	32.914	11987.2	12163.2	0.1461	0.1461	1.4468
369	12752	13216.3	0.1253	0.1162	3.5132	12015.4	11914.4	0.1243	0.1242	-0.847
370	11692.6	18118.4	0.1341	0.1321	35.466	13760.9	14406.8	0.1337	0.1302	4.4836
371	11747.8	19181.2	0.1248	0.1349	38.754	10933.7	11075.8	0.1327	0.138	1.2825
372	13062.8	23773.7	0.1157	0.1304	45.054	12538.9	12606.4	0.1354	0.1377	0.5353
373	12644.5	23541.4	0.116	0.132	46.288	11113.8	11156.3	0.1389	0.1354	0.3811
374	15093.3	20108.2	0.1283	0.1288	24.94	12778.7	13432.6	0.1337	0.1334	4.8674
375	16808.6	17478.8	0.1237	0.1228	3.8344	11985.4	12045.5	0.1391	0.1389	0.4991
376	12295.1	12244.6	0.1116	0.1108	-0.412	13945	14192.5	0.1128	0.1127	1.7438
377	17100.2	17821.5	0.1256	0.1305	4.0474	10725.9	11039.7	0.138	0.1361	2.8432

378	11403.1	17889.9	0.1397	0.1378	36.259	11137.8	11219.6	0.1276	0.1286	0.7294
379	14265.7	21863.2	0.1272	0.1329	34.75	13427.2	14230.8	0.138	0.1408	5.647
380	12812.9	12993.1	0.1292	0.1245	1.3866	10862	16030.4	0.1366	0.1287	32.241
381	13669.3	15515.9	0.1308	0.1319	11.901	12725.6	13040.6	0.1361	0.1374	2.4157
382	13651.6	24758.3	0.1263	0.1303	44.861	10474.1	10826.4	0.138	0.1361	3.2537
383	13993.5	20212.5	0.1318	0.1302	30.768	13325.3	13666.9	0.1272	0.1283	2.4993
384	16173	20692.2	0.1248	0.1319	21.84	13822.7	14008.6	0.1269	0.1285	1.327
385	11663.8	11823	0.133	0.1303	1.3466	11488.8	11642.3	0.1313	0.1292	1.3189
386	11754.7	15196	0.1451	0.1292	22.646	12729	13124.8	0.1413	0.142	3.0161
387	13049.2	21842.2	0.1337	0.1312	40.257	10654.6	10868.3	0.1384	0.135	1.9668
388	11817.7	18443.8	0.1296	0.1338	35.926	12551.5	12716.1	0.1299	0.1299	1.2941
389	11823.8	18461.6	0.1369	0.1402	35.954	10887.6	10906.6	0.1408	0.1377	0.1742
390	12054.7	12058.7	0.1114	0.1116	0.0326	11392.1	11392.1	0.1129	0.1129	0
391	11191.1	14762.1	0.1413	0.1286	24.19	13850.9	14167.7	0.123	0.1237	2.2356
392	12446.2	16217.2	0.1203	0.1295	23.253	11891.1	11891.1	0.1161	0.1159	0
393	12517.6	18881.5	0.1336	0.132	33.705	12106.8	12306.4	0.1292	0.1316	1.6221
394	13515.4	20844.9	0.1343	0.1269	35.162	11969.7	12029.4	0.1431	0.1424	0.4963
395	11491.2	17284.2	0.1389	0.1297	33.516	14911.7	16706.8	0.1341	0.1336	10.745
396	11454.9	11579.9	0.1343	0.1319	1.08	12779.2	12642.2	0.1295	0.1341	-1.083
397	14086.6	14122	0.133	0.1284	0.2504	11980	12225.3	0.1334	0.1333	2.0062
398	11908.2	12458	0.1442	0.1468	4.4137	11047.6	11308.8	0.1338	0.1345	2.3094
399	11793.7	17242.9	0.1252	0.1302	31.602	11509	11683	0.1347	0.1377	1.4891
400	12186.5	11961.4	0.1298	0.1299	-1.882	13063.8	13181.7	0.1299	0.1338	0.8945
401	13191.9	13714.7	0.1274	0.126	3.812	12014.1	12014.1	0.1167	0.1168	0
402	11239	11525.2	0.1321	0.1276	2.4832	11305.7	15588.8	0.1341	0.1283	27.475
403	12332.7	18446.4	0.1265	0.1355	33.143	11993	12014.5	0.143	0.1419	0.179
404	12894.9	13337.9	0.1312	0.1307	3.3215	11711.8	11829.7	0.1273	0.1313	0.9967
405	13137.6	13688.1	0.1122	0.1134	4.0214	11653	11719.5	0.1297	0.1333	0.5673
406	11667.8	16528.9	0.136	0.1274	29.409	13616.2	14468.7	0.1144	0.1148	5.8921
407	11142.2	17407.1	0.1325	0.131	35.99	11769.5	12158.1	0.1349	0.1305	3.1956
408	14038.2	21842.9	0.1219	0.1317	35.731	13776.3	13805.6	0.1293	0.1286	0.2122
409	15117.7	14797.6	0.1343	0.1301	-2.163	14901.8	15123	0.1303	0.1291	1.4625
410	14504.6	14796.9	0.1252	0.1183	1.9757	14237.4	14465.9	0.1272	0.1264	1.5798
411	13153.6	25652.9	0.1132	0.1272	48.725	15218	15984.4	0.1253	0.1243	4.7947
412	11437.1	11427.8	0.1307	0.1345	-0.081	14678.8	14708.1	0.1311	0.1305	0.1991
413	11818.9	13257.4	0.123	0.1289	10.851	11289.9	11333.1	0.1441	0.1437	0.3806
414	13123.4	12911.3	0.1309	0.1257	-1.643	13951	14204.1	0.1244	0.1287	1.7818
415	11818.8	15501.8	0.1394	0.1272	23.758	12845.5	13187	0.1224	0.1239	2.5903
416	14435.7	19681.7	0.1282	0.1323	26.654	10071.1	10687.3	0.1403	0.1398	5.7663
417	11870.4	11819.3	0.1146	0.119	-0.432	10488	10551.2	0.1404	0.1395	0.5984
418	11850.1	18884.6	0.1423	0.1432	37.25	13779.8	14722.3	0.1148	0.1165	6.4014
419	12079.6	24736.5	0.1309	0.1325	51.167	15053.7	15037.4	0.1301	0.1304	-0.109
420	10880.5	16361.9	0.1307	0.1365	33.501	11536.9	11988.4	0.1341	0.1326	3.7661
421	13541	24468.2	0.1129	0.1308	44.659	13804.9	14146.5	0.1239	0.125	2.4146
422	12470.1	14192.9	0.1469	0.1405	12.139	10976.8	13067.5	0.1416	0.1356	15.999
423	10822.3	11302.4	0.1409	0.1388	4.2472	13432.1	13710.5	0.1289	0.1297	2.0303

424	11720.1	15374.2	0.1199	0.1082	23.768	11502	11843.6	0.1255	0.127	2.8841
425	13962.4	22832.8	0.1206	0.1329	38.849	11394	11714.5	0.1362	0.1374	2.7355
426	14093.8	24106.2	0.1123	0.1322	41.535	12263.2	12959.4	0.1297	0.1279	5.3724
427	13454.9	13657	0.1224	0.1181	1.4798	13594.2	13638.5	0.1281	0.1286	0.3252
428	12846.2	13599	0.1245	0.1265	5.536	12070.5	12399	0.1371	0.1427	2.6493
429	11817.9	16178.7	0.1398	0.1282	26.954	12174.3	16003	0.1348	0.1288	23.925
430	12838.6	24199.1	0.1285	0.1313	46.946	13625.2	13838.3	0.1227	0.1244	1.5396
431	13100.9	13398.4	0.1241	0.1215	2.2203	14149.9	15246.3	0.1429	0.1374	7.1913
432	14010.2	15498.8	0.1234	0.1318	9.6048	14201.5	14252.1	0.1297	0.1297	0.3552
433	17064.5	17254.1	0.1289	0.1339	1.0988	12613	13407.1	0.141	0.1391	5.9227
434	12517.6	12400.4	0.1237	0.1245	-0.945	11436.9	11516.5	0.1369	0.1363	0.6914
435	11599.5	11367.4	0.1197	0.1116	-2.041	11756.5	11813.3	0.1306	0.1292	0.4806
436	12494.2	12217	0.125	0.1258	-2.269	12690.7	12756.5	0.1393	0.1401	0.5156
437	12685.2	18833.7	0.1302	0.1279	32.646	14618.8	15116.8	0.1408	0.144	3.2941
438	12800.9	22480.3	0.1371	0.1299	43.057	11128.5	11586.7	0.1371	0.1367	3.9548
439	12219.8	16634.9	0.1457	0.1403	26.541	11958.5	11958.5	0.1136	0.1137	0
440	12106.9	17744.2	0.1209	0.1308	31.77	10936	11156.7	0.1329	0.138	1.9786
441	11635.5	18894.8	0.1408	0.1422	38.419	12420.8	12272.2	0.1306	0.1402	-1.21
442	13171.1	18222	0.1338	0.1329	27.719	11715.8	12001.8	0.133	0.138	2.3831
443	12780.7	12809	0.1181	0.1135	0.2205	14456.1	14598	0.1249	0.1241	0.9722
444	12976.8	12963	0.115	0.1154	-0.106	11376.6	11762.2	0.1452	0.1431	3.279
445	13807	12927	0.1316	0.1251	-6.808	11021.6	11361.9	0.14	0.1358	2.9957
446	11891.9	17418.3	0.1325	0.1361	31.727	14827.6	16059.3	0.1344	0.1365	7.6694
447	12846.4	12901.2	0.1135	0.1131	0.4252	11951.7	12097.5	0.1309	0.129	1.205
448	13055.7	24059	0.1139	0.1314	45.735	14401.7	15451.9	0.1246	0.1243	6.7968
449	12877.7	12637.1	0.1121	0.1144	-1.904	12055.1	12178.3	0.1308	0.1344	1.0121
450	12547.7	20562.8	0.1352	0.1237	38.979	14147.3	14273.4	0.1299	0.1333	0.8841
451	12102.6	18319.2	0.1258	0.1345	33.935	12792.4	12854.6	0.1145	0.1151	0.484
452	12268.7	13044.3	0.1107	0.1155	5.9462	11504.3	11504.3	0.1169	0.1169	0
453	12885.7	26707.5	0.1281	0.1304	51.752	14105.1	14313.6	0.1285	0.1294	1.4566
454	12837.6	24015	0.1119	0.1295	46.543	12510.2	12550.4	0.1352	0.1375	0.3197
455	13299	22890.4	0.1231	0.1328	41.901	11838.8	11885.3	0.1471	0.1442	0.3918
456	11443.3	12816.2	0.1374	0.1443	10.712	14950	15324.7	0.1349	0.1304	2.4453
457	11874.3	14638.3	0.1461	0.1428	18.882	14970	14983.3	0.1241	0.1259	0.0891
458	11782.7	11941.4	0.1137	0.1142	1.329	11774.2	11844.1	0.136	0.1374	0.5903
459	14256.8	22252.2	0.1202	0.1312	35.931	11217.6	11648.3	0.1358	0.1363	3.6979
460	10859.1	10753.7	0.1192	0.1122	-0.98	14147.1	14909.5	0.1285	0.1273	5.1131
461	11453.5	11298.7	0.1344	0.1322	-1.371	11204.3	11315.5	0.1424	0.1416	0.9821
462	12800	19724.3	0.1227	0.1286	35.105	11898.4	16104.7	0.1348	0.1288	26.119
463	12087.3	14536.2	0.1326	0.1361	16.847	12340.5	12553.5	0.1354	0.134	1.6969
464	13011.7	19177.7	0.1168	0.1231	32.152	13932.7	14409.1	0.133	0.1293	3.3062
465	13001.1	13201.8	0.1163	0.1117	1.5203	13528.8	11977.6	0.1199	0.1192	-12.95
466	11447.6	11517.1	0.1122	0.1147	0.6034	13319.9	13602.6	0.1315	0.1319	2.0778
467	11211.1	19639	0.1392	0.1415	42.914	13143.4	13279.8	0.1225	0.1272	1.0271
468	12657.7	12743.3	0.1104	0.1131	0.6714	11760.5	11807.1	0.1416	0.1386	0.3944
469	13112.6	13551.2	0.1213	0.1128	3.2367	10768.2	11338.7	0.1415	0.1384	5.0313

470	14253.9	25922.7	0.1111	0.1248	45.014	13706	13744.1	0.1253	0.1245	0.277
471	13740.5	23797.4	0.1237	0.1326	42.261	11888.5	12023.1	0.1328	0.1307	1.1192
472	14430.2	16519.2	0.1285	0.1296	12.646	12455.6	12586.2	0.1388	0.1409	1.0372
473	14111.6	16050.5	0.128	0.1272	12.08	13755.8	13668.7	0.128	0.1318	-0.638
474	12664.2	12601.6	0.1181	0.1132	-0.497	14034.4	14093	0.1245	0.1245	0.4157
475	13357.8	13222.4	0.1366	0.1318	-1.024	15618.6	15639.1	0.13	0.1297	0.1311
476	16278.1	16608.3	0.1301	0.1279	1.9882	12143.2	12427	0.1439	0.1447	2.2834
477	14264.2	16196.3	0.1252	0.1305	11.929	13270.3	13518.3	0.1255	0.1273	1.8347
478	12992	22206.5	0.1194	0.1344	41.495	13949.1	14271.3	0.1257	0.1264	2.2578
479	12385.5	17338.6	0.1367	0.1386	28.567	11674.2	11657.8	0.1363	0.1367	-0.14
480	14422.8	14159.3	0.1361	0.1313	-1.861	10808.6	12987.3	0.1448	0.1395	16.776
481	13932.4	15529.8	0.1255	0.1346	10.286	13048.8	13612.3	0.127	0.1265	4.1403
482	12550.5	12453.8	0.1254	0.1257	-0.776	11602.8	12005.3	0.1268	0.128	3.3527
483	11535.4	11636.1	0.1143	0.1154	0.8655	11918.2	12152.9	0.1321	0.1337	1.9311
484	13379.9	13101.3	0.1133	0.117	-2.126	15075.4	15854.2	0.1411	0.1433	4.9125
485	13770.5	23064.6	0.1179	0.132	40.296	13476.4	13505.7	0.1296	0.1292	0.2169
486	11915	15863.6	0.1442	0.1422	24.891	11370.9	11431.3	0.1356	0.1347	0.5285
487	13053	24595.7	0.1294	0.1309	46.93	13198.6	13255.5	0.122	0.1234	0.4299
488	12818.6	20786.7	0.1196	0.1236	38.333	12015	12015	0.1181	0.1181	0
489	10905.4	16973.9	0.1306	0.1374	35.752	12947.5	13398.3	0.13	0.1286	3.3646
490	13029.3	13422.9	0.1176	0.1143	2.9326	14015.5	14669.3	0.1354	0.1349	4.457
491	12452	13293.1	0.1293	0.1294	6.3275	10428.6	10437.4	0.1439	0.1425	0.0842
492	12531.1	12743.7	0.1137	0.1122	1.6685	11233.8	11137.8	0.1428	0.1378	-0.863
493	14150.1	14262.1	0.1292	0.1202	0.7856	11982.8	12042.5	0.1416	0.1408	0.4958
494	16741.6	17450.4	0.1241	0.1212	4.0617	10516.9	10997.3	0.1388	0.1379	4.3688
495	12590.1	14266.5	0.1221	0.1291	11.751	12415.2	12736.1	0.1327	0.1404	2.5198
496	11612.7	15674.8	0.1375	0.1343	25.915	12586.3	12656	0.1339	0.1349	0.5508
497	12993.2	22960.7	0.1152	0.1334	43.411	12842.9	12847	0.1143	0.1142	0.0322
498	12097.4	17545.2	0.1266	0.1351	31.05	11002.9	10943.4	0.1362	0.1372	-0.544
499	13031.9	13348.9	0.1305	0.1346	2.3746	12749.9	12749.9	0.122	0.1218	0
500	13573.3	22419.5	0.1206	0.1332	39.457	12954.8	13428.9	0.1443	0.1441	3.5308
501	10697	11579.4	0.132	0.1288	7.6205	12241.3	12262.8	0.1438	0.1428	0.1754
502	15007.1	16284.1	0.1281	0.1307	7.8424	14316.3	14366.9	0.1298	0.1297	0.3524
503	12011.7	14041.3	0.117	0.1081	14.455	11769.7	11832.8	0.1424	0.1416	0.5336
504	15132.4	16181.5	0.127	0.125	6.4837	12433.7	12652.7	0.1344	0.1398	1.7308
505	13000.8	14743.2	0.1155	0.1134	11.819	13493.5	14154	0.1418	0.1438	4.6663
506	10828.4	16298.4	0.139	0.1295	33.561	12600.3	12604.9	0.1292	0.1296	0.0368
507	14009.1	21598.2	0.1217	0.1337	35.138	15846.7	16620	0.1225	0.122	4.6529
508	11461.3	15211	0.1293	0.1321	24.652	14123.4	14174	0.1297	0.1296	0.3572
509	10989.4	15896.8	0.1459	0.1411	30.87	12071.5	12071.5	0.1149	0.115	0
510	12419.8	24031.9	0.1131	0.1302	48.32	10452	10747.8	0.1359	0.1389	2.7522
511	11797.5	15332.6	0.143	0.1408	23.056	12139	12256.9	0.1298	0.1336	0.9619
512	14073.4	16627.3	0.1264	0.1301	15.36	11776.9	11924.9	0.1325	0.1304	1.241
513	12888.8	13695.2	0.1368	0.1333	5.8884	15891.8	15921.1	0.1285	0.1282	0.184
514	13133.3	22079.4	0.124	0.1356	40.518	11910.5	12068	0.1402	0.1412	1.305
515	12340.1	12185.3	0.1337	0.131	-1.271	13243.8	13361.8	0.1291	0.1328	0.8824

516	11545.6	15860	0.1475	0.1418	27.203	11411.4	11289.3	0.1364	0.1346	-1.082
517	12813.8	18822.6	0.1232	0.1289	31.923	13723.4	13780.3	0.1236	0.1249	0.4135
518	13504.8	14009.5	0.1257	0.1245	3.6022	13649.7	15276.3	0.1262	0.1249	10.648
519	11680	11640	0.1163	0.1138	-0.344	13694	13677.6	0.1309	0.1311	-0.12
520	12663.7	12292.8	0.1071	0.1113	-3.017	11637.7	11840.1	0.13	0.1317	1.71
521	13909.8	22277.2	0.1311	0.1323	37.56	11875.8	11929.9	0.1359	0.1371	0.4531
522	13138	23515.1	0.1147	0.1308	44.13	10105	10329.9	0.1384	0.1372	2.1771
523	14370.6	15654.7	0.1232	0.1331	8.2023	11843.7	11849.9	0.1316	0.1311	0.0519
524	11778.1	16168.8	0.1361	0.1363	27.156	11919.7	12003.7	0.1373	0.1449	0.6995
525	12140.1	24291.6	0.1298	0.1325	50.024	13771.5	13976.9	0.1328	0.1319	1.4692
526	13443.5	25894.2	0.1158	0.1268	48.083	11025.2	11144.4	0.133	0.1305	1.0696
527	14239	14946.8	0.1308	0.1305	4.7353	11680.7	11668.8	0.1343	0.1338	-0.102
528	15176.8	15989	0.1284	0.1245	5.0798	12521.4	12524.8	0.1338	0.1343	0.0274
529	12096.5	24217.9	0.1316	0.1309	50.051	11398.1	11445.8	0.1314	0.1314	0.4167
530	13128.5	21060.9	0.1187	0.1236	37.664	13875.7	14144	0.1312	0.1298	1.8971
531	14041.6	14629.5	0.1283	0.129	4.019	11841.9	12370.9	0.1366	0.1368	4.2767
532	15346.5	18514.9	0.1309	0.1332	17.113	11506.9	16266.9	0.1385	0.1294	29.262
533	11505.2	20181.2	0.1356	0.1367	42.991	15874.6	15974.2	0.1285	0.1255	0.6234
534	12657.9	12375.2	0.1171	0.1095	-2.284	14687.4	14985.5	0.1279	0.1252	1.9891
535	10554	14822.3	0.129	0.127	28.796	15630.9	15967.8	0.1306	0.1312	2.1094
536	12802.8	17832.9	0.1196	0.1314	28.207	13221	13249.8	0.1351	0.1341	0.2173
537	12866.3	23025.1	0.1202	0.1335	44.12	11955.8	12189.5	0.1321	0.1328	1.917
538	11953.6	15718.9	0.1268	0.1313	23.954	13167.2	13202	0.1244	0.1274	0.2633
539	12821.5	14160.1	0.1277	0.133	9.4534	10563.2	10873.2	0.1355	0.136	2.8506
540	12437.2	24448.2	0.1141	0.1268	49.129	13634.3	14265.3	0.1356	0.1375	4.4231
541	13878.6	16190.9	0.1276	0.1244	14.282	12085.4	12121.2	0.1331	0.1391	0.2947
542	12341.5	12843.7	0.1191	0.1139	3.9096	12313.7	12502.8	0.134	0.1421	1.5126
543	13294.2	21276.4	0.1262	0.1335	37.517	10465.9	12105.5	0.1403	0.1343	13.544
544	10545.4	18095.6	0.142	0.142	41.724	13450	13954.9	0.1167	0.1162	3.6178
545	12343.5	13899.9	0.1216	0.1288	11.197	11629.2	11670.6	0.1288	0.1291	0.3549
546	12879.9	20726	0.1208	0.1227	37.856	14711.1	15182.4	0.1307	0.1288	3.1042
547	13984.6	18904.9	0.1282	0.1311	26.026	12218.7	12218.7	0.1149	0.115	0
548	12412.5	16642.4	0.1308	0.1337	25.416	11551.2	11555.3	0.1134	0.1132	0.0358
549	15960.4	17483.8	0.1224	0.1244	8.7134	12437.6	12645.4	0.1316	0.1325	1.6431
550	11019.1	11134.3	0.1186	0.1212	1.0353	13153.8	13300.7	0.1161	0.1178	1.1042
551	11721	14998	0.1254	0.1314	21.85	13716.6	14359	0.1416	0.1419	4.4738
552	11540.8	11533.3	0.1113	0.1186	-0.066	14905.3	16042.7	0.1408	0.1375	7.0899
553	11706.3	14895.6	0.1287	0.1314	21.411	14757	15638.8	0.1337	0.134	5.6383
554	15815.5	16854.3	0.1255	0.1252	6.1633	13938.5	13995.5	0.1237	0.125	0.4072
555	13151.4	13759.8	0.1305	0.123	4.4213	11206.1	11465.7	0.1327	0.1346	2.2636
556	13853	13946.8	0.1292	0.1204	0.6723	13398.2	14047	0.1266	0.1249	4.6189
557	12813.3	22901.6	0.1252	0.1311	44.051	11224.7	11262.7	0.1383	0.136	0.3373
558	12317.1	12321	0.1104	0.1106	0.0319	14341.1	19416.9	0.1237	0.1215	26.141
559	11331.2	12232.4	0.1366	0.1248	7.3673	11111.5	11813.6	0.1368	0.1344	5.943
560	11984.8	12611.7	0.137	0.1254	4.971	12789.2	12895.4	0.1144	0.1158	0.8232
561	14097.6	24964.4	0.1124	0.1282	43.529	11078.6	15697.6	0.1385	0.1297	29.425

562	12854.6	13356.7	0.1121	0.116	3.7597	11239.9	11273.5	0.1351	0.1342	0.2984
563	12570.1	21888.8	0.1362	0.1286	42.573	12332.5	12336.6	0.1156	0.1157	0.0336
564	16682.6	17183.8	0.1225	0.1282	2.9163	12071.6	12150.3	0.1241	0.1265	0.6477
565	13003.6	22941.9	0.1227	0.13	43.319	10703	11564.8	0.1391	0.1382	7.4518
566	11210.3	17898.1	0.1449	0.1424	37.366	12014.2	12077.4	0.1384	0.1376	0.5228
567	14044.7	22594.5	0.1209	0.1325	37.84	12671.4	12740.3	0.1268	0.1307	0.5409
568	12610.4	21032.3	0.1276	0.1308	40.043	12116	12424.5	0.1326	0.131	2.4832
569	12490.2	13252.4	0.1114	0.1095	5.7509	11903.1	12009.2	0.1408	0.1374	0.8832
570	11148.6	10966.6	0.1323	0.1334	-1.659	14220.1	14211.3	0.1284	0.1281	-0.062
571	10957.4	15212.3	0.137	0.1362	27.97	12402.7	12537.9	0.1255	0.1258	1.0782
572	14881.4	15528.6	0.1242	0.1223	4.1675	12353.2	12369.1	0.1316	0.1324	0.1282
573	11916.4	15561.4	0.1403	0.1276	23.423	10421.1	11040.6	0.1384	0.1355	5.6109
574	12531.4	16572	0.1438	0.1394	24.382	12070	12187.9	0.1268	0.1309	0.9674
575	13548.7	15167.3	0.1213	0.1323	10.671	12283.7	12346.8	0.1365	0.1358	0.5114
576	10661.1	16365.8	0.1425	0.1295	34.857	11761.3	11902.6	0.1375	0.1356	1.1874
577	11501.9	16730.3	0.1267	0.1322	31.251	11376.1	12337.9	0.14	0.1348	7.7954
578	13124.4	13193	0.1289	0.1302	0.5205	14211.3	14466.6	0.1151	0.1147	1.7651
579	12801.2	22625.8	0.1371	0.1311	43.422	11560.4	11635	0.1439	0.1451	0.6408
580	11506.2	11739.9	0.1298	0.1337	1.9912	11469	11743.6	0.1362	0.1364	2.3383
581	11290.5	17541.7	0.141	0.1392	35.636	12291.6	12271.4	0.136	0.1347	-0.165
582	16327.6	19175.6	0.126	0.1323	14.852	11804.3	15370	0.1388	0.1295	23.199
583	11872.5	18217.5	0.1436	0.1425	34.829	11235.1	11575.2	0.1341	0.1368	2.9387
584	12080.5	14024	0.1348	0.1431	13.859	11760.1	11997.4	0.1354	0.1363	1.9781
585	12906.6	13187.5	0.1421	0.1402	2.1302	10790.4	12898.5	0.1374	0.1328	16.344
586	12052	19295.3	0.1265	0.1334	37.539	12116.7	12252.3	0.135	0.1404	1.1064
587	12572.7	16807.3	0.1363	0.1396	25.195	11766.4	11831	0.141	0.1413	0.5464
588	11946.8	27049.8	0.1197	0.1237	55.834	12176.5	12171.9	0.1421	0.1395	-0.038
589	12828.3	14071.1	0.1129	0.1121	8.8326	13237.5	13891.3	0.1356	0.1349	4.7066
590	11894.9	17559	0.1225	0.1302	32.258	11714	11899	0.1277	0.1283	1.5556
591	14243.2	16779.8	0.1315	0.1292	15.117	13476.7	13662.6	0.1273	0.1285	1.3606
592	13282.3	27800.6	0.1283	0.1264	52.223	12849	13190.6	0.1219	0.1233	2.5896
593	11745.9	14862.7	0.1441	0.1393	20.97	10614.2	10910.3	0.1448	0.1442	2.714
594	11314.6	17709.2	0.1444	0.1413	36.109	13182.5	13203	0.1277	0.1273	0.1553
595	12412.3	14145.3	0.1188	0.1281	12.251	12670.3	12674.4	0.1139	0.1137	0.0327
596	12146.3	11968.5	0.1348	0.1292	-1.485	14065.5	12806.4	0.1243	0.1199	-9.832
597	12939	24458	0.1123	0.1285	47.097	11983.4	12304.3	0.145	0.1443	2.6082
598	15517.7	19080.5	0.1254	0.1306	18.672	12315.3	12365.4	0.135	0.1419	0.4053
599	11601.4	11551.3	0.1293	0.1205	-0.434	11882.4	12650.8	0.1286	0.1285	6.0743
600	10816.4	17821.7	0.136	0.1364	39.307	13381.3	13386	0.1283	0.1286	0.0347
601	13303.6	13979.5	0.1333	0.1318	4.8346	11993.7	11987.9	0.1423	0.1424	-0.049
602	13153.5	13725.3	0.1305	0.124	4.1659	12165	12140.5	0.1293	0.1287	-0.201
603	13546.5	13369.7	0.1364	0.1317	-1.322	12075.1	12959.8	0.1379	0.1379	6.8264
604	11598.1	15141	0.1305	0.1281	23.399	11517.1	11533	0.1339	0.1348	0.1375
605	11459	16823.7	0.1305	0.1369	31.887	11458.8	11539.4	0.1321	0.1362	0.6987
606	11931	17868.6	0.1376	0.1272	33.229	12854.7	12989.9	0.1242	0.1246	1.0407
607	12588.5	23493.8	0.134	0.1319	46.418	11375.9	11469.5	0.1385	0.1383	0.8157

608	17500.9	17412	0.1235	0.1259	-0.51	11964.6	11967.1	0.1374	0.1354	0.021
609	12933.9	22258.4	0.1204	0.1332	41.892	10688.8	11034.8	0.1409	0.1391	3.1357
610	12718.1	12790.7	0.1117	0.115	0.5679	10913.2	14662	0.1409	0.1305	25.568
611	11153.8	11241.3	0.1142	0.1167	0.7783	13177.6	13312.8	0.1261	0.1261	1.0154
612	14728.3	15274	0.1209	0.125	3.5724	13223.6	13223.6	0.1161	0.1161	0
613	12298.3	19217.2	0.1348	0.1399	36.004	14041.7	14923.5	0.1335	0.1336	5.9086
614	13205.2	12208.1	0.1325	0.1284	-8.168	12771.8	13009.8	0.1335	0.1393	1.8293
615	12097.6	19804.6	0.1355	0.1403	38.916	11951.9	12542.9	0.1327	0.1328	4.7119
616	12181.1	16095.3	0.146	0.14	24.319	15199.6	15220.1	0.1288	0.1283	0.1347
617	13910.1	15848.8	0.1244	0.1329	12.233	16087.5	16917.7	0.1243	0.123	4.9071
618	11427.8	11347.4	0.1164	0.1148	-0.708	13089.4	14188.8	0.1442	0.1382	7.748
619	12952.5	13535.8	0.1342	0.1324	4.3096	15862.8	15892.1	0.1287	0.1282	0.1843
620	11961.9	19073.2	0.1283	0.1289	37.284	15097.9	15237.3	0.1297	0.1299	0.9147
621	11415.8	11531.6	0.1288	0.1268	1.004	13868.6	13938	0.13	0.1285	0.498
622	16486.4	17444	0.1246	0.1209	5.4894	13831.5	13970.9	0.1298	0.1293	0.9976
623	10746.8	11666.1	0.1369	0.1397	7.8799	12962	13274	0.1321	0.1344	2.3511
624	11880	11570	0.1097	0.1151	-2.679	12184.1	13213.6	0.1271	0.1265	7.7914
625	11646.4	15870.3	0.1447	0.1408	26.615	11986.5	12231.2	0.1357	0.1312	2.0002
626	13670.8	16197.9	0.1292	0.1302	15.601	11908.7	12323.6	0.1361	0.1411	3.3666
627	14764.5	15634.7	0.13	0.1276	5.5659	11622	11624.5	0.135	0.1333	0.0216
628	12468.6	22383.1	0.1213	0.1335	44.294	10107	10661.8	0.1433	0.1442	5.2036
629	13259.3	20072.6	0.12	0.1228	33.944	12255.1	12434.3	0.138	0.1381	1.4412
630	13491.4	14234.8	0.1283	0.1254	5.222	15796.4	15787.6	0.1294	0.1294	-0.056
631	12282.4	20641.6	0.1231	0.1238	40.497	10914.5	11138.1	0.1361	0.1367	2.0082
632	14345	18351.4	0.1316	0.1334	21.831	12618.9	12657	0.1233	0.1224	0.3008
633	15355.8	21112.2	0.1227	0.1306	27.266	14611.3	15372.6	0.1375	0.1391	4.9521
634	12644.2	19477.9	0.1333	0.1293	35.085	12156.8	12160.9	0.1125	0.1124	0.0341
635	13970.1	19662.1	0.1293	0.1225	28.949	13428.5	13432.6	0.1171	0.117	0.0308
636	12195.1	13422	0.1417	0.1466	9.141	13078.6	13194.5	0.1292	0.1307	0.8781
637	11678.8	11531.3	0.1197	0.1154	-1.279	13486.1	13442.4	0.1295	0.1322	-0.325
638	12885	24375.8	0.113	0.1287	47.14	11051.7	11021.5	0.143	0.1425	-0.274
639	11803	11639.5	0.133	0.1342	-1.405	13584	14238.1	0.1402	0.1406	4.5941
640	12611.7	12382.3	0.1085	0.1172	-1.853	12822.6	13051.2	0.1267	0.1258	1.751
641	12795.6	22515.5	0.1192	0.134	43.17	14212.9	14196.5	0.1328	0.1332	-0.115
642	13983	14633.1	0.1288	0.1282	4.4428	13361.9	13544.8	0.1273	0.1302	1.3508
643	10896	14771.9	0.1322	0.1283	26.239	12719.5	13211.9	0.1431	0.1425	3.7271
644	16839.1	17625.6	0.1244	0.1191	4.462	13904.6	13955.2	0.1297	0.1297	0.3628
645	10557.4	17412.2	0.1364	0.1307	39.368	12207.6	12305.8	0.1404	0.1387	0.7987
646	13365.7	13193.7	0.1349	0.13	-1.303	12930.2	13627.8	0.132	0.1313	5.1194
647	12405.4	13341.8	0.1113	0.115	7.0182	12725.3	13298.5	0.1462	0.1454	4.3104
648	14028.7	23729.5	0.1159	0.1342	40.881	13289.3	13384.7	0.1262	0.1245	0.7131
649	14741.7	14680.2	0.1218	0.1161	-0.419	13576.8	13552.4	0.1311	0.1306	-0.18
650	13841	24937.9	0.1239	0.1339	44.498	12721.5	13095.1	0.1299	0.1298	2.8529
651	12170.3	15621.7	0.146	0.1416	22.094	12595.3	12681	0.1332	0.1326	0.6757
652	12162.4	12273.1	0.1358	0.1369	0.9021	13356.9	13407.6	0.1298	0.1298	0.3776
653	13379.4	21546.6	0.1375	0.1299	37.905	13370.3	13739.6	0.1252	0.1252	2.6883

654	12975.9	12540.9	0.1116	0.1143	-3.469	12165.4	12222.3	0.1248	0.1263	0.4662
655	12204.3	18153.4	0.1423	0.1412	32.771	13499.8	13728.3	0.1247	0.1238	1.6646
656	12359.2	12812.6	0.1237	0.1169	3.5392	14019.7	13975.8	0.1264	0.1256	-0.314
657	16006	16596.5	0.1238	0.1214	3.558	14018.5	14206	0.1278	0.1243	1.3198
658	13642.6	20502.2	0.1313	0.1253	33.458	10708.1	10771.3	0.142	0.1411	0.5862
659	11416.4	19661.4	0.1402	0.1406	41.935	12978.2	12982.8	0.1281	0.1284	0.0358
660	14234.6	14906.1	0.1226	0.1131	4.5046	11830.8	11830.8	0.1153	0.1154	0
661	12831.5	21892.3	0.1223	0.1236	41.388	11398.4	11845.9	0.1283	0.1296	3.7782
662	12861.9	13354.1	0.1292	0.1275	3.6859	11495.8	11809.2	0.1354	0.1339	2.6537
663	11959.6	16441.4	0.1301	0.1307	27.259	12969.4	13103	0.1319	0.1318	1.019
664	12740.3	19838	0.1235	0.1225	35.778	11305.9	15618.5	0.1405	0.1336	27.612
665	13510.7	26375.3	0.1247	0.1233	48.775	13907.6	14252.2	0.1361	0.1361	2.4182
666	12452.4	12456.3	0.1114	0.1116	0.0316	11369.1	11838.8	0.1388	0.1324	3.9681
667	13380	22679.9	0.1192	0.1335	41.005	14628.3	15446.3	0.1284	0.1271	5.2957
668	13034.9	23494	0.1155	0.1315	44.518	11381.1	11713	0.1348	0.1372	2.8334
669	12060.4	12247.3	0.1147	0.1123	1.5258	11259.8	11609	0.1362	0.1322	3.0083
670	11204.1	19899.3	0.1383	0.1418	43.696	12911.3	13057.4	0.1268	0.1251	1.1186
671	12822.4	12795.6	0.1106	0.1116	-0.209	11203.9	11183.7	0.1409	0.1395	-0.181
672	12833.7	25177.5	0.1281	0.1308	49.027	13332.1	13488	0.1342	0.1319	1.1562
673	12353.6	12275.6	0.1345	0.1294	-0.635	12223.9	12223.9	0.1186	0.1186	0
674	12145.3	19114.2	0.1408	0.1401	36.459	11397.9	11706.4	0.1337	0.1321	2.6356
675	12817.4	14896.1	0.1218	0.1121	13.955	12660.1	12672	0.1289	0.1332	0.0934
676	11711.4	12125.7	0.1307	0.1336	3.4167	13460.1	13435.7	0.1322	0.1314	-0.182
677	15050	15018.1	0.1342	0.13	-0.213	12460.5	12663.8	0.1413	0.1435	1.605
678	12844.8	13719	0.1135	0.1149	6.3724	14006.4	13915.6	0.1289	0.1303	-0.652
679	14387.8	17218.3	0.1296	0.131	16.439	11655.2	11643.4	0.1303	0.1345	-0.101
680	13319.5	13182.4	0.1341	0.1295	-1.04	16363	16488.2	0.1277	0.1277	0.7595
681	13170.5	14133.4	0.1255	0.1248	6.8126	11509.2	11920	0.1268	0.1275	3.4462
682	16894.3	16999.9	0.1284	0.1338	0.6215	10889.5	10853.6	0.1364	0.1358	-0.332
683	14076.5	16381.1	0.1279	0.1318	14.068	12088.7	12228.4	0.1395	0.1388	1.1425
684	12556.6	13091.5	0.1282	0.1278	4.0855	14620.5	15546.1	0.1297	0.1301	5.954
685	12015.4	14836.1	0.1192	0.1311	19.013	11002.9	11188.1	0.1424	0.1433	1.6552
686	12945	12666.4	0.1125	0.1164	-2.199	12730.9	12788.1	0.1335	0.1332	0.4472
687	12533.3	12657.1	0.1114	0.1146	0.9785	14191	14221.9	0.1233	0.1242	0.2174
688	12608.4	15750.6	0.1186	0.1329	19.949	12763.6	13019.2	0.1398	0.1398	1.9639
689	12573.8	19271.5	0.1245	0.1336	34.754	13272.9	13329.9	0.1213	0.1227	0.4275
690	10453.4	18891.6	0.1399	0.1419	44.666	11320.6	11582.6	0.1352	0.1418	2.2617
691	11597.9	11847.4	0.1312	0.1293	2.1059	16448.8	16432.4	0.1316	0.1319	-0.1
692	13529.4	14580.7	0.1227	0.1287	7.2104	11851.1	11652.5	0.1315	0.1304	-1.704
693	13011.3	21601.6	0.1308	0.1265	39.767	11286.2	11457.2	0.1325	0.1298	1.4929
694	13741.5	20987.7	0.1259	0.1327	34.526	12134.7	12389.4	0.1334	0.1327	2.0563
695	11055.5	17485.8	0.1346	0.1312	36.774	10401.3	10622	0.1355	0.1379	2.0782
696	11656.5	18000.9	0.1276	0.1363	35.245	12536.6	12527.9	0.1306	0.1303	-0.07
697	15351.7	16274.9	0.128	0.1223	5.6729	12444.4	12507.9	0.1385	0.1391	0.5081
698	12424.2	18072.3	0.1328	0.1263	31.253	11380.8	11764.4	0.132	0.1311	3.2606
699	13162	25504.2	0.123	0.1314	48.393	13289	13264.6	0.1319	0.1312	-0.184

700	11820.4	18832.9	0.1344	0.1397	37.235	14247.5	14418.4	0.1246	0.1244	1.1854
701	11657.6	13602.8	0.121	0.1137	14.3	12830.9	13036.5	0.1348	0.1351	1.5766
702	12134.3	15044.5	0.1464	0.1422	19.344	11908.3	11933.9	0.1403	0.1395	0.2149
703	13016.9	15533.8	0.1232	0.1292	16.203	10641.1	11361.5	0.1439	0.1416	6.3412
704	12634.4	13248.3	0.1342	0.1326	4.6334	12962.7	13608.6	0.1388	0.1406	4.7457
705	12753.6	12632.4	0.1191	0.1131	-0.96	12624.5	12688.5	0.1458	0.1456	0.5039
706	12136.9	17915.7	0.1257	0.1343	32.256	13171.5	13233.7	0.1155	0.1167	0.4702
707	12901	13260.9	0.1267	0.125	2.7135	11063	11211.6	0.1335	0.1368	1.3255
708	13303.6	15366.9	0.1235	0.1289	13.427	11364	11323.8	0.137	0.1356	-0.355
709	11248.2	11289.1	0.1105	0.1125	0.3625	11177.4	11718.4	0.1405	0.1366	4.6166
710	12378.8	13781.7	0.125	0.1317	10.179	11720.2	12217.1	0.1348	0.1356	4.0675
711	12183.4	18833.6	0.1304	0.1267	35.31	12261.2	12547.7	0.1267	0.1263	2.2834
712	11316.6	20418.1	0.1328	0.1403	44.576	11411.7	11548.4	0.1407	0.1429	1.1836
713	12251.1	17917.5	0.132	0.1295	31.625	15896.4	16082.6	0.129	0.1312	1.158
714	14742.3	20286.9	0.122	0.1329	27.331	11814.3	11954	0.1392	0.1383	1.1687
715	13030.5	12864.4	0.1313	0.1257	-1.292	12446.1	12811.4	0.1404	0.1411	2.8515
716	12861.1	22939.7	0.1348	0.1266	43.935	11524.6	11825.7	0.1338	0.1337	2.5467
717	12455.7	14921.8	0.1142	0.1286	16.527	12656.3	12782.6	0.1119	0.1131	0.9885
718	12776.6	15583	0.1234	0.1303	18.009	11955.2	12012.4	0.1327	0.1325	0.4761
719	14424.6	22159.1	0.1194	0.131	34.904	15604.8	15625.3	0.1268	0.1264	0.1312
720	12633.3	21433.2	0.1352	0.1379	41.057	12249.2	12424.1	0.1313	0.1295	1.4077
721	11986.6	19546.7	0.1317	0.127	38.677	14387.9	15269.7	0.1355	0.136	5.7746
722	12991.5	14658.6	0.1199	0.114	11.373	14454.8	14492.8	0.1207	0.12	0.2627
723	11496	11345.7	0.141	0.1301	-1.325	13637.3	13694.3	0.1229	0.1242	0.4161
724	11086.5	10945.6	0.12	0.1164	-1.287	14177.9	14297.5	0.1246	0.1248	0.8364
725	11908	11534.2	0.1183	0.1119	-3.242	11893.7	12028.9	0.1255	0.1259	1.1238
726	10604.7	10669.5	0.1401	0.1396	0.6067	13124.7	13259.9	0.1257	0.126	1.0195
727	11545.4	11327.4	0.1367	0.1318	-1.925	11344	11841.4	0.1359	0.1324	4.2008
728	14614.1	16568.3	0.1281	0.1292	11.795	12272.4	12702.4	0.1314	0.131	3.3852
729	13679.3	21733.2	0.1201	0.1333	37.058	10233.5	10553.2	0.1342	0.1346	3.0298
730	12460.5	12339.7	0.1427	0.1271	-0.979	12029.2	12048.1	0.1392	0.141	0.1569
731	12722.9	14355.3	0.1478	0.1429	11.371	12947.2	13141.1	0.1341	0.1308	1.4758
732	13120.9	21816.7	0.1356	0.1302	39.859	11541.9	11604.8	0.1421	0.1414	0.5423
733	12956.3	24650.4	0.1143	0.1265	47.44	13634.2	14814.2	0.125	0.1244	7.965
734	13063.7	13897.9	0.1296	0.1294	6.0022	10474.1	10791.9	0.1389	0.1415	2.945
735	12755.6	18648.1	0.1389	0.1251	31.598	11325.2	13330.1	0.139	0.137	15.04
736	12414.7	20084.4	0.1351	0.142	38.188	16142.4	16885.4	0.1344	0.1358	4.4001
737	14170.2	16229.1	0.1269	0.1324	12.686	15500.4	15377.8	0.1244	0.1284	-0.797
738	12413.3	20868.9	0.1308	0.1226	40.518	11939.7	11984.1	0.1281	0.1281	0.3701
739	12855.8	12721.4	0.1275	0.1282	-1.057	11427.2	11465	0.1418	0.1388	0.3295
740	14049.9	13991.7	0.1251	0.1239	-0.416	11422.1	11574.6	0.1395	0.1425	1.318
741	11020.4	16166.8	0.1452	0.1433	31.833	12339	12410.5	0.1355	0.1332	0.5762
742	14947.3	14738.6	0.1351	0.1302	-1.416	11473.1	11671.9	0.1341	0.1338	1.7034
743	13350	13262.6	0.1367	0.1321	-0.659	10991.3	11098.9	0.1364	0.1374	0.9696
744	11761.8	17718.9	0.13	0.1296	33.62	12585.7	12614.6	0.1126	0.1122	0.2299
745	11304.9	18613.2	0.1326	0.1284	39.264	13983.6	14287	0.1312	0.1333	2.1238

746	13510	22972.1	0.1321	0.1312	41.19	13212	13216.1	0.1146	0.1145	0.0313
747	12172.3	19573	0.1357	0.141	37.811	15180.5	15342.2	0.124	0.1236	1.0541
748	13269.6	20979.5	0.1264	0.1329	36.749	11207.1	11171.7	0.1339	0.1371	-0.316
749	13537.8	13807.7	0.1219	0.1165	1.9548	13798.1	13924.2	0.1298	0.1334	0.9062
750	12005	14366.3	0.1408	0.1268	16.436	11385.4	11578.2	0.1292	0.1315	1.6648
751	14379.2	19321.3	0.1343	0.1224	25.579	11318.4	11327.7	0.1338	0.1353	0.082
752	12593.1	12809.9	0.1135	0.1121	1.6923	10714.4	10956.1	0.1357	0.1402	2.2065
753	12648.3	24779.8	0.1123	0.1268	48.957	12100.3	12682.6	0.1341	0.1337	4.591
754	12264.3	16953.1	0.1462	0.1424	27.658	11152	11376.9	0.1345	0.1357	1.9767
755	12582.7	18388.1	0.1258	0.1347	31.571	11863.8	11885.3	0.1436	0.1425	0.181
756	13901.9	21406.3	0.1296	0.1278	35.057	11337	15825.5	0.1371	0.1299	28.362
757	14631.9	14692.2	0.136	0.1308	0.4103	12500.1	12715.9	0.1239	0.1287	1.6972
758	12769.3	21788.4	0.138	0.134	41.394	11784	11872.4	0.1347	0.1369	0.7446
759	13155.2	17164.2	0.1327	0.1353	23.357	16202	16217.2	0.1268	0.1293	0.0942
760	10254.7	16316.3	0.1458	0.1429	37.151	13030.9	13494.5	0.1347	0.1355	3.4361
761	11552.1	17755.3	0.1355	0.1377	34.938	12389.7	12634.9	0.1363	0.1363	1.9412
762	11446.4	19750.5	0.1349	0.1377	42.045	11123	11555.8	0.1384	0.1361	3.7452
763	13301	25721.3	0.1143	0.1261	48.288	14718.1	12372.3	0.1229	0.1176	-18.96
764	12220.9	18990.3	0.1315	0.1308	35.647	14237.8	14643.2	0.1153	0.115	2.7682
765	11305.6	17213.5	0.1293	0.1331	34.321	11450.1	11872.9	0.136	0.1407	3.5607
766	11189.1	17167.2	0.1445	0.1425	34.823	11185	11321	0.1399	0.1394	1.2011
767	11156.5	11313.3	0.1335	0.1322	1.3858	12760.9	12896.1	0.1226	0.1228	1.0482
768	11924.4	12180.2	0.1445	0.1434	2.0999	14358	14835.5	0.1263	0.127	3.2185
769	11717.8	11721.7	0.1108	0.1108	0.0336	13162.1	13644.6	0.1312	0.1285	3.5363
770	14988.3	16469.6	0.1341	0.1368	8.9941	14078.5	15120	0.1277	0.1314	6.8885
771	12253.3	14763.2	0.1432	0.1393	17.001	11539.5	11717.6	0.1343	0.1374	1.52
772	12069.7	16518	0.1343	0.1343	26.93	12747.8	12752	0.1173	0.1172	0.0325
773	11840.7	18929.3	0.1356	0.141	37.448	12034.1	11978.9	0.1411	0.14	-0.46
774	15445.5	22365.1	0.1178	0.1288	30.939	11353.6	11640.5	0.1406	0.1349	2.4647
775	12637.3	16168.5	0.1251	0.1274	21.84	10938.3	10954.1	0.1325	0.1321	0.1448
776	12877.5	12810.7	0.1174	0.1125	-0.521	12089.1	12371.4	0.1259	0.1268	2.2825
777	11744.4	12698.3	0.125	0.1296	7.5118	13432.3	13351	0.1286	0.13	-0.609
778	15120.4	19431.3	0.1265	0.1309	22.185	13221.4	13396.8	0.1133	0.1145	1.3089
779	13434.2	19232.2	0.1324	0.1281	30.147	15903.3	16359.2	0.1303	0.1313	2.7869
780	12780.2	19525.4	0.1223	0.1206	34.546	12045.9	12096.5	0.1285	0.1286	0.4185
781	13405.5	13745.1	0.1309	0.1333	2.4706	11778.4	11876.2	0.1343	0.136	0.8241
782	15834.4	21212.7	0.1233	0.1299	25.354	11964	11948.2	0.1374	0.1353	-0.133
783	12486	13919.7	0.1217	0.1098	10.3	14253.1	14378.4	0.1233	0.1221	0.8718
784	16189.6	16512	0.1271	0.1268	1.9527	11285.3	11894.8	0.1362	0.1392	5.1246
785	11755.8	11654.6	0.133	0.1277	-0.868	13695	14576.8	0.1354	0.1355	6.0491
786	14753.5	21508.2	0.123	0.1305	31.405	11579.6	11607.6	0.1342	0.1362	0.2411
787	12256.2	12920.2	0.1457	0.1446	5.1393	11436.9	13716.7	0.1353	0.1348	16.621
788	13757.7	19712.5	0.1315	0.1317	30.208	12094.3	12069.9	0.1322	0.132	-0.202
789	11734	11998.8	0.1376	0.1363	2.2066	11615.9	16269	0.1346	0.1291	28.601
790	16027.4	20757.9	0.123	0.1289	22.789	14068.8	14351.5	0.1286	0.1291	1.9694
791	13123.9	20512.5	0.1192	0.1229	36.02	13804.2	13787.8	0.1321	0.1322	-0.119

792	12016.9	15443.2	0.1447	0.1421	22.187	13469.8	13445.4	0.1318	0.1311	-0.182
793	12689.9	13296.1	0.1306	0.1274	4.5594	11555.7	11943.3	0.1274	0.1281	3.2447
794	11515	18903.6	0.1252	0.135	39.086	14486.2	15140	0.1324	0.1321	4.3184
795	11626.4	12230.5	0.1312	0.1298	4.9389	13002.2	13454	0.1296	0.1325	3.3581
796	13786	20920.6	0.1286	0.1206	34.103	14016.2	14112.2	0.1289	0.1294	0.6807
797	13607.2	18743	0.1304	0.1263	27.401	11094.9	11095.4	0.1414	0.1401	0.0045
798	13158.9	20409.3	0.1247	0.1291	35.525	12187	12923.3	0.1448	0.1451	5.6977
799	12534.8	12459.3	0.1272	0.1223	-0.606	14030.2	14057.4	0.1279	0.1307	0.1931
800	12831.7	12646.7	0.1307	0.1379	-1.463	10647	10732.2	0.1351	0.1352	0.7945
801	15980.9	16133.3	0.1276	0.1322	0.9451	12108.1	12416.6	0.1331	0.1314	2.4848
802	11530.2	12214.4	0.1333	0.1233	5.6017	11379.7	11486.1	0.141	0.1429	0.9271
803	13013.6	19456.5	0.1364	0.1326	33.114	14375.7	14432.7	0.12	0.1213	0.3948
804	13183.5	24082.8	0.1273	0.1298	45.258	15391.1	15552.8	0.1212	0.1208	1.0398
805	11648.7	18569.4	0.1331	0.1395	37.269	12734.9	12739	0.1135	0.1134	0.0325
806	12309	15169.5	0.1286	0.1311	18.857	16145.4	17339.7	0.1278	0.1277	6.8877
807	11653.4	18223.1	0.1373	0.1411	36.051	14691.1	15555.2	0.128	0.1276	5.5553
808	12260.3	12447.7	0.1372	0.135	1.5055	12494.1	12500.3	0.1354	0.1341	0.0492
809	14522.5	14488.7	0.1237	0.1226	-0.234	15245.5	16981.6	0.1319	0.1324	10.224
810	13024.1	21380.9	0.1288	0.1211	39.085	12466.5	13747.7	0.1359	0.1365	9.3194
811	11663.1	11767.7	0.1326	0.1305	0.8885	12699.1	12981.8	0.1285	0.1293	2.1772
812	13370.9	13370.7	0.1136	0.1172	-0.002	13098.6	13088.8	0.1397	0.1386	-0.075
813	12238	15087.5	0.1309	0.1247	18.887	15193.7	15214.2	0.1267	0.1263	0.1348
814	12329.1	19053.1	0.1236	0.1225	35.291	11433.4	11436.8	0.1324	0.133	0.03
815	14671.9	20286.7	0.1284	0.1314	27.677	13951.3	14028.7	0.1123	0.1119	0.5523
816	13637.3	23014.4	0.1237	0.1327	40.744	12656.1	12755.7	0.132	0.1299	0.7807
817	14567.4	14164.9	0.1308	0.1257	-2.841	13142.3	13319.7	0.1316	0.1324	1.3322
818	13768.6	18150.1	0.1345	0.1323	24.14	13760.1	13950.4	0.1261	0.1291	1.3637
819	11214.1	16653.8	0.1463	0.1433	32.664	14394.8	12177.5	0.1224	0.1174	-18.21
820	12953.9	13759.1	0.1262	0.1237	5.852	11634.9	12269	0.1419	0.1369	5.1682
821	11692.3	11885.5	0.1268	0.1261	1.625	11047.4	11472.4	0.1383	0.1349	3.7046
822	11131.8	18363.9	0.1287	0.1356	39.382	12611.3	12653.1	0.1362	0.1358	0.3307
823	12059.7	15567.8	0.1343	0.1361	22.534	12101.6	12155.9	0.1336	0.1331	0.4464
824	12404	18805.7	0.1201	0.1242	34.041	10849.4	10770.2	0.1427	0.1386	-0.735
825	13604.4	21021.7	0.1317	0.13	35.284	11727.1	12056.1	0.1337	0.133	2.7282
826	12676.8	20486.6	0.1287	0.1301	38.122	12581.9	12395.6	0.136	0.1347	-1.503
827	13422.6	14265.8	0.1106	0.1127	5.9107	12027.3	12415.3	0.1352	0.1319	3.1258
828	13333.9	21915.7	0.1195	0.1328	39.158	11956.1	11983.5	0.1418	0.1411	0.2284
829	12334.2	18042.6	0.1222	0.1292	31.639	11256.5	11601.4	0.145	0.1408	2.9728
830	14046.8	18990.5	0.1318	0.1332	26.032	11788.4	11955.1	0.1433	0.1445	1.3943
831	10961.6	17757	0.1447	0.1424	38.269	11464.7	11480.8	0.1406	0.1402	0.1407
832	14588.4	14684	0.1312	0.1302	0.6508	13042.3	13927	0.1367	0.1369	6.3524
833	11856.6	11806.1	0.111	0.1102	-0.428	12368.3	12503.4	0.127	0.1272	1.0812
834	15873.8	21725.4	0.1188	0.1296	26.934	11995.7	11938.3	0.1407	0.1389	-0.481
835	13672.6	14289	0.1287	0.127	4.3135	15098.5	16103.8	0.1227	0.123	6.243
836	11757.3	20155.7	0.1309	0.1223	41.668	12614.9	12527.7	0.1273	0.1309	-0.696
837	14187.9	14426.6	0.1215	0.1167	1.6546	11502.6	11577	0.143	0.1403	0.6422

838	12415.5	17969	0.1213	0.1305	30.906	11531.8	11583.2	0.1285	0.129	0.4439
839	17055	17599.4	0.1231	0.1227	3.0935	13235.1	13517.8	0.1296	0.1302	2.0908
840	11442	15632.7	0.121	0.1244	26.808	12802.7	12859.5	0.1351	0.1351	0.4415
841	12054.2	14148.7	0.1371	0.1241	14.803	12593.9	12644.5	0.1296	0.1289	0.4004
842	15217.3	16007.1	0.1291	0.1256	4.934	11245.2	11482.1	0.1314	0.1282	2.0625
843	13071	23461.5	0.1122	0.1342	44.287	12587.1	12999.1	0.1236	0.1243	3.1694
844	11478.2	11851.9	0.1359	0.1305	3.1529	12171	12228	0.1263	0.1278	0.466
845	14391	14854.9	0.1234	0.1221	3.1231	16089.7	16119	0.1276	0.1272	0.1817
846	11756.9	18237.6	0.1312	0.1277	35.535	11642	12146.1	0.1317	0.1314	4.1502
847	13655.4	14667.4	0.1236	0.131	6.8996	13120.3	13229.2	0.1276	0.1301	0.8232
848	14655.1	18720.2	0.1285	0.1307	21.715	13546.1	13649.4	0.1279	0.132	0.7565
849	12812.3	12952.2	0.1128	0.1131	1.0802	11796.5	12036.8	0.146	0.1458	1.9966
850	14024.1	25107.7	0.1119	0.1303	44.144	13308.5	13379.7	0.1276	0.1239	0.5322
851	14005.4	13536.6	0.1166	0.1233	-3.463	13605.2	14085.9	0.1228	0.1238	3.4126
852	10769.6	14193.8	0.1379	0.136	24.125	9967.34	10312.5	0.1449	0.1436	3.3472
853	11363.7	14974.6	0.1469	0.1424	24.113	15712.9	16576.2	0.1223	0.1212	5.2081
854	14417.9	14501	0.1348	0.1335	0.5733	14517.7	14427.6	0.1269	0.1308	-0.624
855	11172.7	11043.7	0.1202	0.1137	-1.168	13500.7	13557.7	0.1243	0.1257	0.4203
856	13449.9	15107.2	0.122	0.1336	10.97	11847.7	12127.2	0.1383	0.1446	2.3047
857	12174.8	12244.5	0.1105	0.1169	0.5693	10601.1	10922.6	0.1372	0.1331	2.943
858	11420.2	15723.7	0.1306	0.1324	27.37	11995.9	12185.8	0.1279	0.1361	1.5581
859	12040.9	12179.4	0.1392	0.1407	1.1371	10728.3	11119.9	0.1367	0.1367	3.5214
860	11855	20788.9	0.1369	0.1327	42.974	14617.6	14975.9	0.1282	0.1306	2.3924
861	13678.3	14234.9	0.1308	0.1317	3.9099	10773.9	11132.1	0.1325	0.1307	3.218
862	13200.2	22420.5	0.1192	0.133	41.124	12918.2	16474.1	0.1293	0.1249	21.585
863	12741.2	23770.8	0.1247	0.1291	46.4	14172.9	14428.1	0.132	0.1327	1.7684
864	11655.2	14426.5	0.1293	0.1316	19.21	12194.4	12198.8	0.132	0.1305	0.0357
865	12293.6	12513.9	0.1347	0.1384	1.7607	14033.6	14477.8	0.1307	0.1319	3.0681
866	12042.1	15936.7	0.1469	0.1417	24.438	13688.1	14787.7	0.1272	0.1318	7.4355
867	10962.4	17232.9	0.1293	0.1364	36.387	12433.5	12433.5	0.1137	0.1137	0
868	12898	13253	0.1132	0.1119	2.6788	12235.5	12456.8	0.1386	0.1357	1.7768
869	14385.8	20684.2	0.1277	0.1321	30.45	11233.9	11330.2	0.1449	0.1418	0.8497
870	11625.8	11879.1	0.1296	0.134	2.132	11590.8	11984	0.1331	0.1325	3.2818
871	11157.1	18677.2	0.1376	0.1399	40.263	10852.7	10951.5	0.144	0.1424	0.902
872	13413	24483	0.1303	0.132	45.215	13252.7	13410.6	0.1239	0.1286	1.1768
873	11999.7	18223.9	0.1232	0.1283	34.154	11723	11735.5	0.1379	0.1366	0.1066
874	12404.8	19482.5	0.1252	0.1359	36.328	12651.5	12974.6	0.1333	0.1331	2.4896
875	11781.3	15242.5	0.1463	0.1432	22.707	11264.9	11225.4	0.1308	0.1337	-0.352
876	13405.2	13979.1	0.1326	0.1324	4.1051	12127.9	12346.9	0.1311	0.1288	1.774
877	14734.4	20712.8	0.1203	0.1329	28.863	11012.8	11011	0.1358	0.1356	-0.016
878	11424.9	11416.3	0.1328	0.1362	-0.075	11006.5	11033.9	0.1435	0.1424	0.248
879	13336.8	15964.9	0.1389	0.1393	16.461	14537.8	15566.7	0.1275	0.1305	6.6097
880	12758.4	15048.4	0.1416	0.1384	15.218	13226.9	13350.1	0.1372	0.1382	0.9233
881	16097.3	17295.4	0.1272	0.1202	6.9273	13601.3	13651.9	0.1302	0.13	0.3708
882	12341.2	12407.6	0.1203	0.1151	0.5346	11199.7	11471.8	0.1346	0.1381	2.3725
883	12805.1	19317.8	0.1206	0.1235	33.714	12109.5	12161.2	0.1305	0.1305	0.4253

884	14336.2	15977.9	0.1325	0.1312	10.275	11949.6	12171.9	0.1313	0.1327	1.826
885	16172.3	16494.7	0.1256	0.1253	1.9547	12956.4	12973	0.1125	0.1124	0.1277
886	12065.8	12546.2	0.1315	0.1258	3.8288	10905.3	11074	0.1429	0.1429	1.5234
887	14720.2	16468.1	0.1254	0.1301	10.614	12590.6	12924.8	0.1317	0.1407	2.5859
888	12320.8	18662.7	0.127	0.1366	33.982	12133.2	12316.1	0.1459	0.1443	1.4846
889	15024.7	17342.2	0.1256	0.1287	13.363	11821.4	11912.7	0.1353	0.1371	0.7667
890	13615.7	23015.9	0.1273	0.1341	40.843	11805.6	11910	0.1334	0.1388	0.8765
891	11862.5	18539.7	0.1435	0.1416	36.015	12079	12221.6	0.1472	0.1462	1.1671
892	12014.4	13386.3	0.1212	0.1317	10.249	10521.2	10798	0.1438	0.1416	2.5636
893	11829.8	20065.3	0.1345	0.1362	41.044	11047.9	11251.6	0.1283	0.1273	1.8102
894	11627.5	12029.6	0.1314	0.1335	3.3431	13830	13859.3	0.1316	0.1311	0.2113
895	14466.7	14698	0.1226	0.1145	1.5733	12247.3	16133.8	0.1381	0.1304	24.089
896	13824.9	14232.2	0.1297	0.1337	2.8617	13593	14290.7	0.1319	0.1312	4.8819
897	13157.2	23926.4	0.1142	0.1297	45.01	11456.1	11688.1	0.1357	0.1369	1.9846
898	12283.2	15948.1	0.1381	0.1261	22.98	11542.7	11784.5	0.1272	0.1331	2.0525
899	12822.1	13416.7	0.1456	0.1471	4.4317	16872.1	16901.3	0.1283	0.1277	0.1733
900	12650.9	14409.4	0.1248	0.1252	12.203	12714.9	12597.5	0.131	0.1412	-0.932
901	11446.6	11379.8	0.1197	0.1142	-0.587	16213.5	16242.8	0.1287	0.1281	0.1803
902	12761.8	13873.1	0.1336	0.1323	8.0107	11700.4	11807.7	0.1469	0.1439	0.9086
903	13024.9	14348.2	0.1162	0.1121	9.2231	10980.4	11079.7	0.135	0.1357	0.8954
904	12470.4	12508	0.1119	0.1124	0.3004	13733.6	13935.6	0.131	0.1319	1.4502
905	12548.3	22102.6	0.1298	0.136	43.227	16177.6	16277.2	0.1297	0.1281	0.6118
906	11664	16522.8	0.1444	0.142	29.407	12193.9	12193.9	0.1172	0.1173	0
907	12873.5	21559.7	0.1354	0.1301	40.289	12827	13480.8	0.1354	0.1345	4.8499
908	16329.9	17165.7	0.1238	0.1234	4.8693	13807.9	14461.7	0.1337	0.1332	4.521
909	16978.7	20924.5	0.1245	0.1282	18.857	11895	11978.1	0.1344	0.1366	0.6934
910	13897.5	24419.4	0.1255	0.1336	43.088	11471.6	11605.8	0.1442	0.1452	1.1569
911	15016.6	16353	0.123	0.1317	8.1721	12280.6	12934.4	0.1357	0.1351	5.0548
912	16658	17213.1	0.1249	0.1342	3.2248	14882.3	15802.1	0.1364	0.1363	5.821
913	16575.9	16898.3	0.1245	0.1243	1.908	13036.4	13061	0.1263	0.1291	0.188
914	10587.3	10710.5	0.1243	0.1166	1.1505	12034.9	12312.7	0.1325	0.1293	2.2563
915	13014.7	13497.6	0.1278	0.1275	3.5779	11344.7	11570.8	0.1345	0.1339	1.9541
916	12760.8	15880.6	0.1198	0.1306	19.646	11747.9	12125.3	0.1376	0.1455	3.1122
917	11771	11596.4	0.119	0.1167	-1.505	11325.8	11521.7	0.1347	0.1358	1.7002
918	13450.1	23223.8	0.1202	0.1323	42.085	10912.6	10917.3	0.1405	0.1396	0.0433
919	12934.3	21102.6	0.1321	0.1226	38.707	11691	11976.9	0.136	0.1358	2.3863
920	13717.7	22719.1	0.1235	0.133	39.62	11186.8	11190.3	0.1323	0.1328	0.0307
921	11308.5	18434.1	0.1384	0.1421	38.655	11897.6	12738.3	0.131	0.1281	6.6001
922	11765.1	13429.9	0.1161	0.1116	12.397	10823.9	16271.5	0.1382	0.1294	33.479
923	14231.2	13952.4	0.1186	0.1224	-1.998	13922.7	13979.7	0.1237	0.125	0.4076
924	11947.1	23960.1	0.1331	0.1315	50.137	14424.2	15351.9	0.131	0.1305	6.0434
925	14154.8	13933.2	0.1252	0.1248	-1.591	12095.2	12152.2	0.1231	0.1246	0.4689
926	12470.1	12201.6	0.1174	0.1163	-2.2	13216.4	13220.5	0.1143	0.1142	0.0313
927	11905.2	18188.3	0.1303	0.1366	34.545	13210	14371.6	0.1417	0.1365	8.0823
928	12137	14250.7	0.1179	0.1074	14.832	11935.8	12050.8	0.1287	0.1321	0.9541
929	12807.7	13189.7	0.1262	0.1263	2.8956	11888	11577.2	0.138	0.1422	-2.685

930	14761.8	16139.7	0.1222	0.1307	8.5375	12273.2	12565	0.1448	0.1448	2.3226
931	10845.7	15601.5	0.1304	0.1247	30.483	12286.7	12487.5	0.1318	0.1307	1.6083
932	11197.9	16641.5	0.1336	0.1363	32.711	11192.3	15438	0.1358	0.1298	27.502
933	13558.6	19744.4	0.1221	0.1217	31.329	13086.9	13289.3	0.1291	0.1307	1.5235
934	11285.9	18642.6	0.1355	0.1363	39.462	11021	11530.1	0.1358	0.1369	4.4151
935	11917.8	18376.1	0.1323	0.1283	35.145	12107.2	12075.3	0.1287	0.1305	-0.264
936	12909.7	12740.7	0.1143	0.1111	-1.326	12331.4	12593.2	0.1351	0.1352	2.0792
937	12830.5	15769.1	0.1202	0.1062	18.635	14332.7	14580.7	0.1271	0.1286	1.7011
938	13467.7	27347.9	0.1277	0.124	50.754	12187.7	12188.2	0.135	0.1321	0.0041
939	14089.4	24764.5	0.1126	0.1291	43.106	10869.8	11236.2	0.1249	0.1256	3.2612
940	11788	15423.8	0.1296	0.1229	23.573	12593.2	12744.6	0.1399	0.1349	1.1881
941	12362.5	16667.2	0.1446	0.1402	25.828	13426.2	13513.1	0.1144	0.1138	0.6437
942	11855.4	19527.5	0.1356	0.1392	39.289	10600.2	10663.4	0.142	0.1412	0.5921
943	11107.8	14298.6	0.1352	0.1357	22.316	11808.3	16177.4	0.1331	0.1273	27.007
944	13357.6	24018.5	0.1146	0.1302	44.386	14634.6	15386.1	0.1334	0.1327	4.8843
945	12937.7	22926.3	0.1182	0.1322	43.568	11774.7	11914.4	0.1474	0.1465	1.1726
946	12045.7	17510.3	0.1374	0.127	31.208	14573.6	15498.1	0.1283	0.1275	5.9656
947	13872.4	19568	0.1268	0.1272	29.107	11792.8	11846.2	0.1357	0.1361	0.4503
948	12386.7	18439	0.1225	0.1228	32.823	11466.7	11532.9	0.1293	0.1308	0.5747
949	14269.7	20547.9	0.1222	0.1333	30.554	12216.6	12484.6	0.1449	0.1458	2.1466
950	12901.6	12834.8	0.1172	0.1123	-0.52	15122.5	15464.1	0.1255	0.1264	2.2089
951	14810.7	16493	0.1249	0.1263	10.2	15358.3	15271.2	0.1256	0.1288	-0.571
952	12443.1	12216.6	0.1288	0.1248	-1.854	13561.3	13682.5	0.1217	0.1211	0.8859
953	14018.1	21487.3	0.1256	0.1329	34.761	12731.7	12739	0.1389	0.1387	0.0571
954	14646.5	14439	0.136	0.1316	-1.436	11323.2	11529	0.1366	0.1436	1.7848
955	11214.7	17010.2	0.1427	0.1428	34.07	12444.9	12399.7	0.1309	0.1271	-0.364
956	11468.1	11588	0.1142	0.1149	1.0348	13608	13695.8	0.1276	0.128	0.6409
957	11901.1	19027.1	0.1326	0.1352	37.452	12739.5	12862.8	0.128	0.1317	0.9583
958	12074.7	15290.9	0.139	0.1265	21.033	11706.8	12302.5	0.1367	0.1328	4.8423
959	14379.3	15804.7	0.1323	0.1305	9.0188	13328	13511	0.1292	0.1278	1.3542
960	12696.7	12399	0.1098	0.1168	-2.401	11001.4	12157.3	0.1433	0.1366	9.5084
961	13708.7	20136.9	0.1227	0.1224	31.923	11673.9	11677.3	0.1332	0.1337	0.0294
962	12787.5	12791.4	0.1102	0.1105	0.0308	10489.5	10536.1	0.1459	0.1428	0.442
963	12292.6	16856.7	0.1352	0.1383	27.076	12381	12381	0.1161	0.1161	0
964	12664.7	19103.9	0.138	0.1312	33.706	11444.8	11209.2	0.1242	0.1301	-2.102
965	13241.2	14390.6	0.1231	0.1234	7.9867	14491	14956.1	0.1324	0.1295	3.1093
966	12057.8	18759.6	0.128	0.1348	35.724	13053.7	12963.6	0.1323	0.1359	-0.695
967	12055.3	14473	0.1432	0.14	16.705	13090.1	13094.2	0.1174	0.1174	0.0316
968	11906.7	24915.2	0.1344	0.1322	52.211	12409	12111.2	0.1301	0.127	-2.458
969	11426.5	19597	0.1409	0.1409	41.693	10905.3	11516.7	0.142	0.1408	5.3093
970	13748.9	13733.6	0.1368	0.1318	-0.112	11625.8	11535.1	0.1403	0.1341	-0.786
971	11050.7	17448.7	0.1447	0.1431	36.667	11545.5	11740.2	0.1349	0.1345	1.6582
972	13263.1	18971	0.1385	0.1258	30.088	12198.5	12283.1	0.1375	0.1379	0.6891
973	14581.9	23692.4	0.1211	0.1338	38.453	13408	13635.4	0.1285	0.1285	1.6671
974	12243.3	22460.7	0.1375	0.1288	45.49	13944.1	13994.7	0.1299	0.1299	0.3617
975	12042.9	12012.8	0.1315	0.1284	-0.25	12671.8	12655.4	0.1344	0.1347	-0.129

976	13653.8	21566.4	0.1328	0.1311	36.69	10557.7	10817.4	0.1367	0.1402	2.4011
977	14945.6	16210.6	0.1286	0.1323	7.8032	10857.5	10857.1	0.1358	0.1355	-0.004
978	12874.9	13441.7	0.1349	0.1334	4.2166	11983.6	12280.9	0.1336	0.1327	2.421
979	13336.7	13496.4	0.1231	0.1195	1.1833	11423.9	11928	0.1419	0.1375	4.2264
980	13824.9	23152.6	0.1195	0.1317	40.288	13517.1	13946.9	0.1257	0.1273	3.0815
981	13129.7	27024.6	0.1288	0.1298	51.416	11736.3	12000.8	0.1411	0.1353	2.2038
982	16303.5	20795	0.1241	0.1285	21.599	12269.8	12330.7	0.1322	0.1331	0.494
983	13141.6	14833.2	0.1399	0.1368	11.404	11103.4	11107.6	0.1405	0.139	0.0381
984	12261.2	17960.6	0.1245	0.1326	31.733	13963.3	14742.2	0.1418	0.1439	5.2831
985	11653	20128.9	0.1398	0.1419	42.108	12023.2	12027.5	0.1352	0.134	0.0352
986	13553.4	23538.8	0.1168	0.1343	42.421	11211.2	11180	0.1372	0.135	-0.279
987	12204.7	12369	0.1139	0.113	1.328	13722.2	13970.3	0.1255	0.1269	1.7754
988	13572.8	13036.7	0.1365	0.1341	-4.112	12747.8	12828.9	0.1238	0.1258	0.6324
989	11736.7	11945.2	0.1132	0.1121	1.7454	14997.4	15026.7	0.1257	0.125	0.1949
990	12955	13262.4	0.1252	0.1221	2.3176	11339.9	11525.5	0.1307	0.1349	1.6103
991	11524	11624.7	0.1158	0.1165	0.8663	13720.6	13815	0.1276	0.1272	0.6838
992	12195.1	13892.6	0.1345	0.1431	12.219	13037.9	13919.7	0.1317	0.132	6.3347
993	13846	21022.8	0.1237	0.125	34.138	14020.7	17640.2	0.1269	0.1227	20.519
994	12715.7	12556.2	0.135	0.1296	-1.27	12714.7	12698.4	0.1346	0.1346	-0.129
995	10619.9	10876.2	0.1189	0.1175	2.3563	13259	13234.5	0.13	0.1295	-0.185
996	13465.7	12946.3	0.1131	0.1178	-4.012	12441.6	12668.7	0.1342	0.1392	1.792
997	12953.5	13487.5	0.1477	0.1473	3.959	12176.6	12233.6	0.1253	0.1268	0.4658
998	13110.9	22311.4	0.1373	0.1291	41.237	12437.8	12616.7	0.1275	0.1261	1.4174
999	14082	24916.6	0.1131	0.128	43.483	13426.1	14319.6	0.1358	0.1358	6.2396
1000	12875.5	23492.3	0.1146	0.1305	45.193	15292.2	16032.2	0.1349	0.1366	4.616
49	13614.71	13872.78	0.102	0.105	1.8603	11441.61	11452.65	0.105	0.114	0.0964
50	12624.46	13221.57	0.103	0.108	4.5162	12386.62	12952.51	0.068	0.072	4.369
51	12590.48	12783.62	0.103	0.104	1.5108	14842.19	15272.06	0.093	0.103	2.8147
52	12562.87	12932.19	0.103	0.11	2.8559	9929.087	10043.14	0.127	0.122	1.1357
53	12922.58	13065.42	0.103	0.102	1.0933	10043.61	10055.33	0.134	0.13	0.1165
54	13136.4	13143.76	0.104	0.103	0.056	10931.71	11489.58	0.13	0.127	4.8554
55	13700.1	13815.87	0.104	0.104	0.838	13713.56	14610.66	0.114	0.11	6.1401
56	13038.35	12852.99	0.105	0.105	-1.4421	15820.13	15976.24	0.102	0.111	0.9771
57	12607.04	12901.93	0.105	0.11	2.2856	12491.85	13573.05	0.094	0.081	7.9658
58	14145.07	14098.5	0.105	0.105	-0.3303	11882.42	11958.48	0.093	0.094	0.6361
59	13049.29	13329.83	0.105	0.112	2.1046	13755.5	13447.13	0.065	0.067	-2.2932
60	12512.18	13623.14	0.105	0.104	8.1549	12691.14	12662.36	0.095	0.092	-0.2273
61	12118.96	12420	0.105	0.112	2.4238	15478.24	15871.11	0.094	0.101	2.4754
62	12659.92	12571.63	0.105	0.106	-0.7022	12178.46	12155.74	0.086	0.087	-0.1869
63	13015.98	12927.7	0.105	0.106	-0.6829	13042.72	13423.89	0.105	0.118	2.8394
64	12283.94	12234.23	0.106	0.108	-0.4063	12193.73	12139.29	0.091	0.092	-0.4484
65	11922.71	12232.04	0.106	0.113	2.5288	12112.07	12186.72	0.129	0.127	0.6125
66	13542.49	13524.71	0.106	0.107	-0.1315	12641.5	12739.4	0.117	0.122	0.7685
67	14183.77	14688.21	0.106	0.105	3.4343	14111.9	14277.13	0.085	0.093	1.1573
68	13423.17	13492.26	0.106	0.104	0.512	15705.13	16128.9	0.101	0.11	2.6273
69	12726.95	12884.65	0.106	0.103	1.2239	12975.24	13828.11	0.067	0.073	6.1677

70	13624.83	13954.45	0.106	0.112	2.3621	13229.62	13166.9	0.09	0.091	-0.4764
71	12596.92	12963.85	0.106	0.109	2.8304	12599.44	12576.72	0.092	0.093	-0.1807
72	13096.42	12947.72	0.107	0.108	-1.1485	10295.28	11034.44	0.128	0.128	6.6987
73	13718.49	13872.55	0.107	0.104	1.1105	12913.46	13015.5	0.11	0.115	0.784
74	13347.25	14102.26	0.107	0.109	5.3538	16838.76	17007.13	0.105	0.112	0.99
75	13535.15	13772.05	0.107	0.102	1.7201	12981.34	13999.2	0.077	0.095	7.2709
76	13322.04	13719.06	0.107	0.11	2.8939	11825.94	11904.72	0.08	0.084	0.6618
77	13636.63	13569.98	0.107	0.106	-0.4912	11209.34	11571.09	0.111	0.115	3.1263
78	12343.21	12802.16	0.107	0.11	3.5849	11749.05	11686.33	0.093	0.093	-0.5367
79	12884.08	13684.41	0.107	0.107	5.8485	13183.14	13120.42	0.092	0.092	-0.478
80	12039.64	12846.36	0.107	0.114	6.2798	15297.82	15672.29	0.1	0.106	2.3894
81	12927.93	13302.87	0.107	0.099	2.8185	11230.62	11207.9	0.092	0.093	-0.2027
82	12985.18	12987.4	0.107	0.107	0.0171	13802.22	13904.27	0.111	0.116	0.7339
83	11947.18	12248.23	0.107	0.114	2.4578	13036.77	13138.81	0.118	0.123	0.7767
84	12894.88	12884.5	0.107	0.103	-0.0806	13049.56	13282.58	0.077	0.087	1.7543
85	13305.8	13300.44	0.107	0.108	-0.0403	13079.38	13287.07	0.109	0.116	1.5631
86	12938.64	13816.34	0.107	0.106	6.3526	11428.53	11439.58	0.107	0.116	0.0965
87	13642.25	14097.88	0.108	0.109	3.2319	10648.29	10964.01	0.124	0.127	2.8796
88	12786.27	13935.12	0.108	0.111	8.2443	10797.97	10810.4	0.12	0.118	0.1149
89	14015.27	14186.1	0.108	0.104	1.2042	16898.72	17097.51	0.111	0.111	1.1627
90	13392.76	13577.91	0.108	0.109	1.3636	14601.26	15037.41	0.115	0.117	2.9004
91	13300.27	13237.76	0.108	0.107	-0.4722	13922.8	14857.12	0.118	0.113	6.2887
92	12684.83	12697.84	0.108	0.106	0.1025	17281.57	16714.08	0.109	0.11	-3.3953
93	13603.14	14008.62	0.108	0.114	2.8945	12274.52	12223.02	0.09	0.091	-0.4214
94	13416.69	13337.44	0.108	0.103	-0.5942	12958.73	13060.77	0.117	0.122	0.7813
95	13293.97	13267.91	0.108	0.108	-0.1965	12431.56	13579.92	0.076	0.083	8.4563
96	12537.98	12813.58	0.108	0.114	2.1508	12169.82	12267.6	0.078	0.078	0.7971
97	13145.57	13557.61	0.108	0.105	3.0392	11520.73	11902.39	0.097	0.106	3.2066
98	13869.77	13969.68	0.108	0.106	0.7152	12893.49	13056.51	0.086	0.095	1.2485
99	13224.46	14101.61	0.109	0.111	6.2202	16307.29	16172.85	0.104	0.107	-0.8312
100	13721.1	14744.87	0.109	0.108	6.9432	11681	11859.99	0.076	0.081	1.5092
101	13902.11	14517.55	0.109	0.105	4.2393	11969.32	11932.33	0.09	0.095	-0.31
102	12626.3	12887.84	0.109	0.108	2.0294	14106.03	14027.66	0.097	0.103	-0.5587
103	14042.34	13914.3	0.109	0.105	-0.9202	14096.55	14025.54	0.09	0.089	-0.5063
104	13840.18	13834.12	0.109	0.109	-0.0438	15704.72	15511.29	0.103	0.108	-1.247
105	13711.84	13694.06	0.109	0.109	-0.1299	15866.29	15319.63	0.082	0.084	-3.5683
106	12483.67	12967.01	0.109	0.116	3.7275	13427.17	13797.46	0.113	0.116	2.6838
107	14252.76	14552.59	0.109	0.106	2.0603	13168.79	13270.83	0.117	0.122	0.7689
108	13146.4	13045.77	0.109	0.11	-0.7713	12154.05	12140.11	0.115	0.119	-0.1148
109	13044.83	13080.06	0.109	0.106	0.2694	14403.17	14393.38	0.106	0.109	-0.068
110	13445.25	13551.9	0.109	0.107	0.787	15534.51	15528.27	0.104	0.109	-0.0402
111	12827.75	13141.21	0.109	0.116	2.3854	11984.39	11943.64	0.12	0.121	-0.3412
112	13404.39	13514.68	0.109	0.11	0.8161	14126.28	14138.91	0.106	0.109	0.0894
113	14148.03	14768.03	0.109	0.106	4.1983	12086.71	12118.63	0.088	0.086	0.2634
114	13299.39	13337.26	0.11	0.104	0.2839	10592.8	10881.55	0.117	0.115	2.6536
115	13018.41	13026.48	0.11	0.11	0.062	14469.53	13379.95	0.081	0.086	-8.1434

116	13778.8	14287.79	0.11	0.112	3.5624	10777.48	11457.82	0.11	0.109	5.9378
117	12948.58	13437.78	0.11	0.117	3.6405	11618.42	11650.85	0.087	0.087	0.2783
118	14433.03	15355.58	0.111	0.108	6.0079	14448.16	14145.58	0.117	0.114	-2.1391
119	14381.7	15626.05	0.111	0.109	7.9633	12776.15	13143.43	0.122	0.126	2.7944
120	13210.36	14742.82	0.111	0.115	10.395	18069.56	18284.91	0.11	0.11	1.1778
121	14154.07	13671.28	0.115	0.099	-3.5314	12428.9	12603.67	0.072	0.082	1.3866
122	13845.12	13452.99	0.115	0.101	-2.9148	14181.89	14719.63	0.118	0.113	3.6533
123	12980.87	13075.31	0.116	0.114	0.7223	11068.5	11234.18	0.113	0.112	1.4748
124	14249.22	13593.7	0.116	0.101	-4.8222	12282.39	12341.6	0.084	0.086	0.4797
125	13323.32	12667.81	0.117	0.1	-5.1746	13330.27	13454.33	0.077	0.075	0.9221
126	15514.46	15752.54	0.118	0.117	1.5114	14482.61	14860.93	0.108	0.111	2.5457
127	12941.9	12577.6	0.118	0.102	-2.8964	13742.55	13728.62	0.108	0.112	-0.1015
128	15361.64	14121.69	0.118	0.099	-8.7805	11496.83	11943.78	0.128	0.123	3.7421
129	13046.55	12653.96	0.118	0.103	-3.1025	13964.27	13912.76	0.086	0.086	-0.3702
130	16642.15	16892.66	0.118	0.118	1.4829	10043.25	10303.71	0.127	0.125	2.5278
131	17766.77	18066.98	0.119	0.117	1.6616	13477.33	14088.5	0.117	0.112	4.3381
132	14450.07	14494.8	0.119	0.119	0.3086	9902.91	10383.79	0.13	0.121	4.6311
133	13455.98	13116.66	0.119	0.103	-2.587	10968.06	11070.1	0.102	0.109	0.9218
134	14649.55	14900.05	0.119	0.119	1.6812	11405.49	11466.79	0.069	0.082	0.5346
135	13549.79	13718.7	0.119	0.122	1.2312	12360.29	12270.7	0.103	0.111	-0.7301
136	16041.53	16292.03	0.119	0.119	1.5376	10845.31	11097.15	0.078	0.089	2.2694
137	12858.23	12553.46	0.119	0.103	-2.4278	14141.48	13958.05	0.108	0.113	-1.3142
138	13502.51	14575.87	0.12	0.124	7.364	12501.41	12904.08	0.105	0.109	3.1205
139	14155.83	14230.43	0.12	0.111	0.5242	13673.11	14029.8	0.103	0.107	2.5424
140	17008.87	17263.72	0.12	0.119	1.4762	14191.04	14128.32	0.09	0.09	-0.4439
141	13467.7	13785.18	0.12	0.122	2.3031	13202.64	13414.94	0.084	0.092	1.5826
142	15522.54	15801.82	0.12	0.119	1.7674	11026.16	11337.32	0.124	0.122	2.7446
143	16782.66	17082.87	0.12	0.119	1.7574	11960.95	11992.16	0.084	0.084	0.2603
144	14192.78	15270.55	0.12	0.116	7.0578	11559.63	11665.81	0.103	0.109	0.9102
145	16266.89	16517.39	0.12	0.12	1.5166	11422.59	11433.63	0.11	0.119	0.0966
146	14301.58	14540.37	0.12	0.119	1.6422	12397.25	13309.38	0.079	0.086	6.8533
147	14352.14	14590.93	0.12	0.12	1.6365	16219.66	16185.55	0.105	0.109	-0.2107
148	15963.52	16456.03	0.12	0.121	2.9929	12846.66	12850.38	0.091	0.096	0.029
149	12480.36	12211.24	0.12	0.104	-2.2038	12530.17	12632.22	0.111	0.116	0.8078
150	14579.69	14784.84	0.12	0.12	1.3876	15319.06	15717.29	0.101	0.108	2.5337
151	13947.44	14152.59	0.12	0.12	1.4495	13249.04	13635.07	0.127	0.123	2.8312
152	13077.84	12738.52	0.12	0.103	-2.6638	12519.67	12512.6	0.084	0.084	-0.0565
153	14088.62	15495.05	0.121	0.121	9.0767	12925.24	13027.28	0.11	0.115	0.7833
154	14049.62	14862.92	0.121	0.11	5.472	14441.21	14839.45	0.101	0.108	2.6836
155	15878.75	16145.11	0.121	0.12	1.6498	11825.88	11837.9	0.089	0.095	0.1015
156	12774.5	13071.99	0.121	0.123	2.2758	12482.39	12455.53	0.087	0.088	-0.2157
157	12971.47	13960.9	0.121	0.125	7.0871	11876.98	11979.02	0.115	0.121	0.8519
158	17052.62	17220.11	0.121	0.12	0.9726	10261.37	10272.41	0.104	0.114	0.1075
159	16188.95	16563.75	0.121	0.119	2.2628	10911.7	11504.12	0.106	0.113	5.1497
160	14322.88	14400.66	0.121	0.12	0.5401	11105.43	11078.57	0.09	0.09	-0.2425
161	15214.99	15459.04	0.121	0.12	1.5787	9947.372	10022.64	0.127	0.125	0.751

162	15275.99	15526.49	0.121	0.12	1.6134	15201.35	14908.12	0.081	0.085	-1.9669
163	16442.89	16743.1	0.121	0.119	1.793	12438.1	12776.98	0.123	0.118	2.6522
164	12242.37	12184.55	0.121	0.103	-0.4745	11697.7	11931.38	0.109	0.108	1.9585
165	16799.67	17148.87	0.121	0.12	2.0363	11898.24	12384.43	0.095	0.103	3.9258
166	12984.5	13428.35	0.121	0.123	3.3053	12643.73	12745.77	0.115	0.12	0.8006
167	13931.04	13604.01	0.121	0.115	-2.404	12873.93	13805.09	0.094	0.105	6.7451
168	14065.77	15143.54	0.121	0.116	7.117	15375.05	15723.63	0.115	0.117	2.2169
169	14051.58	14302.08	0.121	0.12	1.7515	12681.01	12723.02	0.084	0.091	0.3302
170	14955.45	13392.49	0.121	0.1	-11.67	16163.88	16701.42	0.116	0.112	3.2185
171	14510.84	14743.06	0.121	0.12	1.5751	13853.9	13622.73	0.118	0.116	-1.6969
172	14411.94	14662.44	0.121	0.121	1.7085	12427.16	12897.99	0.068	0.077	3.6504
173	14618.86	14869.36	0.121	0.12	1.6847	11890.54	11901.59	0.107	0.116	0.0928
174	13369.29	14095.93	0.121	0.121	5.155	10989.69	11184.87	0.123	0.121	1.7451
175	12978.56	12639.23	0.121	0.104	-2.6847	10748.21	11076.88	0.122	0.117	2.9671
176	16482.68	16610.17	0.121	0.12	0.7675	11094.39	11344.01	0.073	0.081	2.2005
177	13486.42	13581.94	0.121	0.113	0.7032	13110.44	13933.82	0.073	0.083	5.9092
178	12802.16	12946.42	0.121	0.11	1.1143	15992.98	15861.97	0.083	0.084	-0.8259
179	14889.93	15140.43	0.121	0.121	1.6545	12395.54	12622.7	0.12	0.12	1.7996
180	15927.77	16174.34	0.121	0.12	1.5244	12598.99	12712.75	0.117	0.122	0.8949
181	14526.51	15429.63	0.121	0.117	5.8532	10994.28	10550.85	0.104	0.091	-4.2028
182	16737.62	16905.11	0.121	0.12	0.9908	12763.61	12829.17	0.092	0.094	0.5111
183	13594.73	14868.44	0.121	0.123	8.5665	14382.67	14359.95	0.084	0.085	-0.1582
184	15440.04	14834.34	0.121	0.104	-4.0831	12007.07	12025.95	0.084	0.094	0.1569
185	13439.62	13557.4	0.121	0.121	0.8688	13633.43	13735.48	0.111	0.116	0.7429
186	15184.75	15435.26	0.121	0.121	1.6229	15785.43	15771.49	0.101	0.106	-0.0883
187	13446.84	14567.71	0.121	0.121	7.6942	11564.39	11732.88	0.096	0.101	1.4361
188	13027.84	12688.52	0.121	0.104	-2.6743	11933.45	11957.09	0.123	0.115	0.1977
189	13507.93	14585.7	0.122	0.117	7.3892	13535.77	13637.82	0.11	0.115	0.7483
190	14548.05	15821.76	0.122	0.123	8.0504	11278.63	11609.67	0.113	0.117	2.8514
191	17585.88	17753.37	0.122	0.121	0.9434	12628.4	13010.06	0.099	0.108	2.9336
192	15159.89	13985.58	0.122	0.106	-8.3966	11272.33	11249.61	0.082	0.083	-0.202
193	13911.15	14648.71	0.122	0.121	5.035	10458.2	10553.47	0.129	0.131	0.9027
194	13666.48	14118.32	0.122	0.124	3.2004	10774.21	10936.26	0.119	0.117	1.4817
195	16552.89	17067.03	0.122	0.121	3.0125	13182.31	13284.35	0.108	0.113	0.7682
196	13007.72	13190.57	0.122	0.125	1.3862	9720.803	9853.351	0.127	0.125	1.3452
197	15658	15825.49	0.122	0.121	1.0583	12138.8	12275.12	0.118	0.119	1.1106
198	13519.62	13684.06	0.122	0.123	1.2017	13029.35	13702.07	0.114	0.119	4.9096
199	13729.24	13979.74	0.122	0.121	1.7919	13641.81	13701.9	0.085	0.094	0.4385
200	14440.78	14715.64	0.122	0.121	1.8678	14518.97	14909.01	0.107	0.111	2.6161
201	14692.91	15966.62	0.122	0.123	7.9773	13821.57	14603.03	0.067	0.07	5.3513
202	17846.3	18013.78	0.122	0.121	0.9298	11488.23	11629.73	0.126	0.126	1.2168
203	12438.73	11907.98	0.122	0.104	-4.4571	12818.4	12953.46	0.084	0.086	1.0427
204	13567.22	14644.99	0.122	0.117	7.3593	14983	14852	0.083	0.084	-0.8821
205	15348.06	15506.85	0.122	0.124	1.024	13068.52	13182.28	0.117	0.122	0.863
206	11985.03	13161.75	0.122	0.124	8.9405	13361.48	13307.05	0.087	0.088	-0.4091
207	14201.39	13377.16	0.122	0.1	-6.1615	14631.84	14162.76	0.096	0.078	-3.3121

208	14728.5	14967.29	0.122	0.122	1.5954	10864.24	10964.45	0.09	0.089	0.9139
209	14500.51	14618.3	0.122	0.122	0.8057	11833.24	12813.48	0.073	0.076	7.6501
210	15574.69	15692.47	0.123	0.122	0.7506	11454.72	12178.4	0.068	0.073	5.9423
211	14018.35	14843.48	0.123	0.122	5.5589	12534.91	12887.78	0.1	0.109	2.7381
212	11978.87	11758.04	0.123	0.101	-1.8781	12847.77	12778.19	0.101	0.108	-0.5446
213	13059.2	13176.99	0.123	0.123	0.8938	11619.84	11704.49	0.092	0.094	0.7232
214	14063.91	14909.55	0.123	0.123	5.6718	11958.58	12086.86	0.083	0.088	1.0614
215	15719.13	15846.62	0.123	0.121	0.8045	9990.803	10138	0.123	0.119	1.4519
216	13401.3	14272.29	0.123	0.122	6.1027	15090.93	14959.93	0.084	0.085	-0.8757
217	15543.68	14379.48	0.123	0.106	-8.0962	12534.11	12675.03	0.127	0.129	1.1118
218	13666.45	14644.22	0.123	0.118	6.6768	11326.62	11303.9	0.092	0.092	-0.201
219	13668.47	14010.39	0.123	0.121	2.4405	11681.08	12022.75	0.104	0.113	2.8418
220	12588.14	12705.92	0.123	0.123	0.927	12845.63	13003.7	0.12	0.119	1.2156
221	14763.91	13648.8	0.123	0.105	-8.17	11410.84	11421.88	0.104	0.114	0.0967
222	12282.6	13558.74	0.123	0.123	9.4119	13907.13	13884.71	0.085	0.083	-0.1615
223	15495.13	15622.62	0.123	0.121	0.816	14158.62	14377.23	0.085	0.088	1.5206
224	12973.49	13091.28	0.123	0.123	0.8997	13821.07	13906.63	0.072	0.076	0.6153
225	14305.63	13916.79	0.123	0.114	-2.794	11393.1	12526.38	0.116	0.119	9.0471
226	17441.65	17761.86	0.123	0.122	1.8028	12193.23	12170.5	0.087	0.088	-0.1867
227	13908.99	14811.1	0.123	0.119	6.0908	11065.9	11057.62	0.093	0.09	-0.0749
228	13028.43	14271.43	0.123	0.124	8.7097	10938.78	11692.54	0.1	0.083	6.4465
229	13223.35	13790.87	0.123	0.124	4.1152	12504.52	12623.43	0.086	0.085	0.942
230	14708.71	15358.04	0.123	0.12	4.2279	13517.72	14101.19	0.113	0.11	4.1377
231	14489.74	14607.52	0.123	0.123	0.8063	10620.63	10782.68	0.123	0.12	1.5028
232	14065.21	13477.88	0.123	0.104	-4.3577	11163.18	11195.1	0.095	0.093	0.2852
233	13606.37	13866.88	0.123	0.122	1.8786	11588.13	11566.92	0.076	0.076	-0.1834
234	13167.87	14401.08	0.123	0.118	8.5633	10114.86	10398.29	0.126	0.12	2.7258
235	12912.31	13139	0.123	0.126	1.7253	13504.71	13586.63	0.072	0.076	0.603
236	15210.18	14188.71	0.123	0.106	-7.1992	13000.92	12614.35	0.084	0.089	-3.0645
237	12089.79	11826.83	0.123	0.106	-2.2235	13396.57	14100.71	0.114	0.12	4.9937
238	13981.08	14098.86	0.123	0.123	0.8354	10430.92	10441.97	0.106	0.116	0.1057
239	11430.64	11727.83	0.123	0.127	2.5341	13579.77	13565.83	0.114	0.118	-0.1027
240	15485.93	15653.42	0.123	0.122	1.07	12832.64	12809.92	0.088	0.089	-0.1774
241	16149.78	16317.27	0.123	0.123	1.0264	11926.8	11830.65	0.087	0.086	-0.8127
242	13069.02	13807.59	0.123	0.122	5.349	14632.82	14591.02	0.106	0.11	-0.2865
243	13309.12	13386.9	0.124	0.123	0.581	11843.41	11945.46	0.102	0.107	0.8543
244	13093.47	13359.83	0.124	0.123	1.9937	16264.34	16258.1	0.104	0.109	-0.0384
245	13215.18	13481.04	0.124	0.123	1.9721	12415.3	12392.58	0.086	0.087	-0.1833
246	15433	15600.49	0.124	0.123	1.0736	12203.59	12856.19	0.121	0.116	5.0761
247	12429.97	13563.89	0.124	0.126	8.3598	12766.74	13548.2	0.064	0.068	5.768
248	12394.26	13087.46	0.124	0.124	5.2967	11510.69	11571.61	0.123	0.121	0.5265
249	14570.07	14947.14	0.124	0.123	2.5227	12065.05	12167.1	0.113	0.119	0.8387
250	16056.79	16224.28	0.124	0.123	1.0323	17142.18	17734.85	0.1	0.103	3.3418
251	15858.27	16025.76	0.124	0.123	1.0451	10388.06	10583.24	0.125	0.123	1.8443
252	13309.56	14376.29	0.124	0.124	7.42	13064.5	13159.47	0.13	0.125	0.7217
253	13214.68	13549.53	0.124	0.123	2.4713	13122.16	13224.2	0.109	0.114	0.7717

254	13562.13	13679.92	0.124	0.124	0.861	15831.49	16403.42	0.108	0.111	3.4866
255	12102.17	12729.35	0.124	0.124	4.927	12353.19	12455.24	0.115	0.121	0.8193
256	11899.61	13232.91	0.124	0.127	10.076	14006.49	14103.44	0.116	0.119	0.6874
257	11862.39	13108.41	0.124	0.128	9.5055	13352.26	13136.61	0.086	0.09	-1.6416
258	15864.25	16270.91	0.124	0.123	2.4993	11445.11	11857.12	0.131	0.126	3.4748
259	15988.71	16156.2	0.124	0.123	1.0367	12288.9	12377.98	0.087	0.095	0.7197
260	15814.55	16105.76	0.124	0.123	1.8081	13008.08	12985.36	0.08	0.081	-0.175
261	14030.36	15108.12	0.124	0.119	7.1337	18306.8	18292.87	0.097	0.101	-0.0762
262	13753.97	13871.75	0.124	0.124	0.8491	16396.41	15897.54	0.103	0.083	-3.1381
263	13900	14977.77	0.124	0.119	7.1958	11839.24	12454.56	0.123	0.119	4.9405
264	16196.49	16363.98	0.124	0.123	1.0235	11850.55	12053.78	0.073	0.077	1.686
265	13634.27	13752.05	0.124	0.124	0.8565	15246.04	14872.73	0.103	0.112	-2.51
266	15395.81	15563.3	0.124	0.123	1.0762	16009.42	15961.85	0.081	0.082	-0.298
267	11466.06	11418.99	0.124	0.107	-0.4122	13392.84	13738.53	0.105	0.111	2.5162
268	12611.51	12729.29	0.124	0.124	0.9253	13091.68	13193.73	0.117	0.122	0.7734
269	14198.37	15493.42	0.124	0.118	8.3587	12053.78	12155.82	0.115	0.12	0.8395
270	12938.54	13916.31	0.124	0.119	7.026	12487.04	12589.08	0.118	0.123	0.8106
271	15082.82	15250.31	0.125	0.123	1.0983	12305.68	12407.72	0.112	0.117	0.8224
272	15062.73	15253.15	0.125	0.124	1.2484	11447.83	11761.8	0.11	0.115	2.6694
273	13741.33	12928.31	0.125	0.101	-6.2886	13431.73	13459.34	0.104	0.105	0.2051
274	13795.69	13913.47	0.125	0.125	0.8465	12350.17	12229.38	0.095	0.094	-0.9878
275	13617.82	13735.6	0.125	0.125	0.8575	12400.04	13332.18	0.104	0.107	6.9917
276	14678.8	15047.5	0.125	0.124	2.4502	17867.01	18082.36	0.111	0.11	1.191
277	12774.13	13647.26	0.125	0.118	6.3978	14088.49	14205.06	0.076	0.076	0.8206
278	13564.91	14472.88	0.125	0.12	6.2736	15413.74	15528.21	0.106	0.111	0.7372
279	13902.54	14804.66	0.125	0.119	6.0935	11891.77	12273.43	0.099	0.108	3.1097
280	14770.63	15938.1	0.125	0.119	7.325	12099.99	12444.59	0.102	0.111	2.769
281	12625.42	12743.2	0.125	0.125	0.9243	12783.93	12656.56	0.1	0.106	-1.0063
282	14063.74	14181.52	0.125	0.125	0.8305	10638.06	10749.39	0.123	0.122	1.0357
283	13137.66	14442.08	0.125	0.126	9.0321	16207.98	17082.87	0.099	0.105	5.1214
284	13298.89	13376.67	0.125	0.124	0.5815	13993.91	13979.98	0.108	0.112	-0.0997
285	16355.05	16522.54	0.125	0.124	1.0137	13093.52	14647.58	0.081	0.09	10.61
286	13469.23	14761.73	0.125	0.127	8.7557	12305.62	12642.31	0.093	0.096	2.6632
287	13243.74	13136.04	0.125	0.128	-0.8198	11626.24	12774.02	0.075	0.091	8.9853
288	14218.11	14335.9	0.125	0.125	0.8216	11822.21	11714.93	0.126	0.121	-0.9157
289	15618.09	15785.58	0.125	0.124	1.061	11527.9	11546.47	0.073	0.086	0.1609
290	12325.65	12443.43	0.125	0.125	0.9465	11659.01	11633.15	0.117	0.121	-0.2223
291	14379.07	14649.57	0.125	0.125	1.8465	12422.96	12525	0.116	0.122	0.8147
292	12160.97	13096.4	0.125	0.125	7.1426	15889.05	16351.65	0.118	0.115	2.8291
293	13532.34	13650.12	0.125	0.125	0.8629	13195.11	13582.85	0.127	0.121	2.8547
294	13037.81	14115.58	0.125	0.12	7.6353	11084.59	11181.66	0.129	0.126	0.8681
295	13042.75	14031.02	0.125	0.12	7.0435	15055.81	14843.59	0.101	0.106	-1.4297
296	13309.44	14593.44	0.125	0.12	8.7985	11102.71	11625.94	0.133	0.128	4.5005
297	13342.4	13460.18	0.125	0.125	0.875	12640.44	12952.7	0.108	0.112	2.4107
298	12246.79	13642.97	0.125	0.124	10.234	11111.86	12247.44	0.108	0.108	9.272
299	13358.76	13476.55	0.125	0.125	0.874	11450.05	11942.86	0.126	0.113	4.1264

300	12782.61	13048.97	0.125	0.125	2.0412	11938.81	11913.87	0.083	0.083	-0.2093
301	13585.18	13702.97	0.125	0.125	0.8595	14267.84	13798.56	0.098	0.079	-3.401
302	11906.97	12341.01	0.125	0.126	3.5171	13675.57	14534.39	0.113	0.11	5.9089
303	13124.23	14379.95	0.125	0.126	8.7324	12040.82	12018.1	0.088	0.088	-0.1891
304	12119.11	13555.25	0.125	0.126	10.595	15789.24	16285.05	0.092	0.106	3.0446
305	11778.69	12170.27	0.125	0.126	3.2175	12750.55	12852.6	0.116	0.122	0.794
306	13115.22	14105.83	0.125	0.119	7.0227	14903.44	14889.51	0.107	0.111	-0.0936
307	13714.23	15055.64	0.125	0.12	8.9097	13455.97	13565.59	0.116	0.121	0.8081
308	13966.78	15264.22	0.125	0.121	8.4999	11678.8	12151.19	0.126	0.121	3.8876
309	12706.19	12565.06	0.125	0.128	-1.1232	11030.91	11103.63	0.074	0.094	0.6549
310	12694.77	12812.55	0.126	0.125	0.9193	13927.91	13905.18	0.081	0.081	-0.1634
311	12394.11	13294.68	0.126	0.125	6.7739	9992.813	10146.57	0.122	0.119	1.5154
312	13501.83	13139.89	0.126	0.102	-2.7545	13347.84	13426.63	0.072	0.076	0.5868
313	11517.27	11966.84	0.126	0.126	3.7568	11087.13	12123.21	0.115	0.113	8.5463
314	11484.72	11971.86	0.126	0.125	4.0691	12307.63	12409.67	0.115	0.12	0.8223
315	12950.38	13683.89	0.126	0.127	5.3603	11060.54	11028.83	0.1	0.103	-0.2876
316	13247.22	14524.15	0.126	0.12	8.7918	14084	14027.01	0.092	0.094	-0.4063
317	14010.27	14128.05	0.126	0.125	0.8337	15799.63	15624.48	0.086	0.086	-1.121
318	11928.28	12989.56	0.126	0.127	8.1703	12061.56	12165.2	0.079	0.083	0.8519
319	14353.5	14938.15	0.126	0.125	3.9138	14377.7	14512.76	0.077	0.079	0.9306
320	13981.81	14120.31	0.126	0.125	0.9808	11573.93	11719.7	0.127	0.13	1.2438
321	12711.59	13594	0.126	0.119	6.4912	11525.94	11598.36	0.078	0.083	0.6245
322	13720.27	13838.05	0.126	0.126	0.8511	12302.06	12514.7	0.079	0.077	1.6991
323	12514.97	13131.61	0.126	0.124	4.6958	11878.78	11980.82	0.11	0.115	0.8517
324	13760.57	15058	0.126	0.121	8.6163	11525.85	11904.34	0.073	0.077	3.1794
325	13064.71	13316.55	0.126	0.126	1.8912	10111.57	10193.91	0.12	0.116	0.8077
326	13803.67	15102.85	0.126	0.119	8.6023	12064.08	12654.93	0.109	0.115	4.6689
327	12745.14	13653.11	0.126	0.12	6.6503	12296.12	12633.14	0.104	0.112	2.6677
328	11267.09	11926.86	0.126	0.126	5.5319	11459.17	11554.61	0.128	0.129	0.826
329	12506.53	13584.3	0.126	0.12	7.9339	11149.3	11752.38	0.11	0.11	5.1316
330	12009.88	12127.66	0.126	0.126	0.9712	13232.49	14770.93	0.066	0.069	10.415
331	12192.33	13164.83	0.126	0.127	7.3871	11574.54	11597.3	0.11	0.119	0.1962
332	16473.21	16640.7	0.126	0.125	1.0065	10158.29	10269.63	0.124	0.122	1.0841
333	14263	14533.5	0.126	0.125	1.8612	12812.01	13076.15	0.081	0.093	2.02
334	12227.48	13305.25	0.126	0.12	8.1003	10308.65	10399.77	0.127	0.129	0.8762
335	12996.27	12980.27	0.126	0.097	-0.1232	13538.64	13764.12	0.089	0.087	1.6382
336	14329.33	14496.81	0.126	0.125	1.1553	11041.88	11041.88	0.074	0.074	0
337	13752.32	14719.13	0.126	0.122	6.5684	11533.66	11533.66	0.076	0.076	0
338	11608.07	12035.3	0.126	0.127	3.5498	13820.18	13818.68	0.112	0.116	-0.0109
339	13962.75	13299.27	0.126	0.103	-4.9889	12431.24	12380.95	0.089	0.089	-0.4062
340	13911.77	14791.46	0.126	0.121	5.9473	10933.28	11406.29	0.133	0.129	4.147
341	13200.81	13273.48	0.127	0.125	0.5475	18136.3	18075.08	0.098	0.101	-0.3387
342	12739.23	12857.01	0.127	0.126	0.9161	12388.86	12397.15	0.096	0.093	0.0668
343	12476.47	13118.59	0.127	0.126	4.8947	16612.68	16490.46	0.1	0.104	-0.7411
344	11983.63	12410.86	0.127	0.128	3.4424	12658.87	12607.16	0.086	0.086	-0.4102
345	12383.14	12309.59	0.127	0.128	-0.5975	13859.47	13836.75	0.087	0.087	-0.1642

346	11314.84	11388.99	0.127	0.127	0.651	12271.8	13553.61	0.077	0.094	9.4573
347	14263.46	13390.98	0.127	0.103	-6.5154	11076.73	11072.59	0.076	0.076	-0.0374
348	14171.25	14272.46	0.127	0.126	0.7092	14257.05	14303.62	0.115	0.117	0.3256
349	12396.62	13281.25	0.127	0.127	6.6607	13375.27	13385.86	0.084	0.093	0.0791
350	13309.12	13426.9	0.127	0.127	0.8772	12168.54	12647.71	0.119	0.113	3.7886
351	13263.26	13341.04	0.127	0.126	0.583	12332.29	12323.76	0.117	0.119	-0.0692
352	13237.51	13555.63	0.127	0.131	2.3467	10751.68	11238.46	0.126	0.116	4.3313
353	14213.76	14381.25	0.127	0.126	1.1646	12363.02	12357.07	0.082	0.084	-0.0481
354	16685.63	17292.72	0.127	0.117	3.5107	15705.28	18074.35	0.064	0.102	13.107
355	12766.5	13668.62	0.127	0.121	6.5999	10192.87	10294.92	0.1	0.107	0.9912
356	12261.26	13143.67	0.127	0.12	6.7136	13559.56	13559.56	0.069	0.069	0
357	12700.76	13164.27	0.127	0.127	3.5209	11564.58	11556.29	0.092	0.089	-0.0717
358	14860.21	16027.68	0.127	0.121	7.2841	17706.42	17968.64	0.11	0.11	1.4593
359	14391.82	15803.83	0.127	0.128	8.9346	12730.35	13042.6	0.115	0.121	2.3941
360	13539.08	13951.75	0.127	0.13	2.9578	10960.45	11271.61	0.123	0.121	2.7606
361	12704.58	13582.55	0.127	0.121	6.464	14030.25	14183.26	0.084	0.093	1.0788
362	12556.56	13080.98	0.127	0.127	4.009	13418.96	13383.1	0.09	0.086	-0.2679
363	12286.8	12404.59	0.127	0.127	0.9495	17553.45	17329.31	0.098	0.103	-1.2934
364	13000.47	14307.23	0.127	0.121	9.1336	15733.43	16885.94	0.118	0.112	6.8253
365	11589.17	11706.95	0.128	0.127	1.0061	12848.96	12811.89	0.117	0.12	-0.2893
366	13339.61	14416.29	0.128	0.121	7.4685	15825.31	15902.5	0.103	0.108	0.4854
367	14002.66	14526.2	0.128	0.117	3.6041	12621.9	12592.49	0.081	0.088	-0.2336
368	12338.23	12456.01	0.128	0.127	0.9456	11107.98	11665.85	0.127	0.124	4.7821
369	13438.69	13853.11	0.128	0.105	2.9915	17782.19	18053.2	0.109	0.11	1.5011
370	12298.73	12416.51	0.128	0.127	0.9486	11393.95	11521.94	0.092	0.09	1.1108
371	13346.98	13585	0.128	0.131	1.7521	12397.81	12499.11	0.074	0.086	0.8105
372	12356.14	15486.58	0.128	0.13	20.214	11961.68	12298.79	0.11	0.115	2.741
373	13290.92	13737.7	0.128	0.126	3.2522	14364.77	14377.4	0.106	0.109	0.0879
374	13275.68	14503.95	0.128	0.13	8.4685	16748	17186.95	0.095	0.102	2.5539
375	15314.97	17207.45	0.128	0.129	10.998	11947.28	12109.5	0.123	0.123	1.3396
376	13723.42	14549.27	0.128	0.122	5.6762	13991.4	14136.13	0.087	0.095	1.0238
377	12334.65	12452.43	0.128	0.128	0.9459	9562.519	9666.072	0.132	0.134	1.0713
378	12480.44	12598.23	0.128	0.128	0.9349	13154.88	13967.51	0.117	0.123	5.818
379	14348.4	13082.66	0.128	0.102	-9.6749	12351.6	12312.1	0.071	0.071	-0.3208
380	12392.22	12510	0.128	0.127	0.9415	12927.06	13029.11	0.115	0.121	0.7832
381	12573.99	13193.68	0.128	0.127	4.6969	12264.64	12250.7	0.096	0.101	-0.1137
382	13167.34	13285.12	0.128	0.128	0.8866	13050.41	13044.55	0.1	0.102	-0.0449
383	12433.15	12696.15	0.128	0.092	2.0715	17099.8	17434.62	0.111	0.109	1.9204
384	11789.82	11907.6	0.128	0.128	0.9891	12613.04	12890.24	0.075	0.082	2.1504
385	11699.07	12570.06	0.128	0.128	6.9291	15610.56	15590.11	0.108	0.112	-0.1312
386	13714.41	13881.9	0.128	0.127	1.2065	11906.83	12008.87	0.116	0.121	0.8498
387	13725.81	14502.25	0.128	0.12	5.3539	14125.6	14045.31	0.087	0.087	-0.5717
388	12205.22	15198	0.128	0.131	19.692	16777.18	17220.32	0.105	0.11	2.5733
389	12332.42	13057.55	0.128	0.127	5.5534	16152.06	16573.31	0.101	0.116	2.5417
390	15084.76	14085.78	0.128	0.102	-7.0921	12648.21	13758.2	0.092	0.079	8.0678
391	14141.86	16778.01	0.129	0.126	15.712	14952.5	15084.51	0.118	0.119	0.8751

392	13290.7	14328.59	0.129	0.122	7.2435	14964.22	15124.51	0.118	0.119	1.0598
393	11839.07	12357.43	0.129	0.128	4.1947	11919.99	11937.06	0.093	0.093	0.143
394	14588.13	16480.61	0.129	0.13	11.483	12193.85	12350	0.125	0.126	1.2644
395	12658.21	13377.82	0.129	0.091	5.3791	11885.61	11908.03	0.095	0.093	0.1883
396	13165.31	14047.72	0.129	0.122	6.2815	10444.19	10999.26	0.123	0.126	5.0464
397	12388.04	13685.48	0.129	0.124	9.4804	18807.09	18374.14	0.102	0.092	-2.3563
398	16621.05	17228.99	0.129	0.127	3.5286	11526.57	11725.69	0.102	0.108	1.6981
399	12494.29	12612.07	0.129	0.128	0.9339	13160.18	12790.98	0.082	0.086	-2.8864
400	14820.59	16194.84	0.129	0.129	8.4857	15840.64	15842.06	0.105	0.108	0.009
401	15139.02	16744.69	0.129	0.13	9.5891	11648.36	12616.77	0.078	0.076	7.6755
402	13963.78	15668.81	0.129	0.128	10.882	11971.2	11607.15	0.128	0.122	-3.1365
403	11989.32	12107.1	0.129	0.128	0.9728	12660.77	12319.94	0.083	0.091	-2.7665
404	16910.86	14613.24	0.129	0.105	-15.723	11928.73	12358.15	0.11	0.116	3.4748
405	12669.93	15623.71	0.129	0.131	18.906	16339.28	16333.04	0.104	0.108	-0.0382
406	13626.68	17271.8	0.129	0.128	21.104	11191.2	11408.48	0.072	0.088	1.9045
407	13427.03	15296.08	0.129	0.129	12.219	10478.03	10473.89	0.076	0.076	-0.0395
408	12751.03	13615.92	0.129	0.131	6.352	15740.34	15612.56	0.085	0.086	-0.8185
409	14243.46	13921.52	0.129	0.106	-2.3125	11545.88	12598.36	0.114	0.117	8.3541
410	16011.51	16618.6	0.129	0.119	3.6531	10495.13	10640.9	0.127	0.13	1.3699
411	15057.87	16692.33	0.129	0.13	9.7917	10955.29	11005.79	0.09	0.098	0.4589
412	12495.94	12504.59	0.129	0.093	0.0692	12557.07	12534.35	0.087	0.088	-0.1813
413	14148.63	14683.42	0.129	0.122	3.6421	13650.65	13752.7	0.11	0.115	0.742
414	13033.54	14201.02	0.129	0.122	8.221	10516.01	10527.05	0.108	0.118	0.1049
415	12058.03	14724.95	0.129	0.132	18.112	11035.81	11348.86	0.117	0.122	2.7584
416	14128.93	14838.57	0.129	0.124	4.7824	14596.16	15131.47	0.103	0.115	3.5377
417	13322.67	14823.76	0.129	0.129	10.126	13884.62	13466.46	0.082	0.087	-3.1052
418	15497.47	16507.47	0.129	0.128	6.1184	15892.65	15886.41	0.105	0.11	-0.0393
419	15345.82	16989.43	0.129	0.132	9.6743	14461.79	14614.8	0.082	0.091	1.047
420	12410.41	12735.21	0.13	0.133	2.5504	15637.9	15785.44	0.109	0.11	0.9346
421	12461.4	13236.62	0.13	0.122	5.8566	16153.48	16035.4	0.1	0.104	-0.7363
422	12394.69	13101.12	0.13	0.122	5.3921	12125.37	12663.11	0.126	0.12	4.2466
423	12688.39	13612.72	0.13	0.121	6.7902	17120.61	17429.85	0.103	0.107	1.7742
424	16295.67	17111.27	0.13	0.129	4.7664	12427.27	12456.27	0.091	0.089	0.2328
425	15656.51	16107.33	0.13	0.121	2.7988	11533.31	11386.53	0.114	0.114	-1.289
426	11998.39	12880.5	0.13	0.123	6.8485	10813.77	11445.66	0.128	0.13	5.5208
427	12742.74	13027.99	0.13	0.099	2.1895	11835.05	11850.11	0.091	0.092	0.1271
428	13588.45	13835.04	0.13	0.123	1.7824	17737.64	18332.67	0.111	0.107	3.2457
429	15414.76	17184.14	0.13	0.132	10.297	11897.21	11862.56	0.11	0.115	-0.2921
430	13574.17	14741.64	0.13	0.123	7.9196	11447.95	11789.61	0.106	0.115	2.898
431	14490.76	15246.85	0.13	0.12	4.959	14582.17	15257.52	0.109	0.114	4.4264
432	15605.47	14457.17	0.13	0.1	-7.9428	15069.24	15002.38	0.086	0.087	-0.4457
433	13388.33	14247.6	0.13	0.122	6.031	13674.96	13472.59	0.115	0.113	-1.5021
434	12788.6	13691.51	0.13	0.123	6.5947	13507.93	13483.79	0.083	0.08	-0.179
435	15316.95	15924.04	0.13	0.12	3.8124	11834.76	11954.55	0.082	0.091	1.0021
436	14710.55	16591.82	0.13	0.131	11.339	12520.65	12497.93	0.085	0.085	-0.1818
437	12565.87	15308.57	0.13	0.132	17.916	11851.59	12312.42	0.08	0.09	3.7428

438	13279.99	14654.24	0.13	0.131	9.3778	11194.55	11657.1	0.069	0.079	3.968
439	18443.85	17326.13	0.13	0.109	-6.451	14908.44	15048.65	0.109	0.109	0.9317
440	14374.78	16089.52	0.131	0.132	10.657	17060.98	17318.85	0.107	0.114	1.4889
441	12767.44	13468.1	0.131	0.122	5.2024	12177.86	11779.73	0.13	0.129	-3.3798
442	17815.92	14386.67	0.131	0.107	-23.836	12260.7	12602.37	0.107	0.115	2.7111
443	16333.67	14132.14	0.131	0.106	-15.578	10947.21	11571.35	0.126	0.122	5.3939
444	14712.36	16183.54	0.131	0.134	9.0906	11627.33	11604.61	0.085	0.086	-0.1958
445	14427.21	15147.77	0.131	0.122	4.7569	14569.98	14582.61	0.107	0.11	0.0866
446	16885.44	14633.68	0.131	0.107	-15.388	11423.89	11318.95	0.1	0.108	-0.9271
447	13206.44	14937.46	0.131	0.132	11.588	12435.32	12688.18	0.118	0.117	1.9929
448	17939	15840.91	0.131	0.107	-13.245	15520.72	15527.5	0.103	0.107	0.0436
449	15871.18	14134.63	0.131	0.104	-12.286	11126.95	11330.68	0.128	0.129	1.798
450	17127.37	14588.82	0.131	0.111	-17.401	10527.1	11015.9	0.109	0.112	4.4372
451	17717.83	17013.67	0.131	0.108	-4.1388	12812.39	12804.11	0.089	0.086	-0.0647
452	12189.82	13482.61	0.131	0.125	9.5886	10437.43	11131.52	0.114	0.114	6.2354
453	12891.23	14387.91	0.131	0.132	10.402	16283.53	16889.56	0.112	0.113	3.5882
454	15114.84	16728.16	0.131	0.134	9.6443	13323.63	13209.49	0.102	0.1	-0.8641
455	16469.52	17159.73	0.131	0.127	4.0223	11109.62	11669.59	0.13	0.123	4.7985
456	12199.01	15191.21	0.131	0.129	19.697	12128.45	12234.93	0.095	0.102	0.8703
457	12924.87	15718.98	0.131	0.132	17.775	13874.47	15340.75	0.071	0.081	9.558
458	14921.89	14733.09	0.131	0.122	-1.2815	14882.88	14768.74	0.11	0.108	-0.7729
459	13079.93	15122.51	0.131	0.133	13.507	16239.28	16251.91	0.101	0.104	0.0777
460	12761.82	15766.69	0.131	0.131	19.058	12391.73	12938.76	0.127	0.122	4.2279
461	13016.72	14448.1	0.131	0.134	9.9071	12661.65	12449.43	0.096	0.102	-1.7046
462	12168.19	13867.06	0.131	0.132	12.251	13542.34	13479.62	0.088	0.088	-0.4653
463	11314.77	13932.91	0.131	0.134	18.791	15186.9	15700.58	0.106	0.109	3.2717
464	13567.36	13277.34	0.131	0.099	-2.1843	11271.86	11413.37	0.124	0.124	1.2398
465	13907.72	15612.74	0.131	0.13	10.921	13107.06	13246.89	0.115	0.12	1.0556
466	11959.48	13764.47	0.131	0.135	13.113	12782.37	12768.43	0.113	0.117	-0.1091
467	12760.74	13372.58	0.131	0.134	4.5753	12163.67	12100.95	0.088	0.089	-0.5183
468	17168.28	17010.87	0.131	0.108	-0.9254	16301.37	16381.49	0.103	0.108	0.4891
469	13002.7	14269.97	0.131	0.133	8.8806	11730.53	11741.12	0.087	0.097	0.0902
470	12685.08	14329.12	0.131	0.133	11.473	10786.97	10932.74	0.127	0.13	1.3333
471	15164.67	15771.76	0.131	0.12	3.8492	12780.38	12882.43	0.116	0.121	0.7921
472	14671.2	16400.38	0.131	0.132	10.543	11345.14	11499.19	0.086	0.082	1.3397
473	13134.39	12456.51	0.131	0.126	-5.442	10812.5	11600.37	0.117	0.114	6.7917
474	15282.12	17304.35	0.131	0.132	11.686	12540.62	12661.33	0.095	0.094	0.9534
475	15432.39	13788.62	0.131	0.1	-11.921	14224.88	14818.69	0.118	0.116	4.0072
476	12177.23	15135.78	0.131	0.134	19.547	13916.38	14374.13	0.119	0.115	3.1845
477	12579.12	13333.63	0.131	0.123	5.6587	17822.39	17783.6	0.095	0.099	-0.2181
478	15848.61	14900.64	0.131	0.103	-6.3619	12024.4	11949.26	0.095	0.095	-0.6289
479	16610.53	14009.6	0.131	0.105	-18.565	12468.02	12496.8	0.082	0.084	0.2304
480	13276.97	14806.64	0.131	0.129	10.331	14347.67	14054.95	0.084	0.088	-2.0827
481	12577.49	13460.41	0.131	0.124	6.5593	17109.31	16987.09	0.099	0.103	-0.7195
482	14952.77	13474.47	0.131	0.099	-10.971	13840.45	14492.38	0.089	0.084	4.4984
483	14623.28	16529.9	0.131	0.132	11.534	10972.48	11089.64	0.086	0.094	1.0565

484	16056.08	16819.04	0.131	0.129	4.5363	12612.48	12883.61	0.088	0.09	2.1044
485	12503.93	12733.67	0.131	0.135	1.8042	12292.33	12324.26	0.087	0.087	0.259
486	14072.27	14868.36	0.132	0.121	5.3542	11668.52	11659.82	0.086	0.094	-0.0746
487	11878.28	12433.16	0.132	0.137	4.463	12548.64	12525.92	0.091	0.091	-0.1814
488	19063.64	18362.83	0.132	0.107	-3.8165	11229.93	11289.13	0.083	0.081	0.5244
489	13906.79	14417.23	0.132	0.12	3.5405	16633.28	16915.79	0.108	0.115	1.6701
490	11770.49	13945.26	0.132	0.132	15.595	11630.41	12221.41	0.123	0.119	4.8358
491	14121.06	14295.11	0.132	0.12	1.2176	11432.68	12369.66	0.069	0.07	7.5749
492	12821.53	13453.87	0.132	0.135	4.7001	12438.52	12540.57	0.117	0.122	0.8137
493	12213.45	14643.56	0.132	0.132	16.595	10434.8	10918.32	0.132	0.129	4.4285
494	13670.35	13439.41	0.132	0.099	-1.7183	12213.97	12196.99	0.079	0.086	-0.1393
495	11968.18	13335.44	0.132	0.125	10.253	13724.27	14266.52	0.104	0.108	3.8009
496	17511.24	18500.3	0.132	0.126	5.3462	14854.43	15308.54	0.114	0.112	2.9664
497	16031.82	16621.82	0.132	0.13	3.5496	11575.82	12063.19	0.128	0.124	4.0401
498	14795.64	15812.71	0.132	0.13	6.432	10478.5	10441.43	0.103	0.107	-0.355
499	11770.9	12664.14	0.132	0.099	7.0533	11120.84	11115.4	0.121	0.12	-0.049
500	13351	14311.73	0.132	0.121	6.7129	12840.86	13301.69	0.07	0.079	3.4645
501	11932.17	12919.94	0.132	0.135	7.6453	15292.61	15220.72	0.107	0.11	-0.4723
502	12527.26	13092.84	0.132	0.126	4.3198	10649.43	10645.29	0.078	0.078	-0.0389
503	13330.4	12816.07	0.132	0.125	-4.0132	15766.47	15969.4	0.115	0.115	1.2707
504	12563.7	13683.29	0.132	0.132	8.1821	12808.99	11854.07	0.106	0.106	-8.0556
505	13394.99	16337.68	0.132	0.133	18.012	14003.56	13993.47	0.104	0.111	-0.0721
506	11795.96	14600.58	0.132	0.133	19.209	10846.5	10957.63	0.085	0.083	1.0142
507	16082.45	13921.1	0.132	0.1	-15.526	13834.35	13816.28	0.11	0.114	-0.1308
508	17141.39	15536.76	0.132	0.108	-10.328	11627.75	12529.67	0.1	0.092	7.1983
509	13934.64	14664.15	0.132	0.121	4.9748	13352.55	13497.28	0.085	0.093	1.0723
510	13017.56	12749.02	0.132	0.105	-2.1064	11499.26	11813.23	0.107	0.112	2.6578
511	13259.66	14728.24	0.132	0.132	9.9712	11446.77	11388.19	0.091	0.092	-0.5144
512	12504.45	13505.36	0.132	0.135	7.4112	12702.66	12804.71	0.118	0.123	0.7969
513	14897.92	15928.42	0.132	0.132	6.4696	12188.31	12649.14	0.07	0.079	3.6432
514	13609.02	16485.88	0.132	0.127	17.45	13845.77	13855.27	0.089	0.089	0.0685
515	17729.08	15511.79	0.132	0.107	-14.294	14421.9	15192.14	0.065	0.068	5.07
516	17349	14620.96	0.132	0.109	-18.658	11137.58	11398.03	0.122	0.121	2.2851
517	17406.3	15717.71	0.132	0.108	-10.743	12553.87	12553.87	0.068	0.068	0
518	12669.51	16038.06	0.132	0.131	21.003	11489.91	12162.63	0.108	0.112	5.531
519	16027.27	16538.6	0.132	0.127	3.0918	13537.34	13514.62	0.086	0.087	-0.1681
520	13581.38	14074.24	0.132	0.12	3.5019	16687.29	16764.48	0.102	0.107	0.4605
521	12522.73	13759.78	0.132	0.133	8.9904	11130	10733.73	0.108	0.109	-3.6919
522	13055.2	14396.52	0.132	0.133	9.317	13803.05	13740.33	0.089	0.09	-0.4565
523	11971.08	13513.7	0.132	0.135	11.415	9671.905	10014	0.13	0.122	3.4162
524	14586	13158.49	0.132	0.099	-10.849	16089.91	16632.8	0.121	0.117	3.264
525	12180.87	12414.46	0.132	0.136	1.8816	14865.01	14701.08	0.084	0.085	-1.1151
526	16488.81	16964.29	0.132	0.127	2.8028	13273.46	13375.5	0.107	0.113	0.7629
527	12746.2	14918.2	0.132	0.133	14.559	13379.7	13257.27	0.102	0.1	-0.9235
528	15286.06	14039.18	0.132	0.101	-8.8814	10263.25	10607.55	0.122	0.121	3.2458
529	13737.04	15852.34	0.132	0.131	13.344	10279.59	10273.52	0.128	0.126	-0.059

530	12370.73	13513.14	0.132	0.135	8.4541	12863.81	12849.88	0.113	0.117	-0.1084
531	17744.08	16895.33	0.132	0.112	-5.0236	15862.32	16449.13	0.106	0.109	3.5674
532	16303.75	17269.73	0.132	0.13	5.5935	12986.78	12935.27	0.086	0.086	-0.3982
533	13620.31	14674.39	0.132	0.133	7.1831	11002.23	11383.9	0.101	0.111	3.3527
534	13787.5	14303.8	0.132	0.121	3.6095	11616.64	11829.6	0.109	0.109	1.8003
535	18306.42	16833.86	0.132	0.107	-8.7476	12721.93	13126.36	0.13	0.129	3.0811
536	14376.73	15211.49	0.132	0.129	5.4877	13900.86	14002.91	0.108	0.113	0.7287
537	15245.41	13559.53	0.132	0.1	-12.433	11082.32	11269.51	0.123	0.122	1.6611
538	11404.09	12295.29	0.132	0.125	7.2483	12930.63	12589.79	0.083	0.09	-2.7072
539	16374.61	15135.64	0.133	0.113	-8.1858	11854.52	12216.28	0.107	0.111	2.9612
540	13148.18	14202.26	0.133	0.133	7.4219	11427.95	11156.32	0.13	0.123	-2.4348
541	12792.8	12885.64	0.133	0.12	0.7205	15788.38	15865.58	0.099	0.104	0.4865
542	15279.53	15569.15	0.133	0.13	1.8602	11706.47	12129.65	0.108	0.112	3.4887
543	12936.72	13314.33	0.133	0.132	2.8361	12027.45	12052.72	0.083	0.085	0.2097
544	12049.1	13209.29	0.133	0.136	8.7832	15196.06	15615.4	0.11	0.116	2.6854
545	12756.44	15843.7	0.133	0.13	19.486	11389.84	11832.72	0.112	0.126	3.7428
546	16039.19	15270.22	0.133	0.113	-5.0358	15651.17	15809.25	0.116	0.116	0.9999
547	15755.72	16275.67	0.133	0.131	3.1946	11745.24	12249.31	0.109	0.115	4.1151
548	14678.36	14342.56	0.133	0.096	-2.3413	11257.11	11268.15	0.103	0.113	0.098
549	14474.55	14903.15	0.133	0.122	2.8759	11556.73	11576.23	0.093	0.093	0.1684
550	10998.58	11753.09	0.133	0.123	6.4197	12077.9	12195.68	0.089	0.094	0.9658
551	12762.17	14174.18	0.133	0.132	9.9618	11966.33	11929.26	0.118	0.121	-0.3108
552	12346.47	13503.95	0.133	0.125	8.5714	14003.14	14105.18	0.112	0.117	0.7235
553	16706.47	14778.21	0.133	0.108	-13.048	13818.35	14354.95	0.104	0.108	3.7381
554	17225.3	14876.58	0.133	0.103	-15.788	11743.34	11782.75	0.09	0.091	0.3345
555	15855.14	14734.45	0.133	0.102	-7.6059	14682.59	14551.58	0.084	0.085	-0.9003
556	12414.38	13640.11	0.133	0.132	8.9863	13933.14	14690.96	0.113	0.11	5.1584
557	11791.23	11861.27	0.133	0.136	0.5905	11810.58	12353.34	0.131	0.133	4.3936
558	15432.77	14153.8	0.133	0.101	-9.0363	12308.61	12421.86	0.116	0.121	0.9118
559	12016.64	13107.99	0.133	0.134	8.3259	13902.01	13882.01	0.088	0.084	-0.1441
560	13488.15	13598.26	0.133	0.1	0.8097	13502.13	13492.34	0.108	0.112	-0.0726
561	13059.87	12938.05	0.133	0.1	-0.9415	13136.12	13275.44	0.117	0.122	1.0495
562	15573.63	14618.3	0.133	0.113	-6.5352	13317.29	13300.31	0.079	0.086	-0.1277
563	18427.03	16983.38	0.133	0.109	-8.5004	16392.35	16787.33	0.098	0.103	2.3528
564	12641.7	13695.77	0.133	0.133	7.6964	12548.63	13521.93	0.076	0.084	7.1979
565	13488.09	15643.32	0.133	0.129	13.777	11062.47	11169.96	0.131	0.135	0.9623
566	13067.12	14834.78	0.133	0.131	11.916	12287.74	12389.78	0.098	0.104	0.8236
567	14375.87	16294.08	0.133	0.132	11.772	12937.56	13492.88	0.122	0.117	4.1156
568	12726.39	13358.73	0.133	0.136	4.7335	12104.32	12437.28	0.11	0.115	2.6771
569	13711.5	14436.88	0.133	0.122	5.0245	11511.98	12532.18	0.078	0.075	8.1407
570	14634.37	13615.9	0.133	0.101	-7.48	12016.35	12647.1	0.072	0.077	4.9873
571	12225.1	13046.01	0.133	0.136	6.2924	13393.08	13495.12	0.112	0.117	0.7562
572	11855.2	12272.51	0.133	0.136	3.4004	11056.37	11054.44	0.126	0.125	-0.0174
573	11920.25	12857.51	0.133	0.136	7.2896	12483.75	12488.07	0.109	0.109	0.0345
574	17955.61	16477.61	0.133	0.111	-8.9698	13469.29	13592.64	0.109	0.113	0.9074
575	11689.6	12312.34	0.133	0.092	5.0579	11248.74	11339.45	0.075	0.08	0.8

576	13293.16	15184.93	0.133	0.134	12.458	10661.34	10512.76	0.116	0.115	-1.4133
577	12848.4	14458.97	0.133	0.135	11.139	12634.44	12611.72	0.081	0.082	-0.1802
578	15317.56	16394.13	0.133	0.132	6.5668	12562.25	12699.23	0.082	0.08	1.0787
579	13397.59	13925.6	0.133	0.121	3.7917	14395.33	15659.3	0.109	0.108	8.0717
580	12959.49	14922.16	0.133	0.135	13.153	11946.74	11888.16	0.093	0.093	-0.4927
581	13887.35	15364.51	0.133	0.133	9.6141	11305.07	11316.11	0.106	0.115	0.0976
582	13623.85	13958.81	0.133	0.122	2.3996	12482.49	12469.23	0.081	0.089	-0.1063
583	12944.22	14810.9	0.133	0.134	12.603	14494.95	14363.95	0.083	0.084	-0.912
584	16856.74	14882.41	0.133	0.11	-13.266	10968.07	10945.35	0.091	0.092	-0.2076
585	12583.53	12970.92	0.133	0.097	2.9866	15235.96	15229.72	0.102	0.107	-0.041
586	13152.14	13495.38	0.133	0.121	2.5434	13903.74	14057.67	0.12	0.12	1.095
587	16104.93	16992.57	0.133	0.127	5.2237	10275.07	10386.4	0.125	0.123	1.0719
588	13485.51	14970.75	0.133	0.133	9.9209	12270.26	12261.98	0.093	0.09	-0.0676
589	16802.1	14767.77	0.133	0.11	-13.775	11535.35	11970.7	0.124	0.123	3.6368
590	18672.63	17310.57	0.133	0.112	-7.8684	12870.3	13147.37	0.078	0.08	2.1074
591	13011.72	13338.4	0.133	0.12	2.4491	10665.04	10810.81	0.128	0.131	1.3484
592	13499.92	13694.05	0.134	0.12	1.4176	11727.56	12603.18	0.12	0.123	6.9476
593	17775.14	16641.96	0.134	0.11	-6.8092	12221.53	12198.81	0.082	0.082	-0.1863
594	15097.98	16117.46	0.134	0.134	6.3253	12909.02	13101.57	0.11	0.115	1.4697
595	16746.47	17693.2	0.134	0.128	5.3508	15787.56	15620.7	0.085	0.085	-1.0682
596	13247.64	15082.58	0.134	0.131	12.166	11754.49	13316.86	0.071	0.072	11.732
597	15777.61	16333.21	0.134	0.13	3.4017	11630.26	11952.01	0.114	0.118	2.692
598	18235.86	16585.01	0.134	0.108	-9.9539	11266.38	11635.49	0.079	0.089	3.1723
599	12315.91	14104.11	0.134	0.133	12.679	15920.37	15997.56	0.1	0.105	0.4825
600	10955.45	11809.37	0.134	0.125	7.2309	11272.55	11374.6	0.097	0.103	0.8971
601	11505.48	14231.61	0.134	0.135	19.155	10986.17	11457	0.077	0.087	4.1096
602	12598.8	14416.9	0.134	0.134	12.611	16709.9	16663.54	0.103	0.103	-0.2782
603	15530.49	14399.8	0.134	0.102	-7.8521	13286.31	13261.04	0.081	0.088	-0.1906
604	16130.17	16838.04	0.134	0.131	4.204	11630.94	11966.74	0.101	0.11	2.8062
605	13945.27	14670.96	0.134	0.131	4.9464	12046.18	14275.54	0.073	0.076	15.617
606	18137.18	16629.38	0.134	0.109	-9.0671	12401.23	12442.49	0.119	0.119	0.3316
607	16395.97	14609.13	0.134	0.11	-12.231	18427.36	18256.86	0.096	0.101	-0.9339
608	12381.76	14963.41	0.134	0.133	17.253	12901.93	12867.28	0.11	0.113	-0.2692
609	14100.28	14422.81	0.134	0.123	2.2363	12253.48	12351.77	0.083	0.083	0.7957
610	11067.43	12225.91	0.134	0.137	9.4756	15064.12	15170.31	0.108	0.112	0.7
611	13208.61	15033.37	0.134	0.133	12.138	12190.38	12153.31	0.119	0.122	-0.305
612	12317.05	14214.68	0.134	0.134	13.35	10447.17	10504.96	0.13	0.132	0.55
613	17658.45	18953.08	0.134	0.129	6.8307	12348.54	12469.67	0.082	0.08	0.9714
614	13199.33	14253.41	0.134	0.134	7.3953	11449.97	11450.05	0.128	0.132	0.0008
615	13004.1	13496.96	0.134	0.121	3.6517	12123.84	12096.98	0.092	0.093	-0.2221
616	12219.21	13557.77	0.134	0.134	9.873	10116.66	10145.66	0.125	0.123	0.2858
617	13109.98	13143.48	0.134	0.121	0.2549	11475.96	11462.03	0.095	0.1	-0.1216
618	12301.19	12999.05	0.134	0.121	5.3685	11806.59	12544.82	0.101	0.114	5.8848
619	11230.1	12630.09	0.134	0.137	11.085	12810.76	12912.81	0.116	0.121	0.7903
620	17165.05	16292.09	0.134	0.11	-5.3582	15022.23	15033.15	0.107	0.111	0.0726
621	15521	17029.22	0.134	0.131	8.8567	12357.45	12305.95	0.093	0.094	-0.4186

622	13134.66	14330.66	0.134	0.134	8.3457	13822.4	13811.4	0.086	0.086	-0.0797
623	13674.99	13808.74	0.134	0.123	0.9686	11145.35	13021.53	0.078	0.072	14.408
624	12376.9	13426.04	0.134	0.136	7.8142	13052.6	13108.58	0.11	0.116	0.427
625	13192.17	14246.25	0.134	0.134	7.399	12498.53	12678.36	0.111	0.109	1.4184
626	12850.06	14424.08	0.134	0.133	10.912	17141.32	17053.96	0.097	0.101	-0.5123
627	16085.2	15117.47	0.134	0.115	-6.4014	12675.97	13705.83	0.074	0.082	7.5141
628	13943.47	14671.99	0.134	0.122	4.9653	15157.63	15611.03	0.107	0.108	2.9043
629	13397.62	15136.67	0.134	0.135	11.489	13201.45	13303.49	0.111	0.116	0.7671
630	12555.25	13705.48	0.134	0.134	8.3925	11933.81	12783.02	0.13	0.127	6.6432
631	12629.48	13709.83	0.134	0.135	7.8801	12321.71	12216.77	0.1	0.108	-0.859
632	13191.06	14955.22	0.134	0.132	11.796	11764.11	11741.39	0.084	0.085	-0.1935
633	17141.82	18010.27	0.134	0.128	4.8219	13236.95	13339	0.108	0.113	0.765
634	14702	15356.42	0.134	0.135	4.2616	15990.13	16315.32	0.101	0.105	1.9931
635	12660.46	14543.44	0.134	0.134	12.947	10656.55	11220.14	0.099	0.106	5.023
636	13209.74	13903.59	0.134	0.132	4.9904	11574.27	11539.63	0.097	0.101	-0.3002
637	12954.51	14831.31	0.134	0.134	12.654	15292.98	15451.05	0.116	0.116	1.0231
638	12322.7	13376.78	0.134	0.134	7.8799	11853.1	11830.38	0.086	0.086	-0.1921
639	13206.44	15017.29	0.134	0.134	12.058	12975.53	13077.58	0.111	0.116	0.7803
640	16356.34	15477.71	0.134	0.112	-5.6767	11719.46	11863.1	0.075	0.093	1.2108
641	14070.1	14576.78	0.134	0.122	3.4759	12853.52	12830.8	0.086	0.087	-0.1771
642	12743.81	14527.16	0.134	0.134	12.276	11730.9	11690.73	0.112	0.112	-0.3436
643	17239.44	15580.59	0.134	0.113	-10.647	14223.11	15051.43	0.115	0.111	5.5033
644	15966.06	15613.36	0.135	0.115	-2.259	13894.2	14372.82	0.112	0.109	3.33
645	11955.71	13440.95	0.135	0.134	11.05	14886.52	15255.13	0.101	0.107	2.4163
646	13049.67	14941.43	0.135	0.135	12.661	10617.62	11007.79	0.131	0.122	3.5445
647	16369.18	16830.72	0.135	0.131	2.7423	12663.9	12770.17	0.094	0.095	0.8322
648	12702.76	13783.11	0.135	0.136	7.8382	16011.85	16439.96	0.098	0.109	2.6041
649	14064.7	14773.5	0.135	0.103	4.7978	15118.49	15176.62	0.108	0.111	0.383
650	16557.04	15336.89	0.135	0.115	-7.9557	10429.12	10591.17	0.124	0.121	1.53
651	12372.29	14009.74	0.135	0.132	11.688	15401.79	15836.17	0.1	0.104	2.743
652	13439.64	13536.1	0.135	0.124	0.7127	9910.164	9897.321	0.13	0.134	-0.1298
653	12659.33	13759.68	0.135	0.135	7.9969	18117.99	18061.89	0.111	0.093	-0.3106
654	17972.74	19052.43	0.135	0.128	5.6669	15356.1	16333.04	0.106	0.109	5.9813
655	15815.31	16215.13	0.135	0.13	2.4658	11704.26	12514.79	0.105	0.088	6.4766
656	11887.47	12391.63	0.135	0.127	4.0686	12646.48	12702.43	0.084	0.093	0.4404
657	14393.61	15209.95	0.135	0.131	5.3672	11207.82	11651.71	0.099	0.105	3.8096
658	14774.34	15450.77	0.135	0.131	4.378	11935.11	12358.29	0.107	0.111	3.4242
659	16423.24	15719.67	0.135	0.112	-4.4757	11111.28	11213.33	0.1	0.106	0.91
660	17733.6	17019.15	0.135	0.112	-4.1979	11309.98	11404.12	0.119	0.117	0.8255
661	17237.05	16243.6	0.135	0.113	-6.1159	13048.75	13887.49	0.067	0.073	6.0395
662	12787.17	13968.11	0.135	0.135	8.4545	10724.28	11922.82	0.115	0.112	10.053
663	14639.28	15239.14	0.135	0.134	3.9363	10231.18	10587.2	0.125	0.123	3.3627
664	12401.97	13875.09	0.135	0.136	10.617	15788.25	15969.04	0.111	0.117	1.1322
665	13038.77	14765.39	0.135	0.136	11.694	12540.38	12477.66	0.089	0.09	-0.5027
666	12993.77	14047.84	0.135	0.135	7.5035	10602.64	10613.68	0.105	0.115	0.104
667	15507.44	14407.46	0.135	0.103	-7.6348	12239.73	12318.94	0.092	0.093	0.6429

668	12002.14	13082.49	0.135	0.136	8.258	10707.43	10718.47	0.107	0.117	0.103
669	17195.13	15870.73	0.135	0.112	-8.3449	11301.61	11747.64	0.128	0.123	3.7968
670	14912.39	15408.2	0.135	0.131	3.2178	13856.07	13954.98	0.066	0.069	0.7088
671	12532.68	16064.03	0.135	0.131	21.983	12759.85	12828.73	0.076	0.088	0.5369
672	12148.74	13389.94	0.135	0.137	9.2696	9457.605	9578.229	0.129	0.125	1.2594
673	11462.26	13925.71	0.135	0.134	17.69	12693.52	14520.96	0.075	0.077	12.585
674	12506.7	13587.05	0.135	0.136	7.9513	15709.66	15758.15	0.083	0.084	0.3077
675	15604.41	16510.76	0.135	0.132	5.4894	12972.16	12943.87	0.092	0.094	-0.2185
676	15746.8	16479.6	0.135	0.131	4.4467	12585.19	12798.15	0.107	0.106	1.664
677	11955.61	12377.84	0.135	0.126	3.4112	11441.35	11562.36	0.085	0.087	1.0465
678	11451.13	12693.75	0.135	0.138	9.7892	9851.123	10111.57	0.127	0.125	2.5758
679	16170.99	17080.14	0.135	0.129	5.3229	14972.76	14966.52	0.105	0.11	-0.0417
680	16675.91	16879.74	0.135	0.11	1.2076	13067.66	13049.59	0.112	0.116	-0.1385
681	12429.85	13737.51	0.135	0.134	9.5189	14360.25	14378.24	0.108	0.112	0.1251
682	12715.19	13948.73	0.135	0.136	8.8434	13009.71	12726.99	0.085	0.088	-2.2214
683	17435.67	18515.92	0.135	0.131	5.8341	11316.28	11418.33	0.104	0.11	0.8937
684	13015.25	14388.08	0.135	0.134	9.5414	12008.82	12164.98	0.126	0.123	1.2836
685	13190.9	13350.68	0.135	0.122	1.1968	12684.2	12746.01	0.075	0.086	0.4849
686	13359.23	15250.99	0.135	0.135	12.404	17900.02	18271.27	0.1	0.103	2.0319
687	15227.54	15869.41	0.135	0.13	4.0447	10362.49	10464.54	0.103	0.109	0.9752
688	15338.31	16095.45	0.135	0.131	4.7041	15114.33	15126.96	0.107	0.11	0.0835
689	13125.4	12851.81	0.135	0.124	-2.1287	11878.3	12086.41	0.122	0.12	1.7219
690	13001.32	14897.73	0.135	0.136	12.73	12029.49	13628.02	0.076	0.075	11.73
691	11985.57	12970.91	0.135	0.136	7.5965	11892.95	12616.38	0.103	0.11	5.7341
692	12313.19	12945.53	0.135	0.139	4.8846	12357.55	12541.78	0.121	0.121	1.4689
693	13544.77	14320.25	0.135	0.131	5.4153	13188.61	14175.54	0.095	0.08	6.9622
694	15647.07	16181.46	0.135	0.13	3.3025	13341.24	13877.31	0.118	0.122	3.8629
695	15519.79	16053.47	0.135	0.131	3.3244	13697.13	13648.43	0.091	0.094	-0.3568
696	16050	17015.84	0.135	0.13	5.6761	12581.19	12556.21	0.082	0.09	-0.1989
697	17732.88	15935.38	0.135	0.11	-11.28	13241.42	13218.7	0.085	0.086	-0.1719
698	12702.28	14052.25	0.135	0.131	9.6068	10501.84	10588.83	0.131	0.133	0.8215
699	11504.72	11917.39	0.135	0.138	3.4628	11517.11	11529.54	0.115	0.113	0.1078
700	12526.82	13714.59	0.135	0.137	8.6606	11534.38	12689.07	0.114	0.118	9.0999
701	14558.39	14312.59	0.135	0.102	-1.7174	12894.17	13317.34	0.104	0.109	3.1776
702	12858.94	13637.55	0.135	0.134	5.7093	12030.22	12016.29	0.096	0.101	-0.116
703	17469.77	16652.3	0.135	0.109	-4.909	11602.71	12606.77	0.077	0.089	7.9644
704	14233.5	15259.36	0.135	0.135	6.7228	14000.68	14819	0.097	0.093	5.5221
705	11900.86	13100.09	0.135	0.136	9.1543	11165.81	11518.69	0.101	0.111	3.0635
706	12219.86	13273.94	0.135	0.136	7.941	10821.35	11200.68	0.11	0.115	3.3866
707	16270.68	15585.51	0.135	0.111	-4.3961	13649.39	13586.67	0.091	0.091	-0.4616
708	10666.4	11963.04	0.136	0.137	10.839	11820.1	11911.23	0.124	0.126	0.7651
709	12593.53	14208.24	0.136	0.136	11.365	12129.67	12115.74	0.105	0.109	-0.115
710	12308.49	13141.34	0.136	0.135	6.3376	12393.29	13886.21	0.074	0.092	10.751
711	17243.9	18404.05	0.136	0.132	6.3038	16966.6	17697.19	0.112	0.108	4.1283
712	14121.23	14986.49	0.136	0.133	5.7737	11729.48	11740.52	0.108	0.117	0.094
713	11594.54	11852.77	0.136	0.139	2.1787	14849.8	14827.08	0.087	0.087	-0.1532

714	14597.15	15403.96	0.136	0.133	5.2377	12576.07	12513.35	0.091	0.091	-0.5012
715	12035.07	13185.3	0.136	0.135	8.7236	12547.96	12650	0.111	0.117	0.8067
716	12092.27	13492.64	0.136	0.139	10.379	14757.72	15150.61	0.116	0.114	2.5932
717	15255.62	15731.72	0.136	0.13	3.0264	15741.16	15734.93	0.104	0.109	-0.0396
718	14875.85	15461.86	0.136	0.131	3.7901	14389.48	14659.78	0.117	0.118	1.8438
719	17072.26	16210.32	0.136	0.112	-5.3172	11358.39	11699.72	0.081	0.091	2.9175
720	12182.41	13236.48	0.136	0.136	7.9634	9837.199	9956.661	0.124	0.123	1.1998
721	11776.93	12969.13	0.136	0.136	9.1926	15331.75	15408.95	0.101	0.106	0.501
722	12174.83	13296.28	0.136	0.135	8.4343	12278.4	12268.61	0.116	0.12	-0.0798
723	12892.41	14253.59	0.136	0.135	9.5498	13493.29	12987.76	0.095	0.077	-3.8923
724	13271.2	13972.75	0.136	0.134	5.0208	13047.07	13408.82	0.106	0.11	2.6979
725	16453.54	15606.11	0.136	0.116	-5.4301	10630.3	10732.35	0.099	0.105	0.9508
726	15907.02	16797.72	0.136	0.13	5.3025	15270.81	14683.53	0.096	0.078	-3.9996
727	10638.5	13406.93	0.136	0.134	20.649	12184.7	12434.32	0.071	0.078	2.0075
728	11263.06	13244.41	0.136	0.136	14.96	17641	17279.29	0.099	0.104	-2.0933
729	16397.5	15416.05	0.136	0.115	-6.3664	15578.91	15726.44	0.109	0.11	0.9382
730	12704.5	14369.44	0.136	0.135	11.587	11454.82	11556.33	0.129	0.129	0.8784
731	14353.15	15243.31	0.136	0.133	5.8397	12710.92	12467.7	0.084	0.088	-1.9508
732	11618.38	11560.25	0.136	0.122	-0.5028	14069.2	14462.08	0.098	0.105	2.7166
733	11576.94	13274.59	0.136	0.138	12.789	11923.99	12305.65	0.101	0.11	3.1015
734	11644.98	12847.1	0.136	0.138	9.3571	17421.24	17382.45	0.099	0.103	-0.2231
735	16440.65	17247.5	0.136	0.132	4.6781	10913.41	11015.46	0.106	0.113	0.9264
736	11537.27	12160.82	0.136	0.139	5.1276	16835.05	16972.33	0.099	0.103	0.8088
737	12764.93	14464.83	0.136	0.136	11.752	15711.27	16620.56	0.109	0.105	5.4709
738	11586.22	12562.93	0.136	0.136	7.7746	16887.62	16848.83	0.098	0.103	-0.2302
739	11696.67	13798.96	0.136	0.136	15.235	12966.91	13103.24	0.114	0.115	1.0404
740	17273.98	15789.62	0.136	0.11	-9.4009	12831.66	14340.86	0.075	0.086	10.524
741	12831.26	13885.33	0.136	0.136	7.5913	12140.62	12077.9	0.094	0.095	-0.5193
742	17486.55	16624.94	0.136	0.114	-5.1826	13803.23	13916.99	0.11	0.115	0.8174
743	14032.98	14813.23	0.136	0.133	5.2672	11392.2	11403.24	0.108	0.117	0.0968
744	12208.35	13528.63	0.136	0.137	9.7592	11897.69	11874.97	0.088	0.088	-0.1913
745	11032.47	12108.52	0.136	0.139	8.8867	12390.94	12758.04	0.13	0.132	2.8775
746	17002.34	16415.88	0.136	0.111	-3.5725	15826.24	17127.15	0.08	0.086	7.5957
747	16466.2	17817.65	0.136	0.132	7.5849	13515.71	13493.29	0.085	0.082	-0.1662
748	13590.67	14387.48	0.136	0.134	5.5382	10127.79	10295.69	0.122	0.12	1.6308
749	15502	16514.74	0.136	0.131	6.1323	12153.63	12145.35	0.089	0.087	-0.0682
750	16364.38	17288.42	0.136	0.132	5.3449	12755.97	12858.02	0.115	0.12	0.7936
751	13145.96	13438.24	0.136	0.125	2.1749	13193.79	13131.07	0.09	0.091	-0.4777
752	14676.73	15774.53	0.136	0.134	6.9593	12071.62	12513.21	0.116	0.111	3.529
753	15965.88	16932.35	0.136	0.131	5.7078	14334.92	14303.2	0.087	0.084	-0.2217
754	11147.35	12486.92	0.136	0.137	10.728	14585.23	14718.63	0.113	0.114	0.9063
755	13875.31	14658.65	0.136	0.133	5.3439	12745.86	12723.14	0.088	0.088	-0.1786
756	11941.43	12524	0.136	0.127	4.6516	12661.66	12570.74	0.107	0.104	-0.7233
757	10823.29	13008.49	0.137	0.137	16.798	15034.09	15349.07	0.101	0.107	2.0521
758	14235.52	15069.61	0.137	0.133	5.5349	11565.71	11707.22	0.123	0.123	1.2087
759	12433.85	13646.27	0.137	0.137	8.8846	12291.6	12714.77	0.105	0.109	3.3282

760	13763.53	13513.09	0.137	0.125	-1.8534	11677.77	12161.08	0.118	0.112	3.9742
761	17296.34	15880.55	0.137	0.111	-8.9152	11461.71	11870.87	0.124	0.118	3.4468
762	11785.28	12033.09	0.137	0.135	2.0595	11156.13	11335.96	0.115	0.114	1.5863
763	14724.72	15659.06	0.137	0.134	5.9667	13211.45	13593.11	0.097	0.105	2.8078
764	14559.37	15537.34	0.137	0.133	6.2944	17725.14	17408.78	0.099	0.103	-1.8172
765	11721.37	12775.44	0.137	0.136	8.2508	11557.3	11574.37	0.091	0.089	0.1475
766	15956.61	16761.53	0.137	0.13	4.8022	12857.38	12840.39	0.08	0.087	-0.1323
767	12117.02	13045.37	0.137	0.136	7.1164	14927.68	15543.33	0.09	0.086	3.9609
768	16878.34	16382.45	0.137	0.117	-3.0269	17791.71	17756.86	0.103	0.105	-0.1963
769	11912.43	13062.66	0.137	0.137	8.8055	15152.19	15563.65	0.093	0.103	2.6437
770	12192.64	13246.72	0.137	0.137	7.9573	12386.47	12418.4	0.097	0.094	0.2571
771	16691.86	17615.7	0.137	0.131	5.2444	10889.48	10805.84	0.122	0.114	-0.774
772	15160.32	15941.78	0.137	0.133	4.9019	15089.68	15166.88	0.102	0.107	0.509
773	12200.01	13222.87	0.137	0.137	7.7356	16640.32	16542.95	0.101	0.105	-0.5886
774	12695.78	14627.29	0.137	0.133	13.205	13014.67	13116.72	0.115	0.12	0.778
775	12133.14	13325.35	0.137	0.137	8.9469	13185.09	13214.79	0.112	0.117	0.2248
776	12494.77	13424.13	0.137	0.135	6.9231	13216.07	13921.93	0.114	0.12	5.0701
777	12422.85	13593.34	0.137	0.137	8.6107	13701.84	14076.02	0.108	0.112	2.6583
778	12131.43	13674.08	0.137	0.137	11.282	11946.36	12135.65	0.127	0.127	1.5598
779	11596.01	12506.86	0.137	0.137	7.2828	11880.8	11886.74	0.083	0.091	0.05
780	13212.05	13749.45	0.137	0.134	3.9085	13234.11	13347.87	0.116	0.121	0.8523
781	11743.33	13474.65	0.137	0.137	12.849	12294.07	12740.1	0.123	0.118	3.501
782	11666.2	12293.9	0.137	0.14	5.1057	12158.67	12135.95	0.084	0.085	-0.1872
783	11567.05	13219.33	0.137	0.127	12.499	12351.61	12465.37	0.103	0.108	0.9126
784	12662.26	14135.57	0.137	0.135	10.423	12970.3	12956.36	0.113	0.117	-0.1075
785	16960.47	15804.08	0.137	0.117	-7.317	14224	14337.26	0.111	0.116	0.79
786	12468.56	13953.79	0.137	0.137	10.644	10641.23	10529.77	0.117	0.116	-1.0585
787	11640.86	11297.76	0.137	0.122	-3.0369	13954.94	13923.23	0.096	0.093	-0.2278
788	17428.38	16576.57	0.137	0.114	-5.1387	11025.92	11077.35	0.114	0.109	0.4642
789	11849.72	12704.77	0.137	0.129	6.7301	12714.9	13235.37	0.121	0.116	3.9324
790	15472.5	16506.46	0.137	0.132	6.2639	13141.09	13522.76	0.097	0.105	2.8224
791	12012.28	13497.51	0.137	0.137	11.004	14833.89	14771.16	0.089	0.089	-0.4246
792	11132.32	13264.82	0.137	0.137	16.076	12944.55	13058.31	0.117	0.122	0.8712
793	12923.06	14280.1	0.137	0.137	9.503	12399.82	13499.47	0.063	0.072	8.1459
794	10908.53	11223.13	0.137	0.14	2.8031	11768.47	11874.66	0.102	0.107	0.8942
795	11115.37	11461.35	0.137	0.141	3.0187	14762.17	14773.09	0.106	0.11	0.0739
796	12476.22	14816.4	0.137	0.136	15.795	13060.21	14191.84	0.069	0.076	7.9738
797	11754.17	12192.98	0.138	0.127	3.5989	10983.03	10857.38	0.102	0.108	-1.1573
798	12390.73	12656.83	0.138	0.135	2.1024	14994.83	15007.46	0.107	0.11	0.0842
799	11613.85	12667.93	0.138	0.137	8.3208	13085.95	13199.71	0.117	0.122	0.8618
800	11504.33	12245.2	0.138	0.129	6.0503	12090.26	11478.8	0.069	0.074	-5.3268
801	12160.41	12866.6	0.138	0.134	5.4885	12409.97	12819.64	0.122	0.116	3.1956
802	11998.79	13191	0.138	0.138	9.038	16757.83	16622.68	0.098	0.102	-0.813
803	11579.21	12202.99	0.138	0.127	5.1117	13750.18	16201.97	0.068	0.07	15.133
804	16743.19	17682.59	0.138	0.132	5.3126	15994.93	15914.42	0.083	0.084	-0.5058
805	16673.13	17716.08	0.138	0.132	5.887	12488.75	12613.23	0.113	0.119	0.9868

806	12521.6	13179.2	0.138	0.135	4.9897	13287.39	13258.61	0.089	0.086	-0.2171
807	12095.72	13409.41	0.138	0.136	9.7968	10967.14	11495.87	0.114	0.114	4.5994
808	11950.13	14179.39	0.138	0.135	15.722	11616.35	11998.02	0.101	0.11	3.1811
809	11803.73	12690.95	0.138	0.138	6.9909	12853.43	12830.71	0.082	0.083	-0.1771
810	13104	13818.97	0.138	0.134	5.1739	11761.53	11820.95	0.085	0.087	0.5026
811	11898.17	12258.15	0.138	0.124	2.9367	12660.95	12647.01	0.112	0.117	-0.1102
812	17344.79	16515.4	0.138	0.115	-5.0219	14645.17	15107.77	0.121	0.117	3.062
813	11382.81	12505.97	0.138	0.138	8.981	11388.19	11365.47	0.087	0.088	-0.1999
814	12416.05	13470.12	0.138	0.138	7.8253	12496.74	12781.93	0.11	0.115	2.2311
815	12084.38	13427.3	0.138	0.138	10.001	12615.01	13201.55	0.124	0.119	4.4429
816	11392.15	12024.49	0.138	0.141	5.2588	12712.51	12689.79	0.085	0.085	-0.179
817	12010.53	12634.46	0.138	0.141	4.9383	13001.6	13103.64	0.118	0.123	0.7788
818	11507.69	11987.47	0.138	0.137	4.0023	10372.08	10383.12	0.102	0.112	0.1063
819	12586.61	12743.09	0.138	0.136	1.228	11364.6	11793.42	0.069	0.076	3.6361
820	11345.72	12918.49	0.138	0.137	12.175	10595.58	11215.58	0.127	0.123	5.528
821	11679.71	12923.67	0.138	0.139	9.6254	13655.86	13715.06	0.108	0.112	0.4317
822	11948.04	13641.47	0.138	0.138	12.414	11924.02	11861.3	0.087	0.088	-0.5288
823	12260.78	13764.47	0.138	0.138	10.924	12147.97	12352.65	0.111	0.11	1.657
824	11818.29	12872.37	0.138	0.138	8.1887	11795.29	14274.14	0.076	0.078	17.366
825	12464.59	13057.64	0.138	0.136	4.5418	12080.47	12182.51	0.117	0.123	0.8376
826	11763.82	13150.58	0.138	0.138	10.545	11969.13	11969.13	0.072	0.072	0
827	11169.44	12999.79	0.138	0.139	14.08	16886.68	16764.46	0.099	0.103	-0.729
828	12019.42	12394.93	0.138	0.137	3.0296	11334.34	11311.62	0.089	0.09	-0.2009
829	11429.82	12027.8	0.138	0.137	4.9716	10665.55	10734.93	0.087	0.098	0.6463
830	10714.97	11123.12	0.138	0.141	3.6694	11890.41	11705.14	0.124	0.124	-1.5828
831	12787.29	14503.87	0.138	0.137	11.835	16243.57	16178.83	0.085	0.086	-0.4001
832	10842.76	11918.24	0.138	0.139	9.0238	15399.15	15409.87	0.102	0.106	0.0695
833	11111.18	12385.02	0.138	0.138	10.285	11482.11	11584.16	0.099	0.105	0.8809
834	12216.93	13700.12	0.138	0.138	10.826	12658.06	12926.1	0.118	0.118	2.0736
835	11406.12	12270.41	0.138	0.139	7.0437	11260.02	11909.76	0.096	0.103	5.4555
836	11997.91	13845.75	0.138	0.138	13.346	11511.27	11511.27	0.083	0.083	0
837	11296.27	12893.63	0.138	0.138	12.389	11336.84	11365.84	0.123	0.121	0.2551
838	11412.69	12639.96	0.138	0.139	9.7094	10263.6	10463.42	0.114	0.12	1.9098
839	11867.31	12776.45	0.138	0.14	7.1157	13281.42	13522.84	0.088	0.089	1.7853
840	11546.72	12505.24	0.138	0.141	7.6649	11059.81	11227.5	0.109	0.113	1.4936
841	11129.69	13236.12	0.138	0.138	15.914	11438.82	11890.71	0.13	0.125	3.8003
842	12174.18	12453.21	0.138	0.137	2.2406	13703.11	14069.3	0.104	0.108	2.6027
843	12729	14229.52	0.139	0.137	10.545	13988.7	14002.84	0.078	0.079	0.101
844	11041.01	12037.77	0.139	0.14	8.2803	12193.79	12573.21	0.108	0.115	3.0177
845	12172.03	12465.2	0.139	0.136	2.3519	10295.92	10325.92	0.119	0.114	0.2905
846	11072.4	11971.79	0.139	0.139	7.5126	12857.92	13796.24	0.1	0.097	6.8013
847	11201.31	13015.21	0.139	0.139	13.937	11350.73	11732.39	0.1	0.109	3.2531
848	12302.59	12898.78	0.139	0.137	4.622	11935.7	11952.77	0.086	0.086	0.1428
849	13132.64	13670.04	0.139	0.135	3.9312	14897.46	14849.89	0.083	0.085	-0.3204
850	13155.27	13990.04	0.139	0.135	5.9669	14107.11	14093.17	0.107	0.111	-0.0989
851	11621.72	12507.56	0.139	0.14	7.0825	12720.17	12657.45	0.096	0.097	-0.4955

852	11554	13249.2	0.139	0.138	12.795	11354.56	11460.75	0.104	0.11	0.9265
853	11339.43	13059.43	0.139	0.138	13.171	11024.7	11494.78	0.131	0.128	4.0896
854	11528.33	11772	0.139	0.137	2.07	9419.59	9581.636	0.126	0.123	1.6912
855	10916.07	12114.64	0.139	0.14	9.8935	12860.82	12962.87	0.106	0.112	0.7872
856	12302.7	13600.85	0.139	0.138	9.5446	12617.51	12612.96	0.088	0.095	-0.0361
857	11683.35	12986.51	0.139	0.14	10.035	12286.55	12482.7	0.121	0.122	1.5714
858	12888.02	13516.21	0.139	0.135	4.6477	12049.11	12026.39	0.089	0.089	-0.1889
859	11133.73	11621.79	0.139	0.138	4.1995	11722.74	11702.74	0.096	0.093	-0.1709
860	11745.42	12644.07	0.139	0.137	7.1073	13748.91	13686.19	0.087	0.087	-0.4583
861	13117.1	13832.78	0.139	0.136	5.1738	15109.64	15495.79	0.112	0.11	2.492
862	11726.11	12005.14	0.139	0.138	2.3243	12332.06	12312.06	0.089	0.086	-0.1624
863	11734.95	13104.55	0.139	0.137	10.451	11644.66	11552.15	0.102	0.111	-0.8008
864	10642.84	11664.96	0.139	0.14	8.7623	14898.56	16044.48	0.1	0.108	7.1422
865	11782.19	12662.71	0.139	0.139	6.9537	12552.16	12533.37	0.091	0.094	-0.1499
866	12851.21	13368.11	0.139	0.136	3.8667	12446.31	13200.47	0.111	0.113	5.7131
867	12326.37	13349.23	0.139	0.139	7.6623	12128.21	12206.71	0.127	0.13	0.643
868	11117.16	13504.2	0.139	0.137	17.676	12596.14	13133.89	0.124	0.118	4.0943
869	11500.83	12352.69	0.139	0.141	6.8961	11687.33	11624.61	0.091	0.092	-0.5396
870	11102.2	11345.87	0.139	0.138	2.1477	11897.77	11926.77	0.092	0.089	0.2431
871	10994.38	12158.37	0.139	0.139	9.5736	10375.1	11825.94	0.081	0.074	12.268
872	10984.41	12003.6	0.139	0.139	8.4907	13334.59	13431.15	0.071	0.075	0.719
873	11150.59	11375.69	0.139	0.143	1.9788	11252.39	11311.8	0.091	0.093	0.5252
874	12404.92	12779.22	0.139	0.137	2.929	12525.73	13087.9	0.121	0.12	4.2953
875	11175.85	11424.38	0.14	0.14	2.1754	14556.94	14254.93	0.081	0.085	-2.1186
876	10942.86	11473.07	0.14	0.143	4.6213	10112.32	10296.76	0.123	0.126	1.7912
877	11446.09	12477.01	0.14	0.137	8.2625	14888.17	14916.67	0.083	0.084	0.191
878	10853.11	11616.06	0.14	0.14	6.5681	11036.29	11050.61	0.117	0.116	0.1295
879	11803.71	12793.07	0.14	0.137	7.7336	15497.5	15559.13	0.084	0.086	0.3961
880	11729.36	12887.87	0.14	0.139	8.9892	15584.87	15104.78	0.085	0.088	-3.1784
881	11849.71	13497.13	0.14	0.139	12.206	11238.34	11513.33	0.112	0.118	2.3884
882	11270.74	12184.45	0.14	0.139	7.499	16521.19	16674.08	0.111	0.112	0.917
883	12592.36	13216.62	0.14	0.138	4.7233	12566.71	13039.38	0.097	0.103	3.6249
884	11339.88	12365.68	0.14	0.14	8.2955	15628.64	16097.09	0.12	0.116	2.9102
885	11947.19	12362.91	0.14	0.137	3.3626	12437.34	12574.71	0.121	0.121	1.0924
886	11721.45	12095.75	0.14	0.138	3.0945	11077.79	11242.26	0.112	0.111	1.463
887	11926.89	12929.81	0.14	0.139	7.7566	10398.95	10814.69	0.131	0.121	3.8442
888	10709.91	11695.75	0.14	0.14	8.4291	16582.58	17036.98	0.113	0.113	2.6671
889	11858.44	12106.26	0.14	0.138	2.047	10214.75	10637.92	0.111	0.116	3.978
890	10472.69	11679.94	0.14	0.141	10.336	13244.38	14290.1	0.091	0.077	7.3178
891	10667.13	11621.41	0.14	0.14	8.2114	11683.01	11648.36	0.118	0.123	-0.2974
892	12068.23	12660.86	0.14	0.14	4.6808	15439.61	15976.47	0.112	0.119	3.3603
893	11468.23	11807.17	0.14	0.138	2.8707	10682	10853.21	0.07	0.088	1.5775
894	11332.76	11576.44	0.14	0.139	2.1049	11062.44	12186.08	0.069	0.066	9.2207
895	10959.53	11559.22	0.14	0.139	5.188	14130.98	13922.91	0.107	0.112	-1.4945
896	10761.1	12300.03	0.14	0.139	12.512	15825.84	15743.33	0.085	0.085	-0.5241
897	12034.08	12626.72	0.14	0.14	4.6935	15796.98	16691.09	0.112	0.11	5.3568

898	11673.41	11917.09	0.14	0.139	2.0448	15420.39	15497.59	0.1	0.105	0.4981
899	11430.2	12238.09	0.14	0.139	6.6014	15756.16	15785.78	0.105	0.11	0.1876
900	10269.55	11224.51	0.14	0.143	8.5078	15861.49	15241.7	0.101	0.109	-4.0664
901	12463.58	12980.48	0.14	0.136	3.9821	11480.82	11757.51	0.108	0.113	2.3533
902	10885.41	11776.06	0.14	0.141	7.5632	14970.33	14938.62	0.086	0.082	-0.2123
903	12566.8	13061.28	0.14	0.138	3.7858	17376.03	17806.77	0.099	0.103	2.419
904	10942.52	12003.39	0.14	0.14	8.8381	12165.52	12169.37	0.097	0.101	0.0316
905	11264.11	12192.47	0.14	0.14	7.6142	12245.21	11898.73	0.083	0.091	-2.9119
906	12646.11	13442.92	0.14	0.137	5.9274	14125.5	14227.55	0.111	0.115	0.7172
907	11470.61	11714.28	0.141	0.139	2.0802	13820.92	13702.64	0.114	0.113	-0.8632
908	11379.8	12610.74	0.141	0.142	9.761	12300.11	12390.82	0.078	0.082	0.7321
909	11641.18	12621.88	0.141	0.139	7.7698	12261.33	12363.37	0.113	0.118	0.8254
910	11259.85	12196.02	0.141	0.14	7.6761	10501.73	10584.75	0.121	0.125	0.7843
911	10940.89	11961.83	0.141	0.139	8.535	11162.03	11057.09	0.105	0.113	-0.9491
912	11523.49	12912.58	0.141	0.138	10.758	15032.08	15466.47	0.101	0.105	2.8086
913	10983.4	12195.61	0.141	0.14	9.9397	13272.37	14604.03	0.065	0.067	9.1185
914	12273.41	13182.86	0.141	0.137	6.8987	14042.76	14028.82	0.108	0.112	-0.0993
915	11554.56	11833.6	0.141	0.139	2.358	11622.53	11612.74	0.096	0.1	-0.0843
916	11200.3	11801	0.141	0.14	5.0902	10691.86	10752.75	0.128	0.129	0.5662
917	12900.05	13609.67	0.141	0.138	5.2141	11155.85	11880.29	0.109	0.114	6.0978
918	11820.15	12938.23	0.141	0.139	8.6416	12027.11	12049.87	0.107	0.116	0.1889
919	11288.7	12184.19	0.141	0.141	7.3497	14939.83	15486.94	0.095	0.107	3.5327
920	10340.62	11281.18	0.141	0.141	8.3374	12077.31	12077.31	0.08	0.08	0
921	10995.77	12045.84	0.141	0.14	8.7173	15582.29	15659.48	0.104	0.109	0.4929
922	10170.62	11339.72	0.141	0.141	10.31	17202.23	17824.62	0.11	0.106	3.4917
923	11066.33	11440.63	0.141	0.139	3.2717	15575.61	15919.55	0.111	0.117	2.1605
924	11965.82	13619.05	0.141	0.139	12.139	14956	15637.39	0.113	0.111	4.3574
925	10744.73	11831.98	0.141	0.14	9.1891	14130.01	14430.51	0.119	0.12	2.0824
926	12758.63	13183.81	0.141	0.138	3.225	12409.59	12342.22	0.086	0.086	-0.5458
927	10340.41	10811.9	0.141	0.14	4.3609	15128.53	14237.32	0.095	0.075	-6.2597
928	11501.28	12508.8	0.141	0.138	8.0545	15622.44	16129.25	0.099	0.109	3.1422
929	11678.83	11922.5	0.141	0.14	2.0438	15899.15	16323.33	0.097	0.103	2.5986
930	11952.35	12785.22	0.141	0.137	6.5144	11361.76	12245.35	0.099	0.11	7.2157
931	12622.98	13041.3	0.141	0.138	3.2077	13319.71	13703.68	0.104	0.109	2.8019
932	11130.36	11409.39	0.141	0.14	2.4456	11406.74	11599.67	0.128	0.127	1.6632
933	10859.11	11382.53	0.142	0.14	4.5984	12783.16	13430.24	0.11	0.116	4.818
934	11151.75	12088.18	0.142	0.141	7.7467	13255.92	13320.06	0.068	0.073	0.4815
935	11419.32	11902.03	0.142	0.14	4.0557	11176.34	11223.12	0.121	0.122	0.4168
936	11800.59	12508.58	0.142	0.14	5.66	12258.36	13195.21	0.096	0.083	7.0999
937	11266.37	11545.4	0.142	0.14	2.4168	12718.81	12628.61	0.108	0.104	-0.7143
938	11697.49	12202.8	0.142	0.14	4.1409	11288.93	11777.5	0.133	0.128	4.1484
939	11126.83	11501.13	0.142	0.139	3.2545	10428.46	10688.91	0.125	0.124	2.4367
940	11633.9	12822.42	0.142	0.139	9.269	11374.76	11503.54	0.086	0.092	1.1195
941	12376.27	12784.08	0.142	0.139	3.19	11694.87	11714.37	0.077	0.078	0.1664
942	12040.58	12510.91	0.142	0.14	3.7594	11451.85	11553.9	0.115	0.121	0.8832
943	11122.84	12018.34	0.142	0.142	7.4511	11960.17	11937.45	0.08	0.081	-0.1903

944	11667.69	12818.48	0.142	0.136	8.9776	15973.65	16417.03	0.091	0.105	2.7007
945	11928.6	12398.93	0.142	0.14	3.7933	11820.26	11882.39	0.085	0.082	0.5229
946	11842	12462.63	0.142	0.14	4.9799	10305.3	10413	0.131	0.132	1.0342
947	11064.11	11438.41	0.142	0.14	3.2723	14846.44	15007.62	0.113	0.114	1.074
948	11418.99	11793.29	0.142	0.14	3.1738	10058.6	10351.94	0.126	0.126	2.8337
949	10814.65	11093.68	0.142	0.14	2.5152	10451.64	10684.69	0.117	0.115	2.1812
950	11345.06	12233.86	0.142	0.142	7.2651	12759.84	13784.06	0.094	0.08	7.4304
951	11610.99	11890.02	0.142	0.14	2.3468	11800.05	12722.18	0.074	0.074	7.2482
952	10730	11617.35	0.142	0.141	7.6382	13752.11	13697.67	0.089	0.09	-0.3974
953	11106.72	11556.46	0.142	0.14	3.8917	11959.66	13032.58	0.098	0.084	8.2326
954	11956.22	12299.31	0.142	0.14	2.7895	12398.31	12335.59	0.096	0.097	-0.5085
955	11517.33	12626.15	0.142	0.138	8.7819	15533.77	15402.77	0.084	0.084	-0.8505
956	11018.58	11269.33	0.142	0.141	2.225	12538.57	12477.36	0.115	0.115	-0.4906
957	11581.07	11956.59	0.142	0.141	3.1406	15506.73	15643.63	0.105	0.109	0.8751
958	10769.76	11735.97	0.142	0.141	8.2329	11683.2	11886.46	0.102	0.108	1.71
959	10841.12	11642.56	0.142	0.142	6.8837	10716	10774.99	0.116	0.114	0.5475
960	10988.9	12400.59	0.143	0.142	11.384	12885.43	13558.74	0.118	0.113	4.9659
961	12346.84	13296.71	0.143	0.138	7.1436	12760.25	12812	0.107	0.108	0.4039
962	11699.34	12107.16	0.143	0.139	3.3684	12617.93	12597.81	0.084	0.092	-0.1597
963	12973.72	13669.91	0.143	0.138	5.0929	12402.33	12511.92	0.086	0.095	0.8758
964	10902.57	11766.85	0.143	0.143	7.3451	12026.24	11770.55	0.124	0.125	-2.1722
965	11120.98	12148.9	0.143	0.141	8.4611	15666.79	15619.22	0.082	0.084	-0.3046
966	11585.86	12008.53	0.143	0.14	3.5197	10281.37	10461.19	0.118	0.116	1.719
967	11768.29	12036.82	0.143	0.14	2.2309	14413.68	14504.39	0.071	0.075	0.6254
968	11125.62	11935.35	0.143	0.143	6.7843	15781.08	16390.02	0.1	0.117	3.7153
969	10386.39	10847.14	0.143	0.14	4.2476	10959.83	10970.87	0.107	0.117	0.1006
970	11924.63	12369.22	0.143	0.141	3.5944	12490.59	13027.19	0.105	0.109	4.1191
971	10944.85	11458.77	0.143	0.141	4.4849	12119.82	12479.23	0.086	0.086	2.8801
972	11158.49	12277.54	0.144	0.141	9.1146	14064.2	14799.06	0.115	0.121	4.9655
973	11126.57	11708.03	0.144	0.141	4.9663	16381.7	16655.59	0.098	0.104	1.6444
974	11350.83	11725.13	0.144	0.141	3.1923	11893.28	13645.53	0.082	0.074	12.841
975	11161.37	11977.09	0.144	0.141	6.8107	16135.88	16348.6	0.116	0.117	1.3012
976	11393.65	12106.61	0.144	0.139	5.8891	12191.64	12819.39	0.121	0.116	4.8968
977	11134.47	11473.41	0.144	0.142	2.9542	14554.39	14835.22	0.104	0.109	1.893
978	11942.31	12495.81	0.144	0.142	4.4295	17224.16	17122.66	0.099	0.103	-0.5928
979	10959.86	11944.16	0.144	0.141	8.2408	12237.81	12175.09	0.092	0.092	-0.5152
980	11341.51	11630.04	0.144	0.14	2.4809	12519.78	13063.89	0.122	0.117	4.165
981	10817.16	11382.26	0.144	0.141	4.9647	15338.53	15716.26	0.107	0.118	2.4034
982	11150.06	11648.62	0.144	0.143	4.28	11796.79	14236.69	0.073	0.073	17.138
983	10576.63	11100.04	0.144	0.142	4.7154	13295.8	13677.46	0.098	0.106	2.7905
984	11221.45	11596.97	0.144	0.142	3.238	10857.56	10940.58	0.122	0.126	0.7588
985	10889.82	11229.77	0.144	0.142	3.0272	12079.5	12580.22	0.107	0.109	3.9803
986	10918.44	11118.18	0.144	0.142	1.7965	16338.62	15307.14	0.097	0.073	-6.7385
987	10831.5	11740.81	0.144	0.143	7.7449	14410.58	14359.07	0.09	0.09	-0.3587
988	11463.9	11838.2	0.144	0.142	3.1618	11599.33	11676.73	0.11	0.119	0.6629
989	11656.39	12361.14	0.144	0.14	5.7013	11600.76	11613.19	0.084	0.084	0.107

990	10999.03	11398.77	0.144	0.141	3.5069	11173.56	11380.25	0.115	0.116	1.8162
991	10985.39	11828.47	0.144	0.141	7.1276	10913.52	11371.26	0.121	0.12	4.0253
992	11616.37	12273.09	0.144	0.141	5.3509	11938.31	12291.78	0.106	0.111	2.8756
993	9905.793	10412.64	0.145	0.142	4.8676	10988.7	11074.02	0.125	0.127	0.7704
994	11057.52	11503.03	0.145	0.143	3.873	12319.23	12296.51	0.089	0.089	-0.1848
995	11138.38	12117.32	0.145	0.142	8.0789	17245.76	17617.01	0.099	0.102	2.1073
996	10096.94	10603.79	0.145	0.142	4.7799	11965.64	12079.78	0.084	0.084	0.9449
997	10555.24	11046.4	0.145	0.141	4.4464	9656.981	9969.859	0.125	0.123	3.1382
998	10985.5	11511.84	0.145	0.143	4.5722	11279.39	11258.68	0.119	0.117	-0.184
999	10997.9	11526.76	0.145	0.141	4.5881	12116.83	12089.97	0.087	0.088	-0.2222
1000	9995.584	10338.67	0.147	0.145	3.3185	14180.83	14035.98	0.115	0.114	-1.032

8.3 Submission requirements

For reasons of data protection, the curriculum vitae is not published in the electronic version.

For reasons of data protection, the curriculum vitae is not published in the electronic version.

Eidesstattliche Erklärung

Hiermit versichere ich, Nadav Nir, dass ich die Dissertation Trailing the lanscape selbständig angefertigt habe und keine anderen als die von mir angegebenen Quellen
und Hilfsmittel verwendet habe.

Ich erkläre hiermit, dass die Dissertation bisher nicht in dieser oder anderer Form in einem anderen Prüfungsverfahren vorgelegen hat.

Nadav Nir

21.10.2022